



HAL
open science

Contribution of the DNA sensing pathway STING in neutrophilic allergic asthma exacerbation

Yasmine Messaoud-Nacer

► **To cite this version:**

Yasmine Messaoud-Nacer. Contribution of the DNA sensing pathway STING in neutrophilic allergic asthma exacerbation. Immunology. Université d'Orléans, 2023. English. NNT : 2023ORLE1084 . tel-04770000

HAL Id: tel-04770000

<https://theses.hal.science/tel-04770000v1>

Submitted on 6 Nov 2024

HAL is a multi-disciplinary open access archive for the deposit and dissemination of scientific research documents, whether they are published or not. The documents may come from teaching and research institutions in France or abroad, or from public or private research centers.

L'archive ouverte pluridisciplinaire **HAL**, est destinée au dépôt et à la diffusion de documents scientifiques de niveau recherche, publiés ou non, émanant des établissements d'enseignement et de recherche français ou étrangers, des laboratoires publics ou privés.

UNIVERSITÉ D'ORLÉANS
ÉCOLE DOCTORALE SANTE, SCIENCES BIOLOGIQUES ET CHIMIE DU VIVANT

LABORATOIRE D'IMMUNOLOGIE NEUROGENETIQUE

EXPERIMENTALES ET MOLECULAIRES

UMR7355 – CNRS – Orléans

THÈSE

Présentée par :

Yasmine MESSAOUD NACER

Soutenue le : 09 Octobre 2023

Pour obtenir le grade de : **Docteur de l'Université d'Orléans**

Discipline - Spécialité : Biologie – Immunologie

**Contribution of the DNA sensing pathway STING in
neutrophilic allergic asthma exacerbation**

THÈSE dirigée par :

Valérie QUESNIAUX
Dieudonnée TOGBE

Directrice de Recherche, UMR7355 CNRS, Université d'Orléans.
Professeur des universités, Université d'Orléans, UMR7355 CNRS.

RAPPORTEURS :

Danilo GUERINI
Laurent REBER
Xavier LAHAYE

Directeur de Recherche, Novartis Institute for BioMedical Research, Bâle.
Directeur de Recherche, INFINITY, INSERM U1291, Toulouse
Chargé de recherche, Institut Curie, Inserm U932, Paris.

JURY :

Catherine Mura - Président du Jury Professeur des universités, **Université d'Orléans**, UMR7355 CNRS
Laurent REBER Directeur de Recherche, INFINITY, INSERM U1291, Toulouse
Danilo GUERINI Directeur de Recherche, Novartis Institute for BioMedical Research, Bâle.
Jean-Michel SALLENAVE Professeur des universités, Université de Paris-Cité, INSERM U1152, Paris
Xavier LAHAYE Chargé de recherche, Institut Curie, Inserm U932, Paris.

Remerciements – Acknowledgments

I would like to express my heartfelt appreciation to the members of the jury for honoring me with their presence, for their invaluable contribution, and the time dedicated to evaluating my thesis. My sincere thanks go to each of them for sharing their expertise generously. Thank you to Dr Danilo Guerini, Pr Laurent Reber and Dr Xavier lahaye for taking the time to evaluate this work as rapporteurs. Thank you to Pr Jean-Michel Sallenave for accepting to evaluate my thesis as examiner. Lastly, I would like to thank Pr Catherine Mura for being the chairperson of my thesis jury, which marks the end of this demanding process. I am aware of the opportunity I have been given to receive their evaluation and support.

Dr Valérie Quesniaux. Je vous remercie de m'avoir accueillie dans votre laboratoire et de m'avoir permis de progresser. J'ai beaucoup appris de vous, notamment à modérer mes propos lorsqu'il s'agissait de tirer des conclusions, « It's an over interpretation », I got it ! et je l'ai gravé dans ma tête. Merci de m'avoir aidée à rédiger mes articles, m'épargnant l'angoisse de la page blanche, sans jamais me censurer. Je vous souhaite une très bonne continuation.

Pr Dieudonnée Togbe. Il y a cinq ans, vous avez choisi de me donner une chance et de croire en moi. Les répétitions pour les concours de thèse et vos conseils m'ont été précieux à cette époque, je vous en suis infiniment reconnaissante. Merci de m'avoir fait confiance une seconde fois pour gérer mes projets de thèse. Ce parcours, qui n'a effectivement pas été un long fleuve tranquille (comme vous dites si souvent), m'a permis de me construire, souvent à travers des épreuves. Arrivée au bout de ce fleuve tumultueux, nos chemins vont maintenant bifurquer. Merci de m'avoir prêté cette barque, je vous la renvoie chargée de mes meilleurs vœux pour vos nouvelles fonctions en 2024, et vous souhaite une très bonne continuation.

Dr Bernhard Ryffel. Je vous remercie pour l'intérêt incommensurable que vous témoignez aux projets de tout-un-chacun, ainsi que pour vos précieux conseils, riches de votre expérience. Votre passion pour la science que vous transmettez aux jeunes du laboratoire est admirable.

Elodie Culierier. Chère amie, tu as sans nul doute joué un rôle important durant ces années, il pouvait nous arriver n'importe quoi ce n'était pas grave, nous étions à deux ! Les doutes et les frustrations étaient divisés par deux, la joie des petites victoires au labo était multipliée par deux, et puis un jour tu es partie pour de nouvelles aventures. Merci pour ton soutien infailible, tes encouragements, la force que tu me donnais ainsi que les innombrables heures passées à mes côtés. Je te souhaite tout le bonheur que tu mérites.

Stephanie Rose. Ma profonde reconnaissance pour ton assistance, sache que l'oreille attentive que tu me tendais pour m'écouter parler de mes élans de nouvelles idées de manip comptais énormément pour moi. Te voir donner du crédit à ces idées insufflait de l'espoir en moi. Merci d'avoir partagé ton bureau avec moi, toujours dans une ambiance agréable et positive. Je te souhaite beaucoup de bonheur et une très bonne continuation.

Je tiens à témoigner de ma sincère amitié envers mes amis de l'INEM, qui ont participé au formidable environnement humain et scientifique et qui ont contribué à transformer le quotidien en une extraordinaire aventure. Meriem.T, Asma.O, Sarah.M, Sarah.H-M, Rania.B, Sara.B, Vidian.DC, Mathilde.F, Julie.P, Amandine.F, Alicia, Merci pour tout ... je vous


souhaite beaucoup de bonheur et de réussite. Je souhaite la bienvenue aux nouveaux thésards ainsi qu'à tous les futurs nouveaux thésards de la maison, je croise les doigts pour vous !

Je remercie également tous mes collègues membres de l'INEM. Votre contribution et vos engagements ont rendu notre travail ensemble plus agréable. Merci pour la bienveillance que vous avez souvent témoignée à notre égard. Je vous souhaite beaucoup de bonheur et une bonne continuation dans vos carrières et projets.

Je remercie tous les membres d'Artimmune pour leurs nombreux conseils techniques et pour tout ce que j'ai appris auprès d'eux, ainsi que pour tous les petits moments de partage. Je trouvais souvent refuge chez vous et la nostalgie de mes débuts. Merci à Nathalie et Aurélie qui m'ont épaulé lors de mes débuts périlleux durant mon stage de master. Je vous souhaite à tous beaucoup de bonheur, de beaux projets et une longue vie à votre équipe.

Je n'oublie pas également mes camarades de master auprès de qui j'ai débuté cette aventure Orléanaise. Je remercie chaleureusement Elodie.V, Valentin.B, Christophe.D, et Florestan.C pour leur accueil et leur gentillesse, je vous souhaite à tous une brillante carrière.

A tous les thésards ayant entamé leur parcours l'année de la pandémie du COVID-19, un quotidien marqué par l'isolement, des couvre-feux, de beaucoup de ruptures de stock et de situation particulièrement stressantes. Vous avez tous été si courageux.

My special gratitude to Alexandra Asanovna Elbakyan, the "science's pirate Queen" , without your brave initiative, all this work would not have been possible. Merci pour le soutien

Je tiens à exprimer ma profonde gratitude envers mes parents. Merci à eux de m'avoir transmis la passion des sciences et de m'avoir soutenu dans cette quête éprouvante et de m'avoir écouté râler ! Merci pour l'éducation et les valeurs qui m'ont été inculqués qui ont façonné la personne que je suis aujourd'hui. Je souhaite également adresser mes félicitations à ma chère maman pour son remarquable travail, son dévouement et sa bravoure, une source inépuisable de courage !

Merci à tous ceux qui ont croisé un jour mon chemin, par le plus grand des hasards, et qui ont été une source d'inspiration, de motivation et de bienveillance. Il ne restera de nous que ce que l'on a donné !

List of figures

Figure 01: Predisposing factors of ARDS

Figure 02: Intact alveolar–capillary barrier

Figure 03: Increased permeability in alveolar–capillary barrier.

Figure 04: Macrophages polarization: the “M1 / M2 paradigm “.

Figure 05: Neutrophil-mediated lung injury of the alveolar epithelium via multiple mechanisms.

Figure 06: Neutrophils contribution to health and disease.

Figure 07: Simplified Asthma pathophysiology.

Figure 08: Asthma phenotypes, asthma endotypes and the underlying moldable mechanisms and corresponding treatments.

Figure 09: Biomarkers and associated indicators of asthma endotypes.

Figure 10: cellular and molecular mechanisms governing T2 asthma.

Figure 11: IL-13-STAT6-dependent mechanisms of mucus production.

Figure 12: Cellular and molecular mechanism governing T2-low neutrophilic asthma.

Figure 13: Regulated cell death (RDC) subgroups.

Figure 14: Timeline of the history of cell death research in immunology

Figure 15: The two major apoptotic pathways.

Figure 16: Canonical and noncanonical pathways of pyroptosis.

Figure 17: Necroptosis pathways: “Apoptosis, I got your back !”

Figure 18: Signaling events within the necrosome.

Figure 19: Main molecular mechanism governing NETosis.

Figure 20: “Suicidal” VS “vital” NETs formation.

Figure 21: Caspase-8, a focal point coordinating apoptosis, necroptosis and pyroptosis

Figure 22: A prototypical example of PANoptosome formation (Case of ZBP1-PANoptosome triggered by IAV infection)

Figure 23: Interactome of molecules involved in apoptosis, pyroptosis and necroptosis

Figure 24: Mitochondrial permeabilization as an initiator of inflammation.

Figure 25: Mechanism of cytosolic DNA sensing by the cGAS-STING pathway.

Figure 26: Human vs murine cGAS in DNA detection and cGAMP production.

Figure 27: Propagation of innate responses via the inter-cellular transmission of cGAMP.

Figure 28: DNA-Dependent Regulated Cell Death Pathways.

Figure 29: Proposed mechanism of cGAS-STING-dependent type I IFNs mediating lung immunopathology during severe COVID-19.

Figure 30: Dimeric amidobenzimidazole (diABZI) STING agonist development.

Figure 31: Direct intracellular STING activation strategies.

Figure 32: Immunoblots of phosphorylated STING, cGAS, γ H2AX and Cit-H3 with Actin β as a reference, suggesting the involvement of immune infiltrating cells in the processes of immune exacerbation.

Figure 33: *HIF-1 α* transcripts in lung of STING-dependent asthma exacerbation mice model.

List of tables

Table 01: Macrophages polarization and classification.

Table 02: Major characteristics of asthma phenotype and endotype allowing disease stratification.

Table 03: Signaling pathways involved in asthma pathophysiology.

Table 04: Walter Gottlieb Land's classification of DAMPs.

Abbreviations

ACD: Accidental cell death

ADAR1: Adenosine deaminase acting on RNA 1

AIM2: Absent in Melanoma 2

ALI: Acute lung injury

APAF-1: apoptotic peptidase activating factor 1

ApoEVs: Apoptotic extracellular vesicles

ARDS: Acute respiratory distress syndrome

ARF GTPases: ADP-ribosylation factor

ARG1: Arginase 1

ASC: apoptosis-associated speck-like protein containing a CARD

AT I/II: alveolar type I / II cell

BALF: Bronchoalveolar lavage fluid

BCL-xL: B-cell lymphoma-extra large

BH3-only: Bcl-2 homology 3-only

CARD: Caspase Activation and Recruitment Domain.

C-di-AMP: cyclic diadenosine monophosphate

CG: cathepsin G

cGAMP: Cyclic GMP-AMP

cGAS: Cyclic GMP-AMP Synthase

cIAPs: Cellular inhibitors of apoptosis

CLC: Charcot–Leyden crystals

CLCA: calcium-activated chloride channel 1

COP-II Complex: Coat Protein Complex II

COX-2: cyclooxygenase 2

DAD: diffuse alveolar damage

DAI: DNA-dependent activator of IFN-regulatory factors

DAMP: Danger-associated molecular patterns.

DdC: 2',3'-dideoxycytidine

DDX41: DEAD-box helicase 41.

DEF-1: defensin-1

DEK: Chromatin-binding protein

diABZI: di-Amino Benzimidazole

DISC: death-inducing signaling complex

DMXAA: 5,6-dimethylxanthenone-4-acetic acid

DNA-PK: DNA-dependent protein kinase.

DSB: Double-stranded breaks

dsRNA: double-stranded DNA

ENPP1: ecto-nucleotide pyrophosphatase phosphodiesterase 1

ER: Endoplasmic reticulum

ERAD: ER-associated degradation

F3: Coagulation Factor III

FADD: FAS-associated via death domain

FASL: fas ligand,

HDAC: Histone deacetylase

HDM: House dust mite

HIV: Human Immunodeficiency Virus

HMGB1: High Mobility Group Box 1

HSV: Herpes Simplex Virus

IAV: Influenza A Virus

ICD: Immunogenic cell death

IFIT: Interferon-induced protein with tetratricopeptide repeats

IRF3: Interferon Regulatory Factor 3

ISGs: Interferon-Stimulated Genes

LDH: Lactate Dehydrogenase

LRRC8: Leucine-rich repeat-containing protein 8

MAPK: mitogen-activated proteins kinases

MB21D1: Mab-21 Domain Containing 1

MCP-: monocyte chemotactic protein 1

MLKL: Mixed lineage kinase domain-like protein

MX1: Myxovirus resistance protein 1

NCCD: Nomenclature Committee on Cell Death

NE: Neutrophil elastase

NETs: neutrophil extracellular traps

NK cell: Natural killer cell

NONO: Non-POU domain-containing octamer-binding protein

NOS2: Nitric Oxide Synthase 2

NOX2: ROS producing NADPH oxidase complex.

NOXA: Phorbol-12-myristate-13-acetate-induced protein 1

OAS: 2'-5'-oligoadenylate synthetase

OVA: Ovalbumin

P2X7R: Purinergic P2X7 receptor

PAD4: Peptidyl -arginine deiminase type 4

PANoptosis: (P, pyroptosis; A, apoptosis; N, necroptosis)

PCD: Programmed cell death

pmSTING: plasmatic membrane STING

PNPasep: Olynucleotide phosphorylase

PQBP : polyglutamine-binding protein 1

PR3 : proteinase 3

RBC: RED BLOOD CELL

RCD: Regulated cell death

RETNLA: Resistin-like alpha

RHIM: Receptor-Interacting Protein Homotypic Interaction Motif

RIG-I: retinoic acid receptor responder

RIPA: RLR-induced IRF3-mediated pathway of apoptosis

RIPK1:receptor-interacting serine/threonine protein kinase 1

ROS: reactive oxygen species

SLC19A: solute carrier family 19 member

SPDEF: SAM-pointed domain–containing Ets-like factor

ssDNA: single-stranded DNA

ssRNA: single-stranded RNA

STING: Stimulator of Interferon Genes

TBK1: TANK-Binding Kinase.

TGF β : transforming growth factor

TME: Tumor microenvironment

TMEM173: Transmembrane Protein 173

TNF: tumor necrosis factor

TRADD: TNFRSF1A-associated via death domain

TRAF: TNFR-associated factor

TRAIL: TNF-related apoptosis-inducing ligand

ULK: Unc-51-like autophagy activating kinase

VE-cadherin: vascular endothelial cadherin

VRAC: volume-controlled anion channel

XBP1: X-box binding protein 1

ZBP1: Z-DNA Binding Protein 1

ZO-1: zonula occludens

γ -H2AX: gamma-Histone 2AX

Preface

Human and animal lung are constantly threatened of developing pulmonary disorders, due to their continued exposition to air pollution and airborne viruses, pollutants such as tobacco smoke or occupational exposure for humans, or allergens such as the clinically relevant house dust mite (HDM), pollen and mold.

In the **first Introduction chapter**, we will conduct a brief comprehensive survey analysis of the immunopathology associated with two life-threatening pulmonary conditions, namely Acute Respiratory Distress Syndrome (ARDS) and Neutrophilic Exacerbation of Allergic Asthma, with a description of the main innate immune cells and intracellular mechanisms involved.

In the **second Introduction chapter**, we first will discuss the crucial impact of severe lung injury in the widespreading of inflammation. We will evoke precise concepts of the best described cell death modalities (apoptosis, necroptosis, pyroptosis, and NETosis), following carefully the classifications and recommendations of the National Committee for Cell Death (NCDD), how each cell death is regulated, and what led to the major finding of PANoptosis, a unique cell death modality with significant pathophysiological implications.

In a second step, we aim at uncovering intricate details surrounding the regulation of the innate immune system by cell death, and decipher mechanisms that make a specific cell death "inflammatory", explain the role of danger-associated molecular patterns (DAMPs) released by lytic and non-lytic cell death, with a focus on DNA as a common danger signal in all cell death.

In a third step, we seek to enhance our knowledge of how the cGAS- stimulator of interferon genes (STING) pathway regulates the main cell death modalities while responding to self-DNA, as a positive feed mechanism with deleterious consequences on lung tissue.

Finally, we will explore major advances in the field of immune modulation of the STING pathway as a therapeutic strategy.

In the **third Results chapter**, we will expose our study and the related two manuscripts. In the **final Discussion chapter**, we will discuss the main results and the limitations of the studies, as well as perspectives.

Summary

CHAPTER I: LUNG INFLAMMATION.....	18
I. Acute respiratory distress syndrome.....	18
1. Pathophysiology of ARDS	19
<i>1.a) Lung's epithelial and endothelial barriers damage</i>	<i>20</i>
2. Innate Immune Cells in the Pathogenesis of ARDS: Understanding the Immune-Pathological Landscape.....	23
<i>2.a) Involvement of macrophages</i>	<i>23</i>
<i>2.a.1) Types and origin of macrophages in lung</i>	<i>23</i>
<i>2.a.2) Macrophage polarization: The M1/M2 paradigm</i>	<i>26</i>
<i>2.a.3) Regulation of the M1/M2 balance</i>	<i>27</i>
<i>2.a.4) Role of polarized macrophages in ARDS</i>	<i>28</i>
<i>2.b) Involvement of neutrophils: The role of neutrophils in lung inflammation</i>	<i>29</i>
<i>2.b.1) Oxidative stress</i>	<i>30</i>
<i>2.b.2) Neutrophil degranulation.....</i>	<i>30</i>
<i>2.b.3) Neutrophil extracellular traps (NETs) formation.....</i>	<i>30</i>
<i>2.b.4) Neutrophils heterogeneity: a dual role during inflammation</i>	<i>32</i>
II. Asthma	34
1. Phenotypes and endotypes of asthma	35
2. Asthma biomarkers: A tool for asthma stratification and development of therapeutic targeting strategies.....	37
3. Mechanisms of asthma immune-pathogenesis.....	41
<i>3.a) Type-2 high immune response</i>	<i>41</i>
<i>3.a.1) Mucus production in Th2-high asthma</i>	<i>45</i>
<i>3.a.2) Non type-2 immune response.....</i>	<i>47</i>
<i>3.b) Non type-2 immune response.....</i>	<i>47</i>
CHAPTER II: REGULATION OF INNATE IMMUNITY BY CELL DEATH.....	50
1. Cell death classification	50
1.a) Apoptosis	52
1.b) Pyroptosis.....	55
1.c) Necroptosis	58
1.d) NETotic cell death: Neutrophils extracellular traps (NETs).....	60
<i>1.d.1) Neutrophil intrinsic pathway initiating NETs.....</i>	<i>60</i>
<i>1.d.2) Innate immune pathways initiating NETs.....</i>	<i>61</i>
<i>1.d.3) DNA extrusion from the nucleus to the extracellular compartment</i>	<i>62</i>
<i>1.d.4) An alternative mechanism of NET formation</i>	<i>64</i>
2. PANoptosis: A deadly symphony.	66
2.a) Regulated cell death cross-talks:	67
<i>2.a.1) Apoptosis and pyroptosis</i>	<i>67</i>
<i>2.a.2) Pyroptosis and necroptosis</i>	<i>67</i>
<i>2.a.3) Necroptosis and apoptosis.....</i>	<i>68</i>
<i>2.a.4) PANoptosome and its pathophysiological implication.....</i>	<i>68</i>
3. Role of lytic cell death in the regulation of innate immune inflammation: Self-DNA, the maestro directing the symphony.....	73
3.a) The Role played by DAMPs: the ghost back to hunting you!	75
<i>3.a.1) Focus on DNA as a driver of inflammation and innate immune sensors activation.....</i>	<i>76</i>

4. The cGAS-STING pathway	78
4.a) Role of cGAS-STING pathway in DNA damage and regulated cell death	83
4.a.1) <i>STING and apoptosis</i>	83
4.a.2) <i>STING and necroptosis</i>	84
4.a.3) <i>STING and pyroptosis</i>	84
4.b) cGAS-STING-associated lung diseases	85
4.b.1) <i>STING and DNA in sterile lung conditions: focus on allergic asthma and asthma exacerbation</i>	86
4.b.2) <i>STING and DNA in infectious diseases: focus on respiratory viral infections</i>	88
4.c) Immune-modulation of STING, the central hub of DNA sensing, as a therapeutic strategy	90
4.c.1) <i>STING activation</i>	90
4.c.2) <i>STING inhibition</i>	93
CURRENT CHALLENGES AND AIMS OF THE THESIS	96
RESULTS	98
Article 1: STING agonist diABZI induces PANoptosis and DNA mediated acute respiratory distress syndrome (ARDS)	98
Article 2: STING-dependent induction of neutrophilic asthma exacerbation in response to house dust mite	134
DISCUSSION AND PERSPECTIVES	218
CONCLUSION	232
RESUME DU TRAVAIL DE THESE EN FRANÇAIS	233
REFERENCES	261

'I was really shocked. I thought my immune system was there to protect me'

-Quote from a patient recovering from sepsis-induced ARDS-

Chapter I: Lung inflammation

I. Acute respiratory distress syndrome

Acute respiratory distress syndrome (ARDS) is a clinical syndrome of diffuse lung inflammation and oedema that commonly causes acute respiratory failure (Bos et Ware, 2022). The clinical syndrome ARDS can be caused by a wide range of predisposing factors, including viral infection, bacterial infection and fungal infection to a lesser extent, nonpulmonary sepsis, aspiration of gastric and/or oral and oesophageal contents which can be exacerbated by subsequent infection, and trauma such as blunt, penetrating injuries or burns (Matthay et al, 2019). Among young children, viral infections such as respiratory syncytial virus and influenza virus are the most frequent factors inducing life-threatening ARDS (Nye et al, 2016).

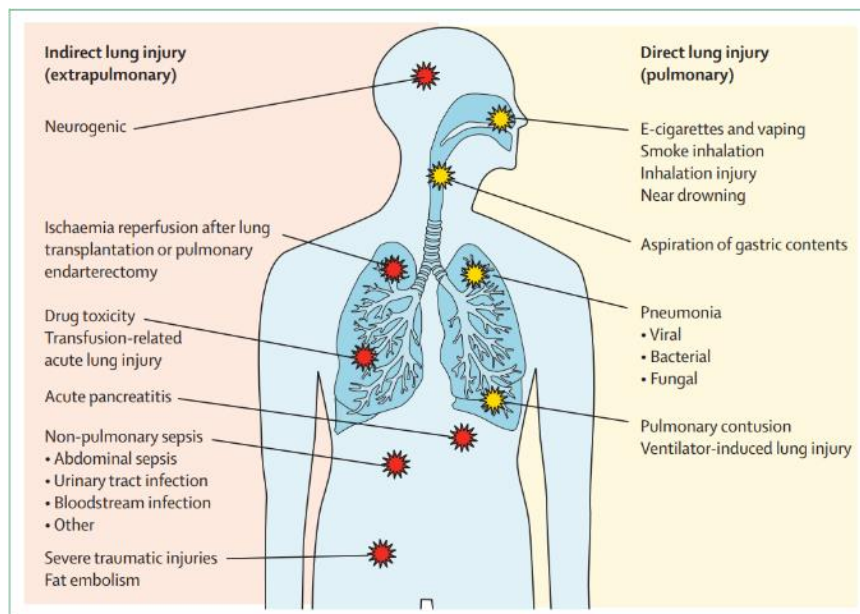


Figure 01: Predisposing factors of ARDS. Acute respiratory distress syndrome can be a result of indirect extrapulmonary lung injury including sepsis, pancreatitis and physical trauma, or of a direct pulmonary lung injury like aspiration of gastric contents or pneumonia which is considered as the most common risk factor (Bos et Ware, 2022).

The LUNG-SAFE study carried out in 2014 by Bellani and collaborators showed that among the 29,144 intensive care patients followed up over 50 countries, the prevalence of ARDS was 10.4% and ARDS was identified in 23% of all ventilated patients (Bellani et al, 2016). ARDS is common in admitted intensive care unit patients but still remains under-recognized and under-treated. During the COVID-19 pandemic, ARDS has gained interest in the field due to the increased incidence of ARDS (Bos et Ware, 2022). Indeed, Severe acute

respiratory syndrome coronavirus 2 (SARS-CoV-2) virus infection (2019) has led to the death of at least 6 million persons, most of them from ARDS (Cascella et al. 2022).

1. Pathophysiology of ARDS

The pathophysiology of ARDS is complex and involves injury and inflammatory pathways that are necessary for host defense to insults and infections, but are deleterious if over-activated (Huppert et al. 2019). In this pathological context, mechanical ventilation can aggravate lung injury and inflammation (Jin et al. 2021).

A normal lung must ease O₂ transfer across the distal alveolar-capillary that begins with inspiration of fresh air and ends at the mitochondrial respiratory chain where O₂ is consumed in the process of oxidative phosphorylation, while eliciting carbon dioxide excretion (Hsia et al, 2016). The alveolar epithelium is composed of a monolayer of alveolar type I (ATI) cells which are responsible of gas exchange, and alveolar type II (ATII) cells, which produce surfactant to reduce surface tension and allow the alveoli to remain open. This epithelium forms a tight barrier that is responsible for the diffusion of oxygen and carbon dioxide, but also restricts the passage of small solutes (Bhattacharya et al. 2013). Under physiological conditions, ATI and ATII cells keep the air space dry by absorbing excess fluid through vectorial ion transport, primarily through apical sodium channels and basolateral Na⁺/K⁺-ATPase pumps. Once the liquid is absorbed, it will be evacuated via the lymphatic network of the lung. Barrier integrity depends on intercellular tight junctions, which are composed of transmembrane claudins and occludins and cytoplasmic zonula occludens (ZO) proteins that anchor tight junctions to the actin cytoskeleton (Matthay et al. 2013. Matthay et al, 2019). Endothelial cells connected by an intact tight junction also play a role in maintaining alveolar homeostasis by regulating the transvascular flux of fluid and inflammatory cells into the interstitial space, preventing them from crossing the epithelial barriers (Müller-Redetzky et al. 2014).

At steady state, alveoli contain alveolar macrophages in the airspace for host defense, while polymorphonuclear leukocytes (neutrophils), erythrocytes, and platelets circulate freely through the endothelial capillary and can be rapidly recruited into the airspace in the context of infection (Matthay et al, 2019. Bos et Ware, 2022).

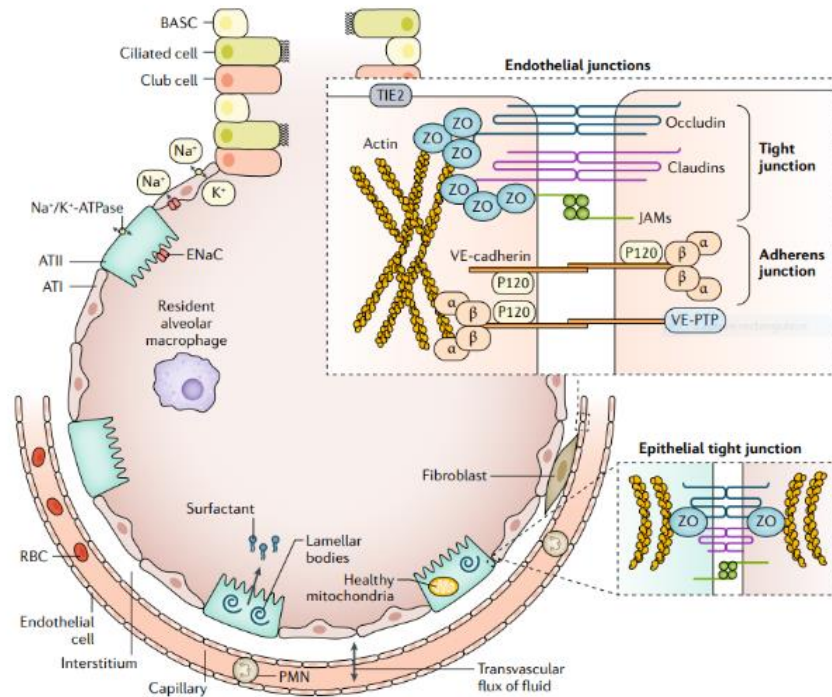


Figure 02: Intact alveolar–capillary barrier. Healthy alveolar–capillary epithelium forms a tight barrier formed by ATI and ATII cells. The barrier is supported by intercellular tight junctions composed of claudins, occludins, and ZO proteins. Endothelial cells regulate fluid influx and are also connected through tight junctions and adherent junctions containing VE-cadherin. TIE2 and VE-PTP help stabilize VE-cadherin. Normally, fluid and solutes move into the interstitial space and lymphatics, while the epithelial barrier remains intact. Alveolar macrophages provide host defense, and the free circulating PMNs can be quickly recruited during infection or injury (Matthay et al, 2019).

One of the hallmark of ARDS is the increased alveolar–capillary permeability to fluid, proteins, neutrophils and red blood cells, leading to their accumulation into the airspace and severe oedema formation (Matthay et al. 2012. Huppert et al. 2019). These phenomena can give rise in some cases to ‘diffuse alveolar damage’ (DAD) and threatens the excretion of carbon dioxide resulting in respiratory failure and mortality (Thille et al, 2013). Post-mortem lung tissues examination from COVID-19 patients revealed that DAD is the prime pattern of lung injury (Carsana et al, 2020). DAD was first defined by Katzenstein in 1976 to describe endothelial and alveolar monolayer cell injury with dying of pneumocytes, hyaline membranes deposition, inflammation (neutrophilic alveolitis) followed by a ATII cell hyperplasia to reorganize the alveoli, and in some cases fibrosis progression (Katzenstein et al, 1976. Lamers et al, 2022).

1.a) Lung’s epithelial and endothelial barriers damage

Injury to the epithelial and endothelial barrier is a typical feature of ARDS. A variety of clinically relevant insults can attack the epithelium directly, such as, bacterial toxins, lytic

viruses, acid, hyperopia, hypoxia and biophysical forces, or indirectly by inducing inflammation (Bos et Ware, 2022). Injured epithelium leads to increased susceptibility to secondary infections, as it is an important barrier to pathogens through the production of defensins and surfactant proteins (Akdis et al. 2021).

Inflammation-induced loosening of the endothelial barrier breakdown can occur through either endothelial junction dysfunction (Claesson-Welsh et al. 2021) or endothelial cell death (Matthay et al. 2012. Cheng et al. 2017). In response to infectious agents, resident macrophages and recruited neutrophils release mediators and danger signals leading to phosphorylation of VE-cadherin and its internalization. VE-cadherin plays a critical role in maintaining the integrity of endothelial cell contacts (Giannotta et al. 2013). It forms cell-cell junctions with TIE2, an endothelial receptor kinase. However, the release of angiopoietin 2 by injured endothelial cells disrupts TIE2-mediated stabilization of VE-cadherin, leading to the formation of gaps between endothelial cells (Matthay et al. 2019). The glycocalyx the layer of glycoproteins and glycolipids that protects endothelial cells, can be easily damaged, exposing adhesion molecules such as P-selectin and E-selectin, which promote leukocyte transmigration (Schmidt et al. 2012). As the capillary endothelium forms a barrier between circulating blood cells and plasma and the lung interstitium and airspace, these events collectively favor edema formation and RBC influx. In the same context, endothelial cells upregulate procoagulant molecules favoring the formation of microvascular pulmonary thrombosis (Livingstone et al 2021).

Lung epithelial injury determines survival in patients with ARDS. Pathogen sensing by innate immune surveillance receptors on alveolar type II (ATII) cells and resident alveolar macrophages induces the secretion of chemokines such as IL-8, which attract immune cells from lung vasculature into the airspace (Thorley et al.2007; Aggarwal et al. 2014). Subsequently, to neutralize infectious agents, neutrophils can produce a variety of tissue stressors including reactive oxygen species (ROS), and form extracellular traps (NETs). NETs are composed of DNA decorated with histones, and proteases such as myeloperoxidase (MPO) and neutrophil elastase (NE), which can be highly immunogenic and harmful when in direct contact with lung tissue and are sufficient to induce epithelial cell death (Radermecker et al. 2020; Ackermann et al. 2021). A previous study has shown that neutrophils undergoing apoptosis induce alveolar epithelial apoptosis through the release of sFasL (Serrao et al. 2001). Moreover, NETs promote thrombosis in the lung (Matthay et al. 2019).

Epithelial cell death by apoptosis or necrosis is a focal point of alveolar injury in ARDS. It can result directly from infecting lytic agents, or from a mechanical stretch which causes surfactant dysfunction normally produced by ATII, increasing the risk of lung injury (Budinger et al. 2011). In addition to neutrophils, macrophages are partially responsible for epithelial cell death through IFN β -dependent release of tumor necrosis factor (TNF) and its TRAIL-dependent activation of death receptors (Högner et al. 2013). Fragile red blood cells which infiltrate the air space, release free hemoglobin, which induces vascular permeability through oxidative mechanisms (Shaver et al, 2018). Alveolar epithelium injury also includes tight junction disruption with the loss of the epithelial glycocalyx, which is proinflammatory (Rizzo et al. 2022).

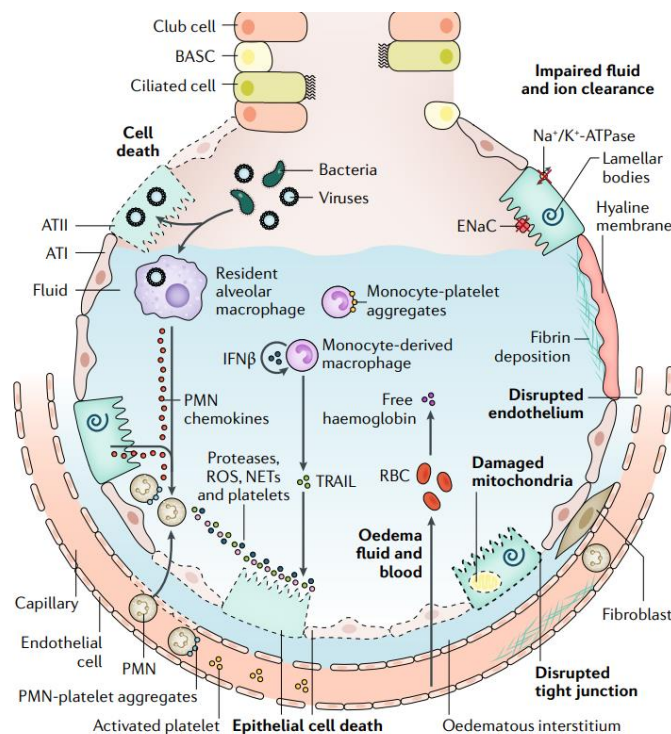


Figure 03: Increased permeability in alveolar–capillary barrier. In the context of ARDS, the integrity of the alveolar barrier is disrupted due to inflammation, leading to the accumulation of fluid in the alveoli (edema). This occurs through the disruption of tight junction, resulting in increased permeability of the endothelial cell layer. Consequently, there is a leakage of water, solutes, leukocytes, platelets, and other inflammatory molecules into the alveolar space (Matthay et al. 2019).

2. Innate Immune Cells in the Pathogenesis of ARDS: Understanding the Immune-Pathological Landscape

The pathogenesis of ARDS is multifactorial and involves excessive activation of multiple immune cells from both the innate and adaptive systems, with a massive release of pro-inflammatory cytokines that mediate the propagation of lung injury (Spadaro et al, 2019; Wong et al, 2019).

Calfee and collaborators stratified ARDS patients into two sub-phenotypes based on blood biomarkers: hypo-inflammatory and hyper-inflammatory. The hyper-inflammatory group was characterized by higher plasma levels of proinflammatory biomarkers including IL-6, IL-8, soluble TNF receptor 1 (sTNFR1), but also alveolar bronchial and endothelial damage biomarkers such as plasminogen activator inhibitor-1 (PAI-1) and protein C, compared to the hypo-inflammatory subgroup. Moreover, the hyper-inflammatory group had fewer ventilator-free and organ failure-free days, and a higher mortality rate (Calfee et al. 2014; Spadaro et al, 2019). This study was updated by another group in 2022 (Duggal et al. 2022).

2.a) Involvement of macrophages

Macrophages in lung tissue are key players of the inflammatory response to ARDS (Liu et al, 2022).

2.a.1) Types and origin of macrophages in lung

Macrophages in lung tissue mainly include three subpopulations including alveolar macrophages (AMs) and pulmonary interstitial macrophages (PIMs). Alveolar macrophages are more abundant and serve as the primary immune sentinels of the airways, express specific surface markers such as Siglec-F and CD11c, and participate in surfactant catabolism (Woo et al, 2021).

Macrophages have historically been described as being derived from blood monocytes that infiltrate target tissue by expressing C-C chemokine receptor type 2 (CCR2) (Krenkel et al., 2018). However, an experimental study has demonstrated that mice lacking CCR2 motifs, have the same number of AMs as the control group, suggesting a minimal contribution of blood monocytes to the AMs pool (Hashimoto et al., 2013).

Recent evidence suggests that pulmonary macrophages are a mixed population of bone marrow-derived blood monocytes and of embryonic-derived primitive macrophages present in the yolk sac or fetal liver (Woo et al, 2021). Yolk sac macrophages are recognized as 'F4/80^{hi}

macrophages' in several tissues including lung. In normal mice, these cells co-exist with 'F4/80^{lo} macrophages', of hematopoietic origin (Davies et al, 2013). Under steady-state, AMs derived from primitive macrophages do not rely on blood monocytes for their renewal (Yona et al. 2012). AMs in the alveolar lumen are mainly derived from fetal liver monocytes (Ginhoux et al. 2016). AMs self-renewal under the stimulation of GM-CSF and TGF- β secreted by ATII cells (Yu et al. 2017). At steady state, AM are maintained quiescent by the alveolar microenvironment through TGF- β , IL-10 and CD200. They promote the differentiation of CD4⁺ T cells into Treg cells through TGF- β (Snelgrove et al. 2008).

AMs can be further divided into two subpopulations based on their origin and function: resident alveolar macrophages (RAMs) and recruited macrophages (RecAMs). RAMs are considered as immunosuppressive and mainly present the M2 phenotype. Conversely, RecAMs highly express M1 markers and increase at the peak of inflammation (Dang et al. 2022). Indeed, they were present in the BALF as early as 3 days in an LPS-induced lung injury model (Janssen et al, 2011). The M1/M2 balance is closely related to macrophage subpopulations (Mould et al, 2019). These findings suggest that a M1/M2 ratio change in ARDS is probably related to a switch in macrophage subgroups.

Pulmonary interstitial macrophages (PIMs) comprise 30–40% of all lung macrophages and are found in the interstitial space of the bronchi and alveoli (Chen et al, 2020). PIMs are initially derived from yolk sac-derived embryonic F4/8 macrophages and can be replenished by circulating monocytes. PIMs are the main source of IL-10, which may be their main mechanism for regulating inflammatory cell infiltration to maintain vascular permeability. Indeed, when PIMs were depleted, proinflammatory factors such as IL-6, CCL2, CCL3, CCL5 and monocyte recruitment increased in the bronchoalveolar lavage after *in vivo* stimulation with poly(I:C) (Ural et al, 2020).

Pulmonary vascular macrophages (PVMs) are a third type of lung macrophages, that are not constitutive but only appear in the lung in conditions of liver dysfunction and bile duct ligation in a monocyte chemotactic protein 1 (MCP-1) dependent manner (Vrolyk et al, 2019). SPIC is the candidate transcription factor that drives the development of PVMs. CD68⁺ PVMs are considered as ARDS promoters of extrapulmonary origin: they exert their pro-inflammatory functions via activation of the NF κ B pathway, secretion of inflammatory mediators (IL-1b, IL-6, IL-8, cyclooxygenase 2 COX-2) and recruitment of neutrophils and platelets (Vrolyk et al, 2020). PVMs are also considered as markers of poor prognosis. Apoptosis of PVMs alleviate lung inflammation (Gill et al, 2008).

Subset	Origin	Biomarker	Functions
AMs <ul style="list-style-type: none"> RAMs RECAMs 	Fetal liver monocytes CD14 ⁺ CD16 ⁻ Monocytes	F4/80 Siglec-F CD11c ⁺ CD11b ⁻ CD206 ⁺ CD64 ⁺ F4/80 CD11c ⁻ CD11b ⁺ CD14 ⁺	Detective microenvironment changes Phagocytosis and cell proliferation Inflammation initiation Pro-inflammatory, Tissue repairment
PIMs <ul style="list-style-type: none"> Vascular-associated IMs Nerve-associated IMs 	Yolk sac-derived F4/80 lineage MΦ; CD14 ⁺ CD16 ⁻ Monocyte	Lyve1 ^{hi} MHCII ^{lo} CD206 ⁺ CD169 ⁺ Lyve1 ^{lo} MHCII ^{hi} CD206 ⁻	Secretion of IL-10 Maintenance of vascular permeability Preventing inflammatory cells infiltration, presentation Regulation of T cell activity Antigen presentation Regulation of T cell activity
PVMs	CD14 ⁻ CD16 ⁺ Monocytes	CD68 ⁺	Secretion of pro-inflammatory

			factors Recruitment of platelets and Neutrophils
--	--	--	--

Table 01: Macrophages polarization and classification. *AMs* alveolar macrophages, *RAMs* resident alveolar macrophages, *RECAMs* recruited alveolar macrophages, *PIMs* pulmonary interstitial macrophages, *IMs* interstitial macrophages, *MΦ* macrophages, *PVMs* pulmonary vascular macrophages (Dang et al, 2022).

2.a.2) Macrophage polarization: The M1/M2 paradigm

Macrophages are highly plastic and can be polarized into different phenotypes under a variety of environmental conditions. For a long time, macrophages have been divided into classical (M1) and alternative (M2) activated macrophages (Murray et al. 2014). The loss of the M1/M2 balance can aggravates lung injury.

When stimulated by Th1 related cytokines, such as interferon γ (IFN- γ) or TNF α macrophages polarize to M1, producing a higher level of TNF- α , IL-1, IL-6, IL-12, chemokine CCL8, IL-23, MCP-1, macrophage inflammatory protein 2 (MIP-2), ROS, and COX-2 and expressing high levels of inducible NO synthase (iNOS). Functionally, this population of macrophages is mainly involved in antimicrobial, and antitumoral activities while participating in lung tissue injury when excessively activated (Aggarwal et al. 2014; Murray et al. 2014; Huang et al. 2018).

Conversely, M2 macrophages are generated in response to Th2 cytokines such as IL-4 and IL-13 as well as anti-inflammatory cytokines such as IL-10 and TGF- β . These macrophages have an anti-inflammatory cytokine profile characterized by low production of IL-12 and high production of IL-1 receptor antagonist, chemokine CCL18, arginase 1 (Arg-1), found in inflammatory zone 1 (Fizz1), chitinase 3-like 3 (Chi313), IL-10, and TGF- β , inhibiting inflammatory cell aggregation and promotes tissue repair (Huang et al. 2018; Shapouri-Moghaddam et al. 2018). M2 macrophages can be further divided into four subtypes: M2a, M2b, M2c and M2d (Figure 3), exerting a vast spectrum of pro-resolving functions (Lee et al. 2021). During the course of ARDS, M2 participate in tissue repair, remodeling and suppression of inflammation (Cheng et al. 2021; Deng et al. 2020)

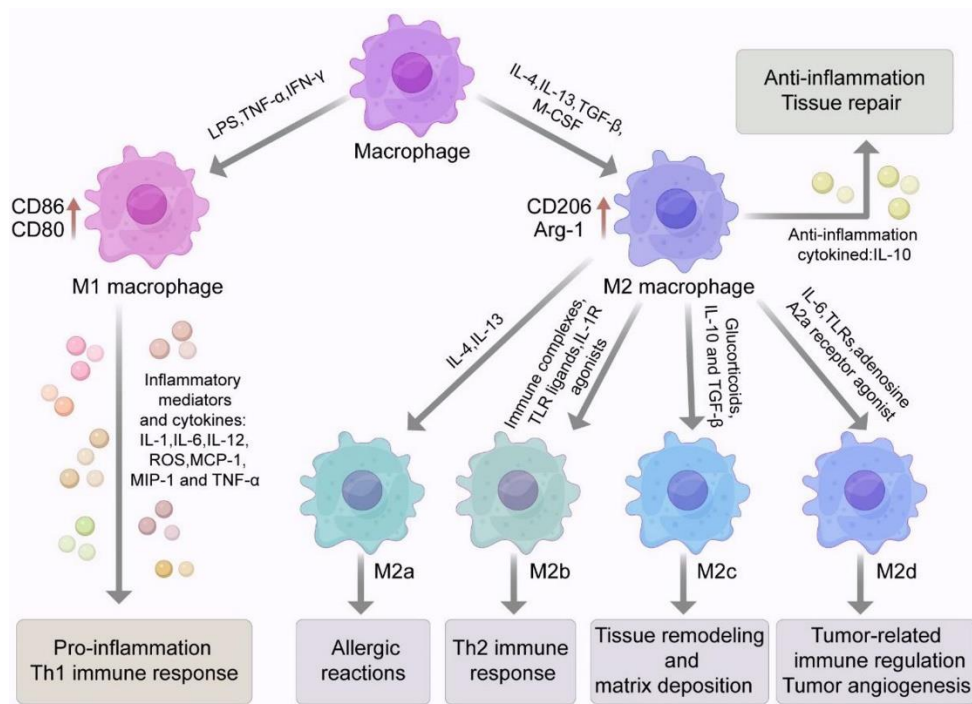


Figure 04: Macrophages polarization: the “M1 / M2 paradigm “. Overview of the dynamic process of macrophage polarization, highlighting the distinct functional phenotypes of M1 and M2 macrophages and their roles in immune responses and tissue homeostasis (Liu et al, 2022).

2.a.3) Regulation of the M1/M2 balance

At the peak of inflammation, single cell sequencing showed that AMs exhibiting the M1 phenotype were enriched in inflammation-related genes such as *NFκB* in a TLR4/MyD88-dependent pathway, leading to the initiation of the exudative phase (Sica et al, 2012). In this phase, several lung inflammatory biomarkers mainly produced by M1 macrophages such as IL-1β, IL-6, IL-8, IL-10 and TNF-α have been reported as a clinical tool for predicting the development, severity and mortality of ARDS in patients with lung injury (Sivapalan et al, 2021; Spadaro et al, 2019; Capelozzi et al, 2017).

Evidence for the involvement of JNK pathway in macrophage polarization have been reported. . In fact, JNK appears to have a dual role, it is required for M1-associated inflammation and fibrosis (Shi et al, 2019). Conversely, in IL-4-stimulated macrophages, a study showed that high expression of JNK and c-Myc transcription could promote the M2 phenotype (Hao et al, 2017). AKT is a family of three serine/threonine protein kinases (Akt1, Akt2 and Akt3) involved in the PI3K/Akt signaling pathway, known to regulate macrophage activation and gene expression with a dual role depending on the Akt isoform. It was shown that Akt1-/-

macrophages express high levels of iNOS, TNF- α and IL-6 and give rise to the M1 phenotype, while Akt1^{+/+} macrophages express high levels of Fizz1, Chi313 and IL-10, leading in M2 phenotype (Arranz et al, 2012).

The Notch signaling pathway, especially Notch1, appears to be exclusively related to M1 macrophages and prevents M2 macrophage differentiation and promotes their apoptosis by binding to Delta-like 4 (Pagie et al, 2018). In the same context, the IFN- γ /JAK/STAT1 signaling pathway is thought to be involved in mediating the M1 phenotype. In contrast, type I IFNs (α - β) exert anti-inflammatory effects via SOCS3 upregulation, which inhibits STAT1 phosphorylation (Zhou et al, 2014), but its role in macrophages polarization remains uncertain. Within the STAT family, STAT6 is recognized as central for M2 polarization *in vivo* under an IL-4/IL-13 rich microenvironment (Sica et al. 2012).

Hypoxic conditions can complicate the course of ARDS in which the HIF family proteins plays an important role. HIF-1 α induces iNOS synthesis and leads to M1 phenotype; conversely, HIF-2 α is known to favor Arg-1 and M2 phenotype (Malyshev et al. 2015). Many other signaling pathways play a critical role in the M1/M2 balance such as the peroxisome proliferator-activated receptor γ (PPAR γ), TGF- β , c-Myc, IRF or the Krüppel-like factor (KLF4 and KLF6) signaling pathways, but they will not be discussed here (Chen et al. 2020).

2.a.4) Role of polarized macrophages in ARDS

M1/M2 macrophages are involved in all stages of ARDS including the exudative phase, the rehabilitation phase and, finally, the fibrotic phase. The M1/M2 paradigm is an oversimplification and cannot fully describe the complex and dynamic changes in different subsets of macrophages, as macrophages can play dual roles during the course of ARDS.

During the exudative phase, the M1 phenotype drives lung tissue damage in ARDS in most reports (Mishra et al. 2021). However, recent studies demonstrated that M1 can attenuate inflammation in LPS-induced lung injury and ventilator-induced lung injury, protecting the integrity of the epithelial barrier (Dolinay et al. 2006). Similarly, fibrosis is a late complication in the course of ARDS in which M2 macrophages promote fibro-proliferation and tissue metalloproteinase inhibition leading to excessive ECM deposition (Mishra et al. 2021). However, contradictory studies revealed that IL-4 polarized M2 macrophages are involved in the antifibrotic process by expressing Arg-1 and resistin-like α genes (D'Alessio et al. 2016).

Targeting macrophages polarization as a therapeutic strategy might show promising results in many preclinical studies, but the fact that macrophages are paradoxally involved in the process

of ARDS makes therapeutic interventions challenging, and further studies are needed to better decipher the functions of different macrophage subtypes in each phase of ARDS.

2.b) Involvement of neutrophils: The role of neutrophils in lung inflammation

Neutrophils are the first and most abundant immune cells to be recruited to the site of pathogenesis within pulmonary tissue, in response to both infectious and sterile inflammatory stimuli (Aulakh. 2018). Neutrophil activation plays a significant role against infections. Nevertheless, their excessive activation contributes to tissue damage and lung dysfunction. Indeed, several reports have associated neutrophilia with lung disease severity and documented its role as a predictor of poor outcome, notably in COVID-19 ARDS patients (Radermecker et al. 2020; Liu et al. 2020).

IL-8 and CXCL5 are the main neutrophil chemoattractant mediators produced by epithelial cells and resident macrophages to drive neutrophil migration to the pathogenic site. It is then not surprising that high CXCL5 concentrations in bronchoalveolar lavage fluid were correlated with neutrophils counts in the injured lung of patients with persistente ARDS (Vassallo et al. 2019). The presence of TNF in the tissue helps neutrophils to progress through the ECM and reach the pathogenic site via enhancement of MMP9 production (Wong et al. 2019).

Once on site, activated neutrophils begin phagocytosis, produce several cytotoxic products, undergo a respiratory burst, ROS release and degranulation of proteolytic enzymes, and form NETs, further enhancing inflammation (Yang et al. 2018).

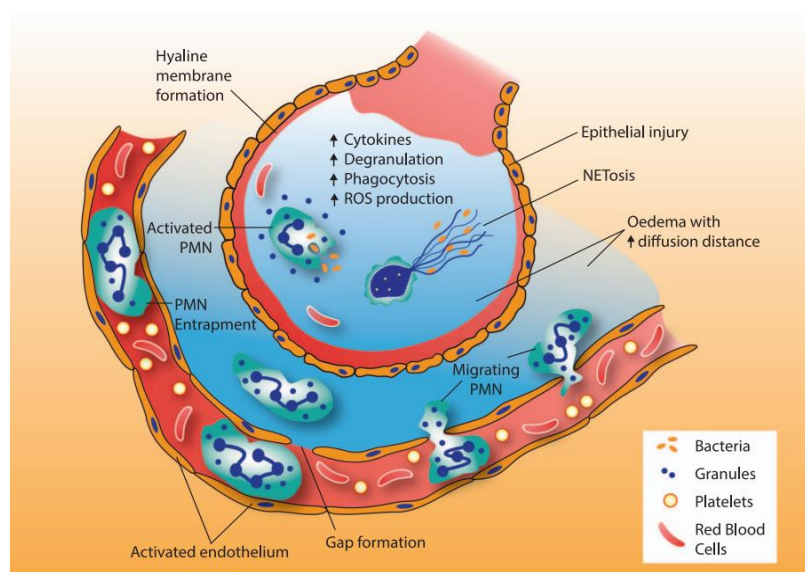


Figure 05: Neutrophil-mediated lung injury of the alveolar epithelium via multiple mechanisms. Neutrophils migrate to the inflamed lung where they undergo respiratory burst, degranulation, ROS production, and NETs formation. These inflammatory responses lead to epithelial damage and cell death that further attract neutrophils and induce endothelium dysfunction. Barrier weakening results in oedema and widening of the interstitium (Vassallo et al. 2019).

2.b.1) Oxidative stress

Activated neutrophils produce a range of toxic ROS as an antimicrobial strategy. However, excessive accumulation of ROS in lung tissue is harmful, causing DNA damage to respiratory epithelial cells, and promoting cell cycle arrest and apoptosis (Park et al. 2019). Another study has shown the potential role of ROS in phosphorylating (MAP) kinases to mediate cell death in response to stress (Usatyuk et al. 2003). ROS also acts on endothelial cells by activating intracellular calcium signals to increase permeability and neutrophil infiltration, further enhancing lung damage (Di et al. 2016).

2.b.2) Neutrophil degranulation

Excessive extracellular degranulation of neutrophils impacts lung injury and ARDS (Liu et al. 2020). Primary granules, also known as azurophilic granules, contain many proteolytic proteins such as MPO, neutrophil elastase (NE) and cathepsin G (Poli & Zanoni. 2022). Apart from its antimicrobial role, NE can degrade extracellular matrix proteins and cleave epithelial-cadherin to disrupt respiratory cell adhesion (Boxio et al. 2016). Moreover, epithelial glycocalyx can be injured by NE (Suzuki et al. 2019). Being immunogenic, the detached glycocalyx can further amplify the inflammation (Rizzo et al. 2022). Neutrophils can release matrix metalloproteinases (MMPs) from the secondary and tertiary granules. Previous reports have linked increased expression of MMPs to inflammation-induced alveolar damage, endothelial damage and ARDS progression (Fligiel et al.2006; Zinter et al. 2019).

2.b.3) Neutrophil extracellular traps (NETs) formation

Neutrophils have the fascinating ability to form NETs, first documented by Brinkmann and collaborators in 2004 for their role in bacterial entrapment (Brinkmann et al. 2004). NETs are a filamentous/cloud-like structure, composed of host DNA fibers containing modified histones coated with cytoplasmic proteases such as NE and MPO that can easily expand and fill the lung alveoli (Vorobjeva1 & Pinegin, 2014; Porto & Stein, 2016).

NETs play a role in the initiation and propagation of inflammation in various sterile and infective lung diseases, including ARDS (Vassallo et al. 2019). Excessive NETs formation may result in accumulation of dense NET plugs, which obstruct small airways within bronchioles (Cortjens et al. 2016). NETs fill the alveoli in areas of histological injury providing evidence for their ability to promote lung damage and impairment of gas exchange (Narasaraju et al. 2011; Juliana et al. 2020; Liu et al. 2016). In COVID-19 ARDS patients, higher NET levels were correlated to severity, mortality and risks of complications with thrombosis and cytokine storm (Liu et al. 2020; Barnes et al. 2020; Zuo et al. 2020). Treatment with DNase I degraded NETs and led to reduced pro-inflammatory cytokines, alleviated lung injury and improved mice survival (Lefrançais et al. 2018), suggesting that an excessive neutrophilic reaction may lead to an adverse and ineffective outcome (Liu et al. 2016; Gan et al. 2018; Lefrançais et al. 2018)

As an example of sterile inflammation-related NETs, NET components were found in the lungs and plasma of transfusion-related acute lung injury (TRALI) patients and mice, triggered by activated platelets, that promote coagulation and thrombosis formation in the lung (Caudrillier et al. 2012; Semeraro et al. 2011). Moreover, NETs induce TF and factor XII-mediated coagulation and formation of lung micro-thrombi (Massberg et al. 2010).

Considering these findings, one can suppose that strategies to reduce neutrophil infiltration may alleviate lung tissue damage. Nevertheless, during neutropenia, cancer patients are at high risk for lung infection and ARDS development (Azoulay & Darmon, 2010). The role of neutrophils in ARDS and lung inflammation in general is complex, and evidence that neutrophils can promote both inflammation and protection are now numerous (Mincham et al. 2021).

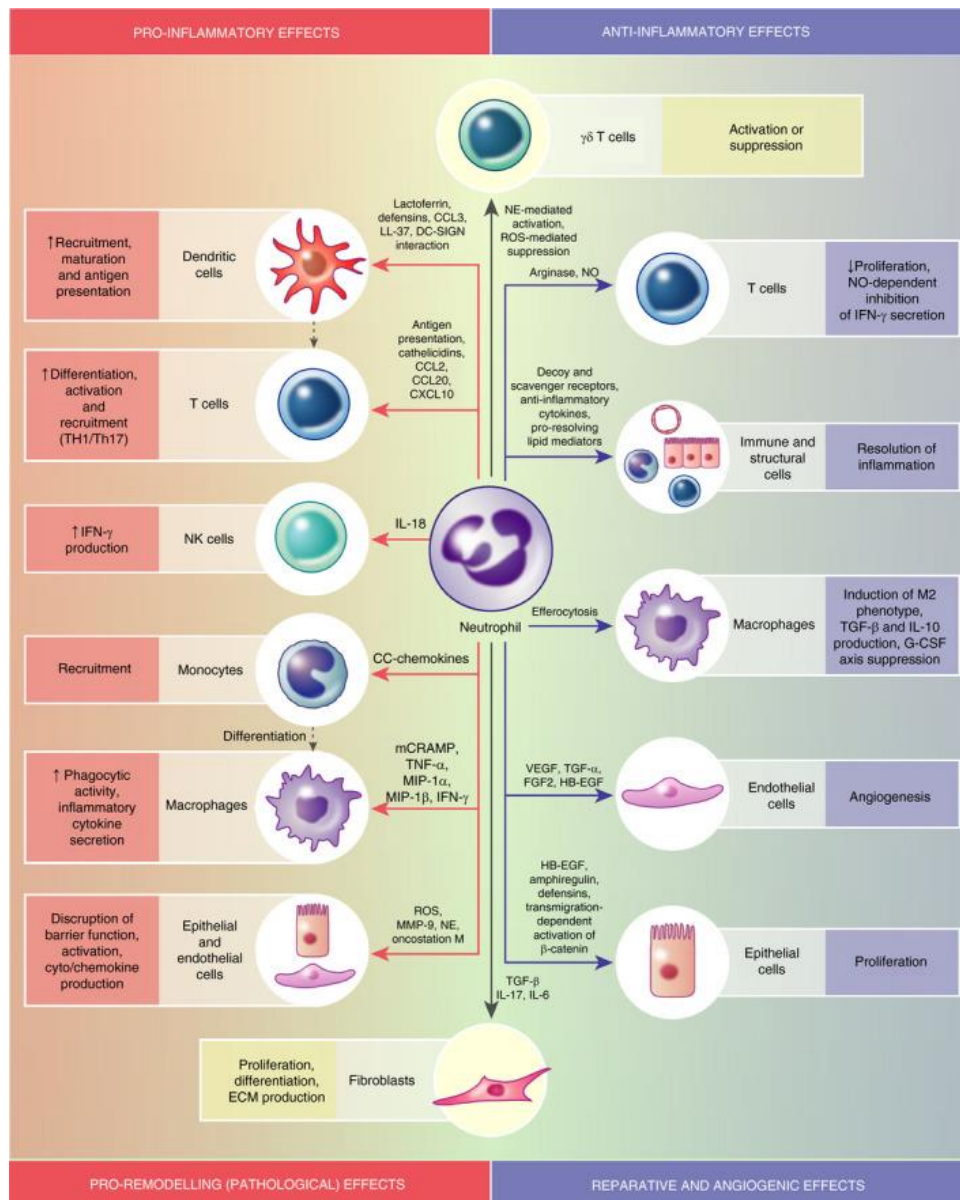


Figure 06: Neutrophils contribution to health and disease. Depending on their microenvironment, age, and maturity, neutrophils can establish several crosstalk with immune and structural cells through its soluble mediators or by a direct cell-cell interaction. The huge heterogeneity of neutrophils reflects their paradoxical action in inflammation. They can initiate inflammation via recruitment of monocytes and DC cells and enhancing their activity or orchestrates the resolution of inflammation. Likewise, neutrophils can drive tissue repair or shift on pathological tissue remodeling (Mincham et al. 2021).

2.b.4) Neutrophils heterogeneity: a dual role during inflammation

Neutrophil heterogeneity may explain their functional complexity. Within 3 hours of intravascular administration of low doses LPS in a human *in vivo* model, immature and less functional neutrophils were released from the bone marrow with impaired ability to generate ROS, reduced interaction with opsonized bacteria and reduced expression of chemokine

receptors such as CD181 and CD182 (Pillay et al. 2010). Another “safe neutrophil” subset with immunosuppressive phenotype described is the CD16^{hi} CD11b^{hi} CD62^{low} that exhibited the ability to suppress T-cell proliferation in human systemic inflammation (Pillay et al. 2012). Conversely, activated tissue neutrophils may have the ability to traffic back to the circulation by a process called reverse-TEM. These neutrophils characterized as ICAM-1^{hi} CXCR1^{low} exhibited enhanced ROS production, enhanced phagocytic capacity and increased longevity (Buckley et al. 2006).

Both animal and human studies have demonstrated the existence of neutrophil CXCR4^{hi} subset and Olfactomedin 4⁺ subset in human which display a higher capacity to undergo NETs (Welin et al. 2013; Rodrigues et al. 2020). Despite their well-described inflammatory and deleterious role in the lung, NET aggregates were shown to promote the resolution of neutrophilic inflammation by degrading cytokines and chemokines and disrupting their own recruitment in other models of acute inflammation (Schauer et al. 2014). Similarly, as a source of TGF- β and IL-10, neutrophils were shown to have a broad anti-inflammatory and repair functions, and demonstrated the potential to reprogram macrophages to a pro-resolving M2-like phenotype that produce IL-10 (Mantovani et al. 2011; Filardy et al. 2010).

Such studies may help shed light on the intricate role of neutrophils in lung injury and the need to no longer consider them as a phenotypically and functionally homogeneous population. New therapeutic strategies should consider the nuances of neutrophil functional behavior.

II. Asthma

Non-communicable diseases (NCDs) represent a major threat to the health, growth, and development in countries worldwide. Asthma is one of the most common NCDs (GAR 2022). It is estimated that more than 350 million people currently suffer from asthma, affecting the quality of life of people of all ages around the world (Athari et al. 2019). According to the Global Asthma Report (GAR) 2022, more than 1,000 individuals die from asthma every day, and many of these deaths are preventable and are due to inappropriate management of asthma in developed countries and to unavailable, unaffordable, or unreliable quality of medicines in low-income countries (GAR 2022).

The Global Initiative for Asthma (GINA) describes asthma as “*a heterogeneous disease, usually characterized by chronic airway inflammation. It is defined by the history of respiratory symptoms such as wheeze, shortness of breath, chest tightness and cough that vary over time and in intensity, together with variable expiratory airflow limitation*”. (GINA 2022)

Allergic asthma is triggered by environmental allergens (e.g. pollen, dust mite). Allergic asthma is the most common asthma phenotype and has been described to occur in about 40-50% of patients with asthma (AAAA, 2019). In the Severe Asthma Research Program (SARP) atopies were found in almost 80% of patients with early-onset asthma and about 50% of patients with late-onset eosinophilic asthma (Moore et al. 2010).

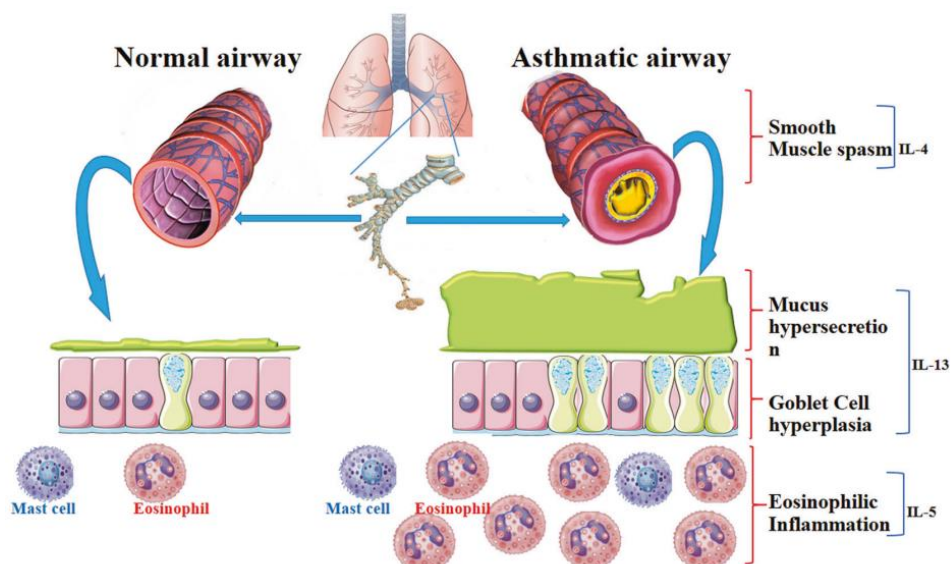


Figure 07: Simplified Asthma pathophysiology. The most common asthma phenotype is associated with Th2 immune response associated with the release of IL-4, IL-5, and IL-13

mediators, characterized by eosinophilic airway inflammation, goblet cell hyperplasia, mucus hypersecretion, airway hyper-responsiveness and shortness of breath. IL-4 has a role in B-cell IgE isotype switching and upregulation of FcεRI on mast cells, leading to histamine release and promotion of allergic symptoms and smooth muscle spasm. IL-5 leads to activation, migration, and accumulation of eosinophils to the airway. IL-13 controls mucus hypersecretion and goblet cell hyperplasia and promotes AHR (Athari et al. 2019).

1. Phenotypes and endotypes of asthma

Given the huge heterogeneity of asthma, several approaches were used to stratify the disease based on phenotypic criteria, the underlying mechanism corresponding to each phenotype and the biomarkers that enable linking disease phenotypes to pathophysiological mechanisms.

Asthma phenotypes	Asthma endotypes
<p>A set of relevant and observable properties allowing patients clustering based on:</p> <ul style="list-style-type: none"> - clinical parameters (age, sex, race, disease onset, triggers, symptoms, etc.) - physiological properties (upper and lower airway patency and hyperreactivity, ventilation pattern, olfaction, skin dryness, etc.) - morphological features (airway smooth muscle hypertrophy, shedding epithelium, mucus production, nasal polyps, etc.) - imaging (bronchial thickness, sinus CT) - clinically relevant outcomes (exacerbations, lung function decline, recurrence of nasal polyps, etc.) - inflammatory parameters (eosinophilic, neutrophilic) - treatment response (responder/nonresponder, corticosteroid sensitive or resistant) 	<p>A set of disease mechanisms explaining each disease phenotype. The main identified endotypes so far:</p> <ul style="list-style-type: none"> - Type 2 high asthma - Non or low-type 2 asthma - Mixed type2/type1 - Mixed type2/type17 - Type 17 asthma - Inflammasome endotype: a subtype of non-type2 with IL-1β, TNFα and NFκB as main mediators - Barrier endotype: a subtype of both type 2 and non-type 2 asthma with severe barrier alteration as a driver of the disease or exacerbation.

Table 02: Major characteristics of asthma phenotype and endotype allowing disease stratification (Agache et al. 2019).

In patients with asthma, phenotype and endotype are prone to overlap and change over time depending on treatment outcome or exposure to airborne infections and pollution. Other

approaches have been proposed to refine the disease stratification such as asthma regiotype (Agache et al. 2019). Regiotype is based on the observation that the regional exposome partially explains the heterogeneity of asthma. Indeed, a recent study showed that sensitization to house dust mite (HDM) allergens Der p 1, 2 and 23 varied considerably across Europe and was predominant in regions where the climate is hot and dry as compared to the humid climate of northern regions (Kiewiet et al 2023).

As with phenotypes and endotypes, biomarkers are also a part of regiotypes. For example, serum periostin is considered as a good indicator of type 2 asthma in the Caucasian population, while it failed to discriminate between allergic asthma and non-allergic asthma in the Chinese population. To date, regiotype is not a widely accepted concept and requires further characterization to establish relevant correlations between regiotypes and asthma phenotypes and endotypes (Agache et al. 2019).

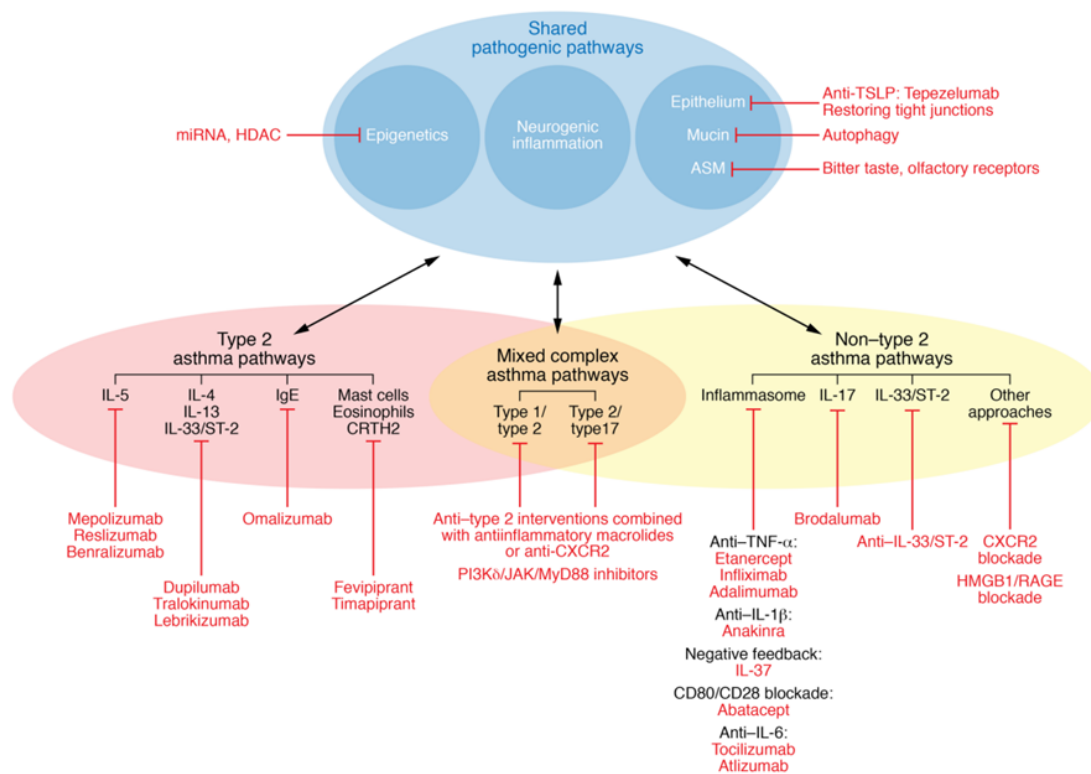


Figure 08: Asthma phenotypes, endotypes and the underlying moldable mechanisms and corresponding treatments. The main asthma phenotypes are type 2-high asthma, type 2-low asthma. These phenotypes can overlap and give rise to mixed granulocytes asthma represented by type2/type1 asthma and type2/type17 asthma. Four main pathways involved in pathophysiology of asthma that showed efficacy: the IgE pathway (omalizumab), the IL-5 pathway (mepolizumab, reslizumab, benralizumab), the IL-4/IL-13 pathway (dupilumab, tralokinumab, lebrikizumab), and the CRTH2 receptor expressed on ILC2 and eosinophils (fevipirant and timapirant). In non-type 2 asthma, three main pathways can be targeted: the inflammasome pathway (using anti-TNF- α , anti-IL-1 β , anti-IL-6, IL-37, or CD80-CD28

blockade), the IL-17 pathway (via brodalumab), or the anti-IL-33 pathway, with additional approaches like CXCR2 and HMGB1/RAGE blockade. For mixed complex endotypes, a combination of anti-type 2 interventions with anti-inflammatory macrolides or anti-CXCR2 may be considered. Alternatively, PI3K δ /JAK/MyD88 inhibitors could address the upstream effects of type 1, type 2, and type 17 cytokines (Agache et al. 2019).

2. Asthma biomarkers: A tool for asthma stratification and development of therapeutic targeting strategies

Biomarkers represent a relevant tool to distinguish between different patient clusters, paving the way for individualized treatment plans. (Kaur et al. 2019; Breiteneder et al. 2020; Agache et al. 2021).

T2-driven allergic asthma is the best characterized endotype and is usually associated with early asthma onset. The most reliable biomarkers are: blood and sputum eosinophil counts, fractional exhaled nitric oxide (F_{ENO}) levels, and specific IgE test results.

Eosinophils: An elevated eosinophil counts in sputum was defined as greater than 2% of the total cell count, whereas an elevated blood eosinophil counts was classified greater than 150 cells/mL. This represents a good indicator of eosinophilic asthma associated with T2 inflammation. However, it is important to note that blood eosinophils are not always reflect the number of eosinophils in the airway walls. Nevertheless, blood eosinophilia predicts response to therapeutic strategies such as anti-IL5, anti-IL-4/IL-13 and anti-IgE. High blood and sputum eosinophilia in individuals with adult-onset asthma has been associated with higher FENO values, the worst lung function with fixed obstruction.

F_{ENO}: Airway epithelial cells and other airway resident cells are responsible for the production of F_{ENO} . According to the 2019 Global Initiative for Asthma guidelines, a F_{ENO} value greater than 25 ppb is indicative of residual T2 and eosinophilic inflammation. However, several studies have shown limitations of this parameter.

IgE levels: The presence of serum-specific IgE and a positive skin test to allergens is associated with atopy in asthma and differentiates allergic asthma from non-allergic asthma.

Non-T2 asthma is independent of T2 inflammatory biomarkers, resistant to corticosteroids, and usually associated with adult-onset asthma as observed in obesity-associated asthma, smoking-associated neutrophilic asthma and paucigranulocytic asthma (i.e., asthma occurring in the context of very low airway levels of neutrophilic and eosinophilic

inflammation) (Sze et al. 2020). Non-T asthma is a more severe form of asthma that is difficult to diagnose due to limited reliable biomarkers.

Current studies suggest that neutrophilic asthma is defined as an increase in neutrophils to above 60% or 76% in induced sputum. Paucigranulocytic asthma is defined as neutrophils < 76% and eosinophils < 3%, whereas mixed granulocytic asthma is defined as neutrophils > 76% and eosinophils > 3% (Yamasaki et al. 2022).

The most relevant non-T2 biomarkers are airway neutrophilia and inflammatory cytokines and mediators such as IL-6 in sputum and serum IL-17 and YKL-40 in serum. IL-6 mediated by Th17 is associated with the severity of asthma in patients with obesity (Peters et al. 2016). Neutrophils and sputum IL-17 were concomitantly associated with non-T2 asthma in obese patients. Moreover, patients with the steroid-resistant asthma phenotype had high plasma IL-17 levels (Chambers et al. 2015; Agache et al. 2010). Another potential non-T2 biomarker is YKL-40, a chitinase-like protein found to be associated with serum neutrophilia and asthma severity (Chupp et al. 2007; Lim et al. 2018).

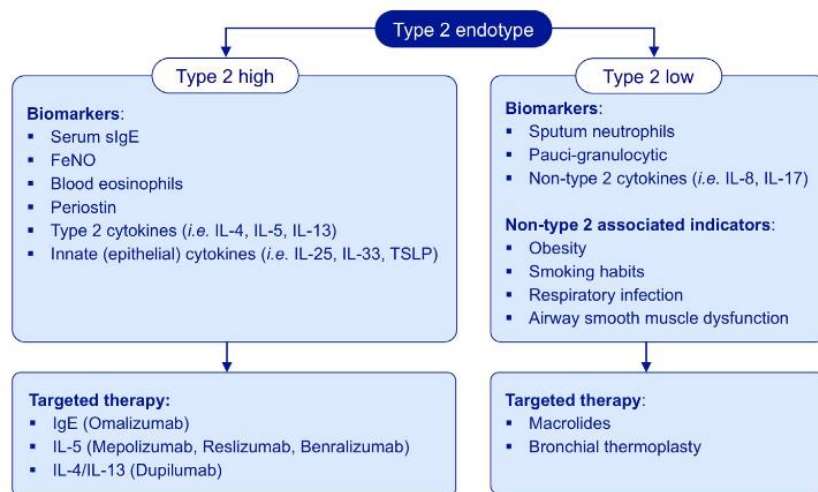


Figure 09: Biomarkers and associated indicators of asthma endotypes. The most predominant asthma are Type 2 high and non-type 2 (or type 2 low) endotypes. Blood and sputum eosinophil counts, FENO values, and specific serum IgE are the most described markers of T2 high asthma which is associated with Th2 cytokines (IL-4, IL-5 and IL-13), and innate epithelial cytokines (IL-25, IL-33 and TSLP) are other complementary markers. Periostin is also a good marker as well but it may be limited by asthma regiotype. Type 2 low asthma presents with predominant airway neutrophilia and pro-inflammatory cytokines such as (IL-6, IL-8 or IL-17) or as paucigranulocytic. It usually occurs in obese population, and as a result of smoking habits or after respiratory infection. Moreover, it can also be the result of psychological aspects such as intense anger, anxiety and depression (Breiteneder et al. 2020).

Other biomarkers have been identified that predict the risk of complications. For example, a defective upregulation of TLR2 and TLR4 on neutrophils was associated with delayed resolution of infection-induced asthma exacerbations (Ekstedt et al. 2020). Sputum TNFR1 and TNFR2 are increased in severe asthma and correlate with worse lung function and uncontrolled asthma. Serum TNFR1 is increased in severe asthma. Further, sputum and serum TNFR2 are often associated with exacerbations (Zounemat Kermani et al. 2021).

A multimorbidity signature of eight genes were systematically overexpressed in all types of multimorbidity of asthma: (CLC, EMR4P, IL-5RA, FRRS1, HRH4, SLC29A1, SIGLEC8 and IL1RL1). Eosinophil-associated immune response and signaling were enriched in the multimorbidity signature (Agache et al. 2021).

Recently, several signaling pathways have been identified for their contribution to asthma pathophysiology that may represent relevant therapeutic targets.

Pathway	Related molecules and actions
- JAK-STAT	- IL-4, IL-5, IL-13, IL-31 and TSLP
- Adiponectin	- AMPK and NF-κB
- Prostaglandin receptor	- CRTH2 and LTB4
- Type I interferon	- PRRs, TLR, RIG-I and MDA5
- Wnt	- WISP-1 and WIF-1. Vit. D, glucocorticoid.
- PI3K/AKT	- miRs
- JNK-Gal-7	- TGF-β
- Nrf2	- ROS
- Foxp3- RORγt	- LncRs ceRs and miRs
- MAPK	- IgE and IL-4
- NF-Kb	- iNOS and COX-2
- CysLT	- eosinophil degranulation
- cAMP	- IL-4, 5, 13 and β2-AR
- Fas	- apoptotic Fas signaling: JNK, NF-kB, p38. nonapoptotic Fas signal: ERK1/2 and p35
- PTHrP/PPARγ	- Leptin
- PAI-1	- PAI-1 t-PA, u-PA, ECM and remodeling
- FcεRI	- TSLP, IL-4, IgE and mast cell Degranulation
- Tim-3-Gal-9	- PI3K/Akt, Th1 apoptosis and inflammation
- TLRs	- NF-κB, AP-1, IRF, SOCS1 and MyD88
- PAR2	- b-Arrestins, cAMP/PKA
- Keap1/Nrf2/ARE	- CHD6, CBP, ARE
- Ca+	- PLCb, ROCK, RhoA

Table 03: Signaling pathways involved in asthma pathophysiology (Athari. 2019).

3. Mechanisms of asthma immune-pathogenesis

The main changes to the airways that occur in asthma including smooth muscle contraction leading to airway narrowing, goblet cell hyperplasia and mucus hypersecretion causing reversible or fixed airway obstruction and potential tissue fibrosis leading to breathing difficulties, are most often a result of exaggerated immune cells in response to an allergen, pollutant or microbial infection.

3.a) Type-2 high immune response

In addition to its role as a physical barrier, the bronchial epithelial cells (BECs) orchestrate the initiation of the immune response during asthma pathophysiology. Upon stimulation with allergens such as HDM, due to their enzymatic activity can directly attack tight junction proteins, resulting in increased permeability. The “barrier endotype” is associated with all asthma phenotypes and is correlated with the severity of asthma (Papi et al. 2018). Furthermore, human BECs express a functional IL-5 receptor and its activation during allergy contributes to barrier dysfunction (Barretto et al. 2020).

The release of IL-33, IL-25 and thymic stromal lymphopoeitin (TSLP) by BECs mainly in a TLR4/Myd88-dependent manner (Cayrol et al. 2018). The IL-33 receptor ST2, is among the most highly replicated susceptibility loci for asthma (Moffatt et al. 2010). Furthermore, IL-33, IL-25 and TSLP were all increased in patients with asthma and correlates with asthma severity (Gasiuniene et al. 2019; Cheng et al. 2014; Ying et al. 2005). The ability of these alarmins in the establishment of allergic asthma resides in the activation of Th2 cells, eosinophils cells, DCs and ILC2 cells.

Activation of IL-33 receptor ST2, IL-25R and TSLPR on the surface of ILC2 leads to cell proliferation and differentiation of ILC2 dependently on c-Myc activation and the release of IL-5, IL-13 and IL-9 (Ye et al. 2020). IL-33 further enhances ILC2 activation during allergy through the upregulation of PPAR- γ which in turn upregulates the IL-33 receptor ST2 (Xiao et al. 2021). Moreover, a positive feedback loop between IL-33 and TSLP fuels inflammation (Toki et al. 2020). ILC2 derived cytokines act directly on the epithelial barrier such as IL-5. The same result was shown for IL-13 when ex vivo ILC2 and human bronchial epithelial cells were co-cultured (Sugita et al. 2018).

ILC2 supports the allergic response by promoting the of polarization of Th0 into Th2 mainly by promoting the migration of DCs to the sentinel lymph node (SLN) through the secretion of IL-13 (Halim et al. 2014).

Epithelial-derived cytokines such as IL-33, TSLP, IL-1 α and GM-CSF instruct a subset of conventional DCs known as type 2 SIRP α^+ CD11b $^+$ cDC2s, to polarize Th2 cells in (SLN) after antigen uptake (Hammad et al. 2021). In T2 high asthma patients, conventional CD1c $^+$ DCs in the lung express Fc ϵ RI. Allergen binding to the IgE/Fc ϵ RI complex on DCs blocks the type I IFN release by pDC and facilitates allergen presentation to memory Th2 lymphocytes (Hammad et al. 2021). This may explain the increased susceptibility to viral infections in allergic asthma (Gill et al. 2018). Monocyte-derived DCs release a panel of chemokines including CCL13, CCL17, CCL18, and CCL24 leading to the accumulation of eosinophils and Th2 cells in the lung, but have no effect on Th2 cell differentiation (Plantinga et al. 2013), (Agache et al. 2021).

After Th2 polarization, patients with allergic asthma can be further divided into type-2 high and type-2 ultra-high with the major signaling signatures IL-4, IL-5, IL-13 and IL-9 (Peters et al. 2019), (Seumois et al. 2020). Similar to ILC2, Th2 cells express the ST2 receptor to response to the epithelial-derived cytokines IL-33 leading to activation of PPAR- γ . PPAR- γ pathway is essential for the pathogenesis of Th2 cells as it contributes to the secretion of Th2 cytokines by upregulating the expression of the IL-33 receptor ST2 (Chen et al. 2017; Tibbitt et al. 2019).

Local interaction of Th2 with B cells mainly through IL-4 and IL-13 induces IgE immunoglobulin class switching and production by B cells (plasmocytes), to promote bronchial hyperresponsiveness. IgE production occurs both in secondary lymphoid organs and also locally in the lung mucosa. IgE has a high affinity receptor Fc ϵ RI that is expressed on mast cells, basophils, eosinophils and also on local structural cells airway smooth muscle cells (ASM), epithelial cells and endothelial cells (Hammad et al. 2021).

Degranulation of mast cells and basophils following IgE binding results in the release of histamine and other mediators such as tryptase, chymase prostaglandin D2 (PGD2), serotonin and Th2 cytokines (IL-4, IL-5, IL-13 and IL-9) (Hammad et al. 2021). On the one hand, it act on submucosal mucus and induce mucus hyperproduction by goblet cells. On the other hand, it will act on ASMs due to their expression of both the high affinity receptor Fc ϵ RI and the low affinity receptor CD23 leading to their proliferation and bronchoconstriction contributing to airway hyper-responsiveness (AHR) (Elieh Ali Komi & Bjermer. 2019). Furthermore, mast cell-derived serotonin acts on nerves to release acetylcholine, thus enhancing AHR (Agache et al. 2021).

IL-5 is the key cytokine that mediates the maturation of eosinophils maturation and mobilization from the bone marrow during allergic inflammation. During the early phase, ILC2-derived IL-5 is the main eosinophils activator. Eosinophils are central to the pathogenesis of allergic asthma and mediate its regulatory functions through their ability to release cytotoxic proteins from their specific granules such as eosinophil cationic protein (ECP), major basic proteins (MBP 1 and 2), eosinophil peroxidase (EPX), eosinophil-derived neurotoxin (EDN) and lipid mediators from lipid bodies (leukotrienes, prostaglandins, platelet-activating factor (PAF). Furthermore, they can fuel the pro-allergic inflammation through potent secretion of (IL-2, IL-3, IL-4, IL-6, IL-13 and GM-CSF) (Novosad et al. 2023).

Patients with asthma, have significant levels of galectin-10 (Gal10), a prominent cytoplasmic protein found in the primary granules of eosinophils (Nyenhuis et al. 2019). This protein forms Charcot–Leyden crystals (CLC). In a humanized mouse model, intratracheal administration of crystalline Gal10 was immunogenic and acted as an adjuvant of type 2 inflammation (Persson et al. 2019). CLC were shown to induce NET in neutrophils (Gevaert et al. 2021), as well as Extracellular Eosinophil Traps (EET) in eosinophils (Persson et al. 2019) EETs are composed of mitochondrial and nuclear DNA decorated with cationic proteins (MBP and ECP) and Charcot–Leyden crystals and have the same function in defense against pathogens as NETs (Novosad et al. 2023). EET have the ability to license the lung epithelial cells to produce IL-33 and TSLP to further support the allergic responses (Hammad et al. 2021).

During the late phases of asthma, eosinophils can represent a risk biomarker as they can be involved in tissue fibrosis stimulated by the actions of ECP, MBP, TGF β , and IL-1 (Novosad et al. 2023).

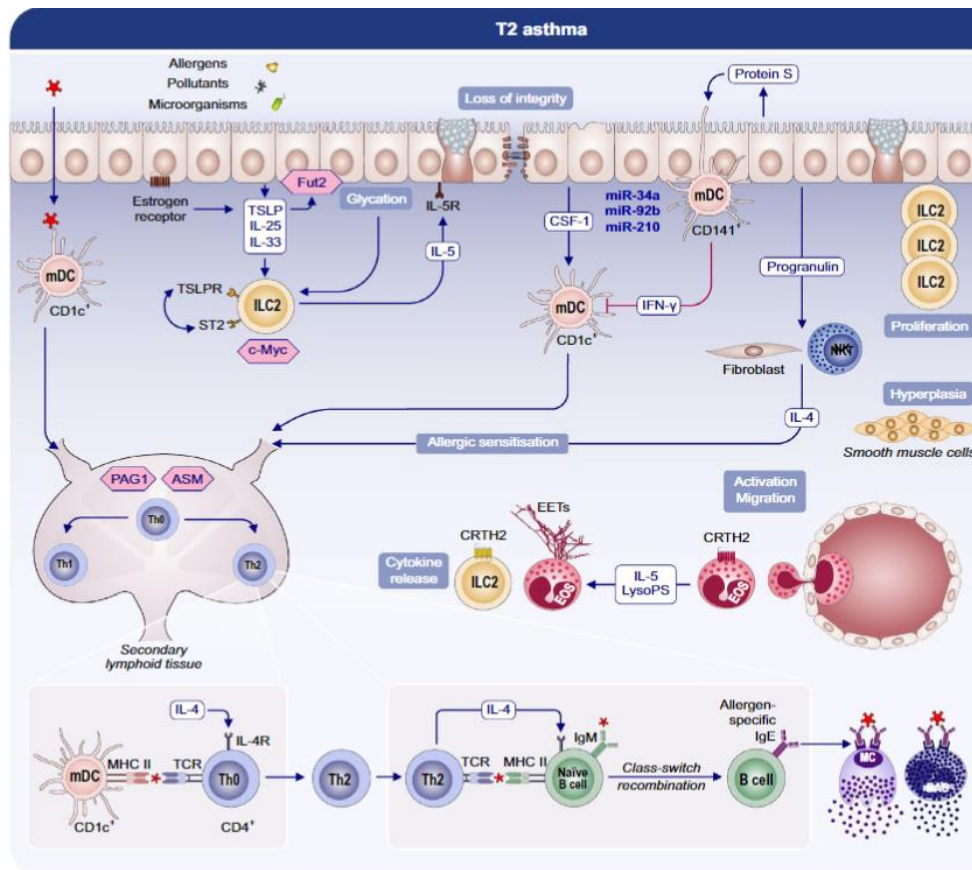


Figure 10: cellular and molecular mechanisms governing T2 asthma. Injury to BECs by allergens, viruses and pollutants leads to loss of barrier integrity and the release of a series of alarmins (IL-33, IL-25 and TSLP). ILC2 cells express the specific receptors for these alarmins, leading to their activation and proliferation in a c-Myc dependent manner. ILC2-derived cytokines (IL-5, IL-13, IL-9) can act on the EBC leading to further impairment of the epithelial barrier. On the other hand, ILC2 recruits eosinophils to lung tissue via IL-5. Besides IL-5, lysophosphatidylserine (LysoPS) induces eosinophil degranulation and EETs. CD1c⁺ myeloid dendritic cells (mDC) are also important contributors to the establishment of T2-high asthma. mDC migrate to secondary lymphoid tissues where they present allergen-antigen where they participate in Th2 polarization, further enhancing IL-5, IL-4 and IL-13 secretion. In turn, Th2 cells stimulate IgE production by B cells and the subsequent activation and degranulation of mast cells and basophils following FcεRI receptor activation. Th2 cytokines and mast cell mediators will set up the hallmark features of asthma: (IL-4 / serotonin: AHR, IL-13: goblet cell hyperplasia and mucus hypersecretion, IgE: airway smooth muscle proliferation and bronchoconstriction) (Agache et al. 2021).

3.a.1) Mucus production in Th2-high asthma

Excessive production of mucus-forming plugs can impair gas exchange and is an important risk factor for asthma exacerbations and mortality. Classically, mucus metaplasia results from increased production and storage of mucins, especially MUC5AC in preexisting secretory cells, including club cells. Patients with Th2-high asthma exhibit increased levels of MUC5AC mRNA within bronchial epithelial cells compared to Th2-low asthma or healthy individuals (Woodruff et al. 2009). Mucus production is mainly driven by IL-13 pathway. However, the EGFR pathway may also be involved (Erle et al. 2014).

o IL-13 signaling pathway

The IL-13 receptor is a heterodimer composed of IL-13R α 1 and IL-4R α subunits. IL-13 binding leads to activation of Jak kinases associated with the cytoplasmic domain of the receptor and subsequent phosphorylation of signal transducer and activator of transcription 6 (STAT6).

Upon IL-13-dependent STAT6 activation, three dependent-pathway are triggered: CLCA1-dependent pathway, Serpin-dependent pathway, and 5-lipoxygenase-1–dependent pathway (Erle et al. 2014; Athari et al. 2019).

The calcium-activated chloride channel 1 (CLCA1), (does not function as an ion channel despite its name) is secreted and cleaved extracellularly. Following the binding to its putative receptor, CLCA1 can induce MUC5AC expression via activation of the MAP kinase MAPK13 (p38 δ -MAPK). A second pathway involves the protease inhibitor Serpin3a, the mouse orthologue of human SERPINB3 and SERPINB4. Both of these pathways converge toward increased expression of the SAM-pointed domain–containing Ets-like factor (SPDEF). SPDEF directly regulates mucin gene transcription through the inhibition of the expression of a FOX family gene, FOXA2. The importance of FOXA2 was demonstrated when experimental deletion of FOXA2 in epithelial cells during fetal development was sufficient to induce IL-13 production and Th2 inflammation in the airway (Chen G et al. 2010).

In the third IL-13-dependent mechanism, STAT6 increases 15-LO-1 which in turn converts arachidonic acid to 15-hydroxyeicosatetraenoic acid, which was shown to enhance MUC5AC expression in human airway epithelial cells.

Later, it was found that phosphorylated STAT6 can directly bind to and activate the MUC5AC promotor region (Wang X et al. 2017).

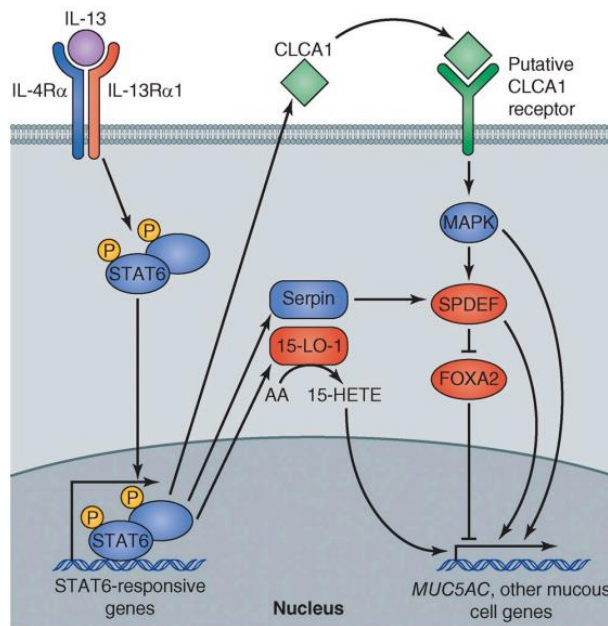


Figure 11: IL-13-STAT6-dependent mechanisms of mucus production. Upon IL-13-dependent STAT6 activation in mucus cell progenitors, like club cells, three dependent-pathway are triggered: CLCA1-dependent pathway, Serpin-dependent pathway, and 5-lipoxygenase-1–dependent pathways. STAT6-dependent activation of CLCA1 and Serpin converge to increase the expression of the pivotal SPDEF. In turn, SPDEF indirectly regulates mucin production through inhibition of FOXA2 expression. The third pathway involves the metabolic production of 15-hydroxyeicosatetraenoic acid by 15-LO-1 in the presence of arachidonic acid. 15-hydroxyeicosatetraenoic acid in turn, enhance MUC5AC expression (Erle et al. 2014).

Following activation of EGFR by its numerous ligands bindings (EGF, TGF- α , heparin-binding EGF, β -cellulin, amphiregulin, epiregulin), the downstream activation of the Ras–Raf–MEK1/2–ERK1/2 pathway ultimately leads to the expression of MUC5AC via the Sp1 transcription factor (Athari et al. 2019).

3.b) Non type-2 immune response

Non or low-type 2 asthma is defined by the absence of the three fundamental type 2 asthma biomarkers (Blood and sputum eosinophilia, increased FeNO and elevated serum IgE). The best identified mechanism explaining the type-2 low phenotype is related to IFN-, TNF- and inflammasome-associated genes and sputum neutrophil increase identified by Kuo et al in a transcriptome associated cluster (TAC) study. This cluster of patients is referred to as “neutrophilic asthma “(TAC2 in this study) (Kuo et al. 2017).

Several studies have found a link between neutrophilic inflammation and development of severe asthma or asthma exacerbations (Jatakanon et al. 1999; Gibson et al 2001). HDM is one of the most clinically relevant aeroallergen involved in the development and exacerbation of allergic asthma, with 90% of cases of childhood asthma due to HDM. In a study, patients with positive serum HDM-specific IgG correlated with sputum neutrophils and also had elevated levels of serum enolase. In the same study, HDM-derived enolase induced barrier disruption in a mouse model. Further strengthening the involvement of neutrophils in severe forms of asthma (Lin et al. 2021).

According to the 2021 international asthma guidelines (GINA), severe asthma is defined as asthma that is uncontrolled despite high-dose ICS long-acting beta, or that requires high-dose ICS-LABA to remain controlled (Agache et al. 2021). This might be explained in part by the observation that glucocorticoids enhance the survival of neutrophils, which express constitutively glucocorticoid receptor β (GR β) (Strickland et al. 2001; Saffar et al. 2011).

In neutrophilic asthma phenotype, the main cytokines involved are IL-17, IFN γ , IL-8 and IL-6 together with TSLP, IL-25 and IL-33, which are released by injured epithelial barrier as it can occur after chronic exposure to benzo(a)pyrene or diesel exhaust particles. This combination was shown to drives steroid resistance (Agache et al. 2021).

Neutrophil counts and IL-8 in patients with asthma were correlated with IL-17 mRNA levels. Besides, IL-17 release was increased in sputum and bronchial biopsies from patients with severe asthma. IL-17 induces GR β on epithelial cells in patients with asthma, which may be involved in corticosteroid resistance, suggesting an important role of IL-17 in neutrophilic exacerbation of asthma (Yamasaki et al. 2022). However, a mouse model using c-di-GMP as an adjuvant resulting in an asthma model with high lung eosinophils counts, low T2 response, and elevated IFN- γ and IL-17 with signs of AHR showed that the contribution of IFN- γ was more important than the contribution of IL-17 in the development of asthma features.

Furthermore, a clinical trial targeting the IL-17 pathway failed to attenuate asthma features (Hammad et al. 2021).

Several reports indicate that neutrophils have an effect on severe asthma through the release of NETs and extracellular DNA (e-DNA). In a clinical study, Lachowicz-Scroggins et al. found a correlation between e-DNA and neutrophils, soluble NETs components and increased caspase-1 activity and IL-1 in the sputum of patients with asthma. Furthermore, they showed that patients with high e-DNA had lower asthma control despite the frequent use of corticosteroids and frequent history of mucus hypersecretion (Lachowicz-Scroggins et al 2019).

A group of researchers has shown in two independent studies that NETs induced by rhinovirus infection or low-dose microbial exposure promote the development of type-2 high asthma (Toussaint et al. 2017; Radermecker et al. 2019).

On the other hand, a study has reported the coexistence of Th17-high signature with Th2-high signature in cluster of patients with asthma (Hammad et al. 2021). This might be partly explained by the finding that IL-17 induces eotaxin expression in human airway smooth muscle cells. Several studies reported the coexistence of neutrophils and eosinophils in severe asthma. Moreover, patients with mixed granulocytic endotype show a rapid decline in respiratory function (Yamasaki et al. 2022).

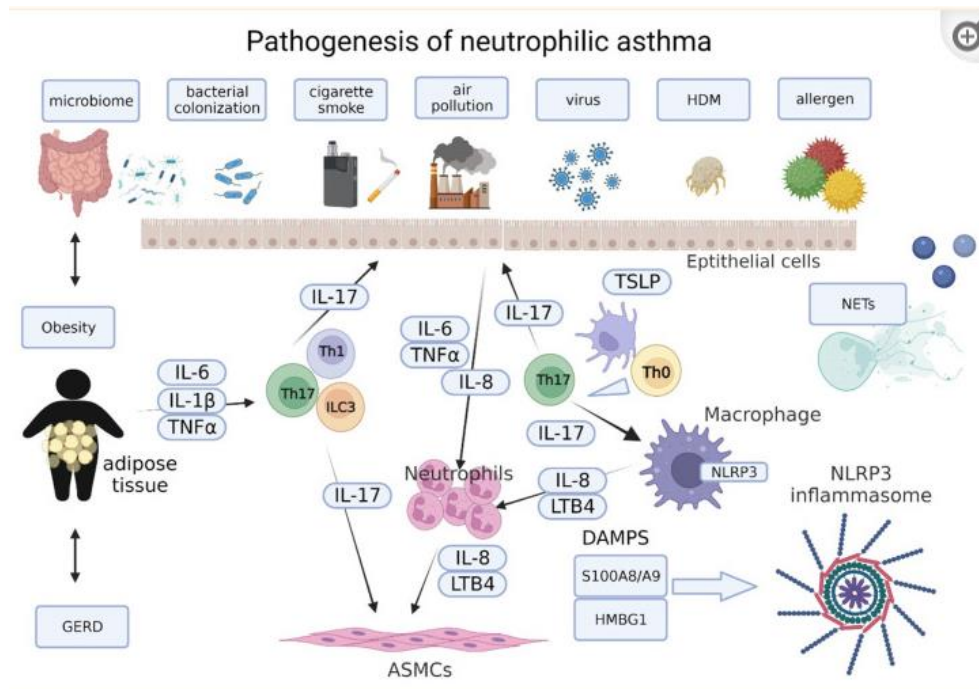


Figure 12: Cellular and molecular mechanism governing T2-low neutrophilic asthma. Pollutants as diesel exhaust particles (DEP) and benzo(a)pyrene, cigarette smoke or even allergens as HDM can damage the airway epithelial and trigger TSLP, IL-25 and IL-33 release. TSLP can drives polarization of Th17 cells and their subsequent release of IL-17. IL-17 can instruct epithelial cells to the release of IL-8 and GM-CSF for neutrophils chemotaxis. The Th17/IL-17 axis is widely found in obesity- and smoking habits-related severe neutrophilic asthma, as well as in microbiome associated neutrophilic inflammation. Neutrophilic asthma is associated with the increased activation of ILC1 and ILC3 as contrast to the involvement of ILC2 in T2-high asthma. Pollutants contributes to the recruitment of pro-inflammatory M1 macrophages, NKT cells and cytotoxic T cell (CTL) in lung tissue. The most prominent signature found in this asthma phenotype/endotype is NLRP3 inflammasome signature, DAMPS such as (HMGB1 and S100A8/A9 protein and NETs formation (Yamasaki et al. 2022).

Chapter II: Regulation of innate immunity by cell death.

In order to prevent deleterious immune responses that can cause pathology, activated immune cells must be eliminated soon after completing their duty, and infected cells tend to undergo “suicide” to prevent the spread of pathogens (Nagata & Tanaka. 2017). Hence, cell death is an important aspect regulating the innate immune system.

1. Cell death classification

The Nomenclature Committee on Cell Death (NCCD) defined a precise nomenclature, and has formulated guidelines for the definition of cell death from the morphological and molecular mechanisms involved. Currently, cell death can be fundamentally divided into accidental cell death (ACD) and regulated cell death (RCD), based on functional aspects (Galluzzi et al. 2018).

ACD is the unexpected, instantaneous and catastrophic cell death corresponding to the disassembly of the plasma membrane caused by severe physical, chemical or mechanical insults (high pressures, temperatures, osmotic forces, extreme pH variations, shear forces) that submerge any possible control mechanisms (Tang et al. 2019). This form of cell death will not be discussed in this document.

By contrast, RCD involves precise signaling cascades and has functional and immunological consequences and hence can be pharmacologically or genetically modulated. RCD is involved in two opposed scenarios: first, RCD occurs in strictly physiological context in the absence of any perturbation of the homeostasis or cell stress, and hence operates as a physiological program for development or tissue turnover. This form of RCD is referred to as programmed cell death (PCD) (Fuchs et al. 2011). Second, RCD can occur under severe and prolonged perturbations of the intracellular or extracellular microenvironment leading to the inevitable failure of the cell to cope with stress and restoring homeostasis (Galluzzi et al. 2015)

RCD can be classified into multiple subgroups based on the signaling pathways involved, referred to as apoptotic or non-apoptotic RCD such as necroptosis, pyroptosis and NETosis, or other less well-studied RCD such as ferroptosis, entotic cell death, parthanatos, lysosome-dependent cell death, autophagy-dependent cell death, alkaliptosis, and oxeiptosis, which may be specific responses to toxins that do not reflect normal physiology (Galluzzi et al. 2018).

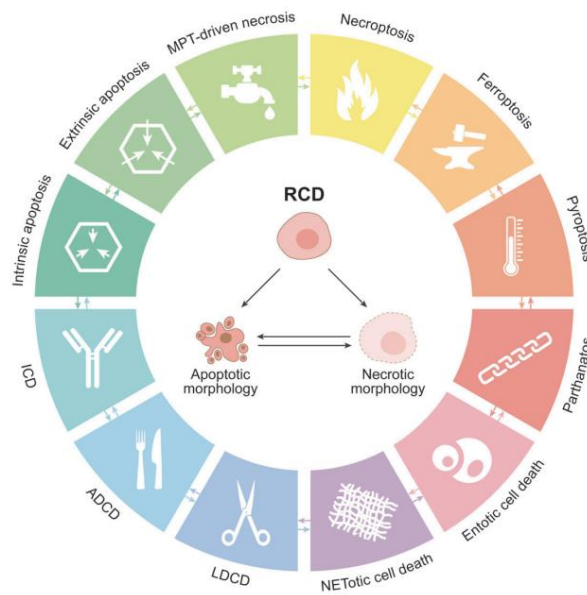


Figure 13: Regulated cell death (RCD) subgroups. Under extreme and irreversible intracellular or extracellular perturbation, cells can activate one or multiple signal transduction cascades that exhibit considerable cross-talk modalities leading to their elimination. Each type of these RCD has a specific immunomodulatory profile ranging from anti-inflammatory to pro-inflammatory and immunogenic. ADCD: autophagy-dependent cell death, ICD: immunogenic cell death, LDCD: lysosome-dependent cell death, MPT: mitochondrial permeability transition (Galluzzi et al. 2018).

Historically, Kerr, Wyllie and Currie were the first research group to observe a specific type of cell death in human tissue in which the cells and nuclei became condensed and fragmented: they named it “Apoptosis” and reported a physiological role for it (Kerr, Wyllie, & Currie. 1975). Around 30 years later, Brad Cookson and coworkers reported a type of cell death dependent on caspase & (CASP1) in macrophages infected by *salmonella* or *Shigella*, accompanied by IL-1 β production formerly known as “leukocytic pyrogen”, which later inspired the name “pyroptosis” (Brennan & Cookson. 2000; Fink & Cookson. 2005). Morphologically, pyroptosis is characterized by chromatin condensation (pyknotic nuclei) and cell swelling with membrane bubbling and rupture. During the same era, Arturo Zychlinsky’s group, paying particular attention to neutrophils, discovered their fascinating and “altruistic” ability to generate extracellular traps, first upon exposure to phorbol myristate acetate or IL-8, then upon exposure to microbes leading to their own death to prevent microbial spread (Brinkmann et al. 2005). Almost simultaneously, in 2005, Yuan and collaborators contributed to the understanding of necroptosis, which had already started in 1996 (Ray et al. 1996), by focusing on the molecular mechanisms behind it (Degterev et al. 2005). The discovery of RPIK1

as a regulator of FasL-induced necroptosis has further improved our understanding of this RCD (Holler et al. 2000)

The observation that cell death may alert the immune system to respond to DAMPs released by dead cells gave rise to the term “immunogenic cell death (ICD)” introduced by Guido Kroemer in 2005, in significant contrast to physiological “silent” efferocytosis in which dead cells are cleared by macrophages without any immune response (Casares et al. 2005). Since then, the field has progressed and several other highly interconnected signaling pathways that regulate RCD have been characterized and are still the subject of intensive research.

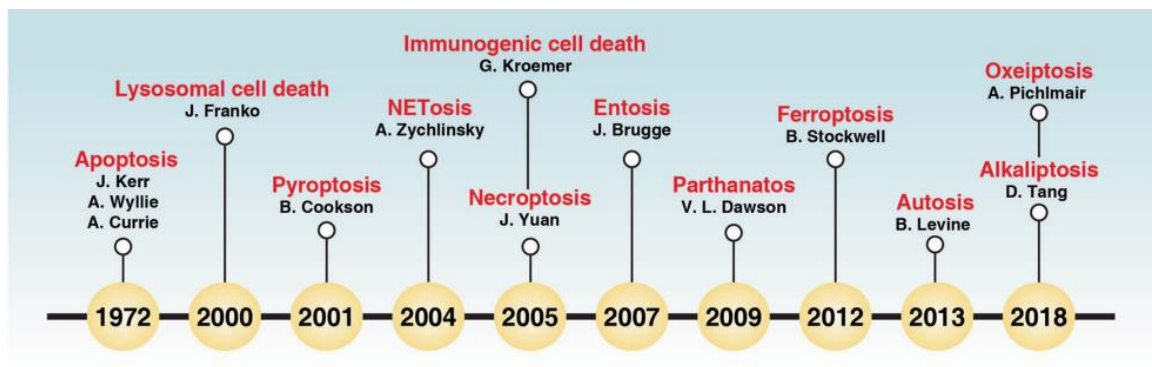


Figure 14: Timeline of the history of cell death research in immunology (Tang et al. 2019)

1.a) Apoptosis

Apoptosis is a PCD, long believed to be the only molecularly controlled type of cell death. Apoptosis can take 16-24 hours or even days from initiation to complete destruction of the cell but parameters like the strength of the stimuli, cell type or variation in the inducing mechanisms can shorten this period (Collins et al. 1997; Rehm et al. 2002). Mechanistically, apoptosis is governed by two main pathways that contribute to the caspase activation cascade: the *intrinsic* and *extrinsic* pathways (Nagata & Tanaka. 2017).

The intrinsic pathway, also called “*mitochondrial pathway*” is triggered by an imbalance in intracellular homeostasis such as growth factor/nutrient deprivation, DNA damage or ER stress, and involves proapoptotic proteins the BCL-2 family such as BAX and BAK which form pores in the mitochondrial membrane causing mitochondrial outer membrane permeabilization (MOMP), and release of cytochrome C in the cytosol. The latter binds and promotes the polymerization of APAF-1 containing a CARD domain that interacts with the CARD domain of the apoptosis initiator pro-caspase-9 to form the apoptosome (Acehan et al. 2002). Within this massive complex, caspase-9 becomes activated and cleaves pro-caspase-3 and pro-caspase-

7 unveiling their apoptotic executioner functions. Once activated, caspase-3 and caspase-7 activate several other procaspases (caspase-2, -6, -8, and -10) creating an apoptosis-amplifying cascade (Slee et al. 1999). Proteins of the IAP family (IAP1/2 and XIAP) can inhibit caspase-3, 7 and -9 activation (Bertheloot et al. 2021). Conversely, caspase-3 has the capacity to process caspase-9 into a p10 fragment lacking the XIAP docking domain, further promoting apoptosis (Slee et al. 1999). A fine balance of expression levels of pro or anti-apoptotic BCL-2 family regulates sensitivity or resistance to apoptosis.

The extrinsic pathway, also known as “*death receptor-mediated apoptosis*”, is initiated by the activation of death receptors triggered by the environment, the immune system, or neighboring cells (Galluzzi et al. 2018). Pro-apoptotic death receptors include TNFR1/2, Fas and TRAIL receptors DR4 and DR5 recognizing their ligand (TNF α , FasL or TRAIL, respectively) (Ketelut-Carneiro & Fitzgerald. 2022). This event leads to the recruitment of adaptor proteins TRADD and FAS-associated protein with dead domains (FADD). Both adaptors contain death domains (DD), that are also present in caspase-8 and are involved in the recruitment of pro-caspase-8 and -10 to form the death inducing signaling complex (DISC) (Boatright et al. 2003; Kischkel et al. 1995). Activation of caspase-8 within the DISC leads to the activation of executioner caspase-3 and caspase-7, either directly through proteolytic cleavage, or indirectly by activating BCL2 protein family member BID, which promotes MOMP and generates feedback into the intrinsic pathway to execute apoptosis (Bertheloot et al. 2021). In some type II cells (such as hepatocytes) the extrinsic pathway may be insufficient and the amplification loop via MOMP may be necessary to execute cell death (Kalkavan et al. 2018).

Extrinsic apoptosis is also regulated by receptor-interacting serine/threonine protein kinase (RIPK)1, which interacts with FADD and TRADD through binding to their death domain. At an early stage of activation, RIPK1 is ubiquitinated into the DISC by cellular inhibitors of apoptosis (cIAPs) and can promote a pro-inflammatory, pro-survival NF κ B signaling pathway. Sustained cellular stress will allow the activation of pro-caspase-8 within the complex and triggers pro-death pathway. In the absence of active caspase-8, RIPK1 induces death through necrosis (Bertheloot et al. 2021).

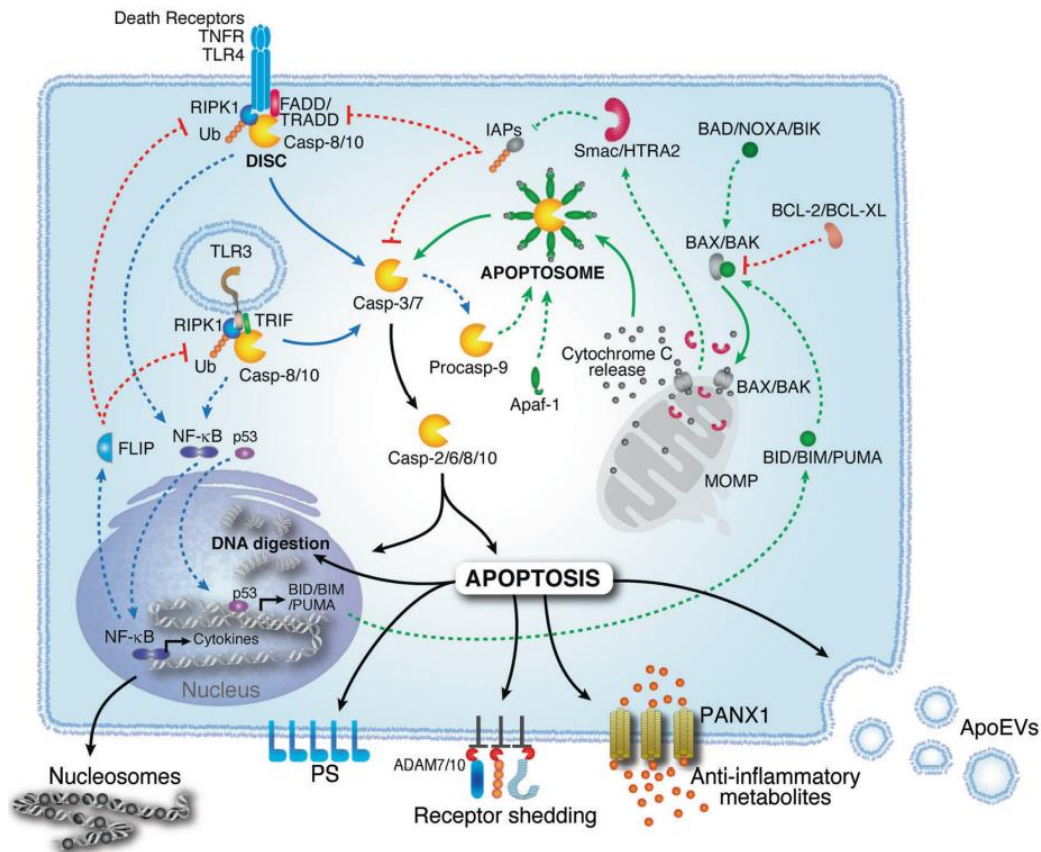


Figure 15: The two major apoptotic pathways. The intrinsic pathway is initiated by a developmental or cellular stress that activates the B cell lymphoma 2 homology 3 (BH3)-only proteins (such as BID, BIM and PUMA) which lead to the assembly of the effector of apoptosis BAX and BAK, which assemble into large complexes causing mitochondrial outer membrane permeabilization (MOMP) and the release of cytochrome C from mitochondria. Cytochrome C binds the apoptotic peptidase-activating factor 1 (APAF-1) to recruit pro-caspase-9 forming the apoptosome initiating the caspase processing cascade. In extrinsic pathway, the engagement of death receptors such as TNFR and FAS recruits pro-caspase-8 through their intracellular adaptor protein (TRADD/FADD) to form the death signaling complex (DISC) which encompasses adaptor FADD/TRADD, RIPK1 and pro-caspase-8 and FLIP, the latter limits caspase-8 activation within the DISC. When anti-apoptotic signals are superior to pro-apoptotic signal, the cellular inhibitor of apoptosis (cIAPs) ubiquitinates RIPK1 and stabilizes the DISC leading to NF κ B activation and survival. Conversely, a sustained cellular stress induces the proteolytic activation of caspase-8 in the DISC leading to downstream caspase cascade that is known to involve caspase-3 and -7. Apoptotic cells release “ghost messages” via the release of nucleosomes, shed receptors to block the intracellular signaling and expose PtdSer molecules on the outer plasma membrane of the apoptotic bodies (ApoEVs) as “eat me signals” for phagocytes (Bertheloot et al. 2021).

Intrinsic and extrinsic apoptosis share common pathway components such as the activation of caspase-3 and -7, which represents the point of no return in apoptosis. They also activate scramblase XKr8 and result in the exposure of PtdSer on the outer layer of the cell membrane, known as the “eat me signal”. Surface PtdSer on apoptotic extracellular vesicles

(ApoEVs) promotes the recruitment of phagocytic cells for the clearance of apoptotic cell and the expression and secretion of TGF- β by these phagocytes, thus underlying the immunosuppressive function of PtdSer (Suzuki et al. 2010; Suzuki et al. 2013; Hoffmann et al. 2005). Furthermore, apoptotic cells shed cell surface proteins under the action of metalloproteinases (ADAM10/17) to detach from their site in the tissue and block signaling in the dying cells. Another recently discovered signature is the release of nucleosome components, which distinguishes apoptosis from other forms of cell death (Tanzer et al. 2020).

1.b) Pyroptosis

Pyroptosis is a form of GSDMD-mediated RCD that occurs in both inflammasome-dependent and independent manner, culminating in the rapid loss of plasma membrane integrity and spilling of intracellular contents (Shi et al. 2015). Activation of the inflammasome including canonical and non-canonical types requires two signals: A priming signal, mediated by the engagement of toll-like receptors (TLRs) or IFN receptors to induce a transcriptional upregulation of inflammasome components through the NF κ B pathway. A sensing signal where a variety of PAMPS and DAMPS activate inflammasome sensors and trigger pro-inflammatory caspase-mediated pyroptosis.

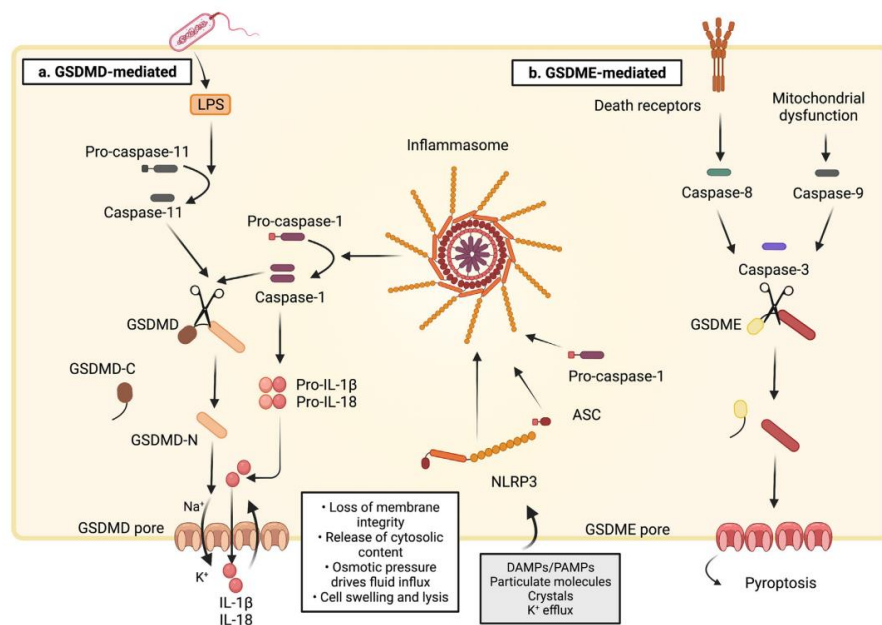


Figure 16: Canonical and noncanonical pathways of pyroptosis. In the canonical pathway, when NLRP3 detects the presence of PAMPs or DAMPs, it recruits the apoptosis-associated speck-like protein containing (ASC) to form a multiprotein complex (inflammasome) that serves as a proteolytic platform to cleave pro-caspase-1. Active caspase-1 cleaves the preforms

of IL-1 β and IL-18. Active caspase-1 also cleaves gasdermin D (GSDMD) into a 31 kDa N-terminal GSDMD that serves as a pore forming protein that controls IL-1 β and IL-18 release and pyroptosis. In the noncanonical pathway, cytosolic LPS activates caspase-11/4/5, triggering pyroptosis by cleaving GSDMD independently of inflammasome activation. Caspase-11 does not permit the release of mature IL-1 β and IL-18. Instead, K⁺ efflux induced by the formation of GSDMD pore lead to NLRP3 inflammasome activation and caspase-1 maturation of IL-1 β and IL-18. Other gasdermin family members can drive pyroptosis such as GSDME which can be cleaved by caspase-3 when the cell is subjected to stress, inducing mitochondrial dysfunction or engagement of cell death receptors (Ketelut-Carneiro & Fitzgerald. 2022).

Canonical pathway: Canonical caspase-1 dependent inflammasome sensors can be divided into NOD-like receptors (including the NLR family pyrin domain-containing 1: NLRP1, NLRP2, NLRP3, NLRP6, NLRP7 and the NLR family CARD domain-containing 4: NLRC4) and the non-NLR such as the absent in melanoma 2 (AIM2) (Tang et al. 2019). Upon PAMPS or DAMPS detection, these sensors assemble with ASC and pro-caspase-1. ASC contains both a pyrin domain (PYD) and a caspase activation and recruitment domain (CARD), with the latter being crucial in mobilizing pro-caspase-1 to form the inflammasome, a cytosolic multiprotein complex responsible for caspase-1 cleavage (Yu et al. 2021). NLRP3 is the best studied inflammasome sensor: it can detect diverse stimuli, including lipopolysaccharide (LPS), metabolites, uric acid crystals, nucleic acids from microbial or host origin and adenosine triphosphate (ATP) (Swanson et al. 2019; Tang et al. 2019). Activated caspase-1 allows the processing of gasdermin D (GSDMD) into a 22 kDa C-terminal (C-GSDMD) and 31 kDa N-terminal (N-GSDMD), which canoligomerize and perforate the cell membrane to form large transmembrane β -barrel pores of around ~10–14 nm (Lieberman et al. 2019; Yu et al. 2021). Further, caspase-1 cleaves the pro forms of IL-1 β and IL-18. At an early stage, GSDMD pores allow the release of mature forms of IL-1 β and IL-18, which recruit immune cells and elicit an inflammatory response. Before the complete loss of membrane integrity, ESCART-dependent membrane repair pathway limits to a certain extent the release of the whole cellular content while allowing cytokine release (Bertheloot et al. 2021). The polybasic motif found in mature IL-1 β enables its relocation to a plasma membrane region enriched with PIP2 phospholipids. Once there, IL-1 β can be released through membrane ruffling independently of GSDMD. In the same context, IL-1 β can also be encapsulated into secretory lysosomes, into ectosomes and exosomes, or released with secretory autophagosomes (Monteleone et al. 2015). In more advanced stages, ESCART can become overwhelmed and full permeabilization occur, allowing DAMPS release such as high mobility group box 1 (HMGB1) which is too large to pass through GDMD pores (Volchuk et al. 2020). ASC specks can also be released from dying cells and

accumulate in tissues or remain in the bloodstream for several days, amplifying thus the inflammation (Franklin et al. 2014).

Non-canonical pathway: In the absence of caspase-1 activation, GSDMD is directly targeted for cleavage. Cytosolic activation of murine caspase-11 and human caspase-4 and -5 by LPS from invading Gram-negative bacteria can cleave GSDMD to N-GSDMD, which can oligomerize and form plasma membrane pores, mediating pyroptosis without enabling maturation of IL-1 β and IL-18 (Shi et al. 2015). Guanylate-binding proteins (GBPs) are essential for LPS-dependent activation of caspase-11 and -4. LPS activation of TLR4 triggers the expression GBPs, which then bind to LPS to form a multimolecular complex with caspase-11 and -4 allowing their activation (Santos et al. 2018; Bertheloot et al. 2021). Several reports have highlighted the interplay between the canonical and non-canonical pyroptosis pathways. Indeed, caspase-11, -4, -5 dependent cleavage of GSDMD leads to K⁺ efflux, which induces the activation of NLRP3 inflammasome, thereby enhancing pyroptosis (Rathinam et al. 2012; Baker et al. 2015).

Absence of GSDMD in murine macrophages does not prevent membrane destabilization as measured by lactate dehydrogenase release (Kayagaki et al. 2015). This finding indicates that GSDMD is not exclusive in the membrane disruption step. Other members of the gasdermin family (such as GSDMA/B/C/E and GSDMA3) may exert comparable roles to GSDMD in pore formation and membrane destabilization (Ding et al. 2016). Upon mitochondrial dysfunction or death receptor activation, caspase-3 is activated and plays a role in GSDME-mediated pyroptosis (Wang et al. 2017). Moreover, under specific conditions in breast cancer, upon TNF- α stimulation, caspase-8 specifically targets GSDMC to release N-GSDMC, leading to pore formation on the cell membrane, which triggers pyroptosis (Hou et al. 2020). In 2020, advances in the field have challenged the conventional understanding that caspases are the only activators of pyroptosis (Yu et al. 2021). Zhang and collaborators found that granzyme B (GzmB) directly cleaves GSDME to induce pyroptosis in cancer cells (Zhang et al. 2020). Simultaneously, Zhou et al showed that NK cells and cytotoxic T lymphocytes (CTLs) exert their cytotoxic effect by releasing Gzma to specifically cleave and activate GSDMB leading to pyroptosis in targeted cells (Zhou et al. 2020). The molecular events of pyroptotic cell death occur rapidly within few minutes (De Vasconcelos et al. 2019).

1.c) Necroptosis

Necroptosis, is a non-caspase-dependent RCD, in which RIPK1, RIPK3 and MLKL (Mixed Lineage Kinase domain-Like protein) are the key molecules of the necroptotic machinery (Galluzzi et al. 2017; Zhan et al. 2021). In striking contrast with apoptosis, deletion of major necroptosis players RIPK3 or MLKL has no effect on development and homeostasis (Shan et al. 2018). It is apparent that necroptosis is a backup mechanism that has evolved to detect pathogens or challenging conditions a cell can face.

The most extensively described necroptosis triggering pathway occurs following the engagement of TNFR1 activated by TNF α (Galluzzi et al. 2017; Zhan et al. 2021). Downstream, active RIPK1 is recruited and form an oligomeric complex with FADD, caspase-8 and -10. When caspase-8 activity is inhibited by caspase inhibitors such as Z-VAD-FMK or by the depletion of FADD, RIPK1 attracts RIPK3 via interactions between their RIP homotypic interacting motif (RHIM), leading to the formation of the hetero-amyloid complex RIPK1/RIPK3 (Vercammen et al. 1998; Mompeán et al. 2018) called “riposome” and RIPK3 autophosphorylation. MLKL is then recruited and phosphorylated to the “necrosome” ultimately leading to necroptosis.

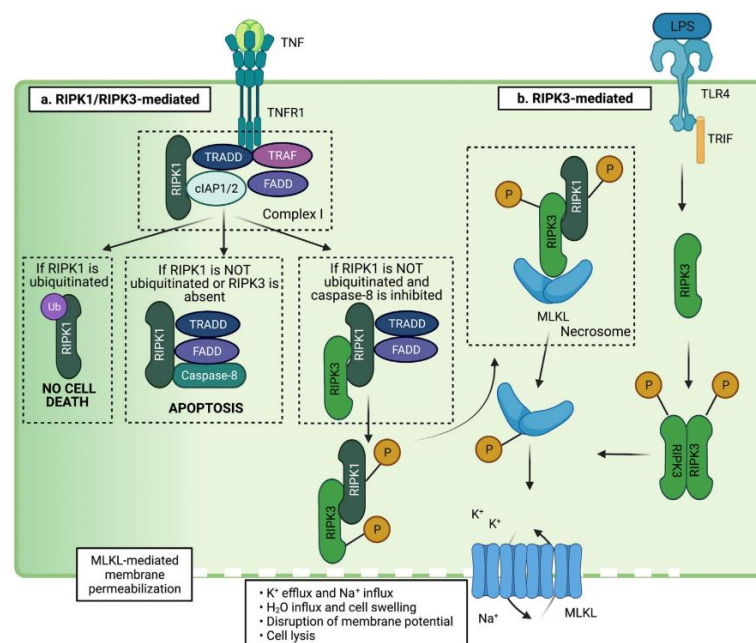


Figure 17: Necroptosis pathway: “Apoptosis, I Got Your Back!”. Following the activation of the death receptor TNFR1, RIPK1 allow the formation of complex I comprising RIPK1, TRADD, FADD, TARF and cIAP. Within this complexe, ubiquitination of RIPK1 promotes cell survival, while RIPK1 desubiquitination promotes the dossciation of RIPK1-TRADD from complex I. When Caspase-8-FADD are available, they are recruited to RIPK-TARDD to initiate apoptosis. However, when apoptosis is blocked, RIPK1 recruits RIPK3 to form the riposome,

allowing phosphorylation of RIPK3 and the subsequent recruitment of MLKL leading to the formation of the necrosome-dependent necrosis. RIPK3 can be alternatively and directly activated following engagement of TLR4 receptors, leading to RIPK3-RIPK3 homodimerization, autophosphorylation and subsequent recruitment of MLKL. Phosphorylation events of MLKL induces their conformational change allowing their insertion in the plasma membrane to initiate osmotic perturbations and cell lysis (Ketelut-Carneiro & Fitzgerald. 2022).

Wu and collaborators have demonstrated that the RIP1–RIP3 heterodimer itself is not sufficient to propagate necroptosis. RIPK1/RIPK3 heterodimerization only serves as a platform that allow the recruitment of free RIPK3 by RIPK3 itself, leading to their autophosphorylation into the scaffold, since downstream necroptosis signaling is triggered by the homodimerization of RIP3-RIP3 but not of RIP1–RIP1 or RIP1–RIP3; this is explained by a higher affinity of RIPK1 for RIPK3 than directly RIPK3 for RIPK3 (Wu et al. 2014). Therefore, high levels of intracellular RIPK3 are critical for the initiation of necroptosis (Ketelut-Carneiro & Fitzgerald. 2022).

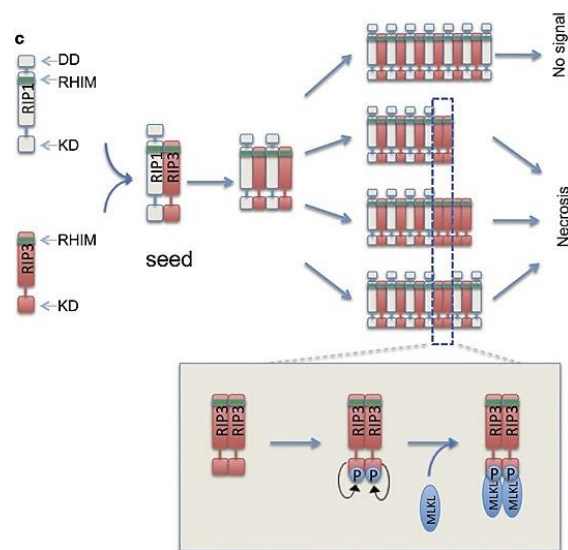


Figure 18: Proposed signaling events within the necrosome. High levels of RIPK3 is a determinant factor for the initiation of necroptosis. The high affinity of RIPK1 for RIPK3 allow its recruitment within the ripotpsosome for the formation of RIPK1-RIPK3 heterodimers. This latter serves as a scaffold for the recruitment of free RIPK3 by RIPK3 responsible for their auto-phosphorylation and recruitment of MLKL leading to the formation of the necrosome (Wu et al. 2014).

Other receptors can trigger necroptosis including Fas/FasL, TLR3/TLR4, and nucleic acid sensors (ZBP1, RIG-I and STING) (DAI et al. 2021; Upton et al. 2012; Schock et al. 2017). These later promote TNF α and IFN-I production, thus amplifying necroptosis in an autocrine manner (Brault et al. 2018). RIPK1 can be dispensable to RIPK3-MLKL dependent necroptosis

downstream of TLR3/4 activation which may promote RIPK3/RIPK3 homo-complex formation (He et al. 2016; Ketelut-Carneiro & Fitzgerald. 2022). Moreover, RIPK3 can be directly targeted by certain virus promoting its binding to ZBP1 to drive necroptosis (Upton et al. 2012; Huang et al. 2015).

RIPK3-dependent phosphorylation of MLKL causes its oligomerization, which subsequently disturbs cellular integrity through two non-exclusive mechanisms as a last step: first, MLKL inserts into the plasma membrane through its ability to bind PIPs and functions as a cation channel permeable to both K^+ efflux and Na^+ influx leading to an increase in cellular osmolality and cell swelling. Second, the N-terminal coiled-coil domain of MLKL forms membrane-disrupting pores to disrupt membrane integrity and kill the cell (Zhang et al. 2018). MLKL activation and plasma membrane trafficking can take approximately 4.5 hours. This process can continue until 7.5 hours after initial necroptosis stimulation, allowing sufficient time to MLKL clusters to increase in size, leading to cell explosion and the spill of DAMPs, including self-DNA (Samson et al. 2020).

1.d) NETotic cell death: Neutrophils extracellular traps (NETs).

In addition to the classical RCD described above, cell death by NETosis is also a form of lytic RCD dependent on ROS and associated with extracellular chromatin extrusion (Galluzzi et al. 2018). The NETotic process is restricted to hematopoietic cells such as eosinophils, dendritic cells, monocytes, macrophages, mast cells, basophils T cells and B cells, but the first and most extensively studied cells forming neutrophil extracellular traps (NETs) are neutrophils, which inspired the term of “NETosis” described for the first time in pathogen killing (Brinkmann et al. 2004).

1.d.1) Neutrophil intrinsic pathway initiating NETs

Production of ROS via NADPH oxidase is crucial during NETosis (Poli & Zanoni. 2023). In inactive neutrophils a fraction of MPO is linked to NE in the azurosome. Upon stimulation by some NET inducers, ROS modulate the release of MPO and NE into the cytosol. When NE is released, it binds F-actin and facilitates its degradation. This step serves to immobilize neutrophils near the microbes that need to be trapped and blocks phagocytosis committing the cell to NETosis (Metzler et al. 2014).

DNA extranuclear extrusion requires chromatin decondensation. This step is supported by NE and MPO, which associate with each other prior to nuclear translocation, where they

initiate the chromatin decondensation process. ROS also participate in the Peptidyl Arginine Deiminase 4 (PAD4) activation, a key calcium-dependent enzyme in NETs formation (Papayannopoulos. 2018; Lewis et al. 2015), which catalyzes the conversion of arginine residues to citrulline on histones H3, H4 and H2A, another mechanism helping chromatin decondensation and DNA extrusion (Nakashima et al. 2013). The level of activation of PAD4 is important in the context of sterile inflammation, however, it is important to note that DNA decondensation can occur in the absence of histone citrullination by PAD4, in which case MPO and NE directly support the decondensation process (Papayannopoulos et al. 2010). Indeed, PAD4 was demonstrated to be dispensable for NET release in PAD4-deficient neutrophils stimulated with group B *Streptococcus* or *C. albicans* (Thiam et al. 2020). Other enzymes contained in the azurosome, such as cathepsin G or proteinase 3 and defensin-1 were shown to participate in the formation of NET.

Kinases activated downstream of increased calcium influx that occurs after neutrophil activation or cytokine signaling pathways have been implicated in the early steps of NADPH oxidase pathway that drives ROS production and NETosis (Thiam et al. 2020). Protein kinase C (PKC α , PKC β 1, PKC ξ), AKT and the RAF-MEK-ERK MAP kinase mediate PMA-, platelet activating factor-, *C. albicans*-, and group B *Streptococcus*-induced NETosis. PI3K involved in autophagy also uncovered a role for NETosis, thus revealing the existence of a cross-talk between autophagy and NETosis. Indeed, in the absence of ATG7 promyelocytes presented a reduced capacity of extracellular DNA release (Ma R. et al. 2016). However, the requirement for each pathway depend on the NET inducer.

1.d.2) Innate immune pathways initiating NETs

The observation that the absence or inhibition of GSDMD led to the prevention of NET formation, confirmed the critical role of GSDMD, activated downstream of canonical and non-canonical inflammasome activation (Sollberger et al. 2018). A study demonstrated that neutrophils exposed to cytosolic LPS or cytosolic Gram-negative bacteria activated NETosis via caspase-11 cleavage of GSDMD (Chen et al. 2018). Cleaved GSDMD forms pores in the granules to release NE, which will itself participate in the proteolytic activation of GSDMD on a different cleavage site from that of caspases (Sollberger et al. 2018; Kambara et al. 2018). Pores can also be formed in the nuclear membrane to allow caspase-11 to act on histone fragmentation and DNA extrusion (Chen et al. 2018). Furthermore, in the context of sterile inflammation both *in vivo* and *in vitro*, Münzer and collaborators recently demonstrated a PAD4-dependent assembly of NLRP3 inflammasome in neutrophils: PAD4 regulates the levels

of NLRP3 and ASC proteins post-transcriptionally, thus implicating NLRP3 in NETosis (Münzer et al. 2021). Consistent with this observation, Desai and collaborators highlighted a role for necrosome components in the induction of NETs. Neutrophils lacking RIPK1 and RIPK3 fail to form NETs when stimulated with PMA and monosodium urate (MSU) crystal, two well-known NET inducers (Desai et al. 2016). However, another research group has challenged this result (Amini et al. 2016). Further investigations are needed to ascertain previous findings. Overall, these data suggest the possible existence of cross-talks between NETosis and other distinct RCDs.

Several studies have identified innate immune receptors as triggers of NET release. A role for TLR2 and TLR4 was described in the context of parasitic infection with *Trypanosoma cruzi* (Sousa-Rocha et al. 2015). TLR7 and TLR8 were shown to drive NETosis in the context of HIV infection (Saitoh et al. 2012). FcγRIIIb (Fc gamma receptor IIIb) on neutrophils engaged by immune complexes has been linked to NETosis occurring in a ROS-dependent manner (Behnen et al. 2014). However, there is no evidence in the literature demonstrating that FcγRIIIb engagement by immune complexes can activate the calcium-dependent enzyme PAD4 to promote further NETosis. It is tempting to speculate that this may be the case. This hypothesis is supported by the fact that neutrophils primed with soluble immune complexes lead to an enhanced Ca²⁺ signal and significant secretion of reactive oxidants (Watson et al. 1997).

1.d.3) DNA extrusion from the nucleus to the extracellular compartment

The nuclear envelope is the first physical obstacle that decondensed chromatin must overcome (Fuchs et al. 2007). Nuclear envelope rupture during NET formation, involved kinases-mediated nuclear lamina phosphorylation-disassembly and discontinuities. PKC-α mediates lamin B phosphorylation and disassembly leading to nuclear envelope rupture (Li Y et al. 2020), (Li M et al. 2022). Cell-cycle proteins also control chromatin extrusion, and cyclin dependent kinase 4/6 (CDK4/6) has been shown to phosphorylate lamin A/C leading to nuclear envelope rupture (Amulic et al. 2017).

After crossing the nuclear barrier, decondensed chromatin must pass through the dense and interconnected network of the cytoskeleton and organelles. To facilitate this, actin filaments, microtubules and vimentin intermediate filaments disassemble prior to chromatin decondensation, the ER vesiculates, cytoplasmic granules disintegrate and mitochondria release mtDNA that can later associate with NETs (Thiam et al. 2020). During this turbulent journey, NETs are adorned with around 330 proteins. Of these, 74 are detected in the neutrophil

proteome independent of the inducer of NETs, with most of proteins originating from the cytoplasm (Petretto et al. 2019; Chapman et al. 2019).

Disrupting the cytoskeleton makes the plasma membrane vulnerable. When combined with the mechanical forces caused by expanding chromatin, this results in breaches of the plasma membrane and the release of NETs into the extracellular space, 3-8 hours after neutrophil activation (Neubert et al. 2018; Papayannopoulos. 2018).

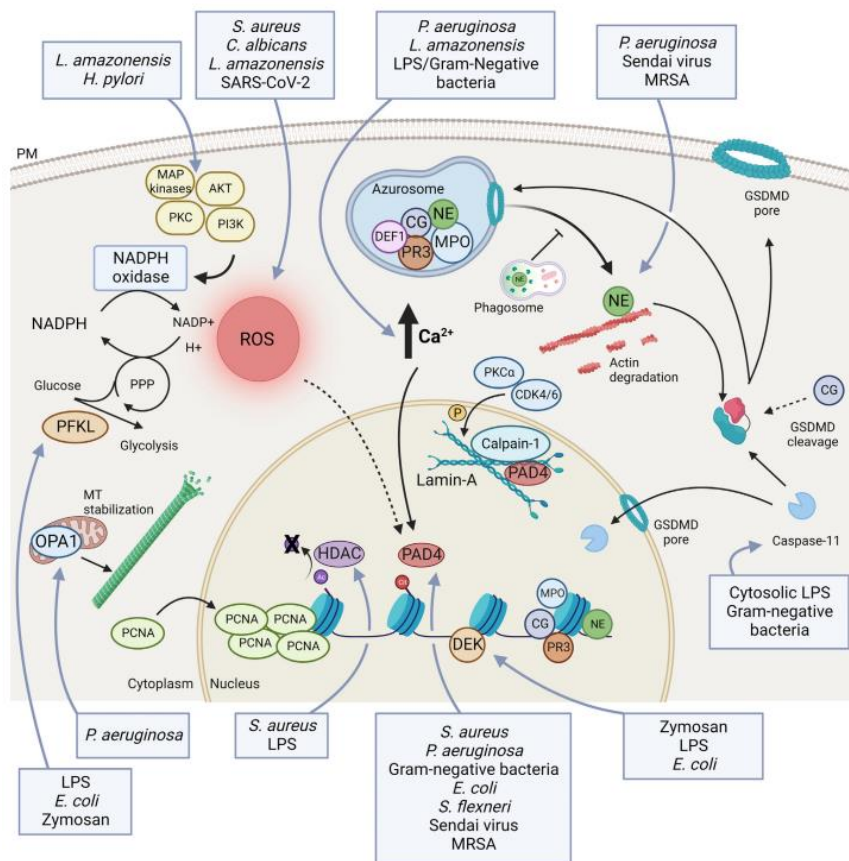


Figure 19: Main molecular mechanism governing NETosis. Neutrophil extracellular traps (NETs) are triggered by microorganisms (bacteria, viruses, fungi) and endogenous stimuli, such as DAMPS, immune complexes and crystals. The induction of reactive oxygen species (ROS) regulated by mitogen-activated proteins kinases (MAPKs), AKT, PIT3 and protein kinase C (PKC) is crucial in the triggering of MPO pathways contained in the azurosome. MPO-mediated oxidative activation of neutrophil elastase (NE) is required for NE-degradation of actin cytoskeleton in the cytoplasm to block phagocytosis and neutrophil chemotaxis migration. Other enzymes contained in the azurosome such as cathepsin G (CG), proteinase 3 (PR3) and defensin-1 (DEF-1) participate in NET formation. Release of granular proteins is facilitated by GasderminD (GSDMD) activation that forms pores in cytoplasmic granules. The release of NE into the cytosol participates in the proteolytic activation of GSDMD which is also necessary to allow NE, MPO, caspase-11 and chromatin-binding protein (DEK) (with similar function as MPO in NET formation), to translocate to the nucleus and drive chromatin decondensation by

processing histones. Increased calcium levels following neutrophil activation mediates protein-arginine deiminase type 4 (PAD4) which citrullinates histones to help chromatin decondensation, that occurs after histone deacetylation by histone deacetylase (HDAC). PAD4, with the help of PKC and CDK4/6, weakens the lamin network responsible for maintaining nuclear integrity and allow, NETs expansion (Poli & Zanoni. 2023).

1.d.4) An alternative mechanism of NET formation

In addition to this classical NET process known as “Suicidal NETs”, Pilszczek and collaborators described an alternative mechanism termed “Vital NETs” in which neutrophil exposure to *Staphylococcus aureus* rapidly induces NETs within 5-60 minutes without cell death. In this process, mitochondrial DNA (mtDNA) and nuclear DNA accompanied by granular proteins are extruded into the extracellular space in a ROS-dependent manner (Pilszczek et al. 2010). Two other studies showed that parasites may also induce rapid vital NETs within 10-30 minutes of neutrophil stimulation (Rochael et al. 2015; Zhou et al. 2020). This process is led by the first neutrophils to arrive at sites of infection or damage, in which the resulting enucleated cytoplasts continue phagocytosis, allowing neutrophils to hit two targets with one shot (Papayannopoulos. 2018).

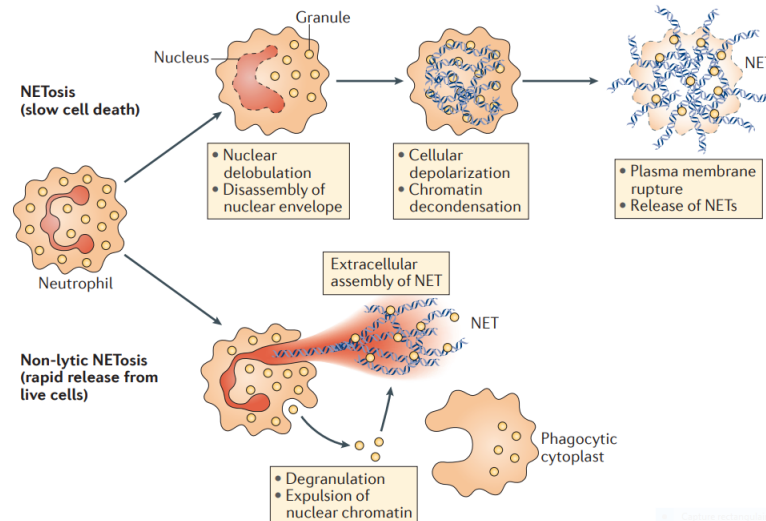


Figure 20: “Suicidal” VS “vital” NETs formation. There are two types of NETs: lytic (also called suicidal) and non-lytic (also called vital) NETs. Lytic NETs are the classical form of NETosis, in which neutrophils release their DNA into the extracellular space after plasma membrane rupture. In contrast, non-lytic or vital NET formation involves a rapid release of DNA of mitochondrial or nuclear origin accompanied by granular proteins, in the absence of plasma membrane breaching and cell death. Besides, the resulting enucleated cytoplast continues its phagocytic activity (Papayannopoulos. 2018).

In the absence of experimental evidence of cell death, the Nomenclature Committee on Cell Death (NCCD) recommends avoiding the use of the term “NETosis”, and discourages the use of alternative terms to describe extracellular DNA extrusion for instance, ETosis (DNA extrusion by eosinophils) (Galluzzi et al. 2018).

2. PANoptosis: A deadly symphony.

Cell death pathways are continuously adapting to the evolution of the exposome including infectious pathogens, allergens and environmental risk factors. Cells display multiple backup RCD programs to ensure the elimination of abnormal cells, when a particular pathway is blocked or suppressed by a pathogen or a danger signal. The key finding that caspase 8 (CASP8) can switch cell death modality from apoptosis to necroptosis depending on its activation status, or even to pyroptosis when caspase-8-dependent apoptosis and MLKL-dependent necroptotic pathways are inhibited, has raised intriguing possibilities of cross-talk and inter-dependency between different types of cell death (Fritsch et al. 2019, Orning & Lien. 2021; (Jiang et al. 2021).

In a murine model of osteomyelitis with the *Pstpip2^{cmo}* mutation, bone inflammation was rescued only when the deletion of NLRP3 or caspase-1 (pyroptotic molecules) was combined to caspase-8/RIPK3 deletion (apoptotic-necroptotic molecules) (Gurung et al. 2016). In the context of *Influenza A* virus (IAV) infection, the combined deletion of RIPK3 and caspase-8 reduced cell death more efficiently than did RIPK3 deletion alone (Kuriakose et al. 2016). These data emphasized the redundancy and the mechanistic overlap between the 3 types of cell death in pathological relevant contexts.

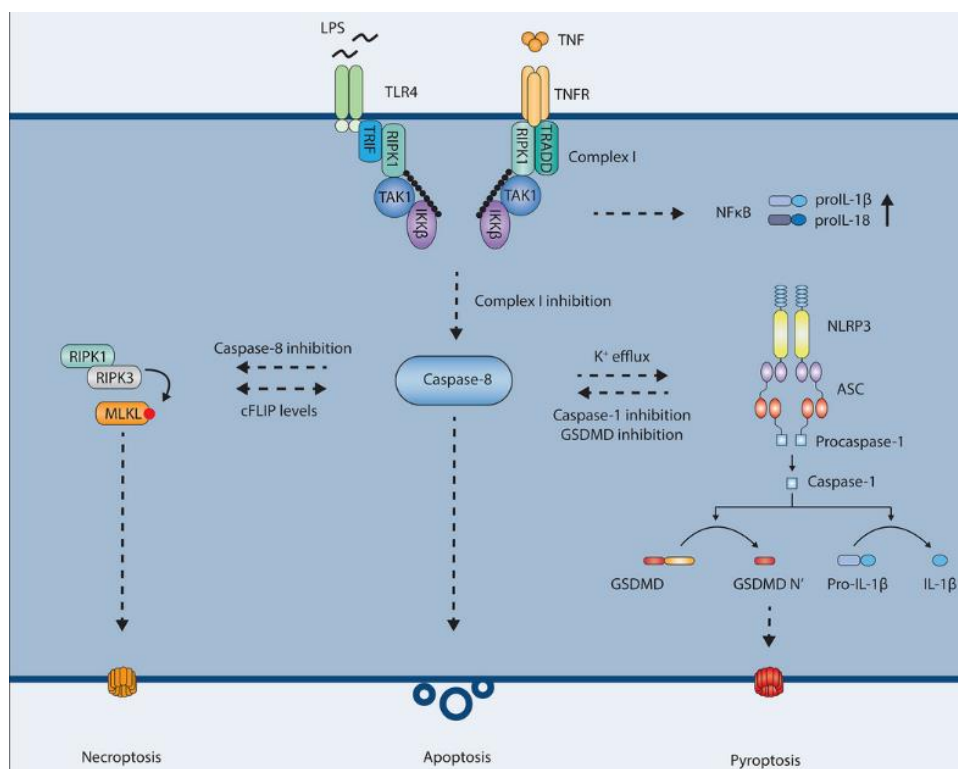


Figure 21: Caspase-8, the core element coordinating apoptosis, necroptosis and pyroptosis. Caspase-8 (CASP-8) plays a versatile role in determining the cell fate. In apoptosis, CASP-8 initiates a cascade of proteolytic events leading to the activation of executioners CASP-3 and -7. In necroptosis, CASP8 is an important negative regulator by limiting RIPK1 activity. In cooperation with cIIP, CASP8 cleaves and inactivates RIPK1 and RIPK3 to limit spontaneous RIPK1-induced necroptosis. Conversely, microbial and mammalian CASP8 inhibitors trigger necroptosis. In pyroptosis, in certain conditions, CASP-8 directly cleaves GSDMD into its active form leading to pore formation, efflux of K⁺ ions that mediates NLRP3 activation and processing and release of IL-1 β and IL-18 further fueling pyroptosis, in this context CASP8 is still able to mediate apoptosis (Orning & Lien. 2021).

2.a) Regulated cell death cross-talks:

2.a.1) Apoptosis and pyroptosis both involve caspase activation, suggesting that they may cross-communicate. Caspase-1 induces apoptosis in GSDMD-deficient cells via the BID-CASP9-CASP3 axis (Tsuchiya et al. 2019). Caspase-8, the initiator of apoptosis, can cleave GSDMD at the same site as caspase-1 to induce pyroptosis (Antonopoulos et al. 2015). In addition, caspase-8 is involved in the activation of NLRP3 inflammasome induced by dsRNA (Kang et al. 2015). In the presence of caspase-1, caspase-8 binds to ASC and acts as a positive regulator of NLRP3 inflammasome and IL-1 production, leading to caspase-1-dependent pyroptosis (Jiang et al. 2021). Other studies have reported a link between other types of inflammasomes (AIM2, NLRC4) and caspase-8 activation or caspase-8 mediated cell death, respectively (Pierini R et al. 2012; Sagulenko V et al. 2013; Lee BL et al. 2018). Additional crosstalks have been observed during chemotherapy. The apoptotic caspase-3 was shown to cleave Gasdermin E (GSDME) driving pyroptosis in several cell types which caused tissue damage and inflammation (Wang Y et al. 2017).

2.a.2) Pyroptosis and necroptosis are both lytic/inflammatory cell death, suggesting an interconnection between them. Reports are indicating that MLKL-mediated necroptosis can act upstream NLRP3 inflammasome to induce pyroptosis. Through its plasma membrane pore formation, MLKL increases potassium efflux in macrophages leading to NLRP3 activation (Gutierrez KD et al. 2017), (Conos SA et al. 2017). Furthermore, another report showed that MLKL-deficient cells failed to trigger ASC oligomerization in response to poly(I:C) and zVAD, two TLR3 ligands known to induce ASC oligomerization and subsequent NLRP3 inflammasome activation (Kang S et al. 2015).

2.a.3) Necroptosis and apoptosis. Genetic studies revealed the existence of a fine balance between *necroptosis* and *apoptosis*. *Caspase-8 (Casp8)* deletion is embryonically lethal, and survival of mice can be rescued by the combined suppression of *Casp8* and *Ripk3* or *Mkl1*, suggesting a role for caspase-8 in avoiding unnecessary necroptosis tissue destruction (Wang & Kanneganti. 2021). Indeed, RIPK1 and RIPK3 are substrates for caspase-8 and several studies have demonstrated that caspase-8 have the ability to destabilize the ripoptosome by forming a heterodimer with cFLIP (Mandal R et al. 2020). Besides, embryonic suppression of RIPK1 leads to both uncontrolled apoptosis and necroptosis, suggesting a role for RIPK1 in the inhibition of apoptosis and necroptosis (Wang & Kanneganti. 2021). Li and collaborators showed that SARS-CoV-2 infection activates a dual mode of cell death (apoptosis /necroptosis) and caspase-8-dependent inflammatory responses that may lead to the lung damage (Li S et al. 2022).

2.a.4) PANoptosome and its pathophysiological implication.

The extensive characterization of cross-talks between each pair of cell death modalities suggests the possible inseparability between apoptosis, pyroptosis and necroptosis. In 2019, professor Kanneganti's team described for the first time a concept of a total cell death called PANoptosis (P, pyroptosis; A, apoptosis; N, necroptosis), a unique innate immune inflammatory PCD, that is mechanistically regulated by a multiprotein PANoptosome complex integrating components from other regulated cell death (Malireddi et al. 2019; Christgen et al. 2020). PANoptosis has been progressively linked to various infectious diseases (Place et al. 2021) as well as sterile inflammation, cancers and cancer therapies (Pan B et al. 2022; Gong L et al. 2023; Sharma et Kanneganti, 2023; Huang J et al. 2022).

The first and best characterized example of PANoptosis was shown in the context of IAV infection, where the suppression of the cytosolic sensor Z-DNA-binding protein 1 (ZBP1) led to complete suppression of IAV-induced PANoptosis, whereas deletion of components from the three RCD individually failed to rescue the cell death (Kuriakose T et al. 2016; Zheng M et al. 2020). Previously known as a nucleic acid innate immune sensor, ZBP1 triggers PANoptosis through the formation of ZBP1-PANoptosome, a platform including NLRP3 inflammasome components, RIPK3, RIPK1 and caspase-8 (Hao Y et al. 2022; Pandian & Kanneganti. 2022).

PANoptosome is composed of PAMPs or DAMPs sensors (ZBP1, AIM2, NLRP3, pyrin), protein adaptors (ASC, FADD) and catalytic effectors (caspase-1, RIPK3, RIPK1, caspase-8) (Zhu et al. 2023). Later, caspase-6 was shown to potentiate the interaction between ZBP1 and RIPK1 promoting ZBP1-PANoptosome (Zheng M et al. 2020). Recently, NLRC4

inflammasome showed a role in PANoptosis upon detection of the T3SS bacterial proteins, leading to the assembly of NAIP-NLRC4 inflammasome and triggers PANoptosis dependently on caspase-1-GSDMD, caspase-8, -3, -7 and MLKL pathways (Sundaram & Kanneganti. 2021). The most up-to-date research in the field identified NLRP12, the cytosolic sensor, as an integral component in driving PANoptosome activation and cell death in a caspase-8/RIPK3-dependent manner. In this context, TLR2/3 activation in response to heme / PAMPs, induces NLRP12, thus opening new therapeutic perspectives in hemolytic disease (Sundaram et al. 2023). Several other potential PANoptosome components remain to be characterized.

Recent studies have shown that the composition of the PANoptosome is dynamic and can vary depending on the diversity of infectious agents or stimuli-mediated alteration of cellular homeostasis (Wang & Kanneganti. 2021; Gullett JM et al. 2022). The formation of this complex relies on homotypic and heterotypic protein interactions between key conserved domains including RIHM, DD, DED, PYD and CARD (Wang & Kanneganti. 2021). The existence of a RIHM domain confers ZBP1 the ability to regulate PANoptosome formation. Indeed, structurally caspase-8 and ZBP1, two main players in the complex have no possibility to directly interact. Instead, it needs to relay on RIPK1 for recruitment through FADD to link the necrotic and apoptotic initiating molecules (Zhu et al. 2023). Additionally, heterotypic interaction has been revealed between the DED of caspase-8 and PYD of ASC linking the apoptotic and pyroptotic initiating molecules (Vajjhala et al. 2015).

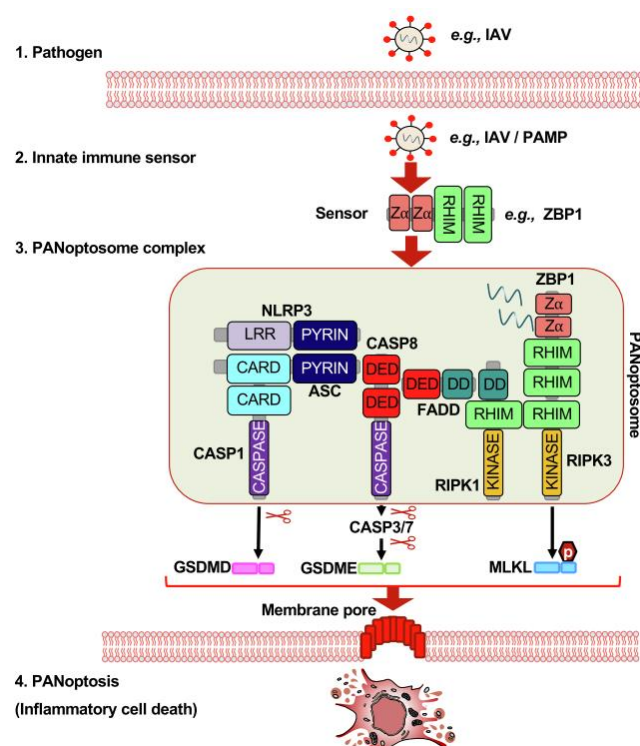


Figure 22: A prototypical example of PANoptosome formation (Case of ZBP1-PANoptosome triggered by IAV infection). PANoptosome composition can vary depending on the signaling trigger. Structurally it is composed of three parts: PAMPs or DAMPs sensors, protein adaptors and catalytic effectors the assembly of these components, relies on homotypic and heterotypic interactions between key conserved domains including RHIM, DD, DED, PYD and CARD leading to lytic cell death. (Wang & Kanneganti. 2021).

To date ZBP1-PANoptosome has been identified in the context of infection with ssRNA virus IAV (Kuriakose T et al. 2016), murine hepatitis virus and SARS-CoV-2 (Karki R et al. 2022), *C albicans* and *A. fumigatus* (Banoth B et al. 2020). Furthermore, this complex has also been implicated in cancer treatment, in a context where ADAR1 sequesters ZBP1 to prevent the ZBP1-RIPK3 interaction and PANoptosis, thereby promoting tumorigenesis. Treatment with nuclear transport inhibitors (KPT-330) blocks ADAR in the nucleus. In combination with IFN, this treatment supports ZBP1-PANoptosome formation and limits tumorigenesis (Karki R et al. 2021).

AIM2 can detect cytosolic dsDNA from invading pathogens or of self-origin. Recently, Lee et al. from Kanneganti's lab, reported a new role for AIM2 in the regulation of the innate immune sensors pyrin and ZBP1 to drive PANoptosis during *Herpes simplex virus 1* (HSV1) and *Francisella novicida* infection. In this context, IFN- β previously found to promote the expression of pyrin and ZBP1 is induced by the AIM2/ASC/CASP1 pathway in bone marrow-derived macrophages (BMDM) to regulate ZBP1 and pyrin which synergize to drive AIM2-mediated multi-protein complex, termed "AIM2-PANoptosome" comprising AIM2, pyrin, ZBP1 ASC, caspase-1, caspase-8, RIPK3, RIPK1 and FADD (Lee S et al. 2021). The same group reported the induction of a RIPK1-PANoptosome which occurs physiologically during *Yersinia pestis* infection through TAK1 inhibition via its YopJ effector in macrophages. Additionally, spontaneous PANoptosis can be triggered by genetic ablation or by pharmacological inhibition of TAK1 (Malireddi et al. 2018; Malireddi et al. 2020).

Additional sensors and interactors are currently under investigation such as TRIF, which can mediate cell death through RHIM-RHIM interaction with RIPK3 following TLR3 activation (Kaiser et al. 2013). RIG-I as another potential candidate, as during Sendai virus (SeV) infection, RIG-I formed a complex with caspase-8 and RIPK1, two major PANoptosis players. This interaction is proposed to be mediated via CARD-CARD interaction (Rajput et al. 2011).

Bioinformatics analysis using the STRING database has supported experimental evidence for PANoptosome assembly. The results showed the existence of several physical crossed interactions between genes from apoptosis, pyroptosis and necroptosis, where caspase-8 appears to be the focal point of these three pathways (Szkларczyk et al. 2019), (Wang & Kanneganti. 2021), (Zhu P et al.2023). This provides unquestionable evidence of pathways cross-talks.

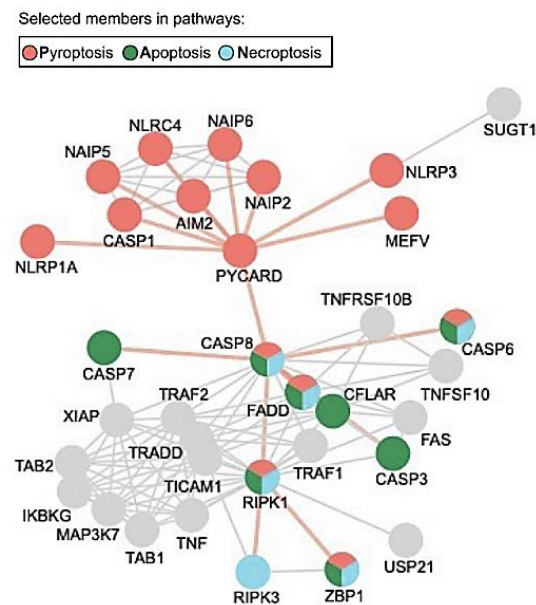


Figure 23: Interactome of molecules involved in apoptosis, pyroptosis and necroptosis (Wang & Kanneganti. 2021).

Given the significance of its implications in physiological and pathophysiological processes, PANoptosis needs to be tightly regulated. It was shown that IRF1 deficiency in IAV-infected macrophages reduces ZBP1, caspase-1, -3, -8, NLRP3 inflammasome and MLKL (Kuriakose T et al. 2018). IRF1 previously known for its role in cell death, acts as an upstream regulator of PANoptosis through transcriptional regulation of ZBP1 (Gullett JM et al. 2022). During IAV-induced PANoptosis, IFN-I increases IRF1 expression, which in turn upregulates ZBP1 transcription (Zhu et al. 2023). Moreover, another study has shown a role for IRF1 in positive regulation of AIM2 inflammasome during *Francisella* infection (Man et al. 2015), suggesting a possible role for IRF1 in the regulation of AIM2-PANoptosome.

Post-translational modification through ubiquitination of ZBP1, as it was detected after IAV infection, can affect PANoptosome assembly (Zhu et al. 2023). Another strategy of negative regulation described in the context of tumorigenesis is ADAR1 sequestration of ZBP1. It was

found that ADAR1 can compete with RIPK3 for the binding of ZBP1, thus affecting the complex stability (Karki R et al. 2021).

3. Role of lytic cell death in the regulation of innate immune inflammation: Self-DNA, the maestro directing the symphony.

What makes a specific cell death become immunogenic/inflammatory ? Regardless of the type of cell death process, dying cells will transmit messages through active secretion of some factors or passive release of the cellular content following the loss of membrane integrity to alert the immune system.

It is well admitted that apoptosis the physiological form of cell death is “immunologically silent” occurring without the release of DAMPs. Apoptotic cells attract professional efferocytes (mostly macrophages) by releasing soluble “find me” signals such as lysophospholipids and nucleotides and they display phosphatylserine (PtdSer) on their outer plasma membrane as an “eat me” signal. Efferocytosis of apoptotic cells leads to an anti-inflammatory outcome with the release of TGF- β and IL-10 to promote resolution of inflammation and tissue repair (Lemke G. 2019). In contrast, following a release of DAMPs, a strong immune response is triggered by necrosis to control infection or tissue damage. The recent focus on cell death has allowed us to realize that this model is an oversimplification of the complex communication between dead cells and efferocytes.

In fact, several factors with variable characteristics must be taken into consideration in the equation of cell death to be able to predict the outcome. In a recent review, Rothlin et al proposed a novel theory with three major’s factors: (1) The identity of the efferocyte; (2) The information code content of the dying cells and their number; (3) The microenvironment in which death occurs, which can largely dictate efferocyte behavior to specify a single output (Rothlin et al. 2021). A study demonstrated that dendritic cells (DC) engulfment of *Citrobacter rodentium*-infected apoptotic cells induces both IL-6 and TGF- β , directing the response toward Th17 polarization, likely via TLR4 recognition of LPS contained in the cell, while DC engulfment of non-infected apoptotic cells resulted in TGF- β release only promoting Treg cell induction (Torchinsky et al. 2009).

Caspase activation during apoptosis induces the cleavage and inactivation of innate immune proteins such as cGAS, IRF3, and MAVS to help maintaining the immune-silent status during physiological processes (Ning X et al 2019). However, this status can be broken in certain cases, such as during severe fever with *thrombocytopenia syndrome virus* (SFTSV) infection which stimulates oxidized mtDNA release from the mitochondria in a BAX/BAK manner that has been shown to be recognized by NLRP3 leading to IL-1 β secretion (Li S et al.

2020). Giampazolias et al. showed that pharmacological caspase inhibition or APAF1 deletion activates NFκB dependent inflammation after the release of SMAC and NIK activation but also the cGAS-STING pathway via mtDNA release both *in vitro* and *in vivo* (Giampazolias E et al. 2017). SMAC release via the BAX/BAK pores can also trigger NLRP3 inflammasome formation via IAP depletion leading to IL-1β secretion in a Gasdermin independent manner (Vince JE et al. 2018).

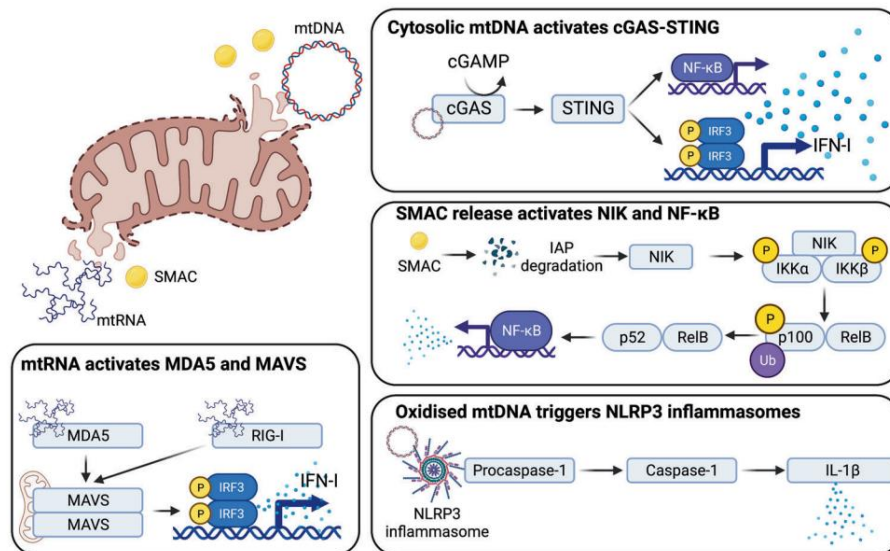


Figure 24: Mitochondrial permeabilization as an initiator of inflammation. BAX/BAK-dependent MOMP has the potential to trigger an immune response under specific circumstances. mtDNA can leak from mitochondria and activate cytosolic immune sensors such as the cGAS-STING pathway leading to type I interferon production and NFκB activation. NFκB can also be activated after SMAC release and its downstream IAP degradation and NIK activation. Infection with certain viruses drives oxidized mtDNA release which can be detected by NLRP3 inflammasome. In pathological conditions where mitochondrial RNA helicase SUV3 and polynucleotide phosphorylase PNPase are inactivated, mtRNA accumulate in the cytoplasm and activate RNA sensors such as RIG-I and MDA5 triggering a type I interferon response (Bock & Riley. 2023).

The timing and efficiency of efferocytosis also instruct the immune response to dead cells. When efferocytosis is overwhelmed, after 15 hours apoptotic cells were shown to release equivalent cellular proteins into the extracellular space as with lytic cell death (Tanzer et al. 2020) by undergoing secondary necrosis (Wang & Labzin. 2023) with release of DAMPs such as HMGB1 and S100 proteins with a strong inflammatory potential (Bertheloot & Latz. 2017).

The removal of necrotic cell death by efferocytes is less efficient than the removal of apoptotic cell death (Krysko DV et al. 2006; Wang Q et al. 2013). One possible explanation is that HMGB1 competes with PtdSer the “eat me” signal for receptor binding on macrophages

and also by sequestering the integrin $\alpha\beta3$ at the surface of phagocytes thus inhibiting efferocytosis in favor of the release of DAMPs and the initiation of inflammatory responses (Liu G et al. 2008; Friggeri A et al. 2010).

To date, there is substantial evidence that activation of programmed necrosis including pyroptosis and necroptosis drives inflammation. On the one hand, activation of pyroptotic pathways is inherently inflammatory by definition. Inflammasome activation drives GSDMD-dependent IL-1 β and IL-18 release. Besides, GSDMD-dependent membrane rupture promotes the release of large DAMPs complexes such as lactate dehydrogenase (LDH) complex and ASC specks. Extracellular ASC specks and smaller soluble metabolic DAMPS such as ATP and uric acid can activate NLRP3 inflammasome assembly in the surrounding cells, thus extending inflammation.

On the other hand, experimental observation that inflammatory process can be inhibited by blocking the function of RIPK3 has prompted researchers to question the role of necroptotic pathway in the fueling of inflammation. Indeed, several reports confirmed that prior to cell demise by pyroptosis, MLKL formed small membrane pores sufficient to allow potassium ions flux. This led to NLRP3 inflammasome activation and the downstream IL-1 β and IL-18 secretion (Conos SA et al. 2017).

Necroptotic pathway potentiates the activation of NF κ B and p38 MAP kinase on a MLKL/RIPK1/RIPK3 fashion (Zhu K et al. 2018). Phosphorylated MLKL is exported from the dying cells in exosomes and can possibly act on other cells to activate NLRP3 inflammasome and inflammation (Yoon S et al. 2017). Furthermore, a study showed that activated MLKL only forms pores with highly phosphorylated inositol phosphates, which may explain why it can be exported in some cases (Dovey et al. 2018). These findings suggest a distinct role for MLKL in inducing inflammation prior to cell demise.

3.a) The Role played by DAMPs: the ghost back to hunting you!

Besides the inflammation that occurs as a result of distinct regulated cell death pathways before cell demise, the release of DAMPs is fundamental to drive innate inflammation following cell death. Among danger signals released from dead cells, we can distinguish two types of DAMPs: (1) constitutive DAMPs (cDAMPs) and inducible DAMPs (iDAMPs).

cDAMPs are present in healthy cells at steady state, but have the ability to elicit an immune response. cDAMPs such as HMGB1, S100 proteins, nucleic acids (including self dsDNA, mtDNA and mtRNA), calreticulin, F-actin and extracellular adenosine triphosphate (eATP) can

be released in the context of accidental necrosis. Conversely, iDAMPs are induced in infected, transformed or damaged cells. They involve IL-1 family members, NF- κ B-induced cytokines (TNF, IL-6) and type I IFN (α , β). Extensive classification of DAMPs was detailed by Walter Gottlieb Land (Table 2) (Land WG. 2018, 2020).

The process of DAMPs sensing is central to detect a perturbation of homeostasis (whether its microbial infection, transformed cell or sterile damaged tissue). Danger signals are sensed by evolutionarily conserved receptors referred to as pattern recognition receptors (PRRs). PRRs highly expressed by immune cells and any other cell susceptible to be infected or transformed to sense DAMPs and/or PAMPs and evoke an innate immune defense strategy (Gong T et al. 2020; Li D, Wu M. 2021). PRRs classically encompass Toll-like receptors (TLRs), NOD-like receptors, retinoic acid inducible gene I-like receptors, C-types lectin receptors, and cytosolic nucleic acids sensors. Non classical PRRs were also identified such as the soluble pattern recognition Pentraxin3 (PTX3) which facilitating pathogen recognition by myeloid cells or the G-protein coupled receptors and ions channels (Porte R et al. 2019; Gong T et al. 2020).

PRRs engagement following DAMPs detection ultimately converge on the production of pro-inflammatory cytokines (TNF, IL-1, IL-6) and type I IFNs through NF- κ B and IRF3 to initiate immune route, only to restore homeostasis, at least at the beginning (Li D, Wu M. 2021).

3.a.1) Focus on DNA as a driver of inflammation and innate immune sensors activation.

Necrosis cell death, including pyroptosis, necroptosis or NETosis have in common the inevitable release of self dsDNA after nuclear and plasma membrane breaching. According to Land WG's classification, nuclear and mitochondrial DNA is classified as an intrinsic DAMP, which can be modified upon injury leading to DNA breaks (Land WG. 2018, 2020).

DNA exert distinct functions depending on its cellular location. When compartmentalized in the nucleus and mitochondria, it carries genetic information. Once in the cytoplasm or outside of the cell, immunity and inflammation become the principal duty of DNA (Pisetsky DS et al. 2012; Singh J et al. 2023). DNases such as the extracellular DNase I, endosomal DNase II or the cytoplasmic TREX1, mitigate this effect by digesting DNA below the level required to activate nucleic acid sensing mechanisms (Paludan SR et al.

Category I: Endogenous DAMPs: Constitutively Expressed Native Molecules (Cat. I DAMPs)	
Class A: DAMPs passively released from Necrotic Cells	Subclass 1: DAMPs except for indirectly NLRP3-activating molecules Subclass 2: DAMPs indirectly activating the NLRP3 inflammasome
Class B: DAMPs exposed on the Cell Surface	Subclass 1: Phagocytosis-facilitating molecules (“chaperones”) Subclass 2: MHC class I chain-related molecules
Category II: Endogenous DAMPs: Constitutively Expressed, Injury-Modified Molecules (Cat. II DAMPs)	
Class A: DAMPs released from the Extracellular Matrix	Subclass 1: Proteoglycans Subclass 2: Glycosaminoglycans Subclass 3: Glycoproteins
Class B: Cell-extrinsic modified DAMPs	Subclass 1: Oxidation-specific epitopes (membrane-bound) Subclass 2: Distinct structural sugar patterns (membrane-bound) Subclass 3: Cell-extrinsic dyshomeostasis-associated molecular patterns Subclass 4: Plasma-derived modified soluble molecules
Class C: Cell-intrinsic modified DAMPs	Subclass 1: Nuclear DNA breaks Subclass 2: Cytosolic DNA (nuclear and mitochondrial) Subclass 3: Cytosolic RNA (accumulated, processed) Subclass 4: Cell-intrinsic dyshomeostasis-associated molecular patterns Subclass 5: Abnormally accumulating metabolic molecules
Category III: Endogenous DAMPs: Inducible DAMPs (Cat. III DAMPs)	
Class A: Native Molecules acting as Inducible DAMPs	Subclass 1: Actively secreted molecules (also passively released) Subclass 2: Cytokines secreted by (DAMP-) activated cells Subclass 3: Full-length interleukin-1 family members Subclass 4: Complement-related and vascular molecules Subclass 5: Galectins Subclass 6: NF-κB signaling in cross-priming Subclass 7: Eicosanoids Subclass 8: Vasoactive Catecholamines, Angiotensin II, Endothelin-1
Class B: Modified Molecules acting as Inducible DAMPs	Subclass 1: Processed interleukin-1 family members Subclass 2: Processed HMGB1 secreted by activated immune cells Subclass 3: Anaphylatoxins C3a and C5a Subclass 4: “Prion-like” polymers (“Specks”) Subclass 5: Lysophospholipids Subclass 6: Peroxiredoxins Subclass 7: Wnt Proteins
Class C: Suppressing/inhibiting DAMPs (“SAMPs”)	Subclass 1: Prostaglandin E2 Subclass 2: Adenosine (extracellular adenosine, cyclic AMP) Subclass 3: Annexin A1 Subclass 4: Specialized proresolving mediators Subclass 5: Lysophosphatidylserine, Lysophosphatidylethanolamine Subclass 6: Angiotensin-(1-7)
Category IV: Exogenous DAMPs (Cat. IV DAMPs)	
Class A: Exogenous DAMPs indirectly sensed by NLRP3	Subclass 1: Aluminium salt Subclass 2: Asbestos fibres Subclass 3: Silica particles Subclass 4: Air pollution—particulate matter
Class B: Exogenous DAMPs sensed by Nociceptors	Subclass 1: Noxious stimuli involved in thermosensation Subclass 2: Non-reactive compounds Subclass 3: Reactive electrophilic compounds Subclass 4: Vanilloids- capsaicin
Class C: Allergens	Subclass 1: Metal Allergens

Table 04: Walter Gottlieb Land’s classification of DAMPs (Land WG. 2018, 2020).

2019). However, when DNA is released in large amounts following tissue injury and cell death or infections, these systems are overwhelmed and innate immune sensors initiate a defense strategy which converge to type I and type II IFN production and pro-inflammatory cytokines and can result in inflammation-related diseases (Roh JS et al. 2018; Royce GH et al. 2019; Fousert E et al. 2020).

Among the nucleic acids sensors, DNA is detected by TLR9 in endosomes, considered to be the first identified DNA-sensing PRR (Hemmi H et al. 2000), ZBP1 (DAI) (Takaoka A et al. 2007), AIM2 (Hornung V et al. 2009), IFI16 (Unterholzner et al. 2010), DDX41, an RNA helicase protein also known to detect cytosolic dsDNA promoting type I IFN (Zhang Z et al. 2011) and cGAS (Sun et al. 2013) one of the best characterized DNA sensors (Ablasser & Chen. 2019). Meanwhile, Barber's lab had shed light on the role of an endoplasmic reticulum adaptor, called "stimulator of interferon genes" STING in innate immune signaling and pointed its requirement for type I IFN production in response to DNA (Ishikawa & Barber. 2008) (Ishikawa & Barber. 2009). Later, STING was shown to function downstream of cytosolic nucleic acid sensors (Ablasser et al. 2013; Gao et al. 2013).

4. The cGAS-STING pathway

When cGAS interacts with cytoplasmic dsDNA, it forms a 2:2 complex in which two cGAS molecules bind to two dsDNA molecules. This combination represents the minimal active enzymatic unit (Li X et al. 2013). cGAS is agnostic to the dsDNA origin, but depends on the length of the DNA (Sun et al. 2013). Longer dsDNA (> 45pb) promotes more efficiently the enzymatic activity of cGAS than short dsDNA (Du & Chen. 2018). Active cGAS catalyzes ATP and GTP into 2'3'-cGAMP (Diner et al. 2013; Ablasser et al. 2013). This endogenous messenger binds to the homodimer adaptor protein STING, localized in the endoplasmic reticulum region (ER). Upon activation, STING undergoes conformational rearrangement, including the bringing of the two wings together with the ligand and the formation of a four anti-parallel β -sheet strands on top of the ligand binding domain, resulting in closed conformation. This new conformation drives a 180° rotation of the ligand-binding domain, eliciting the formation of oligomers through side-by-side assembling of STING dimers. STING oligomers traffics from the ER to the Golgi, in the perinuclear region through the E/R-Golgi intermediate compartment (ERGIC). This translocation is supported by COP-II complex and ARF GTPases. Once in the Golgi region, STING is palmitoylated at residue Cys88/91, a necessary step for its oligomerization. STING oligomers serves as a platform for the recruitment of TBK1, which then proceeds to phosphorylate STING. The C-terminal region of

phosphorylated-STING serves as a docking zone for the recruitment of IRF3 which is also phosphorylated and activated by TBK1. Once activated, the transcription factor IRF3, dimerizes and translocates to the nucleus to activate type I IFN genes. Type I IFNs act through their heterodimeric receptor (IFNAR1-IFNAR2) on an autocrine and paracrine manner to trigger the JAK/STAT1/STAT2 axis and induce the transcription of several interferon-stimulated genes (ISGs).

In the other hand, STING controls the transcription of proinflammatory cytokines through the activation of NFκB pathway in a TRAF6-TBK1 dependent manner in response to dsDNA. Making the downstream kinase TBK1 controlling both dsDNA-mediated IRF3 and NF-κB activation.

Besides IRF3 and NFκB, STING pathway is implicated in the activation of the transcription factor STAT6. STAT6 interacts directly with STING and is subsequently phosphorylated and activated by TBK1, which drives its dimerization, nuclear translocation and subsequent activation (Chen H et al. 2011).

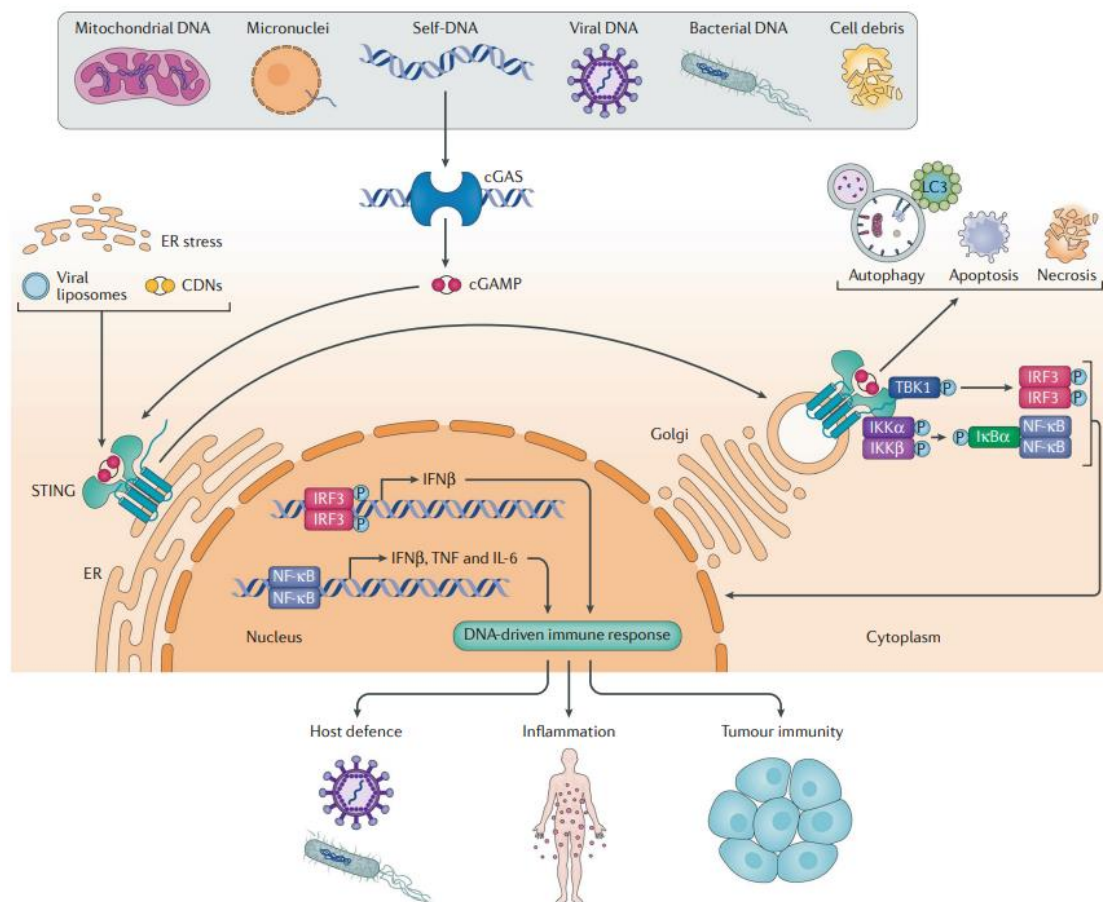


Figure 25: Mechanism of cytosolic DNA sensing by the cGAS-STING pathway. The activation of the cGAS-STING pathway has been implicated in a variety of human and animal diseases including anti-microbial defense, inflammation and auto-inflammation as well as tumor immunity. cGAS acts as an innate immune sensor, recognizing various cytosolic dsDNA forms, including pathogen-derived and self-DNA. Upon its activation by DNA, cGAS catalyzes cGAMP synthesis. In turn, cGAMP activates STING at the ER membrane, leading to STING's translocation to Golgi compartments. Several bacterial CDNs, viral liposomes or synthetic agonists have also the ability to activate STING. Phosphorylated STING recruits TBK1 and I κ B kinase (IKK) for the subsequent phosphorylation of IRF3 and NF- κ B respectively. Phosphorylated IRF3 and NF- κ B translocate to the nucleus to activate transcription of type I IFN (α/β) and pro-inflammatory cytokines (e.g. IL-6, TNF) respectively. Secretion of type I IFNs can stimulate the expression of ISGs through the JAK/STAT signaling pathways, creating a positive feedback loop. Besides its role in inflammation, STING activation can be involved in autophagy as well as several cell death pathways (Motwani et al. 2019)

The structure of the cGAS protein is crucial for its function and enzymatic activity. Studies have shown that the three-dimensional structure of cGAS can vary between species, which can lead to differences in DNA recognition and cGAMP production. The human cGAS (hcGAS) has K187 and L195 mutations compared to the mouse orthologue, which increases its stringency for longer DNA sequences (>45pb). Furthermore, hcGAS is less efficient in cGAMP production than the mouse one (Zhou W et al. 2018; Briard et al. 2020). Besides dsDNA, cGAS can be activated following DNA: RNA hybrids detection, leading to downstream IFN production (Mankan et al. 2014). Other species like ssDNA or dsRNA can also bind to cGAS but do not lead to rearrangement of the catalytic pocket and production of cGAMP (Ablasser et al. 2019).

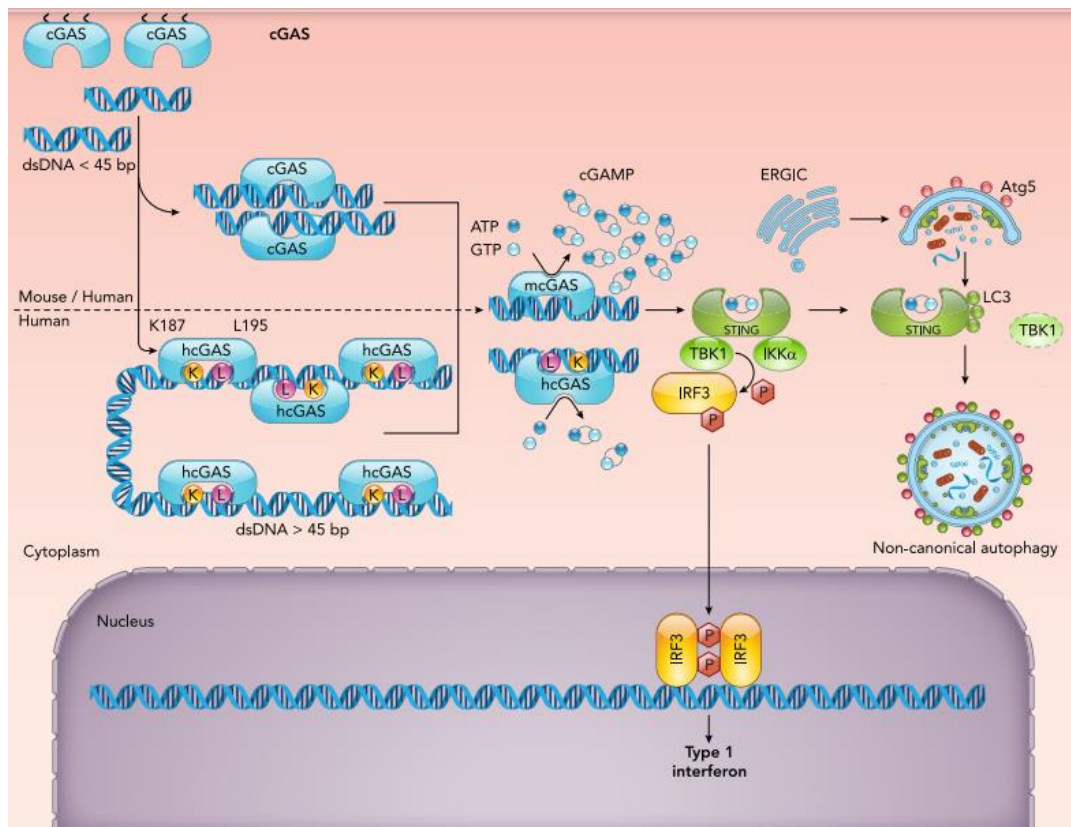


Figure 26: Human cGAS vs murine cGAS in DNA detection and cGAMP production. cGAS is retained near the plasma membrane via its NH₂-terminal-phosphoinositide-binding domain, to facilitate the detection of viral DNA entry and limits its reaction with self-DNA. Upon DNA recognition 2 molecules of cGAS binds 2 dsDNA strands driving catalytic modification in cGAS to permit the synthesis of cGAMP from ATP and GTP. Two mutations in human cGAS (K187 / L195) increase its affinity for longer DNA molecules. The hcGAS has reduced catalytic activity for cGAMP production compared to the mcGAS, which has the ability to bind smaller DNA molecules with higher catalytic activity (Briard et al. 2020).

cGAMP can be transmitted from a “donor cell” to a “recipient cell” for a rapid propagation of innate responses in neighboring cells. When it escapes the proteolytic action of ecto-nucleotide pyrophosphatase phosphodiesterase 1 (ENPP1), a negative regulator of this immune-transmission mechanism (Kato et al. 2018; Carozza et al. 2022), cGAMP can be picked from the extracellular space through various channels to activate intra-cellular STING.

Solute carrier family 19 member 1 (SLC19A1), was the first identified cGAMP importer (Ritchie et al. 2019; Luteijn et al. 2019; Xie et al. 2023). The purinergic P2X7 receptor (P2X7R) was revealed later as another cGAMP importer (Zhou Y et al. 2020). Indeed, when a tissue is severely damaged, a high release of ATP and cGAMP can occur to alert the immune system. Increased levels of extracellular ATP induce the opening of P2X7R channels, which could allow small molecules such as cGAMP, to pass into the cytoplasm (Savio et al. 2018). In

addition, volume-controlled anion channel (VRAC) through its subunit leucine-rich repeat-containing protein 8 (LRRC8) can facilitate the export from the donor cell and also the import of cGAMP in the recipient cell (Zhou C et al. 2020). Gap-junctions between two adjacent cells can be used by cGAMP as a direct cell-cell passage (Ablasser et al. 2013). This strategy protects cGAMP from the action of ENPP1 in the extracellular space.

Recently, a surprising STING localization was described. Li et al. identified an alternatively spliced STING isoform in mouse splenic cells, which lacks one transmembrane domain with an intracytoplasmic N-terminus and a C-terminus outside the cell. This isoform resides in the cell surface, giving it the ability to detect extracellular cGAMP. The pmSTING (plasma membrane STING) isoform triggers the same signaling pathway as the canonical STING, with dimerization and subsequent activation of the TBK1/IRF3/IFN axis. The same isoform was identified in humans (Li et al. 2022). Alternatively, spliced isoforms that have been identified in the cGAS-STING signaling pathway are extensively reviewed here (Liang et al. 2021).

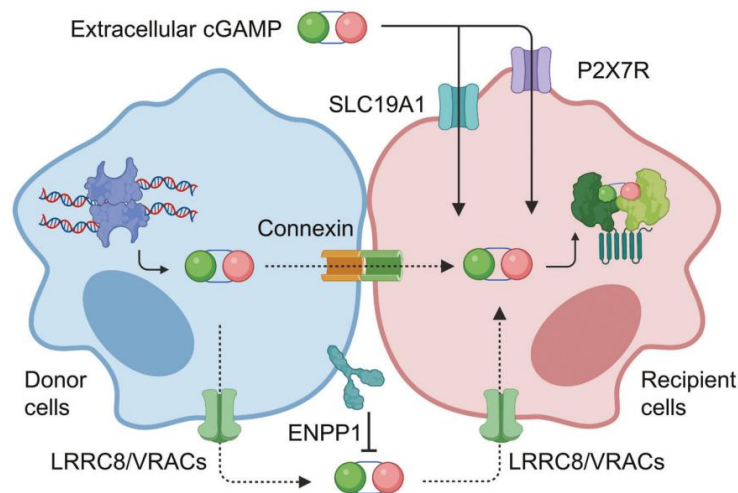


Figure 27: Propagation of innate responses via the inter-cellular transmission of cGAMP.

Endogenous cGAMP production and STING activation is not the only option to initiate innate responses. cGAMP can be released in the extracellular space and be transferred to neighboring cells via transporters, such as LRRRC8/VRAC, P2X7R and SLC19A1. cGAMP can also directly be transmitted to adjacent cells via gap-junctions. cGAMP can be negatively regulated by ENPP1 in the extracellular space (Kim et al. 2023).

cGAS is not strictly necessary for STING activation. Indeed, STING can be directly activated by bacterial cyclic dinucleotides, such as the cyclic di-GMP, cyclic di-AMP and 3'3'-cGAMP, making STING a standalone PRR (Burdette et al. 2011; Moretti et al. 2017). Yet, bacterial dinucleotides have lower affinity for STING than the endogenous 2'3'-cGAMP

(Zhang X et al. 2013). Other DNA sensors can activate STING independently of cGAS such as DDX41 (Cheng Y et al. 2017); IFI16 was shown to detect DNA from different origins driving IFI3 and NF κ B activation (Morrone et al. 2014), and appears to function in this context and cell-specific manner. Indeed, during viral infection IFI16 potentiates cGAS activity leading to increased cGAMP levels and drives STING dimerization and phosphorylation in response to DNA (Jønsson et al. 2017). While in keratinocytes, IFI16 was shown to cooperate with cGAS to activate STING without affecting cGAMP levels (Almine et al. 2017). In sterile conditions, IFI16 was shown to trigger a non-canonical STING pathway by activating the TNF receptor-associated factor 6 (TRAF6) that induces ubiquitination and the subsequent activation of STING (Dunphy et al. 2018).

4.a) Role of cGAS-STING pathway in DNA damage and regulated cell death

When a cell accumulates DNA damage but remains viable and undergoes mitosis, DNA can leak from the nucleus, forming cytoplasmic micronuclei that activate the cGAS-STING pathway (Xu B et al. 2011; Mackenzie et al. 2017; Hintzsche et al. 2017). Various sources have documented that cGAS colocalizes with γ H2AX, a marker of DNA damage enriched in the micronuclei (Yang et al. 2017; Mackenzie et al. 2017). In the best-case scenario, the detection of these accumulated damages by cGAS and the downstream signaling strength triggered by STING lead to the demise of the cell to avoid cellular transformation (Gulen et al. 2017; Cerboni et al. 2017; Brault et al. 2018). Moreover, it is interesting to note that cGAS sensing of double-stranded breaks (DSB) in the nucleus, revealed by γ H2AX/cGAS colocalization results in suppression of DNA repair mechanisms leading to more DNA damage (Liu H et al. 2018).

Cross-talks between the cGAS-STING signaling and regulated cell death (RCD) pathways including apoptosis, pyroptosis and necroptosis have been extensively described (Murthy et al. 2020), conferring an anti-proliferative function to DNA-depend innate immune response. Indeed, myeloid (macrophages) and lymphoid (T/B cells) cells were shown to die following STING activation (Tang et al. 2016; Gulen et al. 2017; Gaidt et al. 2017; Larkin et al. 2017; Kuhl N et al. 2023).

4.a.1) STING and apoptosis

Prior to STING discovery, DMXAA (5,6-dimethylxanthenone-4-acetic acid), a tumor vascular-disrupting agent was recognized for its pro-apoptotic function both *in vivo* and *in vitro* (Ching et al. 2002; Ching et al. 2004). Later, DMXAA was described as an efficient mouse

STING agonist, and this raised question about STING potential role in apoptosis and cell death (Conlon et al. 2013).

Phosphorylated IRF3 can interact with BAX and BAK and drive apoptosis through the mitochondrial pathway downstream of STING. This pathway is also known as the RLR-induced IRF3-mediated pathway of apoptosis (RIPA) (Chattopadhyay et al. 2010; Sze A et al. 2013; Petrasek et al. 2013). Type I IFN production following STING activation induces the expression of TRAIL, which triggers apoptosis through the engagement of death receptors and plays a detrimental role during *Francisella novicida* infection (Zhu Q et al. 2018). Lohard and collaborators, revealed a mechanism by which the activation of STING induces pro-apoptotic secretory phenotype in primary breast tumor cells treated with paclitaxel, an antimitotic agent. This activation drives the production of type I IFN and TNF α , which induce NOXA expression in neighboring cells. These cells become highly sensitive to inhibition of BCL-XL. Moreover, combined with of BH3 mimetics, these apoptotic effects are potentiated (Lohard et al. 2020).

4.a.2) STING and necroptosis

A few years ago, very little was known about the importance of the STING signaling pathway in necroptosis. Early observations indicated that deficiency in IFNAR1 confers resistance to necroptosis during *Salmonella typhimurium* infection *in vivo* in mice (Robinson et al. 2012). Sarhan and al. confirmed this observation showing that natural IFN levels regulated by constitutive low DNA levels sensed via cGAS/STING, play a crucial role in maintaining MLKL expression, predisposing cell to early necroptosis (Sarhan and al. 2019). Simultaneously, Brault et al. revealed that DNA sensing through cGAS-STING activates RIPK3. Extending previous findings, they showed that type I IFN is necessary but not sufficient and that the synergistic signaling of TNF/IFN is responsible for STING-dependent necroptosis in macrophages (Brault et al. 2018). On the other hand, STING priming *in vivo* with high doses of DMXAA had lethal effect. Mice were in part rescued by RIPK3 and MLKL deficiency, providing strong evidence that necroptosis is one of the end-products of STING signaling (Brault et al. 2018).

4.a.3) STING and pyroptosis

The precise mechanism by which STING directly triggers pyroptosis is still to determine. Yet, several studies converge towards the hypothesis that STING enhances pyroptosis by acting on its components. Gaidt et al. demonstrated that during DNA-dependent stress response, STING induces K⁺ efflux to support the lysosomal cell death pathway. K⁺ ions can in turn activate NLRP3 inflammasome (Gaidt et al. 2017). Another study demonstrated that

Chlamydia trachomatis infections in macrophages lead to a GAS-STING-dependent IFN response, which regulates both the canonical inflammasome (caspase-1) and noncanonical inflammasome (caspase-11), resulting in increased IL-1 β production that precedes pyroptotic cell death (Webster et al. 2017). In addition, they showed that inactivated *C. trachomatis* led to a reduced type I IFN response, did not activate inflammasomes and failed to induce IL-1 β and pyroptosis. Interestingly, they demonstrated that exogenous supply of c-di-AMP, rescued inflammasome activation to inactivated bacteria in a STING dependent fashion, thus providing strong evidence that bacterial metabolites sensing by STING is responsible of inflammasome activation and the subsequent pyroptosis, linking indirectly STING to pyroptosis (Webster et al. 2017).

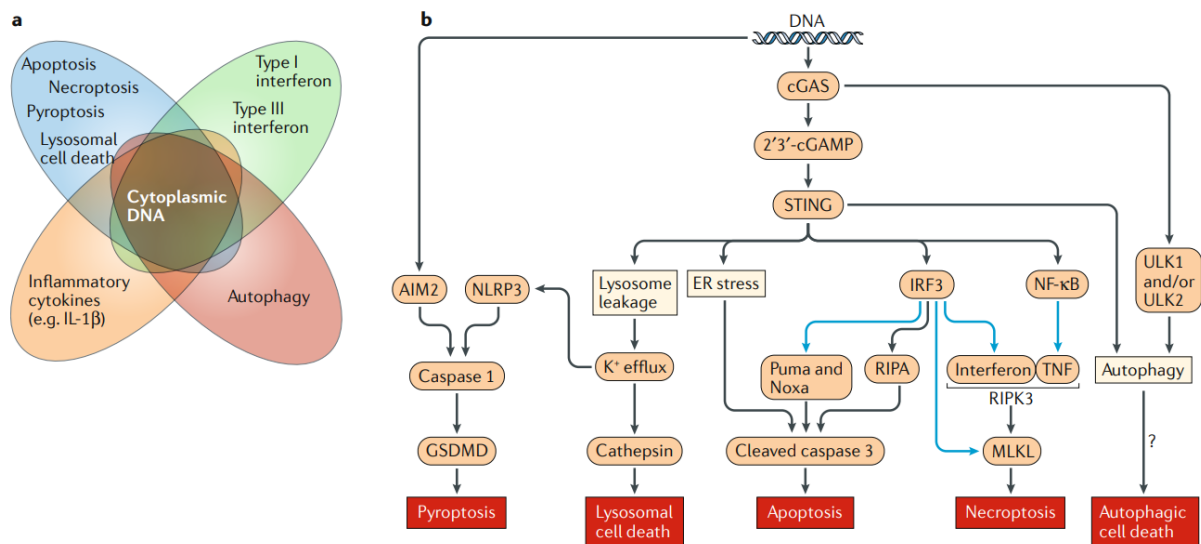


Figure 28: DNA-Dependent Regulated Cell Death Pathways. Outside the nucleus, DNA has many regulatory functions of the innate immune system. DNA is involved in induction of type I IFN, inflammatory cytokines (e.g. IL-1 β , IL-6 and TNF), autophagy and regulation of several regulated cell death pathway including apoptosis, necroptosis and pyroptosis: DNA-dependent GAS-STING activation regulates necroptosis via synergetic effect of IFN and TNF, apoptosis through upregulation of pro-apoptotic protein such as NOXA, and pyroptosis through increasing pyroptosis components such as NLRP3 inflammasome (Paludan et al. 2019).

4.b) cGAS-STING-associated lung diseases

To date, the activation of the DNA-dependent STING pathway has been implicated in a broad spectrum of human and animal diseases, despite their divergent etiologies. Imbalance in the STING pathway was extensively described in tumors such as glioma where STING is epigenetically silenced in a developmentally conserved way (Low et al. 2022), or even during pancreatic tumorigenesis where ferroptotic damage (an iron-dependent cell death) regulates

STING to support tumorigenesis (Dai et al. 2020). Other pathological conditions including neurological disorders, cardiovascular disorders, metabolic diseases, senescence and aging, autoimmune diseases and microbial infection including viral, bacterial and parasitic infections have all been reported to involve the STING pathway in their pathogenesis (Decout et al. 2021; Skopelja-Gardner et al. 2022; Zhang Z et al. 2022). The following section will specifically focus on the potential implications of the STING pathway in lung inflammation.

4.b.1) STING and DNA in sterile lung conditions: focus on allergic asthma and asthma exacerbation.

Several clinical reports demonstrated the correlation between self-DNA accumulation and the severity of multiple sterile lung pathologies. Indeed, extracellular DNA in airway secretion of patients with cystic fibrosis was found to increase the viscosity of airway secretions which leads to the worsening of pulmonary function (Shah et al. 1995; Shah et al. 1995). Later, Benmerzoug et al showed the STING dependence of self-DNA-induced inflammation in a mouse model of silicosis and in human lungs of silicosis patients (Benmerzoug et al. 2018). In chronic obstructive pulmonary disease (COPD), Avriel et al identified DNA levels in serum of COPD patients as a biomarker of poor outcomes and increased risk of exacerbation (Avriel et al. 2016), and another study reported a substantial increase of mtDNA breaks in lung tissue of COPD patients (Pastukh et al. 2011). Subsequently, Nascimento et al. demonstrated in a mouse model of COPD sensitized with cigarette smoke, the STING-dependent lung inflammation that occurs after damage to the respiratory barrier and release of self-DNA (Nascimento et al. 2019). The same observation was made in patients with idiopathic pulmonary fibrosis, where an elevated fraction of mtDNA was found in both bronchoalveolar lavage fluid (BALF) and plasma. This increase in mtDNA levels is associated with reduced survival rates and predicts death in these patients (Ryu et al. 2017).

One of the first experimental evidence that dsDNA could potentiate allergic response was revealed in a mouse model exposed to allergen (ovalbumin), combined with aluminum-based adjuvants (aluminum salts or alum). Alum induced host cell death, releasing dsDNA which rapidly coats injected alum to act as endogenous immunostimulator (McKee et al. 2013). Subsequently, dsDNA supported humoral B cell response with IgG1 production in an IRF3-independent manner, but also classical Th2 responses accompanied with IgE response in a TBK1 and IRF3 dependent manner (Marichal et al. 2011). This observation was further supported by the fact that STING deficiency in mice showed a reduced OVA-specific IgE response (McKee et al. 2013).

In line with the experimental observation, a clinical study reported that a high concentration of extracellular self-dsDNA in patient's sputum positively correlates with more severe asthma accompanied with NETs production (Lachowicz-Scroggins et al. 2019). Together with house dust mites, respiratory viral infection is one of the most common cause of asthma exacerbation. Studies have revealed that rhinoviruses trigger self-dsDNA release associated with NETs induction to boost type-2 allergic inflammation in a setting of airway hypersensitivity (Toussaint et al. 2017; Radermecker et al. 2019). Moreover, injection of mouse dsDNA alone was sufficient to recapitulate many features of rhinovirus-induced type-2 immune responses (Toussaint et al. 2017). On the other hand, a clinical study analyzed gene expression in patients with mild and severe asthma, revealed prominent activation of ISGs. Interestingly, ISG signature was independent of viral genes and unrelated to the increased type 2 inflammation signature. Instead, ISG signature was associated to endoplasmic reticulum (ER) stress, confirmed by an increase in X-box binding protein 1 (XBP1), and also with a reduced lung function (Bhakta et al. 2018). Consequently, these findings raise questions about the potential intervention of the STING pathway, type I IFN production, and subsequent ISG expression.

In early 2020, Han et al. showed for the first time the occurrence of cytoplasmic dsDNA accumulation in airway epithelial cells during allergic inflammation. In this study, deletion of cGAS attenuated OVA- or HDM-induced Th2 immune response in mice, likely via down-regulation of epithelial GM-CSF, IL-25 and IL-33. Furthermore, treatment of human bronchial epithelial cells with a ROS scavenger (which acts on mitochondrial membrane permeabilization) significantly decreased cytosolic dsDNA-positive cells and reduced GM-CSF expression in those cells, suggesting a mitochondrial origin of cytosolic dsDNA which could be sensed by cGAS to mediate asthma pathogenesis (Han et al. 2020). Another group revealed the importance of STING in promoting humoral immunity during house dust mite extract (HDM)-induced allergic asthma. Mice lacking STING showed lower levels of total and HDM-specific IgE and a reduced proportion of B cells and IgE-positive B cells in the airways and lymph nodes, mainly through acting on follicular helper T cells (Nunokawa et al. 2021).

Excessive mucus hypersecretion contributes to airflow obstruction associated with severe asthma phenotypes. Recently, Nishida et al. emphasized a central role for STING but not cGAS in the induction of MUC5AC, one cardinal features of asthma. Oxidative stress induced by H₂O₂ treatment of human bronchial epithelial cells caused mtDNA release into the cytoplasm and subsequently MUC5AC expression. Furthermore, H₂O₂-induced MUC5AC

expression was suppressed in STING deficient cells, highlighting the combined role of oxidative stress, mtDNA and STING in mucin production by airway epithelial cells (Nishida et al. 2023).

Altogether, these studies provide compelling evidence supporting the involvement of self-dsDNA and the cGAS-STING pathway in the pathogenesis of type 2 asthma and asthma exacerbation.

4.b.2) STING and DNA in infectious diseases: focus on respiratory viral infections

The cGAS-STING pathway responds to a variety of DNA viruses including herpes simplex, hepatitis B and cytomegalovirus, to restrict viral dissemination. However, this extends beyond DNA viruses, as the cGAS-STING pathway also plays a crucial role in counteracting RNA viruses either by recognizing viral components or by detecting self DNA from nuclear or mitochondrial origin, which are triggered by the cellular stress induced during viral replication. Human Immunodeficiency Virus (HIV), a ssRNA virus can activate cGAS directly through its retro-transcribed Y-form DNA, possibly with the help of a proximal sensor protein, the polyglutamine-binding protein 1 (PQBP1) (Herzner et al. 2015; Yoh et al. 2015). Subsequently, Lahaye et al. shed light on a novel innate strategy for sensing the presence of HIV in the nucleus. The nuclear Non-POU domain-containing octamer-binding protein (NONO) serves as a sensor of the HIV capsid, associates with nuclear cGAS and facilitates HIV DNA detection (Lahaye et al. 2018).

Viral respiratory infections are among the most common diseases worldwide and represent a significant exacerbation factor for several lung diseases. Holm et al. revealed an unexpected STING function unrelated to cGAS in controlling *Influenza A Virus* (IAV) infection. Virus-cell membrane is sensed by STING, which subsequently stimulates an IFN response (Holm et al. 2016). Another non-canonical function of STING was highlighted during Rhinovirus infection. STING was shown to serve as a host factor to promote RV genome replication, and STING ablation had an antiviral effect *in vitro* (McKnight et al. 2020). Moreover, despite the usurpation of STING during viral replication, the canonical function of STING in the induction of innate inflammation was conserved. STING was suggested to contribute directly to IFN- β induction in response to RV infection *in vitro* (McKnight et al. 2020).

SARS-CoV-2 resulted in a significant loss of life. While most of the clinical research has focused on the fatal outcome of cytokine storm observed in ARDS patients, the underlying

mechanism behind this exacerbated immune response has been less clear. An *in vitro* study showed that SARS-CoV-2 infection induces cell-cell fusion via spike protein and the formation of syncytia. They further demonstrated that cell fusion provokes chromosomal DNA export from the nucleus to the cytoplasm and the subsequent activation of the cGAS-STING-dependent Type I IFNs (Zhou Z et al. 2021). Concurrently, two studies confirmed the pivotal role of STING pathway by demonstrating that STING agonists reduces SARS-CoV-2 viral load through an enhanced type I-IFN response (Humphries et al. 2021; Li M et al. 2021).

Paradoxically, sustained and uncontrolled type I-IFNs could be detrimental and correlate with COVID-19 severity. Recently, Di Domizio et al showed that cGAS–STING pathway drives endothelial dysfunction and type I IFN production (Domizio et al. 2022). Using a lung-on-chip (LoC) model that mimics the alveolar-capillary interface, they revealed that upon SARS-CoV-2 infection, endothelial cells but not epithelial cells, produce high levels of IFN β and eventually die. Moreover, treating LoC with STING inhibitor H-151 abolished this response. Furthermore, mass spectroscopy analysis of cytosolic factors showed that mitochondrial proteins were enriched after infection, suggestive of mitochondrial dysfunction and potential accumulation of mtDNA in the cytosol. In addition, cells incubation with 2',3'-dideoxycytidine (ddC) to deplete mtDNA or with VBIT-4 that inhibits the translocation of mtDNA to the cytosol led to a significant reduction of type I IFN production after infection. *In vivo* inhibition of STING using H-151 in infected K18-hAEC2 mice revealed a reduced lung inflammation (e.g. IL-6, TNF, ISGs) and markers of lung injury (F3, Retnla) at 6 days post-infection, but not at 3 days post-infection. Indicating that STING through type I IFNs mediates a critical contribution to lung immunopathology in the late phase of infections. (Domizio et al. 2022).

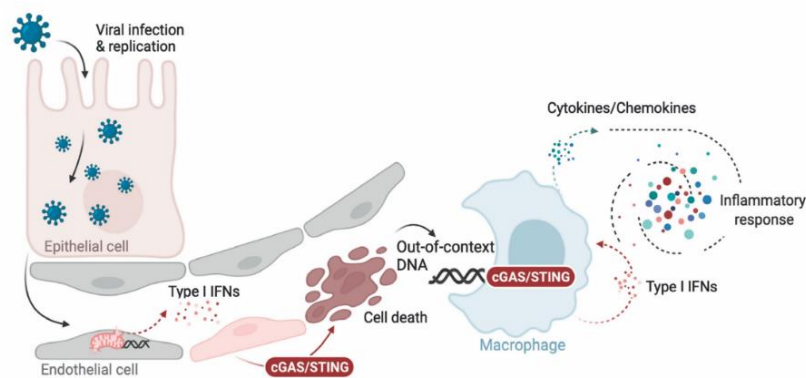


Figure 29: Proposed mechanism of cGAS-STING-dependent type I IFNs mediating lung immunopathology during severe COVID-19. SARS-CoV-2 infection of the alveolar-capillary interface induces mitochondrial dysfunction in endothelial cells with cytoplasmic

accumulation of mtDNA, and the subsequent activation of the cGAS-STING-dependent type I IFNs production driving cell death. Subsequently, perivascular macrophages engulf the dead cells, which in turn activates cGAS that detects damaged DNA from endothelial cells, subsequently activating STING, IRF3, and NF- κ B. This activation amplifies the production of type I IFNs and pro-inflammatory cytokines, contributing to development of severe forms of COVID-19 (Domizio et al. 2022).

Taking together, these studies provide valuable insights into the involvement of the cGAS-STING pathway during respiratory viral infections or chronic lung inflammation, and suggest that this pathway should be finely balanced when considering a therapeutic strategy.

4.c) Immune-modulation of STING, the central hub of DNA sensing, as a therapeutic strategy.

Being sometimes a friend and other times a foe, not only in different diseases but also within the same disease at different stages, tight control of STING activation appears inevitable. Boosting STING in a context of immune-desert TME or early phases of viral infections, holds great promise as a strategy to enhance innate responses for the elimination of transformed or infected cells. In contrast, in autoimmune and auto-inflammatory diseases such as SAVI or SLE, as well as in exaggerated anti-viral response, inhibition of STING became crucial to rescue the deleterious response.

4.c.1) STING activation

The therapeutic potential of activating STING pathway in triggering tumor cell death, (as discussed above), paved the road for the development of several STING agonists. To date, STING activators can be classified into three distinct categories: cyclic dinucleotides (CDNs), chemically modified CDNs and non-nucleotidic small molecules, as extensively reviewed (Ding et al. 2020; Amouzegar et al. 2021; Li Q et al. 2021; Guerini D. 2022; Garland et al. 2022).

All naturally occurring CDNs such as the mammalian non-canonical 2'3'-cGAMP, which exhibits affinity for all hSTING isoforms have limited potential as drug candidates due to their metabolic instability and limited membrane permeability and are susceptible to hydrolytic degradation by ENPP1 in the extracellular space. Several reports suggest that encapsulating cGAMP improves membrane permeability and increases its activity as an effective adjuvant. Endosomal polymersomes encapsulating cGAMP increase its activity by

several orders of magnitude, resulting in improved response to immune checkpoint blockade, inhibition of experimental tumor growth in mice, and increased long-term survival rates when administered both intravenously and intratumorally (Shae et al. 2019). Intranasal administration of lipid nanoparticles-containing cGAMP combined to influenza vaccine, conferred a stronger humoral CD8⁺ T cell immune response against both in early phase of infection (Wang et al. 2020). Subsequently another group confirmed the efficacy of this approach by using cutaneous vaccination to enhance the anti-IAV response in the lung and spleen (Zhu et al. 2022).

CDNs were chemically modified to overcome extracellular hydrolysis and improve membrane permeability and stability. As an example, the promising ML-RR-S2 CDA (ADU-S100) launched by Novartis, known to activate all hSTING isoforms, and the Merck's CDN MK-1454 tested alone or in combination with pembrolizumab respectively (anti-PD-1 antibody), and administrated intratumorally for head and neck cancer patients, showed limited clinical response (NCT04220866, NCT03937141). This could be explained by their high aqueous solubility and their relatively large size (Koshy et al. 2017). CDNs exhibit a higher molecular weight, frequently exceeding 700 Da versus less than 500 Da for the traditional synthetic drug molecules (Li L et al. 2014).

This poor pharmacokinetics prompted researchers to design a next-generation of non-CDN small molecules agonists including diABZI (Ramanjulu et al. 2018), MSA-2 (Pan B et al. 2020) and SR-1717 (Chin et al. 2020). Much attention was crystallized around the potent diABZI described by Ramanjulu and collaborators at GlaxoSmithKline during the anti-Covid research era. First released as ABZI (compound 1), a molecule that binds a subunit of the hSTING homodimer with relatively low potency compared to the natural agonist (cGAMP), a dimer of ABZI (diABZI, compound 2) was then created to increase the potency. Compound 2 yielded in 18-fold higher dose-dependent secretion of IFN- β in human PBMC than cGAMP. Subsequently, compound 2 was further ameliorated to give rise to the diABZI compound 3, which is known to be 400 times more potent than cGAMP *in vitro* in human PBMC. They further showed that unlike other agonists, diABZI maintains an open STING conformation and can bind both the mSTING and several hSTING isoforms (Ramanjulu et al. 2018).

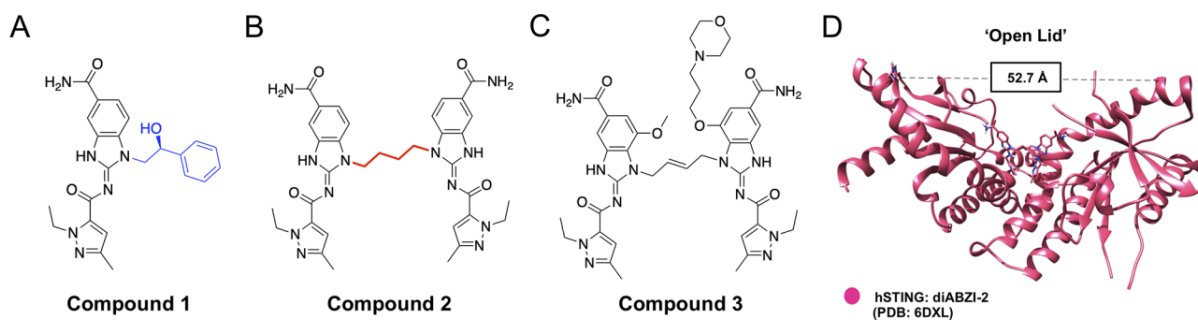


Figure 30: Dimeric amidobenzimidazole (diABZI) STING agonist development. (A) ABZI (compound 1) with relatively low potency (B) diABZI STING agonist (compound 2) with enhanced potency and ~ 18-fold higher *in vitro* activity compared to the natural CDN (C) Fully optimized diABZI STING agonist (compound 3) ~ 400-fold higher *in vitro* activity compared to the natural CDN. (D) The “Open Lid” configuration of hSTING dimer bound to diABZI compound 2 (Garland et al. 2022).

When tested *in vivo* in mice bearing CT26 colorectal tumors at 1.5 mg/Kg intravenously, diABZI showed a promising effect in inhibiting tumors growth. In 2019, the GSK3745417, a diABZI scaffold underwent clinical trials in patients with advanced solid tumors, administered intravenously with and without the anticancer agent, dostarlimab (NCT03843359). The study is expected to be concluded by August 2024. In 2022, GSK3745417 entered a new clinical study planning administration intravenously alone in patients with refractory myeloid malignancies (NCT05424380). The study is expected to end by December 2025.

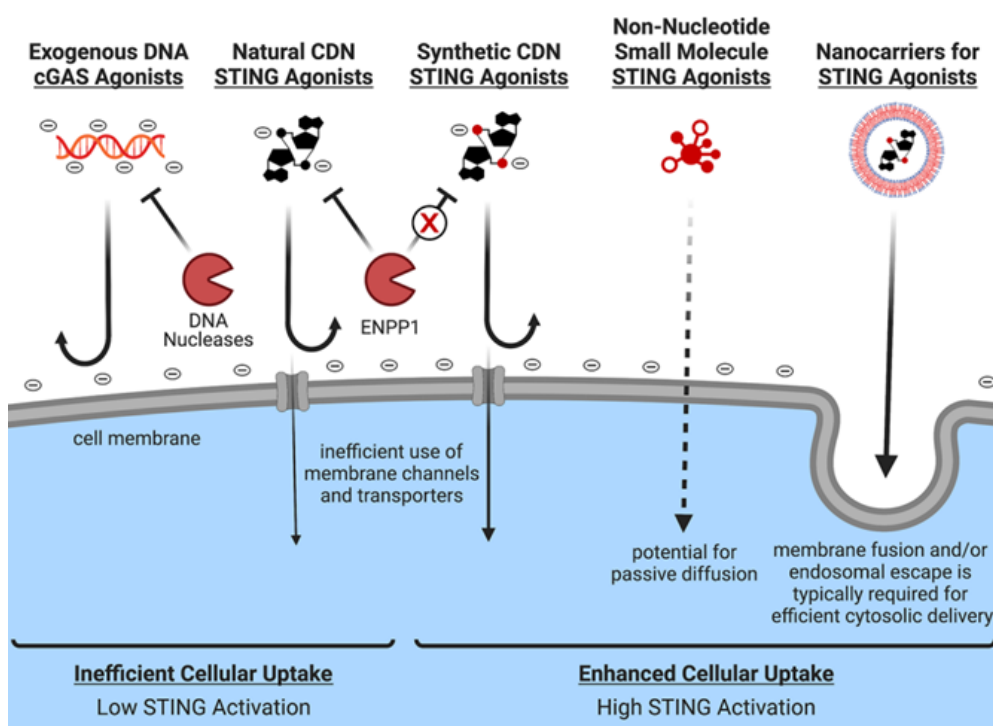


Figure 31: Direct intracellular STING activation strategies. Exogenous DNA activating cGAS and subsequently STING can be degraded by DNA ecto-nucleases before it reaches the cytoplasm. Natural CDNs are relatively small and can be imported by membrane channels and transporter such as LRRC8/VRAC, P2X7R and SLC19A1 but still show moderate membrane permeability due to hydrolytic degradation by ENPP1 in the extracellular space. Modified CDNs are non-hydrolysable and show an enhanced STING activation. Relatively high concentration of CDNs is required to induce measurable STING activation. Non-CDN small molecule STING agonists have the potential to passively cross the plasma membrane. Liposomes encapsulating STING agonists can enhance their cellular permeability (Garland et al. 2022).

STING activation can be enhanced by indirect strategies, such as the use of the phosphonate analogue STF-1084, an ENPP1 inhibitor to prolong the lifespan of extracellular cGAMP (Carozza et al. 2020). When combined with cancer treatment, where tumors were found to highly express ENPP1 at their surface (Li J et al. 2021), STF-1084 enhanced IFN- β production and potentiated the conventional anti-cancer therapeutics (Carozza et al. 2020), (Schadt et al. 2019).

Recently, Ji Y et al. identified a novel endogenous mechanism that modulates baseline STING. They showed that steady-state STING level is negatively regulated by the E3 ubiquitin ligase HRD1 within the ER-associated degradation (ERAD) complex, which is known to target misfolded ER proteins for proteosomal degradation. This, in turn, dampens innate immunity by limiting the size of the STING pool that can be activated. Interestingly, deficiency of SEL1L, an essential cofactor for HRD1 was sufficient to increase STING levels in macrophages, which subsequently ameliorated response to dsDNA and STING agonists, and amplified innate immunity against HSV1 viral infection and tumor growth (Ji Y et al. 2023). Thus, targeting the SEL1L–HRD1 ERAD axis represents a new strategy to enhance STING activation in an indirect manner.

4.c.2) STING inhibition

In interferonopathies or late phase infections, mitigating type I IFN through modulation of STING is of great interest.

To pharmacologically inhibit STING, several small-molecule compounds, including Astin C (Li S et al. 2018), SN-011 (Hong et al. 2021), compound 1 and compound 18 (Siu et al. 2018) target STING ligand-binding pocket. SN-011 demonstrated effectiveness in inhibiting hallmarks of auto-inflammation in the context of SAVI, and significantly reduced inflammatory cytokines including interferons in *Trex1*^{-/-} mice. It also inhibited inflammation induced by 2'3'-

cGAMP, herpes simplex virus type 1 infection or overexpression of cGAS-STING (Hong et al. 2021).

STING palmitoylation of Cys88 and Cys91 residues is a necessary step for STING multimerization and subsequent binding of TBK1 (Mukai et al. 2016). Several chemical molecules, inspired by the naturally occurring nitro-fatty acids (NO₂-FAs) and its mode of action (Hansen et al. 2017), were designed to target these sites, such as the potent nitro-furan derivative H-151, C-170, C-171, C-176 and the C-178 in an irreversible way (Haag et al. 2018). These compounds were effective in disease models such as psoriasis (Pan et al. 2021).

Current challenges and aims of the thesis

In the current, highly concerning climatic context, recent studies indicate that the increasing temperatures we are experiencing are instructing plants to start pollen seasons earlier and make it last longer. Thus, increasing the duration of exposition to pollen. Furthermore, the high atmospheric CO₂ levels resulting from pollution caused by hyper-industrialization, not only weakens respiratory barriers, but also enhances the allergenic potential of pollen (Singh & Kumar. 2022; D'Amato et al. 2023). Indeed, pollutant particles weaken the pollen grain's outer membrane, resulting in smaller fragments that can penetrate more deeply the respiratory airways (Verscheure et al. 2023).

Furthermore, global warming is expected to increase the frequencies of new pandemics (Gupta et al. 2021; Marani et al. 2021), like the one that affected us in 2019, resulting in the death of 6 million people worldwide. The migration of humans and animals as climate refugees will gather hosts whose immune systems have not evolved to counter the same pathogens, thus easing the transmission of viruses and bacteria.

Taken together, these data indicate that in the very near future, respiratory disorders risk to become more prevalent. The World Health Organization (WHO) predicts that by 2050, the prevalence of allergic diseases may double, 50% of the world population could be affected by allergies. In this context, individuals with asthma may develop severe airway inflammation with same characteristics as ARDS. Therefore, it is urgent to understand the mechanisms responsible for exacerbating respiratory pathologies, to develop new therapeutic approaches, and test the safety of these strategies.

As discussed in the introduction, the role of self-DNA in triggering sterile and infectious innate inflammatory responses is now well known. Through the study of these two respiratory disorders, we principally aimed at evaluating and characterizing the role of hyper-activation of the STING pathway in the mediation of (1) potential severe forms of acute respiratory distress syndrome (ARDS), occurring during uncontrolled respiratory viral infection, or (2) severe/exacerbated allergic asthma, which may occur when individuals with asthma are infected with respiratory viruses/bacteria or exposed to air pollution.

Several studies have suggested the use of a STING agonist, such as diABZI, as a therapeutic strategy to reduce SARS-CoV-2 viral load. We sought to determine at steady state the immunomodulatory mechanisms induced by this candidate therapeutic molecule. We wanted to determine whether pharmacological boosting of the STING pathway, is limited to

the activation of the type I IFN pathway, which is highly desirable during viral infection, or whether it may also propagate inflammation and drives positive feedback loops of uncontrolled inflammation and tissue injury. In this latter case, it would be necessary to reassess the risk/benefit ratio of using diABZI or other STING agonists for the treatment of viral infections.

In the Introduction section, we highlighted the involvement of the cGAS-STING pathway in the pathophysiology of classical Th2^{high} asthma and its activation by respiratory viruses and particles pollution. On the other hand, we now know that respiratory viruses such rhinoviruses, SARS-CoV2, or IAV regularly drive asthma exacerbations, with lung neutrophils infiltration and Th1 mediators production. These severe neutrophilic forms of asthma episodes often lead to hospitalizations and render the pathology refractory to conventional treatments.

Based on these information, we evaluated the impact of hyper-activation of the STING pathway on classical Th2^{high} asthma immunopathology. We mimicked viral infection or particle exposure during allergic asthma, using a mouse model of HDM-induced allergic asthma sensitized to STING agonists in the airways. Following this experimental approach, we sought to assess the involvement of the STING pathway in mediating non-classical severe neutrophilic forms of asthma, and its potential to aggravate lung functional function and injury. In which case, careful attention should be payed to mitigating STING hyper-activation in clinical management of severe asthma exacerbation.

Results

Article 1: STING agonist diABZI induces PANoptosis and DNA mediated acute respiratory distress syndrome (ARDS).

Yasmine Messaoud-Nacer, Elodie Culerier, Stéphanie Rose, Isabelle Maillet, Nathalie Rouxel, Sylvain Briault, Bernhard Ryffel, Valerie F. J. Quesniaux, and Dieudonné Togbe.

Cell Death and Disease (2022) 13:269 ; <https://doi.org/10.1038/s41419-022-04664-5>.

The interferons have always been considered to be the ultimate antiviral defense of the body. Indeed, mice lacking IFN α/β -receptor show impaired antiviral response. Furthermore, low IFN production in patients infected with SARS-CoV-2 correlated with low viral clearance, highlighting their clinical and therapeutic importance (Blanco-Melo et al. 2020; Hadjadj et al. 2020).

There are three interferons families: type I (IFN- α/β) and type III (IFN- λ) with canonical anti-viral properties, and type II (IFN- γ) with pro-inflammatory and immunomodulatory properties (Lazear et al. 2019). Anti-viral type I and type III IFNs signal through two distinct heterodimeric receptors namely IFNAR/IFNAR2 and IL28R α /IL10R β , respectively. Both families signal through the JAK1-STAT-1/-2 pathway to activate the heterotrimeric transcription factor complex ISGF3. Activated ISGF3 comprises phosphorylated STAT1 and STAT2, and interferon regulatory factor 9 (IRF9), and translocates to the nucleus to bind the IFN-stimulated response elements (ISREs) in the promoter regions of ISGs (Katze et al. 2002), which encode circa hundred anti-viral proteins, such as OAS, MX1 or IFIT (Lazear et al. 2019).

During the COVID-19 global pandemic, IFN therapy including all subtypes, was clinically administered to patients, in an attempt to manage the crisis. Jhuti et al. reported that among 11 trials examined, 5 studies reported a positive outcome, 4 reported minimal to no difference between IFN and the control, and 2 reported worst patient outcomes than the controls (Jhuti et al. 2022). Later, the discrepancies in these results were partially explained by the timing of IFN administration. Indeed, in acute infections, early administration of type I IFNs in experimental animals induces protective antiviral responses, whereas late administration of IFNs enhances pro-inflammatory cytokine responses and host tissue damage (Davidson et al. 2014; Galani et al. 2017). Moreover, SARS-CoV-2 was found to delay the innate immune response as an immune evasion strategy (Li et al. 2021), highlighting the necessity to adapt the

kinetics of IFN administration to enhance anti-viral immunity while limiting the collateral damage on host tissue.

Li et al suggested the use of the STING agonist diABZI as an alternative therapeutic strategy to enhance type I IFN production during early phases of infection without the collateral damage. Their suggestion was motivated by the transitory character of IFN pathway following STING activation. In this study, they showed transient induction of IFNs and ISG that contributed to lower the viral load, while IFN β treatment led to a sustained ISG expression and was less efficient than diABZI (Li et al. 2021). Another group confirmed the beneficial effect of diABZI on viral clearance (Humphries et al. 2021).

Based on these findings, we sought to evaluate the lung immune landscape modulated by diABZI in immunocompetent mice, and to determine whether the transient type I IFN response reported in previous studies could induce tissue and cellular damage, which in turn could fuel a positive feedback loop between inflammation and damage.

We first investigated the effect of the natural STING agonist cGAMP both *in vivo* by intra-tracheal administration, and *in vitro* in bone marrow-derived macrophages (BMDM) from wild-type and STING^{-/-} mice. cGAMP induced lung neutrophilia as evidenced by CXCL1 (KC) and MPO secretion in BALF, activation of inflammatory pathways including IRF3 and NF κ B, and a massive lung injury associated with self-dsDNA released into the airway. *In vitro* stimulation of BMDM with cGAMP revealed an early production of type I IFNs as early as 2h post-treatment, with downstream ISG production (CXCL10) and expression of several DNA sensors, measured at 4h and further at 16h post treatment.

We next tested the more stable and potent non-CDN STING agonist diABZI, first *in vitro* in both mouse immune cells (BMDM) and human epithelial cells. Likewise, diABZI induced type I IFN (α/β) and other pro-inflammatory cytokines production 16h after treatment, DNA damage evidenced by phosphorylation of γ H2AX and cell death with markers of apoptosis, pyroptosis and necroptosis. *In vivo*, endotracheal administration of diABZI induced the production of IFN- α / IFN- β and pro-inflammatory IL-6 / TNF- α as a result of STING and NF κ B pathway activation, respectively. We revealed the presence of critical amounts of self-dsDNA, in part of mitochondrial origin, indicative of cellular stress. A strong neutrophilic infiltration with the release of NETs was characterized in the lung. Histologically, important peribronchial infiltrates of inflammatory cells spread to lung parenchyma with signs of epithelial injury after diABZI administration.

Next, we further questioned the origin of dsDNA. Up to this point, we knew that dsDNA comes from cellular stress and also from NETosis. Several reports demonstrated that STING may directly mediate apoptosis. Moreover, the deployment of NETs could also be harmful to the lung tissue. We evaluated and showed the occurrence of apoptosis, and the most characterized lytic cell death pyroptosis and necroptosis in lung tissue after diABZI administration. The presence of the 3 cell death markers suggested PANoptosis, which prompted us to evaluate the formation of the PANoptotic complex by assessing the co-localization of caspase-8, ASC and RIPK3 by confocal microscopy.

Knowing the role that DNA can play in inflammation, we hypothesized that the released DNA could act as a second signal to amplify lung inflammation. To address this, we first analyzed the expression of several DNA sensors and found increased levels of cGAS (which was bypassed at the first inflammatory signal during STING priming with diABZI), but also of *Aim2*, *Ifi204*, *Nlrp3*, *Ddx41* and *Tmem173*.

To further characterize the role of DNA in mediating lung injury, diABZI-treated mice received either intratracheal administration of DNAase I, or intraperitoneal administration of Cl-Amidine, an inhibitor of NET formation. The degradation of circulating dsDNA by DNAase I resulted in reduced lung neutrophilia and NETs, and a reduced CD45⁺ necrotic Annexin V⁺ Propidium Iodide (PI)⁺ and apoptotic Annexin V⁺ PI⁻ cells. Likewise, efficient NET inhibition with Cl-Amidine treatment helped to reduce neutrophil infiltration in the lung and revealed the existence of an interplay between STING activation mediating lung damage and NET formation. Indeed, NET inhibition in diABZI treated mice resulted in reduced DNA damage evidenced by phosphorylated histone γ H2AX, but also by all PANoptosis markers assessed. Moreover, lytic cell death assessed by Lactate dehydrogenase (LDH) released in the BALF was attenuated after inhibition. Thus, we provide the first evidence linking NETs to PANoptosis.

Overall, our study demonstrated that therapeutic strategies using the STING agonist diABZI do indeed induce an early induction of type I IFNs, which may be beneficial for infected patients, to overcome viral innate immune evasion. However, the subsequent inflammatory cascade mediating host DNA damage, lytic cell death and lung tissue injury, reveals that the balance between benefit and risk can easily be reversed. This makes it difficult to fully appreciate the antiviral properties of the STING agonist diABZI, and poses additional challenges in defining the right doses and routes of administration to avoid controlling viral infection at the expense of compromising host lung function.

This study was published in *Cell Death and Disease* in March 2022.

ARTICLE OPEN



STING agonist diABZI induces PANoptosis and DNA mediated acute respiratory distress syndrome (ARDS)

Yasmine Messaoud-Nacer^{1,2}, Elodie Culerier^{1,2}, Stéphanie Rose^{1,2}, Isabelle Maillet^{1,2}, Nathalie Rouxel³, Sylvain Briault^{2,4}, Bernhard Ryffel^{1,2,3}, Valerie F. J. Quesniaux^{1,2,5} and Dieudonné Togbe^{1,2,5}

© The Author(s) 2022

Stimulator of interferon genes (STING) contributes to immune responses against tumors and may control viral infection including SARS-CoV-2 infection. However, activation of the STING pathway by airway silica or smoke exposure leads to cell death, self-dsDNA release, and STING/type I IFN dependent acute lung inflammation/ARDS. The inflammatory response induced by a synthetic non-nucleotide-based diABZI STING agonist, in comparison to the natural cyclic dinucleotide cGAMP, is unknown. A low dose of diABZI (1 µg by endotracheal route for 3 consecutive days) triggered an acute neutrophilic inflammation, disruption of the respiratory barrier, DNA release with NET formation, PANoptosis cell death, and inflammatory cytokines with type I IFN dependent acute lung inflammation. Downstream upregulation of DNA sensors including cGAS, DDX41, IFI204, as well as NLRP3 and AIM2 inflammasomes, suggested a secondary inflammatory response to dsDNA as a danger signal. DNase I treatment, inhibition of NET formation together with an investigation in gene-deficient mice highlighted extracellular DNA and TLR9, but not cGAS, as central to diABZI-induced neutrophilic response. Therefore, activation of acute cell death with DNA release may lead to ARDS which may be modeled by diABZI. These results show that airway targeting by STING activator as a therapeutic strategy for infection may enhance lung inflammation with severe ARDS.

Cell Death and Disease (2022)13:269; <https://doi.org/10.1038/s41419-022-04664-5>

INTRODUCTION

Stimulator of interferon genes (STING) is recognized as crucial in host immune responses against tumors [1], as the absence of STING leads to defective CD8⁺ T cell priming [2]. Cyclic dinucleotide (CDN) and non-nucleotidyl STING agonists are in development for cancer immunotherapy [1, 3]. Interesting activities in inhibiting infection by SARS-COV2, the agent responsible for COVID-19, in vitro and in vivo in mice have recently been reported [4, 5]. However, the clinical development of CDN STING agonists is hampered by limited bioavailability and adverse effects. In cancer therapy, subcutaneous or intratumor routes of administration are most frequent [3] while intravenous administration may lead to systemic inflammation with release type I IFN and cytokines in the bloodstream [6]. This triggered the development of encapsulated nanoparticulate forms of STING agonists [7], such as lysosomes loaded with cGAMP for airway delivery in the treatment of lung metastasis [8].

We showed the critical role of the STING pathway in sterile lung inflammation [9] after airway exposure to silica microparticles [10] or cigarette smoke [11], involving lung cell damage, cell death, and self-dsDNA release in the bronchoalveolar space that triggers STING activation and downstream type I IFN responses. We hypothesized that STING agonists administered in the airways for anticancer or anti-COVID treatment might induce an inflammatory response,

fueled by STING-mediated cell death [12], and we questioned whether STING agonists induce acute respiratory distress syndrome (ARDS), through programmed cell death PANoptosis, including pyroptosis, apoptosis, necroptosis pathways [13].

Here we addressed the lung inflammatory response induced by endotracheal administration of an endogenous CDN cGAMP, STING agonist, and a non-nucleotide-based synthetic STING agonist comprising two linked, symmetry-related amidobenzimidazole-based compounds (diABZI) selected for its enhanced binding to STING and higher potency [14]. We show that airway application of STING agonists triggered a neutrophilic response in the bronchoalveolar space, induced cell death with the loss of epithelial barrier function and release of self-dsDNA, neutrophil extracellular traps (NETs), and lung inflammation. We hypothesized and showed that self-dsDNA release was accompanied by upregulation of DNA sensors such as cyclic GMP-AMP synthase (cGAS), IFN-γ-inducible protein 16 (IFI16) mouse orthologue IFI204, or DEAD-box helicase 41 (DDX41) that trigger type I IFN response through STING, TANK-binding kinase 1 (TBK1) and IFN regulatory factor 3 (IRF3) activation, as well as upregulation of Toll-like receptor 9 (TLR9) and the inflammasomes NLRP3 and AIM2. Markers of apoptosis, pyroptosis, and necroptosis were also present and colocalized in airway recruited inflammatory cells, indicative of STING-dependent PANoptosis.

¹CNRS - UMR7355, 45071 Orleans Cedex 2, France. ²Experimental and Molecular Immunology and Neurogenetics, University of Orleans, Rue de la Ferrollerie, 45071 Orleans, Cedex 2, France. ³Artimmune SAS, 13 Avenue Buffon, 45100 Orleans, Cedex 2, France. ⁴Genetics department, Regional Hospital Orleans (CHRO), Orleans 45100, France.

⁵email: quesniaux@cnrs-orleans.fr; dtogbe@cnrs-orleans.fr
Edited by Professor Mauro Piacentini

Received: 15 September 2021 Revised: 25 January 2022 Accepted: 11 February 2022
Published online: 25 March 2022

RESULTS
cGAMP local administration triggers airway neutrophilic inflammation

We first addressed the effect of the natural cyclic dinucleotide STING ligand cGAMP in the airways. Endotracheal administration of cGAMP (1, 3, or 10 µg) for 3 consecutive days induced airway

inflammation within 24 h (Fig. 1A). The neutrophilic attracting chemokine CXCL1/KC was released in the bronchoalveolar lavage fluid (BALF; Fig. 1B), and this was accompanied by increased neutrophil recruitment (Fig. 1C) and myeloperoxidase (MPO), a marker of neutrophil presence and activation in the BALF (Fig. 1D) and in the lung tissue (Fig. 1E). cGAMP-induced airway

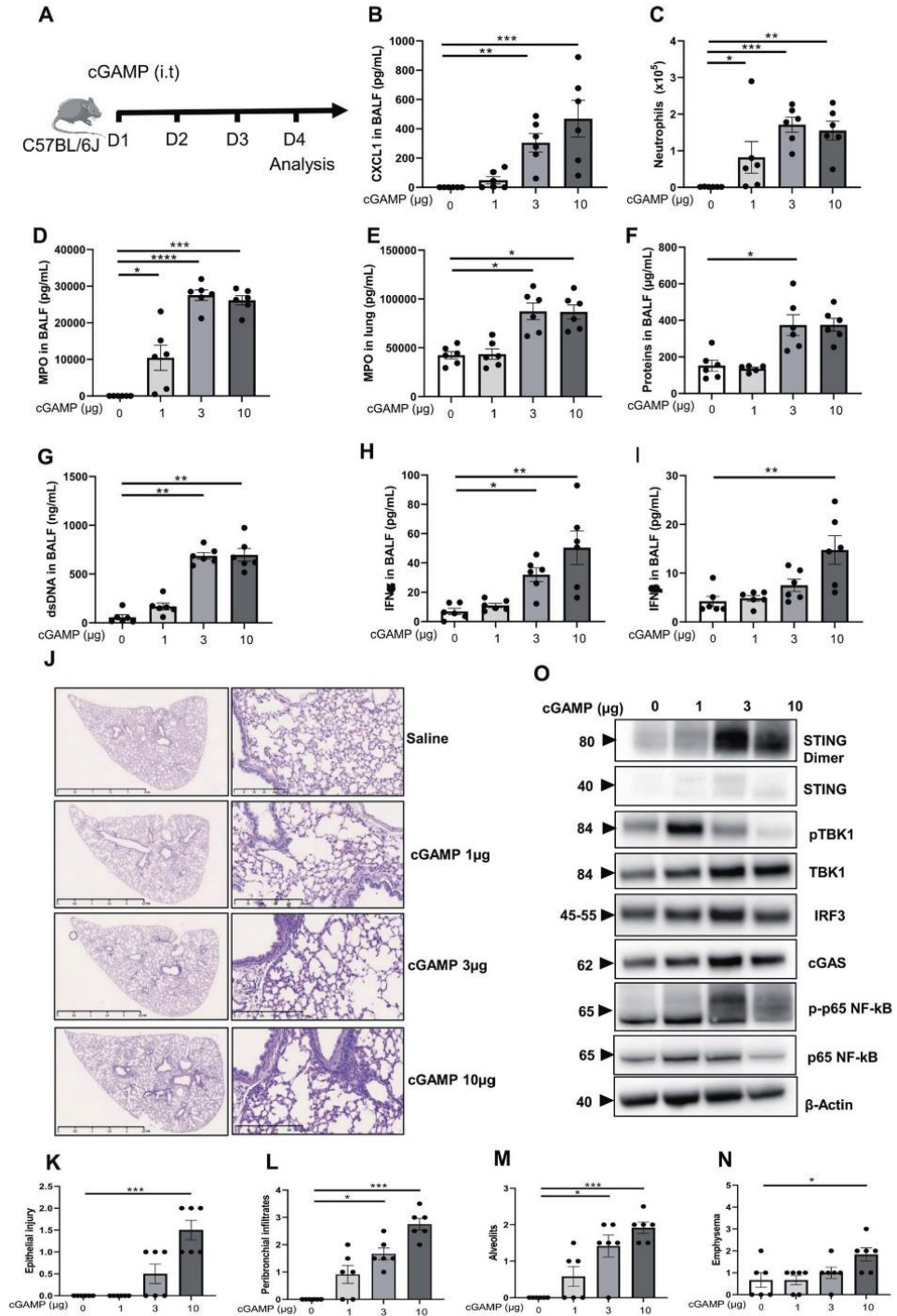


Fig. 1 Endotracheal cGAMP induces neutrophilic inflammation, protein extravasation, and self-dsDNA release in the airways. **A** cGAMP (1, 3, or 10 μg , i.t.) or saline were administered daily in WT mice for 3 consecutive days, and parameters analyzed on day 4. **B** Concentration of CXCL1/KC in bronchoalveolar lavage fluid (BALF) determined by ELISA. **C** Neutrophils counts in BALF. **D, E** Myeloperoxidase (MPO) concentration in BALF (**D**) and in the lung (**E**) determined by ELISA. **F** Concentration of proteins in BALF. **G** Concentration of extracellular dsDNA in the acellular fraction of BALF. **H, I.** Concentration of IFN α and IFN β in BALF determined by Luminex immunoassay. **J–N.** Lung tissue histology PAS staining (**J**), with pathology scoring of the presence of epithelial injury (**K**), peribronchial infiltration of inflammatory cells (**L**), alveolitis (**M**), and emphysema (**N**). Bars, left panels: 2.5 mm, right panels: 250 μm . **O** Immunoblots of STING pathway activation in the lung tissue in response to cGAMP, including STING dimer, STING, phospho-TBK1, TBK1, IRF3, cGAS, phosphorylated NF- κB p65 (p-p65-NF- κB), and p65 NF- κB , with β -actin as a reference. Graph data were presented as mean \pm SEM with $n = 6$ mice per group. Each point represents an individual mouse. * $p < 0.05$, ** $p < 0.01$, *** $p < 0.001$, **** $p < 0.0001$ (Nonparametric Kruskal–Wallis with Dunn post test).

dysfunction was evidenced by increased total protein extravasation (Fig. 1F), self-dsDNA release in the bronchoalveolar space (Fig. 1G), and IFN α and IFN β in the airways (Fig. 1H, I).

Thus, the natural CDN STING ligand cGAMP is a potent inducer of neutrophilic inflammation in the airways that may cause cell damage and lung dysfunction. Indeed, airway cGAMP resulted in acute alveolitis with thickened alveolar septae containing inflammatory cells, partial disruption of the alveolar membrane and rarefaction of alveoli, acute bronchiolitis with cell death and a beginning of remodeling with peribronchial infiltrates, visible 24 h after 1 μg , and further increased after 3–10 μg cGAMP endotracheal administration (Fig. 1J–N), but no mucus secretion (PAS staining). These are typical features following a massive injury with inflammation and incipient emphysema, repair, and fibrosis (Fig. 1J–N).

STING activation triggers several inflammatory pathways including IRF3 and NF- κB activation. We show that cGAMP administration at 1 to 10 μg increased STING dimers, TBK1 phosphorylation (pTBK1), IRF3, cGAS, NF- κB , and NF- κB p65 subunit phosphorylation (p-p65 NF- κB) in the lung tissue (Fig. 1O and Supplemental Fig. S5A). We next asked whether both pathways were functionally activated following the administration of cGAMP in the airways. Indeed, the chemokine *Cxcl10* mRNA, a typical Interferon-stimulated gene (ISG) downstream of IRF3/type I IFN, was overexpressed in the lung tissue after administration of 3–10 μg cGAMP in the airways (Supplemental Fig. S1A). CXCL10/IP-10 was increased in the BALF after 10 μg cGAMP administration (Supplemental Fig. S1B), as were TNF α and IL-6, both triggered in response to NF- κB pathway (Supplemental Fig. S1C, D). Interestingly, the expression of STING gene *Tmem173* doubled in the lung 1 day after cGAMP administration (Supplemental Fig. S1E).

Thus, airway cGAMP administration induces strong lung inflammation and injury, associated with dsDNA release, type I IFN and inflammatory cytokines in the lung, and overexpression of STING transcript.

Amplification loop of STING pathway activation

Since airway cGAMP administration induced extracellular dsDNA release in the BALF, we hypothesized that this dsDNA might act as a danger signal, activate DNA sensors, and induce further type I IFN response.

We analyzed the kinetics of cGAMP-induced responses in vitro in bone marrow-derived macrophages (Fig. 2). Type I IFN α and IFN β release at 4 h, further increased 16 h after macrophage activation by cGAMP (Fig. 2A, B). CXCL10 was also strongly increased at 4–16 h (Fig. 2C). *Irfn3* gene was already overexpressed 2 h after cGAMP addition (Fig. 2D), and phosphorylation of STING, TBK1 and IRF3 occurred already at 1 h, while STAT1 phosphorylation was delayed to 2 h (supplemental Fig. S2 and S5G). ISG includes DNA sensors such as cGAS, AIM2, or IFI204, and we verified their expression. There was overexpression of cGAS gene *Mb21d1*, *Aim2*, and *Ifi204* genes at 4–16 h (Fig. 2E–G), while *Ddx41* and *Nlrp3* genes were barely affected (Fig. 2H, I). STING gene *Tmem173* itself was overexpressed at 16 h (Fig. 2J), CXCL1 and IL-10 were increased at 16 h (Fig. 2K, L). We verified that the effects of cGAMP was indeed mediated by STING using *Tmem173*-

deficient (*STING*^{-/-}) macrophages. As expected, *Irfn3*, *Irfn2*, and *Irfn4* genes expression, and IFN α and IFN β release were abrogated in *STING*^{-/-} macrophages (Fig. 2M–Q).

Thus, activation of STING by the natural CDN agonist cGAMP triggers a well-coordinated expression of type I IFNs and ISGs including several DNA sensors that may contribute to downstream chemokines and cytokines release.

Synthetic STING agonist diABZI triggers potent inflammation in murine macrophages and human epithelial cells

To further characterize the effects of triggering STING activation in the airways, we turned to the recently developed and highly potent synthetic, non-nucleotidyl molecule diABZI [14]. We first checked the response induced by diABZI on murine macrophages. DiABZI at 1 μM induced the release of IFN α , IFN β , CXCL10, IL-6, TNF α , CXCL1, and IL-10 at 16 h (Fig. 3A–G), similar to the natural CDN cGAMP, and this was abrogated in *STING*^{-/-} macrophages (Fig. 3A–G).

DiABZI at 0.3–1 μM induced the phosphorylation of STING and downstream TBK1 kinase, together with STAT1 phosphorylation, similar to cGAMP (Fig. 3H and supplemental Fig. S5B). The relative reduction of STING protein in conditions when STING is phosphorylated is intriguing, not due to antibody artifact as it is seen in independent blots, and might be related to the STING protein turnover in cells in culture in vitro. DNA damage was revealed by phosphorylated- γH2AX (p γH2AX ; Fig. 3H and supplemental Fig. S4A). Indeed, cell death was also induced, as documented by immunoblots with elevated caspase 3, cleaved Gasdermin D (GSDMD) as a marker of pyroptosis, elevated Mixed Lineage Kinase domain Likepseudokinase (MLKL), and phospho-MLKL as a marker of necroptosis (Fig. 3I and supplemental Fig. S4A). This was suggestive of PANoptosis, and confirmed as the Z-DNA-binding protein 1 (ZBP1) was also upregulated (Fig. 3I and supplemental Fig. S5B). These responses were reduced in *STING*^{-/-} mice (Fig. 3H, I), documenting the STING dependence of the induced responses.

We next characterized the response induced by diABZI on primary human airway epithelial cells (hAEC). DiABZI at 1–10 μM induced the expression of IFN β , IL-1 β , and IL-8 (Fig. 3J–L). Indeed, diABZI induced the phosphorylation of STING and downstream TBK1 kinase, as well as overexpression of cGAS, but it also induced cell death, documented by cleaved Caspase 3 as a marker of apoptosis and DNA damage with increased p γH2AX (Fig. 3M and supplemental Fig. S5C).

Thus, diABZI induced activation of the STING pathway and cell death with upregulation of markers of apoptosis, pyroptosis, and necroptosis, indicative of STING-dependent PANoptosis, a term recently introduced [13].

Airway administration of STING agonist diABZI triggers neutrophilic inflammation and NET formation

Endotracheal administration of diABZI for 3 consecutive days induced a strong airway inflammation within 24 h (Fig. 4A). CXCL1 was released in the bronchoalveolar space after 0.1–1 μg diABZI administration (Fig. 4B), alongside neutrophil recruitment (Fig. 4C) and increased MPO (Fig. 4D). Protein extravasation in the

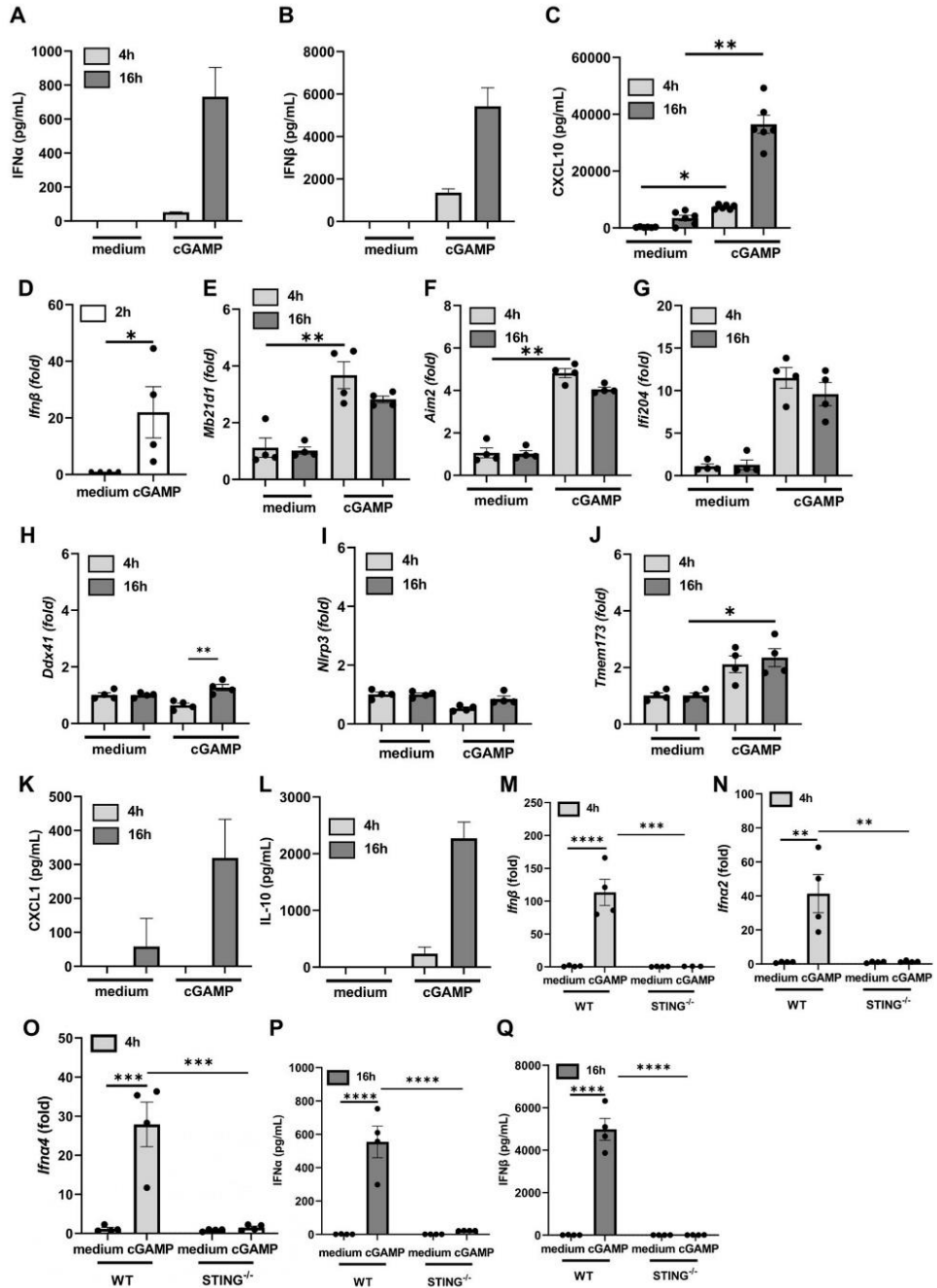
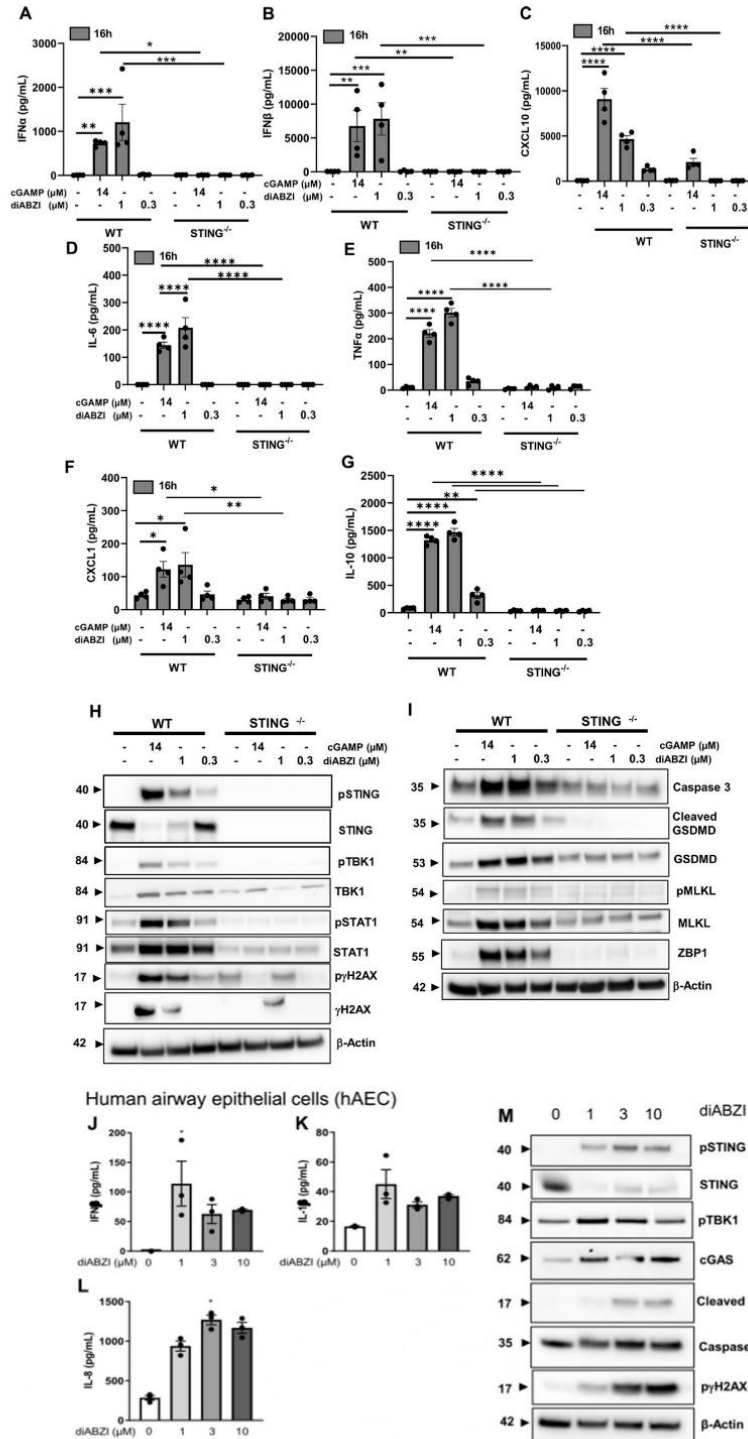


Fig. 2 cGAMP-induced type I IFN macrophage response and DNA sensor expression. Bone marrow-derived macrophages from wild-type (A–L) and STING^{-/-} (M–Q) mice were unstimulated or stimulated with cGAMP (14 μM) for 4 or 16 h as indicated. **A–C** Protein concentrations of IFNα (A) and IFNβ (B) in macrophage culture supernatant determined by multiplex immunoassay, and of CXCL10 quantified by ELISA (C). **D–J** *Ifnb*, *Mb21d1*, *Aim2*, *Ifi204*, *Ddx41*, *Nlrp3*, and *Tmem173* transcripts measured by real-time PCR. **K, L** CXCL1 (K) and IL-10 (L) protein concentration quantified by ELISA. **M–O** *Ifnb1*, *Ifna2*, and *Ifna4* transcripts measured by real-time PCR in macrophages from WT and STING^{-/-}. **P, Q** Comparison of protein levels of IFNα (P) and IFNβ (Q), in the supernatant of WT and STING^{-/-} macrophages. Data were presented as mean ± SEM with *n* = 4 mice. **p* < 0.05, ***p* < 0.01, ****p* < 0.001, *****p* < 0.0001 (A–L Nonparametric Kruskal–Wallis with Dunn post test. M–Q Two-way Anova with Tukey post test).



bronchoalveolar space (Fig. 4E), indicative of disruption of the respiratory barrier, was accompanied by self-dsDNA release (Fig. 4F), suggesting cell damage and/or cell death. As cell stress or death may release mitochondrial DNA in the cytosol or

extracellularly, that acts as a strong danger signal recognized by nucleic acid sensors such as cGAS, we quantified nuclear and mitochondrial DNA released in the BALF in response to diABZI or cGAMP. While nuclear DNA was barely released, there was a

Fig. 3 **DiABZI-induced type I IFN response in human alveolar epithelial cells.** **A–G** Bone marrow-derived macrophages (BMDM) from wild-type and STING^{-/-} mice were unstimulated or stimulated with cGAMP (14 μM) or diABZI (0.3 or 1 μM) for 16 h. Protein concentrations of IFNα (A) and IFNβ (B) in macrophage culture supernatant determined by multiplex immunoassay, of CXCL10 (C), IL-6 (D), TNFα (E), CXCL1 (F), and IL-10 (G) quantified by ELISA. **H, I** Immunoblots of STING axis (H), including phospho-STING, STING, phospho-TBK1, TBK1, phospho-STAT1, STAT1, DNA damage as revealed by phospho-γH2AX, γH2AX and of cell death axis (I) including Caspase 3, cleaved Gasdermin D, Gasdermin D, phospho-MLKL, MLKL, and ZBP1 in WT and STING^{-/-} macrophages, with β-actin as a reference. **J–L** Human alveolar epithelial cells (hAEC) were unstimulated or stimulated with diABZI (1, 3, or 10 μM) for 24 h. Protein levels of IFNβ (J), IL-1β (K), and IL-8 (L) were released in the culture supernatant. **M** Immunoblots of STING axis, including phospho-STING, STING, phospho-TBK1, cGAS, and cell death markers cleaved Caspase 3, Caspase 3, and phospho-γH2AX with β-actin as a reference. **p* < 0.05, ***p* < 0.01, ****p* < 0.001, *****p* < 0.0001, (A–G; two-way Anova with Tukey post test. J–L; nonparametric Kruskal–Wallis with Dunn post test). Data were presented as mean ± SEM and are representative of two independent experiments with *n* = 4 (A–G) and *n* = 3 (J–L) independent cultures.

strong increase in mtDNA after diABZI 1 μg and to a lesser extent after exposure to cGAMP 10 μg (Fig. 4G, H), with a 35- to 42-fold mtDNA/nDNA ratio after cGAMP and diABZI exposure, respectively.

We next asked whether both IRF3 and NF-κB pathways were activated following STING activation by diABZI administration. Although no phosphorylated TBK1, IRF3, or p65 NF-κB could be detected at this time point (not shown), there was a functional activation of these pathways. Indeed, IFNα and IFNβ were released in the BALF after administration of diABZI at 0.1–1 μg (Fig. 4I, J), as was CXCL10, downstream of type I IFN/IRF3, after 1 μg diABZI (Fig. 4K), and both IL-6 and TNFα, triggered in response of NF-κB pathway (Fig. 4L, M).

DiABZI activating neutrophilic responses, we further investigated the formation of NETs, a neutrophil innate effector mechanism. Indeed, NETs comprising neutrophil-derived DNA, citrullinated histone H3 (Cit-H3), and MPO were increased by diABZI administration in the airways (Fig. 4N–R).

Histologically, marked inflammatory cell infiltration in the lung parenchyma was visible 24 h after three doses of 0.01 μg, and furthermore 0.1–1 μg diABZI endotracheal administration (Fig. 4S–W) with signs of epithelial injury, alveolitis, and emphysema, but no mucus secretion revealed by PAS staining.

Thus, the synthetic, non-nucleotidyl, STING ligand diABZI is a potent inducer of neutrophilic inflammation in the airways that may cause cell damage, dsDNA release and NETosis, and lung dysfunction.

DiABZI-induced pulmonary cell death by PANoptosis

As STING may mediate apoptosis [12, 15], we characterized the mode of cell death induced by diABZI in the lung. Airway administration of diABZI at 0.1 and more at 1 μg induced caspase 3 cleavage in the lung tissue, indicative of STING activation-induced apoptosis (Fig. 5A and supplemental Fig S5D). The occurrence of pyroptosis and necroptosis in diABZI-induced pulmonary cell death was assessed by immunoblots of cleaved Gasdermin D (GSDMD) and phosphorylated MLKL. Indeed, GSDMD and MLKL were increased in the lung, with the presence of cleaved GSDMD and phosphorylated MLKL (54 kD lower band) after administration of diABZI at 0.1 and further augmented at 1 μg (Fig. 5A, B). These data were suggestive of PANoptosis induced in the lung after exposition to diABZI, and was confirmed as the Z-DNA-binding protein 1 (ZBP1) was also upregulated (Fig. 5A, B). DNA damage was documented as increased levels of pyH2AX after diABZI treatment (Fig. 5A, B). Cit-H3 detection provided evidence of pulmonary NETosis triggered by diABZI administration (Fig. 5A, B).

To further characterize PANoptosis we next analyzed ASC-Caspase 8-RIPK3 complex formation [16, 17]. Indeed, in sterile inflammation, the Caspase 8-RIPK3 shared by apoptosis and necroptosis is generally associated with ASC, the adapter protein of inflammasomes [18], these molecular interactions likely serving as the backbone for PANoptosome formation. Confocal microscopy analysis of immunofluorescence labeling shows increased Caspase 8, ASC, and RIPK3 protein expression in BAL cells of mice

exposed to diABZI 1 μg as compared to saline controls, and colocalization of these PANoptosome components, indicative of PANoptosis complex (Fig. 5C).

Therefore, triggering airway STING activation by local administration of a potent STING agonist, diABZI, induced lung cell death through apoptosis, necroptosis, and pyroptosis, with evidence of PANoptosis complex formation, indicating STING-induced PANoptosis.

DiABZI-induced nucleic acid sensors and inflammasome expression

We next asked whether triggering the STING pathway induced further DNA sensors expression. We report STING overexpression and activation visible by increased STING dimers in immunoblots of lung tissue after endotracheal administration of 0.1–1 μg diABZI (Fig. 5D, E and supplemental Fig S5E). cGAS protein expression was also strongly increased in the lung after the diABZI challenge (Fig. 5D, E). DNA sensors cGAS gene *Mb21d1* and AIM2 are ISG, and their messages increased after the diABZI challenge, as were *Tmem173*, *Ifi204*, *Nlrp3*, less *Ddx41*, and >200-fold *Cxcl10* (Fig. 5F).

Therefore, triggering airway STING activation by local administration of the potent STING agonist diABZI induced DNA damage and overexpression of DNA sensors and inflammasomes that may fuel further inflammatory responses.

Self-dsDNA release contributes to diABZI-induced airway inflammation

To evaluate the contribution of the self-dsDNA released after diABZI administration to the induced lung inflammation through secondary responses, we treated mice receiving local airway diABZI with DNase I (Fig. 6A). Pulmozyme DNase I treatment at 50 μg i.t. on the 3 consecutive days of diABZI administration efficiently abrogated dsDNA in the BALF (Fig. 6B), and reduced neutrophil recruitment and CXCL10 release in the airways (Fig. 6C, D), while other parameters such as IFNα, IFNβ (Fig. 6E, F), MPO, IL-6, or TNFα were barely affected (Supplemental Fig. S3A–C).

DNase I treatment resulted in the impairment of NETs formation as evidenced by DNA, MPO and citrullinated Histone 3 immunofluorescence analysis (Fig. 6G), and decreased ZBP1 protein in the airways (Fig. 6H).

The CD45⁺ inflammatory cells recruited in the airways after diABZI local administration showed increased frequency and absolute counts of necrotic Annexin V⁺ Propidium Iodide (PI)⁺ and apoptotic Annexin V⁺ PI⁻ cells, that were largely abrogated by the DNase I treatment (Fig. 6I, J and supplemental Fig. S3D).

To evaluate the interplay between STING activation and NETs formation, we treated mice receiving local airway diABZI with Cl-amidine, an inhibitor of peptidyl arginine deiminase 4 (PAD4), an enzyme essential for NET formation (Fig. 6K). Cl-amidine treatment at 200 μg i.p. on the 3 consecutive days of diABZI administration efficiently prevented neutrophil recruitment and NETs in the BALF (Fig. 6L, M). Treatment with Cl-amidine also reduced NETs formation as evidenced by Cit-H3 immunoblot, and the expression of STING protein in the lung (Fig. 6N, O).

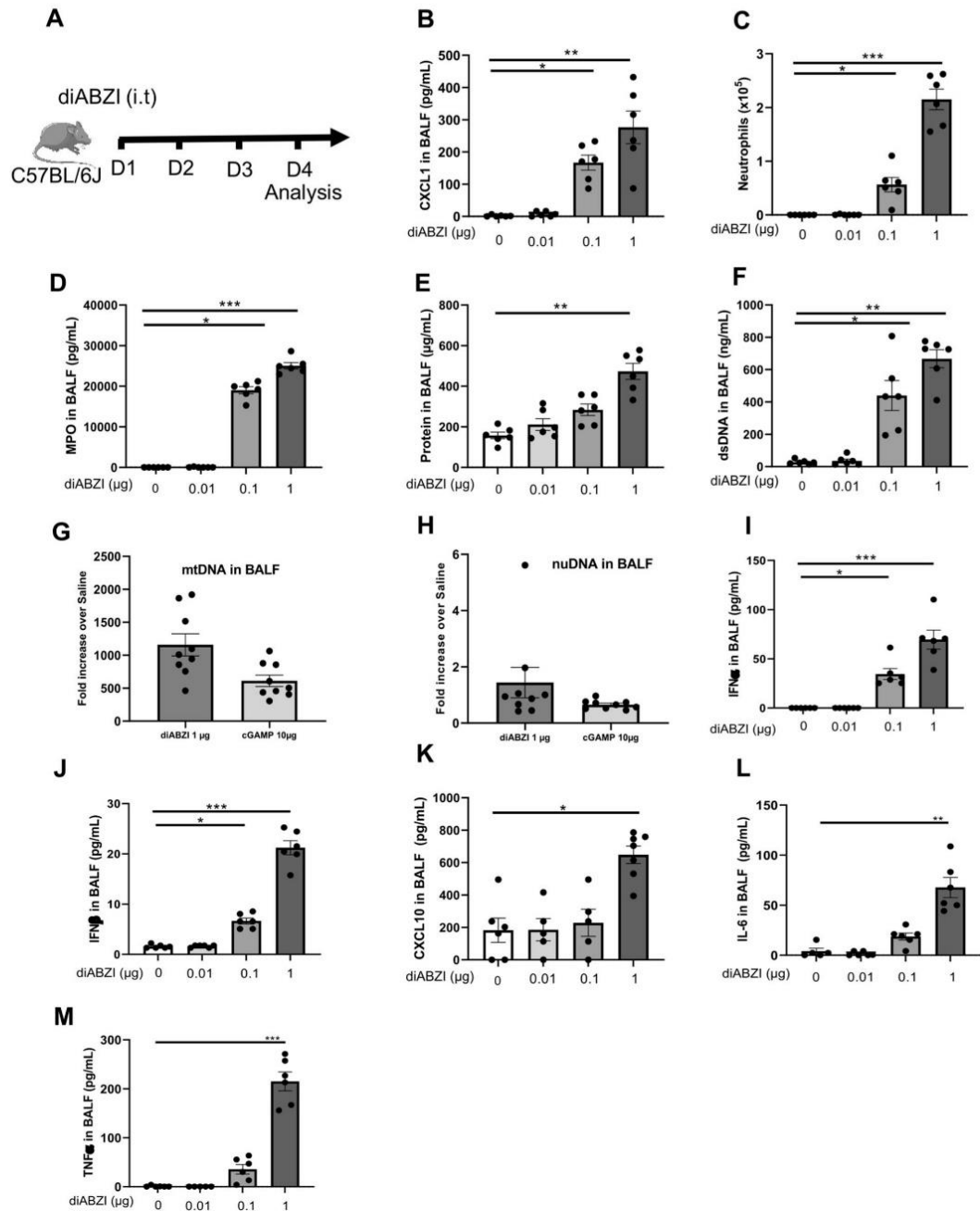


Fig. 4 STING agonist diABZI triggers neutrophilic airway inflammation. **A** STING agonist diABZI (0.01, 0.1, or 1 μg , i.t.) DMSO (0.25%) vehicle or saline were administered daily in WT mice for 3 consecutive days and parameters were analyzed on day 4. **B** Concentration of CXCL1/KC in the bronchoalveolar lavage fluid (BALF) determined by ELISA. **C** Neutrophils counts in BAL. **D** Concentration of myeloperoxidase (MPO) in BALF determined by ELISA. **E** Concentration of proteins in BALF. **F** Concentration of extracellular dsDNA in the acellular fractions of BAL. **G, H** Mitochondrial DNA (mtDNA) (**G**) and nuclear DNA (nDNA) (**H**) in the BALF after diABZI or cGAMP administration. **I–M** IFN α (**I**) and IFN β (**J**) determined by multiplex immunoassay, and CXCL10 (**K**), IL-6 (**L**), and TNF α (**M**) quantified by ELISA in the BALF. **N** Visualization of NETs in BAL and lung with the staining of DNA dye DAPI (cyan), MPO (green), and citrullinated Histone 3 (red). Bars, 20 μm . **O, P** Quantification of Cit-H3 staining intensity (**O**) and MPO staining intensity (**P**) in the lung. **Q, R** Correlation between MPO and Cit-H3 after diABZI administration at 0.1 μg (**Q**) and 1 μg (**R**). **S–W** Lung tissue histology PAS staining (**S**), with pathology scoring of the presence of epithelial injury (**T**), peribronchial infiltration of inflammatory cells (**U**), alveolitis (**V**), and emphysema (**W**). Bars, left panels: 2.5 mm, right panels: 250 μm . Graph data were presented as mean \pm SEM with $n = 5–6$ mice per group. Each point represents an individual mouse. * $p < 0.05$, ** $p < 0.01$, *** $p < 0.001$, **** $p < 0.0001$ (Nonparametric Kruskal–Wallis with Dunn post test).

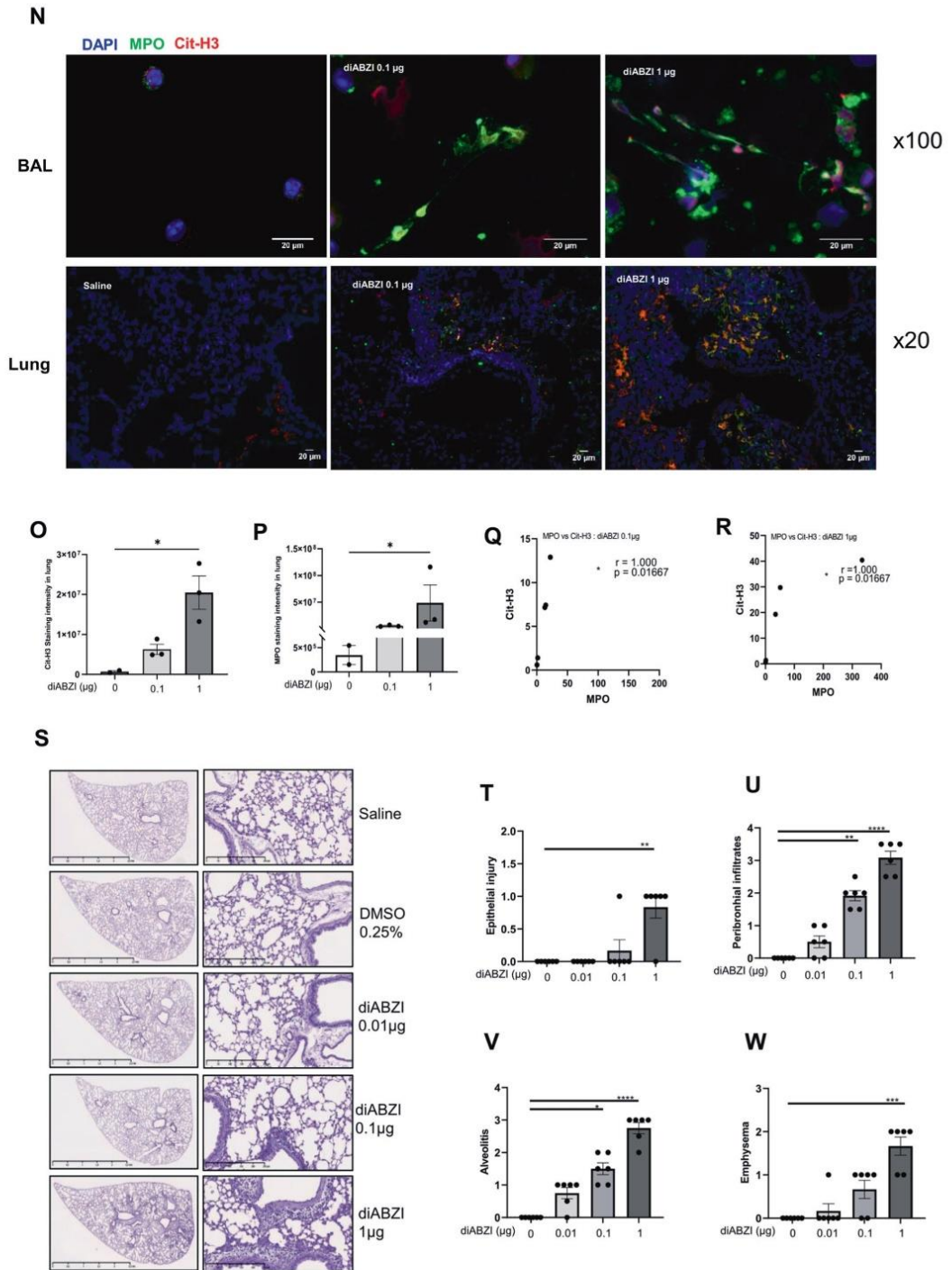


Fig. 4 (Continued)

To determine the link between NETosis and PANoptosis, we evaluated PANoptosis markers following Cl-amidine treatment in diABZI exposed mice. Cl-amidine treatment reduced diABZI-induced PANoptosis as evidenced by reduced cleaved caspase

3, caspase 3, cleaved GSDMD, GSDMD, pMLKL, MLKL, and ZBP1 proteins in lung, assessed by western blot (Fig. 6N, O and supplemental Fig S5F). Caspase 8, ASC, and RIPK3 protein expression in BAL cells was also reduced after Cl-amidine

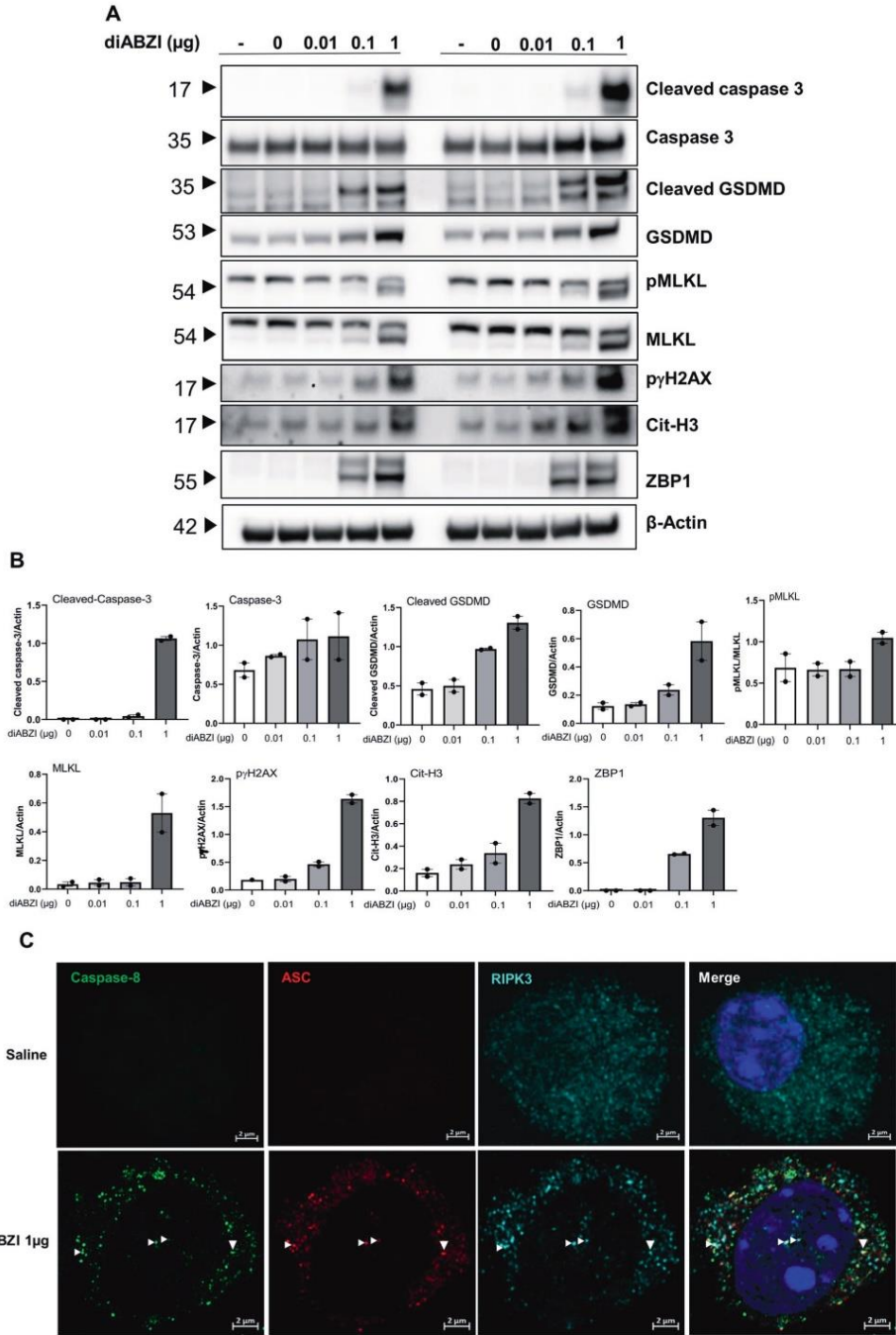


Fig. 5 (Continued)

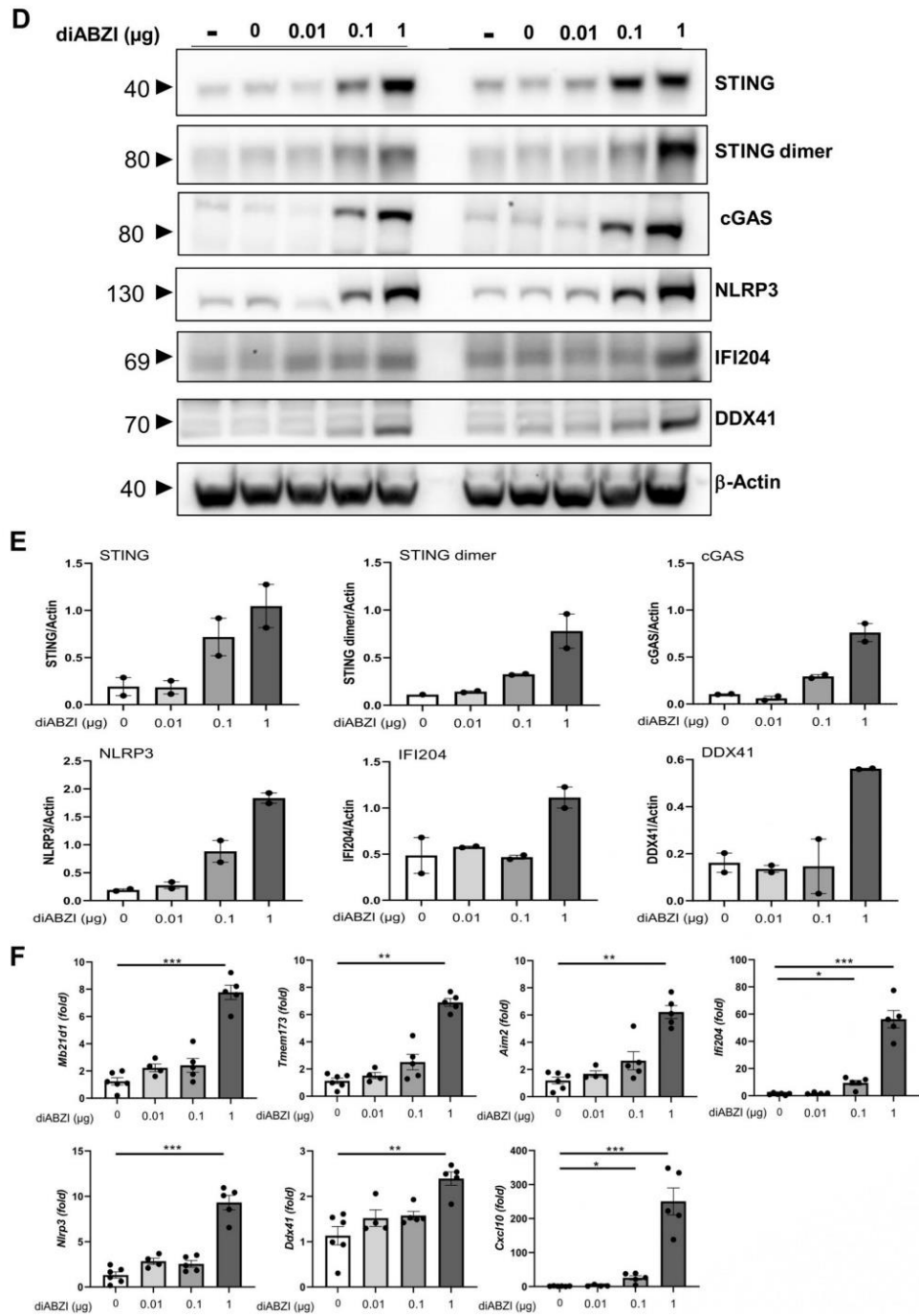


Fig. 5 (Continued)

treatment, as seen by immunofluorescence (Fig. 6P). The diABZI-induced release of dsDNA in the BALF (Fig. 6Q), damaged DNA documented by immunoblot of γH2AX in the lung (Fig. 6N, O), and overall lytic cell death measured by

Lactate dehydrogenase (LDH) release in the BALF (Fig. 6R) were alleviated by Cl-amidine treatment.

Thus, the airway inflammatory response to diABZI local administration is in part dependent on the released dsDNA and NET formation.

Fig. 5 Airway diABZI induces lung tissue PANoptosis and damage and STING pathway activation. diABZI (0.01, 0.1, or 1 μg , i.t.) or saline were administered daily in WT mice for 3 consecutive days as in Fig. 4 and parameters analyzed on day 4. **A** Immunoblots of cleaved Caspase 3, Caspase 3, cleaved Gasdermin D, Gasdermin D, phospho-MLKL, MLKL, phospho- γH2AX , citrullinated Histone 3 (Cit-H3), and ZBP1 with β -actin as a reference. **B** Immunoblot quantification of cleaved Caspase 3, Caspase 3, cleaved Gasdermin D, Gasdermin D, pMLKL, MLKL, phospho- γH2AX , citrullinated Histone 3 (Cit-H3), and ZBP1, normalized to β -actin. **C** Confocal microscopy showing Caspase 8 (green), ASC (red), RIPK3 (far-red/turquoise blue), and DNA dye DAPI (cyan) in BAL cells of mice exposed to saline or diABZI 1 μg , showing the colocalization of PANoptosome components. Bars, 2 μm . **D** Immunoblots of STING axis in the lung of WT mice including STING and STING dimer, cGAS, NLRP3, IFI204, DDX41 with β -actin as reference. **E** Immunoblot quantification of STING and STING dimer, cGAS, NLRP3, IFI204, and DDX41 normalized to β -actin. **F** *Mb21d1*, *Tmem173*, *Aim2*, *Ifi204*, *Nlrp3*, *Ddx41*, and *Cxcl10* transcripts were measured by real-time PCR. * $p < 0.05$, ** $p < 0.01$, *** $p < 0.001$. (Nonparametric Kruskal–Wallis test followed by Dunn post test). Graph data from real-time PCR are presented as mean \pm SEM with $n = 4$ –6 mice per group. Immunoblots representative of $n = 2$ samples from two independent experiments, quantified in bar graphs with $n = 2$.

DNA sensors dependence of diABZI-induced airway inflammation

As STING agonist cGAMP may activate alternative, noncanonical inflammasome priming, we first verified that the inflammatory airway response to diABZI administration is dependent on the STING pathway (Fig. 7A–D). Indeed, the recruitment of neutrophils and dsDNA release in the airways seen after endotracheal administration of 0.1–1 μg diABZI for 3 consecutive days in wild-type mice was absent in STING^{-/-} mice (Fig. 7A, B), as well as MPO release in BALF (Supplemental Fig. S4A). Further, IFN α and IFN β release in the airways was absent in STING^{-/-} mice (Fig. 7C and Supplemental Fig. S4B), as were both CXCL10, downstream of IRF3/type I IFN (Fig. 7D), and NF κ B-dependent IL-6 and TNF α (Supplemental Fig. S4C, D).

As dsDNA was released and cGAS expression was increased after diABZI administration, we then assessed the contribution of self-dsDNA-induced secondary responses, in cGAS-deficient mice. Interestingly, the airway inflammation induced by local diABZI administration was retained in cGAS^{-/-} mice, in terms of neutrophil recruitment, MPO, dsDNA, or cytokine release in the airways, including IFN α and IFN β , CXCL10, IL-6, or TNF α (Fig. 7E–H and supplemental Fig. S4E–H). This indicated a cGAS-independent response to diABZI and downstream dsDNA released. Similarly, while NLRP3 and AIM2 expression was increased after diABZI administration, the response to airway diABZI administration was unaffected in NLRP3^{-/-} and AIM2^{-/-} mice, in terms of neutrophil recruitment, MPO, dsDNA, or cytokine release in the airways, including IFN α and IFN β , CXCL10, IL-6, or TNF α (Fig. 7I–P and supplemental Fig. S4I–P). As expected, the inflammatory responses to diABZI were abrogated in IFNAR^{-/-} mice (Fig. 7I–L and supplemental Fig. S4I–L), and the neutrophilic response was reduced in TLR9^{-/-} mice (Fig. 7R–U and supplemental Fig. S4R–U).

Thus, the airway inflammatory response to diABZI local administration is fully dependent on STING and IFNAR, and extracellular DNA and TLR9 are central to diABZI-induced neutrophilic response, independently of cGAS, NLRP3, and AIM2 pathways.

DISCUSSION

Immunotherapy with STING agonists is promising in oncology including lung cancer, and in fighting SARS-COV2 airway infection in mice [4, 5]. As the STING pathway fuels sterile lung inflammation after exposure to silica microparticles [10] or cigarette smoke [11], we characterized the lung inflammatory response induced by endotracheal administration of STING agonists, endogenous CDN cGAMP, and synthetic diABZI. STING agonists triggered a neutrophilic response in the bronchoalveolar space, a strong pulmonary inflammatory response with loss of epithelial barrier function and ARDS, cell death and release of self-dsDNA, NETs formation, and type I IFN responses. Further, we show that STING agonists induce programmed cell death with features of pyroptosis, apoptosis, and necroptosis, indicative of

STING-dependent PANoptosis and that extracellular dsDNA is central to diABZI-induced neutrophilic response.

We questioned the origin of dsDNA released after administration of STING agonists in the airways. cGAMP has noncanonical functions in inflammasome activation, enhancing the expression of inflammasome components such as NLRP3 through IFN-I-dependent response, while activating the inflammasomes through an AIM2, NLRP3, ASC, and caspase-1 dependent process [19]. STING activation may orchestrate a lysosomal cell death program engaging NLRP3 inflammasome after cytosolic DNA recognition [12]. The complex interactions of cGAS-STING signaling and different cell death pathways has been reviewed recently [20] and the role of STING in PANoptosis questioned. Here, we show that triggering STING directly via diABZI STING agonist administration triggered apoptosis, NETosis, and DNA damage, as evidenced by an increased presence of cleaved caspase 3, Cit-H3, and γH2AX in the lung of treated mice. In addition, we show in the same setting that markers of pyroptosis, apoptosis, and necroptosis were present, and colocalized in inflammatory cells recruited in the airways, indicative of STING-induced PANoptosis.

The ectopic presence of nucleic acids in the cytosol represents a danger signal activating the cytosolic surveillance system, which may, in turn, activate DNA sensors. This is particularly the case for mitochondrial DNA, released after cellular and mitochondrial stress. Here, exposure to STING agonists yielded predominantly release of mitochondrial DNA over nuclear DNA in the airway. Self-dsDNA was an integral part of the response, as degradation of extracellular DNA by local administration of DNase I prevented diABZI-induced neutrophilic response in the airways. The expression of several DNA sensors, including cGAS, NLRP3, AIM2, IFI204, and DDX41, was increased after STING agonist-induced lung inflammation. While the airway inflammatory response to diABZI was fully dependent on STING and type I IFN, as expected, we showed that TLR9 is central to diABZI-induced neutrophilic response, independently of cGAS, NLRP3, and AIM2 pathways. Although CpG nucleotides are likely masked by methylation in mammalian self-DNA, cationic antimicrobial peptides such as LL37, human β -defensin (hBD)2, hBD3, or lysozyme condense self-DNA into particles that are endocytosed and trigger TLR9 activation and type I response in pDC and psoriatic skin lesions [21, 22].

In conclusion, the present findings establish that administration of STING agonists in the airways, besides activating type I IFN response, induces PANoptosis, dsDNA release, and NETosis, leading to neutrophilic lung inflammation and ARDS in a cGAS-independent, TLR9-dependent manner. Targeting STING activation as a therapeutic strategy for local cancer metastasis or infection may thus include a component of lung inflammation.

METHODS

Mice

Female C57BL/6J mice were purchased from Janvier Laboratories (Le Genest St Isle, France). Wild-type mice and mice deficient for STING

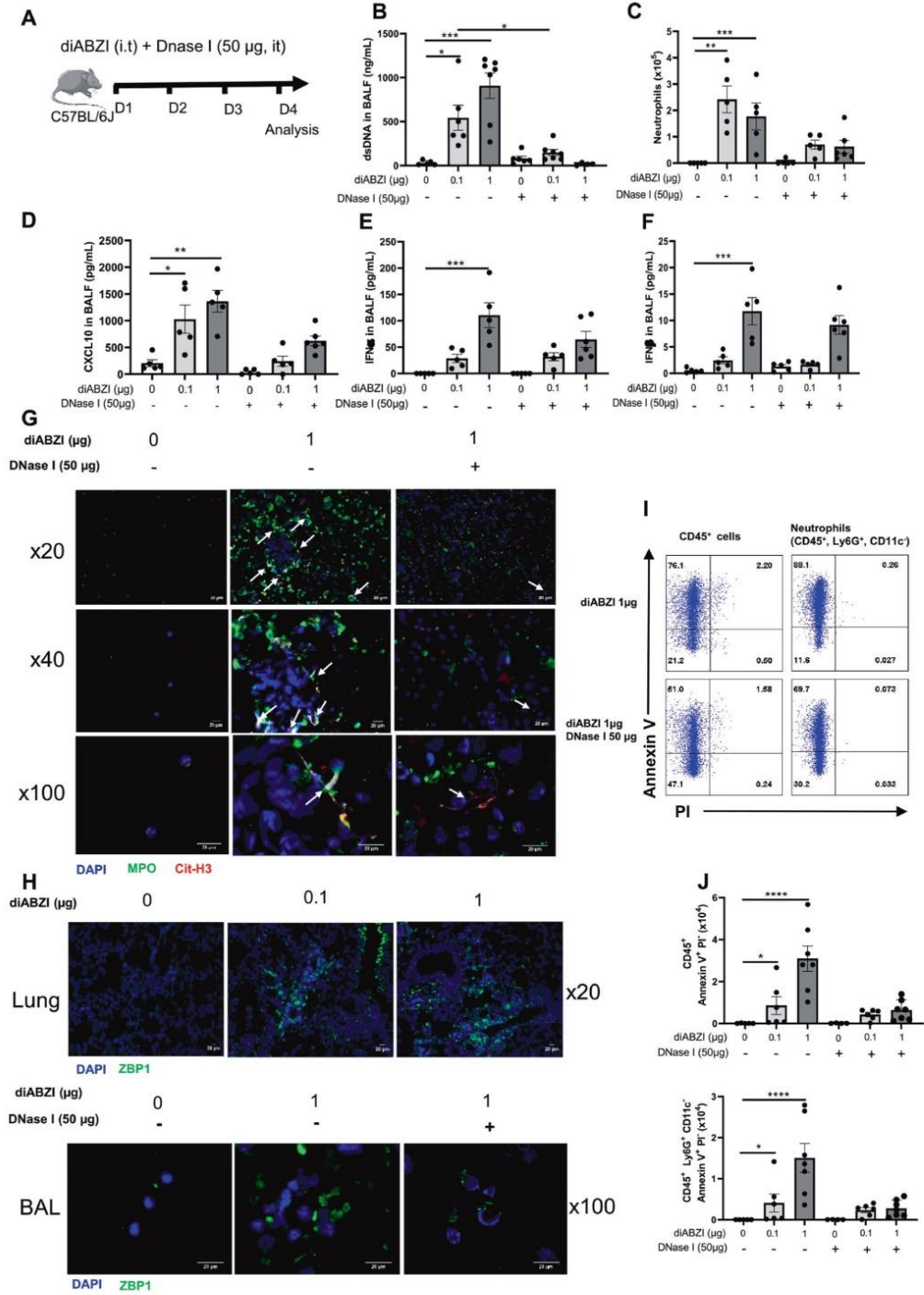


Fig. 6 (Continued)

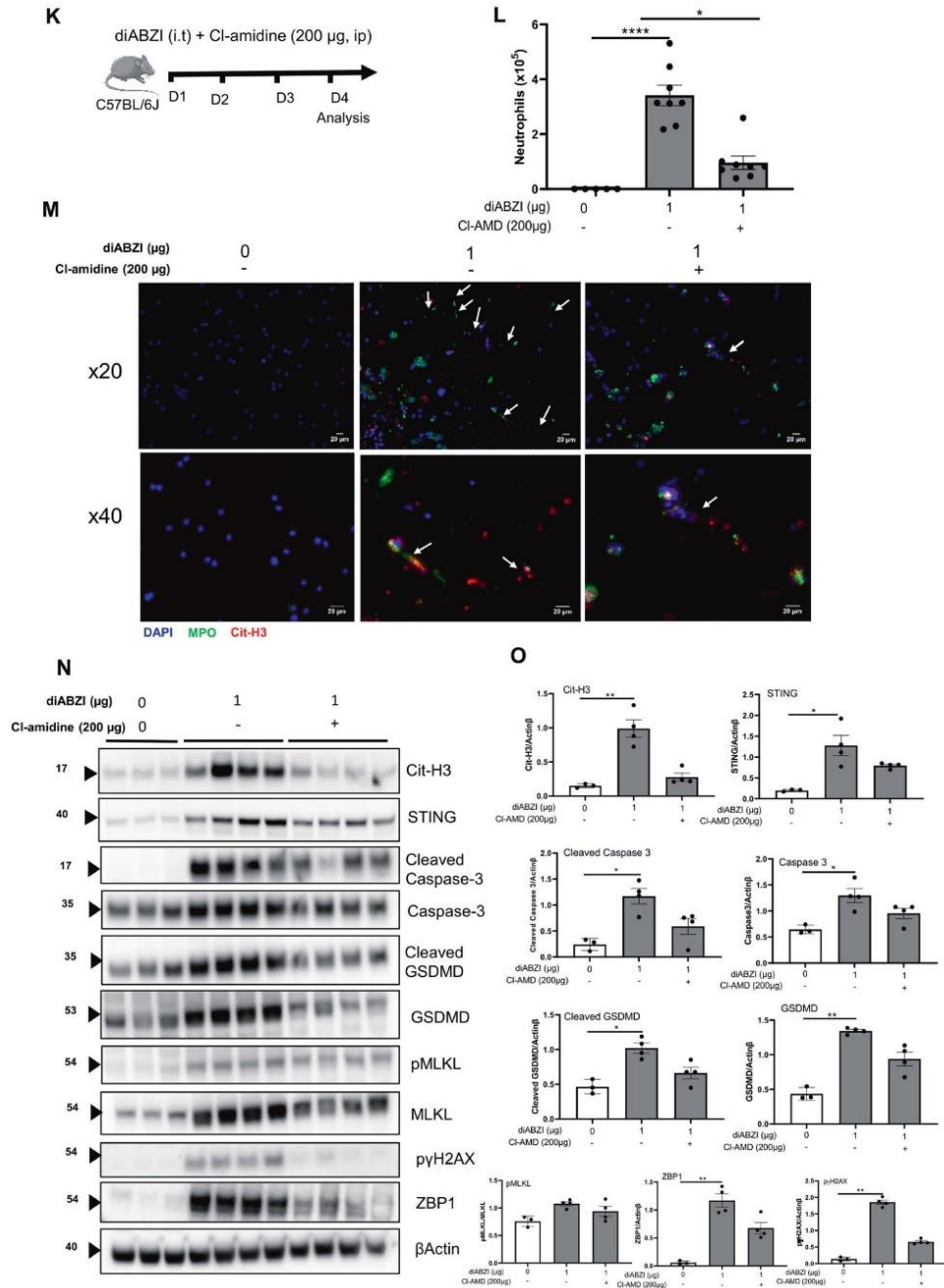


Fig. 6 (Continued)

(STING^{-/-}) [23], cGAS (cGAS^{-/-}) [24], IFNAR (IFNAR^{-/-}) [25], TLR9 (TLR9^{-/-}) [26], NLRP3 (NLRP3^{-/-}) [27], AIM2 (AIM2^{-/-}) [28] were bred and housed under specific pathogen-free conditions at CNRS animal facility (TAAM UAR44, Orleans, France). They were maintained in a 12-h light-dark cycle with food and water ad libitum, following European and local legislation. Age-matched, 8- to 12- week-old mice were used for

experiments. All animal experiments complied with the French Government animal experiment regulations and ARRIVE guidelines. The protocols were submitted to the “Ethics Committee for Animal Experimentation of CNRS Campus Orleans” (CCO) under numbers CLE CCO 2015-1087 and CLE CCO 2020-2018 and approved by the French Minister under APAFIS #19361 and #25360.

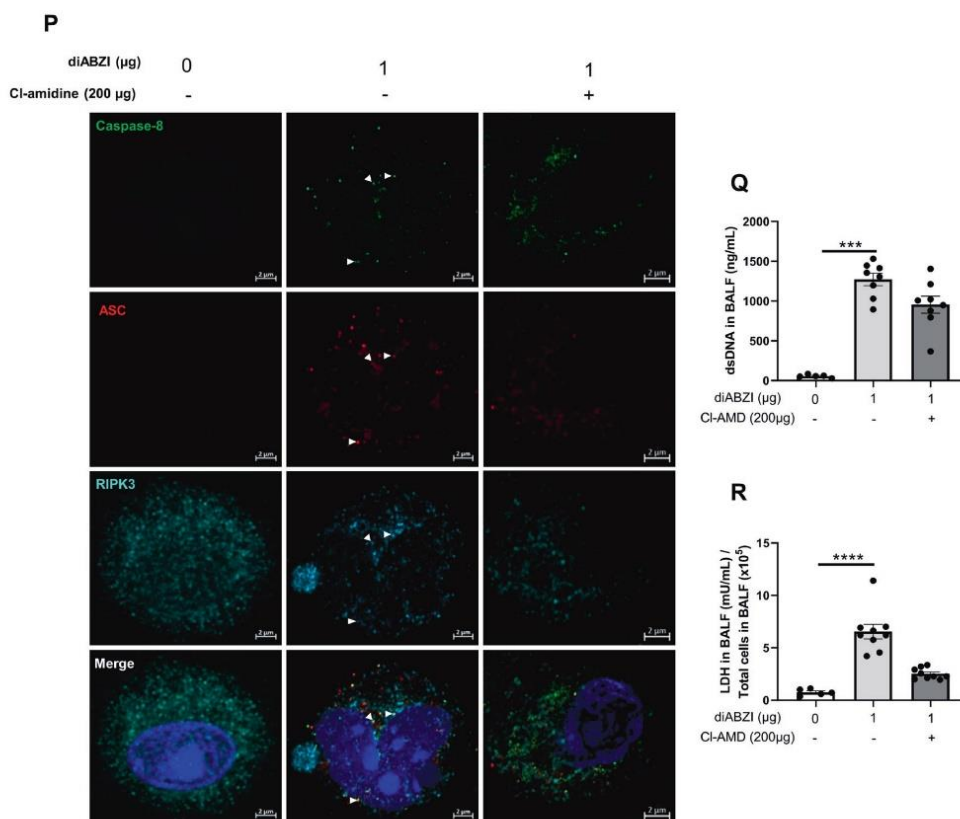


Fig. 6 DNase I treatment or NET inhibition reduce diABZI-induced neutrophilic airway inflammation. **A** diABZI (0.1 or 1 µg, i.t.) were administered with DNase I (50 µg/mouse, i.t.) daily in WT mice for 3 consecutive days and parameters were analyzed on day 4. **B** Extracellular dsDNA in acellular fraction of BAL. **C** Neutrophils counts in BAL. **D** Concentration of CXCL10 in BALF, determined by ELISA. **E, F** IFN α (**E**) and IFN β (**F**) in BALF are determined by multiplex immunoassay. **G** Visualization of NETs with staining of DNA (DAPI, cyan), MPO (green), and Cit-H3 (red) in cells from BAL. Bars 20 µm, magnification x20 upper panels, x40 middle panels, x100 lower panels. **H** Visualization of PANoptosis with stainings of ZBP1 (vert) and DNA (DAPI, cyan) in cells from lung and BAL. Bars 20 µm, magnification x20 (Lung), x100 (BAL). **I, J** Annexin V/PI flow cytometry analysis pre-gated on singlet cells, and CD45⁺ (leukocytes) or CD45⁺Ly6G⁺CD11c⁺ (neutrophils). **K** diABZI (1 µg, i.t.) was administered alone or with Cl-amidine (200 µg/mouse, i.p.) daily in WT mice for 3 consecutive days and parameters were analyzed on day 4. **L** Neutrophils counts in BAL. **M** Visualization of NETs with staining of DNA (DAPI, cyan), MPO (green), and Cit-H3 (red) in cells from BAL; Bars 20 µm, magnification x20 upper panels, x40 lower panels. **N** Immunoblots of Cit-H3, STING, cleaved caspase 3, caspase 3, cleaved Gasdermin D, Gasdermin D, phospho-MLKL, MLKL, phospho- γ H2AX, and ZBP1 in the lung of WT mice exposed to diABZI alone or treated with Cl-amidine, with β -actin as reference. **O** Immunoblot quantification of Cit-H3, STING, cleaved caspase 3, caspase 3, cleaved GSDMD, GSDMD, phospho- γ H2AX and ZBP1 normalized to β -actin, and phospho-MLKL normalized to MLKL. **P** Confocal microscopy showing Caspase 8 (green), ASC (red), RIPK3 (far-red/turquoise blue), and DNA dye DAPI (cyan) in BAL from mice challenged with diABZI at 1 µg and treated with Cl-amidine or saline. PANoptosome formation is illustrated by colocalization of the components of PANoptosome in the merged image (indicated by arrowheads). Bars, 2 µm. **Q** Concentration of extracellular dsDNA in the acellular fraction of BALF. **R** Lactate dehydrogenase (LDH) quantification in the acellular fraction of BALF. Graph data were presented as mean \pm SEM with $n = 5-8$ mice/group. Each point represents an individual mouse. * $p < 0.05$, ** $p < 0.01$, *** $p < 0.001$. (Nonparametric Kruskal-Wallis test followed by Dunn post test).

In vivo animal experiments

Mice were anesthetized with 2% Isoflurane (ISO-VET, Netherlands) and challenged intratracheally (i.t.) with cGAMP (1–10 µg in 40 µL, Invitrogen, California) or diABZI, a STING agonist 3 (0.01 to 1 µg in 40 µL, Cayman chemicals, Michigan) or saline (NaCl 0.9%) for 3 consecutive days. Bronchoalveolar lavage (BAL) was performed 24 h after the last challenge by flushing lung tissue four times with 0.5 mL of cold NaCl 0.9% via a cannula inserted in the trachea. BALF was collected, cells counted and cytopspins performed. The supernatant of the first lavage was collected after centrifugation and stored at -80°C for dsDNA quantification. The left lung lobe was harvested for histology, the post caval lung for RNA extraction and qPCR analysis, and the right lobes for Western blots analysis and cytokines measurement. Protein extravasation in the BALF was measured by Pierce[™] BCA Protein Assay (ThermoFisher[™], Massachusetts).

Immunoblots

Lung tissues were homogenized in T-PER[™] buffer supplemented with a cocktail containing protease and phosphatase inhibitors (halt[™], ThermoFisher). Total protein was extracted and quantified by using Pierce[™] BCA Protein Assay Kit (ThermoFisher[™]). Total protein (40 µg) was treated with NuPAGE[™] LDS sample buffer and sample reducing agent (ThermoFisher[™]), and heated 10 min at 70°C . Samples were resolved on 4–12% polyacrylamide gel (Bolt[™] Mini protein gel, ThermoFisher) and run at 160 V for 45 min using the Mini gel Tank (ThermoFisher[™]). Total proteins were electroblotted to 0.2 µm nitrocellulose membrane (Amersham[™], UK) using a Trans-Blot SD Transfer System (Bio-Rad, California) at 100 V for 45 min. Successful protein transfer was confirmed by using Ponceau S staining. Membranes were blocked with 5% nonfat milk (Cell signaling, Massachusetts) in 1X TBST (20 mM Tris Base,

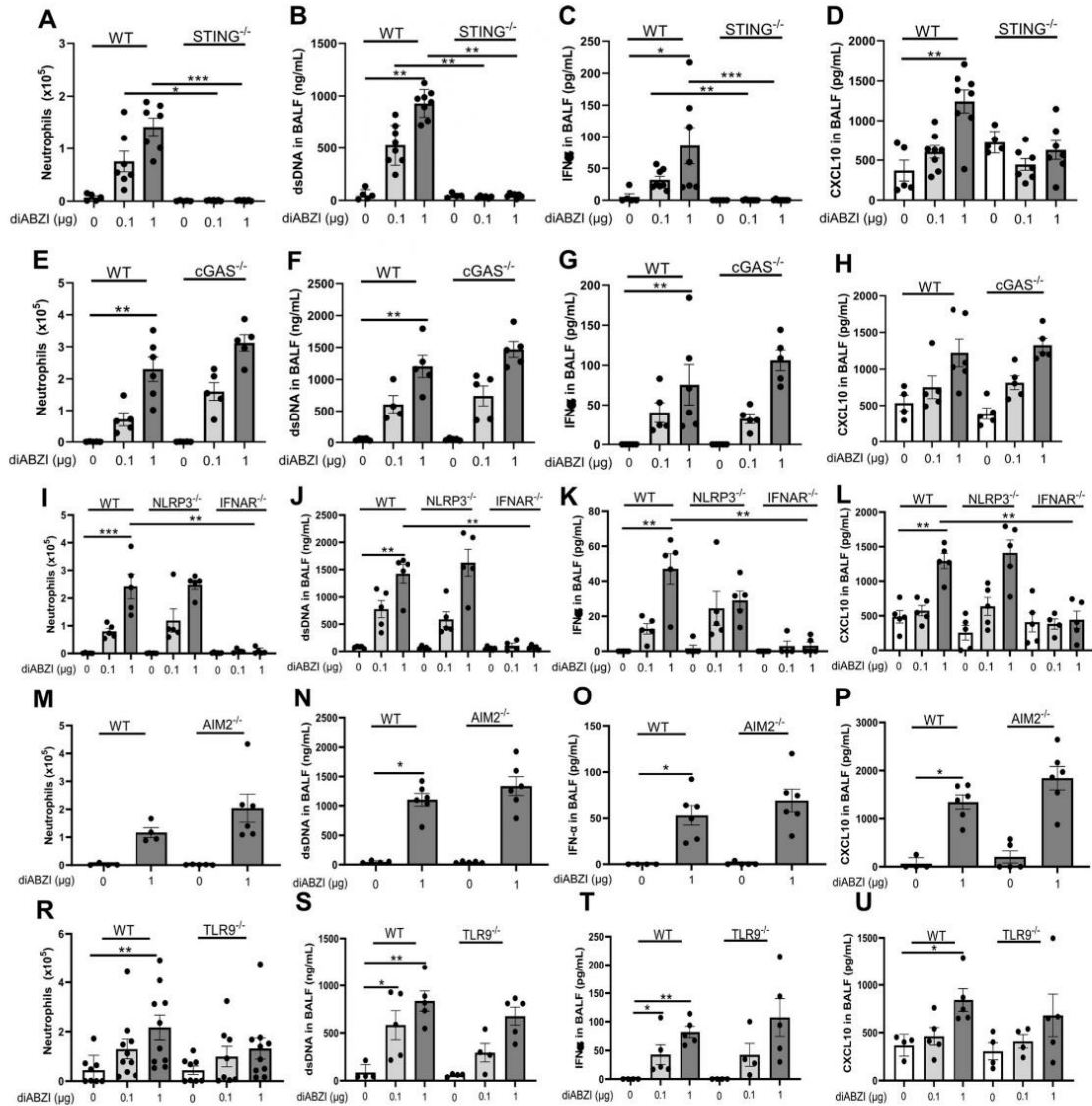


Fig. 7 **STING is the major sensor of diABZI-induced lung inflammation.** DiABZI (0.1 or 1 μg , i.t.) or saline were administered daily in $\text{STING}^{-/-}$, $\text{cGAS}^{-/-}$, $\text{NLRP3}^{-/-}$, $\text{IFNAR}^{-/-}$, $\text{AIM2}^{-/-}$, $\text{TLR9}^{-/-}$, and WT mice for 3 consecutive days and parameters analyzed on day 4. **A–D** Neutrophils (**A**), concentrations of dsDNA (**B**), $\text{IFN}\alpha$ (**C**), and CXCL10 (**D**) in BALF in WT and $\text{STING}^{-/-}$ mice. **E–H.** Neutrophils (**E**), dsDNA (**F**), $\text{IFN}\alpha$ (**G**), and CXCL10 (**H**) concentration in BALF in WT and $\text{cGAS}^{-/-}$ mice. **I–L** Neutrophils (**I**), dsDNA (**J**), $\text{IFN}\alpha$ (**K**), and CXCL10 (**L**) concentration in BALF in WT and $\text{NLRP3}^{-/-}$ and $\text{IFNAR}^{-/-}$ mice. **M–P** Neutrophils (**M**), dsDNA (**N**), $\text{IFN}\alpha$ (**O**), and CXCL10 (**P**) concentration in BALF in WT and $\text{AIM2}^{-/-}$ mice. **R–U** Neutrophils (**R**), dsDNA (**S**), $\text{IFN}\alpha$ (**T**), and CXCL10 (**U**) concentration in BALF in WT and $\text{TLR9}^{-/-}$ mice. Graph data were presented as mean \pm SEM with $n = 4$ –10 mice/group, each point representing an individual mouse. * $p < 0.05$, ** $p < 0.01$, *** $p < 0.001$. (Nonparametric Kruskal–Wallis test followed by Dunn post test).

150 mM sodium chloride, and 0.05% Tween-20 pH 7.6) for 1 h at room temperature.

Full membranes or portions of membranes were incubated overnight using primary antibodies from rabbit anti-phospho-STING (#72971 1/500; Cell signaling), anti-STING (#13647 1/500; Cell signaling), anti-phospho-TBK1 (#5483 1/500; Cell signaling), anti-TBK1 (#3504 1/500; Cell signaling), anti-phospho-IRF3 (#4947 1/500; Cell signaling), IRF3 (#4302 1/500; Cell signaling), anti-phospho-NF- κB (#3031 1/500; Cell signaling), anti-NF- κB (#4764 1/500; Cell signaling), anti-cGAS (#31659 1/500; Cell signaling), anti-NLRP3 (#15101 1/500; Cell signaling), anti-MLKL (#37705 1/500; Cell

signaling), anti-phospho-MLKL (#37333 1/500; Cell signaling), anti-GSDMD (#ab209845 1/500; Abcam), anti-cleaved GSDMD (#10137 1/500; Cell signaling), anti-cleaved Caspase 3 (#9661 1/500), anti-Caspase 3 (#9662 1/500; Cell signaling), anti-phospho- γH2AX (#9718 1/500; Cell signaling), anti- γH2AX (#7631 1/500; Cell signaling), anti-histone H3 (#ab5103 1/500; Abcam, UK), anti-IFI204 (#ab228512 1/500; Abcam), anti-phospho-STAT1 (#9167 1/500; Cell signaling), anti-STAT1 (#14994 1/500; Cell signaling), mouse anti-ZBP1 (#5C-271483 1/300; Santa Cruz, Texas), and anti actin (#A3854 1/10000; Sigma-Aldrich, Massachusetts). Membranes were washed in TBS-T three times for 10 min each at room temperature, and then

incubated with goat anti-rabbit-IgG-HRP-conjugate (#7074 1/2000; Cell signaling) or horse anti-mouse-IgG-HRP-conjugate (#7076 1/2000; Cell signaling) diluted in 5% nonfat milk in TBS-T for 1 h at RT.

The membranes were washed three times in TBS-T. Protein bands were visualized following exposure of the membrane to Amersham ECL™ prime substrate solution (Cytiva, Massachusetts) on film (PXi gel doc system*, India), and quantified by densitometry analysis using ImageJ software. Uncropped immunoblot gels are shown in Supplemental Fig. S5.

Immunofluorescence staining of lung and BAL cells

Lungs were fixed with 4% formalin for 72 h, embedded in paraffin, and sectioned at 3 µm. Lung sections were dewaxed and rehydrated, then heated 20 min at 80 °C in citrate buffer 10 mM pH = 6 for antigen retrieval (unmasking step). Lung sections were permeabilized in PBS 0.5% triton X-100, blocked with 5% FCS for 1 h at RT, and then incubated overnight with primary goat antibodies to MPO (1:40, R&D systems, Minneapolis) and rabbit anti-H3-citrulline (1:100, Abcam, UK) or mouse anti-ZBP1 (1:100, Santa Cruz, Texas). After washing, the sections were incubated with donkey anti-rabbit IgG secondary antibodies conjugated with AlexaFluor568 (1:500, Invitrogen, Massachusetts) and anti-goat IgG secondary antibodies conjugated with AlexaFluor488 (1:200, Invitrogen) or with goat anti-mouse IgG conjugated with AlexaFluor488 in 1% FCS. Following washing, lung sections were stained with DAPI (1:1000) for 10 min, washed with PBS, and mounted onto microscope slides (Fluoromount-G, Invitrogen).

Cytospin slides were fixed in 4% PFA. Cells were washed three times in TBS, incubated 15 min in TBS-0.3% Triton X-100, then washed three times in TBS, blocked in TBS-10% FCS for 45 min and incubated overnight at 4 °C with primary antibodies to MPO (1:40, R&D systems), and to histone H3-citrulline (1:100, Abcam) for NETs visualization. For PANoptosome visualization slides were incubated with primary antibodies from mouse anti-ZBP1 (1:100, Santa Cruz), rat anti-Caspase 8 (1: 100, Enzo Lifesciences, France), goat anti-ASC (1:50, Abcam), and mouse anti-RIPK3 (B-2) Alexa Fluor® 647 (1:30, Santa Cruz Biotechnology). After washing, slides were incubated as described above for NETs formation and ZBP1 detection. For analysis of PANoptosome formation, slides were incubated with donkey anti-goat IgG secondary antibodies conjugated with AlexaFluor488 (1:200, Invitrogen) and goat anti-rat secondary antibodies Alexa Fluor 546. Slides were stained using DAPI for 10 min. For NETs and ZBP1 visualization, cells were observed using a Leica DM 6000B microscope (Leica Camera, Wetzlar, Germany), images were acquired using MetaMorph® software, and were treated using ImageJ software. For PANoptosome visualization, cells were observed using a Zeiss LSM 980 microscope coupled with a Zeiss Airyscan 2 device (Carl Zeiss Co. Ltd., Jena, Germany). Images were acquired using Zeiss LSM Image Browser (Carl Zeiss Co. Ltd., Jena, Germany).

Flow cytometry

Bronchoalveolar lavage cells were counted and plated on a 96 well plate for extracellular staining. Different subsets of lung infiltrating cells or resident cells were detected by flow cytometry in BAL cell suspensions using a mix of the following fluorochrome-conjugated antibodies against mouse (CD45-PE-Cy7 1/200, eBiosciences, California), (Siglec F-PE-CF59, 1/300, BD Bioscience, New Jersey), (Ly6G-FITC, 1/200), (CD3-AF700, 1/100, BD bioscience), (B220-BV711, 1/200), (Epcam-5B645, 1/100, Invitrogen, Massachusetts), (CD11c-BV605, 1/200), (F4/80-BV42, 1/200), and (Fc Block, 1/200) to avoid nonspecific binding. Early apoptosis to late apoptosis/necrosis in the detected cell populations was assessed by using Annexin V-APC and Propidium Iodide Apoptosis Detection Kit I (BD Bioscience). All staining reactions were performed at RT for 20 to 30 min. Flow cytometry analyses were performed on an LSR Fortessa X-20 flow cytometer (Becton Dickinson, New Jersey). The gating strategy was set up according to FMO control for all antibodies. Analysis and graphical output were performed using FlowJo™ software (Tree Star, Ashland, OR).

Cell Culture and stimulation

Bone marrow-derived macrophages (BMDMs) were generated by differentiating mouse bone marrow cells for 10 days in DMEM medium (Life Technologies) supplemented with 10% heat-inactivated fetal calf serum (FCS, Life Technologies, Massachusetts), 100 U/mL penicillin, 100 µg/mL streptomycin (Gibco, Australia), 2 mM glutamine (Sigma-Aldrich, Missouri), 20% horse serum, and 30% (v/v) L929 conditioned medium as a source of

M-CSF. On day 10, BMDMs were seeded in 24 wells plate at 10⁶ cells/well and stimulated with cGAMP (14 µM) or diABZI (0.3 and 1 µM) in DMEM containing 0.2% heat-inactivated FCS.

Human airway epithelial cells (hAEC, Epithelix, Switzerland), passage 1, isolated from bronchial biopsies were maintained in 75 cm² flasks in the hAEC growth medium (Epithelix) and incubated at 37 °C and 5% CO₂. hAEC (passage 8) were seeded in 24 wells plate at 5 × 10⁵ cells/well and stimulated after 4 h when they reached 80% confluence. Cells were stimulated with diABZI (1; 3 and 10 µM) and 2',3'-cGAMP (14 µM) diluted in DMEM (Life Technologies, Massachusetts) supplemented with 2 mM L-glutamine, 2 mM of sodium pyruvate, 100 U/mL penicillin, 100 µg/mL streptomycin (Life Technologies), and 0.2% heat-inactivated FCS for 24 h at 37 °C and 5% CO₂.

Double-stranded DNA measurement in BALF

dsDNA was measured in the acellular fraction of the BALF using Quant-iT PicoGreen (Invitrogen, Massachusetts) according to the manufacturer's protocol.

Quantification of mitochondrial versus nuclear DNA

Mitochondrial and nuclear DNA were quantified as described previously [10]. Briefly, total DNA released in the BALF was purified using NucleoSpin Tissue Genomic DNA from tissue (Macherey-Nagel) and quantified by real-time PCR (10 ng/well). Primers for mouse mtDNA (mMitoF1 and mMitoR1) and mouse B2M (mB2MF1 and mB2MR1) that do not co-amplify nuclear mitochondrial insertion sequences (NumtS), mouse fragments of the mitochondrial genome present in the nuclear genome in the form of pseudogenes, were used [29]. The quantitative real-time PCR were performed in AriaMx Real-Time PCR System.

Lactate dehydrogenase (LDH) measurement in BALF

Cytotoxicity was determined by quantifying lactate dehydrogenase (LDH) released in the acellular fraction of the BALF using LDH-Glo™. Cytotoxicity assay kit (Promega) according to the manufacturer's instructions.

Quantification of mRNA expression by RT-qPCR analysis

Total mRNA was extracted using TRIzol (TRI-Reagent, Sigma-Aldrich, Germany) and reverse transcribed in cDNA with GoScript™ Reverse Transcription kit (Promega, Wisconsin). Genes mRNA expression were analyzed using GoTaq™ qPCR Master Mix (Promega). All primer sequences used were from Qiagen: *Tmem173* (#QT00261590), *Mb21d1* (#QT00131929), *Nlrp3* (#QT00122458), *Ifi204* (#QT01753535), *Ddx41* (#QT00137130), *Aim2* (#QT00266819), *Cxcl10* (#QT00093436), *Ifna2* (#QT00253092), *Ifna4* (#QT01774353), and *Ifnβ1* (#QT00249662). RNA expression was normalized to *Rn18s* expression (Qiagen, Maryland). Data were analyzed using the comparative analysis of relative expression by $\Delta\Delta C_t$ methods.

Histology

Lung left lobe was removed and fixed in 4% formalin, embedded in paraffin, sectioned at 3 µm, stained with periodic acid-Schiff (PAS), and blindly scored by an anatomo-pathologist. Semi-quantitative scoring (0–5) of airway inflammation and damage including epithelial injury, peribronchial infiltrates, alveolitis, and emphysema severity was performed.

Measurement of cytokine levels

MPO, IL-6, TNFα, CXCL1, IL-10, and CXCL10 concentrations in BALF or cell culture supernatant were measured by ELISA (R&D System, Minneapolis). IFNα and IFNβ levels were measured in BALF or cell culture supernatant by multiplex immunoassay according to manufacturers' instructions (ProcartaPlex, Life Technologies, Massachusetts). Data were acquired on Luminex equipment (MagPix, Bio-Rad, California) and analyzed using Bioplex Manager software (Bio-Rad).

Statistical analysis

Statistic analysis was performed with GraphPad Prism 8.0 software (San Diego). Statistical significance was determined by one-way ANOVA followed by Kruskal–Wallis multiple-comparisons tests or two-way ANOVA followed by Dunn post test as indicated in figure legends. *P* value < 0.05 was considered significant. **p* < 0.05, ***p* < 0.01, ****p* < 0.001 and *****p* < 0.0001. All data were shown as mean ± SEM.

DATA AVAILABILITY

All datasets generated and analysed during this study are included in this published article and its Supplementary Information files. Additional data are available from the corresponding author on reasonable request.

REFERENCES

- Motedayen Aval L, Pease JE, Sharma R, Pinato DJ. Challenges and opportunities in the clinical development of STING agonists for cancer immunotherapy. *J Clin Med*. 2020;9:3323.
- Woo SR, Fuertes MB, Corrales L, Spranger S, Furdyna MJ, Leung MY, et al. STING-dependent cytosolic DNA sensing mediates innate immune recognition of immunogenic tumors. *Immunity*. 2014;41:830–42.
- Le Naour J, Zitvogel L, Galluzzi L, Vacchelli E, Kroemer G. Trial watch: STING agonists in cancer therapy. *Oncoimmunology*. 2020;9:1777624.
- Humphries F, Shmuel-Galia L, Jiang Z, Wilson R, Landis P, Ng SL, et al. A diaminobenzimidazole STING agonist protects against SARS-CoV-2 infection. *Sci Immunol*. 2021;6:eabi9002.
- Li M, Ferretti M, Ying B, Descamps H, Lee E, Dittmar M, et al. Pharmacological activation of STING blocks SARS-CoV-2 infection. *Sci Immunol*. 2021;6:eabi9007.
- Gajewski TF, Higgs EF. Immunotherapy with a sting. *Science*. 2020;369:921–2.
- Hanson MC, Crespo MP, Abraham W, Moynihan KD, Szeto GL, Chen SH, et al. Nanoparticle STING agonists are potent lymph node-targeted vaccine adjuvants. *J Clin Invest*. 2015;125:2532–46.
- Liu Y, Crowe WN, Wang L, Lu Y, Petty WJ, Habib AA, et al. An inhalable nanoparticle STING agonist synergizes with radiotherapy to confer long-term control of lung metastases. *Nat Commun*. 2019;10:5108.
- Benmerzoug S, Ryffel B, Togbe D, Quesniaux VFJ. Self-DNA sensing in lung inflammatory diseases. *Trends Immunol*. 2019;40:719–34.
- Benmerzoug S, Rose S, Bounab B, Gosset D, Duneau L, Chenuet P, et al. STING-dependent sensing of self-DNA drives silica-induced lung inflammation. *Nat Commun*. 2018;9:5226.
- Nascimento M, Gombault A, Lacerda-Queiroz N, Panek C, Savigny F, Sbeity M, et al. Self-DNA release and STING-dependent sensing drives inflammation to cigarette smoke in mice. *Sci Rep*. 2019;9:14848.
- Gaidt MM, Ebert TS, Chauhan D, Ramshorn K, Pinci F, Zuber S, et al. The DNA inflammasome in human myeloid cells is initiated by a STING-cell death program upstream of NLRP3. *Cell*. 2017;171:1110–24 e1118.
- Samir P, Malireddi RKS, Kanneganti TD. The PANoptosome: a deadly protein complex driving pyroptosis, apoptosis, and necroptosis (PANoptosis). *Front Cell Infect Microbiol*. 2020;10:238.
- Ramanjulu JM, Pesiridis GS, Yang J, Concha N, Singhaus R, Zhang SY, et al. Design of amidobenzimidazole STING receptor agonists with systemic activity. *Nature*. 2018;564:439–43.
- Gulen MF, Koch U, Haag SM, Schuler F, Apetoh L, Villunger A, et al. Signalling strength determines proapoptotic functions of STING. *Nat Commun*. 2017;8:427.
- Christgen S, Zheng M, Kesavardhana S, Karki R, Malireddi RKS, Banoth B, et al. Identification of the PANoptosome: a molecular platform triggering pyroptosis, apoptosis, and necroptosis (PANoptosis). *Front Cell Infect Microbiol*. 2020;10:237.
- Wang Y, Kanneganti TD. From pyroptosis, apoptosis and necroptosis to PANoptosis: a mechanistic compendium of programmed cell death pathways. *Comput Struct Biotechnol J*. 2021;19:4641–57.
- Fritsch M, Gunther SD, Schwarzer R, Albert MC, Schorn F, Werthenbach JP, et al. Caspase-8 is the molecular switch for apoptosis, necroptosis and pyroptosis. *Nature*. 2019;575:683–7.
- Swanson KV, Junkins RD, Kurkjian CJ, Holley-Guthrie E, Pendse AA, El Morabiti R, et al. A noncanonical function of cGAMP in inflammasome priming and activation. *J Exp Med*. 2017;214:3611–26.
- Murthy AMV, Robinson N, Kumar S. Crosstalk between cGAS-STING signaling and cell death. *Cell Death Differ*. 2020;27:2989–3003.
- Lande R, Chamilos G, Ganguly D, Demaria O, Frasca L, Durr S, et al. Cationic antimicrobial peptides in psoriatic skin cooperate to break innate tolerance to self-DNA. *Eur J Immunol*. 2015;45:203–13.
- Lande R, Gregorio J, Facchinetti V, Chatterjee B, Wang YH, Homey B, et al. Plasmacytoid dendritic cells sense self-DNA coupled with antimicrobial peptide. *Nature*. 2007;449:564–9.
- Ahn J, Gutman D, Saijo S, Barber GN. STING manifests self DNA-dependent inflammatory disease. *Proc Natl Acad Sci USA*. 2012;109:19386–91.
- Li XD, Wu J, Gao D, Wang H, Sun L, Chen ZJ. Pivotal roles of cGAS-cGAMP signaling in antiviral defense and immune adjuvant effects. *Science*. 2013;341:1390–4.
- Muller U, Steinhoff U, Reis LF, Hemmi S, Pavlovic J, Zinkernagel RM, et al. Functional role of type I and type II interferons in antiviral defense. *Science*. 1994;264:1918–21.
- Hemmi H, Takeuchi O, Kawai T, Kaisho T, Sato S, Sanjo H, et al. A Toll-like receptor recognizes bacterial DNA. *Nature*. 2000;408:740–5.

- Martinon F, Petrilli V, Mayor A, Tardivel A, Tschopp J. Gout-associated uric acid crystals activate the NALP3 inflammasome. *Nature*. 2006;440:237–41.
- Jones JW, Kayagaki N, Broz P, Henry T, Newton K, O'Rourke K, et al. Absent in melanoma 2 is required for innate immune recognition of *Francisella tularensis*. *Proc Natl Acad Sci USA*. 2010;107:9771–6.
- Malik AN, Czajka A, Cunningham P. Accurate quantification of mouse mitochondrial DNA without co-amplification of nuclear mitochondrial insertion sequences. *Mitochondrion*. 2016;29:59–64.

ACKNOWLEDGEMENTS

The authors thank Glen N. Barber for sharing the STING-deficient mice, to Zhijian J. Chen for providing cGAS-deficient mice (University of Texas Southwestern Medical Center, Dallas), to Vijay Dixit and Thomas Henry for sharing AIM2-deficient mice (Max Planck Institute of Biochemistry, 82152 Martinsried, Germany). The skillful assistance of David Gosset, running the P@CYFIC platform (CNRS UPR 4301, Orleans) is gratefully acknowledged.

AUTHOR CONTRIBUTIONS

YM-N performed most experiments with the assistance of EC, SR, IM, and N.R. YM-N, DT, BR, and VQ conceived the project, designed the experiments, analyzed and interpreted the data. DT, BR, and VFJQ wrote the manuscript. All authors had the opportunity to discuss the results and comment on the manuscript.

FUNDING

This work was supported by CNRS, University of Orleans, "Fondation pour la Recherche Médicale"(EQU202003010405) and European funding in Region Centre-Val de Loire (FEDER N° EX010381).

COMPETING INTERESTS

The authors declare no competing interests

ETHICS STATEMENT

All animal experiments complied with the French Government animal experiment regulations and ARRIVE guidelines. The protocols were submitted to the "Ethics Committee for Animal Experimentation of CNRS Campus Orleans" (CCO) under numbers CLE CCO 2015-1087 and CLE CCO 2020-2018 and approved by the French Minister under APAFIS #19361 and #25360.

ADDITIONAL INFORMATION

Supplementary information The online version contains supplementary material available at <https://doi.org/10.1038/s41419-022-04664-5>.

Correspondence and requests for materials should be addressed to Valerie F. J. Quesniaux or Dieudonné. Togbe.

Reprints and permission information is available at <http://www.nature.com/reprints>

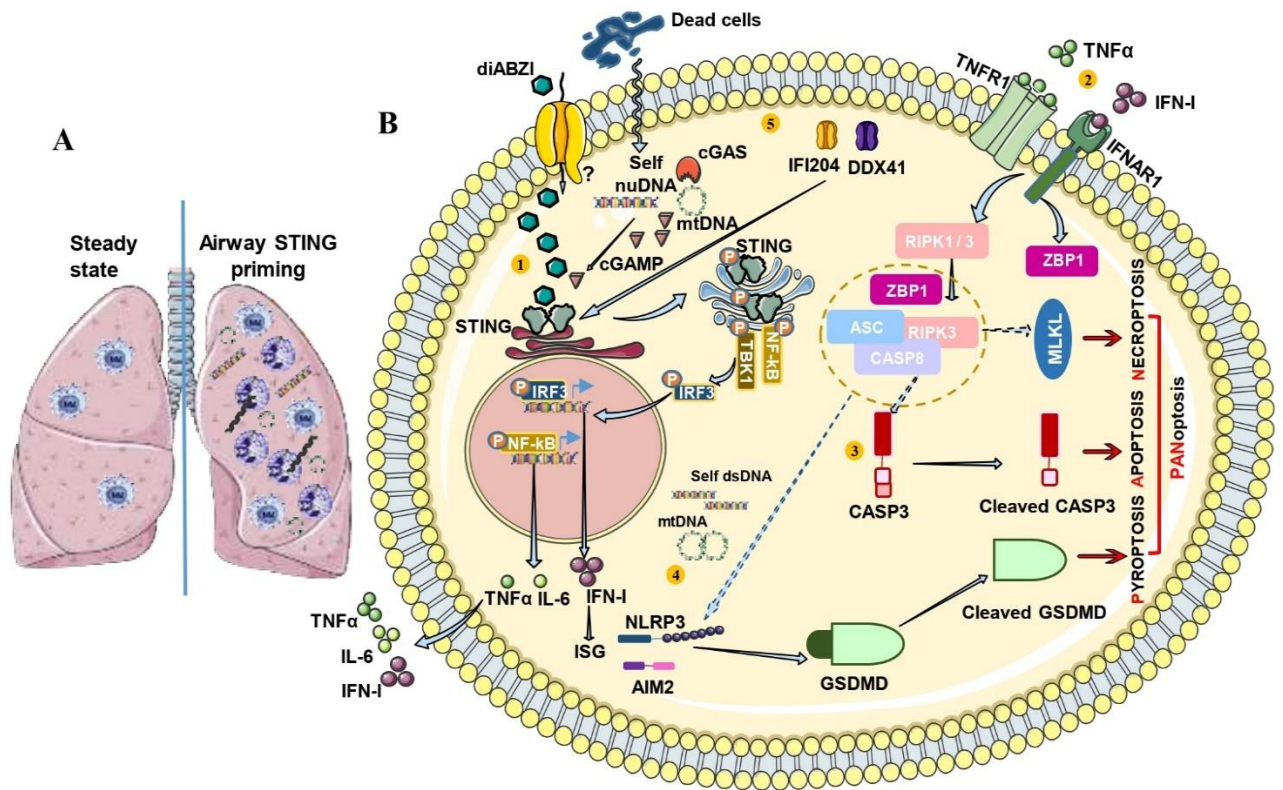
Publisher's note Springer Nature remains neutral with regard to jurisdictional claims in published maps and institutional affiliations.



Open Access This article is licensed under a Creative Commons Attribution 4.0 International License, which permits use, sharing, adaptation, distribution and reproduction in any medium or format, as long as you give appropriate credit to the original author(s) and the source, provide a link to the Creative Commons license, and indicate if changes were made. The images or other third party material in this article are included in the article's Creative Commons license, unless indicated otherwise in a credit line to the material. If material is not included in the article's Creative Commons license and your intended use is not permitted by statutory regulation or exceeds the permitted use, you will need to obtain permission directly from the copyright holder. To view a copy of this license, visit <http://creativecommons.org/licenses/by/4.0/>.

© The Author(s) 2022

Graphical abstract

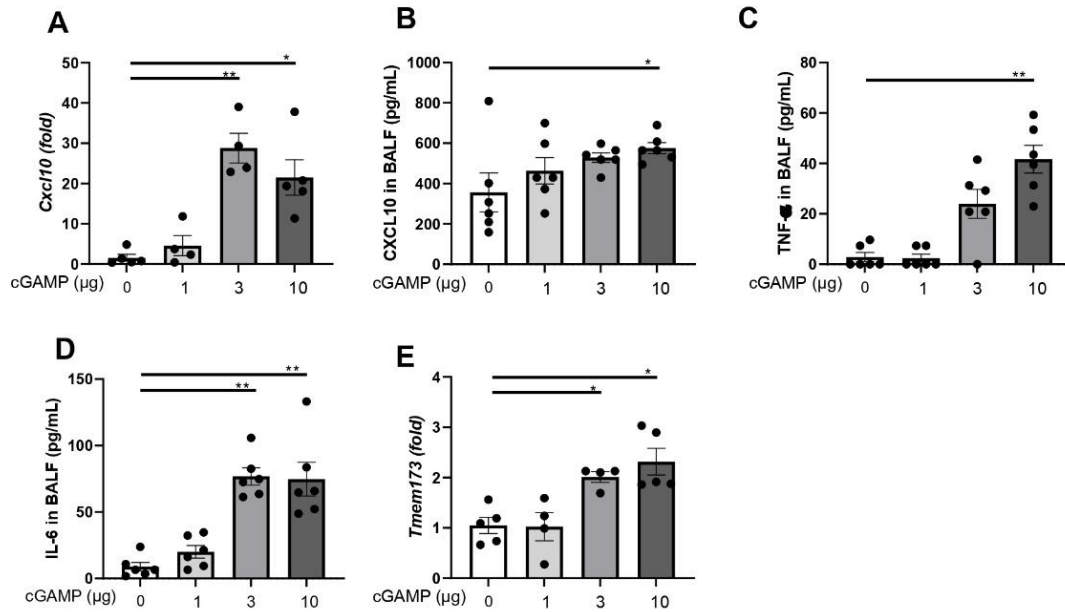


STING agonist diABZI induces neutrophilic lung inflammation and PANoptosis

STING agonist diABZI induces neutrophilic lung inflammation and PANoptosis

A, Airway STING priming induce a neutrophilic lung inflammation with epithelial barrier damage, double-stranded DNA release in the bronchoalveolar space, cell death, NETosis and type I interferon release. B, **1.** The diamidobenzimidazole (diABZI), a STING agonist is internalized into the cytoplasm through unknown receptor and induce the activation and dimerization of STING followed by TBK1/IRF3 phosphorylation leading to type I IFN response. STING activation also leads to NF-κB activation and the production of pro-inflammatory cytokines TNFα and IL-6. **2.** The activation of TNFR1 and IFNAR1 signaling pathway results in ZBP1 and RIPK3/ASC/CASP8 activation leading to MLKL phosphorylation and necroptosis induction. **3.** This can also leads to Caspase-3 cleavage and apoptosis induction. **4.** Self-dsDNA or mtDNA sensing by NLRP3 or AIM2 induces inflammasome formation leading to Gasdermin D cleavage enabling Gasdermin D pore formation and the release mature IL-1β and pyroptosis. NLRP3 inflammasome formation can be enhanced by the ZBP1/RIPK3/CASP8 complex. **5.** A second signal of STING activation with diABZI induces cell death and the release of self-DNA which is sensed by cGAS and form 2'3'-cGAMP leading to STING hyper activation, the amplification of TBK1/IRF3 and NF-κB pathway and the subsequent production of IFN-I and inflammatory TNFα and IL-6. This also leads to IFI204 and DDX41 upregulation thus, amplifying the inflammatory loop. The upregulation of apoptosis, pyroptosis and necroptosis is indicative of STING-dependent PANoptosis.

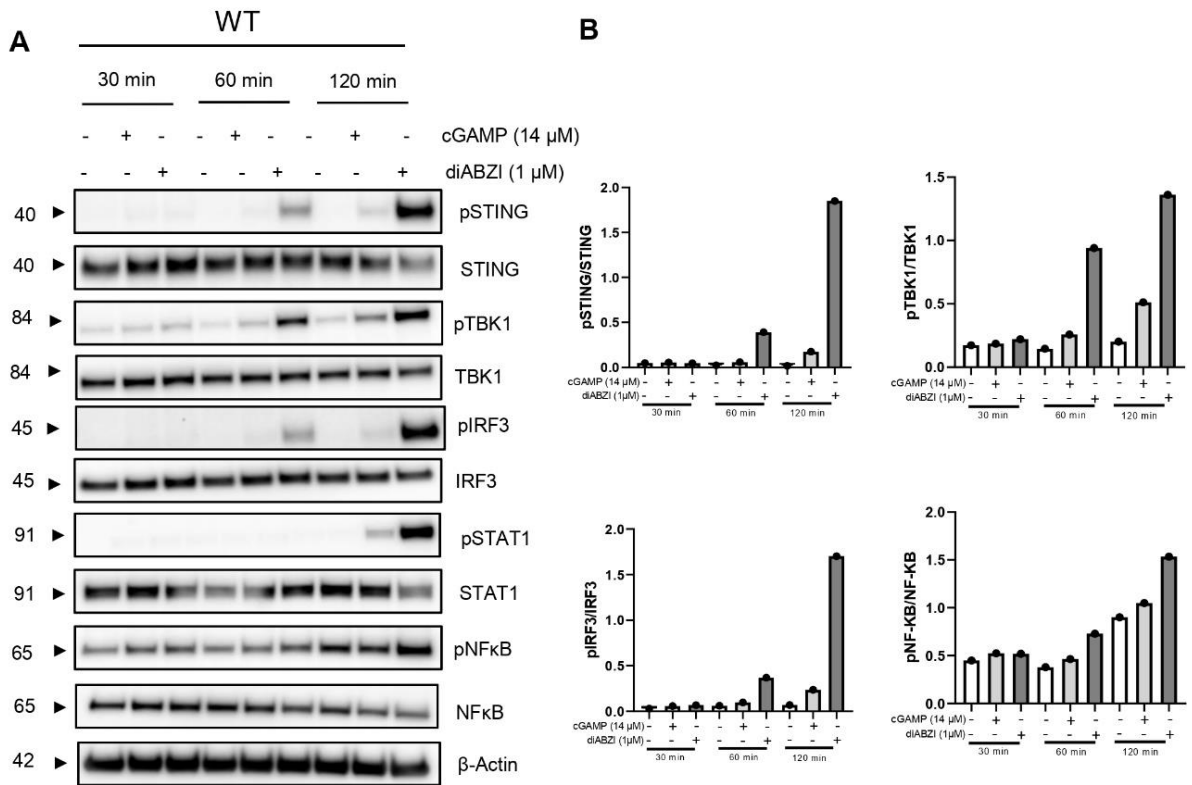
Supplemental Figure S1 related to Figure 1



Supplemental Figure S1. cGAMP induced airway inflammation.

cGAMP (1, 3 or 10 µg, i.t.) or saline were administered daily in WT mice for 3 consecutive days and parameters analyzed on day 4 as described in Figure 1. **A-B.** *Cxcl10* transcripts (**A**), measured by real-time PCR and concentration of CXCL10 in BALF determined by ELISA (**B**), concentration of TNFα (**C**) and IL-6 (**D**) in BALF determined by ELISA. **D.** *Tmem173* transcripts measured by real-time PCR. Data are presented as mean ± SEM with n= 5-6 mice per group. Each point represents an individual mouse. *p < 0.05, **p < 0.01, ***p < 0.001, ****p < 0.0001 (Non-parametric Kruskal–Wallis test followed by Dunn post-test).

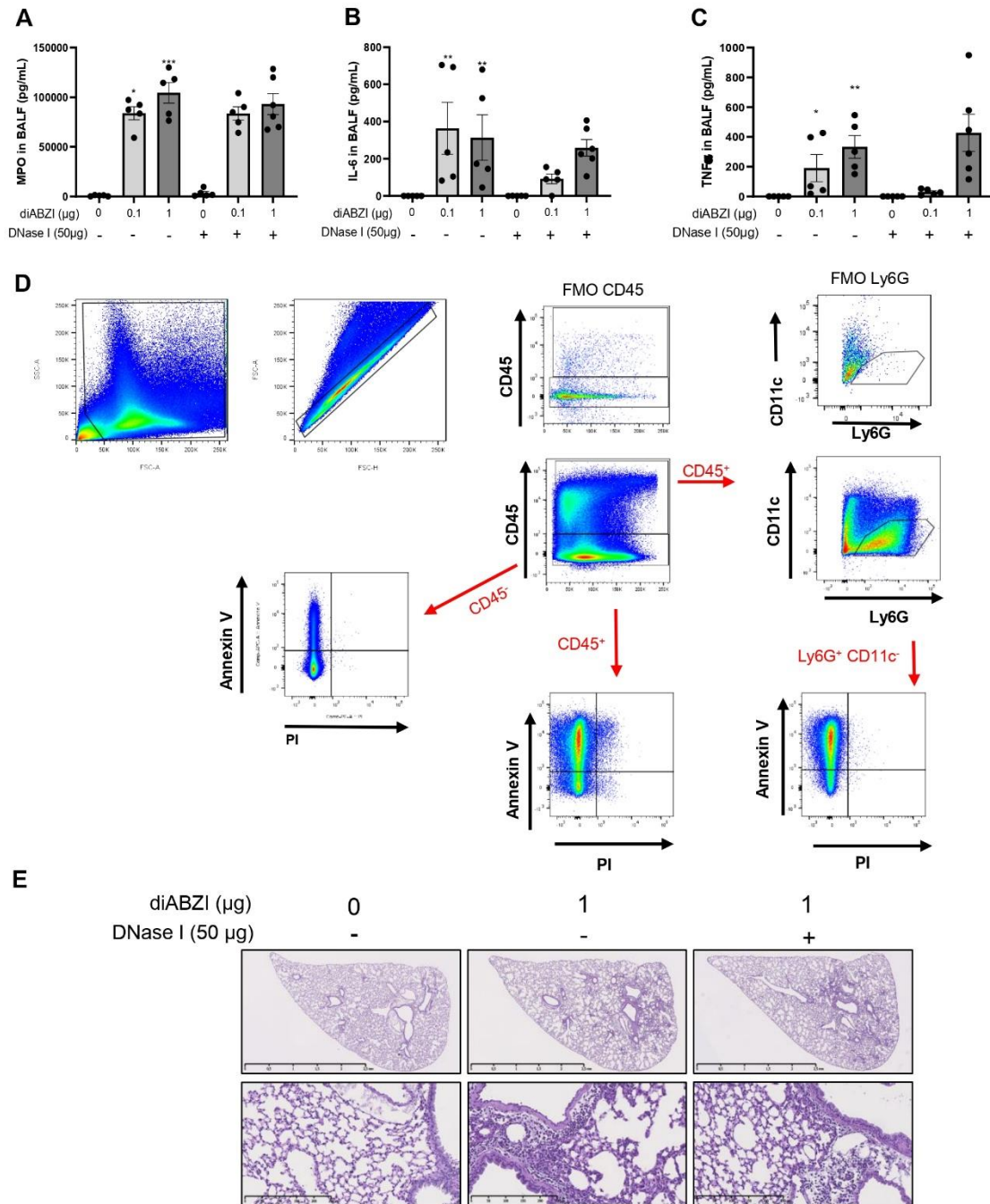
Supplemental Figure S2 related to Figure 3



Supplemental Figure S2. diABZI induced STING axis activation at an early time-point.

A. Kinetic analysis of STING axis and NFkB axis by immunoblot at 30 min, 60 min and 120 min post-stimulation with cGAMP and diABZI, including phospho-STING, STING, phospho-TBK1, TBK1, phospho-IRF3, IRF3, phospho-STAT1, STAT1, phospho-NFkB, NFkB with β -actin obtained from BMDM lysate. **B.** Immunoblot quantification of pSTING, pIRF3, pTBK1 and pNFkB normalized to their total form.

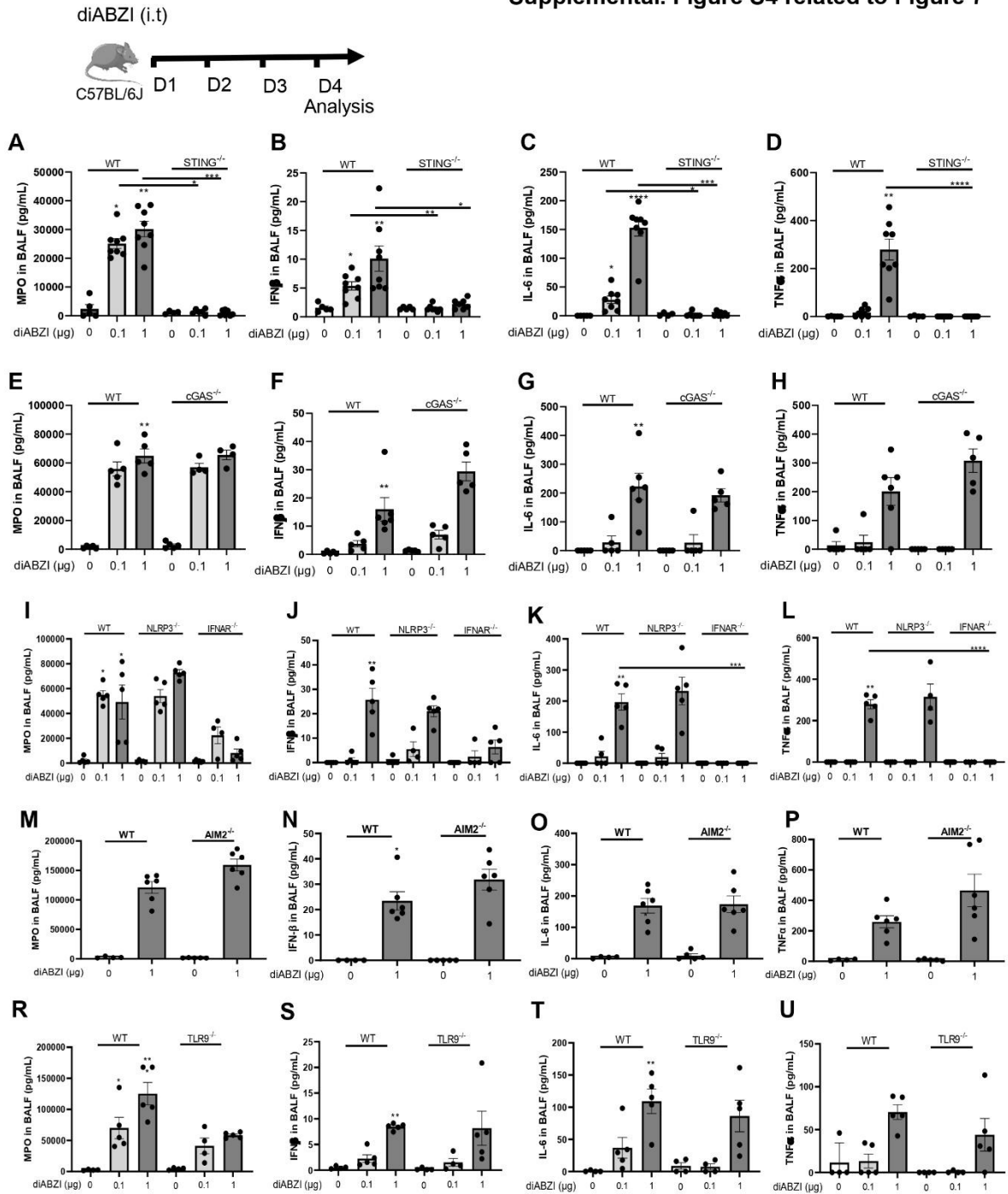
Supplemental Figure S3 related to Figure 6



Supplemental Figure S3. DNase I treatment reduced diABZI induced airway inflammation.

diABZI (0.1 or 1 µg, i.t.) were administered with DNase I (50µg/mouse, i.t.) daily in WT mice for 3 consecutive days and parameters analyzed on day 4. **A-C**, Concentration of MPO (**A**), IL-6 (**B**) and TNFα (**C**) in BALF, determined by ELISA. **D**, gating strategy of Annexin V/PI staining of pre-gated singlets (SSC-A/SSC-H), CD45⁺ (leukocytes) and CD45⁺Ly6G⁺CD11c⁻ cells (neutrophils). **E**, Lung tissue histology PAS staining. Bars, upper panels: 2.5 mm, lower panels: 250 µm. Data are presented as mean ± SEM with n= 5-6 mice per group. Each point represents an individual mouse. *p < 0.05, **p < 0.01, ***p < 0.001, ****p < 0.0001 (Non-parametric Kruskal-Wallis test followed by Dunn post-test).

Supplemental. Figure S4 related to Figure 7



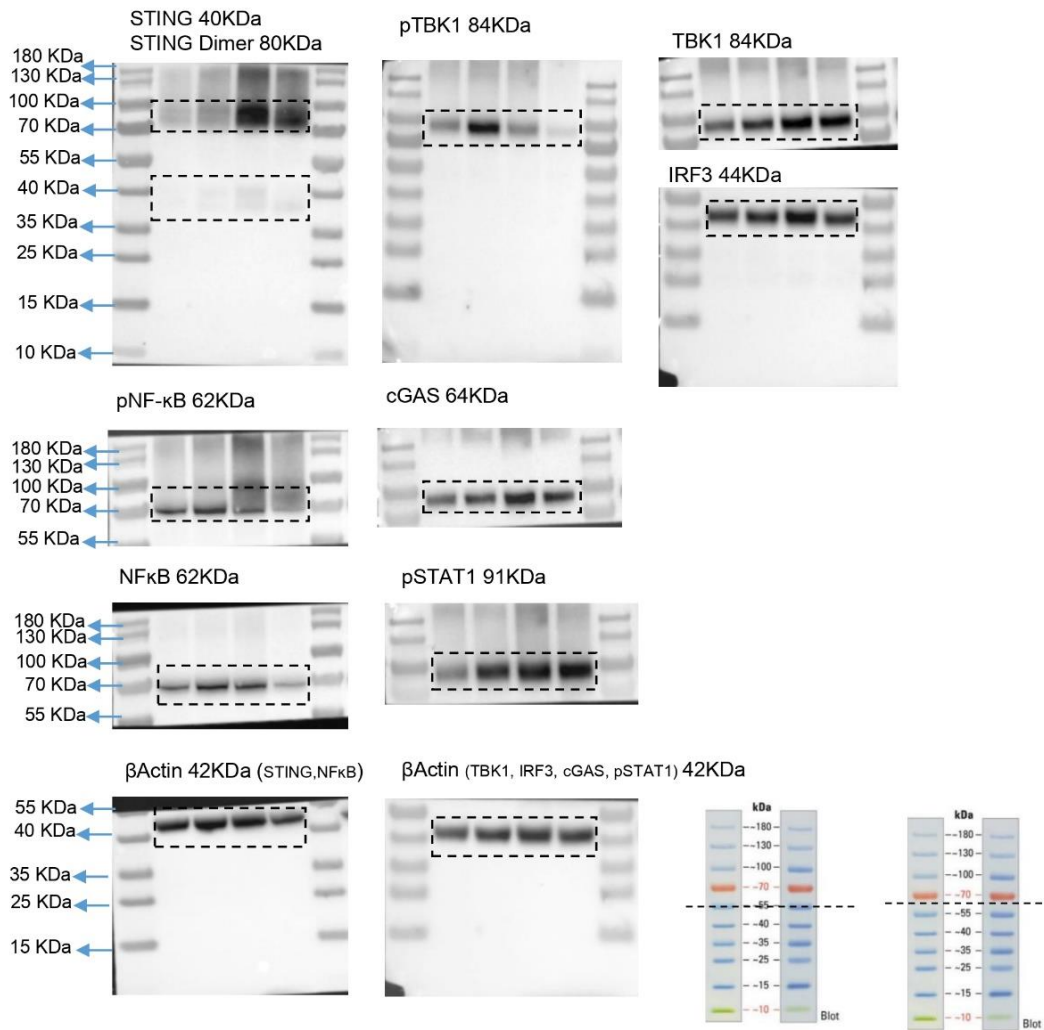
Supplemental Figure S4. STING is a major sensor of diABZI induced lung inflammation

DiABZI (0.1 or 1 μ g, i.t.) or saline were administered daily in STING^{-/-}, cGAS^{-/-}, NLRP3^{-/-}, IFNAR^{-/-}, TLR9^{-/-}, AIM2^{-/-} and WT mice for 3 consecutive days and parameters analyzed on day 4. **A-D**. Concentrations of MPO (**A**), IFN β (**B**), IL-6 (**C**) and TNF α (**D**) in BALF in WT and STING^{-/-} mice. **E-H**. Concentrations of MPO (**E**), IFN β (**F**), IL-6 (**G**) and TNF α (**H**) in BALF in WT and cGAS^{-/-} mice. **I-L**. Concentrations of MPO (**I**), IFN β (**J**), IL-6 (**K**) and TNF α (**L**) in BALF in WT and NLRP3^{-/-} and IFNAR^{-/-} mice. **M-P**. Concentrations of MPO (**M**), IFN β (**N**), IL-6 (**O**) and TNF α (**P**) concentration in BALF in WT and AIM2^{-/-} mice. **R-U**. Concentrations of MPO (**R**), IFN β (**S**), IL-6 (**T**) and TNF α (**U**) in BALF in WT and TLR9^{-/-} mice. Graph data are presented as mean \pm SEM with n=5-6 mice/group. Each point represents an individual mouse. *p < 0.05, **p < 0.01, ***p < 0.001. (Non-parametric Kruskal–Wallis test followed by Dunn post-test).

Supplemental Figure 5: full Western blots

Supplemental Figure S5A related to Figure 10

cGAMP *in vivo*



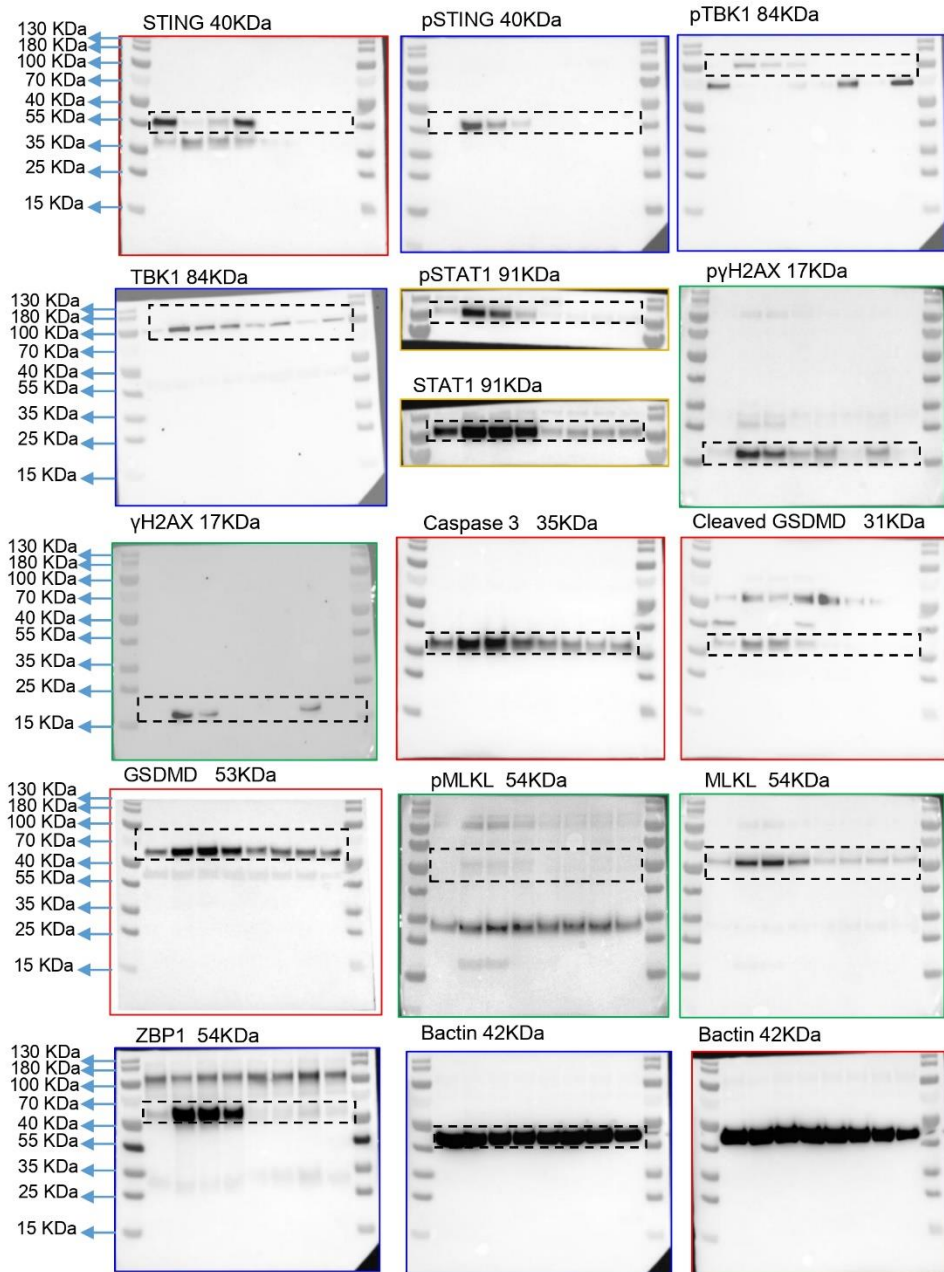
Supplemental Figure S5. Uncropped immunoblots of the different figures

A. Immunoblots related to Figure 10, immunoblots of STING Dimers, STING, phospho-TBK1, TBK-1, IRF3, cGAS, pNF-κB, NF-κB, pSTAT1 with β-actin obtained from lungs tissue lysate.

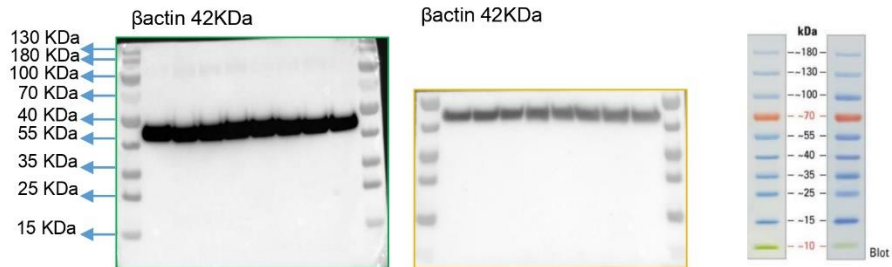
Supplemental Figure 5: full Western blots

Supplemental Figure S5B related to Figure 3H-I

Macrophages (BMDM)



Supplemental Figure S5B related to Figure 3H-I

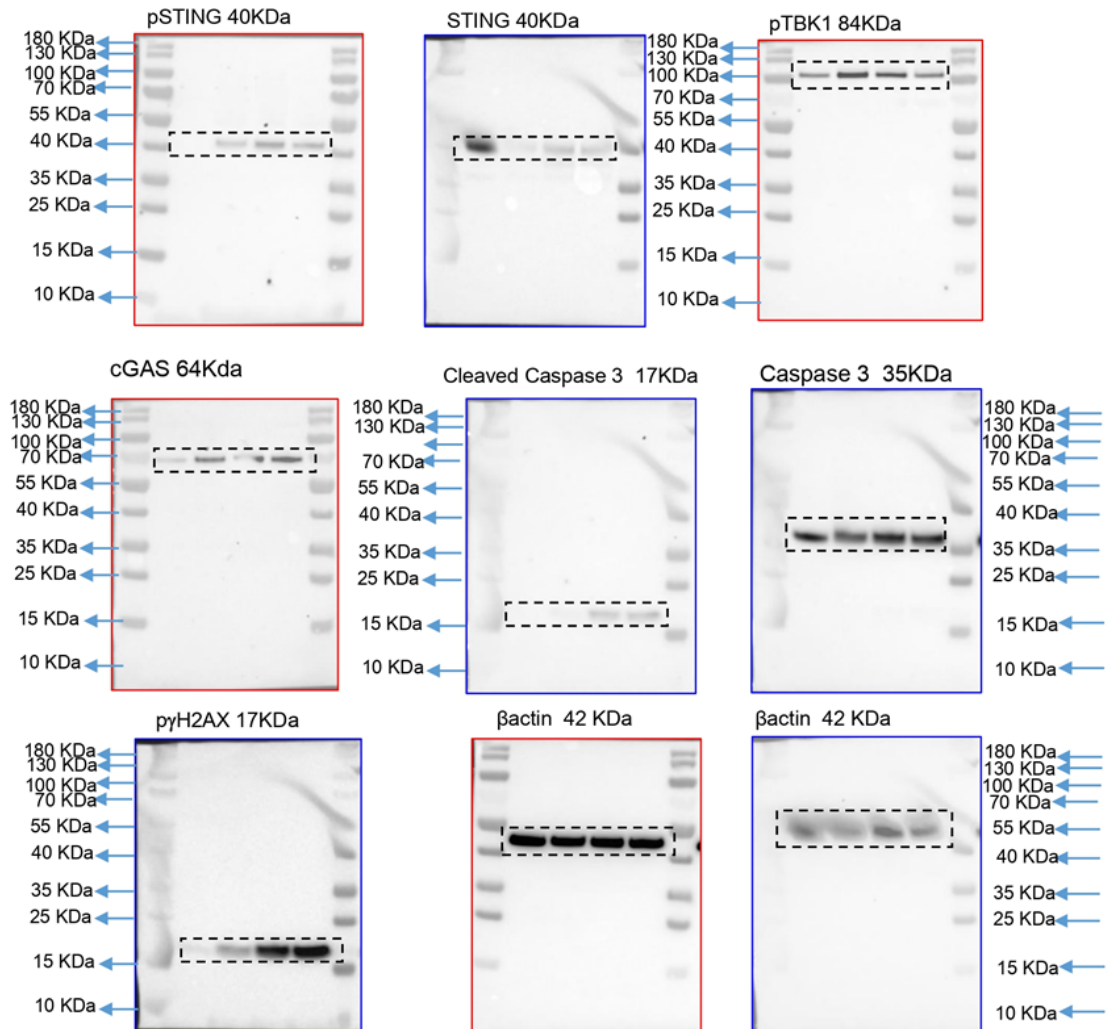


Supplemental Figure S5. Uncropped immunoblots of the different figures

B. Immunoblots related to **Figure 3H**, immunoblots of STING, phospho-STING, phospho-TBK1, TBK1, phospho-STAT1, STAT1, phospho- γ H2AX, γ H2AX. **Figure 3I**, immunoblots of Caspase-3, Cleaved GSDMD, GSDMD, phospho-MLKL, MLKL, ZBP1 with β -actin obtained from BMDM lysate.

Supplemental Figure S5C related to Figure 3M

Human airway epithelial cells (hAEC)

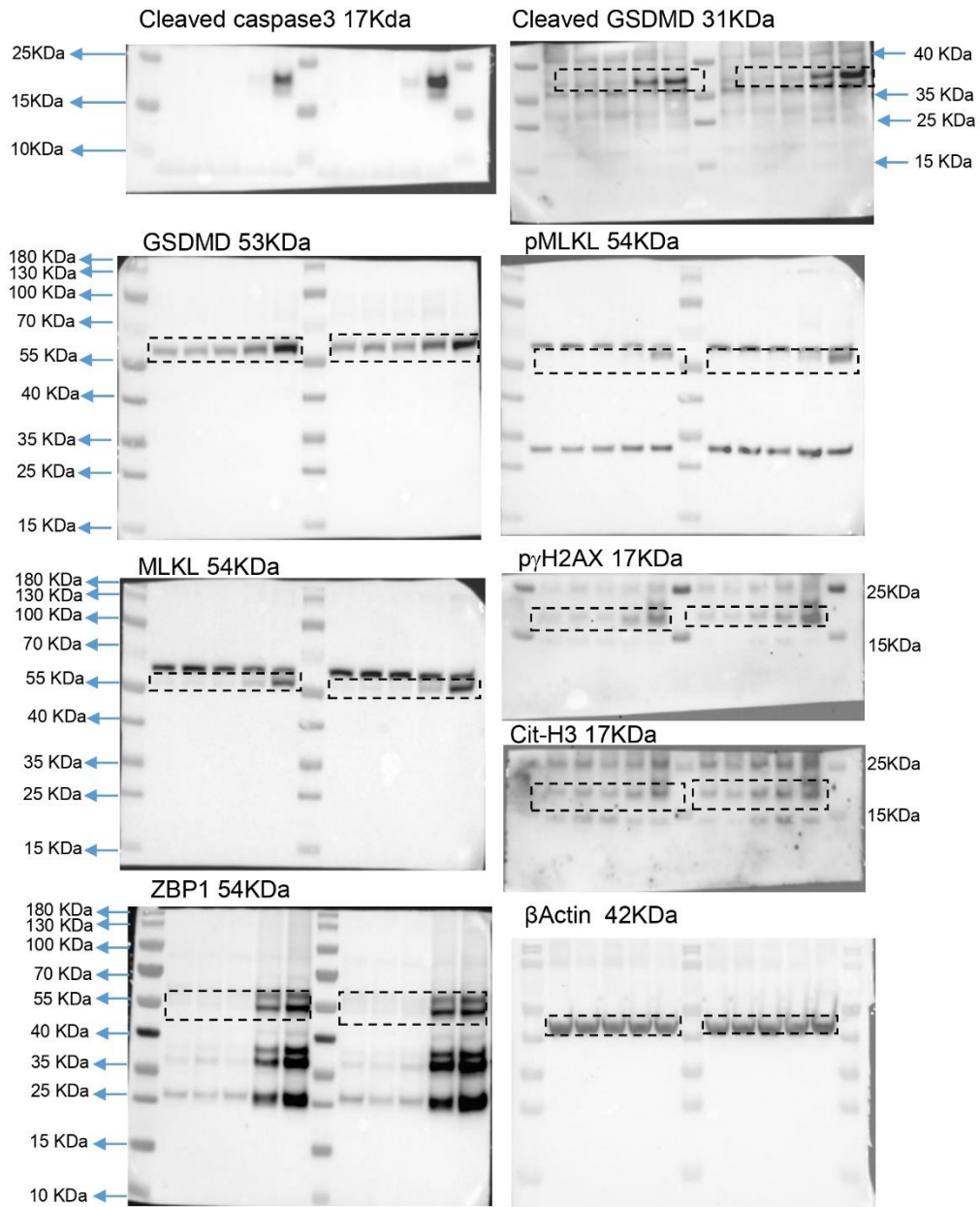


Supplemental Figure S5C Uncropped immunoblots of the different figures

C. Immunoblots related to Figure 3M, immunoblots of phospho-STING, STING, phospho-TBK1, cGAS, Cleaved caspase-3, Caspase-3, phospho- γ H2AX, with β -actin obtained from human airway epithelial cells lysate.

Supplemental Figure S5D related to Figure 5A

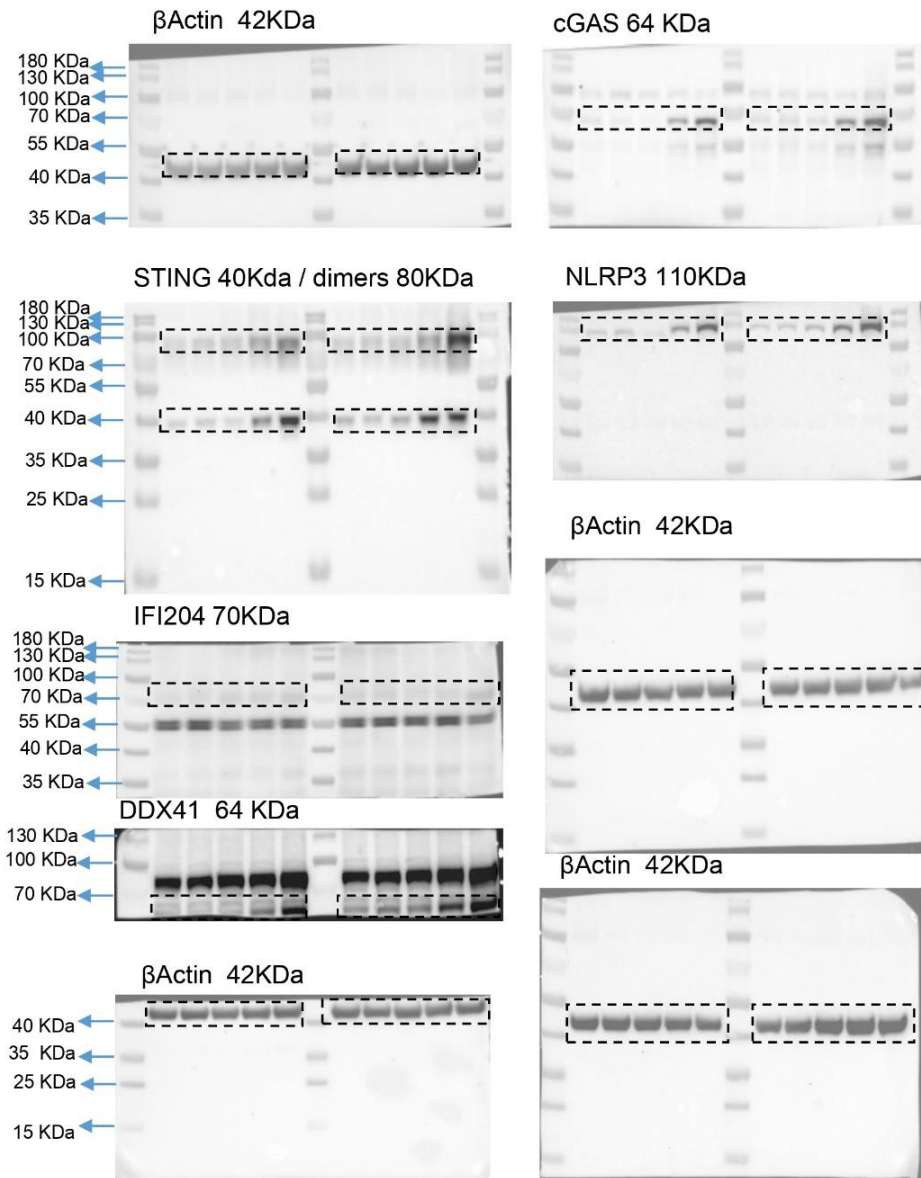
In vivo



Supplemental Figure S5D Uncropped immunoblots of the different figures

D. Immunoblots related to Figure 5A, immunoblots of cleaved caspase-3, cleaved GSDMD, GSDMD, phospho-MLKL, MLKL, phospho- γ H2AX, Cit-H3, ZBP1 with β -actin obtained from lungs tissue lysate.

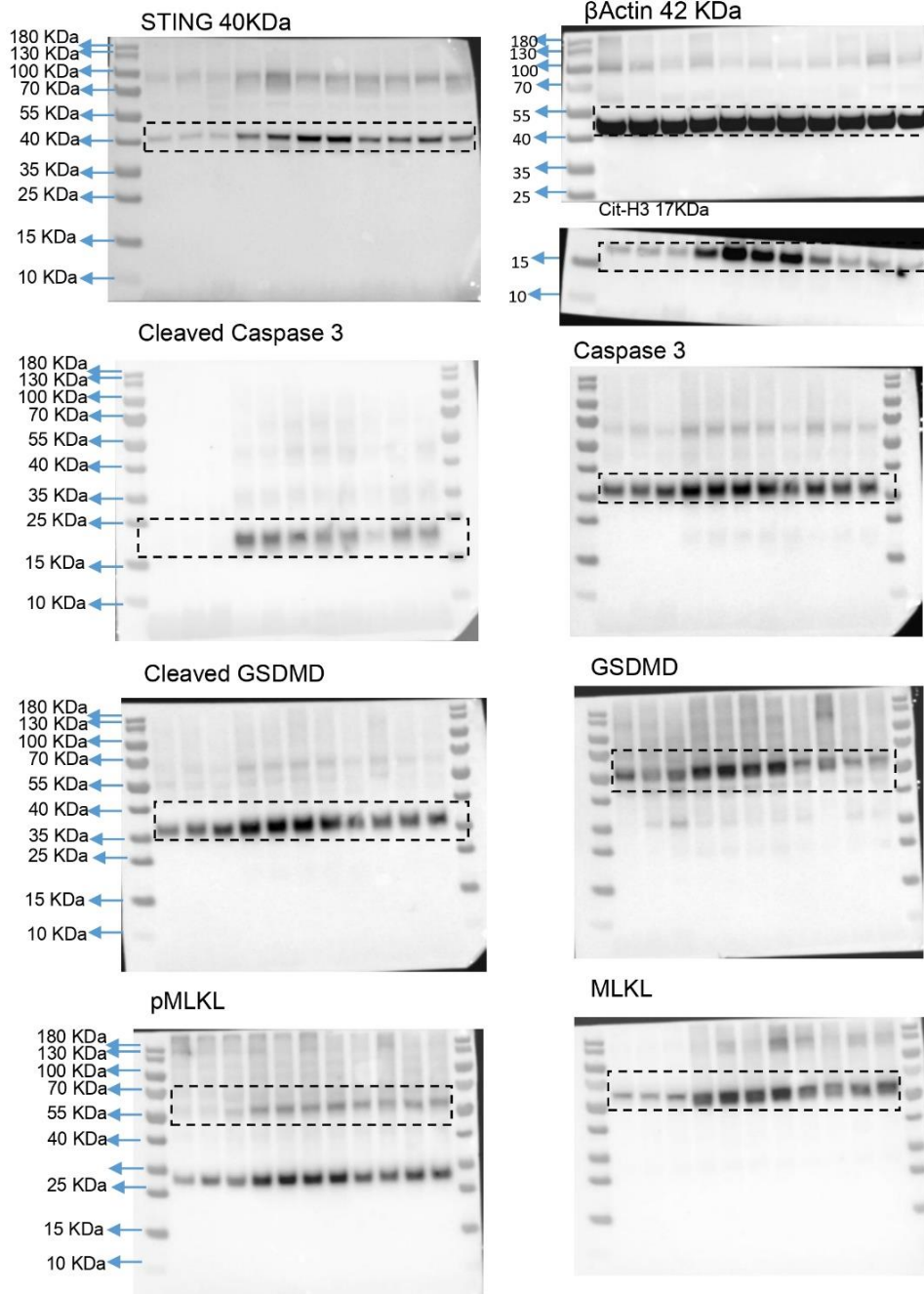
Supplemental Figure S5E related to *Figure 5D*



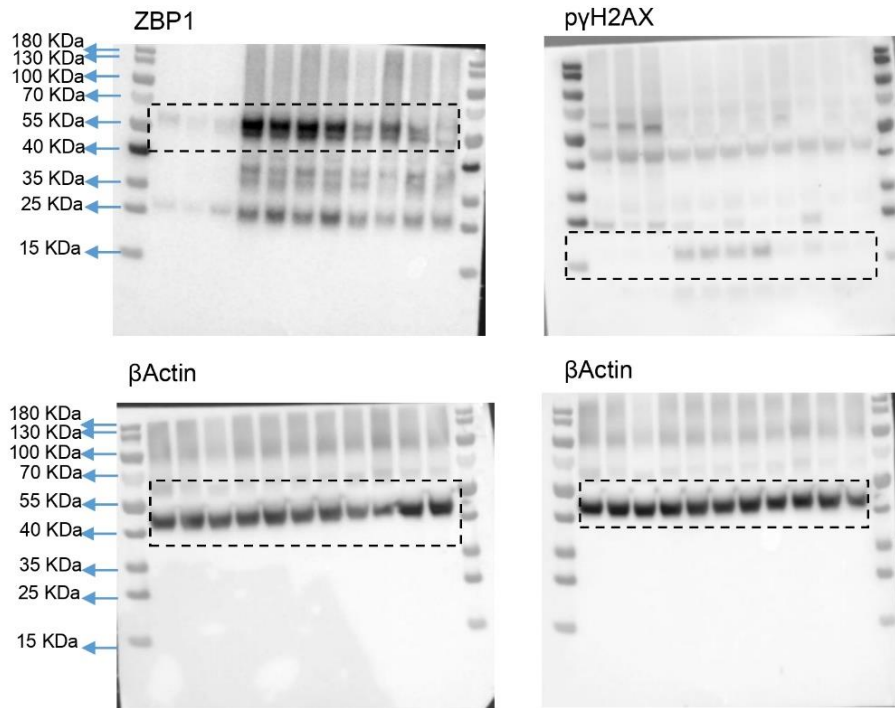
Supplemental Figure S5E Uncropped immunoblots of the different figures

E. Immunoblots related to Figure 5D, immunoblots of cGAS, STING, NLRP3, IFI204, DDX41 with β-actin obtained from lungs tissue lysate.

Supplemental Figure S5F related to Figure 6N



Supplemental Figure S5F related to Figure 6N

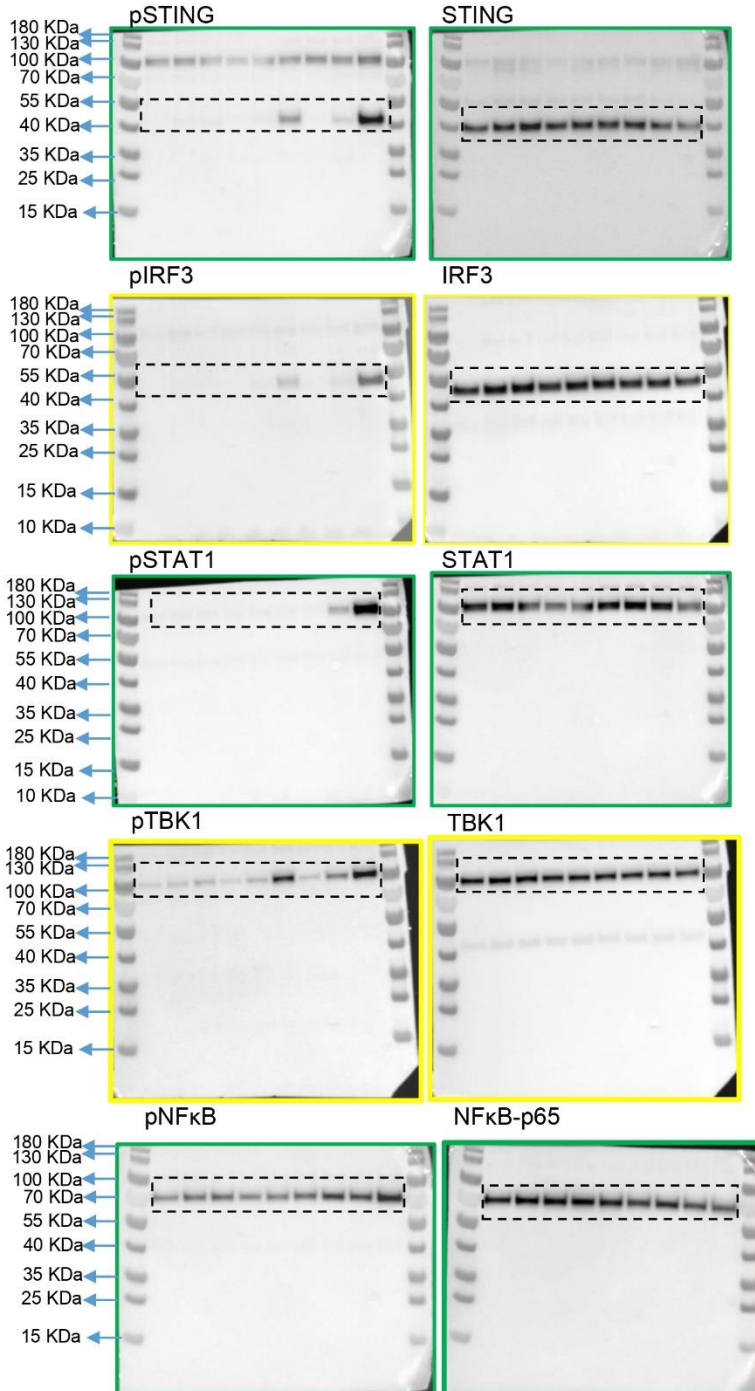


Supplemental Figure S5F Uncropped immunoblots of the different figures

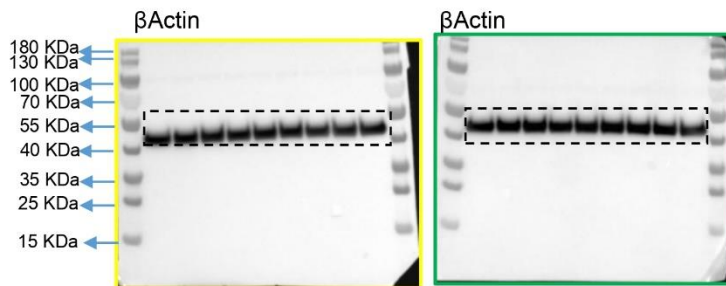
F. Immunoblots related to Figure 6N, immunoblots of Cit-H3, STING, Cleaved caspase-3, Caspase-3, Cleaved-GSDMD, GSDMD, phospho-MLKL, MLKL, phospho-γH2AX, ZBP1 with b-actin obtained from lungs tissue lysate.

Supplemental Figure S5G related to Figure S2

BMDM



Supplemental Figure S5G related to *Figure S2*



Supplemental Figure S5G Uncropped immunoblots of the different figures

G. Immunoblots related to Figure S2, immunoblots of phospho-STING, STING, phospho-IRF3, IRF3, phospho-STAT1, STAT1, phospho-TBK1, TBK1, phospho-NF κ B, NF κ B with β -actin obtained from BMDM lysate.

Article 2: **STING-dependent induction of neutrophilic asthma exacerbation in response to house dust mite.**

Yasmine Messaoud-Nacer, Elodie Culerier, Stéphanie Rose, Isabelle Maillet, Bernard Malissen, Urszula Radzikowska, Milena Sokolowska, Gabriel VL da Silva, Michael R Edwards, David J Jackson, Sebastian L Johnston, Bernhard Ryffel, Valerie F. Quesniaux, and Dieudonné Togbe*

Submitted article. 2023

Persistent uncontrolled asthma despite high-dose oral corticosteroids (OCS) treatment is a hallmark of severe asthma exacerbations. In a subgroup of patient with asthma, there is evident involvement of neutrophils in the lungs, which increases disease severity and correlates with corticosteroid insensitivity. Understanding the immuno-inflammatory pathways that drive neutrophilic asthma will help select more appropriate treatments (Nair et al. 2020; Ragnoli et al. 2022)

In this study, we hypothesized that the DNA sensing pathway cGAS-STING plays a role in neutrophilic asthma exacerbation following viral infection or exposure to pollution, and thus may represent a new therapeutic target. To test this hypothesis, we specifically targeted STING *in vivo* in mice, with STING agonists (cGAMP, diABZI) during allergic responses to house dust mite (HDM), and analyzed inflammatory parameters.

STING agonists, especially diABZI, induced a strong neutrophil infiltration in the lung, and type 1 (Th1) immune response besides the preexisting Th2 immune response, while worsening HDM-induced lung resistance, thus mimicking the most important neutrophilic asthma exacerbation hallmarks. Furthermore, we demonstrated for the first time that infiltrated neutrophils following STING hyperactivation exhibit a pro-inflammatory N1 profil (NOS2⁺ ARG1⁻) with strong NET release, unlike the HDM-induced neutrophils with a N2 profil (NOS2⁺ ARG1⁻). Locally in lung tissue, we showed important increased leukocyte infiltration, epithelial injury, with decreased goblet cells. We also showed evidences of DNA damage and cell death markers suggestive of PANoptotic cell death.

Despite the highly pathogenic role played by pro-inflammatory neutrophils in neutrophilic asthma exacerbation, alveolar macrophages were found to be one of the main lung cell types responsible for the uptake of the natural STING agonist cGAMP *in vivo* (She et al. 2021). We investigated the contribution of macrophages and granulocytes using conditional STING-deficient mice. Inflammatory parameters assessed such as neutrophil infiltration, type

I IFN and NET release were partially reduced in conditional STING deficient mice compared to wild-type controls. These results suggested that inflammatory cells play a role in shaping the exacerbated response, but are not exclusively.

The previous results, prompted us to question the role of structural lung epithelial cells. We showed that STING agonists further weaken the HDM-induced barrier disruption *in vivo* in mice by down-regulating tight junctions. Moreover, human bronchial epithelial cells and air-liquid bronchial epithelial cell cultures mimicking the respiratory barrier showed the ability to respond to STING agonists with evidence of STING pathway activation, pro-inflammatory cytokine induction and DNA damage that will further fuel the inflammation.

To further validate the relevance of our mouse model of neutrophilic exacerbation, we tested whether the STING pathway was also hyperactivated in patients with asthma undergoing respiratory infections, or in patients with severe asthma as compared to healthy controls. To this purpose, we analyzed with the help of collaborators, publicly available data from bronchial epithelial cells stimulated *in vitro* with RV-A16 rhinovirus, bronchial brushings from patients with asthma and healthy controls experimentally infected with rhinovirus *in vivo*, and PBMC from patients with severe asthma and controls. Indeed, we found an increased expression of the STING pathway in bronchial epithelial cells from patients with asthma compared to the controls after rhinovirus infection. This expression was accompanied by an increase in several PANoptosis-related genes, and a decreased expression of several tight junction genes, after rhinovirus infection in patients with asthma as compared to the controls. Furthermore, by analyzing the neutrophil signature in bronchial brushings from experimentally infected individuals, we found that NOS2 was increased while ARG1 was decreased after rhinovirus infection in patients with asthma as compared to the controls.

These results indicate that uncontrolled STING activation, e.g. after rhinovirus infection, may drive neutrophilic exacerbation in patients with asthma, and shift the immune response from a classical Th2-high response to a mixed Th1/Th2 response. Therefore, considering STING inhibitors as therapeutic strategy, alone or in combination with other treatments, may improve the condition of patients with severe asthma.

This article has been submitted to the *Journal of Allergy and Clinical Immunology* in July 2023.

STING-dependent induction of neutrophilic asthma exacerbation in response to house dust mite.

Yasmine Messaoud-Nacer, PhD¹, Elodie Culerier, MSc¹, Stéphanie Rose, MSc¹, Isabelle Maillat, MSc¹, Bernard Malissen, PhD², Urszula Radzikowska, PhD^{3,4}, Milena Sokolowska, MD^{3,4}, Gabriel VL da Silva, PhD⁵, Michael R Edwards, PhD⁶, David J Jackson, PhD⁶, Sebastian L Johnston, MD, PhD⁶, Bernhard Ryffel, MD, PhD¹, Valerie F. Quesniaux, PhD¹, and Dieudonné Togbe, PhD^{1*}

¹*Experimental and Molecular Immunology and Neurogenetics, INEM UMR7355 University of Orleans and CNRS, 3B Rue de la Ferrollerie 45100 Orleans-Cedex 2, France.*

²*Centre d'Immunophénomique (CIPHE), Aix Marseille Université, INSERM, CNRS, 13288, Marseille, France.*

³*Swiss Institute of Allergy and Asthma Research (SIAF), University of Zurich, Herman-Burchard-Strasse 9, 7265 Davos Wolfgang, Switzerland*

⁴*Christine Kühne – Center for Allergy Research and Education (CK-CARE), Herman-Burchard-Strasse 1, 7265 Davos Wolfgang, Switzerland⁵Artimmune SAS, 13 Avenue Buffon, 45071 Orleans-Cedex 2, France.*

⁵*Ribeirão Preto Medical School, University of Sao Paulo. Avenida Bandeirantes, 3900 - CEP 14049-900. Ribeirao Preto, Sao Paulo, Brazil.*

⁶*National Heart and Lung Institute, Imperial College Londont, London W2 1PG, United Kingdom; Asthma UK Centre in Allergic Mechanism of Asthma, London, United Kingdom; Imperial College Healthcare NHS Trust, The Bays, S Wharf Rd, London W2 1NY, United Kingdom.*

**Corresponding author: Dieudonné Togbe (dtogbe@cnrs-orleans.fr)*

Author Contributions

Y.M.-N. performed most experiments with the assistance of E.C. and S.R. B.M. generated the STING-OST^{fl} mouse model. Y.M.-N., D.T., B.R. and V.Q. conceived the project and designed the experiments, Y.M.-N., D.T., B.R., V.Q., G.dS., M.E., D.J., S.J., M.S. and U.R. analyzed and interpreted the data. Y.M.-N, D.T., B.R. and V.Q. wrote the manuscript. All authors had the opportunity to discuss the results and comment on the manuscript.

Funding Statement

This work was supported by CNRS, University of Orleans, ‘Fondation pour la Recherche Médicale’ (FRM EQU202003010405), Region Centre-Val de Loire (ExAsPIR17 N° 2021-00144721), European funding in Region Centre-Val de Loire (FEDER EUROFerri N° EX010381 and TARGET-Ex N° EX016008), ANR-10-INSB-07 and CIPHE (supported by the “investissement d’avenir programme PHENOMIN” (French National infrastructure for mouse

Phenogenomics). The human in vivo work was supported by the European Research Council (ERC FP7 Advanced grant number 233015); a Chair from Asthma UK (CH11SJ); the Medical Research Council Centre (grant number G1000758); National Institute of Health Research (NIHR) Biomedical Research Centre (grant number P26095); Predicta FP7 Collaborative Project (grant number 260895); and the NIHR Biomedical Research Centre at Imperial College London.

Running head: STING activation induces neutrophilic asthma exacerbation

Total word count: text: 3426 words

This article has an online data supplement, which is accessible at JACI online Repository Materials.

Abstract (250 words)

Background: Severe refractory, neutrophilic asthma remains an unsolved clinical problem. STING agonists induce a neutrophilic response in the airways, suggesting that STING activation may contribute to trigger neutrophilic exacerbation.

Objectives: Determine whether STING-induced neutrophilic lung inflammation mimics severe asthma.

Methods: We developed new models of neutrophilic lung inflammation induced by house dust mite (HDM) plus STING agonists diamidobenzimidazole (diABZI) or cGAMP in wild-type, and conditional-STING-deficient mice. We measured DNA damage, cell death, NETs, cGAS/STING pathway activation by immunoblots, N1/N2 balance by flow cytometry, lung function by plethysmography, and Th1/Th2 cytokines by multiplex. We evaluated diABZI effects on human airway epithelial cells from healthy or patients with asthma, and validated the results by transcriptomic analyses of rhinovirus infected healthy controls *vs* patients with asthma.

Results:

DiABZI administration during HDM challenge increased airway resistance, neutrophil recruitment in the airways with prominent NOS2⁺ARG1⁻ type 1 neutrophils, protein extravasation, cell death by PANoptosis, NETs formation, extracellular dsDNA release, DNA sensors activation, IFN γ , IL-6 and CXCL10 release. Functionally, STING agonists exacerbated HDM-induced lung resistance, while TLR3 agonist Poly(I:C) spared lung function. DiABZI caused DNA damage, epithelial barrier damage, and STING pathway activation in human airway epithelial cells exposed to HDM, in line with DNA-sensing and PANoptosis pathways upregulation and tight-junction downregulation induced by rhinovirus challenge in patients with asthma.

Conclusions: Triggering STING in allergic context may shape the inflammatory response toward mixed Th1/Th2 immune responses and recapitulate features of severe neutrophilic asthma. Thus, targeting STING pathway might be considered in severe asthma including seasonal respiratory viral exacerbation.

Key Message

- STING agonists trigger neutrophilic asthma development and PANoptosis.
- STING agonists induce N2 versus N1 neutrophil polarization.
- Human transcriptome GEO database analysis reveals DNA sensing pathway activation and NOS2/ARG1 imbalance following rhinovirus infection in patients with asthma.

Capsule summary

STING activation during allergic challenge mimics severe neutrophilic asthma exacerbation, with switch toward N1 neutrophil polarization and lung functional damage, highlighting the importance of controlling STING during asthma attacks.

Keys words: DNA sensing, cGAMP, diABZI, cell death, PANoptosis, lung inflammation, neutrophils, neutrophil extracellular traps, airway hyperresponsiveness, asthma exacerbation, asthma endotypes.

Abbreviations

AIM2: absent in melanoma 2, BAL, BronchoAlveolar Lavage; BALF, BronchoAlveolar Lavage Fluid; cGAMP: cyclic Guanosine monophosphate-Adenosine MonoPhosphate, cGAS: cyclic GMP-AMP synthase, DDX41: DEAD-box helicase 41, diABZI: symmetry-related amidobenzimidazole-based compounds, GSDMD: Gasdermin D, GEO: Gene Expression Omnibus, hAEC, human airway epithelial cells, HBEC: human bronchial epithelial cells, HDM: house dust mite, HE: hematoxylin and eosin, IFI204: IFN- γ -Inducible protein 204, IRF3: IFN regulatory factor 3, ISG: Interferon Stimulated Gene, LDH: Lactate DeHydrogenase, MLKL: Mixed Lineage Kinase domain Likepseudokinase, MPO: myeloperoxidase, NETs: Neutrophil Extracellular Traps, NLRP3: NOD-, LRR- and Pyrin Domain-Containing Protein 3, PAS: Periodic acid Schiff, RNA-Seq : RNA sequencing, STING: STimulator of INterferon Genes, TBK1: TANK-binding kinase 1, WT: wild type, ZBP1: Z-DNA-Binding Protein 1.

Introduction (455 words)

The most common reaction to several allergens such as house-dust mite (HDM) in allergic asthma endotype is IgE production depending on high Th2 responses with IL-4, IL-5 and IL-13 release, mucus overproduction, eosinophil recruitment, epithelial metaplasia and airway remodeling ¹. The ability of an allergen to initiate the first steps of type 2 immune response is based on direct epithelial cell damage and damage of associated cells forming the respiratory barrier. Allergenic toxins or proteases may cause necrotic cell death leading to a strong Th2 response ². Severe asthma is often associated with Th2 low and mixed endotype, increased neutrophils and extracellular DNA (eDNA) in patient sputum, with an increase in type 1 cytokines IL-1 β and IL-6 at the late onset of the disease, and unresponsiveness to corticosteroids or specific biologicals ^{1, 3-6}. However, the molecular mechanism underlying severe neutrophilic asthma is more complex and remains unsolved.

Extracellular host-derived DNA has been associated with allergic type 2 immune responses. Indeed, host DNA released from dying cells acts as a damage associated molecular pattern (DAMP) that mediates e.g. the adjuvant activity of alum ⁷. The detection of extracellular host-derived dsDNA is ensured by cyclic GMP–AMP synthase (cGAS) which converts ATP and GTP into cyclic dinucleotide 2'3'cGAMP. The latter, in turn binds and activates the ER-resident adaptor protein Stimulator of Interferon Genes (STING) which activates the transcription factors NF-kB and IRF3, and the production of pro-inflammatory cytokines including tumor necrosis factor (TNF α), IL-6 and type I IFNs (IFN α/β) ⁸.

Cytosolic dsDNA accumulated in airway epithelia of ovalbumin (OVA)- or HDM-challenged mice ⁹. Deletion of cGAS in airway epithelial cells attenuated OVA or HDM induced allergic airway inflammation, while cGAS promoted Th2 immunity likely by regulating airway

epithelial GM-CSF⁹. Further, 2'3'cGAMP, produced after activation of cGAS by extracellular DNA, was shown to function as an adjuvant promoting type 2 allergic lung inflammation when administered during sensitization with HDM, with increased of serum IgE and eosinophils in the airways, an effect mediated by IL-33 and STING signaling pathway¹⁰.

Recently, we showed that endotracheal administration of cGAMP or the synthetic STING agonist diamidobenzimidazole (diABZI) led to lung inflammation with neutrophilic response in the broncho-alveolar space, cell death via PANoptosis, loss of epithelial barrier function, and release of self-dsDNA and NETs¹¹.

Here, we asked whether activating STING pathway during challenges after immunization with the widely distributed house-dust mite allergen might affect the allergic response and trigger a neutrophilic exacerbation. We show that cGAMP and furthermore diABZI administration during challenge exacerbated HDM-induced lung resistance, neutrophil recruitment, protein extravasation and extracellular dsDNA release in the airways, with an overexpression of Th1 cytokine IFN γ . We report differential expression of DNA-sensing and PANoptosis pathways after rhinovirus challenge in patients with asthma.

Methods (565 words)

Mice

Female C57BL/6Rj mice were purchased from Janvier Laboratories (Le Genest St Isle, France). Wild type mice and mice deficient for STING (STING^{-/-})¹², cGAS (cGAS^{-/-})¹³ were bred and housed under specific pathogen free conditions at CNRS animal facility (TAAM UAR44, Orleans, France). STING-OST^{fl} were crossed to LysM^{Cre} mice to generate STING-OST^{fl} LysM^{Cre} mice. They were maintained in a 12-h light-dark cycle with food and water ad libitum, following European and local legislation. Age-matched, 8- to 12- week-old mice were used for experiments. All animal experiments complied with the French Government animal experiment regulations and ARRIVE guidelines. The protocols were submitted to the “Ethics Committee for Animal Experimentation of CNRS Campus Orleans” under the number CLE CCO 2019-2017 and 2020-2006, and approved by the French Minister under APAFIS #25876 and #26195.

Induction of allergic airway inflammation and bronchoalveolar lavage (BAL)

Mice were anesthetized with 2% Isoflurane (ISO-VET, Netherlands) were sensitized with HDM on day 0 and 7 (25 µg/mouse, i.n.) and challenged with HDM (Stallergenes Greer) intranasally on 3 consecutive days (10 µg/mouse, i.n. on day 14-16), in the absence or together with cGAMP (at 1, 3 or 10 µg/mouse, i.t.), diABZI compound 3 (at 0.1 or 1 µg/mouse, i.t) or Poly(I:C) (at 60 or 200 µg/mouse, i.t). Mice were analyzed on day 17, 24 hours after the last HDM instillation (Fig. 1A).

Bronchoalveolar lavage (BAL) was performed 24h after the last challenge by flushing lung tissue four times with 0.5 mL of cold NaCl 0.9% via tracheal intubation with a cannula. BALF was collected, cells counted and cytopins performed. The supernatant of the first lavage was collected after centrifugation and stored at -80°C for dsDNA and mediator quantifications. The left lung lobe was harvested for histology, the post caval lung for RNA extraction and qPCR analysis and the right lobes for Western blot analysis and cytokine measurement. Protein

extravasation in the BALF was measured by Pierce™ BCA Protein Assay (ThermoFisher®, Massachusetts).

Cell Culture and stimulation

Human airway epithelial cells (hAEC; Epithelix, Switzerland) isolated from bronchial biopsies (passage 1) were maintained in 75 cm² flasks in the hAEC serum-free culture medium (Epithelix). hAEC (passage 8) were seeded in 24-wells plate at 5×10^5 cells/well, when they reached 80% confluence. Cells were stimulated with HDM at 100 µg/mL alone or in combination with diABZI (10 µM), cGAMP (14 µM) or Poly(I:C) (100 µg/mL) for 2 or 24h at 37°C and 5% CO₂. Human airway bronchial epithelium (MUCILAIR™; Epithelix, Switzerland), from a single healthy or donor with asthma were maintained in MUCILAIR™ serum-free medium (Epithelix) and stimulated on the apical face, with HDM at 100 µg/mL alone or in combination with diABZI, cGAMP or Poly(I:C) as above for 6h. Supernatant from hAEC and MUCILAIR™ cultures were collected for mediator measurements and cells harvested for mRNA and proteins analysis.

Statistical Analysis

Statistical analysis was performed with GraphPad Prism 9.0 software (San Diego). To determine whether the data come from Gaussian distribution, column statistic using Shapiro-Wilk normality test is performed before running the statistical analysis. Statistical significance was determined by non-parametric Kruskal-Wallis multiple-comparisons tests followed by Dunn post-test or two-way ANOVA followed by Dunn post-test as indicated in figure legends. All data are shown as mean ± SEM. Saline control data are compared with HDM group. HDM +/- agonist groups are compared. P value <0.05 was considered significant. *p <0.05, **p <0.01, ***p <0.001 and ****p <0.0001.

Results (2614 words)

Synthetic STING agonist diABZI triggers a neutrophilic asthma exacerbation in HDM sensitized mice.

To evaluate how STING activation by agonists modulate type 2 immune response, we tested their effects during the challenge phase of HDM-induced allergic lung inflammation in mice. We compared the effect of the natural STING agonist cGAMP, and of the potent, non-nucleotidyl STING agonist diABZI¹⁴, to the TLR3 agonist dsRNA Poly(I:C), all known to induce IRF3-type 1 IFN response. Wild type BL6 (WT) mice sensitized with HDM on day 0 and 7 (25 µg/mouse, i.n.) and challenged on day 14-16 (10 µg/ mouse, i.n.) received either diABZI (1 µg/mouse, i.t.), cGAMP (10 µg/mouse, i.t.), or Poly(I:C) (200 µg/mouse, i.t.), doses determined from previous titrations (**Suppl Fig E1-3**), and were analyzed on day 17, 24-hours after the last challenge (**Fig 1A**). First, we evaluated airway hyperresponsiveness (AHR), one of the hallmarks of allergic asthma known to correlate with disease severity^{15, 16}. There was a significant increase of AHR in HDM-challenged WT mice at a dose of 200 mg/mL of methacholine (MCh), as compared to saline control (**Fig 1B**). Administration of diABZI during HDM challenge further increased AHR significantly, while cGAMP increased AHR only at 200 mg/mL of MCh, and Poly(I:C) had no effect, compared to untreated HDM-challenged mice (**Fig 1B**). DiABZI and cGAMP administration had little effect on eosinophil recruitment in the airways (**Fig 1C**), while they strongly increased neutrophil recruitment (**Fig 1D**) in HDM-challenged mice. Interestingly, diABZI and cGAMP promoted a subsets of neutrophils expressing inducible nitric oxide synthase (iNOS/NOS2) corresponding to type 1 neutrophils (N1, NOS2⁺ARG1⁻) while decreased the frequency of arginase 1 (ARG1) expressing type 2 neutrophils (N2, NOS2⁻ARG1⁺) (**Fig 1E, Suppl Fig E4A-D**). This increase in N1 neutrophils

was associated with higher myeloperoxidase (MPO) in BALF and lung (**Fig 1F-G**), total protein extravasation (**Suppl Fig E4E**) and dsDNA release in BALF (**Fig 1H**). There was also an increase in macrophages, but not in lymphocytes influx in BAL (**Suppl Fig E4A-C**) or Th2 cytokines IL-4, IL-5 and IL-13 (**Suppl Fig E4F-K**). The exacerbation effect was observed especially with diABZI, inducing a strong IFN γ response (**Fig 1I**) with CCL11, IL-6 and TNF release in the airways (**Suppl Fig E4L-P**). Further, IFN α/β , the end-products of STING pathway activation were increased in BALF upon diABZI administration (**Fig 1J, K**).

STING agonists induced a narrowing of the airways with severe infiltration of inflammatory cells in the peribronchial area, epithelial injury, bronchiolitis, alveolitis and decreased goblet cells hyperplasia and production of mucus together with a decrease in *Muc5ac* transcripts in the lung compared to HDM-challenged mice (**Fig 1L-P**), while TLR3 agonist caused no major changes (**Fig 1L-O**). Muc5AC protein concentration doubled in BALF after administration of STING or TLR3 agonists while it was essentially unaffected in the lung (**Fig 1Q-R**). STAT6, the transcription factor involved in *Muc5ac* gene induction and mucus hypersecretion¹⁷ was phosphorylated in the lung of HDM challenged mice and this was increased by STING or TLR3 agonists (**Fig 1S, Suppl Fig E4Q**).

Thus, administration of the potent STING agonist diABZI during HDM challenge augmented HDM-induced lung resistance, together with a strong neutrophilic response characterized by neutrophil recruitment, MPO expression, protein extravasation, overexpression of Th1 cytokine IFN γ and extracellular dsDNA release in the airways.

NETosis and PANoptosis as main sources of airway dsDNA fueling STING-triggered exacerbation of HDM inflammation.

Extracellular dsDNA release is an active process in several chronic inflammatory diseases. Therefore, we first assessed the ability of neutrophils to form NETs^{18,19}. Indeed, MPO staining demonstrated that unlike HDM-treated mice that showed localized cellular staining, the lung of cGAMP- and more importantly diABZI-challenged mice exhibited the typical morphological shape of NETs (**Fig 2A**), with citrullinated histone H3 (Cit-H3) revealed by immunoblot (**Fig 2B, suppl Fig E5A**). In contrast, Poly(I:C) did not result in the formation of NET, with intracellular MPO staining and absence of Cit-H3 (**Fig 2A-B**). DNA damage was documented by increased γ H2AX after both diABZI and cGAMP challenges, but less after Poly(I:C) administration (**Fig 2B, suppl Fig E5A**).

NETs comprise host DNA fibers coated with cytoplasmic proteases, making host DNA available to activate DNA sensors. Indeed, cGAS, IFI204 and/or DDX41 expression increased in the lung of HDM and STING agonist challenged mice (**Fig 2C, suppl Fig E5B**). Further, there was evidence of inflammasome activation, likely involving AIM2 and/or NLRP3, with non-canonical caspase-11 upregulation, resulting in cleavage of IL-1 β and IL-18 release after STING trigger (**Fig 2D, suppl Fig E5C**).

NETs associated molecules such as MPO, neutrophil elastase and defensins may promote lung injury, and directly induce epithelial and endothelial cell death^{18,20}. HDM-immunized and challenged mice co-administered with STING or TLR3 agonists induced caspase 3 cleavage indicative of apoptosis in the lung tissue, but also cell death markers of necroptosis and pyroptosis with upregulation of Mixed Lineage Kinase domain Likepseudokinase (MLKL) and Gasdermin D (GSDMD), and GSDMD cleavage indicative of PANoptosis (**Fig 2E, suppl Fig E5D**). We further assessed specific components of the macromolecular complexes regulating PANoptosis by immunoblot. Indeed, Z-DNA binding protein 1 (ZBP1), caspase-8 and RIPK3 were upregulated after challenge with STING or TLR3 agonists in HDM-treated mice (**Fig 2E, suppl Fig E5D**). We also demonstrated a co-localization of PANoptosis components Caspase-

8, ASC and RIPK3 proteins in macrophages from BAL cells (**Fig 2F**) which is absent in neutrophils (**Suppl Fig E5E**).

Therefore, neutrophils induced during HDM challenge with STING agonists undergo NETs formation, expose host DNA to activate innate immune DNA sensors, inducing lung tissue damage and death by PANoptosis, amplifying DNA release as a positive feedback loop.

STING dependence of the neutrophilic exacerbation of HDM-induced response.

To evaluate the STING specificity of diABZI induced asthma exacerbation, response to the extracellularly released dsDNA, mice deficient for STING ($STING^{-/-}$) or cGAS ($cGAS^{-/-}$) were sensitized and challenged with HDM with or without diABZI as above (**Fig 3A**). DiABZI-induced increase of neutrophils was absent in the airways of HDM-challenged $STING^{-/-}$ mice, and reduced in $cGAS^{-/-}$ mice (**Fig 3B**), as were total inflammatory cells, macrophages and lymphocytes, or the decreased recruitment of eosinophils (**Suppl Fig E6A-D**). In addition, diABZI-induced increase of MPO and extracellular dsDNA (**Fig 3C-E**), or protein extravasation, $IFN\gamma$, TNF, IL-6, and CXCL10 (**Fig 3F-K**) release were abolished in the airways of HDM-challenged $STING^{-/-}$ mice, while they were barely affected in $cGAS^{-/-}$ mice. Because allergic airway inflammation triggers Th2 immune response, we evaluated Th2 cytokines and found increased IL-4 and IL-5 transcripts and proteins in HDM-challenged mice (**Suppl Fig E6E, F and H, I**). DiABZI further increased Th2 cytokine IL-13 and chemokines CCL11 and CCL24 in the airways, and this was absent in $STING^{-/-}$ and reduced in $cGAS^{-/-}$ mice (**Suppl Fig E6 G, J-L**). Pulmonary CXCR2⁺ and CXCR4⁺ expressing neutrophils subsets increased after diABZI challenge were reduced in $STING^{-/-}$ and $cGAS^{-/-}$ mice (**Suppl Fig E6 O-R**).

The increased leukocyte infiltration, epithelial injury, with decreased goblet cells, mucus staining (**Fig 3L-O**) and *Muc5ac* transcript expression (**Fig 3P**) after diABZI administration in HDM-challenged WT mice were abolished in $STING^{-/-}$ mice, while they were barely affected

in cGAS^{-/-} mice. DiABZI and HDM co-administration upregulated *Tmem173* (STING) transcript expression in WT and cGAS^{-/-} mice (**Fig 3Q**), while the increase in *Mb21d1* (cGAS) transcripts was abolished in STING^{-/-} mice (**Fig 3R**).

IL-13 mRNA expression, a Th2 cytokine necessary for mucus metaplasia, increased after diABZI and HDM co-administration in WT mice, while it was barely affected in STING^{-/-} or cGAS^{-/-} mice. IL-13 binding triggers a STAT6-dependent transcriptional program involving the activation of *Serpin1* and *Clca1* (protein calcium-activated chloride channel 1) whose transcripts were overexpressed after diABZI administration in HDM-challenged WT mice but not in STING^{-/-} mice (**Fig 3S-V**). On the other hand, the transcripts for *Socs1*, a negative regulator of *Muc5ac* expression²¹, was overexpressed after diABZI co-administration in WT mice but not in STING^{-/-} mice (**Fig 3W**), in line with the fact that STING activation was shown to enhance SOCS1 expression²².

Thus, diABZI-induced asthma exacerbation is mediated by STING pathway activation in terms of neutrophil recruitment, release of extracellular dsDNA and pro-inflammatory cytokines in the airways, increased epithelial injury with decreased goblet cells and mucus production, while the involvement of cGAS is more limited.

STING-deficient macrophages and granulocytes mitigate asthma exacerbation in vivo.

Neutrophilic inflammation is observed during asthma exacerbation but also in the airways of patients with severe asthma²³. In addition to neutrophils, macrophages are one of the main lung cell types responsible for the uptake of cGAMP *in vivo*²⁴. We investigated the contribution of both cell types in mice by generating conditional STING deficient mice. We crossed mice carrying STING-OST floxed alleles (STING-OST^{fl}) with LysM^{cre} transgenic mice expressing Cre under the control of the LysM promotor to obtain STING-OST^{fl}LysM^{cre/+} mice deficient for STING gene in myeloid cells such as granulocytes and macrophages, as well as STING-

OST^{fl}LysM^{+/+} control mice (**Suppl Fig E7 A-D**). Administration of cGAMP during HDM challenges resulted in a reduction of eosinophils and an increase in total cells, neutrophils, MPO and self dsDNA in BALF of STING-OST^{fl}LysM^{+/+} control mice (**Fig4 A-E** and **Suppl Fig E7E, G**). These parameters were partially reduced in STING-OST^{fl}LysM^{cre/+} suggesting that myeloid cells, but also other cell types contribute to shape the neutrophilic response after STING trigger (**Fig4 A-E**). cGAMP induced an increase in type I IFN α/β , as well as pro-inflammatory cytokines TNF α and IL-6 production in HDM-treated STING-OST^{fl}LysM^{+/+} control mice that were partially reduced in STING-OST^{fl}LysM^{cre/+} (**Fig 4 F-I**). The increase in peribronchial leukocytes infiltration and epithelial injury following cGAMP administration in STING-OST^{fl}LysM^{+/+} mice was abrogated in STING-OST^{fl}LysM^{cre/+} (**Fig 4J, K**). Moreover, protein extravasation in BALF was reduced in STING-OST^{fl}LysM^{cre/+} mice in comparison with control mice (**Suppl Fig E7F**), which was suggestive of a less severe barrier disruption. Neutrophils infiltrating the lung of mice lacking STING in granulocytes/macrophages, were tested for their ability to form NETs. BAL cells from STING-OST^{fl}LysM^{+/+} control mice challenged with HDM and cGAMP showed the formation of a weblike structure positive for MPO and Cit-H3 staining (**Fig 4L**), suggestive of NET formation. In contrast, this process was reduced in STING-OST^{fl}LysM^{cre/+} group (**Fig 4L**), in line with the reduced histopathological damage observed.

Thus, these data indicate that granulocytes/macrophages, but also other cell types, contribute to the development of STING-dependent neutrophilic asthma exacerbation *in vivo*.

Epithelial cells respond to diABZI and may contribute to STING agonist-induced neutrophilic asthma exacerbation.

Allergens cause airway epithelium damage and structural changes including downregulation of group I tight junction and extracellular matrix (ECM) expression which are often associated with asthma exacerbations and severity²⁵⁻²⁷. The transmembrane proteins Zona-occludens-1

(ZO-1) are scaffold proteins important for cell-cell adhesion in healthy tissue and main regulators of epithelial permeability in allergic lung inflammation²⁶. After confirming the role of diABZI on immune cells infiltration, we investigated its effect on human airway epithelium. HDM led to ZO-1 downregulation in lung tissue compared to saline control (**Fig 5A**), as expected²⁶. STING agonists DiABZI and cGAMP, and Poly(I:C) further downregulated ZO-1 expression as evidenced by immunofluorescence staining (**Fig 5A**). To evaluate the ability of diABZI to activate STING pathway in epithelial cells, human airway epithelial cells (hAEC) from bronchial biopsies were stimulated for 2h or 24h with HDM alone or in combination with diABZI, cGAMP or Poly(I:C). There was evidence of STING pathway activation with the detection of phosphorylated STING, TBK1 and IRF3 when hAEC were co-stimulated with diABZI detectable at an early stage, 2h post stimulation (**Fig 5B, suppl Fig E8A**). cGAMP and Poly(I:C) co-stimulation also induced TBK1 phosphorylation at 2h, that persisted after 24h with diABZI and cGAMP. Moreover, there was evidence of epithelial DNA damage in hAEC, revealed by phosphorylation of γ H2AX at 2h and 24h post stimulation (**Fig 5C, suppl Fig E8A**), and some activation of necroptosis with the phosphorylation of MLKL at 2h (**Fig 5C, suppl Fig E8A**). Activating STING with diABZI in cells sensitized with HDM yielded in the secretion of inflammatory cytokines starting from 2h post stimulation that were sustained after 24h, such as CXCL8, IFN β , CXCL10, IL-6 and TNF- α (**Fig 5 D-M**).

To further characterize the contribution of epithelial barrier, air liquid interface (ALI) culture of bronchial epithelial cells isolated from the lung of healthy donor and patient with asthma were performed and stimulated for 16h with HDM alone or in combination with diABZI, cGAMP or Poly(I:C) (**Fig 5 N**). DiABZI induced an increased release of lactate dehydrogenase (LDH), IFN α , IFN β , IFN λ , CXCL10, IL-6 and TNF- α protein and overexpression of *MUC5AC* transcript in healthy epithelial cells sensitized with HDM (**Fig 5 O-V**), and less in epithelial cells from patient with asthma (**Fig 5 O-V**). Further, diABZI induced epithelial DNA damage

evidenced by the phosphorylation of γ H2AX in epithelial cells from patient with asthma, compared to healthy cells (**Fig 5 W**).

Thus, diABZI affected airway epithelium cells by activating STING pathway, impairing tight junctions, and inducing epithelial DNA damage, necroptosis and secretion of inflammatory cytokines, that may further fuel the lung inflammation.

Viral infection of human bronchial epithelial cells from patients with asthma aggravates inflammation and weakens epithelial barrier both *in vitro* and *in vivo*.

To ascertain the clinical relevance of these findings, we first analyzed the different expression of STING and PANoptosis pathways in PBMC from healthy controls or patients with severe asthma (**Suppl FigE9**). Indeed, host double-stranded DNA released by NETosis promote rhinovirus-induced asthma exacerbations²⁸. Therefore, we analyzed DNA-sensing, PANoptosis, tight junction, and neutrophils gene signatures from two independent studies addressing Rhinovirus (RV) infection in patients with asthma, either *in vitro* in differentiated primary bronchial epithelial cells (HBECs) from healthy and individuals with asthma²⁹, or *in vivo* in bronchial brushing from intranasally RV infected healthy controls and patients with asthma^{30,31} (**Supl FigE10**).

Human epithelial cells from patients with asthma stimulated *in vitro* with RV-A16 (**Fig. 6A**) showed an upregulation of genes involved in DNA-sensing and STING pathway (**Fig.6B**) such as the DNA sensors ZBP1, IFI16 and the cytosolic TRIM21. *IRF3* responsible of type I/III IFNs induction and anti-viral defense was also upregulated in the cells of these patients, concomitant with *IFN- λ* expression, while STING itself was not significantly downregulated. Analysis of tight-junction gene sets (**Fig.6C**) revealed the reduced expression of a whole cluster of genes such as *OCN*, *CLD3*, *CLDN4*, *NRAS*, *HCLS1*, *MYH10* in virus-infected cells from patients with asthma in comparison to the controls. Moreover, analysis of PANoptosis related genes set

revealed the upregulation and a tendency to upregulation of several components of the PANoptosome such as the pivotal *ZBP1*, *PYCARD*, *CASPASE-8*, *RIPK1*, *CASPASE-1*, and *FADD* after viral infection of the cells from patients with asthma compared to the controls (**Fig.6D**), which was not visible before RV infection (**Suppl Fig E10A-D**). Mucus genes such as *MUC5AC* and *MUC5B* were also upregulated (**Suppl Fig E10E-F**).

Bronchial brushings from patients with asthma experimentally infected *in vivo* with RV-A16³⁰ (**Fig. 6E**) showed a decrease in a group of tight junction-related gene such as *CLDN15*, *TJAP1*, *AKT2*, *SRC*, *CGN*, *EXOC3*, *LLG2*, *CLDN22*, compared to similarly infected healthy controls, while *CLDN12* and *MYL12B* genes were increased (**Fig. 6F**). PANoptosis components showed a tendency toward an increase 4 days after *in vivo* infection in patients with asthma compared to controls (**Fig.6G**), in contrast to the non-infected controls and patients with asthma, where the PANoptosis components were downregulated (**Suppl Fig E9G-I**). Moreover, the gene expression of IL-18 (*IL18*) was higher after infection in patients with asthma compared to healthy individuals (**Fig.6G**), in line with inflammasome activation³¹. Interestingly, the NOS2/ARG1 gene expression balance was disrupted in bronchial brushings. *NOS2* was significantly increased after infection in patients with asthma compared to the controls, while *ARG1* was downregulated in patients with asthma (**Fig.6H-I**). Overall, these analyses show an involvement of DNA sensing pathway, weakening of the epithelial barrier and upregulation of pro-inflammatory markers such as *NOS2* after RV infection in patients with asthma.

Discussion (791 words)

Here we demonstrate the existence of a tight link between STING activation during type 2 allergic response challenge and asthma exacerbation, with reproduction of hallmark features of severe asthma and epithelial damage. Indeed, administration of synthetic STING agonist diABZI during HDM challenge induces asthma exacerbation by increasing epithelial damage, dsDNA release, DNA damage, cell death by NETosis and PANoptosis, and neutrophils influx in the lung. We highlight the partial requirement for STING expression in granulocytes/macrophages to induce asthma exacerbation. We show that co-stimulation of human epithelial cells with diABZI and HDM induces IL-6, TNF- α , type I IFN α/β and type III IFN λ release *in vitro*, with DNA damage and cell death. These results have important implications revealing STING agonists as inducers of asthma exacerbation and offer a mechanism through which dsDNA release after cell death triggers Th1 response and promotes neutrophilic asthma exacerbation.

Host DNA released from dying cells was shown to mediate alum adjuvant activity ⁷, and cGAMP may function as a type 2 adjuvant promoting allergic asthma when administered during sensitization with HDM ¹⁰. Our previous findings showing neutrophilic response induced by STING agonists in the airways ¹¹ prompted us to ask whether triggering STING during HDM-challenge might affect the allergic response and promote a neutrophilic exacerbation.

The potent STING agonist diABZI administered during HDM-challenge strongly exacerbated neutrophil recruitment and the release of IFN γ , CXCL1/KC and CXCL10/IP10 in the airways. It induced some cell stress with extracellular dsDNA release, mobilized DNA sensors, and promoted an IFN α/β response. Importantly, administration of diABZI during HDM-challenge functionally exacerbated HDM-induced lung resistance, while Poly(I:C) did not affect lung function. We verified that diABZI-induced neutrophilic response in HDM-challenged mice is fully dependent on STING pathway, as it is absent in STING-deficient mice, and showed a

limited involvement of cGAS. The increased neutrophil recruitment, together with the presence of extracellular DNA, MPO and Cit-H3 was indicative of NETs formation, that were indeed visible in the airways of HDM challenged mice after cGAMP or diABZI administration. Thus, STING agonist induction of NETosis may contribute to the neutrophilic exacerbation of HDM-induced responses.

STING agonists led to a reduction of goblet cell numbers and of mucus transcript in the lung of HDM-challenged mice, together with a strong release of mucus protein in the airways. A possible explanation is that diABZI induced epithelial barrier damage, documented by epithelium cell tight junction ZO-1 protein expression, leading to Goblet cells shedding and release of their mucus content, that may clog the airspace and contribute to the exacerbation of HDM-induced lung resistance.

Several soluble mediators regulate the recruitment of neutrophils in the airways ²³. Indeed, diABZI induced IFN γ , CXCL1/KC and CXCL10/IP10 release *in vivo* in the BAL of HDM-challenged mice, and CXCL8 *in vitro* in the supernatant of human epithelial cells. These mediators are potent neutrophil chemoattractants in the lung, CXCL10 facilitating the recruitment of Th1 cells producing IFN γ which, in turn, upregulates chemotaxis receptors of human neutrophils ³². Functional type I IFN signaling in neutrophils induces neutrophil maturation, and limits their lifespan by acting on both extrinsic and intrinsic apoptosis pathways but also by influencing the NETosis process ³³. Indeed, we show increased mature neutrophils expressing high CXCR2 or CXCR4 in the airways after diABZI during HDM-challenge.

Type I IFNs are essential regulators of neutrophil polarization, as shown in cancer, driving neutrophils from anti-inflammatory, pro-tumoral N2 phenotype into pro-inflammatory, anti-tumoral N1 capable of cytotoxicity ^{33, 34}. Here, we demonstrate that STING agonists strongly induced N1 (NOS2⁺ARG1⁻) subset. This phenotypic shift from N2 (ARG1⁺NOS2⁻) observed at HDM baseline response toward N1 pro-inflammatory after STING agonist challenge, may

shape neutrophils function and enroll them in NETs formation process, in part responsible of lung tissue damage. Conversely, the N2 (ARG1⁺ NOS2⁻) profile of Poly(I:C)-induced neutrophils may explain the lack of NET in the lung of Poly(I:C) treated HDM challenged mice. NOS2 and ARG1 are important enzymes regulating both macrophage and neutrophil functions and markers of alternative activation ^{35, 36}. NOS2 has multiple roles in the airways, its expression being highest in severe asthma, while ARG1 decreases ³⁷⁻⁴⁰. We report increased NOS2 expression in RV-A16 infected patients with asthma, as compared to healthy controls. Further, transcriptomic analyses of RV-A16 infected cells from patients with asthma also indicated an involvement of DNA sensing, PANoptosis, and weakening of the epithelial barrier. Our study is the first to demonstrate the induction of this particular subset of N1, NOS2⁺ARG1⁻ neutrophils following STING activation.

Triggering STING in an allergic context may shape the inflammatory response toward a mixed Th1/Th2 immune response and recapitulate features of severe neutrophilic asthma with increased lung resistance, NETosis and PANoptosis, increased epithelial injury, release of extracellular dsDNA and pro-inflammatory cytokines in the airways. Thus, targeting the STING pathway might be considered in severe asthma including seasonal respiratory viral exacerbation.

Acknowledgements

The authors thank Glen N. Barber for sharing the STING-deficient mice, to Zhijian J. Chen for providing cGAS-deficient mice (University of Texas Southwestern Medical Center, Dallas), to Nicolas Manel for sharing STING-OST^{fl} mice (Institut Curie, PSL Research University, INSERM U932, Paris, France). The skillful assistance of David Gosset, running the MO2VING platform (CNRS UPR 4301, Orleans) and Marie-Laure Dessain (TAAM, CNRS UAR44) are gratefully acknowledged.

Conflict of interest statement

M.S. reports research grants from Swiss National Science Foundation (nr 310030_189334/1), Novartis Foundation for Medical-Biological Research, GSK, and Stiftung vorm. Buendner Heilstaette Arosa; speaker's fee from AstraZeneca; voluntary positions in the European Academy of Allergy and Clinical Immunology (EAACI) as Executive Board member and Basic and Clinical Immunology Section Chair. S.L.J. reports grants/contracts from European Research Council ERC FP7 grant number 233015, Chair from Asthma UK CH11SJ, Medical Research Council Centre grant number G1000758, NIHR Biomedical Research Centre grant number P26095, Predicta FP7 Collaborative Project grant number 260895, NIHR Emeritus NIHR Senior Investigator; consulting fees from Lallemand Pharma, Bioforce, resTORbio, Gerson Lehrman Group, Boehringer Ingelheim, Novartis, Bayer, Myelo Therapeutics GmbH; patents issued/licensed: Wark PA, Johnston SL, Holgate ST, Davies DE. Anti-virus therapy for respiratory diseases. UK patent application No. GB 0405634.7, 12March 2004. Wark PA, Johnston SL, Holgate ST, Davies DE. Interferon-Beta for Anti-Virus Therapy for Respiratory Diseases. International Patent Application No. PCT/GB05/50031, 12 March 2004. Davies DE, Wark PA, Holgate ST, Johnston SL. Interferon Lambda therapy for the treatment of respiratory disease. UK patent application No. 6779645.9, granted 15th August 2012; Participation on a data safety monitoring board or advisory board: Enanta Chair of DSMB, Virtus Respiratory

Research Ltd Shareholder and Board membership. All other authors declare no competing interests

Ethics Statement

All animal experiments complied with the French Government animal experiment regulations and ARRIVE guidelines. The protocols were submitted to the “Ethics Committee for Animal Experimentation of CNRS Campus Orleans” under the number CLE CCO 2019-2017 and 2020-2006, and approved by the French Government animal experiment regulatory authorities under APAFIS #25876 and #26195. In vivo rhinovirus infection in controls and patients with asthma was approved by the St. Mary`s Hospital Research Ethics Committee (United Kingdom), permission number 09/H0712/59 (observational trial registration number NCT01159782) ^{30, 31}.

Data Availability Statement

All datasets generated and analyzed during this study are included in this published article and its Supplementary Information files. Publicly available Transcriptome data from bronchial brushings from control individuals and patients with asthma infected in vivo with RV are available under accession number: GSE185658 ³¹. Publicly available RNAseq data GSE61141 were downloaded from the NCBI gene expression omnibus ^{29, 31}. Additional data are available from corresponding author on reasonable request. The PBMCs scRNAseq datasets from patients with severe asthma and control individuals analyzed in the present study, have been deposited in the Sequence Read Archive (SRA) repository under the accession number GSE172495 ⁴¹.

References:

1. Hammad H, Lambrecht BN. The basic immunology of asthma. *Cell* 2021; 184:1469-85.
2. Schiffers C, Hristova M, Habibovic A, Dustin CM, Danyal K, Reynaert NL, et al. The Transient Receptor Potential Channel Vanilloid 1 Is Critical in Innate Airway Epithelial Responses to Protease Allergens. *Am J Respir Cell Mol Biol* 2020; 63:198-208.
3. Agache I. Severe asthma phenotypes and endotypes. *Semin Immunol* 2019; 46:101301.
4. Cardoso-Vigueros C, von Blumenthal T, Ruckert B, Rinaldi AO, Tan G, Dreher A, et al. Leukocyte redistribution as immunological biomarker of corticosteroid resistance in severe asthma. *Clin Exp Allergy* 2022; 52:1183-94.
5. Fahy JV. Type 2 inflammation in asthma--present in most, absent in many. *Nat Rev Immunol* 2015; 15:57-65.
6. Lambrecht BN, Hammad H, Fahy JV. The Cytokines of Asthma. *Immunity* 2019; 50:975-91.
7. Marichal T, Ohata K, Bedoret D, Mesnil C, Sabatel C, Kobiyama K, et al. DNA released from dying host cells mediates aluminum adjuvant activity. *Nat Med* 2011; 17:996-1002.
8. Decout A, Katz JD, Venkatraman S, Ablasser A. The cGAS-STING pathway as a therapeutic target in inflammatory diseases. *Nat Rev Immunol* 2021; 21:548-69.
9. Han Y, Chen L, Liu H, Jin Z, Wu Y, Wu Y, et al. Airway Epithelial cGAS Is Critical for Induction of Experimental Allergic Airway Inflammation. *J Immunol* 2020; 204:1437-47.
10. Ozasa K, Temizoz B, Kusakabe T, Kobari S, Momota M, Coban C, et al. Cyclic GMP-AMP Triggers Asthma in an IL-33-Dependent Manner That Is Blocked by Amlexanox, a TBK1 Inhibitor. *Front Immunol* 2019; 10:2212.

11. Messaoud-Nacer Y, Culerier E, Rose S, Maillet I, Rouxel N, Briault S, et al. STING agonist diABZI induces PANoptosis and DNA mediated acute respiratory distress syndrome (ARDS). *Cell Death Dis* 2022; 13:269.
12. Ahn J, Gutman D, Saijo S, Barber GN. STING manifests self DNA-dependent inflammatory disease. *Proc Natl Acad Sci U S A* 2012; 109:19386-91.
13. Li XD, Wu J, Gao D, Wang H, Sun L, Chen ZJ. Pivotal roles of cGAS-cGAMP signaling in antiviral defense and immune adjuvant effects. *Science* 2013; 341:1390-4.
14. Ramanjulu JM, Pesiridis GS, Yang J, Concha N, Singhaus R, Zhang SY, et al. Design of amidobenzimidazole STING receptor agonists with systemic activity. *Nature* 2018; 564:439-43.
15. Chapman DG, Irvin CG. Mechanisms of airway hyper-responsiveness in asthma: the past, present and yet to come. *Clin Exp Allergy* 2015; 45:706-19.
16. Lemanske RF, Jr., Busse WW. Asthma: clinical expression and molecular mechanisms. *J Allergy Clin Immunol* 2010; 125:S95-102.
17. Wang X, Li Y, Luo D, Wang X, Zhang Y, Liu Z, et al. Lyn regulates mucus secretion and MUC5AC via the STAT6 signaling pathway during allergic airway inflammation. *Sci Rep* 2017; 7:42675.
18. Porto BN, Stein RT. Neutrophil Extracellular Traps in Pulmonary Diseases: Too Much of a Good Thing? *Front Immunol* 2016; 7:311.
19. Vorobjeva NV, Pinegin BV. Neutrophil extracellular traps: mechanisms of formation and role in health and disease. *Biochemistry (Mosc)* 2014; 79:1286-96.
20. Radermecker C, Detrembleur N, Guiot J, Cavalier E, Henket M, d'Emal C, et al. Neutrophil extracellular traps infiltrate the lung airway, interstitial, and vascular compartments in severe COVID-19. *J Exp Med* 2020; 217.

21. Chen L, Xu J, Deng M, Liang Y, Ma J, Zhang L, et al. Telmisartan mitigates lipopolysaccharide (LPS)-induced production of mucin 5AC (MUC5AC) through increasing suppressor of cytokine signaling 1 (SOCS1). *Bioengineered* 2021; 12:3912-23.
22. Zhang CX, Ye SB, Ni JJ, Cai TT, Liu YN, Huang DJ, et al. STING signaling remodels the tumor microenvironment by antagonizing myeloid-derived suppressor cell expansion. *Cell Death Differ* 2019; 26:2314-28.
23. Ray A, Kolls JK. Neutrophilic Inflammation in Asthma and Association with Disease Severity. *Trends Immunol* 2017; 38:942-54.
24. She L, Barrera GD, Yan L, Alanazi HH, Brooks EG, Dube PH, et al. STING activation in alveolar macrophages and group 2 innate lymphoid cells suppresses IL-33-driven type 2 immunopathology. *JCI Insight* 2021; 6.
25. Akdis CA. Does the epithelial barrier hypothesis explain the increase in allergy, autoimmunity and other chronic conditions? *Nat Rev Immunol* 2021; 21:739-51.
26. Tan HT, Hagner S, Ruchti F, Radzikowska U, Tan G, Altunbulakli C, et al. Tight junction, mucin, and inflammasome-related molecules are differentially expressed in eosinophilic, mixed, and neutrophilic experimental asthma in mice. *Allergy* 2019; 74:294-307.
27. Xiao C, Puddicombe SM, Field S, Haywood J, Broughton-Head V, Puxeddu I, et al. Defective epithelial barrier function in asthma. *J Allergy Clin Immunol* 2011; 128:549-56 e1-12.
28. Toussaint M, Jackson DJ, Swieboda D, Guedan A, Tsourouktsoglou TD, Ching YM, et al. Host DNA released by NETosis promotes rhinovirus-induced type-2 allergic asthma exacerbation. *Nat Med* 2017; 23:681-91.

29. Bai J, Smock SL, Jackson GR, Jr., MacIsaac KD, Huang Y, Mankus C, et al. Phenotypic responses of differentiated asthmatic human airway epithelial cultures to rhinovirus. *PLoS One* 2015; 10:e0118286.
30. Jackson DJ, Makrinioti H, Rana BM, Shamji BW, Trujillo-Torralbo MB, Footitt J, et al. IL-33-dependent type 2 inflammation during rhinovirus-induced asthma exacerbations in vivo. *Am J Respir Crit Care Med* 2014; 190:1373-82.
31. Radzikowska U, Eljaszewicz A, Tan G, Stocker N, Heider A, Westermann P, et al. Rhinovirus-induced epithelial RIG-I inflammasome suppresses antiviral immunity and promotes inflammation in asthma and COVID-19. *Nat Commun* 2023; 14:2329.
32. Bonecchi R, Polentarutti N, Luini W, Borsatti A, Bernasconi S, Locati M, et al. Up-regulation of CCR1 and CCR3 and induction of chemotaxis to CC chemokines by IFN-gamma in human neutrophils. *J Immunol* 1999; 162:474-9.
33. Pylaeva E, Lang S, Jablonska J. The Essential Role of Type I Interferons in Differentiation and Activation of Tumor-Associated Neutrophils. *Front Immunol* 2016; 7:629.
34. Wang X, Qiu L, Li Z, Wang XY, Yi H. Understanding the Multifaceted Role of Neutrophils in Cancer and Autoimmune Diseases. *Front Immunol* 2018; 9:2456.
35. Garcia-Navas R, Gajate C, Mollinedo F. Neutrophils drive endoplasmic reticulum stress-mediated apoptosis in cancer cells through arginase-1 release. *Sci Rep* 2021; 11:12574.
36. Murray PJ. Macrophage Polarization. *Annu Rev Physiol* 2017; 79:541-66.
37. Cloots RHE, Poynter ME, Terwindt E, Lamers WH, Kohler SE. Hypoargininemia exacerbates airway hyperresponsiveness in a mouse model of asthma. *Respir Res* 2018; 19:98.

38. Litonjua AA, Lasky-Su J, Schneiter K, Tantisira KG, Lazarus R, Klanderman B, et al. ARG1 is a novel bronchodilator response gene: screening and replication in four asthma cohorts. *Am J Respir Crit Care Med* 2008; 178:688-94.
39. Maarsingh H, Dekkers BG, Zuidhof AB, Bos IS, Menzen MH, Klein T, et al. Increased arginase activity contributes to airway remodelling in chronic allergic asthma. *Eur Respir J* 2011; 38:318-28.
40. Yamamoto M, Tochino Y, Chibana K, Trudeau JB, Holguin F, Wenzel SE. Nitric oxide and related enzymes in asthma: relation to severity, enzyme function and inflammation. *Clin Exp Allergy* 2012; 42:760-8.
41. Chen A, Diaz-Soto MP, Sanmamed MF, Adams T, Schupp JC, Gupta A, et al. Single-cell characterization of a model of poly I:C-stimulated peripheral blood mononuclear cells in severe asthma. *Respir Res* 2021; 22:122.

Figure 1

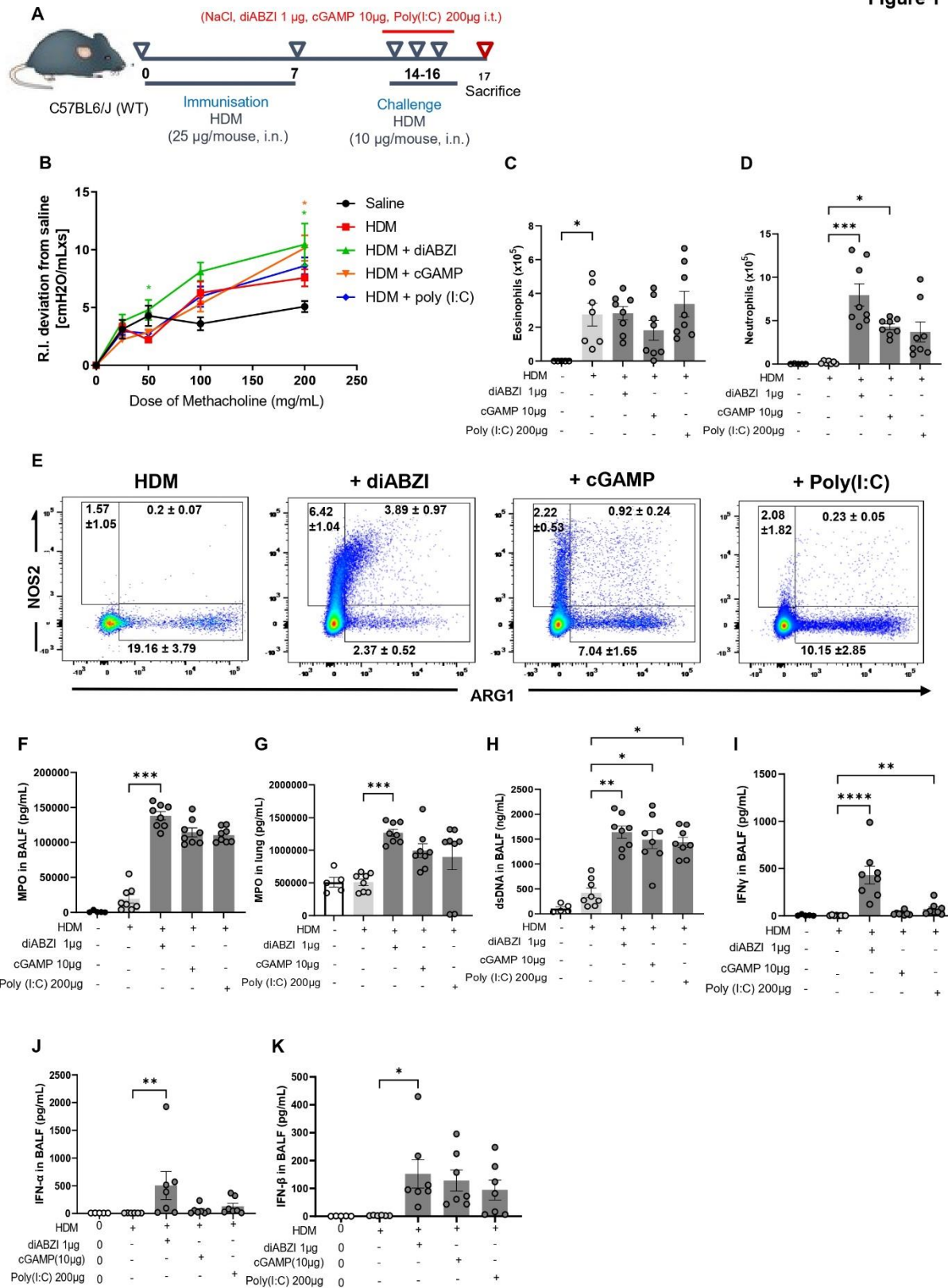


Figure 1 continued

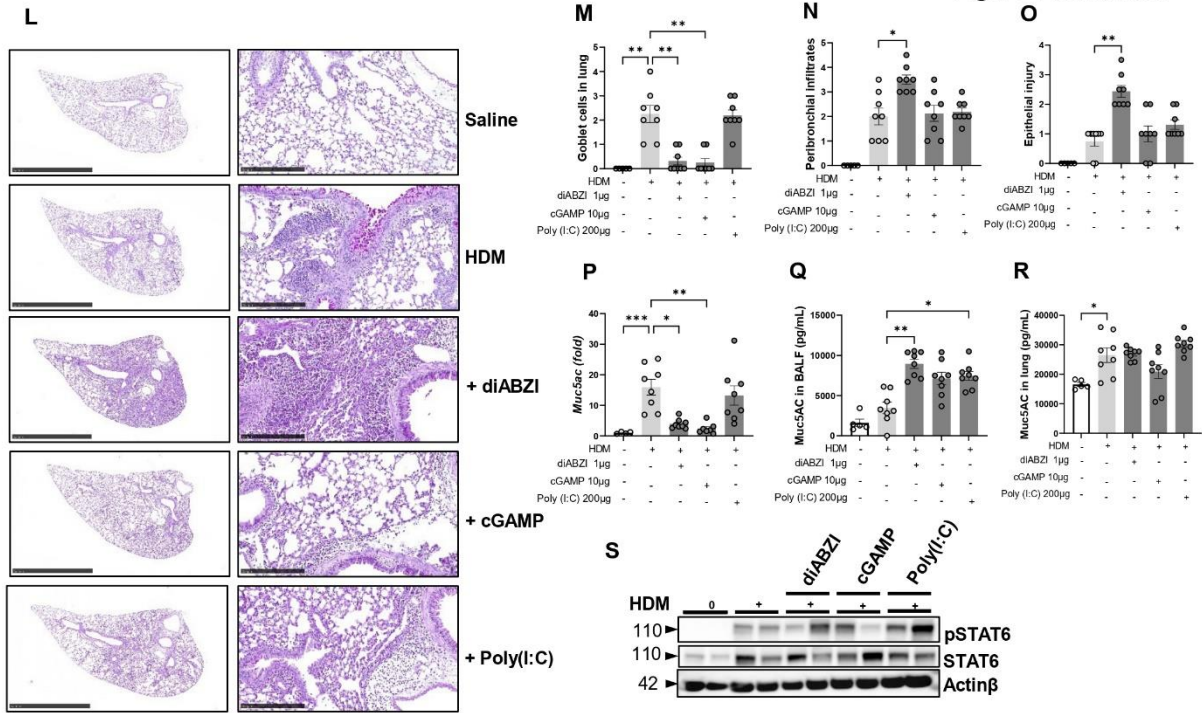


Figure 1: Endogenous STING agonists promote lung neutrophilia and exacerbate allergic airway inflammation.

(A) Mice sensitized with HDM on day 0 and 7 (25 µg/mouse, i.n.) and challenged with HDM on day 14-16 (10 µg/mouse, i.n.) received either diABZI (1 µg/mouse, i.t.), cGAMP (10 µg/mouse, i.t.), or Poly(I:C) (200 µg/mouse, i.t.) on day 14-16, and were analyzed on day 17. (B) Airway resistance to increased doses of methacholine (50-200 mg/mL Mch) was measured 24h after the last HDM/agonist challenges. (C) Eosinophil and (D) neutrophil counts in BAL. (E) Flow cytometry analysis of NOS2/ARG1 expressing neutrophils pre-gated on singlet cells, and CD45⁺CD11b⁺Ly6G⁺F4/80⁻SiglecF⁻ cells. (F, G) Myeloperoxidase (MPO) concentrations in BALF and lung determined by ELISA. (H) dsDNA measured in the acellular fraction of the BAL. (I) IFN γ , (J) IFN- α and (K) IFN- β concentrations in BALF measured by multiplex immunoassay. (L) Histology of lung sections stained with PAS, with semi quantitative pathology scoring of (M) goblet cells, (N) peribronchial infiltrates and (O) epithelial injury. Bars, left panel: 2.5 mm, right panel: 250 µm. (P) *Muc5ac* transcripts measured by real-time PCR (Q, R) *Muc5ac* protein in BALF and lung measured by ELISA. (S) Immunoblots of phospho-STAT6 and STAT6 with Actin β as a reference. Data were presented as mean \pm SEM with n = 8 mice per group. Each point represents an individual mouse. *p < 0.05, **p < 0.01, ***p < 0.001, ****p < 0.0001 (Nonparametric Kruskal–Wallis with Dunn’s post-test).

Figure 2

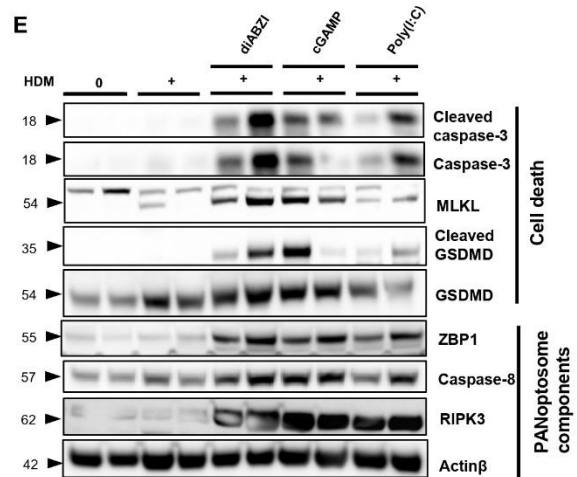
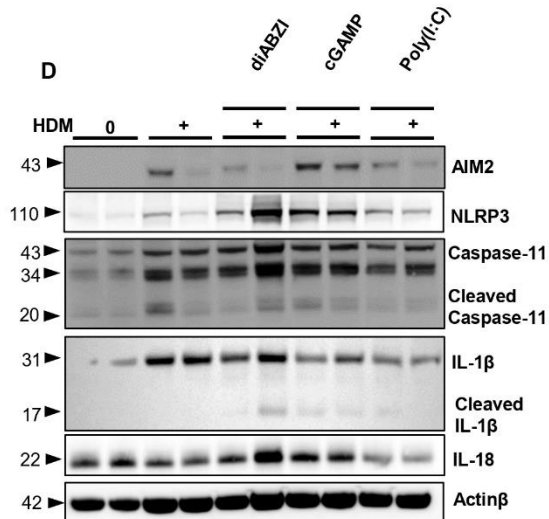
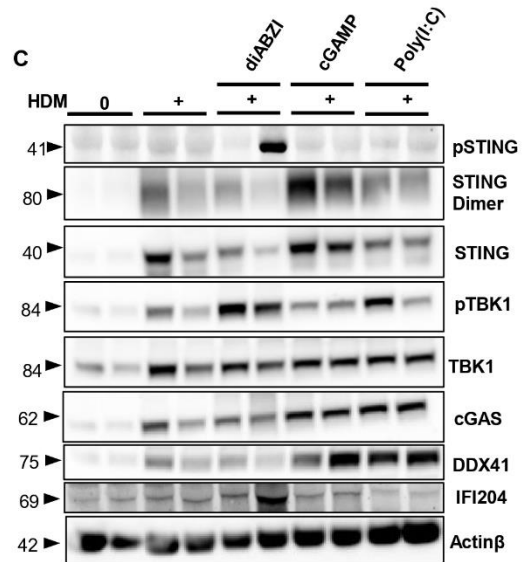
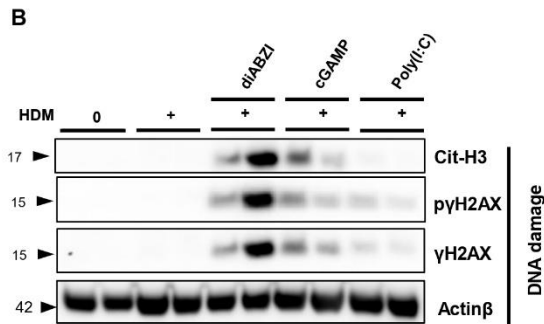
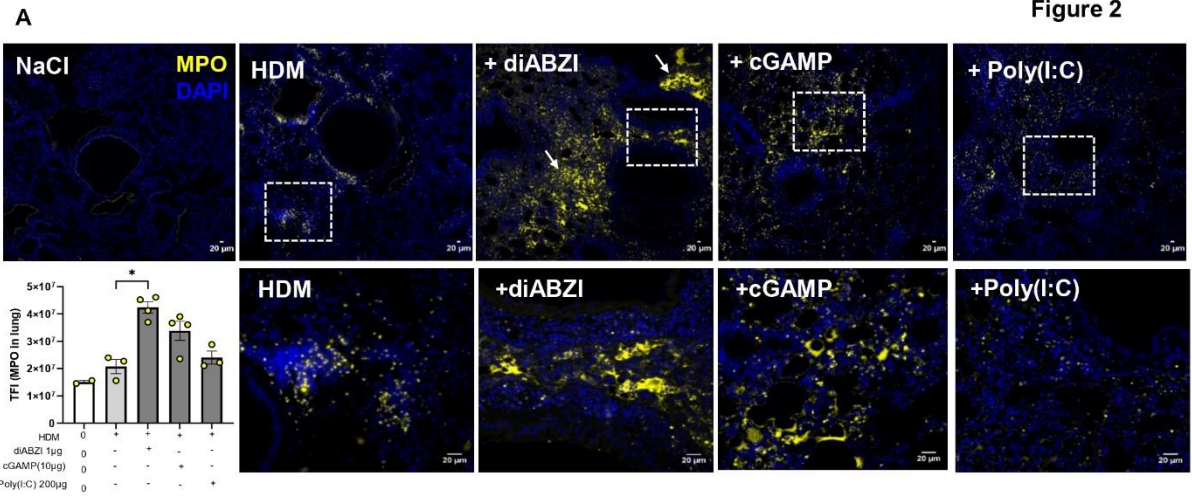


Figure 2 continued

F

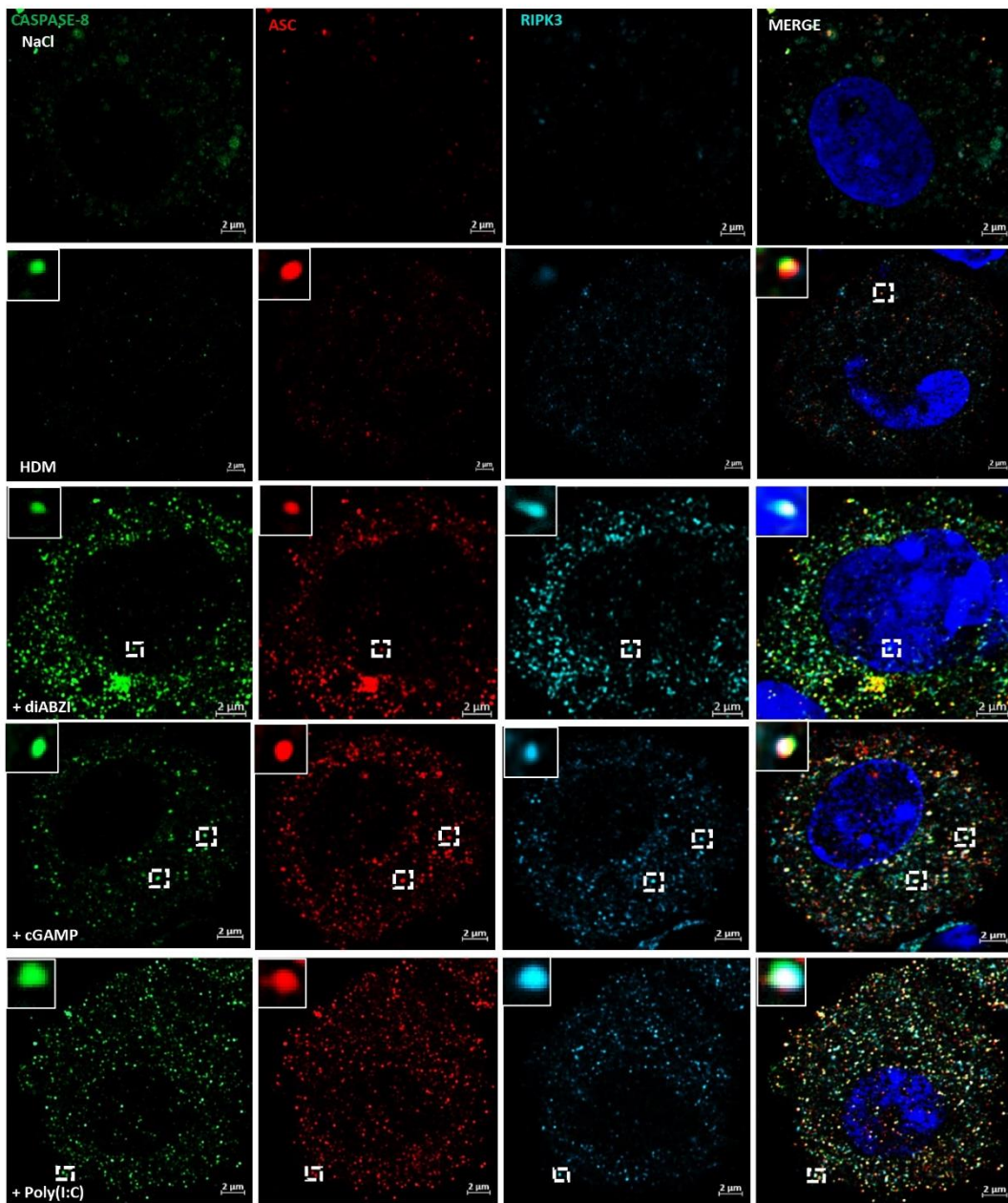


Figure 2: NETosis, apoptosis, pyroptosis and necroptosis (PANoptosis) as main sources of airway dsDNA exacerbating HDM-induced lung inflammation.

Mice sensitized and challenged with HDM received either diABZI, cGAMP, or Poly(I:C) as in Figure 1, and were analyzed on day 17. **(A)** Visualization of NETs formation in lung tissue with the staining of DNA dye DAPI (Blue) and MPO (Yellow). Bars (20 μ m). Tissue fluorescence intensity (TFI) of MPO staining in lung. **(B)** Immunoblot highlighting DNA damage with expression of Cit-H3 phospho- γ H2AX and γ H2AX with Actin β as a reference. **(C)** Immunoblot of STING axis including phospho-STING, STING dimer, STING, phospho-TBK1, TBK1 and DNA sensors including cGAS, DDX41 and IFI204 with Actin β as a reference. **(D)** Immunoblot of inflammasome activation including AIM2, NLRP3, Caspase-11, cleaved caspase-11, IL-1 β , cleaved IL-1 β and IL-18 with Actin β as a reference. **(E)** Immunoblot of cell death axis showing cleaved caspase-3, caspase-3, MLKL, cleaved GSDMD, GSDMD, ZBP1, caspase-8, and RIPK3 with Actin β as a reference. **(F)** Confocal microscopy showing Caspase-8 (green), ASC (red), RIPK3 (far-red/turquoise blue) and DNA dye DAPI (cyan) in BAL cells showing the colocalization of PANoptosome components. Bars, 2 μ m.

Figure 3

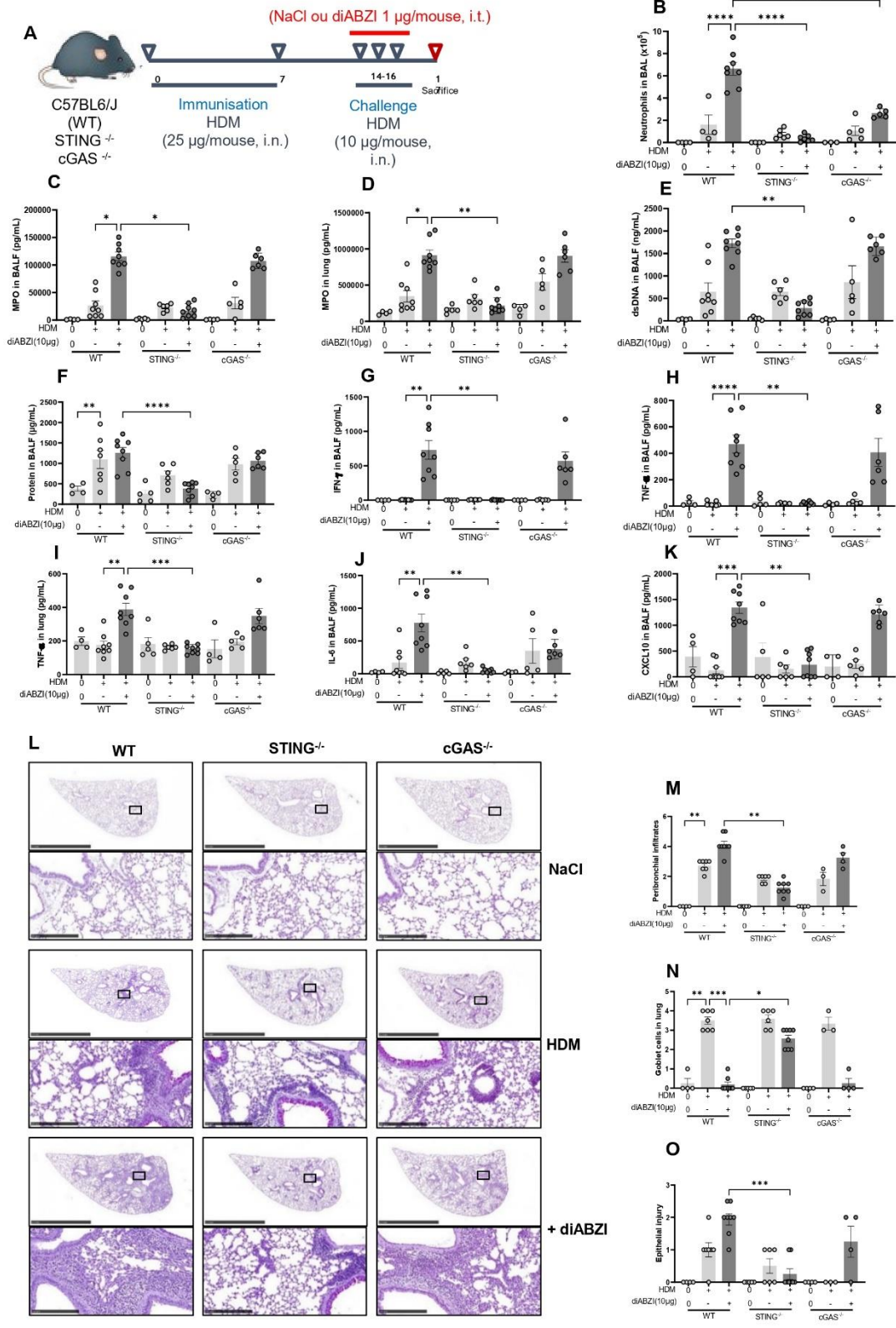


Figure 3 continued

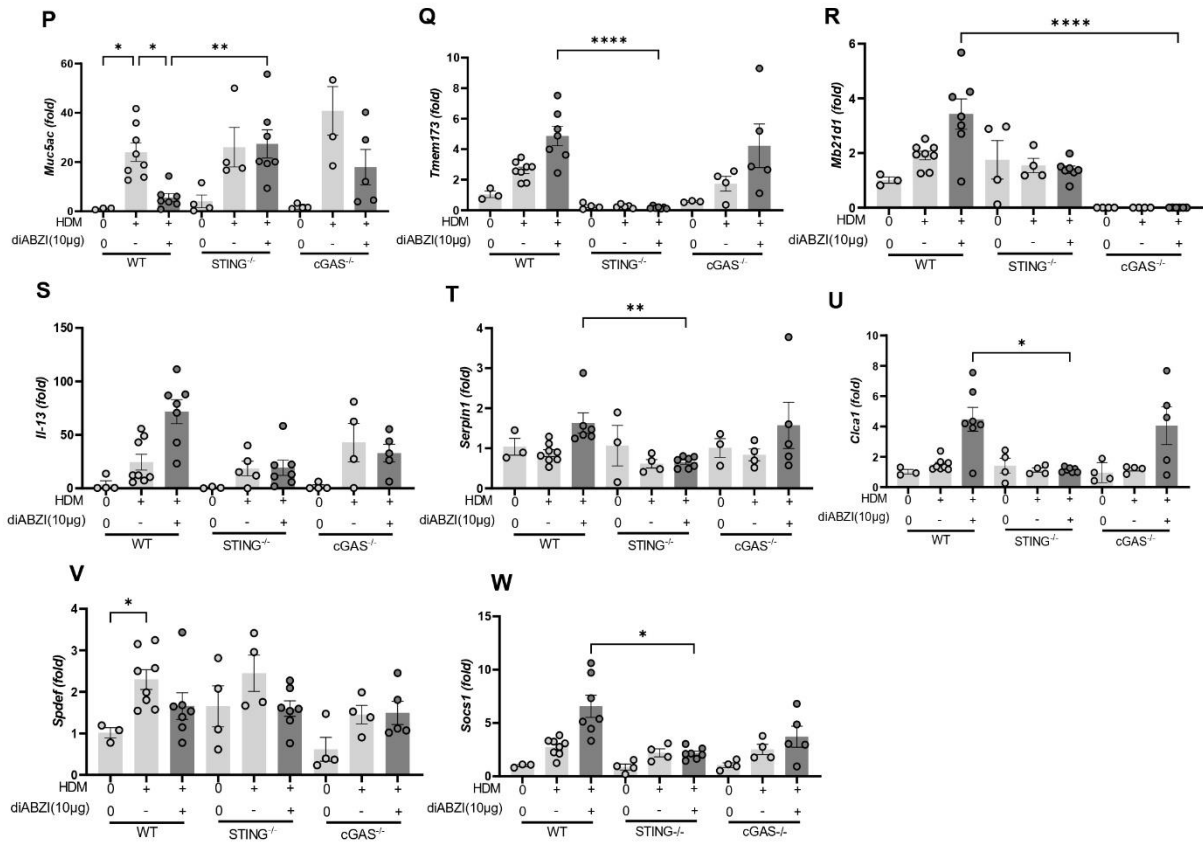


Figure 3: STING dependence of the neutrophilic airway inflammation exacerbation.

(A) Wild-type (WT), *STING*^{-/-} or *cGAS*^{-/-} mice were sensitized with HDM on day 0 and 7 (25 µg/mouse, i.n.), challenged with HDM on day 14-16 (10 µg/mouse, i.n.) without or with diABZI (1 µg/mouse, i.t.), and analyzed on day 17. **(B)** Neutrophils count in BAL. **(C, D)** MPO concentration in BALF and lung determined by ELISA. **(E)** dsDNA concentration in the BAL acellular fraction. **(F)** Protein concentration in BALF. **(G)** IFN-γ in BALF determined by multiplex immunoassay. **(H, I)** TNF-α in BALF and lung determined by ELISA. **(J)** IL-16 and **(K)** CXCL10/IP-10 concentration in BALF measured by ELISA. **(L)** Histology of lung tissues stained with PAS of WT, *STING*^{-/-} and *cGAS*^{-/-} mice, with semi quantitative pathology scoring of **(M)** peribronchial infiltrates, **(N)** goblet cells and **(O)** epithelial injury. Bars, upper panel: 2.5 mm, lower panel: 250 µm. **(P-W)** *Muc5ac*, *Tmem173*, *Mb21d1*, *Il-13*, *Serpin1*, *Clc1*, *Spdef* and *Socs1* transcripts measured by real-time qPCR. Data were presented as mean ± SEM with n = 6 ~ 8 mice per group. Each point represents an individual mouse. *p < 0.05, **p < 0.01, ***p < 0.001, ****p < 0.0001 (Nonparametric Kruskal–Wallis with Dunn’s post-test).

Figure 4

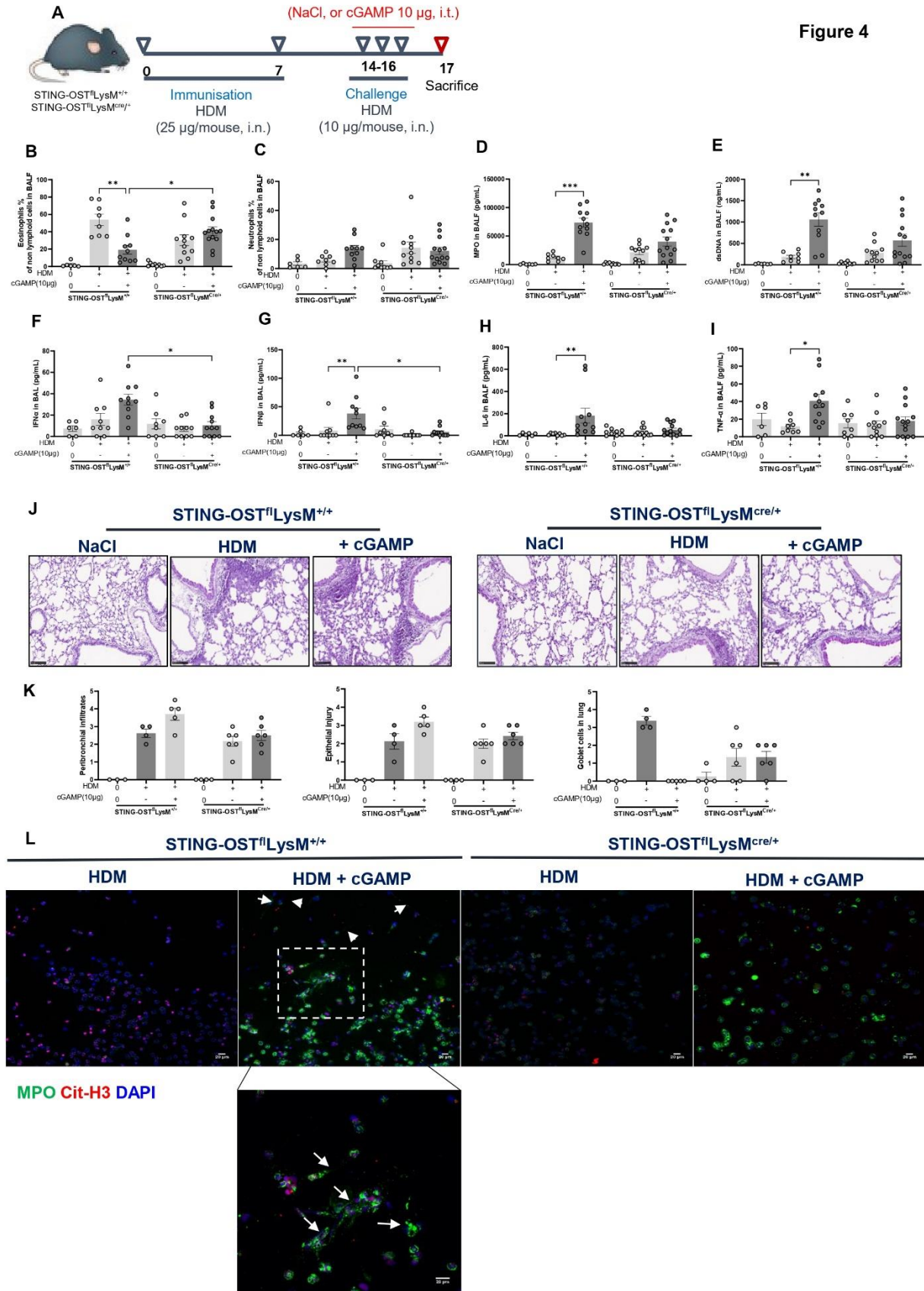
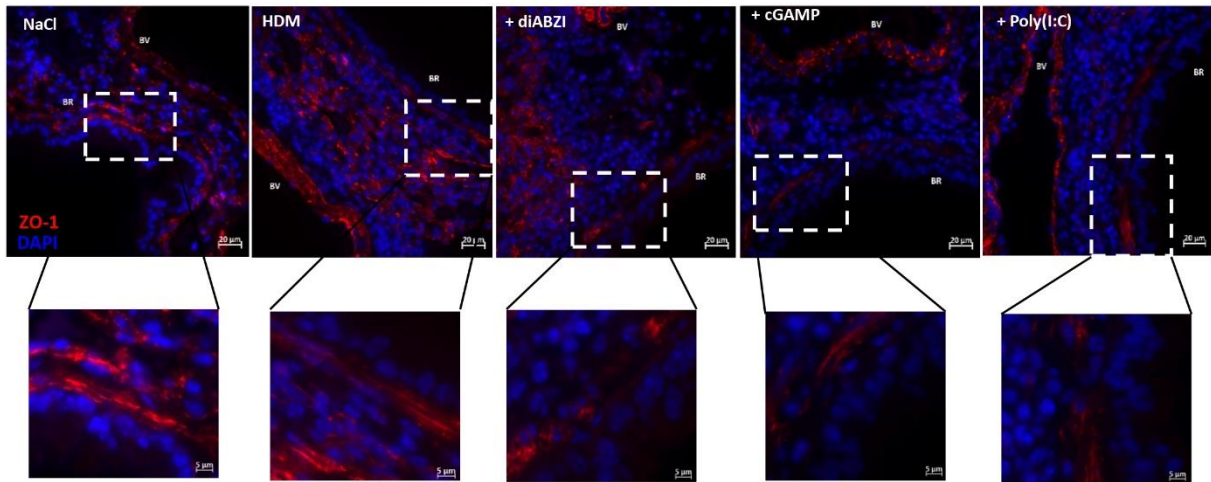


Figure 4: STING-deficient macrophages and granulocytes mitigates asthma exacerbation *in vivo* in the lung.

(A) STING-OST^{fl}LysM^{cre/+} or STING-OST^{fl}LysM^{+/+} mice were sensitized with HDM on day 0 and 7 (25 µg/mouse, i.n.), challenged with HDM on day 14-16 (10 µg/mouse, i.n.) without or with cGAMP (10 µg/mouse, i.t.), and analyzed on day 17. **(B)** Eosinophils and **(C)** Neutrophils counts in BAL. **(D)** MPO concentration in BALF measured by ELISA. **(E)** dsDNA measured in the acellular fraction of the BAL. **(F)** Concentration of IFN- α and **(G)** IFN- β in BALF measured by luminex immunoassay. **(H)** IL-6 concentration **(I)** and TNF- α concentration in BALF measured by ELISA. **(J)** Lung tissue histology with PAS staining of STING-OST^{fl}LysM^{cre/+} or STING-OST^{fl}LysM^{+/+} mice with semi quantitative pathology scoring of **(K)** peribronchial infiltrates, epithelial injury and goblet cells. **(L)** Visualization of NET in BAL with the staining of DNA dye DAPI (blue), MPO (Green), CitH3 (Red). Bars, 20 µm. Data were presented as mean \pm SEM with n = 8 ~ 13 mice per group. Each point represents an individual mouse. *p < 0.05, **p < 0.01, ***p < 0.001, ****p < 0.0001 (Nonparametric Kruskal–Wallis with Dunn’s post-test).

A Lung tissue

Figure 5



Human Alveolar Epithelial Cell (hAEC)

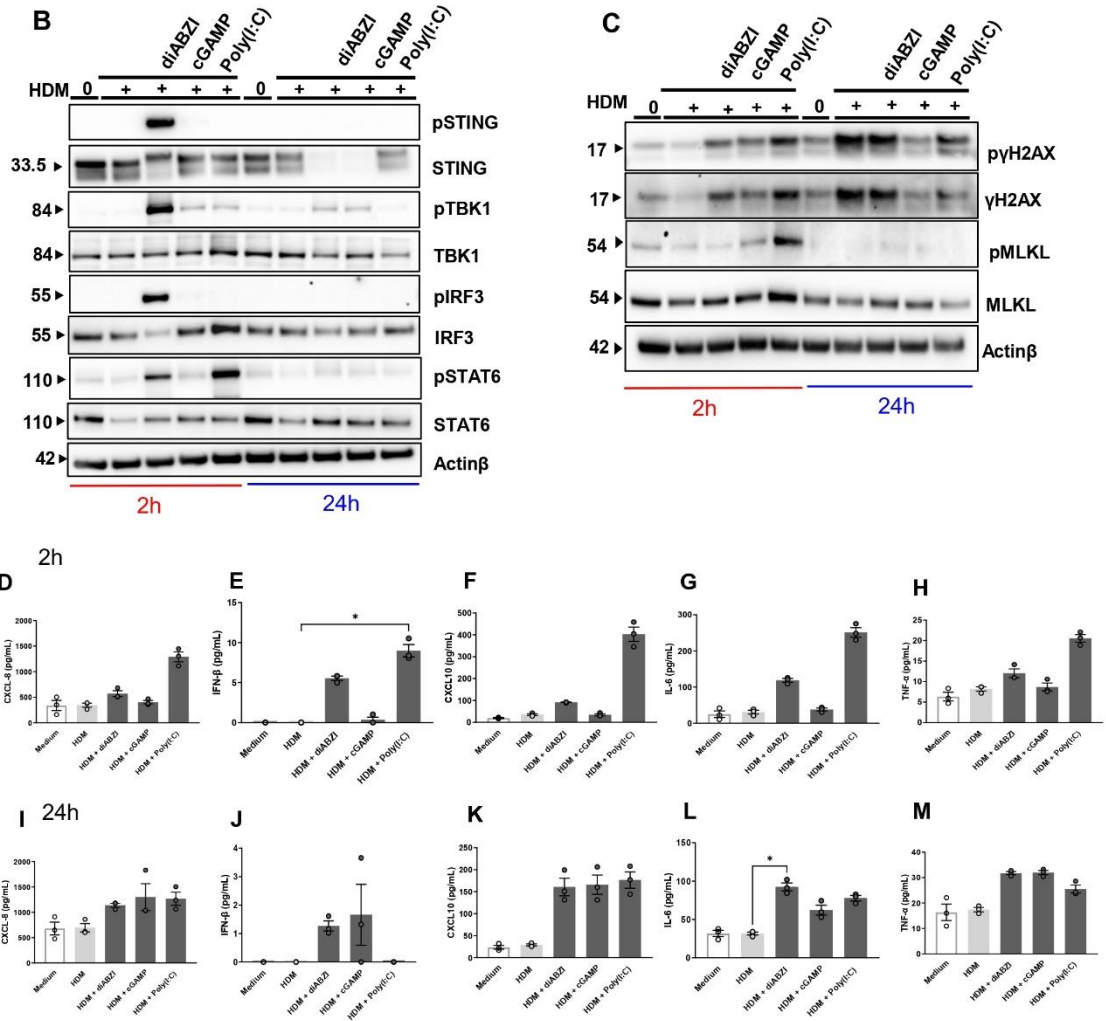
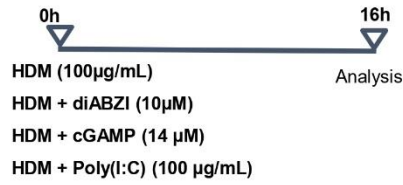
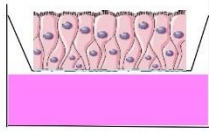


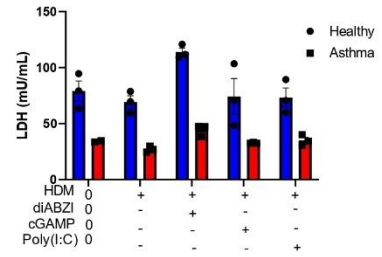
Figure 5 continued

N

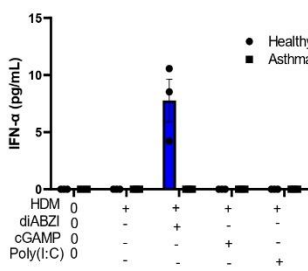
Healthy or donor with asthma



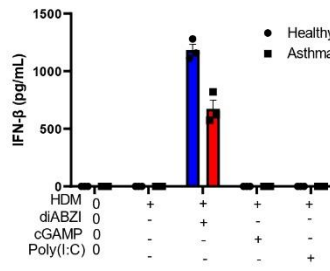
O



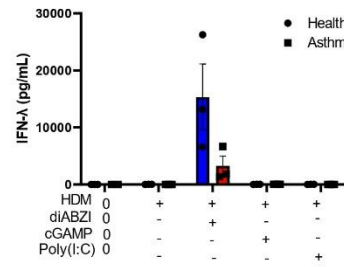
P



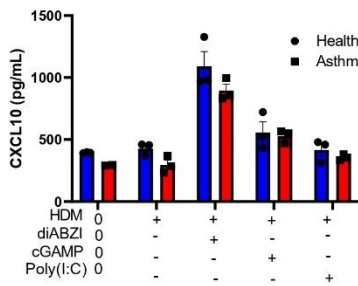
Q



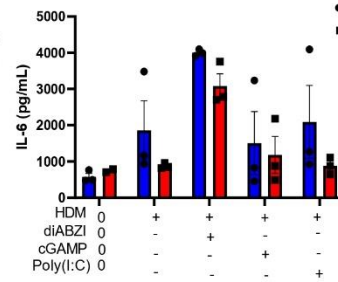
R



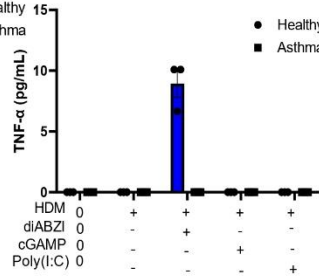
S



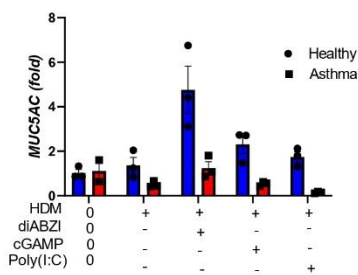
T



U



V



W

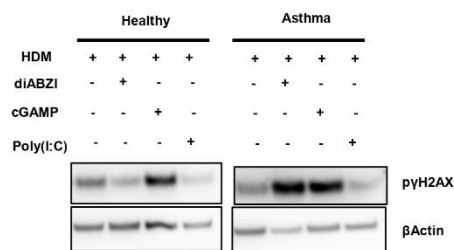


Figure 5. Epithelial cells contribute to the process of STING agonists-induced neutrophilic asthma exacerbation.

(A) Immunofluorescence staining of Zonulin-1 (ZO-1) (RED) in lung tissue sections from mice treated by HDM and challenged or not with diABZI, cGAMP, or Poly(I:C) as in Figure 1, counterstained with DAPI (Blue). Upper panel: 20µm, lower panel: 5µm. Immunoblots of human airway epithelial cell (hAEC) stimulated with HDM at 100 µg/mL alone or in combination with diABZI (10 µM), cGAMP (14 µM) or Poly(I:C) (100 µg/mL) for 2 or 24h showing (B) STING pathway activation including phospho-STING, STING, phospho-TBK1, TBK1, phospho-IRF3, IRF3, phospho-STAT6 and STAT6, with Actinβ as a reference. (C) DNA damage and cell death axis including phospho-γH2AX, γH2AX, phospho-MLKL, MLKL and Actinβ as a reference. (D-M) Cytokines concentration of (D, I) IL-8/CXCL8, (E, J) IFN-β, (F, K) IP-10/CXCL10, (G, L) IL-6 and (H, M) TNF-α in cell culture supernatant were measured by multiplex immunoassay at 2h (D-H) and 24h (I-M). Data were presented as mean ± SEM with n = 3 independent wells from the same donor. (N) Human airway epithelium (MUCILAIR™) from a single healthy or donor with asthma were restimulated on the apical face, with HDM at 100 µg/mL alone or in combination with diABZI at 10 µM, cGAMP at 14 µM or Poly(I:C) at 100 µg/mL. At 6h post-stimulation, (O) Lactate dehydrogenase (LDH) concentration was determined in the supernatant. (P-U) Multiplex immunoassay of IFN-α (P), IFN-β (Q), IFN-λ (R), IP-10/CXCL-10 (S), IL-6 (T) and TNF-α (U) concentrations in the supernatant. (V) *MUC5AC* transcripts measured by real-time PCR. (W) Immunoblot from epithelial cell homogenates from healthy and patients with asthma showing the expression of phospho-γH2AX with Actinβ as a reference. Data were presented as mean ± SEM with n = 3 independent wells from the same donor. *p < 0.05. (D-M) Nonparametric Kruskal–Wallis with Dunn’s post-test.

Figure 6

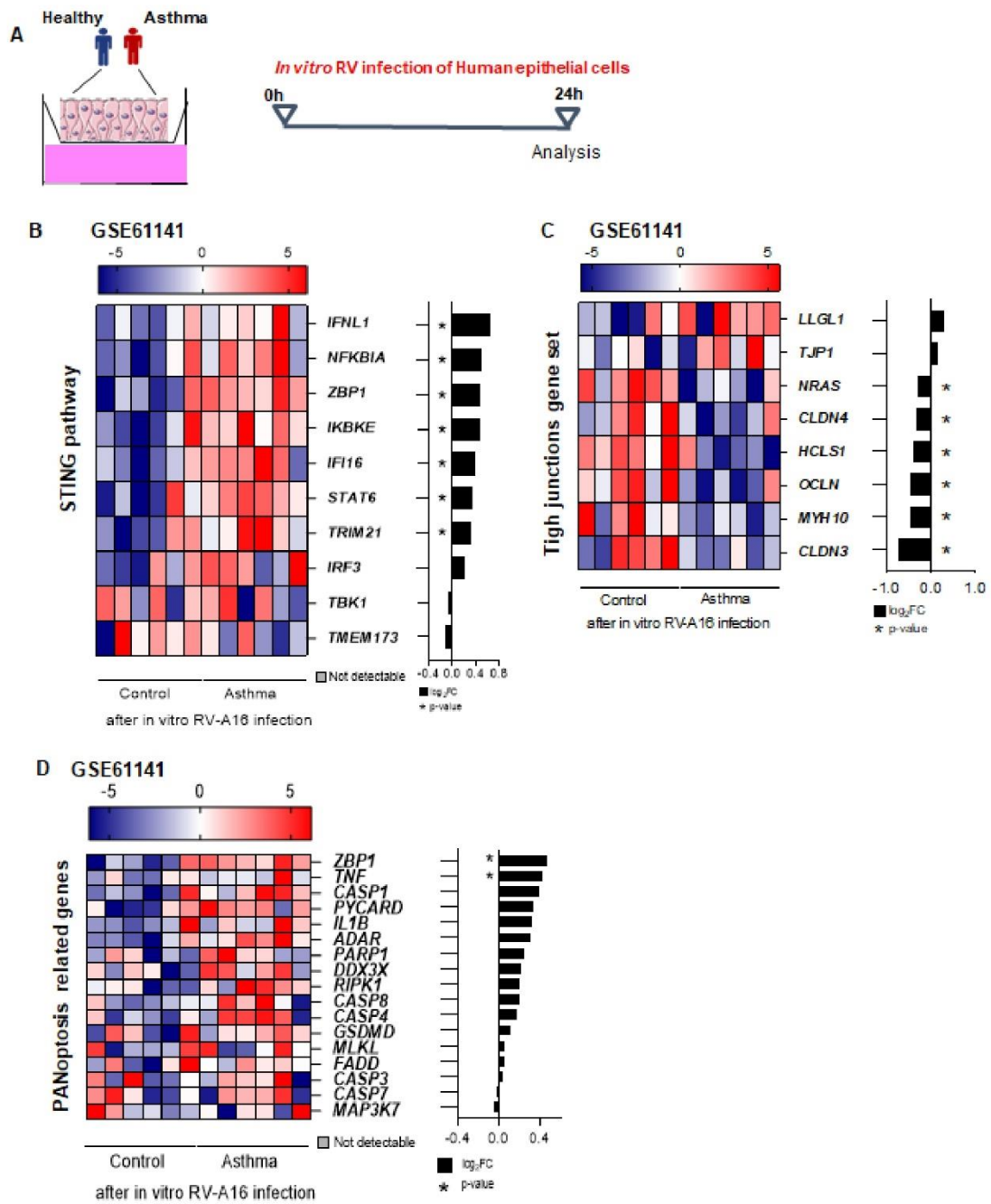


Figure 6 continued

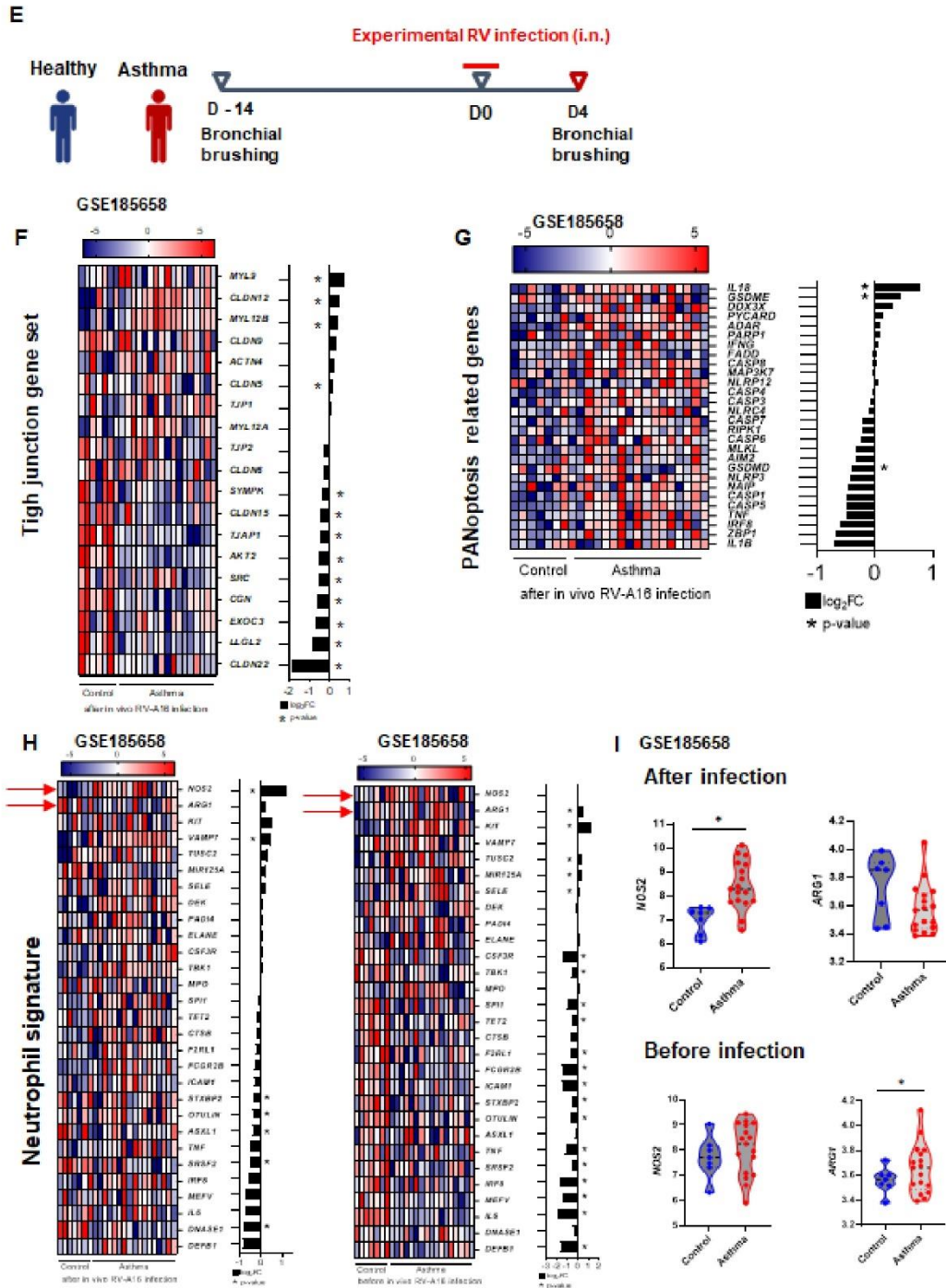
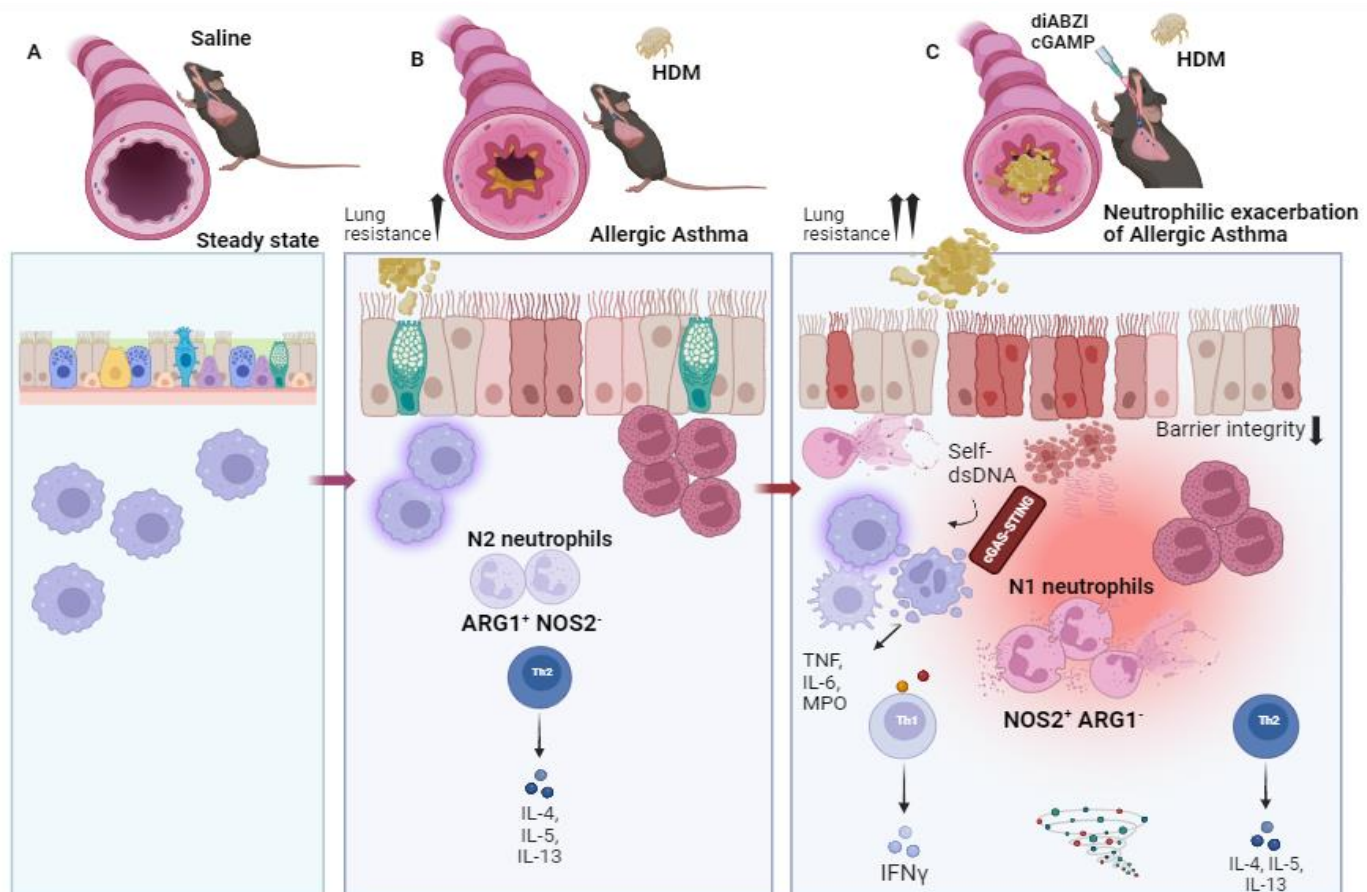


Figure 6. Upregulation of DNA sensing and PANoptosis pathways upon rhinovirus infection in patients with asthma

(A) Human bronchial epithelial cells (HBECs) from patients with asthma (n = 6) and healthy controls (n=6), were infected with RV-A16 for 24h, and subjected to transcriptome analysis. (B-E) Heatmaps presented together with the corresponding log₂ fold change (FC) expression changes (black bars) of (B) STING pathway-related genes, (C) Tight junction genes set, (D) PANoptosis-related genes, after in vitro RV-A16 infection in controls compared to HBEC from patients with asthma. Transcriptomic data were processed with the workflow available on <https://github.com/uzh/ezRun>.

(E) Experimental in vivo RV RV-A16 infection in patients with asthma (n=17) and healthy individuals (n=7): Transcriptomic analysis of bronchial brushings 14 days before and 4 days after in vivo infection. (F-G) Heatmaps presented together with the corresponding log₂ fold change (FC) expression changes (black bars) of (F) Tight junction genes set, (G) PANoptosis-related genes, after in vivo RV-A16 infection in controls compared to patients with asthma. (H) Heatmaps of neutrophilic signature before (right panel) and after (left panel) infection in controls compared to patients with asthma. (I) Violin plots representing gene expressing of *NOS2* and *ARG1* in healthy individual and patients with asthma, before (lower set) and after (Upper set) infection. Data was analyzed with Bioconductor microarray analysis workflow [<https://www.bioconductor.org/packages/release/workflows/vignettes/arrays/inst/doc/arrays.html>].

All Heatmaps display normalized gene expression across the groups (row normalization). Asterisks demonstrate significantly changed genes with threshold $p < 0.05$. p-value: * < 0.05 ; ** < 0.005 ; *** < 0.0005 , **** < 0.00005 . Publicly available data under accession number: GSE185658 and GSE61141. Source data are provided as Source Data files.



Created in BioRender.com

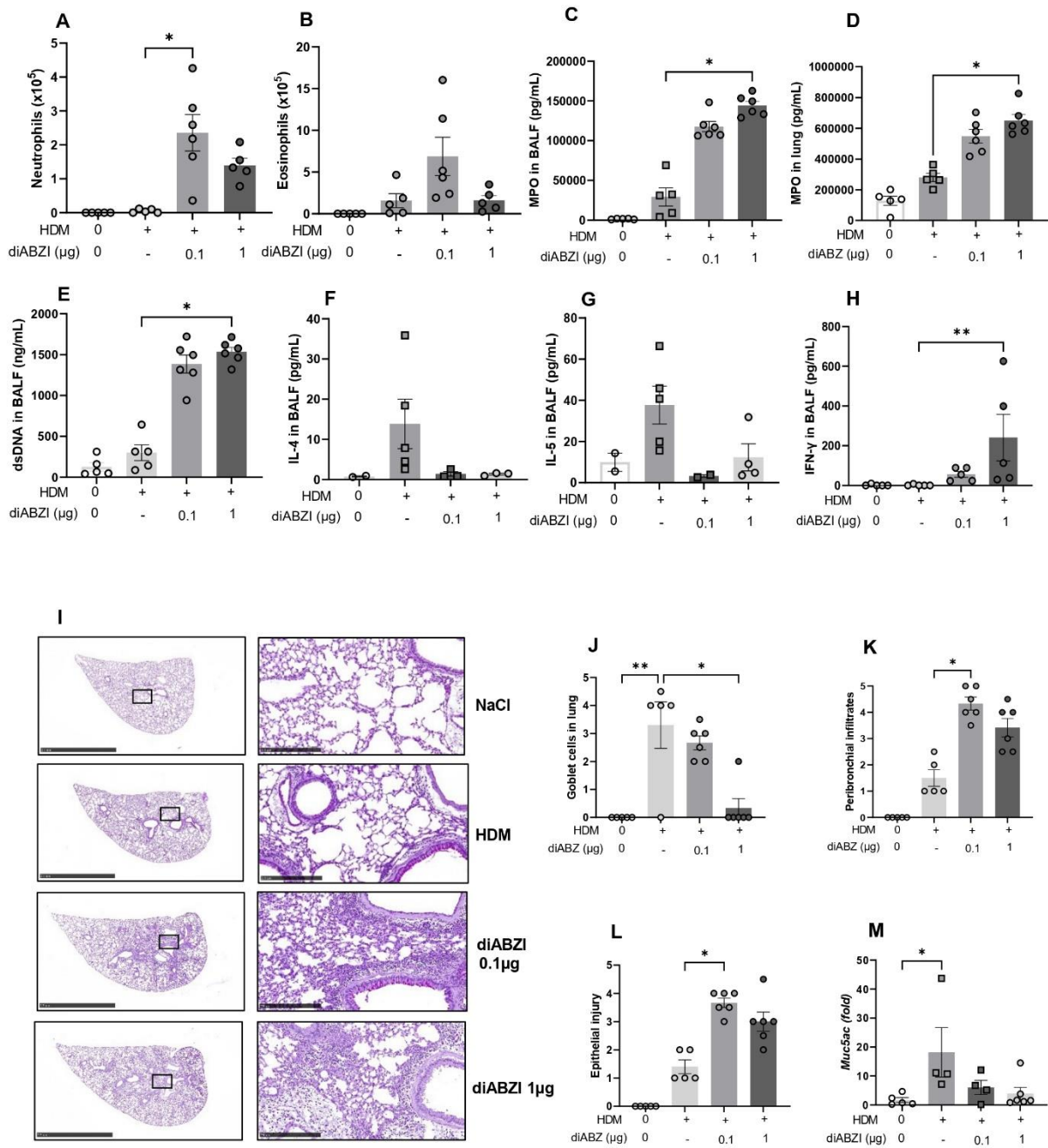
Figure 7: Graphical abstract

STING agonists in the lung mediates neutrophilic exacerbation of allergic asthma *in vivo*.

(A) Healthy airway epithelium with the presence of alveolar macrophages providing host defense (B) intranasal HDM sensitization induces allergic airway response characterized by an increase in goblet cells and mucus hypersecretion, important infiltration of eosinophils, macrophages, and to a lesser extent N2 neutrophils ($ARG1^{+} NOS2^{-}$) together with Th2 cytokines signature (IL-4, IL-5, IL-13) leading to an increase in lung resistance. (C) Intratracheal administration of STING agonists (diABZI, cGAMP) in HDM sensitized mice, promotes airways neutrophils infiltration, with prominent pro-inflammatory N1 ($NOS2^{+} ARG1^{-}$) profile and NETs formation. STING agonists caused epithelial barrier damage, cell death and extracellular self-dsDNA release accompanied by Th1 and pro-inflammatory cytokine signature ($IFN\gamma$, TNF, IL-6, MPO) besides the Th2 cytokines. STING agonists increased mucus

secretion in the airways and functionally worsen lung function by amplifying lung resistance. **Created with BioRender.com**

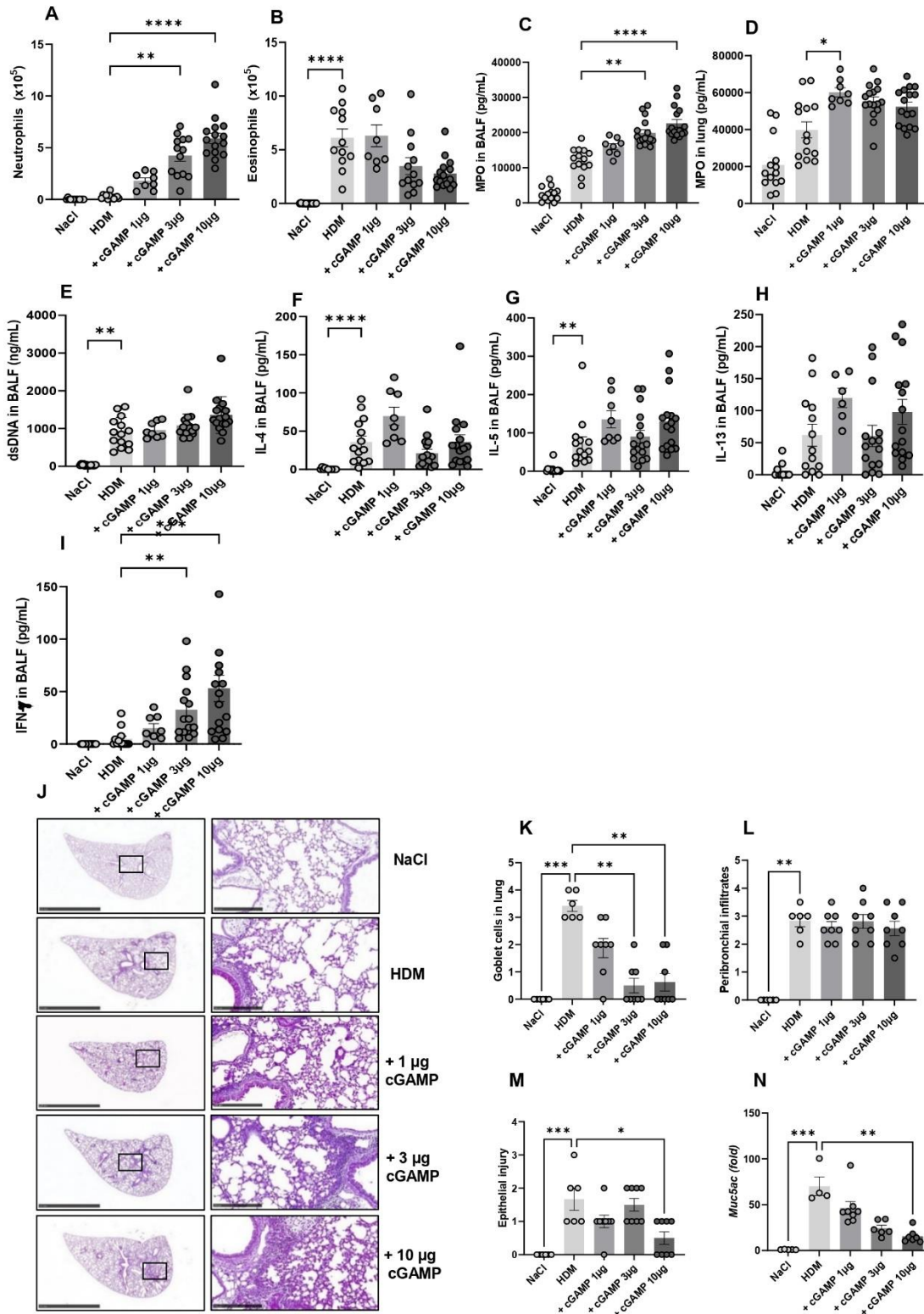
Suppl Fig.E1



Suppl E1: Synthetic STING agonist diABZI triggers neutrophilic asthma exacerbation in HDM sensitized mice, induces DNA damages and upregulation of DNA sensors.

(A) Neutrophils and (B) Eosinophils counts in BAL. (C, D) MPO concentration in BALF and lung. (E) Concentration of extracellular dsDNA in the acellular fraction of the BALF. (F) IL-4, (G) IL-5 and (H) IFN- γ concentrations in BALF quantified by Luminex immunoassay. (I) Lung tissue histology PAS staining Bars, left panel: 2.5mm, right panel: 250 μ m, with pathology scoring of (J) goblet cells (K) Peribronchial infiltrates (L) Epithelial injury. (M) *Muc5ac* transcripts measured by real-time PCR. Data were presented as mean \pm SEM with n = 4-6 mice per group. Each point represents an individual mouse. *p < 0.05, **p < 0.01 (Nonparametric Kruskal–Wallis with Dunn’s post-test).

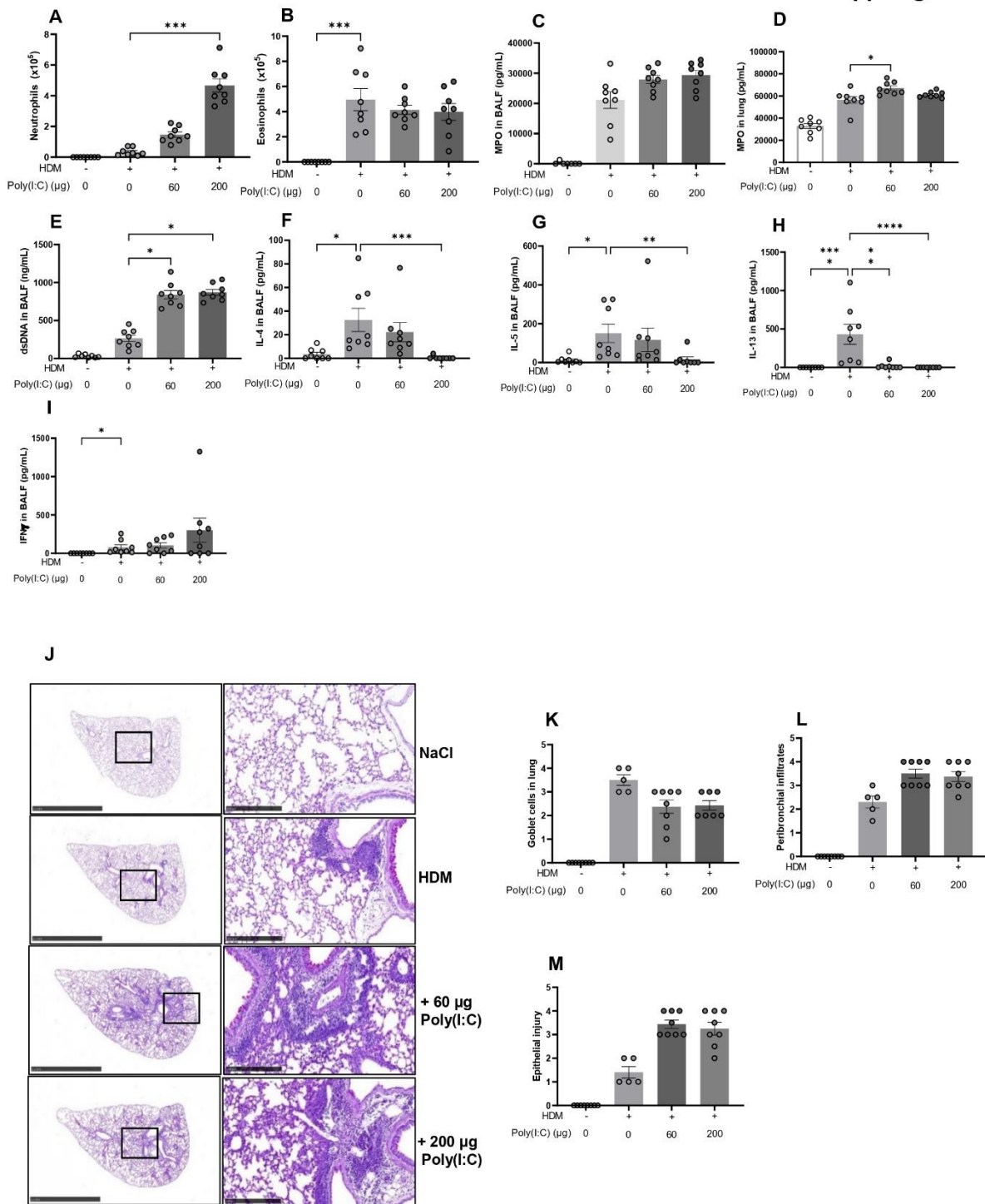
Suppl Fig.E2



Suppl E2: Endogenous STING agonist 2'3'-cGAMP promotes lung neutrophilia, NETs formation, DNA damage and exacerbate the inflammatory response to House dust mite.

(A) Neutrophils and (B) Eosinophils counts in BAL. (C, D) MPO concentration in BALF and lung. (E) Concentration of extracellular dsDNA in the acellular fraction of the BALF. (F) IL-4, (G) IL-5 and (H) IL-13 and (I) IFN- γ concentrations in BALF quantified by Luminex immunoassay. (J) Lung tissue histology PAS staining Bars, left panel: 2.5mm, right panel: 250 μ m, with pathology scoring of (K) goblet cells (L) Peribronchial infiltrates (M) Epithelial injury. (N) *Muc5ac* transcripts measured by real-time PCR. Data were presented as mean \pm SEM with n = 6-15 mice per group. Each point represents an individual mouse. *p < 0.05, **p < 0.01, ***p < 0.001, ****p < 0.0001 (Nonparametric Kruskal–Wallis with Dunn's post-test).

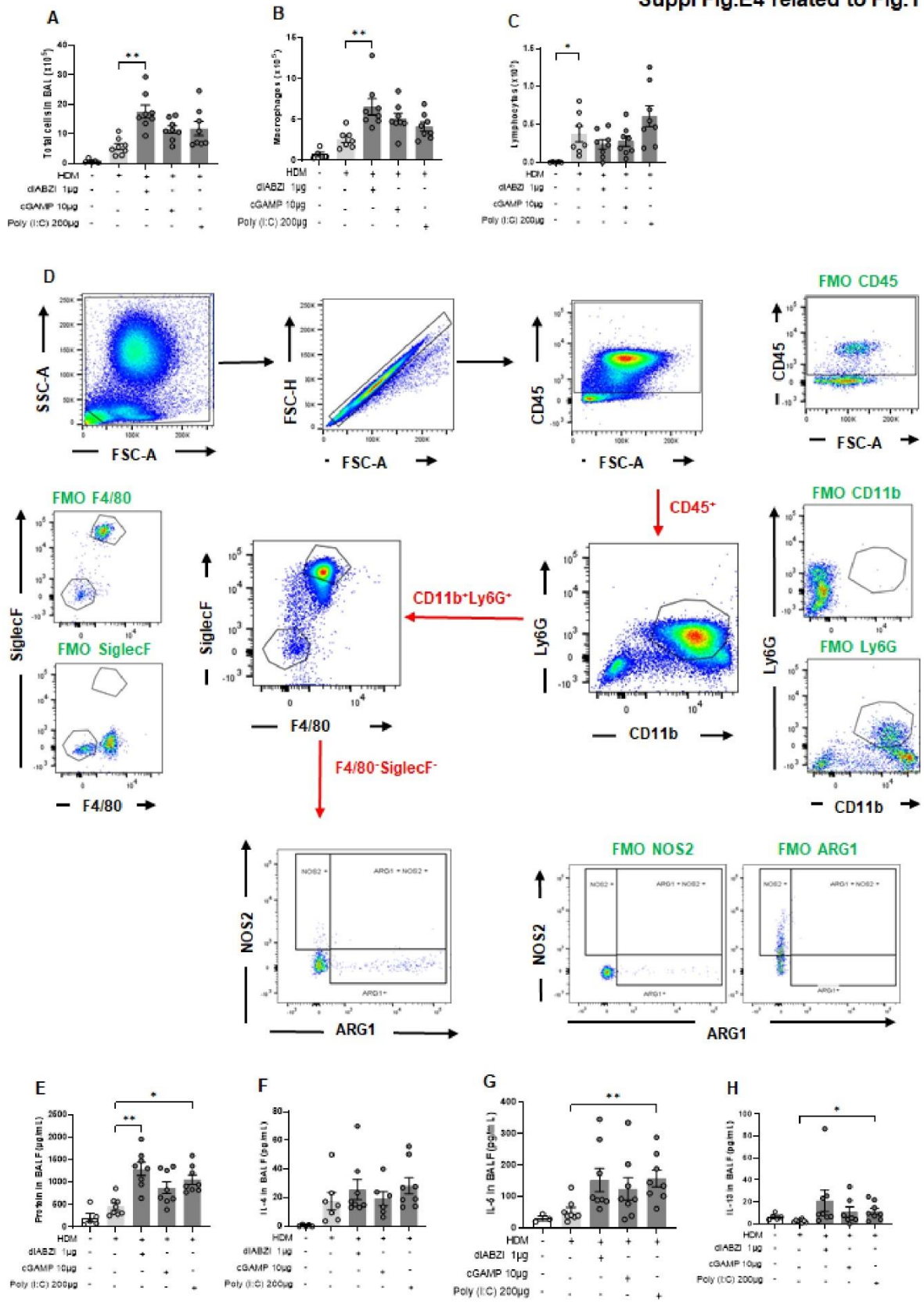
Suppl Fig.E3



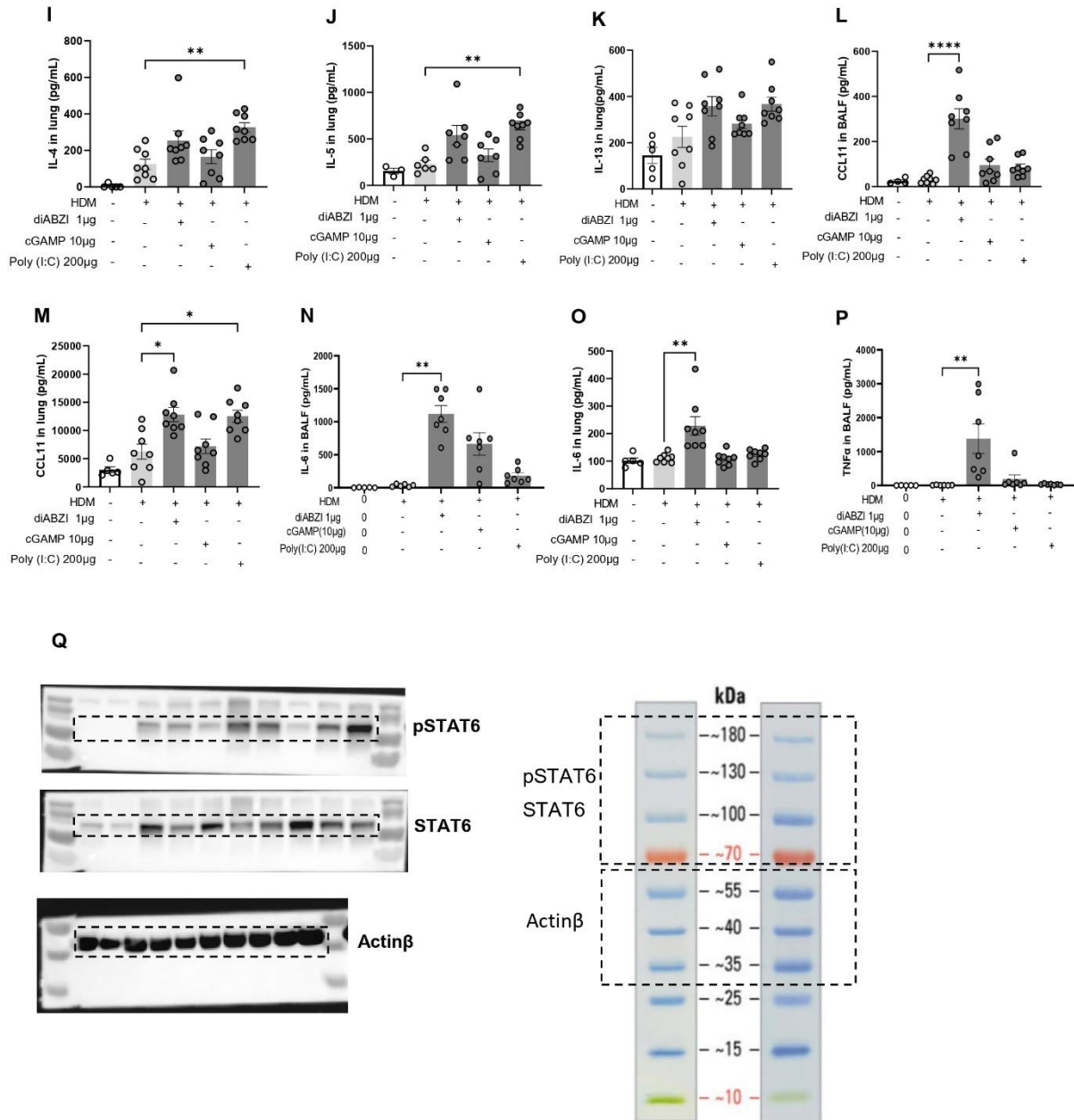
Suppl E3: Effect of Poly(I:C) on allergic asthma response to house dust mite

(A) Neutrophils and (B) Eosinophils counts in BAL. (C, D) MPO concentration in BALF and lung. (E) Concentration of extracellular dsDNA in the acellular fraction of the BALF. (F) IL-4, (G) IL-5 and (H) IL-13 and (I) IFN- γ concentrations in BALF quantified by Luminex immunoassay. (J) Lung tissue histology PAS staining Bars, left panel: 2.5mm, right panel: 250 μ m, with pathology scoring of (K) goblet cells (L) Peribronchial infiltrates (M) Epithelial injury. Data were presented as mean \pm SEM with n = 8 mice per group. Each point represents an individual mouse. *p < 0.05, **p < 0.01, ***p < 0.001, ****p < 0.0001 (Nonparametric Kruskal–Wallis with Dunn’s post-test).

Suppl Fig.E4 related to Fig.1



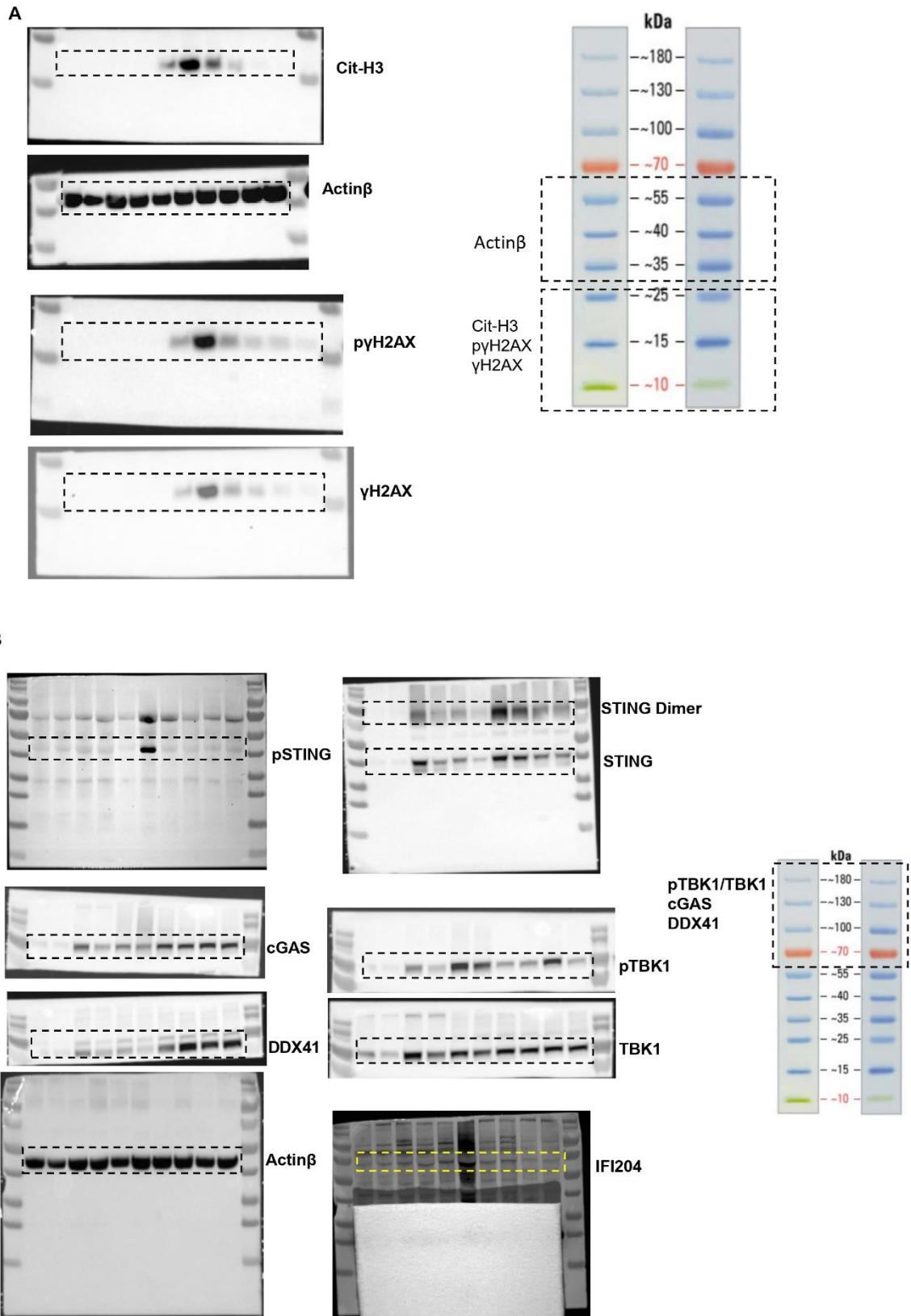
Suppl Fig.E4 related to Fig.1



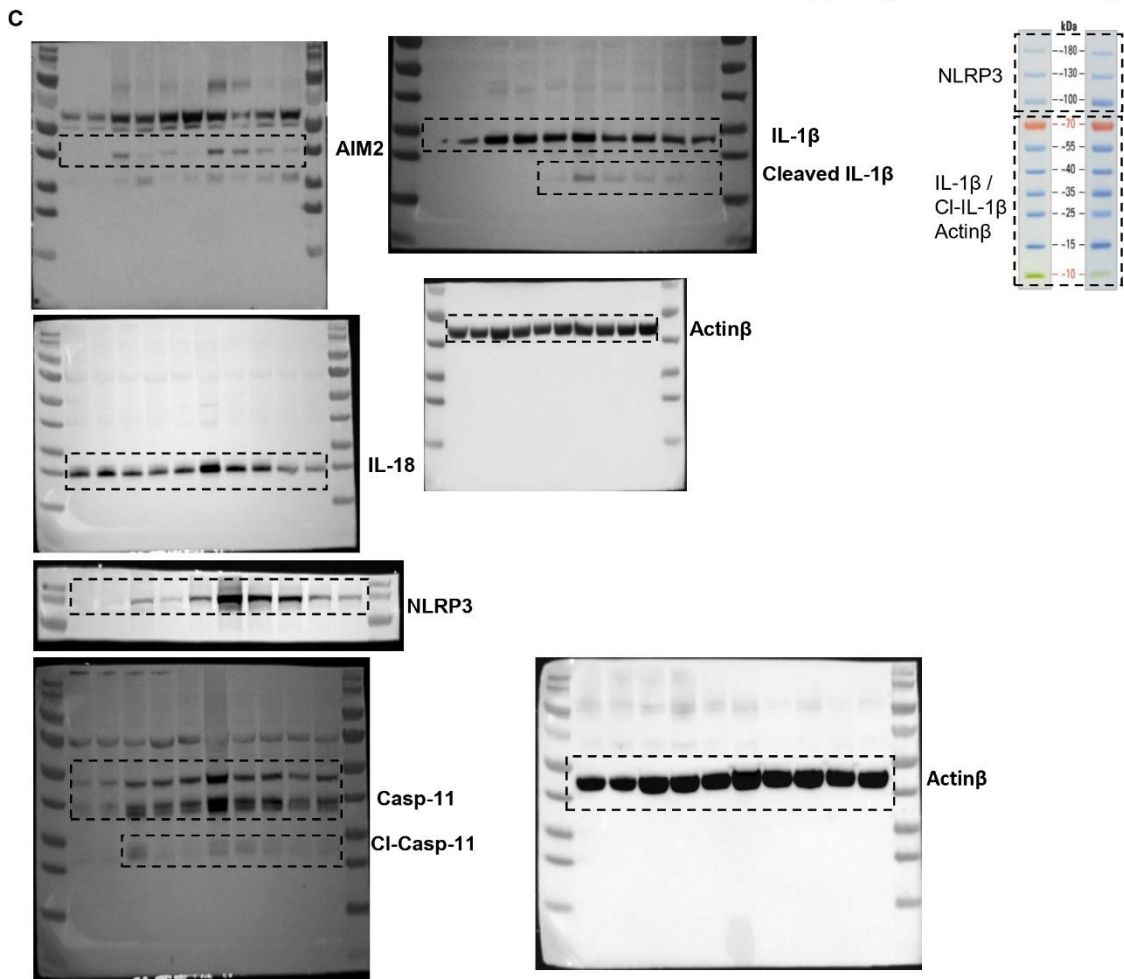
Suppl E4 related to Fig.1:

(A), Total cells (B) macrophages and (C) lymphocytes counts in BAL. (D) Gating strategy of NOS2/ARG1 staining of pre-gated singlets (SSC-A/SSC-H), CD45⁺ (leukocytes) and CD45⁺CD11b⁺Ly6G⁺F4/80⁻SiglecF⁻ (neutrophils). (E) Concentration of proteins in BALF. (F-K) Th2 cytokines (F, I) IL-4, (G, J) IL-5 and (H, K) IL-13 in BALF and lung determined by multiplex immunoassay. (L, M) Eotaxine1 (CCL11) in BALF and lung measured by ELISA. (N, O) IL-6 concentrations in BALF and lung determined by ELISA. (P) TNF- α concentration in BALF determined by ELISA. (Q) Uncropped immunoblots of p STAT6, STAT6, Actin β . Data are presented as mean \pm SEM with n = 8 mice per group. Each point represents an individual mouse. *p < 0.05, **p < 0.01 (Nonparametric Kruskal–Wallis with Dunn’s post-test).

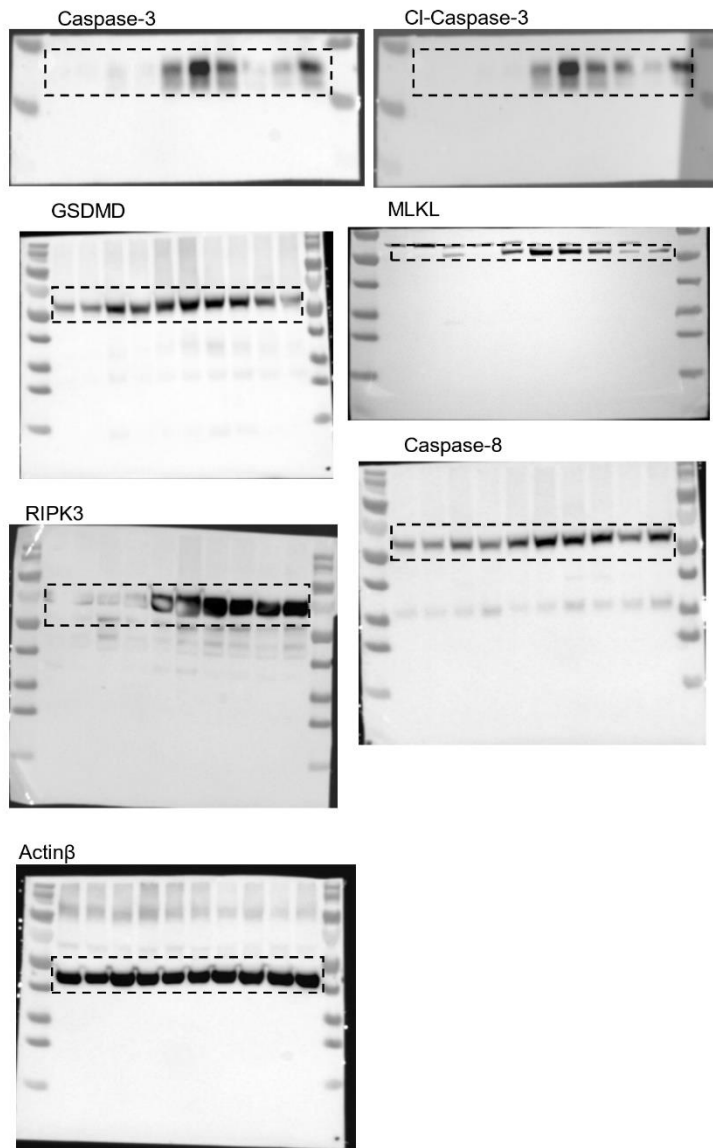
Suppl Fig.E5 related to Fig.2



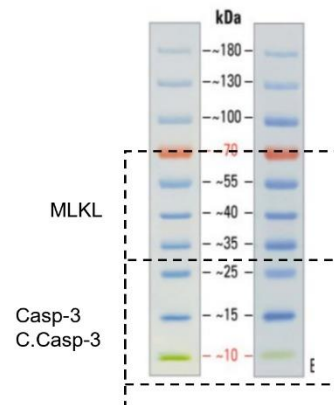
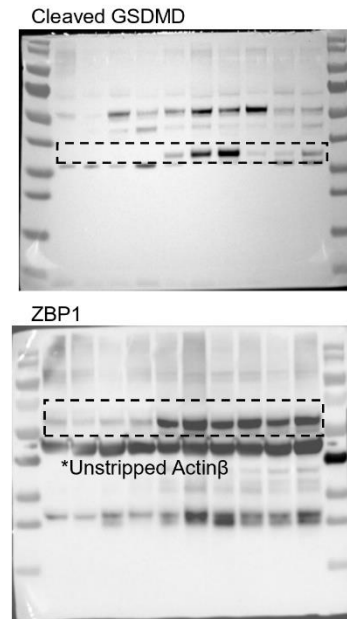
Suppl Fig. E5 related to Fig.2



D

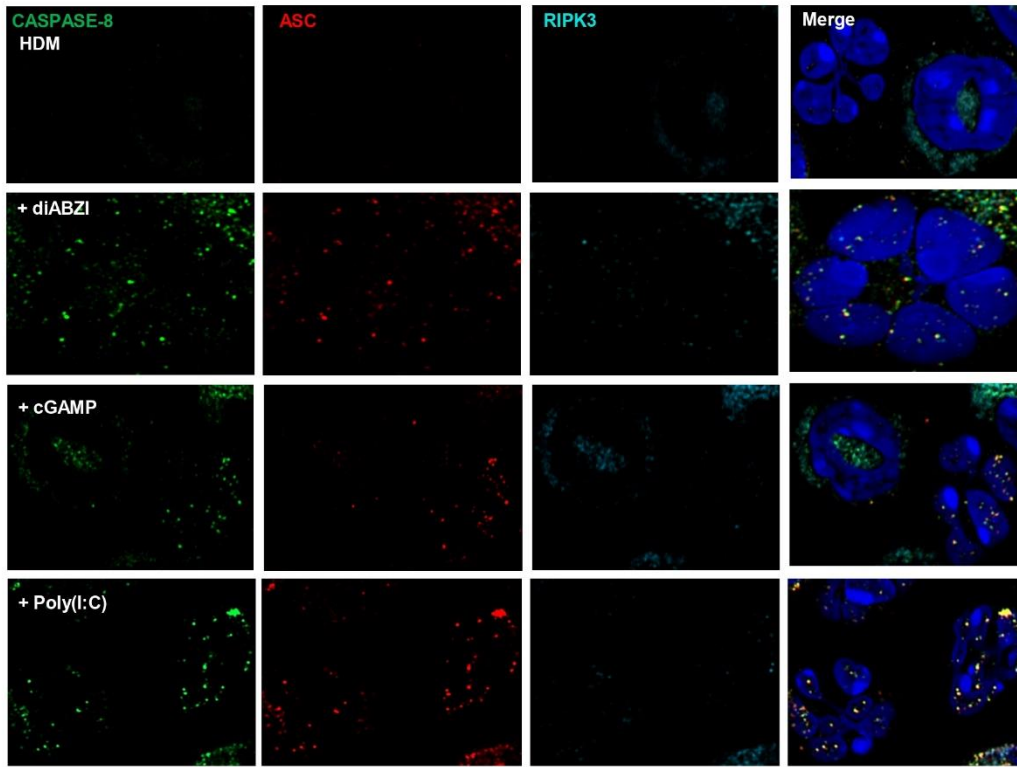


Suppl Fig. E5 related to Fig.2



Suppl Fig. E5 related to Fig.2

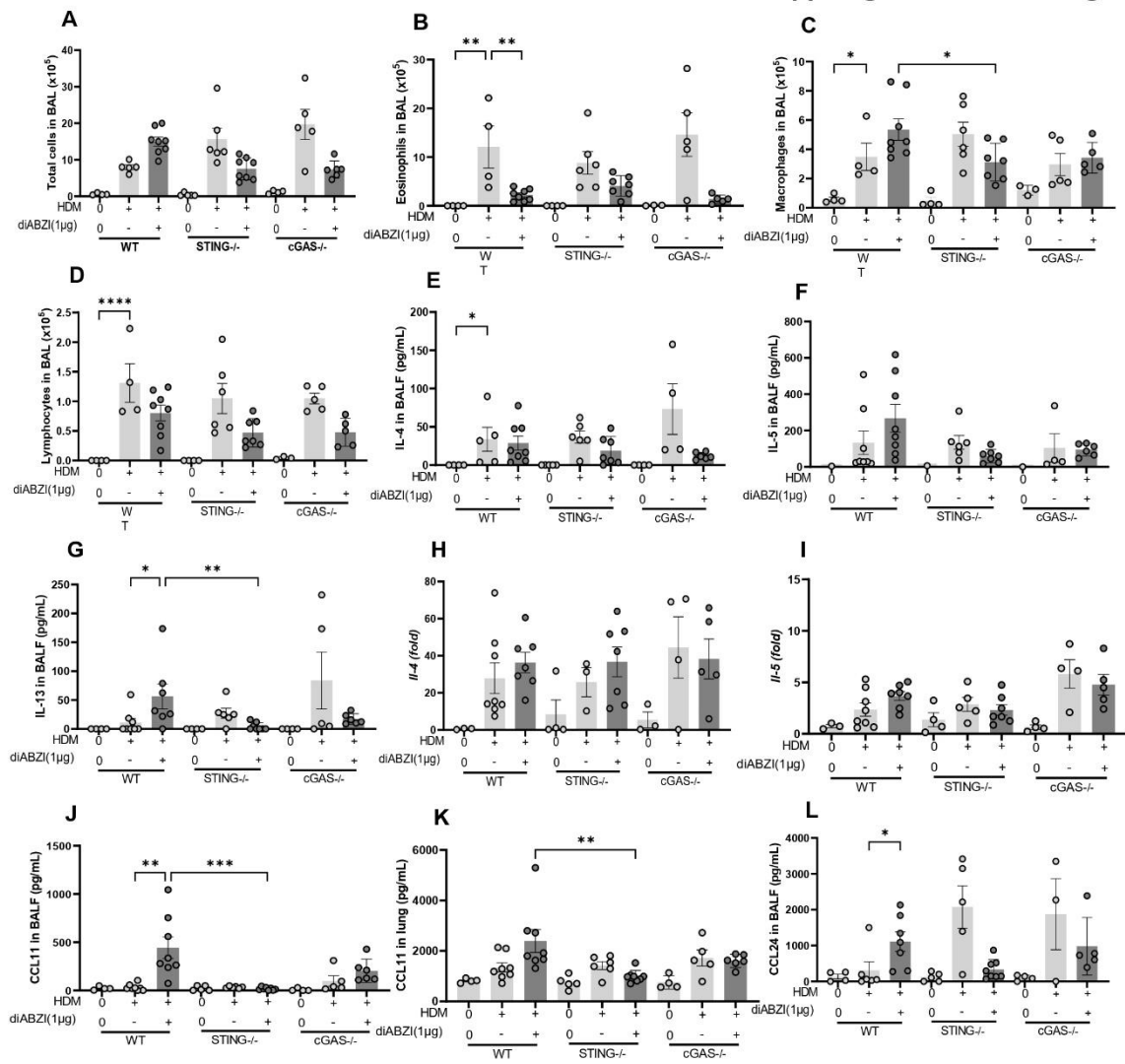
E



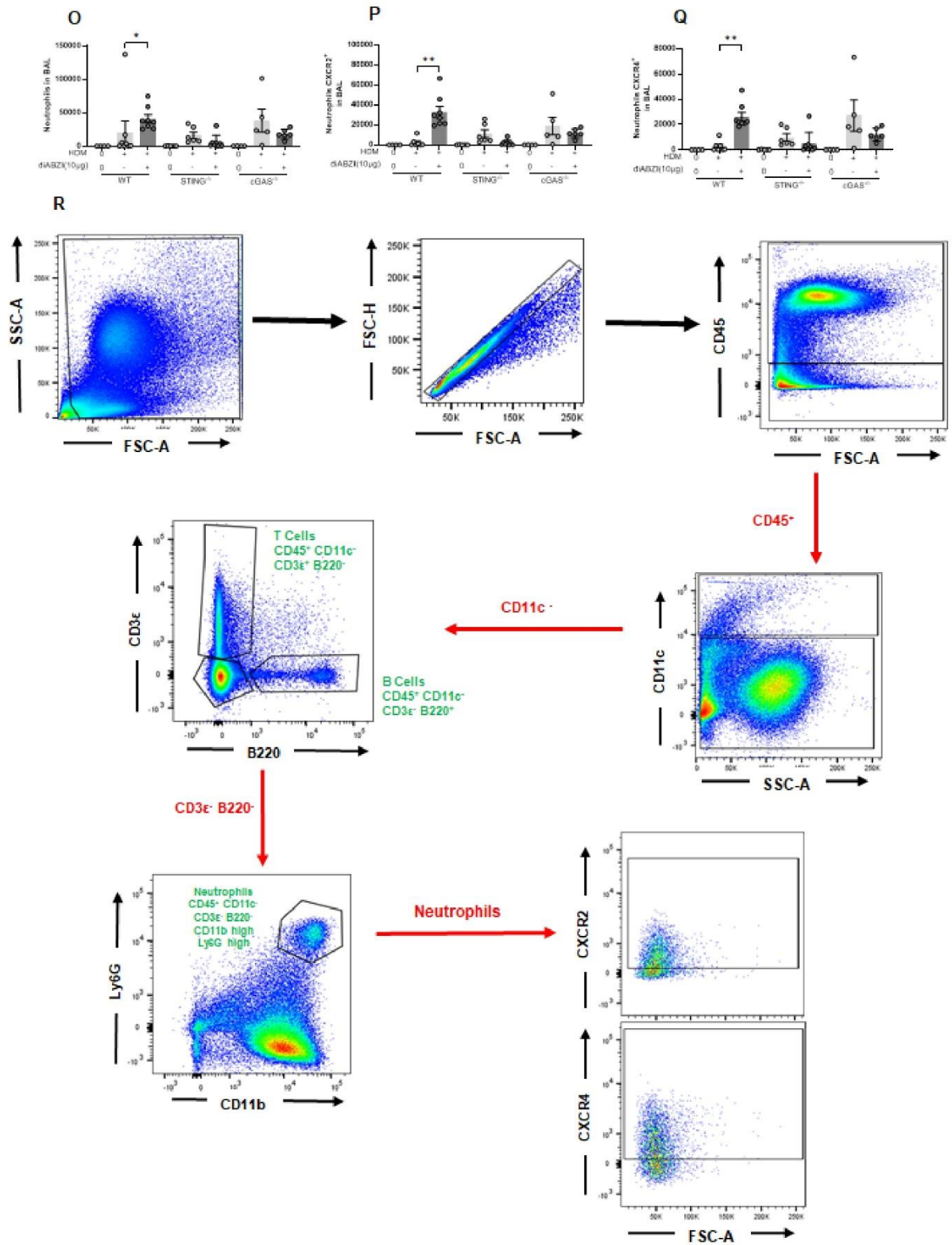
Suppl E5 related to Fig.2:

(A-D) Uncropped immunoblots of Cit-H3, p γ H2AX, γ H2AX, pSTING, STING, pTBK1, TBK1, cGAS, DDX41, Ifi204, AIM2, NLRP3, CASP-11, cleaved CASP-11, cleaved IL-1 β , IL-18, CASP-3, cleaved CASP-3, GSDMD, cleaved GSDMD, MLKL, ZBP1, RIPK3, CASP-8 and Actin β . **(E)** Confocal microscopy showing Caspase-8 (green), ASC (red), RIPK3 (far-red/turquoise blue), and DNA dye DAPI (cyan) in granulocytes from BAL of mice treated by HDM challenged or not with diABZI 1 μ g, cGAMP 10 μ g, or Poly(I:C) 200 μ g.

Suppl Fig. E6 related to Fig.3



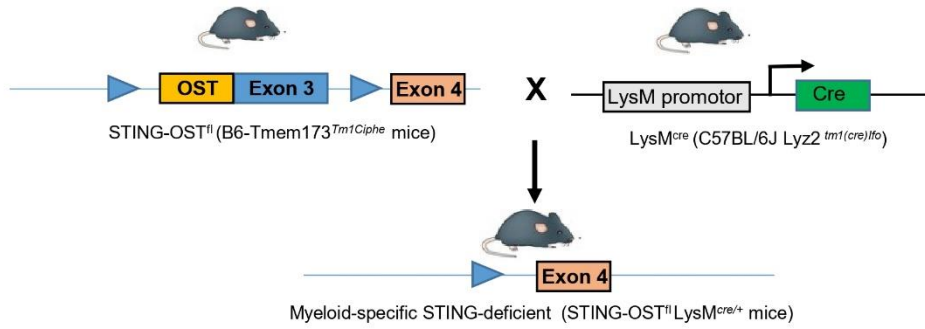
Suppl Fig. E6 related to Fig.3



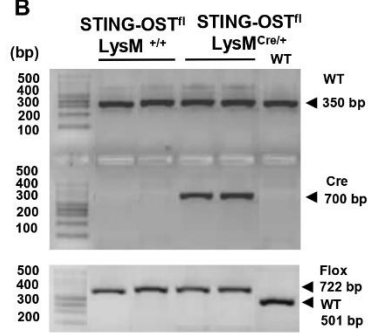
Suppl E6 related to Fig.3:

(A) total cells, (B) eosinophils, (C) macrophages and (D) lymphocytes counts in BAL. (E-G): Th2 cytokines (E) IL-4, (F) IL-5 and (G) IL-13 concentration in BALF measured by multiplex immunoassay. (H) *Il-4* and (I) *Il-5* transcripts in lung analyzed by real time qPCR. (J-L) Eotaxins (J, K) CCL11 concentrations in BALF and lung, (L) CCL24 concentration in BALF determined by ELISA. Flow cytometry analysis of (O) Neutrophils in BAL (P) Neutrophils expressing CXCR2⁺ in BAL (Q) Neutrophils expressing CXCR4⁺ in BAL (R) Gating strategy of CXCR2 and CXCR4 staining of pre-gated singlets (SSC-A/SSC-H), CD45⁺ CD11c⁻ and CD45⁺CD11c⁻CD3-B220⁻CD11⁺Ly6G^{high} (neutrophils). Data are presented as mean ± SEM with n = 6 ~ 8 mice per group. Each point represents an individual mouse. *p < 0.05, **p < 0.01, ***p < 0.001, ****p < 0.0001 (Nonparametric Kruskal–Wallis with Dunn’s post-test).

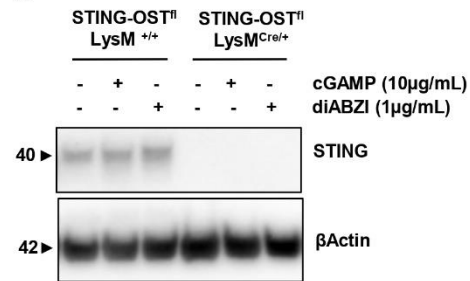
A



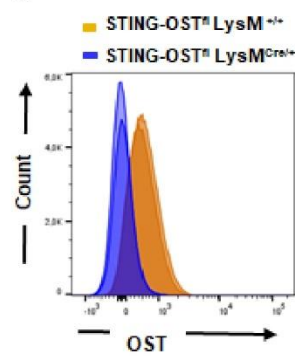
B



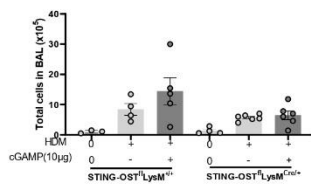
C



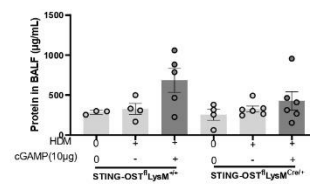
D



E



F

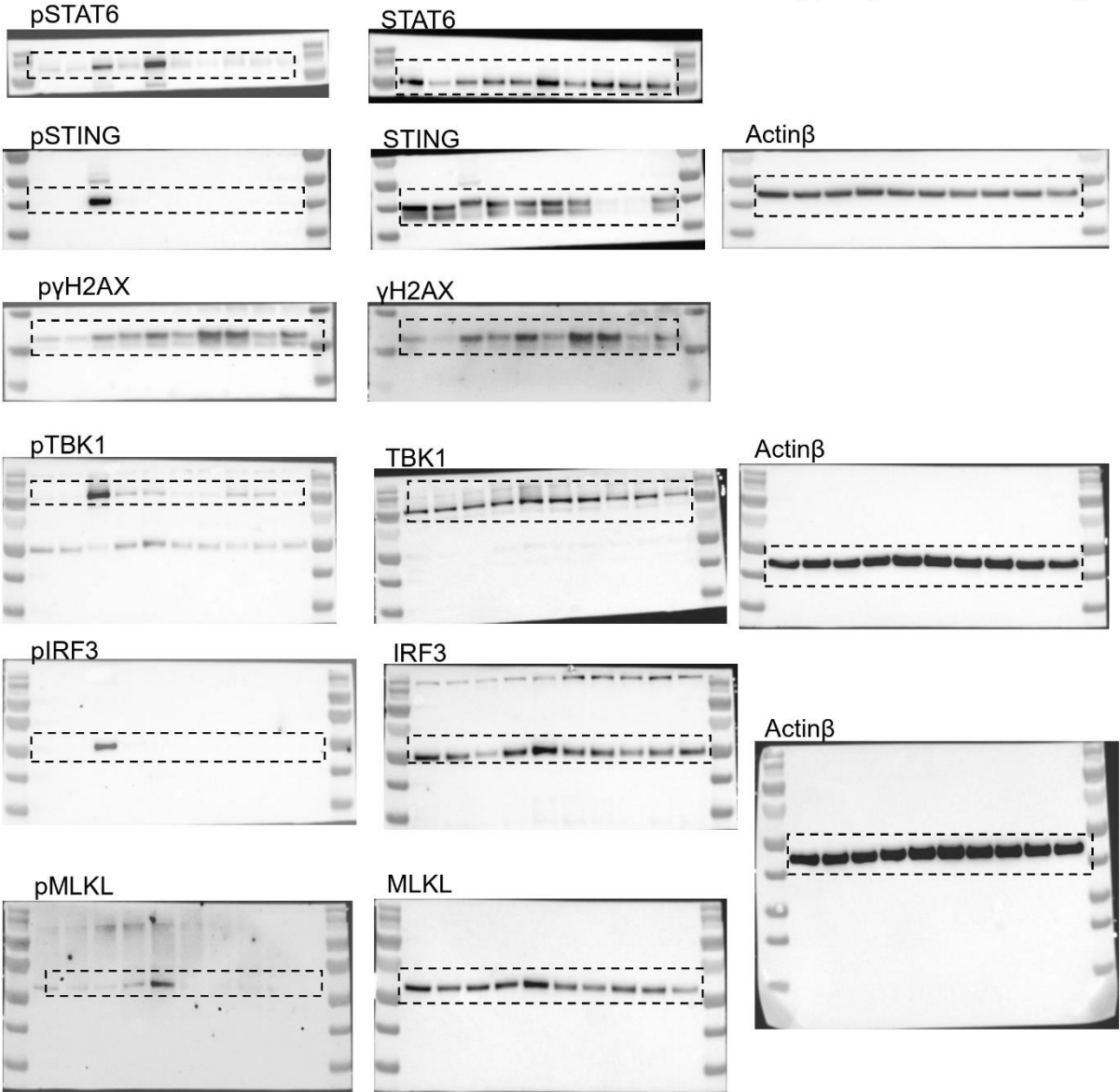


Suppl E7 related to Fig.4: Generation, identification and induction of allergic lung inflammation in myeloid-specific STING-deficient (STING-OST^{fl}LysM^{Cre/+}) mice.

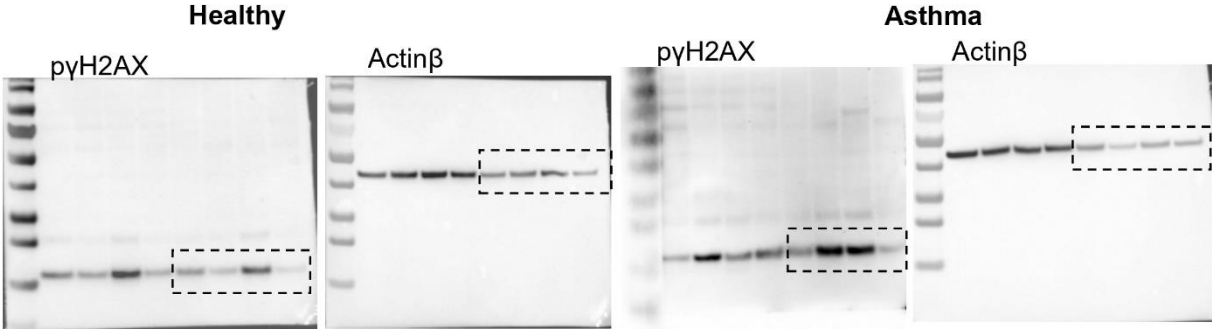
(A) Mice conditionally containing a loxP sequence flanking the third exon of STING gene (STING-OST^{fl/fl}) were crossed with Lysozyme M^{Cre} mice, which expressed Cre recombinase downstream of the lysozyme LysM promoter (LysM^{Cre}). (B) Mice were genotyped using PCR analysis of DNA obtained from tail snip. STING-deficient (STING-OST^{fl}LysM^{Cre/+}) mice have a 722-bp product for the loxP-targeted allele and a 700-bp product for the LysM^{Cre} allele. STING-OST^{fl/fl} mice have a 722-bp product for the loxP-targeted allele and a 501-bp product for the WT allele. (C) STING protein expression of STING-OST in BMDMs by immunoblot. (D) Flow cytometry analysis of OST producing cells in STING-OST^{fl}LysM^{Cre/+} BMDMs. All genotypes were generated on C57BL6/N background. Data are presented from one experiment (n = 2, B–D). (E) total cells count in BAL (F) Proteins level in BALF. (G) Gating strategy of Neutrophils (CD45⁺CD11c⁻CD3⁻B220⁻CD11b^{high} Ly6G^{high}) and Eosinophils (CD45⁺CD11c⁻CD3⁻B220⁻SiglecF⁺IAIE⁻CD11b⁺Ly6G⁻) cells in BAL pre-gated on singlets (SSC-A/SSC-H), CD45⁺CD11c⁻ and non-lymphoid cells CD3⁻B220⁻. Data are presented as individual mouse.

Suppl Fig.E8 related to Fig.5

A

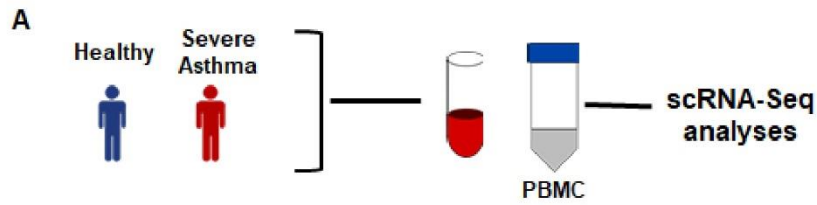


B

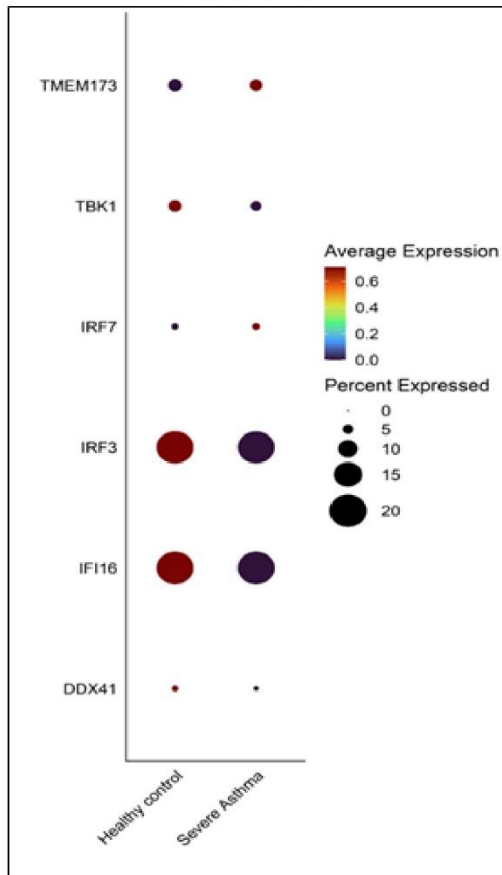


Suppl E8 related to Fig.5:

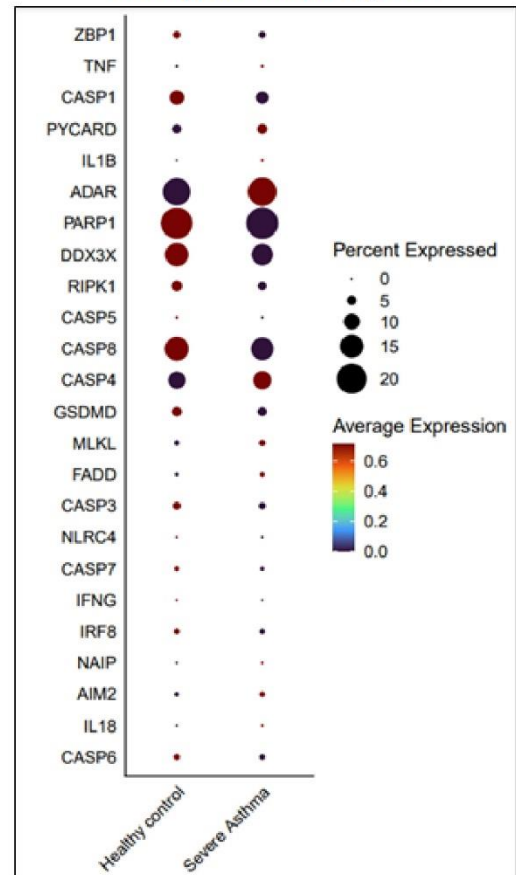
(A) Uncropped immunoblots of pSTAT6, STAT6, pSTING, STING p γ H2AX, γ H2AX, pTBK1, TBK1, pIRF3, IRF3, p MLKL, MLKL, p γ H2AX and Actin β . (B) Uncropped immunoblots of p γ H2AX and Actin β of cells from healthy controls and patient with asthma.



B GSE172495
STING pathway



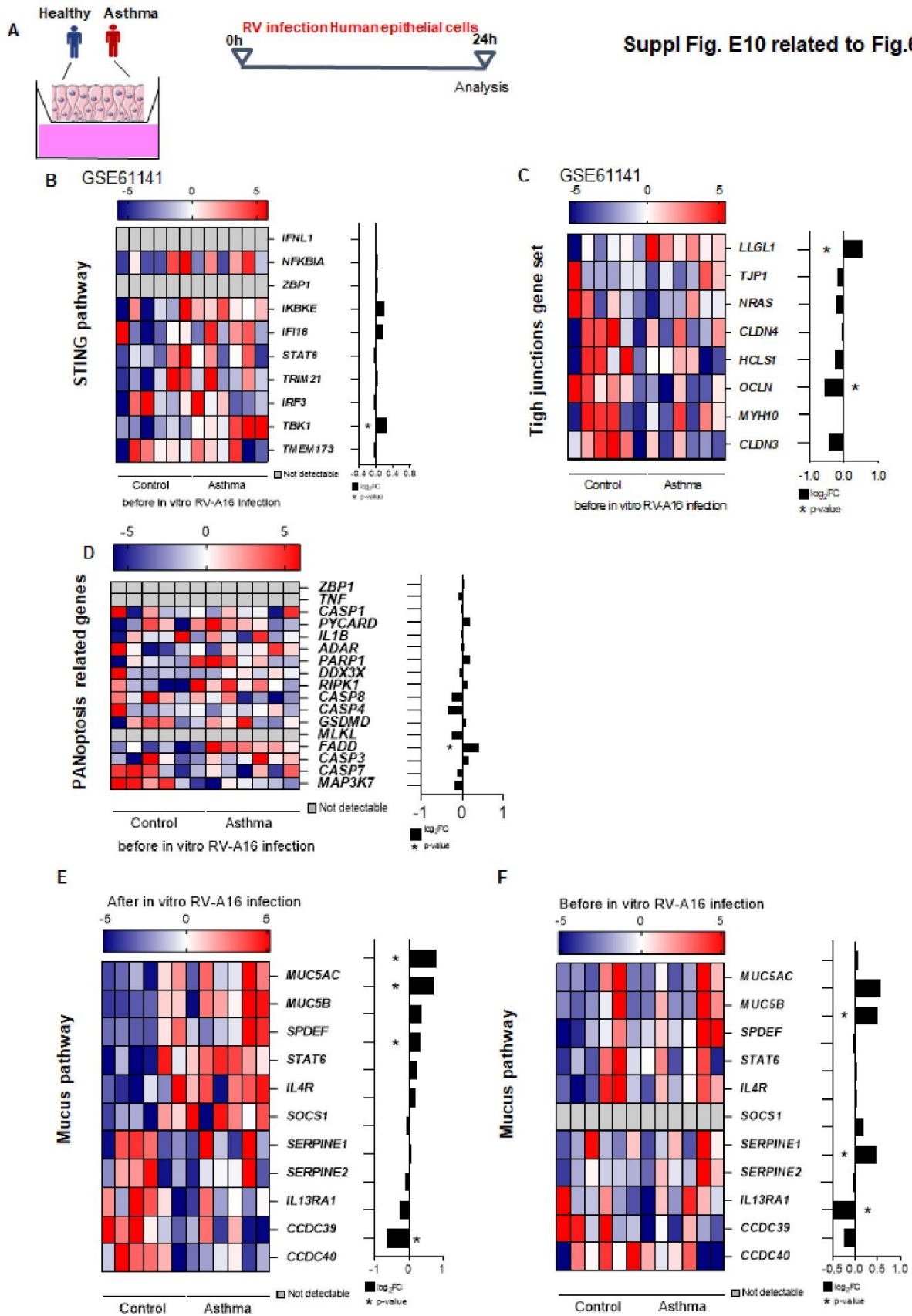
C GSE172495
PANoptosis related genes



Suppl E9 related to Fig.6: Single-cell RNAseq of PBMCs from healthy individuals or patients with severe asthma

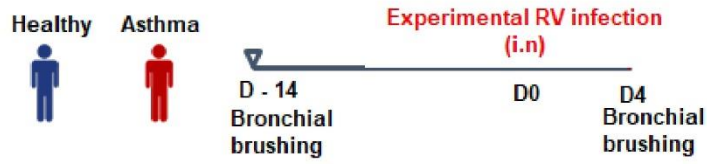
(A) PBMC cells isolated from whole blood of 5 patients with severe asthma A (n=6099) and 3 healthy individuals (n=3315), and subjected to gene profiling using scRNA-Seq as described in the original study ¹. (B-C) Dot-plots showing the expression of (B) STING pathway-related genes and (C) PANoptosis-related genes. Publicly available data under accession number: GSE172495.

Suppl Fig. E10 related to Fig.6

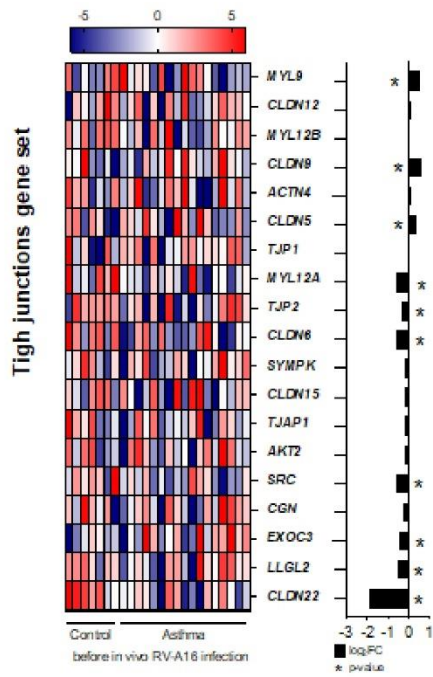


Suppl Fig. E10 related to Fig.6

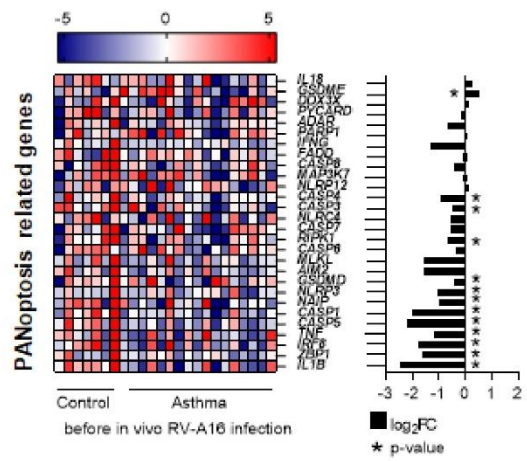
G



H GSE185658



I GSE185658



Suppl E10 related to Fig.6: Upregulation of DNA sensing and PANoptosis pathways upon rhinovirus infection in patients with asthma, as compared to non-infected individuals

(A) Human bronchial epithelial cells (HBECs) from patients with asthma (n = 6) and healthy controls (n=6), were infected with RV-A16 for 24h, and subjected to transcriptome analysis.

(B-D) Heatmaps presented together with the corresponding log₂ fold change (FC) expression changes (black bars) of (B) STING pathway-related genes, (C) Tight junction genes set, (D) PANoptosis-related genes, before *in vitro* RV-A16 infection in controls compared to HBEC from patients with asthma. (E-F) Heatmaps of mucus pathway (E) after and (F) before *in vitro* RV-A16 infection in controls compared to HBEC from patients with asthma.

(G) Experimental *in vivo* RV infection in patients with asthma (n=17) and healthy individuals (n=7): Transcriptomic analysis of bronchial brushings 14 days before and 4 days after the infection Heatmaps presented together with the corresponding log₂ fold change (FC) expression changes (black bars) of (H) Tight junction genes set, (I) PANoptosis-related genes, 14 days before *in vivo* RV-A16 infection in controls compared to patients with asthma.

Data was analyzed by the Bioconductor microarray analysis workflow available here [<https://www.bioconductor.org/packages/release/workflows/vignettes/arrays/inst/doc/arrays.html>].

All Heatmaps displays normalized gene expression across the groups (row normalization).

Asterisks demonstrate significantly changed genes with threshold $p < 0.05$. p-value: * < 0.05 .

Publicly available data under accession number: GSE185658 and GSE61141.

Online supplemental materials

Methods

Airway resistance measurement

Mice were anesthetized with intraperitoneal (i.p.) injection of a solution containing ketamine (100 mg/kg, Merial) and xylazine (10 mg/kg, Bayer), paralyzed using D-tubocurarine (0.125%, Sigma), and intubated with an 18-gauge catheter. Respiratory frequency was set at 140 breaths per min with a tidal volume of 0.2 ml and a positive end-expiratory pressure of 2 ml H₂O. Increasing concentrations of aerosolized methacholine (25, 50, 100 and 200 mg/mL) were administered. Airway resistance was measured using a ventilator (Elan Series Mouse RC Site, Buxco, Electronics) and BioSystem X.A. software (Buxco Electronics). Baseline resistance was restored before administering the subsequent doses of methacholine.

Immunoblots

Lung tissues were homogenized in T-PER™ buffer supplemented with a cocktail containing protease and phosphatase inhibitors (halt™, ThermoFisher). Total protein was extracted and quantified by using Pierce™ BCA Protein Assay Kit (ThermoFisher®). Total protein (40 µg) was treated with NuPAGE™ LDS sample buffer and sample reducing agent (ThermoFisher®), and heated 10 min at 70°C. Samples were resolved on 4-12% polyacrylamide gel (Bolt™ Mini protein gel, ThermoFisher) and run at 160V for 45min using the Mini gel Tank (ThermoFisher®). Total protein was electroblotted to 0.2 µm nitrocellulose membrane (Amersham™, UK) using a Trans-Blot SD Transfer System (Bio-Rad, California) at 100V for 45 min. Successful protein transfer was confirmed by using Ponceau S staining. Membranes were blocked with 5% nonfat milk (Cell signaling, Massachusetts) in 1X TBS-T (20 mM Tris Base, 150 mM sodium chloride, and 0.05% Tween-20 pH 7.6) for 1h at room temperature.

Full membranes or portions of membranes were incubated overnight using primary antibodies from rabbit anti-phospho-STAT6 (#56554 1/500; Cell signaling), anti-STAT6 (#5397 1/500;

Cell signaling), anti-histone H3 (#ab281584 1/500; Abcam, UK), anti-phospho- γ H2AX (#9718 1/500; Cell signaling), anti- γ H2AX (#7631 1/500; Cell signaling), anti-phospho-STING (#72971 1/500; Cell signaling), anti-STING (#13647 1/500; Cell signaling), anti-phospho-TBK1 (#5483 1/500; Cell signaling), anti-TBK1 (#3504 1/500; Cell signaling), anti-phospho-IRF3 (#4947 1/500; Cell signaling), IRF3 (#4302 1/500; Cell signaling), anti- cGAS (#31659 1/500; Cell signaling), anti-DDX41 (#15076 1/500; Cell signaling), anti-IFI204 (#ab228512 1/500; Abcam), anti-AIM2 (#63660 1/500; Cell signaling), anti-NLRP3 (#15101 1/500; Cell signaling), anti-caspase-11/cleaved-caspase-11 (#NB120-10454 1/500; Novus), anti-IL-1 β (#12426 1/500; Cell signaling), anti-IL-18 (#57058 1/500; Cell signaling), anti-cleaved caspase-3 (#9661 1/500), anti-caspase-3 (#9662 1/500; Cell signaling), anti-MLKL (#37705 1/500; Cell signaling), anti-cleaved GSDMD (#10137 1/500; Cell signaling), anti-GSDMD (#ab219800 1/500; Abcam), mouse anti-ZBP1 (#SC-271483 1/300; Santa Cruz, Texas), anti-caspase-8 (#4927 1/500; Cell signaling), anti-RIPK3 (#95702, 1/500, Cell signaling) and anti-actin β (#A3854 1/10000; Sigma-Aldrich, Massachusetts). Membranes were washed in TBS-T three times for 10 min each at room temperature, and then incubated with goat anti-rabbit-IgG-HRP-conjugate (#7074 1/2000; Cell signaling) or horse anti-mouse-IgG-HRP-conjugate (#7076 1/2000; Cell signaling) diluted in 5% non-fat milk in TBS-T for 1h at RT. The membranes were washed three times in TBS-T. Protein bands were visualized following exposure of the membrane to Amersham ECLTM prime substrate solution (Cytiva, Massachusetts) on film iBright 1500 (Invitrogen, Massachusetts).

Immunofluorescence staining of lung and BAL cells

Lungs were fixed with 4% formalin for 72h, embedded in paraffin and sectioned at 3 μ m. Lung sections were dewaxed and rehydrated, then heated 20 min at 80°C in citrate buffer 10 mM pH=6 for antigen retrieval (unmasking step). Lung sections were permeabilized in PBS 0.5% triton X-100, blocked with 5% FCS for 1h at RT and then incubated overnight with primary

goat antibodies to MPO (1:40, R&D systems, Minneapolis) or rabbit antibodies to ZO-1 (1:200, Abcam, UK). After washing, the sections were incubated with donkey anti-goat IgG secondary antibodies conjugated with AlexaFluor488 (1:200, Invitrogen) and goat anti-rabbit IgG secondary antibodies conjugated with AlexaFluor 568 (1:500, Invitrogen, Massachusetts) in 1% FCS. Following washing, lung sections were counterstained with DAPI (1:1000) and mounted onto microscope slides (Fluoromount-G, Invitrogen). Cytospin slides were fixed in 4% PFA. Cells were washed 3 times in TBS, incubated 15 min in TBS-0.3% Triton X-100, then washed 3 times in TBS, blocked in TBS-10% FCS for 45 min and incubated overnight with primary antibodies to MPO (1:40, R&D systems), and to histone H3-citrulline (1:100, Abcam) for NETs visualization. For PANoptosome visualization slides were incubated with primary antibodies from mouse anti-ZBP1 (1:100, Santa Cruz), rat anti-Caspase 8 (1: 100, Enzo Lifesciences, France), goat anti-ASC (1:50, Abcam), and mouse anti-RIPK3 (B-2) conjugated to Alexa Fluor® 647 (1:30, Santa Cruz Biotechnology). After washing, slides were incubated as described above for NETs formation detection. For the analysis of PANoptosome components, slides were incubated with donkey anti-goat IgG secondary antibodies conjugated with AlexaFluor488 (1:200, Invitrogen) and goat anti-rat secondary antibodies Alexa Fluor 546. Slides were counterstained using DAPI for 10 min. For NETs visualization, lung tissue and cells were observed using a Leica DM 6000B microscope (HAMAMATSU ORCA-Fusion C14440 Camera, Japan), images were acquired using MetaMorph® software and were treated using ImageJ software. For PANoptosome visualization, cells were observed using a Zeiss LSM 980 confocal microscope coupled with a Zeiss Airyscan 2 device (Carl Zeiss Co. Ltd., Jena, Germany). Images were acquired using Zeiss LSM Image Browser (Carl Zeiss Co. Ltd., Jena, Germany).

Flow cytometry

Bronchoalveolar lavage cells were counted and plated on a 96 well plate for extracellular staining. Different subsets of lung infiltrating cells or resident cells were detected by flow cytometry in BAL cell suspensions using a mix of the following fluorochrome-conjugated antibodies against mouse NOS2 PE-Cy7 (1/100 eBioscience), Arginase1-PE (1/100 eBioscience), Siglec F-PE-Cf59 (1/300, BD), CD45-PerCP (1/200, Biolegend), MPO-FITC (1/200, ThermoFisher), CD11b-BV786 (1/200, Fisher scientific), LY-6G-BV605 (1/100, BD), F4/80- BV421 (1/200, Biolegend), CD45-APC (1/200, Biolegend), F4/80-PE/Cy7 (1/200, Biolegend), Siglec F-PE-Cf59 (1/300, BD), CD3e-PE (1/100, BD), CD193 (CCR3)-PercPVio700 (1/50, Miltenyi Biotec), CD182 (CXCR2)-R718 (1/100, BD), CD11b-BV786 (1/200, Fisher scientific), CD45R/B220-BV711 (1/200, BD), CD11c-BV605 (1/200, BD), Ly-6G-BV510 (1/100, BD), IA/IE-eF450 (1/200, Fisher scientific), CD184 (CXCR4)-PE (1/100, Biolegend) and Fc Block (1/200) to avoid nonspecific binding. All staining reactions were performed at RT for 20 to 30 min. Flow cytometry analyses were performed on LSR Fortessa X-20 flow cytometer (Becton Dickinson, New Jersey). Gating strategy was set up according to FMO controls for all antibodies. Analysis and graphical output were performed using FlowJo™ software (Tree Star, Ashland, OR).

Lactate dehydrogenase (LDH) Measurement

Cytotoxicity was determined by quantifying lactate dehydrogenase (LDH) released in the supernatant of human epithelial cells using LDH-Glo™- Cytotoxicity assay kit (Promega) according to the manufacturer's instructions.

Quantification of mRNA expression by RT-qPCR analysis

Total mRNA was extracted using TRIzol (TRI-Reagent, Sigma-Aldrich, Germany) and reverse transcribed in cDNA with GoScript™ Reverse Transcription kit (Promega, Wisconsin). Genes

mRNA expression were analyzed using GoTaq®qPCR Master Mix (Promega). All primer sequences used were from Qiagen: *Tmem173* (#QT00261590), *Mb21d1* (#QT00131929), *Ifi204* (#QT01753535), *Aim2* (#QT00266819), *Serpinb2* (#QT01052345), *Clac1* (#QT00164290); *Spdef* (#QT0010719), *Socs1* (#QT01059268), *Hif1- α* (#QT01039542), *Osm* (#QT00263193), *Tlr-9* (#QT01043049), *IL-4* (#QT00160678), *IL-5* (#QT00099715), *IL-13* (#QT00099554). *Muc5ac* (Forward: CAGCCGAGAGGAGGGTTTGATCT. Reverse: AGTCTCTCTCCGCTCCTCTCAAT), *MUC5AC* (#QT00088991), RNA expression was normalized to *Rn18s* expression (Qiagen, Maryland). Data were analyzed using the comparative analysis of relative expression by $\Delta\Delta$ Ct methods.

Histology

Lung left lobe was removed and fixed in 4% formalin, embedded in paraffin, sectioned at 3 μ m, stained with periodic acid-Schiff (PAS) and blindly scored by an anatomic-pathologist. Semi quantitative scoring (0-5) of Goblet cell and airway inflammation including epithelial injury, and peribronchial infiltrates severity were performed.

Double-stranded DNA Measurement in BALF

dsDNA was measured in the acellular fraction of the BALF using Quant-iT PicoGreen (Invitrogen, Massachusetts) according to the manufacturer's protocol.

Measurement of cytokine levels

MPO, IL-6, TNF α , CCL11, CCL24, CXCL1, and CXCL10 concentrations in BALF and lung homogenate were measured by ELISA (R&D System, Minneapolis). IFN α , IFN β , IFN- γ , IL-4, IL-5 and IL-13, levels in BALF and lung homogenate, and IFN α , IFN β , IFN- γ , CXCL-8 CXCL-10, IL-6, TNF- α levels in cell culture supernatant were quantified by multiplex immunoassay according to manufacturers' instructions (ProcartaPlex, Life Technologies, Massachusetts).

Data were acquired on Luminex equipment (MagPix, BioRad, California) and analyzed using Bioplex Manager software (BioRad).

MUC5AC measurements

MUC5AC levels were quantified in the acellular fraction of the BALF and lung homogenate using the Mouse MUC5AC (Mucin-5 subtype AC) ELISA kit (Elabscience[®], Texas) according to the manufacturer's instructions.

Dose response study of STING agonists

Mice were anesthetized with 2% Isoflurane (ISO-VET, Netherlands) and sensitized with HDM on day 0 and 7 (25 µg/mouse, i.n.) and challenged with HDM intranasally on 3 consecutive days (10 µg/mouse, i.n. on day 14-16), in the absence or together with cGAMP (at 1, 3 or 10 µg/mouse, i.t.), diABZI compound 3 (at 0.1 or 1 µg/mouse, i.t) or Poly(I:C) (at 60 or 200 µg/mouse, i.t). Mice were analyzed on day 17, 24 hours after the last HDM instillation.

Bronchoalveolar lavage (BAL) was performed 24h after the last challenge by flushing lung tissue four times with 0.5 mL of cold NaCl 0.9% via tracheal intubation with a cannula. BALF was collected, cells counted and cytopins performed. The supernatant of the first lavage was collected after centrifugation and stored at -80°C for dsDNA and mediators quantification. The left lung lobe was harvested for histology, the post caval lung for RNA extraction and qPCR analysis and the right lobes for Western blot analysis and cytokine measurement. Protein extravasation in the BALF was measured by Pierce[™] BCA Protein Assay (ThermoFisher[®], Massachusetts).

Single cell RNA sequencing analysis

We re-analyzed single-cell transcriptomic data (GSE172495) from Human Asthma PBMC and control PBMC ¹. The dataset was downloaded and the RDS file was imported into R ²

environment version v4.3.0 and Seurat v4.3.0³ by filtering genes expressed in at least 200 cells and cells expressing at least 3 genes. For the pre-processing step, outlier cells were filtered out based on three metrics ($nCount_RNA < 4000$, $nFeature_RNA \geq 200$ & $nFeature_RNA < 2500$ and mitochondrial percentage expression < 5). The top 2,000 variable genes were then identified using the ‘vst’ method using the *FindVariableFeatures* function. Percent of mitochondrial genes was regressed out in the scaling step, and Principal Component Analysis (PCA) was performed using the top 2,000 variable genes and the top 50 PCs were selected for dimension reduction by Uniform Manifold Approximation and Projection (UMAP). Clusters were identified using the authors annotation. Then, differential gene expression analysis was performed using *FindAllMarkers* function in Seurat with default parameters to obtain a list of significant gene markers for each cluster of cells. Visualization of genes illustrating expression levels was performed using R/Seurat commands (DimPlot, FeaturePlot and DotPlot) using ggplot2⁴ and scCustomize⁵ R packages.

In vitro RV-A16 infection of human bronchial epithelial cells

Human bronchial epithelial cells (HBECs) obtained from six healthy individuals and six patients diagnosed with asthma were infected with RV-A16 at an MOI of 10 for 24h and subjected to sequencing using the Illumina HiSeq 2000 platform as described^{6,7}. Transcriptome data were processed with the workflow available here [<https://github.com/uzh/ezRun>] using the edgeR R package⁷. Presented gene sets were curated from GSEA and MSigDB Database (Broad Institute, Massachusetts Institute of Technology, and Reagent of the University of California, USA). Full sets of analyzed genes are described in Supplementary Table 1. Asterisks demonstrate significantly changed genes with threshold $p < 0.05$. Heatmaps display normalized gene expression across the gene in the groups (row normalization).

Transcriptome analyses of experimental in vivo RV-A16 infection in humans

Transcriptomics of bronchial brushings obtained from control individuals (n=7) and patients with asthma (n=17) 14 days before and 4 days after experimental RV-A16 infection in vivo⁶⁻⁸ were collected and analyzed as previously described⁷ with Affymetrix HuGene 1.0 array and Transcriptome Analysis Console v4.0 (Santa Clara, United States). Data was analyzed by the Bioconductor microarray analysis workflow available here [<https://www.bioconductor.org/packages/release/workflows/vignettes/arrays/inst/doc/arrays.html>]. Presented gene sets were curated from GSEA and MSigDB Database (Broad Institute, Massachusetts Institute of Technology, and Reagent of the University of California, USA). Full sets of analyzed genes are described in Supplementary Table 2. Asterisks demonstrate significantly changed genes with threshold $p < 0.05$. Heatmaps display normalized gene expression across the gene in the groups (row normalization).

References

1. Chen A, Diaz-Soto MP, Sanmamed MF, Adams T, Schupp JC, Gupta A, et al. Single-cell characterization of a model of poly I:C-stimulated peripheral blood mononuclear cells in severe asthma. *Respir Res* 2021; 22:122.
2. Team RC. R: A Language and Environment for Statistical Computing_. R Foundation for Statistical Computing,. <https://www.R-project.org/>, 2023.
3. Hao Y, Hao S, Andersen-Nissen E, Mauck WM, 3rd, Zheng S, Butler A, et al. Integrated analysis of multimodal single-cell data. *Cell* 2021; 184:3573-87 e29.
4. Wickham H. *ggplot2: Elegant Graphics for Data Analysis*. ; 2016.
5. Marsh S. *scCustomize: Custom Visualizations & Functions for Streamlined Analyses of Single Cell Sequencing*_. R package version 1.1.1. <https://CRAN.R-project.org/package=scCustomize>, 2023.
6. Jackson DJ, Makrinioti H, Rana BM, Shamji BW, Trujillo-Torralbo MB, Footitt J, et al. IL-33-dependent type 2 inflammation during rhinovirus-induced asthma exacerbations in vivo. *Am J Respir Crit Care Med* 2014; 190:1373-82.
7. Radzikowska U, Eljaszewicz A, Tan G, Stocker N, Heider A, Westermann P, et al. Rhinovirus-induced epithelial RIG-I inflammasome suppresses antiviral immunity and promotes inflammation in asthma and COVID-19. *Nat Commun* 2023; 14:2329.
8. Farne H, Lin L, Jackson DJ, Rattray M, Simpson A, Custovic A, et al. In vivo bronchial epithelial interferon responses are augmented in asthma on day 4 following experimental rhinovirus infection. *Thorax* 2022; 77:929-32.

Discussion and perspectives

This work aimed at enhancing our understanding of the involvement of STING, the key nod of DNA sensing pathways, in lung inflammation, and how the activation of this innate immune defense pathway, which is supposed to confer host protection, can in some circumstances lead to deleterious outcomes in lung inflammation.

Although the two respiratory diseases that we have studied differ in their pathophysiological processes, in both cases significant pulmonary inflammation can cause important breathing difficulties, being sometimes fatal. We have demonstrated that the inflammation induced following the activation of STING pathway resulted in lung neutrophilia with NETs formation, and severe lung tissue injury characterized by lytic cell death, which in turn drives massive self-dsDNA release, a major danger signal for the innate immune surveillance system.

The lung is a vital organ that is particularly susceptible to inflammation amplification. The high availability of oxygen in the lung tissue compared to other tissues, results in a greater capacity to produce ROS. The ROS-producing NADPH oxidase complex of innate immune cells, reduces oxygen to superoxide anion and releases it into the extracellular space. Because superoxide anion is instable, it is rapidly converts to hydrogen peroxide (H_2O_2). The enzyme myeloperoxidase (MPO) which is highly expressed by immune cells, uses H_2O_2 to produce a range of tissue damaging ROS. ROS are central to NETs formation making the lung a favorable environment for NETs formation and, consequently, exposing it to the damaging effects of NETs.

We have identified STING agonists including diABZI, as potent NETs activators. This activation correlates with increased pulmonary neutrophil influx accompanied by MPO upregulation. This aspect of tissue susceptibility must be considered in lung diseases in which STING is involved in the pathophysiology, or in therapeutic strategies aiming at enhancing STING activation in lung tissue.

In the healthy settings, surfactant protein D produced by ATII cells is responsible for the clearance of dying cells including NETs (Cahilog et al. 2020). However, in lung diseases where the lung barrier is compromised by apoptosis or necrosis of epithelial cells, there is evidence of altered surfactant protein levels, as reported in ARDS and allergic immune response (Choi et al. 2020). This results in the accumulation of persistent NETs. In our murine model of asthma exacerbation, we demonstrated evidence of lung barrier disruption through visualization

of decrease in the ZO-1 tight junction. We also reported a reduced expression of tight junction genes in bronchial brushings from patients with asthma compared to controls. This may result in altered levels of surfactant protein, explaining the persistence of damaging NETs in the lung parenchyma that we visualized in both models. Assessing lung surfactant levels as risk biomarker could help predict severity in lung neutrophilic inflammation.

Moreover, NETs could directly destabilize the epithelial barrier. Recently Sun and collaborators, demonstrated a correlation between NETs infiltration, sepsis-induced intestinal barrier dysfunction and enterocyte injury in sepsis patients, occurring via TLR9-ER stress pathway and apoptosis. Moreover, PAD4 deficiency mitigated intestinal barrier disruption (Sun et al. 2021). Even if this is another pathological model, it would be interesting to document whether we observe the same correlation in our models of pulmonary inflammation.

Several studies linked excessive NETs formation to lung injury in a context of ALI / ARDS, or experimental allergic asthma (Lefrançois et al. 2018; Barnes et al. 2020; Thierry et al. 2020; Radermecker et al. 2019). NETs directly mediate their damaging effects on lung tissue through by-products. The most abundant NETs by-products are histones, elastases and MPO. In a mouse model of LPS-induced lung injury, NET-derived histones induced cytotoxicity and cell death of both epithelial and endothelial cells (Saffarzadeh et al. 2012). They further demonstrated the harmful potential of histones using neutralizing anti-histone antibodies or a polyanionic compound which masks histones, ultimately resulted in a decrease in NETs-induced cytotoxicity, while blocking elastase had no effect and MPO moderately decreased NETs-mediated cytotoxicity (Saffarzadeh et al. 2012). On the other hand, during COVID-19 pathogenesis, elastases seemed to be the most important NETs proteins responsible for endothelial damage (Thierry et al. 2020).

We showed an increased expression of both MPO and citrullinated-histones after STING activation, forming a cloud-like structure filling the lung alveoli indicative of NETs formation. We confirmed the harmful effect on lung tissue through PAD4 inhibition of NETs formation themselves, that resulted in downregulation of DNA damage and several types of cell death. It would be interesting, in future characterization to determine which NETs by-products are most responsible for tissue injury after STING hyper-activation in our models. Targeting specifically the most damaging by-product proteins may be of particular interest in pathogen-induced immune exacerbation, to benefit from the pathogen-trapping function without collateral lung damage.

In our ARDS mouse model, we had evidence of lytic cell death by measuring LDH in bronchoalveolar lavage. In accordance with the NCDD recommendation, we can assume that the NETs in this model originate from a cell death process and not from viable neutrophils. Recently, Stojkov and collaborators described the GSDMD-independent process of viable NETs. They showed that inflammasome activation resulted in GSDMD cleavage in neutrophils but did not lead to membrane rupture and cell death, yet forming NETs. Moreover, GSDMD^{-/-} neutrophils were still able to form NETs in the same conditions (Stojkov et al. 2023). On the other hand, another study demonstrated that cytosolic LPS and cytosolic Gram-negative bacteria elicited neutrophil caspase-11 activation and subsequent GSDMD cleavage and plasma membrane rupture allowing DNA extrusion and thus NETosis (Chen and al. 2018).

The GSDMD cleavage that we detected in lung tissue may not be sufficient to ascertain the viability status of the NETs observed. Further studies to delineate the contribution of other immune infiltrating cells, epithelial and endothelial cells, through *ex vivo* isolation of NETs, and assessing GSDMD cleavage specifically in neutrophils could allow us to ascertain the viability status of NETs.

How do neutrophils choose between staying alive or dying during releasing NETs is less documented. Neutrophils express relatively low levels of caspase-1 resulting in low capacity for GSDMD cleavage (Chen and al. 2018). From the two previous studies demonstrating viable and suicidal NETs, it is tempting to speculate that non-canonical inflammasome activation of caspase-11 leads to sufficient GSDMD cleavage which in turn serves to membrane breaching and NETosis. While canonical-inflammasome activation relying on caspase-1, its low levels of expression will lead to insufficient GSDMD cleavage. Thus, NETs occur without cell lysis, and the pool of cleaved GSDMD will probably serve to ease IL-1 β secretion from the neutrophil.

When studying neutrophils, it is essential to regard them as a heterogeneous population, likely with distinct functions. Several studies identified neutrophil subsets expressing distinct surface markers and displaying higher ability to perform NETs. Olfactomedin 4 (OLFM4⁺) neutrophils were increased in septum of patients with uncontrolled asthma (Mincham et al. 2021). This subset has an important capacity to form NETs compared to OLFM4⁻ neutrophils (Mincham et al. 2021). Likewise, CXCR4^{hi} neutrophils were also increased in asthma patients and associated with a higher ability to form NETs. In a mouse model of HDM-induced asthma exacerbated by low doses of LPS, Radermecker and collaborators identified a CXCR4^{hi}CD49d^{hi}Lamp-1^{hi} neutrophils subset found in the lung which were prone to NETs

release and supported HDM-uptake by dendritic cells *in vivo*. Furthermore, adaptive transfer of these neutrophil subsets in HDM-treated mice resulted in amplification of allergic inflammation including airway eosinophilia, type 2 immunity, peribronchial inflammation and increased mucus hyper-section compared to control mice (Radermecker et al. 2018).

Our study of exacerbated allergic asthma identified another neutrophil subset associated with NETs release. STING hyper-activation during allergic response in mice led to a N1 neutrophil polarization $\text{NOS2}^+\text{ARG1}^-$, while neutrophils in HDM baseline mice or Poly(I:C) exacerbated mice were alternatively activated $\text{ARG1}^+\text{NOS2}^-$. Functionally, $\text{NOS2}^+\text{ARG1}^-$ neutrophils were enrolled in NETs formation, confirmed by Cit-Histone 3 expression, while the $\text{ARG1}^+\text{NOS2}^-$ neutrophils did not produce NETs. The same imbalance of NOS2 vs ARG1 expressing neutrophil populations were found in bronchial brushing of patients with asthma exacerbated by rhinoviruses.

The phenotypic classification of neutrophil subsets in N1 vs N2 profiles has been first described in cancer. However, very little is known about such plasticity in other chronic and acute inflammatory conditions. In mouse model of myocardial infraction, the two subpopulations N1 and N2 were sequentially detected. N1 neutrophils were isolated during early inflammatory phase of myocardial infraction and produced high levels of pro-inflammatory cytokines such as $\text{TNF-}\alpha$ and $\text{IL-1}\beta$, while the N2 neutrophils were concomitant with the resolving phase and showed anti-inflammatory markers such as IL-10 release (Ma Y et al. 2016). More recently, the phenotypic and functional differences of N1 and N2 population has been investigated. In coherence with our findings, among various parameters analyzed, N1 neutrophils as compared to N2, revealed significant higher levels of NO suggestive of higher NOS2 expression, as well as increased ROS and expression of NADPH oxidase subunits, important for NETs release (Mihaila et al. 2021).

Recently, Shin et al demonstrated that intratracheal challenge with diesel exhaust particles related to traffic-air pollution in HDM-mice, exacerbated asthma Th2 and Th17 immune responses and airway hyperresponsiveness (AHR), through induction of a specific neutrophil subset coexpressing Ly6G and SiglecF in the lung. These SiglecF⁺ neutrophils were promoted by ATP, a potent danger signal, and resulted in enhanced NETs release capacity (Shin et al. 2022). This study reinforced a previous study in line with our findings, in which PM2.5 air pollution-induced asthma exacerbation of OVA-treated mice. The authors showed that PM2.5 significantly increased neutrophils numbers and NETs (REF). Subsequently, NETs, probably through elastase, increased quinone oxidoreductase1 (NQO1) expression, which in

turn aggravated mucus hyper-secretion by upregulating MUC5AC and STAT6 expression, in accordance with our findings (He et al. 2021).

On the other hand, the specific involvement of the cGAS/STING pathway in the context of diesel particule-mediated lung injury through the lung flora has very recently been established (Sun M et al. 2023).

Given the exacerbation parameters described in these studies, reminiscent of some of our observations, it would be interesting to assess the contribution of the STING pathway in these exacerbation models. Further, it would be interesting to determine whether the exacerbation-related neutrophil subsets are context-dependent, or if several of these markers can be expressed simultaneously in various severe lung inflammation situations, thus opening ways for multi-target therapeutic strategies.

Neutrophils subsets mediating lung tissue injury are currently under investigation in other types of lung inflammation; as an example, the “Rogue” neutrophil-subset expression DEspR⁺ were identified in LPS-induced acute inflammation in BALF of human, and were associated with disease severity (Carstensen et al. 2022).

Since a shift in neutrophil profile can be followed by a change in their functional behavior, deeper comprehensive characterization of neutrophils subsets is imperative. This will help in guiding prediction of disease outcome, especially in neutrophilic asthma exacerbation, in which neutrophils are challenging the efficacy of current asthma therapeutics, mostly targeting eosinophils while prolonging neutrophils lifespan and their potential deleterious effect.

Despite their major contribution in our models, neutrophils express critically low levels of STING and cGAS (Xia et al. 2015). This may mean that they are not the primary cells responding to STING agonists. Instead, it is highly possible that alveolar macrophages known for their high levels of STING expression or epithelial cells are the actual first cells responding and initiating STING priming, followed by neutrophils as “responder” cells.

Analysis of lung tissue in our asthma exacerbation model revealed a clear difference in terms of phosphorylated STING, DNA damage with phosphorylated γ H2AX and citrullinated histone3 and cGAS between the experimental conditions where bronchoalveolar lavage was performed (BAL), or not performed (NO), which means when all immune cells infiltrating the lung were kept and processed with the lung tissue. This result strongly suggests the contribution

of immune infiltrating cells, particularly alveolar macrophages in activating STING in response to diABZI, in line with the study of She and collaborators, presenting alveolar macrophages as the main cell type in lung taking up extracellular cGAMP (She et al. 2021).

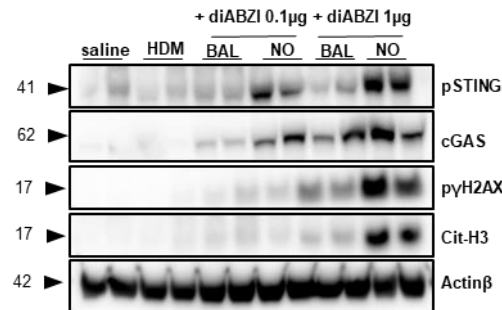


Figure 32: Immunoblots of phosphorylated STING, cGAS, p γ H2AX and Cit-H3 with Actin β as a reference, suggesting the involvement of immune infiltrating cells in the processes of immune exacerbation. BAL: BAL was performed on the lung before analysis. NO: BAL not performed before analysis. (Supplementary data not included in the submitted manuscript).

Moreover, our *in vitro* studies of macrophages and human epithelial cells, showed that both cell types can respond to STING agonists and mount an efficient innate immune response with type I IFN production, TNF- α , IL-6, induction of several DNA sensors, signs of DNA damage with p γ H2AX and markers of regulated cell death, which strongly suggest collaboration of both cell types during the initiation process.

What makes STING agonists, including the naturally occurring cGAMP, preferentially target macrophages or epithelial cells, both known to highly express STING in the lung is not yet documented. Intuitively, one could speculate that small molecule agonists such as diABZI depend on the presence or not, and the frequency of the newly described plasmatic membrane STING (pmSTING) (Li X et al. 2022). CDN agonists and chemically modified CDN might be contingent upon the frequency of specific membrane channels and transporters such as available on each cell types and also on pmSTING.

In this context, we could imagine two possible scenarios:

The first one based on the epithelial barrier hypothesis proposed by Akdis C (Akdis C. 2021), in which epithelial cells are first to be fragilized and injured by STING agonists (the DAMP here), leading to cell death and massive DNA release. This would in turn activate the DNA sensors machinery in macrophages along with efferocytosis in an attempt to clear dead cells, at least in early stages, and also attract neutrophils and their subsequent deleterious effects leading to more damage. In other terms, scenario 1 supports cell death leading to hyperinflammation.

In the second scenario, alveolar macrophages are the first to sense and respond to STING agonists resulting in important cytokines secretion (IFN α , IFN β , TNF α , IL-6, CXCL10) and subsequent neutrophil infiltration and NETs formation. In turn, NETs filling the alveoli harm lung tissue through their by-products and lead to massive cell death from the epithelial barrier and lung parenchyma. In other terms, this scenario supports the idea of inflammation leading to cell death, and subsequent fueling a second wave of exacerbated inflammation.

Our result from *in vitro* studies showed that macrophages fully responded to diABZI from phosphorylation of STING to phosphorylation of IRF3, as early as 60min after stimulation. A further comparative *in vitro* study confronting epithelial cells vs macrophages, and also a kinetic *in vivo* study may help address this question.

Whichever scenario, massive DNA release is the final outcome. In this work we focused our attention around self-dsDNA released from leaky inflammatory lung tissue.

In addition to the DNA exposed by NETs, we showed in lung tissue markers of apoptosis, necroptosis and pyroptosis, participating in the net increase of free dsDNA measured in BAL and evidence of the formation of PANoptotic complexe likely in macrophages. Moreover, we revealed the presence of mtDNA in BAL of ARDS mice.

It is possible that inflammatory cytokines released soon after STING agonist priming in our models, especially TNF- α , actively participate to mtDNA release. In context of inflammatory arthritis, Willemsen et al showed that prolonged IFN stimulation has an inhibitory effect on the PINK1-mediated mitophagy mechanism, triggering mitochondrial stress followed by mtDNA release and a subsequent dominant IFN signature through ISGs upregulation in a cGAS-STING dependent fashion (Willemsen et al. 2021). Thus cGAS-STING pathway could utilize the TNF-PINK1 inhibition axis as a positive feedback mechanism to enhance its own activation. This indicates that focusing on the inhibition of STING pathway and its direct IFN production is not the only option to consider for interferonopathies, since there are additional upstream regulatory mechanisms such as the TNF-PINK1 axis.

Furthermore, TNF- α is involved in impairment of dead cells engulfment by macrophages (McPhillips et al. 2007), resulting in an accumulation of dead cell debris. In the absence of efficient clearance mechanisms, apoptosis which is known for its silent immune status, will turn into lytic cell death, and release the content of its apoptotic bodies within 15h (Tanzer et al. 2020).

We reported upregulation of TNF- α during both mice lung conditions. In a more clinically relevant context, such as chronic asthma exacerbation in humans, involving more prolonged exposure to TNF- α compared to our models, we can imagine that there will be risks of “weaponizing” apoptosis, even during tissue turnover by making it lytic and inflammatory. This could be potentially relevant during chronic inflammatory bowel diseases where the intestinal epithelium is the most rapidly self-renewing (3–4 days).

Among the various effects of TNF- α , a study from Kanneganti’s lab showed a synergetic action of TNF- α with IFN- γ in driving PANoptosis in cytokine storm-mediating SARS-CoV2 mortality (Karki et al. 2021). Among all pro-inflammatory cytokines found to be up-regulated in patients with COVID-19, concomitant TNF- α and IFN- γ treatment induced important cell death with markers of PANoptosis in BMDM cells and THP-1 cell lines. They further revealed that PANoptosis markers were dependent on STAT1/IRF1 axis after synergetic TNF- α and IFN- γ stimulation. In this specific setting, STAT1/IRF1 pathway was found to control iNOS expression and up-regulate NO secretion leading to cell death, while Nos2^{-/-} BMDMs were protected. This experimental observation is consistent with data from patients with severe and critical COVID-19 expressing significantly higher levels of NOS2 compared to healthy controls (Karki et al. 2021).

We demonstrated the occurrence of PANoptosis in both ARDS model and neutrophilic asthma exacerbation model following challenges with STING agonists. We provided evidence for up-regulation of apoptosis, necroptosis and pyroptosis markers, as well as upregulation of components from the PANoptotic complex such as ZBP1, caspase-8 and RIPK3 in lung tissue. Furthermore, confocal microscopy performed on the cellular fraction of BAL allowed us to visualize the formation of the PANoptotic complex composed of caspase-8, ASC and RIPK3 in macrophages but not neutrophils. In our work, we stated the occurrence of PANoptosis as a downstream indirect consequence of STING activation, and demonstrated a link between NETs and PANoptosis markers in the lung. However, it would be interesting in future studies to gain insight on the precise molecular mechanisms involved in these processes.

Consistent with Karki’s study, we demonstrated augmented levels of both TNF- α and IFN- γ during neutrophilic exacerbation of allergic asthma. Indeed, the allergic response has shifted from classical Th2 with type 2 cytokines towards a mixed Th2/Th1 response with induction of IFN- γ , TNF- α and type I IFN after STING agonists treatment. Thus, it is plausible that synergism between TNF- α and IFN- γ would be at the origin of the inflammatory PANoptotic process leading to massive lytic cell death and injury.

In fact, the synergy between TNF- α and IFN- γ is not a new concept and has been documented in the literature since 1998, Zhang et al. demonstrated their synergetic role in mediating anti-toxoplasmatic effects through enhancement of NO production by macrophages (Zhang et al. 1998). The combination was involved in progression of various inflammatory diseases such as in Alzheimer progression where it correlates with NO levels (Belkhefha et al. 2014). Besides, the downstream mechanism of action of TNF- α and IFN- γ was also well documented in autoimmune diabetes during which TNF- α and IFN- γ acts through STAT1-IRF1 to mediate beta cell apoptosis (Suk et al. 2001a), or in ME-180 cervical cancer cells in which TNF- α and IFN- γ lead to apoptosis or necroptosis depending on caspases activation status (as early proof for regulated cell death (RCD) pathway overlap) in a STAT1-IRF1 and, concomitant inhibition of TNF α -induced pro-survival NF κ B pathway (Suk et al. 2001b). Apart from NF κ B pathway inhibition, these studies are coherent with Karki's study.

Interestingly, consistent with Karki's study, we reported up regulation in NOS2 expression in neutrophils *in vivo* after STING priming of HDM-treated mice, suggestive of higher NO production, while HDM-control mice showed an alternative polarization with ARG1 neutrophilic signature. In this model, we did not investigate polarization of alveolar macrophages, but we can suggest an M2 profile in HDM-treated mice and an M1 pro-inflammatory profile in exacerbated groups, known to express high levels of NOS2 and NO. Taken together, all these informations further reinforce the hypothesis of the involvement of TNF- α plus IFN- γ through the STAT1-IRF1-NO axis in mediating PANoptosis during neutrophilic exacerbation of allergic asthma.

To address this hypothesis, we could treat HDM-sensitized mice with a combination of TNF- α and IFN- γ intratracheally during HDM challenges and re-assess all exacerbation parameters considered in the original model in term of lung resistance, differential cells infiltration, dsDNA released in BAL, occurrence of N1 neutrophils and NETs release, tissue and epithelial injury and cell death markers and PANoptosis in order to fully verify if we could recapitulate STING agonists-induced exacerbation of allergic asthma then, assess the upregulation of the STAT1-IRF1-NO axis. TNF- α administration can be challenging *in vivo*, to encounter this, we could also administer neutralizing antibodies to verify if it blocks STING agonist's effect on PANoptosis.

Regarding our ARDS model, IFN- γ levels were not assessed in those settings, which make it difficult to speculate about the underlying mechanism of PANoptosis, especially considering the synthetic pharmacological nature of the trigger.

Given our findings, we could intuitively imagine that preventing lung macrophages apoptosis or necrosis can be beneficial to the host. Indeed, several reports showed that preventing alveolar macrophages apoptosis and necroptosis during the early stage of inflammation can help decrease the severity of ARDS (Dang et al.2022). In fact, the context holds greater complexity, the type of lung macrophages, whether it is PVM, RAM, or RecAM has its importance. In a mouse model of influenza A and LPS induced acute lung injury, recruited macrophages (RecAM) accumulates in the lung during early phases of inflammation and progressively decline by apoptosis during resolving phase, as indicated by the high levels of death receptor Fas expressed on RecAM as compared to resident AMs (REF). Furthermore, apoptosis inhibition of RecAM in this setting delayed the resolution of ALI, highlighting the protective role of apoptosis. The resident AMs persist along with lung injury (Janssen et al. 2011).

A better characterization of the differential role of each lung macrophage type and their fate during lung diseases could guide us distinguish between protective cell death known as tolerogenic cell death (TCD) and immunogenic cell death (ICD) potentially harmful. We can assume that protective cell death occurs when phagocytosis mechanisms are efficient. More attention should be placed on ensuring that they are not overwhelmed in pathologies where tissue injury is significant.

In clinically relevant models of ARDS and asthma exacerbation using respiratory virus and bacteria, microbial antigens (PAMPs) represents a significant factor, which our models do not consider due to the molecular nature of our triggers. Immunological cell death (ICD) is defined by collaboration between inflammation, antigenicity (eg. PAMPs or cancer neo-antigens) and adjuvanticity (eg. self-dsDNA) to activate efficiently adaptive immunity and establish a memory. Even in the absence of PAMPs, the concept of ICD is not entirely to be excluded from our models, especially considering that we recapitulated cardinal hallmarks of ARDS and neutrophilic asthma exacerbation. ICD is not associated with a specific RCD (apoptosis, necrosis) and it does not describe one of the many ways a cell can die, but instead it guides the outcome of the communication between innate immunity in response to DAMPs released or exposed by one or several RCD to amplify the inflammation.

According to the NCDD guidelines, only six DAMPs enable a specific RCD to be qualified as ICD: Calreticulin (CALR), ATP, HMGB1, type I IFN, cancer cell derived nucleic acids, and, annexin A1 (ANXA1) (Galluzi et al. 2018). Given the prominent STING activation and subsequent type I IFN production, we could possibly consider ICD in our models.

One of the most life threatening symptom of airway inflammatory disease is lung desaturation and breathing difficulties. In setting of mucus hypersecretion such as during allergic asthma attacks, free dsDNA from NETs present in the bronchoalveolar space can contribute to high viscosity of mucus which will functionally increase airway hyperresponsiveness (AHR) (Linssen et al. 2021). Considering the strong increase in dsDNA originating from NETs and other RCD in our asthma exacerbation model, we can suggest that beside its role in inflammation, DNA possibly contributes to exacerbate AHR that we revealed after STING agonists treatment.

Inflammation itself, through inflammatory cells, can participate in exacerbation of AHR. Deletion of HIF-1 α in myeloid cells using cell specific mice, or systemic inhibition of HIF-1 α with YC-1, decreased AHR and goblet cell hyperplasia in a murine model of OVA-induced asthma (Crotty et al. 2013).

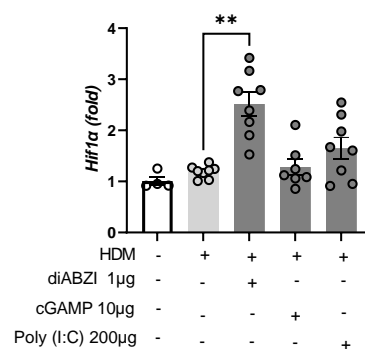


Figure 33: *HIF-1 α* transcripts in lung of STING-dependent asthma exacerbation mice model.

This aspect has not been deeply explored yet in our experimental models. However, we observed upregulation of HIF-1 α after diABZI treatment in HDM-sensitized mice, along with an exacerbation of AHR. HIF-1 α was first associated with hypoxia. Nevertheless, there is now evidence that HIF-1 α can also be activated in a normoxic environment, as well as during inflammatory responses induced by signals such as LPS, TNF- α and GM-CSF (Byrne et al. 2013). Further investigations are required to address the possible link between HIF-1 α and the exacerbation of AHR in our airway inflammatory disease models.

To open up new perspectives, it is crucial to further explore certain key aspects. First, it would be interesting to validate the corticosteroids resistance in our STING-dependent neutrophilic asthma exacerbation murine model.

In the literature, patients with asthma are often considered as homogenous and equally exposed to risks of exacerbation and development of severe forms. Nevertheless, two asthmatic populations need further attention, elderly or aging population and obese patients. Indeed, loss of nuclear envelope integrity in normal aging through, among other factors, Lamin A aberrant splicing event leads to DNA damage (Scaffidi & Misteli. 2006) and undesired molecular exchanges between nucleus and cytoplasm (Robijns et al. 2018). This suggests a chronic STING-related inflammation, further exposing elderly asthma patients to neutrophilic exacerbation.

On the other hand, a recent study revealed a non-canonical role for STING in metabolic homeostasis. At steady state, STING was found to interact with and inhibit the fatty acid desaturase 2 (FADS2)-dependent polyunsaturated fatty acids (PUFAs) desaturation. Conversely, during chronic inflammation, STING activation followed by its degradation increased Fads2-dependent desaturase activity and led to augmented omega-6 derivatives accompanied by an increase in the omega-6/omega-3 ratio that further fuelled the inflammation (Vila et al. 2022). Thus, in a context of obesity-associated chronic inflammation, the development of STING-dependent neutrophilic asthma exacerbation in obese patients with asthma multiplies comorbidities.

Therapeutic strategies using STING antagonists may face predictable limitations. Inhibiting DNA sensing pathway for long periods of time may expose the host to immunoparalysis and increased tolerance towards opportunistic microbes and tumor development. For long-term treatment, strategies targeting DNA to mitigate the inflammation could be safer for the host defense.

Likewise, strategies based on STING agonists especially in oncology which already showed limitations, should examine other pathways directly connected to the STING pathway. Indeed, as evoked in the introduction chapter, the SEL1L–HRD1 ERAD axis controls the pool of activable STING (Ji Y et al. 2023). Consequently, evaluating the activation of this axis in patient biopsies before clinical studies may help predict treatment efficacy, as tumors may downregulate STING. Further, in the absence of STING in tumors cells, STING agonists risk to be picked-up by T cells present in the tumor microenvironment known to highly express STING, leading to their demise by apoptosis. This stands in complete contrast with the aim of transforming “cold tumors” into “hot tumors”.

Furthermore, STING agonists modulate a metabolic pathway which could dampen STING activation. STING agonists were shown to fit into the crystal structure of FADS2 and directly activate its dependent PUFAs desaturation activity leading to PUFAs accumulation. In turn, PUFAs were shown to inhibit STING (Vila et al. 2022).

Finally, studies often focus on how to handle inflammation but little attention is given to what is following the post-airway injury phase that could impact future functional behavior of the immune system. In patients with systemic inflammation, phagocytosis alternations in AMs and circulating monocytes persisted over six months after resolution of inflammation (Roquilly et al. 2020). The experimental mouse model revealed that resident AMs that persist after resolution of inflammation bear epigenetic alterations of the signal-regulatory protein α (SIRP α), a negative regulator of phagocytosis, allowing the development of paralyzed AMs (Roquilly et al. 2020). Such immunoparalysis predisposes individuals to serious life-threatening issues.

Conclusion

This thesis work allowed us to evaluate the contribution of cGAS-STING pathway in the development of severe forms of airway inflammatory diseases often associated with lung tissue injuries. Recently, Singh et al qualified the role of DNA in the regulation of the innate responses as “moonlighting” (Singh et al. 2023). Indeed, when massively released from injured tissue after STING hyper-activation, self-dsDNA triggers a second wave of inflammation and impairs lung function leading sometimes to severe uncontrolled forms of asthma with modified immune landscape, irresponsive to conventional treatments. On the other hand, this work allowed us to evaluate potential threatening side effects of STING agonist-based treatments mediated by cell stress/death and self-dsDNA release and how strategies targeting free self-dsDNA alleviate lung inflammation without impairing the host defense elements. Overall, these studies uncover a potential overlap between ARDS and episodes of asthma exacerbation.

Résumé du travail de Thèse en Français

Important : La version originale de ce document est rédigée en anglais, et s'articule autour des chapitres décrit ci-dessous. Pour de plus amples détails sur l'état de l'art de la présente thématique, veuillez-vous référer à la partie en anglais

L'appareil respiratoire humain et animal est constamment menacé en raison de son exposition continue à la pollution de l'air, aux pathogènes aéroportés, aux polluants tels que la fumée de tabac ou l'exposition professionnelle, ou encore aux allergènes tels que les acariens, le pollen et la moisissure.

Dans le premier chapitre d'introduction de ce document, nous réaliserons une analyse approfondie des réponses immunopathologiques associées à deux affections pulmonaires potentiellement mortelles, à savoir le Syndrome de Détresse Respiratoire Aiguë (ARDS) et l'exacerbation neutrophilique de l'asthme allergique, avec une description du rôle des principales cellules immunitaires innées et des mécanismes intracellulaires impliqués.

Dans le second chapitre d'introduction, nous discuterons d'abord de l'impact crucial des lésions pulmonaires sévères sur la propagation et aggravation des affections inflammatoires pulmonaire. Nous aborderons les concepts précis des modalités de mort cellulaire les mieux décrites (apoptose, nécroptose, pyroptose et NETose), en suivant attentivement les classifications et recommandations du Comité National pour la Mort Cellulaire (NCDD), comment chaque type de mort cellulaire est régulé, et ce qui a conduit à la découverte majeure de la PANoptose, une modalité unique de mort cellulaire avec des implications pathophysiologiques significatives.

Dans un deuxième temps, nous visons à élucider comment les voies complexes de mort cellulaire régulent la réponse immunitaire innée, et à comprendre les mécanismes qui rendent une mort cellulaire spécifique "inflammatoire". Nous décrypterons également le rôle des signaux de danger (DAMPs) libérés par la mort cellulaire lytique et non lytique, en mettant l'accent sur l'ADN comme signal de danger commun à toutes les morts cellulaires.

Dans un troisième temps, nous chercherons à approfondir notre compréhension de la manière dont la voie cGAS-STING régule les principales modalités de mort cellulaire en réponse à l'ADN du soi, en tant que mécanisme de rétroaction positive ayant des conséquences délétères sur le tissu pulmonaire. Enfin, nous explorerons les avancées majeures dans le domaine de la modulation immunitaire de la voie STING comme stratégie thérapeutique.

Dans le troisième chapitre des résultats, nous exposerons nos études et les deux manuscrits associés. Dans le chapitre final de discussion, nous aborderons les principaux résultats et les limites des études, ainsi que les perspectives.

Enjeux actuels et objectifs de la thèse

Dans le contexte climatique actuel très préoccupant, de récentes études indiquent que l'augmentation des températures que nous connaissons, induit des perturbations dans les périodes de pollinisation, les faisant débiter de manière précoce et à les prolonger. Ainsi, la durée d'exposition au pollen s'en trouve augmentée. De plus, les niveaux élevés de CO₂ atmosphérique résultant de la pollution due à l'hyper-industrialisation affaiblissent non seulement les barrières respiratoires, mais renforcent également le potentiel allergisant du pollen (Singh & Kumar, 2022; D'Amato et al., 2023). En effet, les particules polluantes affaiblissent la membrane externe du grain de pollen, résultant en des fragments plus petits capables de pénétrer plus profondément dans les voies respiratoires (Verscheure et al., 2023).

De plus, le réchauffement climatique devrait augmenter la fréquence des pandémies émergentes (Gupta et al., 2021; Marani et al., 2021), comme celle qui nous a affecté en 2019, entraînant la mort de 6 million de personnes dans le monde. La migration des humains et des animaux en tant que réfugiés climatiques rassemblera des hôtes dont les systèmes immunitaires n'ont pas évolué pour contrer les mêmes agents pathogènes, facilitant ainsi la transmission de virus et de bactéries.

Pris ensemble, ces données indiquent qu'à l'avenir, les troubles respiratoires risquent de devenir plus courants. En effet, l'organisation mondiale de la santé (OMS) prévoit qu'en 2050, la prévalence des maladies allergiques pourrait doubler, affectant 50 % de la population mondiale. Dans ce contexte, les personnes asthmatiques peuvent développer une inflammation sévère des voies respiratoires présentant les mêmes caractéristiques que le SDRA. Il est donc urgent de comprendre les mécanismes responsables de l'exacerbation des pathologies respiratoires, de développer de nouvelles approches thérapeutiques et de tester la sécurité de ces stratégies.

Comme discuté dans l'introduction, le rôle de l'ADN du soi dans le déclenchement des réponses inflammatoires innées stériles et infectieuses est désormais bien connu. À travers l'étude de ces deux troubles respiratoires, notre objectif principal est d'évaluer et de caractériser le rôle de l'hyperactivation de la voie STING dans la médiation des (1) formes potentiellement graves du syndrome de détresse respiratoire aiguë (ARDS), survenant lors d'une infection virale

respiratoire non contrôlée, ou (2) d'asthme allergique aggravé/exacerbé, pouvant survenir lorsque des individus asthmatiques sont infectés par des virus/bactéries respiratoires ou exposés à la pollution atmosphérique.

Plusieurs études ont suggéré l'utilisation d'un agoniste de STING, tel que le diABZI, comme stratégie thérapeutique pour réduire la charge virale du SARS-CoV-2 durant la pandémie Covid-19. Nous avons cherché à comprendre les mécanismes immunomodulateurs induits par cette molécule thérapeutique candidate dans des organismes immunocompétants et immunodéficients pour plusieurs éléments de la voie cGAS-STING. Nous voulions déterminer si booster pharmacologiquement la voie STING se limite à l'activation de la voie de l'IFN de type I, ce qui serait bénéfique pour l'hôte lors d'une infection virale, ou si cela peut également propager l'inflammation et entraîner des boucles de rétroaction positive d'inflammation non contrôlée, entraînant des lésions tissulaires. Dans ce scénario, il serait nécessaire de réévaluer le rapport bénéfice/risque de l'utilisation du diABZI ou d'autres agonistes de STING pour le traitement des infections virales.

Dans la section Introduction, nous avons souligné l'implication de la voie cGAS-STING dans la physiopathologie de l'asthme classique à dominance Th2 et son activation par les virus respiratoires ou la pollution atmosphérique telle que les particules de diesel. D'autre part, nous savons maintenant que les virus respiratoires tels que les rhinovirus, le SARS-CoV2 ou l'IAV entraînent régulièrement des exacerbations de l'asthme, avec infiltration neutrophilique pulmonaire et production de médiateurs Th1. Ces formes sévères d'épisodes d'asthme neutrophiliques entraînent souvent des hospitalisations et rendent la pathologie réfractaire aux traitements conventionnels.

Sur la base de ces informations, nous avons évalué l'impact de l'hyperactivation de la voie STING sur l'immunopathologie de l'asthme classique à dominance Th2. Nous avons mimé l'infection virale ou l'exposition aux particules polluantes pendant les réponses allergiques, en utilisant un modèle murin d'asthme allergique induit par les HDM sensibilisé aux agonistes de STING dans les voies respiratoires. En suivant cette approche expérimentale, nous avons évalué l'implication de la voie STING dans la médiation de formes sévères non classiques d'asthme neutrophilique, et son potentiel à aggraver la fonction pulmonaire et les lésions. Dans ce contexte, une attention particulière devrait être portée à l'atténuation de l'hyperactivation des voies STING dans la prise en charge clinique de l'exacerbation sévère de l'asthme.

Résultats

Article 1: STING agoniste diABZI induit la PANoptose et un syndrome de détresse respiratoire aiguë (ARDS) médié par l'ADN du soi.

Yasmine Messaoud-Nacer, Elodie Culerier, Stéphanie Rose, Isabelle Maillet, Nathalie Rouxel, Sylvain Briault, Bernhard Ryffel, Valérie F. J. Quesniaux, et Dieudonnée Togbe. *Cell Death and Disease* (2022) 13:269; <https://doi.org/10.1038/s41419-022-04664-5>.

Les interférons ont toujours été considérés comme étant la première ligne de défense de l'organisme contre les infections ou les cellules transformées. En effet, les souris dépourvues du récepteur IFN α/β montrent une réponse antivirale altérée. De plus, une faible production d'interférons chez les patients infectés par le SARS-CoV-2 est corrélée à une faible clairance virale, soulignant leur importance clinique et thérapeutique (Blanco-Melo et al. 2020 ; Hadjadj et al. 2020).

Il existe trois familles d'interférons: les interférons de types I (IFN- α/β) et III (IFN- λ) avec des propriétés antivirales canoniques, et le type II (IFN- γ) avec des propriétés pro-inflammatoires et immunomodulatrices (Lazear et al. 2019). Les IFN de type I et de type III signalent à travers deux récepteurs hétérodimériques distincts, à savoir IFNAR/IFNAR2 et IL28R α /IL10R β , respectivement. Les deux familles signalent à travers la voie JAK1-STAT1/-2 pour activer le complexe de transcription hétérotrimérique ISGF3. L'ISGF3 activé comprend STAT1 et STAT2 phosphorylés, ainsi que le facteur de régulation de l'interféron 9 (IRF9), et transloque dans le noyau pour se fixer et activer les éléments de réponse stimulés par les IFN ou 'ISRE' dans les régions promotrices des ISGs (Katze et al. 2002), qui encodent environ une centaine de protéines antivirales, telles que OAS, MX1 ou IFIT (Lazear et al. 2019).

Pendant la pandémie mondiale de COVID-19, la thérapie par les IFN, incluant tous les sous-types, a été administrée cliniquement aux patients, dans une tentative de gérer la crise. Jhuti et al. ont rapporté que parmi 11 essais examinés, 5 études ont rapporté un résultat positif, 4 ont rapporté peu ou pas de différence entre le groupe traité l'IFN et le groupe contrôle, et 2 études ont déclaré aggravation des manifestations cliniques chez les patients traités par rapport aux contrôles (Jhuti et al. 2022). Plus tard, ces incohérences jugeant de l'efficacité du traitement aux interférons dans ce contexte infectieux, ont été partiellement expliquées par le timing de l'administration des IFNs. En effet, lors des infections aiguës, une administration précoce des IFN de type I chez dans un modèle murin induit des réponses antivirales protectrices, tandis

qu'une administration tardive des IFN amplifie la production de cytokines pro-inflammatoires induisant des dommages tissulaire chez l'hôte (Davidson et al. 2014; Galani et al. 2017). De plus, il a été découvert que le SARS-CoV-2 retardait la réponse immunitaire innée comme stratégie d'évasion immunitaire (Li et al. 2021), soulignant la nécessité d'adapter la cinétique de l'administration des IFNs pour améliorer la réponse immune antivirale tout en limitant les dommages collatéraux aux tissus hôtes.

Li et al. ont suggéré l'utilisation de l'agoniste STING diABZI comme une stratégie thérapeutique alternative pour améliorer la production des IFN de type I durant les phases précoces de l'infection tout en limitant les dommages collatéraux. Leur suggestion était motivée par le caractère transitoire de la stimulation de la production des IFNs après l'activation aiguë de la voie STING. Dans cette étude, les auteurs ont montré que l'agoniste de STING a induit la production des IFNs et des ISGs de manière transitoire, ce qui a contribué à réduire la charge virale, tandis que le traitement par IFN β a conduit à une expression soutenue des ISGs et a été moins efficace que diABZI (Li et al. 2021). Un autre groupe a confirmé l'effet bénéfique de diABZI sur la clairance virale (Humphries et al. 2021).

Sur la base de ces résultats, nous avons cherché à évaluer le paysage immunitaire pulmonaire modulé par diABZI chez des souris immunocompétentes, et à déterminer si la réponse transitoire des IFN de type I rapportée dans les études précédentes pouvait induire des dommages tissulaires et cellulaires, ce qui pourrait à son tour alimenter une boucle de rétroaction positive entre inflammation et dommages.

Nous avons d'abord étudié l'effet de l'agoniste naturel de STING, cGAMP, à la fois in vivo par administration intra-trachéale, et in vitro dans des macrophages dérivés de la moelle osseuse (BMDM) de souris de type sauvage et STING^{-/-}. L'agoniste endogène cGAMP a induit une neutrophilie pulmonaire comme en témoigne la sécrétion de CXCL1 (KC) et de MPO dans les lavages broncho-alvéolaire (BALF), l'activation des voies inflammatoires incluant IRF3 et NF κ B, et des lésions pulmonaire massives associée à une libération d'ADN double brin du soi dans les voies respiratoires. La stimulation in vitro des BMDM avec cGAMP a révélé une production précoce des IFN de type I dès 2 heures après le traitement, avec une production d'ISGs (CXCL10) et l'expression de plusieurs senseurs d'ADN, mesurée à 4 et 16 heures après le traitement.

Nous avons ensuite testé l'agoniste STING non-CDN diABZI connu pour être plus stable que l'agoniste endogène, d'abord in vitro dans les cellules immunitaires de souris (BMDM) et les cellules épithéliales humaines. De même, diABZI a induit la production d'IFN de type I (α/β) et d'autres cytokines pro-inflammatoires 16 heures après le traitement, des dommages d'ADN mis en évidence par la phosphorylation de γ H2AX et la mort cellulaire avec des marqueurs d'apoptose, de pyroptose et de nécroptose au niveau du tissu pulmonaire. In vivo, l'administration intratrachéale de diABZI a induit la production d'IFN- α / IFN- β et des cytokines pro-inflammatoires IL-6 / TNF- α résultant de l'activation des voies STING et NF κ B, respectivement. Nous avons révélé la présence de quantités critiques d'ADN double brin du soi, en partie d'origine mitochondriale, témoignant du stress cellulaire induit par le traitement. Une forte infiltration neutrophilique avec la libération de NETs a été caractérisée dans le poumon. Sur le plan histopathologique, d'importants infiltrats péribronchiques de cellules inflammatoires se sont étendus au parenchyme pulmonaire avec des signes de lésion épithéliale après administration de diABZI.

Nous avons ensuite voulu déterminer précisément l'origine de l'ADN double brin détectée dans les voies respiratoire. Plusieurs rapports ont démontré que STING pouvait directement activer les voies pro-apoptotique. Nous avons évalué et montré l'occurrence de l'apoptose, ainsi que la mort cellulaire lytique la plus caractérisée, la pyroptose et la nécroptose dans le tissu pulmonaire après l'administration de diABZI. La présence des 3 marqueurs de mort cellulaire suggérait la PANoptose. Nous avons par la suite confirmé la formation du complexe PANoptotique en évaluant la co-localisation de la caspase-8, ASC et RIPK3 par microscopie confocale.

Connaissant le rôle que l'ADN peut jouer dans l'inflammation, nous avons émis l'hypothèse que l'ADN libéré pourrait agir comme un second signal pour amplifier l'inflammation pulmonaire. Pour aborder cette question, nous avons d'abord analysé l'expression de plusieurs capteurs d'ADN et trouvé des niveaux accrus de cGAS (qui a été contourné au premier signal inflammatoire lors de l'amorçage de STING avec diABZI), mais aussi de Aim2, Ifi204, Nlrp3, Ddx41 et Tmem173.

Afin de caractériser davantage le rôle de l'ADN dans la médiation des lésions pulmonaires, des souris traitées au diABZI ont reçu soit une administration intratrachéale de DNAase I, soit une administration intrapéritonéale de Cl-Amidine, un inhibiteur de la formation de NET. La dégradation de l'ADN double brin du soi la DNAase I a entraîné une diminution de

l'infiltration des neutrophiles au niveau pulmonaire, une réduction dans la proportion de NETs ainsi qu'une diminution de l'infiltration des cellules immunes CD45⁺ nécrotiques annexine V⁺ iodure de propidium (PI)⁺ et des cellules annexine V⁺ apoptotiques PI⁻. De même, l'inhibition des NET avec le traitement à la Cl-Amidine a contribué à réduire l'infiltration des neutrophiles dans le poumon et a révélé l'existence d'une interaction entre l'activation de STING médiée par les lésions pulmonaires et la formation de NET. En effet, l'inhibition des NETs chez les souris traitées par diABZI a entraîné une réduction des dommages à l'ADN, comme en témoignent la phosphorylation de l'histone γ H2AX, mais aussi tous les marqueurs de la PANoptose évalués. De plus, la mort cellulaire lytique évaluée par libération de lactate déshydrogénase (LDH) dans les lavages broncho-alvéolaire a été atténuée après l'inhibition. Ainsi, nous présentons les premières preuves établissant un lien entre les NET et la PANoptose.

Dans l'ensemble, notre étude a démontré que les stratégies thérapeutiques utilisant l'agoniste de STING diABZI induisent en effet une induction précoce des IFN de type I, ce qui peut être bénéfique pour les patients infectés afin de contrer l'évasion immunitaire virale innée. Cependant, la cascade inflammatoire subséquente, conduisant à des dommages d'ADN de l'hôte, à l'activation de mécanismes de mort cellulaire lytique et les lésions tissulaires pulmonaires, révèle que la balance entre les bénéfices et les risques peut être facilement inversé. Cela rend difficile l'appréciation complète des propriétés antivirales de l'agoniste de STING diABZI, et pose des défis supplémentaires pour définir les doses et les voies d'administration adéquates afin de contrôler l'infection virale sans compromettre la fonction pulmonaire de l'hôte.

Article 2: Induction STING-dépendante de l'exacerbation d'asthme de type neutrophilique en réponse aux acariens domestiques.

Yasmine Messaoud-Nacer, Elodie Culerier, Stéphanie Rose, Isabelle Maillet, Bernard Malissen, Urszula Radzikowska, Milena Sokolowska, Gabriel VL da Silva, Michael R Edwards, David J Jackson, Sebastian L Johnston, Bernhard Ryffel, Valerie F. Quesniaux, et Dieudonnée Togbe* Article soumis. 2023

La persistance de la réponse allergique malgré un traitement aux corticostéroïdes oraux (OCS) à haute dose caractérise les exacerbations sévères de l'asthme. Chez un sous-groupe de patients asthmatiques, il existe une implication évidente des neutrophiles dans les poumons, ce qui augmente la gravité de la maladie et corrèle avec une insensibilité aux corticostéroïdes. Comprendre les voies immuno-inflammatoires qui conduisent à l'asthme neutrophilique aiderait à sélectionner des traitements plus appropriés (Nair et al. 2020; Ragnoli et al. 2022).

Dans cette étude, nous avons émis l'hypothèse que la voie de détection de l'ADN cGAS-STING joue un rôle dans l'exacerbation de l'asthme neutrophilique suite à une infection virale ou à une exposition à la pollution, et pourrait ainsi représenter une nouvelle cible thérapeutique. Pour tester cette hypothèse, nous avons spécifiquement ciblé STING *in vivo* chez des souris, avec des agonistes de STING (cGAMP, diABZI) au cours des réponses allergiques aux acariens domestique (HDM), et analysé les paramètres inflammatoires.

Les agonistes de STING, en particulier diABZI, ont induit une forte infiltration de neutrophiles dans les poumons et une réponse immunitaire de type 1 (Th1) en plus de la réponse immunitaire Th2 préexistante, tout en aggravant la résistance pulmonaire induite par les HDM, mimant ainsi les principaux marqueurs de l'exacerbation de l'asthme neutrophilique. De plus, nous avons démontré pour la première fois que les neutrophiles infiltrés suite à l'hyperactivation de STING présentent un profil pro-inflammatoire N1 (NOS2+ ARG1-) avec un fort potentiel à former des NETs, contrairement aux neutrophiles induits par les HDM, qui présenterait plus un profil N2 (NOS2+ ARG1-). Localement, au niveau du tissu pulmonaire, nous avons montré une importante augmentation de l'infiltration des leucocytes et des lésions épithéliales, avec une diminution dans le nombre de goblets cells. Nous avons également montré des preuves de dommages à l'ADN et des marqueurs de mort cellulaire suggérant une mort cellulaire de type PANoptotique.

Malgré le rôle hautement pathogène joué par les neutrophiles pro-inflammatoires dans l'exacerbation de l'asthme neutrophilique, les macrophages alvéolaires se sont révélés être l'un des principaux types de cellules pulmonaires responsables de la captation et l'intégration de l'agoniste naturel de STING cGAMP *in vivo* (She et al. 2021). Nous avons investigué la contribution des macrophages et des granulocytes en utilisant des souris déficientes conditionnelles pour la protéine adaptatrice STING. Les paramètres inflammatoires évalués, tels que l'infiltration de neutrophiles, la libération de type I IFN et de NET, étaient partiellement réduits chez les souris déficientes en STING de manière conditionnelle par rapport aux témoins de type sauvage. Ces résultats suggèrent que les cellules inflammatoires jouent un rôle dans la formation de la réponse exacerbée, mais ne sont pas exclusives à ces réponses pathologique dans ce contexte spécifique.

Les résultats précédents nous ont incités à nous interroger sur le rôle des cellules épithéliales pulmonaires structurelles. Nous avons montré que les agonistes de STING affaiblissent davantage l'intégrité de la barrière épithéliale initié par l'allergène HDM *in vivo* chez les souris en agissant directement sur les jonctions serrées. De plus, les cellules épithéliales bronchiques humaines et les cultures cellulaires épithéliales bronchiques air-liquide imitant la barrière respiratoire ont montré la capacité de répondre aux agonistes de STING avec des preuves d'activation de la voie STING, d'induction de cytokines pro-inflammatoires ainsi que des dommages d'ADN qui alimenteront davantage l'inflammation.

Pour valider davantage la pertinence de notre modèle murin d'exacerbation neutrophilique, nous avons testé si la voie STING était également hyperactivée chez les patients asthmatiques souffrant d'infections respiratoires, ou chez les patients atteints d'asthme sévère en comparaison aux témoins sains. À cet effet, nous avons analysé les données disponibles publiquement provenant de cellules épithéliales bronchiques stimulées *in vitro* au rhinovirus RV-A16, des prélèvements bronchiques de patients asthmatiques et de témoins sains infectés expérimentalement par le rhinovirus *in vivo*, et des PBMC de patients atteints d'asthme sévère et de témoins. En effet, nous avons trouvé une expression accrue de la voie STING dans les cellules épithéliales bronchiques des patients asthmatiques par rapport aux témoins après infection par le rhinovirus. Cette expression était accompagnée d'une augmentation de plusieurs gènes liés à la PANoptose, et d'une diminution de l'expression de plusieurs gènes de jonctions serrées, après infection par le rhinovirus chez les patients asthmatiques par rapport aux témoins. De plus, en analysant la signature des neutrophiles au niveau des prélèvements bronchiques

d'individus infectés expérimentalement, nous avons trouvé que NOS2 était augmenté tandis qu'ARG1 était diminué après infection par le rhinovirus chez les patients asthmatiques par rapport aux témoins, ce qui est en adéquation avec nos résultats expérimentaux.

Ces résultats indiquent que l'activation incontrôlée de STING, par exemple après une infection par le rhinovirus, peut entraîner une exacerbation neutrophilique chez les patients asthmatiques, et faire basculer la réponse immunitaire d'une réponse classique à dominance Th2 vers une réponse mixte Th1/Th2. Par conséquent, envisager les inhibiteurs de STING comme stratégie thérapeutique, seuls ou en combinaison avec d'autres traitements, pourrait améliorer l'état et le quotidien des patients atteints d'asthme sévère.

Discussion

Ce travail de thèse visait à approfondir notre compréhension du rôle de STING dans l'inflammation pulmonaire, situé à l'intersection de plusieurs voies de détection de l'ADN, et comment l'activation de cette voie de défense immunitaire innée, censée conférer une protection à l'hôte, peut dans certaines circonstances conduire à des effets délétères sur l'intégrité du tissu pulmonaire.

Bien que les deux maladies respiratoires que nous avons étudiées diffèrent par leurs processus physiopathologiques, dans les deux cas, une inflammation pulmonaire exacerbée ou persistante peut entraîner d'importantes difficultés respiratoires, parfois fatales. Nous avons démontré que l'inflammation induite suite à l'activation de la voie STING a entraîné une neutrophilie pulmonaire avec formation de NETs, accompagnés de lésions sévères du tissu pulmonaire caractérisées par une mort cellulaire de type lytique, qui à son tour provoque une libération massive de dsDNA du soi, considéré en tant que signal de danger majeur (DAMP) par les systèmes de surveillance de l'immunité innée.

Le poumon est un organe vital particulièrement susceptible à l'amplification de l'inflammation. La haute disponibilité en oxygène dans le tissu pulmonaire comparé à d'autres tissus, résulte en une plus grande capacité à produire des ROS. Le complexe NADPH oxydase des cellules immunitaires innées réduit l'oxygène en anion superoxyde et le libère dans l'espace extracellulaire. Considérant la nature instable de l'anion superoxyde, ce dernier peut rapidement être converti en peroxyde d'hydrogène (H_2O_2). L'enzyme myéloperoxydase (MPO), fortement exprimée par les cellules immunitaires, utiliserait le H_2O_2 pour produire une gamme de ROS qui endommagerait les tissus. Les ROS sont centraux dans la formation des NETs, faisant du poumon un environnement favorable à la formation des NETs et, par conséquent, l'exposant aux effets potentiellement dommageables des NETs.

Nous avons identifié des agonistes de STING, dont le diABZI, comme de puissants inducteurs de NETs. Cette activation corrèle avec une augmentation de l'afflux de neutrophiles au niveau du poumon accompagnée d'une surexpression de la MPO. De ce fait, cet aspect de susceptibilité tissulaire doit donc être pris en considération dans les pathologies pulmonaire où STING est clairement impliqué, et pour lesquelles on envisagerait des stratégies thérapeutiques visant à renforcer l'activation de STING au niveau de ce tissu.

Dans un contexte physiologique, la protéine de surfactant D produite par les cellules ATII est responsable de la clairance des cellules mortes, y compris les NETs (Cahilog et al. 2020). Cependant, dans les pathologies où la barrière pulmonaire est endommagée par induction d'apoptose de nécrose des cellules épithéliales, les études ont décrit l'altération des niveaux de production de surfactant, comme rapporté dans le SDRA ou les réponses inflammatoires allergiques (Choi et al. 2020). Par conséquent, cela entraînerait l'accumulation et la persistance des NETs au niveau du tissu pulmonaire. Dans notre modèle murin d'exacerbation de l'asthme, nous avons montré des preuves de rupture de la barrière respiratoire via visualisation de la protéine de jonction ZO-1. Nous avons également constaté une réduction de l'expression des gènes impliqués dans l'établissement des jonctions serrées dans des échantillons bronchoscopiques de patients asthmatiques en comparaison aux témoins sains. Cela pourrait entraîner une altération des niveaux de protéines du surfactant, ce qui expliquerait la persistance des NETs dommageables dans le parenchyme pulmonaire que nous avons visualisé dans les deux modèles. L'évaluation des niveaux de surfactant pulmonaire en tant que biomarqueur de risque pourrait aider à prédire la gravité de l'inflammation neutrophilique pulmonaire.

De plus, les NETs pourraient directement déstabiliser la barrière épithéliale. Récemment, Sun et ses collaborateurs ont démontré une corrélation entre l'infiltration des NETs, le dysfonctionnement de la barrière intestinale induite par septicémie ainsi qu'une lésion des entérocytes chez ces patients où l'axe TLR9-ER et l'apoptose seraient impliqués. Par ailleurs, les auteurs ont démontré que l'absence de PAD4, dont la fonction est essentielle à la formation des NETs a atténué la perturbation observée sur la barrière intestinale. (Sun et al. 2021). Bien qu'il s'agît ici d'un autre contexte pathologique, il serait intéressant de vérifier si nous observons la même corrélation dans nos modèles d'inflammation pulmonaire.

Plusieurs études ont établi un lien entre la formation excessive de NETs et les lésions pulmonaires dans un contexte d'ALI / ARDS, ou d'asthme allergique expérimental (Lefrançais et al. 2018 ; Barnes et al. 2020 ; Thierry et al. 2020 ; Radermecker et al. 2019). Les NETs médient directement leurs effets dommageables sur le tissu pulmonaire par le biais de molécules fixées sur les filaments d'ADN. Les composants les plus abondants des NETs sont les histones, les élastases et la MPO. Dans un modèle murin de lésions pulmonaires induites par le LPS, les histones dérivées des NET ont induit la cytotoxicité et la mort cellulaire des cellules épithéliales et endothéliales (Saffarzadeh et al. 2012). Dans cette études les auteurs ont ensuite démontré le potentiel nocif des histones en utilisant des anticorps anti-histones neutralisants ou un composé polyanionique qui masque les histones, ce qui a entraîné une diminution de la cytotoxicité

induite par les NETs, tandis que l'inhibition des élastases (NE) n'a eu aucun effet, tandis que la MPO a modérément diminué la cytotoxicité médiée par les NETs (Saffarzadeh et al. 2012). D'autre part, au cours de la pathogenèse de COVID-19, les élastases semblent être les composants les plus importantes des NETs, responsables des dommages endothéliaux (Thierry et al. 2020).

Nous avons montré une augmentation de l'expression de la MPO et des histones citrullinées après l'activation de STING, formant une structure en nuage remplissant la surface des alvéoles pulmonaires, typique de la présence de NETs. Nous avons confirmé l'effet délétère sur le tissu pulmonaire par l'inhibition de la formation des NETs via l'inhibition de PAD4, ce qui a entraîné une diminution des dommages d'ADN et une diminution de plusieurs marqueurs de différents types de mort cellulaire. Il serait intéressant, dans le cadre de futurs travaux de déterminer spécifiquement quels composants dérivés des NETs seraient les plus impliqués dans l'induction des lésions tissulaires après hyperactivation de STING dans nos modèles. Neutraliser spécifiquement les protéines les plus à risque des NETs pourrait être particulièrement intéressant dans les exacerbations de réponses inflammatoires induites par des agents infectieux, afin de bénéficier de la fonction de piégeage des agents pathogènes sans compromettre l'intégrité du tissu pulmonaire.

Dans notre modèle de souris ARDS, nous avons démontré la survenue de mort cellulaire de type lytique en mesurant la LDH dans le lavage broncho-alvéolaire. Conformément à la recommandation de la NCDD, nous pouvons supposer que les NETs dans ce modèle proviennent d'un processus de mort cellulaire et non de neutrophiles viables. Récemment, Stojkov et ses collaborateurs ont démontré que le processus au cours duquel un neutrophile viable formerait un NETs serait indépendant de la GSDMD. Ils ont montré que l'activation de l'inflammasome entraînait le clivage de la GSDMD avec formation de mais ne conduirait pas à la rupture de la membrane et à la mort de la cellule. De plus, les neutrophiles GSDMD^{-/-} ont conservé la capacité à former des NETs dans les mêmes conditions expérimentales. (Stojkov et al. 2023). En revanche, une autre étude a démontré que le LPS cytosolique et les bactéries Gram négatives cytosoliques induisaient l'activation de la caspase-11, suivi du clivage de la GSDMD entraînant une rupture de la membrane plasmique qui permet l'extrusion de l'ADN et donc la NETose (Chen et al. 2018).

Le clivage du GSDMD que nous avons détecté dans le tissu pulmonaire peut ne pas être suffisant pour vérifier la viabilité des NET observées. En effet, La GSDMD clivée pourrait émaner d'autres types cellulaires ou encore être le résultat de l'activation d'une autre modalité

de mort cellulaire. Afin d'écartier la contribution d'autres sources, il serait intéressant d'effectuer une isolation *ex vivo* des NETs et d'évaluer spécifiquement le clivage des GSDMD au niveau des neutrophiles afin d'établir le statut de viabilité des NETs, bien que cette technique pourrait s'avérer particulièrement challengeante.

Il est essentiel de les considérer les neutrophiles comme une population hétérogène, susceptible d'avoir des fonctions distinctes. Plusieurs études ont identifié des sous-types de neutrophiles exprimant des marqueurs de surface distincts et présentant une plus grande capacité à effectuer des NET. Les neutrophiles olfactoméline 4 (OLFM4⁺) ont augmenté dans les crachats de patients souffrant d'asthme non contrôlé (Mincham et al. 2021). Ce sous-type a une capacité importante à former des NETs par rapport aux neutrophiles OLFM4. (Mincham et al. 2021). De même, les neutrophiles CXCR4^{hi} étaient également plus nombreux chez les patients asthmatiques et associés à une plus grande capacité à former des NETs. Dans un modèle murin d'asthme induit par l'HDM et exacerbé par de faibles doses de LPS, Radermecker et ses collaborateurs ont identifié un sous-type de neutrophiles CXCR4^{hi}CD49d^{hi}Lamp-1^{hi} présents dans les poumons, qui étaient enclins à libérer des NETs et à favoriser « l'up-take » de l'HDM par les cellules dendritiques *in vivo*. En outre, le transfert adaptatif de ces sous-types de neutrophiles chez des souris traitées par HDM a entraîné une amplification de l'inflammation allergique, y compris l'éosinophilie des voies respiratoires, l'immunité de type 2, l'inflammation péribronchique et l'augmentation de l'hyper-section du mucus par rapport aux souris témoins (Radermecker et al. 2018).

Notre étude de l'asthme allergique exacerbé a identifié un autre sous-type de neutrophiles associé à la libération de NETs. L'hyperactivation de STING au cours de la réponse allergique chez les souris a conduit à une polarisation des neutrophiles N1 NOS2⁺ARG1⁻, alors que les neutrophiles présents chez le groupe de souris représentant notre ligne de base d'asthme allergique à HDM, ou encore des souris exacerbées Poly(I:C) étaient alternativement activés ARG1⁺NOS2⁻. Sur le plan fonctionnel, les neutrophiles NOS2⁺ARG1⁻ ont participé à la formation de NETs, confirmée par l'expression de Cit-Histone 3, alors que les neutrophiles ARG1⁺NOS2⁻ n'ont pas produit de NETs. De manière intéressante, le même déséquilibre entre les populations de neutrophiles exprimant la NOS2 et celles exprimant l'ARG1 a été retrouvé dans les biopsies bronchiques de patients souffrant d'asthme exacerbé par des rhinovirus en comparaison aux témoins sains.

La classification phénotypique des sous-types de neutrophiles en profils N1 et N2 a été décrite pour la première fois dans le cancer. Cependant, on en sait encore très peu sur cette

plasticité dans d'autres contextes d'inflammations chroniques et aiguës. Dans un modèle murin d'infarctus du myocarde, les deux sous-populations N1 et N2 ont été séquentiellement détectées. Les neutrophiles N1 ont été isolés pendant la phase inflammatoire précoce de l'infarctus du myocarde et ont produit des niveaux élevés de cytokines pro-inflammatoires telles que le TNF- α et l'IL-1 β , tandis que les neutrophiles N2 étaient concomitants de la phase de résolution et ont montré des marqueurs anti-inflammatoires tels que la libération d'IL-10 (Ma Y et al. 2016). Plus récemment, les différences phénotypiques et fonctionnelles des populations N1 et N2 ont été étudiées. En cohérence avec nos résultats, parmi les différents paramètres analysés, les neutrophiles N1 comparés aux N2, ont révélé des niveaux significativement plus élevés de NO suggérant une expression plus élevée de NOS2, ainsi qu'une augmentation des ROS et de l'expression des sous-unités de la NADPH oxydase, importante pour la libération des NETs (Mihaila et al. 2021).

Récemment, Shin et al. ont démontré qu'une exposition intratrachéale à des particules de diesel liées à la pollution de l'air dans des souris HDM exacerbait les réponses immunitaires Th2 et Th17 de l'asthme et l'hyperréactivité des voies aériennes (AHR), par l'induction d'un sous-type spécifique de neutrophiles coexprimant Ly6G et SiglecF dans le poumon. Ces neutrophiles SiglecF⁺ sous l'effet l'ATP, un puissant signal de danger retrouvé dans l'environnement inflammatoire, amplifie leur capacité à libérer des NETs (Shin et al. 2022). Cette étude a complété une étude antérieure conforme à nos résultats, dans laquelle la pollution atmosphérique par les particules PM_{2,5} a provoqué une exacerbation de l'asthme chez des souris traitées à l'OVA. Les auteurs ont démontré que les PM_{2.5} augmentaient de manière significative le nombre de neutrophiles et de NETs. Par la suite, les NETs, probablement par le biais des neutrophiles élastase, ont augmenté l'expression de la quinone oxydoréductase1 (NQO1), qui à son tour a aggravé l'hypersécrétion de mucus en augmentant l'expression de MUC5AC et STAT6, en accord avec nos résultats (He et al. 2021). Par ailleurs, l'implication spécifique de la voie cGAS/STING dans le contexte des lésions pulmonaires provoquées par les particules de diesel via la flore pulmonaire a été très récemment établie (Sun M et al. 2023).

Étant donné les paramètres d'exacerbation décrits dans ces études, qui rappellent certaines de nos observations, il serait intéressant d'évaluer la contribution de la voie STING dans ces modèles d'exacerbation. En outre, il serait intéressant de déterminer si les sous-ensembles de neutrophiles liés à l'exacerbation sont contexte dépendant, ou si plusieurs de ces marqueurs peuvent être exprimés simultanément dans diverses inflammations pulmonaires sévères, ouvrant ainsi la voie à des stratégies thérapeutiques multi-cibles.

Étant donné qu'un changement dans le profil des neutrophiles peut être suivi d'un changement de la fonction de la cellule, il est impératif d'approfondir la caractérisation des sous-types de neutrophiles. Cela permettra de prédire la sévérité des pathologies inflammatoires, ce qui serait particulièrement utile dans l'exacerbation de l'asthme neutrophile, dans laquelle les neutrophiles challenge l'efficacité des traitements actuels de l'asthme, qui ciblent principalement les éosinophiles tout en prolongeant la durée de vie des neutrophiles et leur effet délétère potentiel.

Malgré leur contribution majeure dans nos modèles, les neutrophiles expriment des niveaux extrêmement faibles de STING et de cGAS (Xia et al. 2015). Cela peut signifier qu'ils ne sont pas les principales cellules répondant aux agonistes STING. En revanche, il est très probable que les macrophages alvéolaires, connus pour leurs niveaux élevés d'expression de STING, ou les cellules épithéliales soient les premières cellules à répondre et activer STING, suivies par les neutrophiles en tant que cellules "répondeuses".

L'analyse du tissu pulmonaire dans notre modèle d'exacerbation de l'asthme a révélé une nette différence en termes de phosphorylation de STING, de dommages à l'ADN avec γ H2AX phosphorylé et histone3 citrulliné et cGAS entre les conditions expérimentales où le lavage broncho-alvéolaire a été effectué (BAL), ou non effectué (NO), ce qui signifie que toutes les cellules immunitaires infiltrant le poumon ont été conservées et traitées avec le tissu pulmonaire. Ce résultat suggère fortement la contribution des cellules immunitaires infiltrant le poumon, en particulier les macrophages alvéolaires, dans l'activation de STING en réponse au diABZI, conformément à l'étude de She et de ses collaborateurs, présentant les macrophages alvéolaires comme le principal type de cellule dans le poumon intégrant le cGAMP extracellulaire (She et al. 2021).

De plus, nos études *in vitro* sur les macrophages et les cellules épithéliales humaines ont montré que les deux types de cellules peuvent répondre aux agonistes STING et monter une réponse immunitaire innée efficace avec production d'IFN de type I, TNF- α , IL-6, induction de plusieurs senseurs d'ADN, signes de dommages à l'ADN avec γ H2AX et marqueurs de mort cellulaire régulée, ce qui suggère fortement une collaboration des deux types de cellules pendant le processus d'initiation.

Ce qui fait que les agonistes de STING, y compris le cGAMP naturel, ciblent préférentiellement les macrophages ou les cellules épithéliales, tous deux connus pour exprimer fortement STING dans le poumon, n'est pas encore documenté. Intuitivement, on pourrait

supposer que les agonistes de petit poids moléculaire tels que le diABZI dépendent de la présence ou non, et de la fréquence d'expression du STING membranaire (pmSTING) récemment décrite (Li X et al. 2022). Les agonistes de type CDN et les CDN chimiquement modifiés pourraient dépendre de la fréquence de canaux et de transporteurs spécifiques décrits dans l'introduction exprimés de manière ubiquitaire et également des pmSTING.

Dans ce contexte, nous pourrions imaginer deux scénarios possibles :

Le premier est basé sur l'hypothèse de la barrière épithéliale proposée par Akdis C (Akdis C. 2021), dans laquelle les cellules épithéliales sont d'abord fragilisées et blessées par les agonistes STING (le DAMP ici), ce qui entraîne la mort cellulaire et la libération massive d'ADN. Cela activerait à son tour la machinerie des senseurs d'ADN dans les macrophages ainsi que l'efférocytose pour tenter d'éliminer les cellules mortes. Ceci aboutirait ultérieurement à la chimioattraction des neutrophiles aux effets potentiellement délétères entraînant d'avantage de dommages. En d'autres termes, le scénario 1 soutient l'hypothèse de la mort cellulaire qui serait à l'origine de l'hyperinflammation.

Dans le second scénario, les macrophages alvéolaires sont les premiers à détecter les agonistes STING et à y répondre, ce qui entraîne la sécrétion d'importantes cytokines (IFN α , IFN β , TNF α , IL-6, CXCL10), puis l'infiltration de neutrophiles et la formation de NETs. À leur tour, les NETs qui remplissent les alvéoles endommagent le tissu pulmonaire par leurs sous-produits et conduisent à une mort cellulaire massive au niveau de la barrière épithéliale et du parenchyme pulmonaire. En d'autres termes, ce scénario soutient l'idée selon laquelle l'inflammation conduit à la mort cellulaire et alimente par la suite une seconde vague d'inflammation exacerbée.

Les résultats de nos études *in vitro* ont montré que les macrophages réagissaient pleinement au diABZI en passant de la phosphorylation de STING à la phosphorylation d'IRF3, dès 60 minutes après la stimulation. De plus amples investigations *in vitro* confrontant les cellules épithéliales et les macrophages, ainsi qu'une étude cinétique *in vivo* pourraient nous aider à répondre à cette question.

Quel que soit le scénario, la libération massive d'ADN semble inéluctable. Dans ce travail, nous avons concentré notre attention sur l'ADN double bin du soi émanant du tissu pulmonaires rendu « perméable » par l'inflammation.

En plus de l'ADN exposé par les NETs, nous avons montré dans le tissu pulmonaire des marqueurs d'apoptose, de nécroptose et de pyroptose, participant à l'augmentation de l'ADNdb libre mesuré dans le BALF avec preuves de formation du complexe PANoptotique probablement dans les macrophages. De plus, nous avons révélé la présence d'ADNmt (mitochondrial) dans le BALFs de souris atteintes de ARDS.

Il est possible que les cytokines inflammatoires libérées peu après la prise en charge de l'agoniste STING dans nos modèles, en particulier le TNF- α , participent activement à la libération de l'ADNmt. Dans le contexte de l'arthrite inflammatoire, Willemsen et al. ont montré qu'une stimulation IFN prolongée a un effet inhibiteur sur le mécanisme de mitophagie médié par PINK1, déclenchant un stress mitochondrial suivi d'une libération d'ADNmt et d'une signature IFN dominante subséquente par le biais d'une régulation à la hausse des ISG d'une manière dépendante de cGAS-STING (Willemsen et al. 2021). Ainsi, la voie cGAS-STING pourrait utiliser l'axe d'inhibition TNF-PINK1 comme un mécanisme de rétroaction positive pour renforcer sa propre activation. Cela indique que se concentrer sur l'inhibition de la voie STING et sa production directe d'IFN n'est pas la seule option à envisager pour les interféronopathies, puisqu'il existe d'autres mécanismes de régulation en amont tels que l'axe TNF-PINK1.

De plus, le TNF- α est impliqué dans l'altération de la phagocytose des cellules mortes par les macrophages (McPhillips et al. 2007), ce qui entraîne une accumulation de débris de cellules mortes. En l'absence de mécanismes d'élimination efficaces, l'apoptose, connue pour son statut immunitaire silencieux, se transforme en mort cellulaire lytique et libère le contenu de ses corps apoptotiques en l'espace de 15 heures (Tanzer et al. 2020).

Nous avons rapporté une augmentation de la régulation du TNF- α dans modèles murins d'inflammation pulmonaire. Dans un contexte plus relevant sur le plan clinique, tel que l'exacerbation de l'asthme chronique chez l'homme, impliquant une exposition plus prolongée au TNF- α par rapport à nos modèles, nous pouvons imaginer qu'il existe un risque potentiel que l'apoptose soit « instrumentalisée » au profil de l'amplification de l'inflammation, même durant les processus physiologiques de renouvellement cellulaire des tissus, en la rendant lytique et inflammatoire. Ceci pourrait être potentiellement pertinent au cours des maladies inflammatoires chroniques de l'intestin où l'épithélium intestinal se renouvelle très rapidement (3-4 jours).

Parmi les divers effets du TNF- α , une étude du laboratoire du Pr Kanneganti a montré une action synergique du TNF- α et de l'IFN- γ dans la stimulation de la PANoptose dans la mortalité due au SRAS-CoV2 causée par la tempête de cytokines (Karki et al. 2021). En effet, le traitement concomitant au le TNF- α et l'IFN- γ a induit une mort cellulaire importante avec des marqueurs de PANoptose dans les cellules BMDM et les lignées cellulaires THP-1. L'étude a également révélé que les marqueurs de PANoptose dépendaient de l'axe STAT1/IRF1 après une stimulation synergique par le TNF- α et l'IFN- γ . Dans ce contexte spécifique, la voie STAT1/IRF1 contrôle l'expression de l'iNOS et augmente la sécrétion de NO conduisant à la mort cellulaire, alors que les BMDM NOS2^{-/-} sont protégées. Cette observation expérimentale est cohérente avec les données de patients atteints de forme grave de COVID-19 exprimant des niveaux significativement plus élevés de NOS2 par rapport aux témoins sains (Karki et al. 2021).

Nous avons montré l'expression des marqueurs PANoptotiques dans le modèle de ARDS et dans le modèle d'exacerbation de l'asthme neutrophilique après l'administration d'agonistes STING. Nous avons mis en évidence la régulation à la hausse des marqueurs d'apoptose, de nécroptose et de pyroptose, ainsi que la régulation à la hausse des composants du complexe PANoptotique tels que ZBP1, la caspase-8 et RIPK3 dans le tissu pulmonaire. De plus, la microscopie confocale réalisée sur la fraction cellulaire du BAL nous a permis de visualiser la formation du complexe PANoptotique composé de la caspase-8, de l'ASC et de RIPK3 dans les macrophages mais pas dans les neutrophiles. Dans notre travail, nous avons décrit l'activation de la PANoptose en tant que conséquence indirecte survenant en aval de l'activation de STING, et démontré un lien entre les NETs et les marqueurs de PANoptose dans le poumon. Cependant, il serait intéressant dans de futures études d'avoir un aperçu des mécanismes moléculaires précis impliqués dans ces processus.

En accord avec l'étude de Karki, nous avons démontré une augmentation des niveaux de TNF- α et d'IFN- γ pendant l'exacerbation neutrophilique de l'asthme allergique. En effet, la réponse allergique est passée d'une réponse Th2 classique caractérisée par une production de cytokines de type 2 à une réponse mixte Th2/Th1 avec induction de l'IFN- γ , du TNF- α et de l'IFN de type I après un traitement par agonistes STING. Il est donc plausible que la synergie entre le TNF- α et l'IFN- γ soit à l'origine du processus inflammatoire PANoptotique conduisant à une mort cellulaire lytique massive et à des lésions.

En réalité, la synergie entre le TNF- α et l'IFN- γ n'est pas un concept nouveau et a été documentée dans la littérature depuis 1998, Zhang et al. ont démontré leur rôle synergique dans

la médiation des effets anti-toxoplasmiques par l'amélioration de la production de NO par les macrophages (Zhang et al. 1998). Cette combinaison a été impliquée dans la progression de diverses maladies inflammatoires, comme dans la progression de la maladie d'Alzheimer, où elle est corrélée aux niveaux de NO (Belkhefha et al. 2014). En outre, le mécanisme d'action en aval du TNF- α et de l'IFN- γ a également été bien documenté dans le diabète auto-immun au cours duquel le TNF- α et l'IFN- γ agissent par l'intermédiaire de STAT1-IRF1 pour médier l'apoptose des cellules bêta (Suk et al. 2001a), ou dans les cellules cancéreuses du col de l'utérus ME-180 dans lesquelles le TNF- α et l'IFN- γ conduisent à l'apoptose ou à la nécroptose en fonction de l'état d'activation des caspases.

En accord avec l'étude de Karki, nous avons révélé une régulation à la hausse de l'expression de NOS2 dans les neutrophiles *in vivo* après l'administration des agonistes de STING chez les souris traitées par HDM, ce qui suggère une production plus élevée de NO, tandis que les souris témoins HDM ont montré une polarisation alternative avec une signature neutrophilique ARG1. Dans ce modèle, nous n'avons pas étudié la polarisation des macrophages alvéolaires, mais nous pouvons suggérer un profil M2 chez les souris traitées par HDM et un profil M1 pro-inflammatoire dans les groupes exacerbés, connus pour exprimer des niveaux élevés de NOS2 et de NO. L'ensemble de ces informations renforce l'hypothèse de l'implication du TNF- α et de l'IFN- γ via l'axe STAT1-IRF1-NO dans la médiation de la PANoptose au cours de l'exacerbation neutrophilique de l'asthme allergique.

Pour tester cette hypothèse, nous pourrions traiter des souris sensibilisées à la HDM avec une combinaison de TNF- α et d'IFN- γ par voie intratrachéale pendant les challenges HDM et réévaluer tous les paramètres d'exacerbation considérés dans le modèle original en termes de résistance pulmonaire, d'infiltration différentielles de cellules immunitaire, dsDNA libéré dans le BAL, infiltration de neutrophiles N1 et libération de NETs, lésions tissulaires et épithéliales, marqueurs de mort cellulaire et PANoptose afin de vérifier pleinement si nous pouvons récapituler l'exacerbation de l'asthme allergique induite par les agonistes STING, puis évaluer l'activation de l'axe STAT1-IRF1-NO. L'administration de TNF- α peut représenter un défi *in vivo*, pour y parvenir, nous pourrions également administrer des anticorps neutralisants pour vérifier s'ils bloquent l'effet de l'agoniste STING sur la PANoptose.

En ce qui concerne notre modèle ARDS, les niveaux d'IFN- γ n'ont pas été évalués dans ces conditions, ce qui rend difficile de spéculer sur le mécanisme sous-jacent de la PANoptose.

Au vu de nos résultats, nous pourrions intuitivement penser que la prévention de l'apoptose ou de la nécrose des macrophages pulmonaires peut être bénéfique pour l'hôte. En effet, plusieurs rapports ont montré que la prévention de l'apoptose et de la nécroptose des macrophages alvéolaires au stade précoce de l'inflammation pouvait contribuer à diminuer la sévérité de l'ARDS (Dang et al.2022). En réalité, le contexte est plus complexe, le type de macrophages pulmonaires, qu'il s'agisse de PVM, RAM ou RecAM a son importance. Dans un modèle murin de lésion pulmonaire aiguë induite par la grippe A et le LPS, les macrophages recrutés (RecAM) s'accumulent dans le poumon pendant les premières phases de l'inflammation et diminuent progressivement par apoptose pendant la phase de résolution, comme l'indiquent les niveaux élevés du récepteur de mort Fas exprimé sur les RecAM par rapport aux AM résidents. En outre, l'inhibition de l'apoptose des RecAM dans ce contexte a retardé la résolution de l'ALI, soulignant le rôle protecteur de l'apoptose. Les macrophages alvéolaires résidents, quant à eux persistent et sont détectés au niveau des lésions pulmonaire (Janssen et al. 2011).

Une meilleure caractérisation du rôle différentiel de chaque type de macrophage pulmonaire et de leur devenir au cours des pathologies pulmonaires pourrait nous aider à distinguer la mort cellulaire protectrice, connue sous le nom de mort cellulaire tolérogène (TCD), de la mort cellulaire immunogène (ICD), potentiellement délétère. Nous pouvons supposer que la mort cellulaire protectrice se produit lorsque les mécanismes de phagocytose sont efficaces. De ce fait, il conviendrait de veiller davantage à ce qu'ils ne soient pas surchargés dans les pathologies où les lésions tissulaires sont récurrentes.

Dans les modèles cliniques pertinents d'ARDS et d'exacerbation de l'asthme utilisant des virus et des bactéries affectant le système respiratoire, les antigènes microbiens (PAMPs) représentent un facteur important, que nos modèles ne prennent pas en compte en raison de la nature pharmacologique de notre signal déclencheur. La mort cellulaire immunologique (ICD) est caractérisée une trinité comprenant l'inflammation, l'antigénicité (par exemple les PAMPs ou les néo-antigènes tumoraux) et l'adjuvantité (par exemple l'ADN du soi) pour activer efficacement l'immunité adaptative et établir une mémoire. Même en l'absence de PAMPs, le concept de ICD n'est pas totalement à exclure de nos modèles, surtout si l'on considère que nous avons récapitulé les principales caractéristiques de l'ARDS et de l'exacerbation de l'asthme neutrophilique. L'ICD n'est pas associée à une modalité de RCD spécifique (apoptose, nécrose) et ne décrit pas l'une des nombreuses façons dont une cellule peut mourir, mais elle influencerait plutôt la résultante de la communication entre l'immunité innée en réponse aux DAMPs libérés ou exposés par un ou plusieurs RCD pour amplifier l'inflammation.

Selon les lignes directrices de la NCDD, seuls six DAMP permettent à un RCD spécifique d'être qualifié d'immunogénique : la calréticuline (CALR), l'ATP, l'HMGB1, l'IFN de type I, les acides nucléiques dérivés de cellules cancéreuses et l'annexine A1 (ANXA1) (Galluzi et al. 2018). Compte tenu de l'activation prééminente de STING et de la production subséquente d'IFN de type I, nous pourrions éventuellement considérer la notion de mort cellulaire immunogénique (ICD) dans nos modèles.

La désaturation des poumons en oxygène et les difficultés respiratoires constituent l'un des symptômes les plus préoccupants des pathologies inflammatoires des voies respiratoires. En cas d'hypersécrétion de mucus, comme lors des crises d'asthme allergique, l'ADNdb libre provenant des NETs présents dans l'espace broncho-alvéolaire peut provoquer une augmentation de la viscosité du mucus, qui entraîne à son tour un accroissement de l'hyperréactivité bronchique (Linssen et al. 2021). Compte tenu de la forte augmentation de l'ADNdb provenant des NETs et d'autres RCD dans notre modèle d'exacerbation de l'asthme, nous pouvons suggérer qu'en plus de son rôle dans l'inflammation, l'ADN contribue peut-être à exacerber l'hyperréactivité bronchique que nous avons observé après le traitement par agonistes STING.

L'inflammation elle-même, par l'intermédiaire des cellules inflammatoires, peut participer à l'exacerbation de l'hyperréactivité bronchique. En effet, dans une étude, la suppression de HIF-1 α dans les cellules myéloïdes à l'aide de souris à cellules spécifiques, ou l'inhibition systémique de HIF-1 α avec YC-1, a atténué l'hyperréactivité bronchique et l'hyperplasie des cellules caliciformes dans un modèle murin d'asthme induit par l'OVA (Crotty et al. 2013).

Cet aspect n'a pas encore été exploré en profondeur dans nos modèles expérimentaux. Cependant, nous avons observé une régulation à la hausse de HIF-1 α après un traitement au diABZI chez des souris sensibilisées à l'HDM, ainsi qu'une exacerbation de l'hyperréactivité bronchique. L'HIF-1 α a d'abord été associé à l'hypoxie. Néanmoins, il est désormais prouvé que HIF-1 α peut également être activé dans un environnement normoxique, ainsi que lors de réponses inflammatoires induites par des signaux tels que LPS, TNF- α et GM-CSF (Byrne et al. 2013). De plus amples études sont nécessaires afin de comprendre le lien possible entre HIF-1 α et l'exacerbation de l'hyperréactivité bronchique dans nos modèles de maladies inflammatoires des voies respiratoires.

Pour ouvrir de nouvelles perspectives, il serait crucial d'explorer davantage certains aspects clés. Tout d'abord, il serait intéressant de valider la résistance aux corticostéroïdes dans notre modèle murin d'exacerbation de l'asthme neutrophile dépendant de STING.

Dans la littérature, les patients asthmatiques sont souvent considérés comme étant homogènes et exposés de la même manière aux risques d'exacerbation et de développement de formes sévères. Néanmoins, deux populations asthmatiques méritent une attention particulière : les personnes âgées ou vieillissantes et les patients obèses. En effet, la perte de l'intégrité de l'enveloppe nucléaire observé au cours du processus physiologique de vieillissement normal à travers, entre autres facteurs, l'épissage aberrant de la Lamin A conduisant à des dommages d'ADN (Scaffidi & Misteli. 2006) et à des échanges moléculaires indésirables entre le noyau et le cytoplasme (Robijns et al. 2018). Cela suggère une inflammation chronique liée à STING, exposant davantage les patients asthmatiques âgés à une exacerbation de type neutrophilique.

D'autre part, une récente étude a révélé un nouveau rôle non canonique de STING dans la régulation de l'homéostasie métabolique. En absence de signal inflammatoire, STING interagit avec la désaturase d'acides gras 2 (FADS2) et inhibe son activité qui consiste à générer des acides gras polyinsaturés (PUFAs) et acides gras polyinsaturés à longue chaînes (LC-PUFAs) à partir des acides gras essentiels.

A l'inverse, lors d'une inflammation chronique, l'activation de STING suivie de sa dégradation augmente l'activité de FADS2 et conduit à une accumulation des dérivés oméga-6 accompagnée d'une augmentation du ratio oméga-6/oméga-3 qui alimente davantage l'inflammation (Vila et al. 2022). Ainsi, dans un contexte d'inflammation chronique associée à l'obésité, le développement d'une exacerbation neutrophilique de l'asthme dépendante de STING chez les patients obèses asthmatiques risque d'engendrer davantage de problème métabolique

Les stratégies thérapeutiques se basant sur des antagonistes de STING peuvent être confrontées à des limitations prévisibles. L'inhibition de la voie de détection de l'ADN pendant de longues périodes peut exposer l'hôte à une « paralysie immunitaire » et à une tolérance accrue à l'égard des pathogènes opportunistes et du développement de tumeurs. Pour un traitement à long terme, les stratégies ciblant l'ADN pour atténuer l'inflammation pourraient être plus sûre pour l'hôte.

De même, les stratégies basées sur les agonistes de STING, en particulier en oncologie, qui ont déjà montré leurs limites pour certains, devraient examiner d'autres voies directement

connectées à la voie STING. En effet, comme évoqué dans le chapitre d'introduction, l'axe SEL1L-HRD1 ERAD contrôle le pool de STING activable (Ji Y et al. 2023). Par conséquent, l'évaluation de l'activation de cet axe dans les biopsies de patients avant les études cliniques peut aider à prédire l'efficacité du traitement, car les tumeurs peuvent réguler STING à la baisse. De plus, en l'absence de STING dans les cellules tumorales, les agonistes de STING risquent d'être captés par les cellules T présentes dans le microenvironnement tumoral et connues pour exprimer fortement STING, ce qui entraînerait leur déclin par apoptose. Ceci est en totale contradiction avec l'objectif de transformer les "cold tumors" en "hot tumors".

En outre, les agonistes de STING modulent le métabolisme des lipides qui pourrait interférer avec l'activation de STING. Il a été démontré que les agonistes de STING y compris le cGAMP « fittent » dans la structure cristalline de FADS2 et augmente son activité des desaturation des omega-3 et omega-6, ce qui entraîne une accumulation de PUFAs. A l'inverse, il a été démontré que ces PUFAs peuvent à leur tour inhiber STING (Vila et al. 2022).

Conclusion

Ce travail de thèse nous a permis d'évaluer la contribution de la voie cGAS-STING dans le développement de formes sévères de maladies inflammatoires des voies respiratoires, souvent associées à des lésions pulmonaires. Récemment, Singh et al. ont qualifié le rôle de l'ADN dans la régulation des réponses immunitaires innées de "travail dissimulé" (Singh et al. 2023). En effet, lorsque l'ADN double brin du soi est massivement libéré par les tissus endommagés suite à une hyperactivation de STING, il déclenche une seconde vague d'inflammation et altère la fonction pulmonaire, conduisant parfois à des formes sévères et incontrôlées d'asthme avec modification du type de réponse immunitaire, la rendant ainsi réfractaire aux traitements conventionnels dans certains cas.

D'autre part, ce travail nous a permis d'évaluer les effets secondaires potentiellement délétères des traitements basés sur l'utilisation des agonistes de STING, médiés par le stress cellulaire/la mort cellulaire et la libération d'ADN double brin du soi, ainsi que la manière dont les stratégies ciblant l'ADN double brin du soi libre atténuent l'inflammation pulmonaire sans compromettre les éléments de défense de l'hôte. Dans l'ensemble, ces études révèlent une possible similarité en terme de réponses physiopathologique entre le SDRA et les épisodes d'exacerbation de l'asthme.

Poison is in everything, and no thing is without poison. The dosage makes it either a poison or a remedy.

Theophrastus von Hohenheim (1493/1494 – 24 September 1541).

References

- Ablasser, A., & Chen, Z. J.** (2019). cGAS in action: Expanding roles in immunity and inflammation. *Science* (New York, N.Y.), 363(6431), eaat8657. <https://doi.org/10.1126/science.aat8657>
- Ablasser, A., Goldeck, M., Cavlar, T., Deimling, T., Witte, G., Röhl, I., Hopfner, K. P., Ludwig, J., & Hornung, V.** (2013). cGAS produces a 2'-5'-linked cyclic dinucleotide second messenger that activates STING. *Nature*, 498(7454), 380–384. <https://doi.org/10.1038/nature12306>
- Ablasser, A., Schmid-Burgk, J. L., Hemmerling, I., Horvath, G. L., Schmidt, T., Latz, E., & Hornung, V.** (2013). Cell intrinsic immunity spreads to bystander cells via the intercellular transfer of cGAMP. *Nature*, 503(7477), 530–534. <https://doi.org/10.1038/nature12640>
- Acehan, D., Jiang, X., Morgan, D. G., Heuser, J. E., Wang, X., & Akey, C. W.** (2002). Three-dimensional structure of the apoptosome: implications for assembly, procaspase-9 binding, and activation. *Molecular cell*, 9(2), 423–432. [https://doi.org/10.1016/s1097-2765\(02\)00442-2](https://doi.org/10.1016/s1097-2765(02)00442-2)
- Ackermann, M., Anders, H. J., Bilyy, R., Bowlin, G. L., Daniel, C., De Lorenzo, R., Egeblad, M., Henneck, T., Hidalgo, A., Hoffmann, M., Hohberger, B., Kanthi, Y., Kaplan, M. J., Knight, J. S., Knopf, J., Kolaczowska, E., Kubes, P., Leppkes, M., Mahajan, A., Manfredi, A. A., ... Herrmann, M.** (2021). Patients with COVID-19: in the dark-NETs of neutrophils. *Cell death and differentiation*, 28(11), 3125–3139. <https://doi.org/10.1038/s41418-021-00805-z>
- Agache, I., & Akdis, C. A.** (2019). Precision medicine and phenotypes, endotypes, genotypes, regiotypes, and theratypes of allergic diseases. *The Journal of clinical investigation*, 129(4), 1493–1503. <https://doi.org/10.1172/JCI124611>
- Agache, I., Ciobanu, C., Agache, C., & Anghel, M.** (2010). Increased serum IL-17 is an independent risk factor for severe asthma. *Respiratory medicine*, 104(8), 1131–1137. <https://doi.org/10.1016/j.rmed.2010.02.018>
- Aggarwal, N. R., King, L. S., & D'Alessio, F. R.** (2014). Diverse macrophage populations mediate acute lung inflammation and resolution. *American journal of physiology. Lung cellular and molecular physiology*, 306(8), L709–L725. <https://doi.org/10.1152/ajplung.00341.2013>
- Akdis C. A.** (2021). Does the epithelial barrier hypothesis explain the increase in allergy, autoimmunity and other chronic conditions?. *Nature reviews. Immunology*, 21(11), 739–751. <https://doi.org/10.1038/s41577-021-00538-7>
- Almine, J. F., O'Hare, C. A., Dunphy, G., Haga, I. R., Naik, R. J., Atrih, A., Connolly, D. J., Taylor, J., Kelsall, I. R., Bowie, A. G., Beard, P. M., & Unterholzner, L.** (2017). IFI16 and cGAS cooperate in the activation of STING during DNA sensing in human keratinocytes. *Nature communications*, 8, 14392. <https://doi.org/10.1038/ncomms14392>

- Amini, P., Stojkov, D., Wang, X., Wicki, S., Kaufmann, T., Wong, W. W., Simon, H. U., & Yousefi, S. (2016).** NET formation can occur independently of RIPK3 and MLKL signaling. *European journal of immunology*, 46(1), 178–184. <https://doi.org/10.1002/eji.201545615>
- Amouzegar, A., Chelvanambi, M., Filderman, J. N., Storkus, W. J., & Luke, J. J. (2021).** STING Agonists as Cancer Therapeutics. *Cancers*, 13(11), 2695. <https://doi.org/10.3390/cancers13112695>
- Amulic, B., Knackstedt, S. L., Abu Abed, U., Deigendesch, N., Harbort, C. J., Caffrey, B. E., Brinkmann, V., Heppner, F. L., Hinds, P. W., & Zychlinsky, A. (2017).** Cell-Cycle Proteins Control Production of Neutrophil Extracellular Traps. *Developmental cell*, 43(4), 449–462.e5. <https://doi.org/10.1016/j.devcel.2017.10.013>
- Antonopoulos, C., Russo, H. M., El Sanadi, C., Martin, B. N., Li, X., Kaiser, W. J., Mocarski, E. S., & Dubyak, G. R. (2015).** Caspase-8 as an Effector and Regulator of NLRP3 Inflammasome Signaling. *The Journal of biological chemistry*, 290(33), 20167–20184. <https://doi.org/10.1074/jbc.M115.652321>
- Arranz, A., Doxaki, C., Vergadi, E., Martinez de la Torre, Y., Vaporidi, K., Lagoudaki, E. D., Ieronymaki, E., Androulidaki, A., Venihaki, M., Margioris, A. N., Stathopoulos, E. N., Tschlis, P. N., & Tsatsanis, C. (2012).** Akt1 and Akt2 protein kinases differentially contribute to macrophage polarization. *Proceedings of the National Academy of Sciences of the United States of America*, 109(24), 9517–9522. <https://doi.org/10.1073/pnas.1119038109>
- Athari S. S. (2019).** Targeting cell signaling in allergic asthma. *Signal transduction and targeted therapy*, 4, 45. <https://doi.org/10.1038/s41392-019-0079-0>
- Athari S. S. (2019).** Targeting cell signaling in allergic asthma. *Signal transduction and targeted therapy*, 4, 45. <https://doi.org/10.1038/s41392-019-0079-0>
- Aulakh G. K. (2018).** Neutrophils in the lung: "the first responders". *Cell and tissue research*, 371(3), 577–588. <https://doi.org/10.1007/s00441-017-2748-z>
- Avriel, A., Rozenberg, D., Raviv, Y., Heimer, D., Bar-Shai, A., Gavish, R., Sheynin, J., & Douvdevani, A. (2016).** Prognostic utility of admission cell-free DNA levels in patients with chronic obstructive pulmonary disease exacerbations. *International journal of chronic obstructive pulmonary disease*, 11, 3153–3161. <https://doi.org/10.2147/COPD.S113256>
- Azoulay, E., & Darmon, M. (2010).** Acute respiratory distress syndrome during neutropenia recovery. *Critical care (London, England)*, 14(1), 114. <https://doi.org/10.1186/cc8198>
- Baker, P. J., Boucher, D., Bierschenk, D., Tebartz, C., Whitney, P. G., D'Silva, D. B., Tanzer, M. C., Monteleone, M., Robertson, A. A., Cooper, M. A., Alvarez-Diaz, S., Herold, M. J., Bedoui, S., Schroder, K., & Masters, S. L. (2015).** NLRP3 inflammasome activation downstream of cytoplasmic LPS recognition by both caspase-4 and caspase-5. *European journal of immunology*, 45(10), 2918–2926. <https://doi.org/10.1002/eji.201545655>
- Banoth, B., Tuladhar, S., Karki, R., Sharma, B. R., Briard, B., Kesavardhana, S., Burton, A., & Kanneganti, T. D. (2020).** ZBP1 promotes fungi-induced inflammasome activation and pyroptosis, apoptosis, and necroptosis

(PANoptosis). *The Journal of biological chemistry*, 295(52), 18276–18283.
<https://doi.org/10.1074/jbc.RA120.015924>

Barnes, B. J., Adrover, J. M., Baxter-Stoltzfus, A., Borczuk, A., Cools-Lartigue, J., Crawford, J. M., Daßler-Plenker, J., Guerci, P., Huynh, C., Knight, J. S., Loda, M., Looney, M. R., McAllister, F., Rayes, R., Renaud, S., Rousseau, S., Salvatore, S., Schwartz, R. E., Spicer, J. D., Yost, C. C., ... Egeblad, M. (2020). Targeting potential drivers of COVID-19: Neutrophil extracellular traps. *The Journal of experimental medicine*, 217(6), e20200652.
<https://doi.org/10.1084/jem.20200652>

Barnes, B. J., Adrover, J. M., Baxter-Stoltzfus, A., Borczuk, A., Cools-Lartigue, J., Crawford, J. M., Daßler-Plenker, J., Guerci, P., Huynh, C., Knight, J. S., Loda, M., Looney, M. R., McAllister, F., Rayes, R., Renaud, S., Rousseau, S., Salvatore, S., Schwartz, R. E., Spicer, J. D., Yost, C. C., ... Egeblad, M. (2020). Targeting potential drivers of COVID-19: Neutrophil extracellular traps. *The Journal of experimental medicine*, 217(6), e20200652.
<https://doi.org/10.1084/jem.20200652>

Barretto, K. T., Brockman-Schneider, R. A., Kuipers, I., Basnet, S., Bochkov, Y. A., Altman, M. C., Jarjour, N. N., Gern, J. E., & Esnault, S. (2020). Human airway epithelial cells express a functional IL-5 receptor. *Allergy*, 75(8), 2127–2130. <https://doi.org/10.1111/all.14297>

Behnen, M., Leszczyc, C., Möller, S., Batel, T., Klinger, M., Solbach, W., & Laskay, T. (2014). Immobilized immune complexes induce neutrophil extracellular trap release by human neutrophil granulocytes via FcγRIIIB and Mac-1. *Journal of immunology* (Baltimore, Md. : 1950), 193(4), 1954–1965.
<https://doi.org/10.4049/jimmunol.1400478>

Belkhef, M., Rafa, H., Medjeber, O., Arroul-Lammali, A., Behairi, N., Abada-Bendib, M., Makrelouf, M., Belarbi, S., Masmoudi, A. N., Tazir, M., & Touil-Boukoffa, C. (2014). IFN-γ and TNF-α are involved during Alzheimer disease progression and correlate with nitric oxide production: a study in Algerian patients. *Journal of interferon & cytokine research : the official journal of the International Society for Interferon and Cytokine Research*, 34(11), 839–847. <https://doi.org/10.1089/jir.2013.0085>

Bellani, G., Laffey, J. G., Pham, T., Fan, E., Brochard, L., Esteban, A., Gattinoni, L., van Haren, F., Larsson, A., McAuley, D. F., Ranieri, M., Rubinfeld, G., Thompson, B. T., Wrigge, H., Slutsky, A. S., Pesenti, A., LUNG SAFE Investigators, & ESICM Trials Group (2016). Epidemiology, Patterns of Care, and Mortality for Patients With Acute Respiratory Distress Syndrome in Intensive Care Units in 50 Countries. *JAMA*, 315(8), 788–800.
<https://doi.org/10.1001/jama.2016.0291>

Benmerzoug, S., Rose, S., Bounab, B., Gosset, D., Duneau, L., Chenuet, P., Mollet, L., Le Bert, M., Lambers, C., Geleff, S., Roth, M., Fauconnier, L., Sedda, D., Carvalho, C., Perche, O., Laurenceau, D., Ryffel, B., Apetoh, L., Kiziltunc, A., Uslu, H., ... Quesniaux, V. F. J. (2018). STING-dependent sensing of self-DNA drives silica-induced lung inflammation. *Nature communications*, 9(1), 5226. <https://doi.org/10.1038/s41467-018-07425-1>

Bertheloot, D., & Latz, E. (2017). HMGB1, IL-1α, IL-33 and S100 proteins: dual-function alarmins. *Cellular & molecular immunology*, 14(1), 43–64. <https://doi.org/10.1038/cmi.2016.34>

Bertheloot, D., Latz, E., & Franklin, B. S. (2021). Necroptosis, pyroptosis and apoptosis: an intricate game of cell death. *Cellular & molecular immunology*, 18(5), 1106–1121. <https://doi.org/10.1038/s41423-020-00630-3>

Bhakta, N. R., Christenson, S. A., Nerella, S., Solberg, O. D., Nguyen, C. P., Choy, D. F., Jung, K. L., Garudadri, S., Bonser, L. R., Pollack, J. L., Zlock, L. T., Erle, D. J., Langelier, C., Derisi, J. L., Arron, J. R., Fahy, J. V., & Woodruff, P. G. (2018). IFN-stimulated Gene Expression, Type 2 Inflammation, and Endoplasmic Reticulum Stress in Asthma. *American journal of respiratory and critical care medicine*, 197(3), 313–324. <https://doi.org/10.1164/rccm.201706-1070OC>

Bhattacharya, J., & Matthay, M. A. (2013). Regulation and repair of the alveolar-capillary barrier in acute lung injury. *Annual review of physiology*, 75, 593–615. <https://doi.org/10.1146/annurev-physiol-030212-183756>

Blanco-Melo, D., Nilsson-Payant, B. E., Liu, W. C., Uhl, S., Hoagland, D., Møller, R., Jordan, T. X., Oishi, K., Panis, M., Sachs, D., Wang, T. T., Schwartz, R. E., Lim, J. K., Albrecht, R. A., & tenOever, B. R. (2020). Imbalanced Host Response to SARS-CoV-2 Drives Development of COVID-19. *Cell*, 181(5), 1036–1045.e9. <https://doi.org/10.1016/j.cell.2020.04.026>

Boatright, K. M., & Salvesen, G. S. (2003). Mechanisms of caspase activation. *Current opinion in cell biology*, 15(6), 725–731. <https://doi.org/10.1016/j.ceb.2003.10.009>

Bock, F. J., & Riley, J. S. (2023). When cell death goes wrong: inflammatory outcomes of failed apoptosis and mitotic cell death. *Cell death and differentiation*, 30(2), 293–303. <https://doi.org/10.1038/s41418-022-01082-0>

Bos, L. D. J., & Ware, L. B. (2022). Acute respiratory distress syndrome: causes, pathophysiology, and phenotypes. *Lancet (London, England)*, 400(10358), 1145–1156. [https://doi.org/10.1016/S0140-6736\(22\)01485-4](https://doi.org/10.1016/S0140-6736(22)01485-4)

Boxio, R., Wartelle, J., Nawrocki-Raby, B., Lagrange, B., Malleret, L., Hirche, T., Taggart, C., Pacheco, Y., Devouassoux, G., & Bentaher, A. (2016). Neutrophil elastase cleaves epithelial cadherin in acutely injured lung epithelium. *Respiratory research*, 17(1), 129. <https://doi.org/10.1186/s12931-016-0449-x>

Brault, M., Olsen, T. M., Martinez, J., Stetson, D. B., & Oberst, A. (2018). Intracellular Nucleic Acid Sensing Triggers Necroptosis through Synergistic Type I IFN and TNF Signaling. *Journal of immunology (Baltimore, Md.: 1950)*, 200(8), 2748–2756. <https://doi.org/10.4049/jimmunol.1701492>

Brault, M., Olsen, T. M., Martinez, J., Stetson, D. B., & Oberst, A. (2018). Intracellular Nucleic Acid Sensing Triggers Necroptosis through Synergistic Type I IFN and TNF Signaling. *Journal of immunology (Baltimore, Md.: 1950)*, 200(8), 2748–2756. <https://doi.org/10.4049/jimmunol.1701492>

Brault, M., Olsen, T. M., Martinez, J., Stetson, D. B., & Oberst, A. (2018). Intracellular Nucleic Acid Sensing Triggers Necroptosis through Synergistic Type I IFN and TNF Signaling. *Journal of immunology (Baltimore, Md.: 1950)*, 200(8), 2748–2756. <https://doi.org/10.4049/jimmunol.1701492>

Breiteneder, H., Peng, Y. Q., Agache, I., Diamant, Z., Eiwegger, T., Fokkens, W. J., Traidl-Hoffmann, C., Nadeau, K., O'Hehir, R. E., O'Mahony, L., Pfaar, O., Torres, M. J., Wang, D. Y., Zhang, L., & Akdis, C. A. (2020). Biomarkers for diagnosis and prediction of therapy responses in allergic diseases and asthma. *Allergy*, 75(12), 3039–3068. <https://doi.org/10.1111/all.14582>

Brennan, M. A., & Cookson, B. T. (2000). Salmonella induces macrophage death by caspase-1-dependent necrosis. *Molecular microbiology*, 38(1), 31–40. <https://doi.org/10.1046/j.1365-2958.2000.02103.x>

- Briard, B., Place, D. E., & Kanneganti, T. D. (2020).** DNA Sensing in the Innate Immune Response. *Physiology (Bethesda, Md.)*, 35(2), 112–124. <https://doi.org/10.1152/physiol.00022.2019>
- Brinkmann, V., Reichard, U., Goosmann, C., Fauler, B., Uhlemann, Y., Weiss, D. S., Weinrauch, Y., & Zychlinsky, A. (2004).** Neutrophil extracellular traps kill bacteria. *Science (New York, N.Y.)*, 303(5663), 1532–1535. <https://doi.org/10.1126/science.1092385>
- Brinkmann, V., Reichard, U., Goosmann, C., Fauler, B., Uhlemann, Y., Weiss, D. S., Weinrauch, Y., & Zychlinsky, A. (2004).** Neutrophil extracellular traps kill bacteria. *Science (New York, N.Y.)*, 303(5663), 1532–1535. <https://doi.org/10.1126/science.1092385>
- Brinkmann, V., Reichard, U., Goosmann, C., Fauler, B., Uhlemann, Y., Weiss, D. S., Weinrauch, Y., & Zychlinsky, A. (2004).** Neutrophil extracellular traps kill bacteria. *Science (New York, N.Y.)*, 303(5663), 1532–1535. <https://doi.org/10.1126/science.1092385>
- Buckley, C. D., Ross, E. A., McGettrick, H. M., Osborne, C. E., Haworth, O., Schmutz, C., Stone, P. C., Salmon, M., Matharu, N. M., Vohra, R. K., Nash, G. B., & Rainger, G. E. (2006).** Identification of a phenotypically and functionally distinct population of long-lived neutrophils in a model of reverse endothelial migration. *Journal of leukocyte biology*, 79(2), 303–311. <https://doi.org/10.1189/jlb.0905496>
- Budinger, G. R., Mutlu, G. M., Urich, D., Soberanes, S., Buccellato, L. J., Hawkins, K., Chiarella, S. E., Radigan, K. A., Eisenbart, J., Agrawal, H., Berkelhamer, S., Hekimi, S., Zhang, J., Perlman, H., Schumacker, P. T., Jain, M., & Chandel, N. S. (2011).** Epithelial cell death is an important contributor to oxidant-mediated acute lung injury. *American journal of respiratory and critical care medicine*, 183(8), 1043–1054. <https://doi.org/10.1164/rccm.201002-0181OC>
- Burdette, D. L., Monroe, K. M., Sotelo-Troha, K., Iwig, J. S., Eckert, B., Hyodo, M., Hayakawa, Y., & Vance, R. E. (2011).** STING is a direct innate immune sensor of cyclic di-GMP. *Nature*, 478(7370), 515–518. <https://doi.org/10.1038/nature10429>
- Byrne, A. J., Jones, C. P., Gowers, K., Rankin, S. M., & Lloyd, C. M. (2013).** Lung macrophages contribute to house dust mite driven airway remodeling via HIF-1 α . *PloS one*, 8(7), e69246. <https://doi.org/10.1371/journal.pone.0069246>
- Cahilog, Z., Zhao, H., Wu, L., Alam, A., Eguchi, S., Weng, H., & Ma, D. (2020).** The Role of Neutrophil NETosis in Organ Injury: Novel Inflammatory Cell Death Mechanisms. *Inflammation*, 43(6), 2021–2032. <https://doi.org/10.1007/s10753-020-01294-x>
- Calfee, C. S., Delucchi, K., Parsons, P. E., Thompson, B. T., Ware, L. B., Matthay, M. A., & NHLBI ARDS Network (2014).** Subphenotypes in acute respiratory distress syndrome: latent class analysis of data from two randomised controlled trials. *The Lancet. Respiratory medicine*, 2(8), 611–620. [https://doi.org/10.1016/S2213-2600\(14\)70097-9](https://doi.org/10.1016/S2213-2600(14)70097-9)
- Capelozzi, V. L., Allen, T. C., Beasley, M. B., Cagle, P. T., Guinee, D., Hariri, L. P., Husain, A. N., Jain, D., Lantuejoul, S., Larsen, B. T., Miller, R., Mino-Kenudson, M., Mehrad, M., Raparia, K., Roden, A., Schneider, F., Sholl, L. M., & Smith, M. L. (2017).** Molecular and Immune Biomarkers in Acute Respiratory Distress Syndrome:

A Perspective From Members of the Pulmonary Pathology Society. *Archives of pathology & laboratory medicine*, 141(12), 1719–1727. <https://doi.org/10.5858/arpa.2017-0115-SA>

Carozza, J. A., Böhnert, V., Nguyen, K. C., Skariah, G., Shaw, K. E., Brown, J. A., Rafat, M., von Eyben, R., Graves, E. E., Glenn, J. S., Smith, M., & Li, L. (2020). Extracellular cGAMP is a cancer cell-produced immunotransmitter involved in radiation-induced anti-cancer immunity. *Nature cancer*, 1(2), 184–196. <https://doi.org/10.1038/s43018-020-0028-4>

Carozza, J. A., Cordova, A. F., Brown, J. A., AlSaif, Y., Böhnert, V., Cao, X., Mardjuki, R. E., Skariah, G., Fernandez, D., & Li, L. (2022). ENPP1's regulation of extracellular cGAMP is a ubiquitous mechanism of attenuating STING signaling. *Proceedings of the National Academy of Sciences of the United States of America*, 119(21), e2119189119. <https://doi.org/10.1073/pnas.2119189119>

Carsana, L., Sonzogni, A., Nasr, A., Rossi, R. S., Pellegrinelli, A., Zerbi, P., Rech, R., Colombo, R., Antinori, S., Corbellino, M., Galli, M., Catena, E., Tosoni, A., Gianatti, A., & Nebuloni, M. (2020). Pulmonary post-mortem findings in a series of COVID-19 cases from northern Italy: a two-centre descriptive study. *The Lancet. Infectious diseases*, 20(10), 1135–1140. [https://doi.org/10.1016/S1473-3099\(20\)30434-5](https://doi.org/10.1016/S1473-3099(20)30434-5)

Carstensen, S., Müller, M., Tan, G. L. A., Pasion, K. A., Hohlfeld, J. M., Herrera, V. L. M., & Ruiz-Opazo, N. (2022). "Rogue" neutrophil-subset [DE_{sp}R+CD11b+/CD66b+] immunotype is an actionable therapeutic target for neutrophilic inflammation-mediated tissue injury - studies in human, macaque and rat LPS-inflammation models. *Frontiers in immunology*, 13, 1008390. <https://doi.org/10.3389/fimmu.2022.1008390>

Casares, N., Pequignot, M. O., Tesniere, A., Ghiringhelli, F., Roux, S., Chaput, N., Schmitt, E., Hamai, A., Hervas-Stubbs, S., Obeid, M., Coutant, F., Métivier, D., Pichard, E., Aucouturier, P., Pierron, G., Garrido, C., Zitvogel, L., & Kroemer, G. (2005). Caspase-dependent immunogenicity of doxorubicin-induced tumor cell death. *The Journal of experimental medicine*, 202(12), 1691–1701. <https://doi.org/10.1084/jem.20050915>

Cascella et al. 2022. <https://www.ncbi.nlm.nih.gov/books/NBK554776/>

Caudrillier, A., Kessenbrock, K., Gilliss, B. M., Nguyen, J. X., Marques, M. B., Monestier, M., Toy, P., Werb, Z., & Looney, M. R. (2012). Platelets induce neutrophil extracellular traps in transfusion-related acute lung injury. *The Journal of clinical investigation*, 122(7), 2661–2671. <https://doi.org/10.1172/JCI61303>

Cayrol, C., Duval, A., Schmitt, P., Roga, S., Camus, M., Stella, A., Burlet-Schiltz, O., Gonzalez-de-Peredo, A., & Girard, J. P. (2018). Environmental allergens induce allergic inflammation through proteolytic maturation of IL-33. *Nature immunology*, 19(4), 375–385. <https://doi.org/10.1038/s41590-018-0067-5>

Carboni, S., Jeremiah, N., Gentili, M., Gehrmann, U., Conrad, C., Stolzenberg, M. C., Picard, C., Neven, B., Fischer, A., Amigorena, S., Rieux-Laucat, F., & Manel, N. (2017). Intrinsic antiproliferative activity of the innate sensor STING in T lymphocytes. *The Journal of experimental medicine*, 214(6), 1769–1785. <https://doi.org/10.1084/jem.20161674>

Chambers, E. S., Nanzer, A. M., Pfeffer, P. E., Richards, D. F., Timms, P. M., Martineau, A. R., Griffiths, C. J., Corrigan, C. J., & Hawrylowicz, C. M. (2015). Distinct endotypes of steroid-resistant asthma characterized by IL-

17A(high) and IFN- γ (high) immunophenotypes: Potential benefits of calcitriol. *The Journal of allergy and clinical immunology*, 136(3), 628–637.e4. <https://doi.org/10.1016/j.jaci.2015.01.026>

Chapman, E. A., Lyon, M., Simpson, D., Mason, D., Beynon, R. J., Moots, R. J., & Wright, H. L. (2019). Caught in a Trap? Proteomic Analysis of Neutrophil Extracellular Traps in Rheumatoid Arthritis and Systemic Lupus Erythematosus. *Frontiers in immunology*, 10, 423. <https://doi.org/10.3389/fimmu.2019.00423>

Chattopadhyay, S., Marques, J. T., Yamashita, M., Peters, K. L., Smith, K., Desai, A., Williams, B. R., & Sen, G. C. (2010). Viral apoptosis is induced by IRF-3-mediated activation of Bax. *The EMBO journal*, 29(10), 1762–1773. <https://doi.org/10.1038/emboj.2010.50>

Chen, G., Wan, H., Luo, F., Zhang, L., Xu, Y., Lewkowich, I., Wills-Karp, M., & Whitsett, J. A. (2010). Foxa2 programs Th2 cell-mediated innate immunity in the developing lung. *Journal of immunology (Baltimore, Md. : 1950)*, 184(11), 6133–6141. <https://doi.org/10.4049/jimmunol.1000223>

Chen, H., Sun, H., You, F., Sun, W., Zhou, X., Chen, L., Yang, J., Wang, Y., Tang, H., Guan, Y., Xia, W., Gu, J., Ishikawa, H., Gutman, D., Barber, G., Qin, Z., & Jiang, Z. (2011). Activation of STAT6 by STING is critical for antiviral innate immunity. *Cell*, 147(2), 436–446. <https://doi.org/10.1016/j.cell.2011.09.022>

Chen, K. W., Monteleone, M., Boucher, D., Sollberger, G., Ramnath, D., Condon, N. D., von Pein, J. B., Broz, P., Sweet, M. J., & Schroder, K. (2018). Noncanonical inflammasome signaling elicits gasdermin D-dependent neutrophil extracellular traps. *Science immunology*, 3(26), eaar6676. <https://doi.org/10.1126/sciimmunol.aar6676>

Chen, K. W., Monteleone, M., Boucher, D., Sollberger, G., Ramnath, D., Condon, N. D., von Pein, J. B., Broz, P., Sweet, M. J., & Schroder, K. (2018). Noncanonical inflammasome signaling elicits gasdermin D-dependent neutrophil extracellular traps. *Science immunology*, 3(26), eaar6676. <https://doi.org/10.1126/sciimmunol.aar6676>

Chen, T., Tibbitt, C. A., Feng, X., Stark, J. M., Rohrbeck, L., Rausch, L., Sedimbi, S. K., Karlsson, M. C. I., Lambrecht, B. N., Karlsson Hedestam, G. B., Hendriks, R. W., Chambers, B. J., Nylén, S., & Coquet, J. M. (2017). PPAR- γ promotes type 2 immune responses in allergy and nematode infection. *Science immunology*, 2(9), eaal5196. <https://doi.org/10.1126/sciimmunol.aal5196>

Chen, X., Tang, J., Shuai, W., Meng, J., Feng, J., & Han, Z. (2020). Macrophage polarization and its role in the pathogenesis of acute lung injury/acute respiratory distress syndrome. *Inflammation research : official journal of the European Histamine Research Society ... [et al.]*, 69(9), 883–895. <https://doi.org/10.1007/s00011-020-01378-2>

Cheng, D., Xue, Z., Yi, L., Shi, H., Zhang, K., Huo, X., Bonser, L. R., Zhao, J., Xu, Y., Erle, D. J., & Zhen, G. (2014). Epithelial interleukin-25 is a key mediator in Th2-high, corticosteroid-responsive asthma. *American journal of respiratory and critical care medicine*, 190(6), 639–648. <https://doi.org/10.1164/rccm.201403-0505OC>

Cheng, K. T., Xiong, S., Ye, Z., Hong, Z., Di, A., Tsang, K. M., Gao, X., An, S., Mittal, M., Vogel, S. M., Miao, E. A., Rehman, J., & Malik, A. B. (2017). Caspase-11-mediated endothelial pyroptosis underlies endotoxemia-induced lung injury. *The Journal of clinical investigation*, 127(11), 4124–4135. <https://doi.org/10.1172/JCI94495>

Cheng, P., Li, S., & Chen, H. (2021). Macrophages in Lung Injury, Repair, and Fibrosis. *Cells*, 10(2), 436. <https://doi.org/10.3390/cells10020436>

- Cheng, Y., Liu, Y., Wang, Y., Niu, Q., Gao, Q., Fu, Q., Ma, J., Wang, H., Yan, Y., Ding, C., & Sun, J. (2017).** Chicken DNA virus sensor DDX41 activates IFN- β signaling pathway dependent on STING. *Developmental and comparative immunology*, 76, 334–342. <https://doi.org/10.1016/j.dci.2017.07.001>
- Chin, E. N., Yu, C., Vartabedian, V. F., Jia, Y., Kumar, M., Gamo, A. M., Vernier, W., Ali, S. H., Kissai, M., Lazar, D. C., Nguyen, N., Pereira, L. E., Benish, B., Woods, A. K., Joseph, S. B., Chu, A., Johnson, K. A., Sander, P. N., Martínez-Peña, F., Hampton, E. N., ... Lairson, L. L. (2020).** Antitumor activity of a systemic STING-activating non-nucleotide cGAMP mimetic. *Science (New York, N.Y.)*, 369(6506), 993–999. <https://doi.org/10.1126/science.abb4255>
- Ching, L. M., Cao, Z., Kieda, C., Zwain, S., Jameson, M. B., & Baguley, B. C. (2002).** Induction of endothelial cell apoptosis by the antivascular agent 5,6-Dimethylxanthenone-4-acetic acid. *British journal of cancer*, 86(12), 1937–1942. <https://doi.org/10.1038/sj.bjc.6600368>
- Ching, L. M., Zwain, S., & Baguley, B. C. (2004).** Relationship between tumour endothelial cell apoptosis and tumour blood flow shutdown following treatment with the antivascular agent DMXAA in mice. *British journal of cancer*, 90(4), 906–910. <https://doi.org/10.1038/sj.bjc.6601606>
- Choi, Y., Jang, J., & Park, H. S. (2020).** Pulmonary Surfactants: a New Therapeutic Target in Asthma. *Current allergy and asthma reports*, 20(11), 70. <https://doi.org/10.1007/s11882-020-00968-8>
- Christgen, S., Zheng, M., Kesavardhana, S., Karki, R., Malireddi, R. K. S., Banoth, B., Place, D. E., Briard, B., Sharma, B. R., Tuladhar, S., Samir, P., Burton, A., & Kanneganti, T. D. (2020).** Identification of the PANoptosome: A Molecular Platform Triggering Pyroptosis, Apoptosis, and Necroptosis (PANoptosis). *Frontiers in cellular and infection microbiology*, 10, 237. <https://doi.org/10.3389/fcimb.2020.00237>
- Chupp, G. L., Lee, C. G., Jarjour, N., Shim, Y. M., Holm, C. T., He, S., Dziura, J. D., Reed, J., Coyle, A. J., Kiener, P., Cullen, M., Grandsaigne, M., Dombret, M. C., Aubier, M., Pretolani, M., & Elias, J. A. (2007).** A chitinase-like protein in the lung and circulation of patients with severe asthma. *The New England journal of medicine*, 357(20), 2016–2027. <https://doi.org/10.1056/NEJMoa073600>
- Claesson-Welsh, L., Dejana, E., & McDonald, D. M. (2021).** Permeability of the Endothelial Barrier: Identifying and Reconciling Controversies. *Trends in molecular medicine*, 27(4), 314–331. <https://doi.org/10.1016/j.molmed.2020.11.006>
- Collins, J. A., Schandi, C. A., Young, K. K., Vesely, J., & Willingham, M. C. (1997).** Major DNA fragmentation is a late event in apoptosis. *The journal of histochemistry and cytochemistry: official journal of the Histochemistry Society*, 45(7), 923–934. <https://doi.org/10.1177/002215549704500702>
- Conlon, J., Burdette, D. L., Sharma, S., Bhat, N., Thompson, M., Jiang, Z., Rathinam, V. A., Monks, B., Jin, T., Xiao, T. S., Vogel, S. N., Vance, R. E., & Fitzgerald, K. A. (2013).** Mouse, but not human STING, binds and signals in response to the vascular disrupting agent 5,6-dimethylxanthenone-4-acetic acid. *Journal of immunology (Baltimore, Md. : 1950)*, 190(10), 5216–5225. <https://doi.org/10.4049/jimmunol.1300097>
- Conos, S. A., Chen, K. W., De Nardo, D., Hara, H., Whitehead, L., Núñez, G., Masters, S. L., Murphy, J. M., Schroder, K., Vaux, D. L., Lawlor, K. E., Lindqvist, L. M., & Vince, J. E. (2017).** Active MLKL triggers the

NLRP3 inflammasome in a cell-intrinsic manner. *Proceedings of the National Academy of Sciences of the United States of America*, 114(6), E961–E969. <https://doi.org/10.1073/pnas.1613305114>

Conos, S. A., Chen, K. W., De Nardo, D., Hara, H., Whitehead, L., Núñez, G., Masters, S. L., Murphy, J. M., Schroder, K., Vaux, D. L., Lawlor, K. E., Lindqvist, L. M., & Vince, J. E. (2017). Active MLKL triggers the NLRP3 inflammasome in a cell-intrinsic manner. *Proceedings of the National Academy of Sciences of the United States of America*, 114(6), E961–E969. <https://doi.org/10.1073/pnas.1613305114>

Cortjens, B., de Boer, O. J., de Jong, R., Antonis, A. F., Sabogal Piñeros, Y. S., Lutter, R., van Woensel, J. B., & Bem, R. A. (2016). Neutrophil extracellular traps cause airway obstruction during respiratory syncytial virus disease. *The Journal of pathology*, 238(3), 401–411. <https://doi.org/10.1002/path.4660>

Crotty Alexander, L. E., Akong-Moore, K., Feldstein, S., Johansson, P., Nguyen, A., McEachern, E. K., Niciatia, S., Cowburn, A. S., Olson, J., Cho, J. Y., Isaacs, H., Jr, Johnson, R. S., Broide, D. H., & Nizet, V. (2013). Myeloid cell HIF-1 α regulates asthma airway resistance and eosinophil function. *Journal of molecular medicine (Berlin, Germany)*, 91(5), 637–644. <https://doi.org/10.1007/s00109-012-0986-9>

Dai, E., Han, L., Liu, J., Xie, Y., Zeh, H. J., Kang, R., Bai, L., & Tang, D. (2020). Ferroptotic damage promotes pancreatic tumorigenesis through a TMEM173/STING-dependent DNA sensor pathway. *Nature communications*, 11(1), 6339. <https://doi.org/10.1038/s41467-020-20154-8>

Dai, W., Cheng, J., Leng, X., Hu, X., & Ao, Y. (2021). The potential role of necroptosis in clinical diseases (Review). *International journal of molecular medicine*, 47(5), 89. <https://doi.org/10.3892/ijmm.2021.4922>

D'Alessio, F. R., Craig, J. M., Singer, B. D., Files, D. C., Mock, J. R., Garibaldi, B. T., Fallica, J., Tripathi, A., Mandke, P., Gans, J. H., Limjunyawong, N., Sidhaye, V. K., Heller, N. M., Mitzner, W., King, L. S., & Aggarwal, N. R. (2016). Enhanced resolution of experimental ARDS through IL-4-mediated lung macrophage reprogramming. *American journal of physiology. Lung cellular and molecular physiology*, 310(8), L733–L746. <https://doi.org/10.1152/ajplung.00419.2015>

D'Amato, G., & D'Amato, M. (2023). Climate change, air pollution, pollen allergy and extreme atmospheric events. *Current opinion in pediatrics*, 35(3), 356–361. <https://doi.org/10.1097/MOP.0000000000001237>

Dang, W., Tao, Y., Xu, X., Zhao, H., Zou, L., & Li, Y. (2022). The role of lung macrophages in acute respiratory distress syndrome. *Inflammation research: official journal of the European Histamine Research Society ... [et al.]*, 71(12), 1417–1432. <https://doi.org/10.1007/s00011-022-01645-4>

Davidson, S., Crotta, S., McCabe, T. M., & Wack, A. (2014). Pathogenic potential of interferon $\alpha\beta$ in acute influenza infection. *Nature communications*, 5, 3864. <https://doi.org/10.1038/ncomms4864>

Davies, L. C., Jenkins, S. J., Allen, J. E., & Taylor, P. R. (2013). Tissue-resident macrophages. *Nature immunology*, 14(10), 986–995. <https://doi.org/10.1038/ni.2705>

De Vasconcelos, N. M., Van Opendenbosch, N., Van Gorp, H., Parthoens, E., & Lamkanfi, M. (2019). Single-cell analysis of pyroptosis dynamics reveals conserved GSDMD-mediated subcellular events that precede plasma membrane rupture. *Cell death and differentiation*, 26(1), 146–161. <https://doi.org/10.1038/s41418-018-0106-7>

- Decout, A., Katz, J. D., Venkatraman, S., & Ablasser, A. (2021).** The cGAS-STING pathway as a therapeutic target in inflammatory diseases. *Nature reviews. Immunology*, 21(9), 548–569. <https://doi.org/10.1038/s41577-021-00524-z>
- Degterev, A., Huang, Z., Boyce, M., Li, Y., Jagtap, P., Mizushima, N., Cuny, G. D., Mitchison, T. J., Moskowitz, M. A., & Yuan, J. (2005).** Chemical inhibitor of nonapoptotic cell death with therapeutic potential for ischemic brain injury. *Nature chemical biology*, 1(2), 112–119. <https://doi.org/10.1038/nchembio711>
- Deng, H., Wu, L., Liu, M., Zhu, L., Chen, Y., Zhou, H., Shi, X., Wei, J., Zheng, L., Hu, X., Wang, M., He, Z., Lv, X., & Yang, H. (2020).** Bone Marrow Mesenchymal Stem Cell-Derived Exosomes Attenuate LPS-Induced ARDS by Modulating Macrophage Polarization Through Inhibiting Glycolysis in Macrophages. *Shock (Augusta, Ga.)*, 54(6), 828–843. <https://doi.org/10.1097/SHK.0000000000001549>
- Desai, J., Kumar, S. V., Mulay, S. R., Konrad, L., Romoli, S., Schauer, C., Herrmann, M., Bilyy, R., Müller, S., Popper, B., Nakazawa, D., Weidenbusch, M., Thomasova, D., Krautwald, S., Linkermann, A., & Anders, H. J. (2016).** PMA and crystal-induced neutrophil extracellular trap formation involves RIPK1-RIPK3-MLKL signaling. *European journal of immunology*, 46(1), 223–229. <https://doi.org/10.1002/eji.201545605>
- Diner, E. J., Burdette, D. L., Wilson, S. C., Monroe, K. M., Kellenberger, C. A., Hyodo, M., Hayakawa, Y., Hammond, M. C., & Vance, R. E. (2013).** The innate immune DNA sensor cGAS produces a noncanonical cyclic dinucleotide that activates human STING. *Cell reports*, 3(5), 1355–1361. <https://doi.org/10.1016/j.celrep.2013.05.009>
- Ding, C., Song, Z., Shen, A., Chen, T., & Zhang, A. (2020).** Small molecules targeting the innate immune cGAS–STING–TBK1 signaling pathway. *Acta pharmaceutica Sinica. B*, 10(12), 2272–2298. <https://doi.org/10.1016/j.apsb.2020.03.001>
- Ding, J., Wang, K., Liu, W., She, Y., Sun, Q., Shi, J., Sun, H., Wang, D. C., & Shao, F. (2016).** Pore-forming activity and structural autoinhibition of the gasdermin family. *Nature*, 535(7610), 111–116. <https://doi.org/10.1038/nature18590>
- Dolinay, T., Kaminski, N., Felgendreher, M., Kim, H. P., Reynolds, P., Watkins, S. C., Karp, D., Uhlig, S., & Choi, A. M. (2006).** Gene expression profiling of target genes in ventilator-induced lung injury. *Physiological genomics*, 26(1), 68–75. <https://doi.org/10.1152/physiolgenomics.00110.2005>
- Domizio, J. D., Gulen, M. F., Saidoune, F., Thacker, V. V., Yatim, A., Sharma, K., Nass, T., Guenova, E., Schaller, M., Conrad, C., Goepfert, C., de Leval, L., Garnier, C. V., Berezowska, S., Dubois, A., Gilliet, M., & Ablasser, A. (2022).** The cGAS-STING pathway drives type I IFN immunopathology in COVID-19. *Nature*, 603(7899), 145–151. <https://doi.org/10.1038/s41586-022-04421-w>
- Dovey, C. M., Diep, J., Clarke, B. P., Hale, A. T., McNamara, D. E., Guo, H., Brown, N. W., Jr, Cao, J. Y., Grace, C. R., Gough, P. J., Bertin, J., Dixon, S. J., Fiedler, D., Mocarski, E. S., Kaiser, W. J., Moldoveanu, T., York, J. D., & Carette, J. E. (2018).** MLKL Requires the Inositol Phosphate Code to Execute Necroptosis. *Molecular cell*, 70(5), 936–948.e7. <https://doi.org/10.1016/j.molcel.2018.05.010>

- Downey, G. P., Worthen, G. S., Henson, P. M., & Hyde, D. M.** (1993). Neutrophil sequestration and migration in localized pulmonary inflammation. Capillary localization and migration across the interalveolar septum. *The American review of respiratory disease*, 147(1), 168–176. <https://doi.org/10.1164/ajrccm/147.1.168>
- Du, M., & Chen, Z. J.** (2018). DNA-induced liquid phase condensation of cGAS activates innate immune signaling. *Science (New York, N.Y.)*, 361(6403), 704–709. <https://doi.org/10.1126/science.aat1022>
- Duggal, A., Kast, R., Van Ark, E., Bulgarelli, L., Siuba, M. T., Osborn, J., Rey, D. A., Zampieri, F. G., Cavalcanti, A. B., Maia, I., Paisani, D. M., Laranjeira, L. N., Serpa Neto, A., & Deliberato, R. O.** (2022). Identification of acute respiratory distress syndrome subphenotypes de novo using routine clinical data: a retrospective analysis of ARDS clinical trials. *BMJ open*, 12(1), e053297. <https://doi.org/10.1136/bmjopen-2021-053297>
- Dunphy, G., Flannery, S. M., Almine, J. F., Connolly, D. J., Paulus, C., Jønsson, K. L., Jakobsen, M. R., Nevels, M. M., Bowie, A. G., & Unterholzner, L.** (2018). Non-canonical Activation of the DNA Sensing Adaptor STING by ATM and IFI16 Mediates NF- κ B Signaling after Nuclear DNA Damage. *Molecular cell*, 71(5), 745–760.e5. <https://doi.org/10.1016/j.molcel.2018.07.034>
- Ekstedt, S., Tufvesson, E., Bjermer, L., Kumlien Georén, S., & Cardell, L. O.** (2020). A new role for "eat me" and "don't eat me" markers on neutrophils in asthmatic airway inflammation. *Allergy*, 75(6), 1510–1512. <https://doi.org/10.1111/all.14179>
- Elieh Ali Komi, D., & Bjermer, L.** (2019). Mast Cell-Mediated Orchestration of the Immune Responses in Human Allergic Asthma: Current Insights. *Clinical reviews in allergy & immunology*, 56(2), 234–247. <https://doi.org/10.1007/s12016-018-8720-1>
- Erle, D. J., & Sheppard, D.** (2014). The cell biology of asthma. *The Journal of cell biology*, 205(5), 621–631. <https://doi.org/10.1083/jcb.201401050>
- Filardy, A. A., Pires, D. R., Nunes, M. P., Takiya, C. M., Freire-de-Lima, C. G., Ribeiro-Gomes, F. L., & DosReis, G. A.** (2010). Proinflammatory clearance of apoptotic neutrophils induces an IL-12(low)IL-10(high) regulatory phenotype in macrophages. *Journal of immunology (Baltimore, Md.: 1950)*, 185(4), 2044–2050. <https://doi.org/10.4049/jimmunol.1000017>
- Filippi M. D.** (2016). Mechanism of Diapedesis: Importance of the Transcellular Route. *Advances in immunology*, 129, 25–53. <https://doi.org/10.1016/bs.ai.2015.09.001>
- Filippi M. D.** (2019). Neutrophil transendothelial migration: updates and new perspectives. *Blood*, 133(20), 2149–2158. <https://doi.org/10.1182/blood-2018-12-844605>
- Fink, S. L., & Cookson, B. T.** (2005). Apoptosis, pyroptosis, and necrosis: mechanistic description of dead and dying eukaryotic cells. *Infection and immunity*, 73(4), 1907–1916. <https://doi.org/10.1128/IAI.73.4.1907-1916.2005>
- Fligiel, S. E., Standiford, T., Fligiel, H. M., Tashkin, D., Strieter, R. M., Warner, R. L., Johnson, K. J., & Varani, J.** (2006). Matrix metalloproteinases and matrix metalloproteinase inhibitors in acute lung injury. *Human pathology*, 37(4), 422–430. <https://doi.org/10.1016/j.humpath.2005.11.023>

- Fousert, E., Toes, R., & Desai, J. (2020).** Neutrophil Extracellular Traps (NETs) Take the Central Stage in Driving Autoimmune Responses. *Cells*, 9(4), 915. <https://doi.org/10.3390/cells9040915>
- Franklin, B. S., Bossaller, L., De Nardo, D., Ratter, J. M., Stutz, A., Engels, G., Brenker, C., Nordhoff, M., Mirandola, S. R., Al-Amoudi, A., Mangan, M. S., Zimmer, S., Monks, B. G., Fricke, M., Schmidt, R. E., Espevik, T., Jones, B., Jarnicki, A. G., Hansbro, P. M., Busto, P., ... Latz, E. (2014).** The adaptor ASC has extracellular and 'prionoid' activities that propagate inflammation. *Nature immunology*, 15(8), 727–737. <https://doi.org/10.1038/ni.2913>
- Friggeri, A., Yang, Y., Banerjee, S., Park, Y. J., Liu, G., & Abraham, E. (2010).** HMGB1 inhibits macrophage activity in efferocytosis through binding to the alphavbeta3-integrin. *American journal of physiology. Cell physiology*, 299(6), C1267–C1276. <https://doi.org/10.1152/ajpcell.00152.2010>
- Fritsch, M., Günther, S. D., Schwarzer, R., Albert, M. C., Schorn, F., Werthenbach, J. P., Schiffmann, L. M., Stair, N., Stocks, H., Seeger, J. M., Lamkanfi, M., Krönke, M., Pasparakis, M., & Kashkar, H. (2019).** Caspase-8 is the molecular switch for apoptosis, necroptosis and pyroptosis. *Nature*, 575(7784), 683–687. <https://doi.org/10.1038/s41586-019-1770-6>
- Fuchs, T. A., Abed, U., Goosmann, C., Hurwitz, R., Schulze, I., Wahn, V., Weinrauch, Y., Brinkmann, V., & Zychlinsky, A. (2007).** Novel cell death program leads to neutrophil extracellular traps. *The Journal of cell biology*, 176(2), 231–241. <https://doi.org/10.1083/jcb.200606027>
- Fuchs, Y., & Steller, H. (2011).** Programmed cell death in animal development and disease. *Cell*, 147(4), 742–758. <https://doi.org/10.1016/j.cell.2011.10.033>
- Gaidt, M. M., Ebert, T. S., Chauhan, D., Ramshorn, K., Pinci, F., Zuber, S., O'Duill, F., Schmid-Burgk, J. L., Hoss, F., Buhmann, R., Wittmann, G., Latz, E., Subklewe, M., & Hornung, V. (2017).** The DNA Inflammasome in Human Myeloid Cells Is Initiated by a STING-Cell Death Program Upstream of NLRP3. *Cell*, 171(5), 1110–1124.e18. <https://doi.org/10.1016/j.cell.2017.09.039>
- Gaidt, M. M., Ebert, T. S., Chauhan, D., Ramshorn, K., Pinci, F., Zuber, S., O'Duill, F., Schmid-Burgk, J. L., Hoss, F., Buhmann, R., Wittmann, G., Latz, E., Subklewe, M., & Hornung, V. (2017).** The DNA Inflammasome in Human Myeloid Cells Is Initiated by a STING-Cell Death Program Upstream of NLRP3. *Cell*, 171(5), 1110–1124.e18. <https://doi.org/10.1016/j.cell.2017.09.039>
- Galani, I. E., Triantafyllia, V., Eleminiadou, E. E., Koltsida, O., Stavropoulos, A., Manioudaki, M., Thanos, D., Doyle, S. E., Kotenko, S. V., Thanopoulou, K., & Andreakos, E. (2017).** Interferon- λ Mediates Non-redundant Front-Line Antiviral Protection against Influenza Virus Infection without Compromising Host Fitness. *Immunity*, 46(5), 875–890.e6. <https://doi.org/10.1016/j.immuni.2017.04.025>
- Galluzzi, L., Bravo-San Pedro, J. M., Kepp, O., & Kroemer, G. (2016).** Regulated cell death and adaptive stress responses. *Cellular and molecular life sciences: CMLS*, 73(11-12), 2405–2410. <https://doi.org/10.1007/s00018-016-2209-y>
- Galluzzi, L., Kepp, O., Chan, F. K., & Kroemer, G. (2017).** Necroptosis: Mechanisms and Relevance to Disease. *Annual review of pathology*, 12, 103–130. <https://doi.org/10.1146/annurev-pathol-052016-100247>

- Galluzzi, L., Vitale, I., Aaronson, S. A., Abrams, J. M., Adam, D., Agostinis, P., Alnemri, E. S., Altucci, L., Amelio, I., Andrews, D. W., Annicchiarico-Petruzzelli, M., Antonov, A. V., Arama, E., Baehrecke, E. H., Barlev, N. A., Bazan, N. G., Bernassola, F., Bertrand, M. J. M., Bianchi, K., Blagosklonny, M. V., ... Kroemer, G. (2018).** Molecular mechanisms of cell death: recommendations of the Nomenclature Committee on Cell Death 2018. *Cell death and differentiation*, 25(3), 486–541. <https://doi.org/10.1038/s41418-017-0012-4>
- Gan, T., Yang, Y., Hu, F., Chen, X., Zhou, J., Li, Y., Xu, Y., Wang, H., Chen, Y., & Zhang, M. (2018).** TLR3 Regulated Poly I:C-Induced Neutrophil Extracellular Traps and Acute Lung Injury Partly Through p38 MAP Kinase. *Frontiers in microbiology*, 9, 3174. <https://doi.org/10.3389/fmicb.2018.03174>
- Gao, P., Ascano, M., Zillinger, T., Wang, W., Dai, P., Serganov, A. A., Gaffney, B. L., Shuman, S., Jones, R. A., Deng, L., Hartmann, G., Barchet, W., Tuschl, T., & Patel, D. J. (2013).** Structure-function analysis of STING activation by c[G(2',5')pA(3',5')p] and targeting by antiviral DMXAA. *Cell*, 154(4), 748–762. <https://doi.org/10.1016/j.cell.2013.07.023>
- Garland, K. M., Sheehy, T. L., & Wilson, J. T. (2022).** Chemical and Biomolecular Strategies for STING Pathway Activation in Cancer Immunotherapy. *Chemical reviews*, 122(6), 5977–6039. <https://doi.org/10.1021/acs.chemrev.1c00750>
- Gasiuniene, E., Janulaityte, I., Zemeckiene, Z., Barkauskiene, D., & Sitkauskiene, B. (2019).** Elevated levels of interleukin-33 are associated with allergic and eosinophilic asthma. *Scandinavian journal of immunology*, 89(5), e12724. <https://doi.org/10.1111/sji.12724>
- Gevaert, E., Delemarre, T., De Volder, J., Zhang, N., Holtappels, G., De Ruyck, N., Persson, E., Heyndrickx, I., Verstraete, K., Aegerter, H., Nauwynck, H., Savvides, S. N., Lambrecht, B. N., & Bachert, C. (2020).** Charcot-Leyden crystals promote neutrophilic inflammation in patients with nasal polyposis. *The Journal of allergy and clinical immunology*, 145(1), 427–430.e4. <https://doi.org/10.1016/j.jaci.2019.08.027>
- Giampazolias, E., Zunino, B., Dhayade, S., Bock, F., Cloix, C., Cao, K., Roca, A., Lopez, J., Ichim, G., Proics, E., Rubio-Patiño, C., Fort, L., Yatim, N., Woodham, E., Orozco, S., Taraborrelli, L., Peltzer, N., Lecis, D., Machesky, L., Walczak, H., ... Tait, S. W. G. (2017).** Mitochondrial permeabilization engages NF- κ B-dependent anti-tumour activity under caspase deficiency. *Nature cell biology*, 19(9), 1116–1129. <https://doi.org/10.1038/ncb3596>
- Giannotta, M., Trani, M., & Dejana, E. (2013).** VE-cadherin and endothelial adherens junctions: active guardians of vascular integrity. *Developmental cell*, 26(5), 441–454. <https://doi.org/10.1016/j.devcel.2013.08.020>
- Gibson, P. G., Simpson, J. L., & Saltos, N. (2001).** Heterogeneity of airway inflammation in persistent asthma : evidence of neutrophilic inflammation and increased sputum interleukin-8. *Chest*, 119(5), 1329–1336. <https://doi.org/10.1378/chest.119.5.1329>
- Gill, M. A., Liu, A. H., Calatroni, A., Krouse, R. Z., Shao, B., Schiltz, A., Gern, J. E., Togias, A., & Busse, W. W. (2018).** Enhanced plasmacytoid dendritic cell antiviral responses after omalizumab. *The Journal of allergy and clinical immunology*, 141(5), 1735–1743.e9. <https://doi.org/10.1016/j.jaci.2017.07.035>

- Gill, S. S., Suri, S. S., Janardhan, K. S., Caldwell, S., Duke, T., & Singh, B. (2008).** Role of pulmonary intravascular macrophages in endotoxin-induced lung inflammation and mortality in a rat model. *Respiratory research*, 9(1), 69. <https://doi.org/10.1186/1465-9921-9-69>
- Ginhoux, F., & Guillemins, M. (2016).** Tissue-Resident Macrophage Ontogeny and Homeostasis. *Immunity*, 44(3), 439–449. <https://doi.org/10.1016/j.immuni.2016.02.024>
- Gong, L., Huang, D., Shi, Y., Liang, Z., & Bu, H. (2023).** Regulated cell death in cancer: from pathogenesis to treatment. *Chinese medical journal*, 136(6), 653–665. <https://doi.org/10.1097/CM9.0000000000002239>
- Gong, T., Liu, L., Jiang, W., & Zhou, R. (2020).** DAMP-sensing receptors in sterile inflammation and inflammatory diseases. *Nature reviews. Immunology*, 20(2), 95–112. <https://doi.org/10.1038/s41577-019-0215-7>
- Guerini D. (2022).** STING Agonists/Antagonists: Their Potential as Therapeutics and Future Developments. *Cells*, 11(7), 1159. <https://doi.org/10.3390/cells11071159>
- Gulen, M. F., Koch, U., Haag, S. M., Schuler, F., Apetoh, L., Villunger, A., Radtke, F., & Ablasser, A. (2017).** Signalling strength determines proapoptotic functions of STING. *Nature communications*, 8(1), 427. <https://doi.org/10.1038/s41467-017-00573-w>
- Gullett, J. M., Tweedell, R. E., & Kanneganti, T. D. (2022).** It's All in the PAN: Crosstalk, Plasticity, Redundancies, Switches, and Interconnectedness Encompassed by PANoptosis Underlying the Totality of Cell Death-Associated Biological Effects. *Cells*, 11(9), 1495. <https://doi.org/10.3390/cells11091495>
- Gupta, S., Rouse, B. T., & Sarangi, P. P. (2021).** Did Climate Change Influence the Emergence, Transmission, and Expression of the COVID-19 Pandemic?. *Frontiers in medicine*, 8, 769208. <https://doi.org/10.3389/fmed.2021.769208>
- Gurung, P., Burton, A., & Kanneganti, T. D. (2016).** NLRP3 inflammasome plays a redundant role with caspase 8 to promote IL-1 β -mediated osteomyelitis. *Proceedings of the National Academy of Sciences of the United States of America*, 113(16), 4452–4457. <https://doi.org/10.1073/pnas.1601636113>
- Gutierrez, K. D., Davis, M. A., Daniels, B. P., Olsen, T. M., Ralli-Jain, P., Tait, S. W., Gale, M., Jr, & Oberst, A. (2017).** MLKL Activation Triggers NLRP3-Mediated Processing and Release of IL-1 β Independently of Gasdermin-D. *Journal of immunology (Baltimore, Md. : 1950)*, 198(5), 2156–2164. <https://doi.org/10.4049/jimmunol.1601757>
- Haag, S. M., Gulen, M. F., Reymond, L., Gibelin, A., Abrami, L., Decout, A., Heymann, M., van der Goot, F. G., Turcatti, G., Behrendt, R., & Ablasser, A. (2018).** Targeting STING with covalent small-molecule inhibitors. *Nature*, 559(7713), 269–273. <https://doi.org/10.1038/s41586-018-0287-8>
- Hadjadj, J., Yatim, N., Barnabei, L., Corneau, A., Boussier, J., Smith, N., Péré, H., Charbit, B., Bondet, V., Chenevier-Gobeaux, C., Breillat, P., Carlier, N., Gauzit, R., Morbieu, C., Pène, F., Marin, N., Roche, N., Szwebel, T. A., Merklings, S. H., Treluyer, J. M., ... Terrier, B. (2020).** Impaired type I interferon activity and inflammatory responses in severe COVID-19 patients. *Science (New York, N.Y.)*, 369(6504), 718–724. <https://doi.org/10.1126/science.abc6027>

- Halim**, T. Y., Steer, C. A., Mathä, L., Gold, M. J., Martinez-Gonzalez, I., McNagny, K. M., McKenzie, A. N., & Takei, F. (2014). Group 2 innate lymphoid cells are critical for the initiation of adaptive T helper 2 cell-mediated allergic lung inflammation. *Immunity*, 40(3), 425–435. <https://doi.org/10.1016/j.immuni.2014.01.011>
- Hammad**, H., & Lambrecht, B. N. (2021). The basic immunology of asthma. *Cell*, 184(6), 1469–1485. <https://doi.org/10.1016/j.cell.2021.02.016>
- Han**, Y., Chen, L., Liu, H., Jin, Z., Wu, Y., Wu, Y., Li, W., Ying, S., Chen, Z., Shen, H., & Yan, F. (2020). Airway Epithelial cGAS Is Critical for Induction of Experimental Allergic Airway Inflammation. *Journal of immunology* (Baltimore, Md. : 1950), 204(6), 1437–1447. <https://doi.org/10.4049/jimmunol.1900869>
- Hansen**, A. L., Buchan, G. J., Rühl, M., Mukai, K., Salvatore, S. R., Ogawa, E., Andersen, S. D., Iversen, M. B., Thielke, A. L., Gunderstofte, C., Motwani, M., Møller, C. T., Jakobsen, A. S., Fitzgerald, K. A., Roos, J., Lin, R., Maier, T. J., Goldbach-Mansky, R., Miner, C. A., Qian, W., ... Holm, C. K. (2018). Nitro-fatty acids are formed in response to virus infection and are potent inhibitors of STING palmitoylation and signaling. *Proceedings of the National Academy of Sciences of the United States of America*, 115(33), E7768–E7775. <https://doi.org/10.1073/pnas.1806239115>
- Hao**, J., Hu, Y., Li, Y., Zhou, Q., & Lv, X. (2017). Involvement of JNK signaling in IL4-induced M2 macrophage polarization. *Experimental cell research*, 357(2), 155–162. <https://doi.org/10.1016/j.yexcr.2017.05.010>
- Hao**, Y., Yang, B., Yang, J., Shi, X., Yang, X., Zhang, D., Zhao, D., Yan, W., Chen, L., Zheng, H., Zhang, K., & Liu, X. (2022). ZBP1: A Powerful Innate Immune Sensor and Double-Edged Sword in Host Immunity. *International journal of molecular sciences*, 23(18), 10224. <https://doi.org/10.3390/ijms231810224>
- Hashimoto**, D., Chow, A., Noizat, C., Teo, P., Beasley, M. B., Leboeuf, M., Becker, C. D., See, P., Price, J., Lucas, D., Greter, M., Mortha, A., Boyer, S. W., Forsberg, E. C., Tanaka, M., van Rooijen, N., García-Sastre, A., Stanley, E. R., Ginhoux, F., Frenette, P. S., ... Merad, M. (2013). Tissue-resident macrophages self-maintain locally throughout adult life with minimal contribution from circulating monocytes. *Immunity*, 38(4), 792–804. <https://doi.org/10.1016/j.immuni.2013.04.004>
- He**, X., Zhang, L., Xiong, A., Ran, Q., Wang, J., Wu, D., Niu, B., Liu, S., & Li, G. (2021). PM2.5 aggravates NQO1-induced mucus hyper-secretion through release of neutrophil extracellular traps in an asthma model. *Ecotoxicology and environmental safety*, 218, 112272. Advance online publication. <https://doi.org/10.1016/j.ecoenv.2021.112272>
- Hemmi**, H., Takeuchi, O., Kawai, T., Kaisho, T., Sato, S., Sanjo, H., Matsumoto, M., Hoshino, K., Wagner, H., Takeda, K., & Akira, S. (2000). A Toll-like receptor recognizes bacterial DNA. *Nature*, 408(6813), 740–745. <https://doi.org/10.1038/35047123>
- Herzner**, A. M., Hagmann, C. A., Goldeck, M., Wolter, S., Kübler, K., Wittmann, S., Gramberg, T., Andreeva, L., Hopfner, K. P., Mertens, C., Zillinger, T., Jin, T., Xiao, T. S., Bartok, E., Coch, C., Ackermann, D., Hornung, V., Ludwig, J., Barchet, W., Hartmann, G., ... Schlee, M. (2015). Sequence-specific activation of the DNA sensor cGAS by Y-form DNA structures as found in primary HIV-1 cDNA. *Nature immunology*, 16(10), 1025–1033. <https://doi.org/10.1038/ni.3267>

- Hintzsche**, H., Hemmann, U., Poth, A., Utesch, D., Lott, J., Stopper, H., & Working Group “In vitro micronucleus test”, Gesellschaft für Umwelt-Mutationsforschung (GUM, German-speaking section of the European Environmental Mutagenesis and Genomics Society EEMGS) (2017). Fate of micronuclei and micronucleated cells. *Mutation research. Reviews in mutation research*, 771, 85–98. <https://doi.org/10.1016/j.mrrev.2017.02.002>
- Hoffmann**, P. R., Kench, J. A., Vondracek, A., Kruk, E., Daleke, D. L., Jordan, M., Marrack, P., Henson, P. M., & Fadok, V. A. (2005). Interaction between phosphatidylserine and the phosphatidylserine receptor inhibits immune responses in vivo. *Journal of immunology (Baltimore, Md. : 1950)*, 174(3), 1393–1404. <https://doi.org/10.4049/jimmunol.174.3.1393>
- Högner**, K., Wolff, T., Pleschka, S., Plog, S., Gruber, A. D., Kalinke, U., Walmrath, H. D., Bodner, J., Gattenlöhner, S., Lewe-Schlosser, P., Matrosovich, M., Seeger, W., Lohmeyer, J., & Herold, S. (2013). Macrophage-expressed IFN- β contributes to apoptotic alveolar epithelial cell injury in severe influenza virus pneumonia. *PLoS pathogens*, 9(2), e1003188. <https://doi.org/10.1371/journal.ppat.1003188>.
- Holler**, N., Zaru, R., Micheau, O., Thome, M., Attinger, A., Valitutti, S., Bodmer, J. L., Schneider, P., Seed, B., & Tschopp, J. (2000). Fas triggers an alternative, caspase-8-independent cell death pathway using the kinase RIP as effector molecule. *Nature immunology*, 1(6), 489–495. <https://doi.org/10.1038/82732>
- Holm**, C. K., Rahbek, S. H., Gad, H. H., Bak, R. O., Jakobsen, M. R., Jiang, Z., Hansen, A. L., Jensen, S. K., Sun, C., Thomsen, M. K., Laustsen, A., Nielsen, C. G., Severinsen, K., Xiong, Y., Burdette, D. L., Hornung, V., Lebbink, R. J., Duch, M., Fitzgerald, K. A., Bahrami, S., ... Paludan, S. R. (2016). Influenza A virus targets a cGAS-independent STING pathway that controls enveloped RNA viruses. *Nature communications*, 7, 10680. <https://doi.org/10.1038/ncomms10680>
- Hong**, Z., Mei, J., Li, C., Bai, G., Maimaiti, M., Hu, H., Yu, W., Sun, L., Zhang, L., Cheng, D., Liao, Y., Li, S., You, Y., Sun, H., Huang, J., Liu, X., Lieberman, J., & Wang, C. (2021). STING inhibitors target the cyclic dinucleotide binding pocket. *Proceedings of the National Academy of Sciences of the United States of America*, 118(24), e2105465118. <https://doi.org/10.1073/pnas.2105465118>
- Hornung**, V., Ablasser, A., Charrel-Dennis, M., Bauernfeind, F., Horvath, G., Caffrey, D. R., Latz, E., & Fitzgerald, K. A. (2009). AIM2 recognizes cytosolic dsDNA and forms a caspase-1-activating inflammasome with ASC. *Nature*, 458(7237), 514–518. <https://doi.org/10.1038/nature07725>
- Hsia**, C. C., Hyde, D. M., & Weibel, E. R. (2016). Lung Structure and the Intrinsic Challenges of Gas Exchange. *Comprehensive Physiology*, 6(2), 827–895. <https://doi.org/10.1002/cphy.c150028>
- Hsia**, C. C., Hyde, D. M., & Weibel, E. R. (2016). Lung Structure and the Intrinsic Challenges of Gas Exchange. *Comprehensive Physiology*, 6(2), 827–895. <https://doi.org/10.1002/cphy.c150028>
- Huang**, J., Jiang, S., Liang, L., He, H., Liu, Y., Cong, L., & Jiang, Y. (2022). Analysis of PANoptosis-Related LncRNA-miRNA-mRNA Network Reveals LncRNA SNHG7 Involved in Chemo-Resistance in Colon Adenocarcinoma. *Frontiers in oncology*, 12, 888105. <https://doi.org/10.3389/fonc.2022.888105>
- Huang**, X., Xiu, H., Zhang, S., & Zhang, G. (2018). The Role of Macrophages in the Pathogenesis of ALI/ARDS. *Mediators of inflammation*, 2018, 1264913. <https://doi.org/10.1155/2018/1264913>

Huang, Z., Wu, S. Q., Liang, Y., Zhou, X., Chen, W., Li, L., Wu, J., Zhuang, Q., Chen, C., Li, J., Zhong, C. Q., Xia, W., Zhou, R., Zheng, C., & Han, J. (2015). RIP1/RIP3 binding to HSV-1 ICP6 initiates necroptosis to restrict virus propagation in mice. *Cell host & microbe*, 17(2), 229–242. <https://doi.org/10.1016/j.chom.2015.01.002>

Humphries, F., Shmuel-Galia, L., Jiang, Z., Wilson, R., Landis, P., Ng, S. L., Parsi, K. M., Maehr, R., Cruz, J., Morales-Ramos, A., Ramanjulu, J. M., Bertin, J., Pesiridis, G. S., & Fitzgerald, K. A. (2021). A diamidobenzimidazole STING agonist protects against SARS-CoV-2 infection. *Science immunology*, 6(59), eabi9002. <https://doi.org/10.1126/sciimmunol.abi9002>

Humphries, F., Shmuel-Galia, L., Jiang, Z., Wilson, R., Landis, P., Ng, S. L., Parsi, K. M., Maehr, R., Cruz, J., Morales-Ramos, A., Ramanjulu, J. M., Bertin, J., Pesiridis, G. S., & Fitzgerald, K. A. (2021). A diamidobenzimidazole STING agonist protects against SARS-CoV-2 infection. *Science immunology*, 6(59), eabi9002. <https://doi.org/10.1126/sciimmunol.abi9002>

Huppert, L. A., Matthay, M. A., & Ware, L. B. (2019). Pathogenesis of Acute Respiratory Distress Syndrome. *Seminars in respiratory and critical care medicine*, 40(1), 31–39. <https://doi.org/10.1055/s-0039-1683996>

Ishikawa, H., & Barber, G. N. (2008). STING is an endoplasmic reticulum adaptor that facilitates innate immune signalling. *Nature*, 455(7213), 674–678. <https://doi.org/10.1038/nature07317>

Ishikawa, H., Ma, Z., & Barber, G. N. (2009). STING regulates intracellular DNA-mediated, type I interferon-dependent innate immunity. *Nature*, 461(7265), 788–792. <https://doi.org/10.1038/nature08476>

Janssen, W. J., Barthel, L., Muldrow, A., Oberley-Deegan, R. E., Kearns, M. T., Jakubzick, C., & Henson, P. M. (2011). Fas determines differential fates of resident and recruited macrophages during resolution of acute lung injury. *American journal of respiratory and critical care medicine*, 184(5), 547–560. <https://doi.org/10.1164/rccm.201011-1891OC>

Janssen, W. J., Barthel, L., Muldrow, A., Oberley-Deegan, R. E., Kearns, M. T., Jakubzick, C., & Henson, P. M. (2011). Fas determines differential fates of resident and recruited macrophages during resolution of acute lung injury. *American journal of respiratory and critical care medicine*, 184(5), 547–560. <https://doi.org/10.1164/rccm.201011-1891OC>

Jatakanon, A., Uasuf, C., Maziak, W., Lim, S., Chung, K. F., & Barnes, P. J. (1999). Neutrophilic inflammation in severe persistent asthma. *American journal of respiratory and critical care medicine*, 160(5 Pt 1), 1532–1539. <https://doi.org/10.1164/ajrccm.160.5.9806170>

Jhuti, D., Rawat, A., Guo, C. M., Wilson, L. A., Mills, E. J., & Forrest, J. I. (2022). Interferon Treatments for SARS-CoV-2: Challenges and Opportunities. *Infectious diseases and therapy*, 11(3), 953–972. <https://doi.org/10.1007/s40121-022-00633-9>

Ji, Y., Luo, Y., Wu, Y., Sun, Y., Zhao, L., Xue, Z., Sun, M., Wei, X., He, Z., Wu, S. A., Lin, L. L., Lu, Y., Chang, L., Chen, F., Chen, S., Qian, W., Xu, X., Chen, S., Pan, D., Zhou, Z., ... Qi, L. (2023). SEL1L-HRD1 endoplasmic reticulum-associated degradation controls STING-mediated innate immunity by limiting the size of the activable STING pool. *Nature cell biology*, 25(5), 726–739. <https://doi.org/10.1038/s41556-023-01138-4>

- Jiang, M., Qi, L., Li, L., Wu, Y., Song, D., & Li, Y. (2021).** Caspase-8: A key protein of cross-talk signal way in "PANoptosis" in cancer. *International journal of cancer*, 149(7), 1408–1420. <https://doi.org/10.1002/ijc.33698>
- Jin, S., Ding, X., Yang, C., Li, W., Deng, M., Liao, H., Lv, X., Pitt, B. R., Billiar, T. R., Zhang, L. M., & Li, Q. (2021).** Mechanical Ventilation Exacerbates Poly (I:C) Induced Acute Lung Injury: Central Role for Caspase-11 and Gut-Lung Axis. *Frontiers in immunology*, 12, 693874. <https://doi.org/10.3389/fimmu.2021.693874>
- Jønsson, K. L., Laustsen, A., Krapp, C., Skipper, K. A., Thavachelvam, K., Hotter, D., Egedal, J. H., Kjolby, M., Mohammadi, P., Prabakaran, T., Sørensen, L. K., Sun, C., Jensen, S. B., Holm, C. K., Lebbink, R. J., Johannsen, M., Nyegaard, M., Mikkelsen, J. G., Kirchhoff, F., Paludan, S. R., ... Jakobsen, M. R. (2017).** IFI16 is required for DNA sensing in human macrophages by promoting production and function of cGAMP. *Nature communications*, 8, 14391. <https://doi.org/10.1038/ncomms14391>
- Juliana, A., Zonneveld, R., Plötz, F. B., van Meurs, M., & Wilschut, J. (2020).** Neutrophil-endothelial interactions in respiratory syncytial virus bronchiolitis: An understudied aspect with a potential for prediction of severity of disease. *Journal of clinical virology : the official publication of the Pan American Society for Clinical Virology*, 123, 104258. <https://doi.org/10.1016/j.jcv.2019.104258>
- Kaiser, W. J., Sridharan, H., Huang, C., Mandal, P., Upton, J. W., Gough, P. J., Sehon, C. A., Marquis, R. W., Bertin, J., & Mocarski, E. S. (2013).** Toll-like receptor 3-mediated necrosis via TRIF, RIP3, and MLKL. *The Journal of biological chemistry*, 288(43), 31268–31279. <https://doi.org/10.1074/jbc.M113.462341>
- Kalkavan, H., & Green, D. R. (2018).** MOMP, cell suicide as a BCL-2 family business. *Cell death and differentiation*, 25(1), 46–55. <https://doi.org/10.1038/cdd.2017.179>
- Kambara, H., Liu, F., Zhang, X., Liu, P., Bajrami, B., Teng, Y., Zhao, L., Zhou, S., Yu, H., Zhou, W., Silberstein, L. E., Cheng, T., Han, M., Xu, Y., & Luo, H. R. (2018).** Gasdermin D Exerts Anti-inflammatory Effects by Promoting Neutrophil Death. *Cell reports*, 22(11), 2924–2936. <https://doi.org/10.1016/j.celrep.2018.02.067>
- Kang, S., Fernandes-Alnemri, T., Rogers, C., Mayes, L., Wang, Y., Dillon, C., Roback, L., Kaiser, W., Oberst, A., Sagara, J., Fitzgerald, K. A., Green, D. R., Zhang, J., Mocarski, E. S., & Alnemri, E. S. (2015).** Caspase-8 scaffolding function and MLKL regulate NLRP3 inflammasome activation downstream of TLR3. *Nature communications*, 6, 7515. <https://doi.org/10.1038/ncomms8515>
- Kang, S., Fernandes-Alnemri, T., Rogers, C., Mayes, L., Wang, Y., Dillon, C., Roback, L., Kaiser, W., Oberst, A., Sagara, J., Fitzgerald, K. A., Green, D. R., Zhang, J., Mocarski, E. S., & Alnemri, E. S. (2015).** Caspase-8 scaffolding function and MLKL regulate NLRP3 inflammasome activation downstream of TLR3. *Nature communications*, 6, 7515. <https://doi.org/10.1038/ncomms8515>
- Karki, R., Lee, S., Mall, R., Pandian, N., Wang, Y., Sharma, B. R., Malireddi, R. S., Yang, D., Trifkovic, S., Steele, J. A., Connelly, J. P., Vishwanath, G., Sasikala, M., Reddy, D. N., Vogel, P., Pruett-Miller, S. M., Webby, R., Jonsson, C. B., & Kanneganti, T. D. (2022).** ZBP1-dependent inflammatory cell death, PANoptosis, and cytokine storm disrupt IFN therapeutic efficacy during coronavirus infection. *Science immunology*, 7(74), eabo6294. <https://doi.org/10.1126/sciimmunol.abo6294>

- Karki, R., Sharma, B. R., Lee, E., Banoth, B., Malireddi, R. K. S., Samir, P., Tuladhar, S., Mummareddy, H., Burton, A. R., Vogel, P., & Kanneganti, T. D. (2020).** Interferon regulatory factor 1 regulates PANoptosis to prevent colorectal cancer. *JCI insight*, 5(12), e136720. <https://doi.org/10.1172/jci.insight.136720>
- Karki, R., Sharma, B. R., Tuladhar, S., Williams, E. P., Zalduondo, L., Samir, P., Zheng, M., Sundaram, B., Banoth, B., Malireddi, R. K. S., Schreiner, P., Neale, G., Vogel, P., Webby, R., Jonsson, C. B., & Kanneganti, T. D. (2021).** Synergism of TNF- α and IFN- γ Triggers Inflammatory Cell Death, Tissue Damage, and Mortality in SARS-CoV-2 Infection and Cytokine Shock Syndromes. *Cell*, 184(1), 149–168.e17. <https://doi.org/10.1016/j.cell.2020.11.025>
- Karki, R., Sundaram, B., Sharma, B. R., Lee, S., Malireddi, R. K. S., Nguyen, L. N., Christgen, S., Zheng, M., Wang, Y., Samir, P., Neale, G., Vogel, P., & Kanneganti, T. D. (2021).** ADAR1 restricts ZBP1-mediated immune response and PANoptosis to promote tumorigenesis. *Cell reports*, 37(3), 109858. <https://doi.org/10.1016/j.celrep.2021.109858>
- Kato, K., Nishimasu, H., Oikawa, D., Hirano, S., Hirano, H., Kasuya, G., Ishitani, R., Tokunaga, F., & Nureki, O. (2018).** Structural insights into cGAMP degradation by Ecto-nucleotide pyrophosphatase phosphodiesterase 1. *Nature communications*, 9(1), 4424. <https://doi.org/10.1038/s41467-018-06922-7>
- Katze, M. G., He, Y., & Gale, M., Jr (2002).** Viruses and interferon: a fight for supremacy. *Nature reviews Immunology*, 2(9), 675–687. <https://doi.org/10.1038/nri888>
- Katzenstein, A. L., Bloor, C. M., & Leibow, A. A. (1976).** Diffuse alveolar damage--the role of oxygen, shock, and related factors. A review. *The American journal of pathology*, 85(1), 209–228.
- Kaur, R., & Chupp, G. (2019).** Phenotypes and endotypes of adult asthma: Moving toward precision medicine. *The Journal of allergy and clinical immunology*, 144(1), 1–12. <https://doi.org/10.1016/j.jaci.2019.05.031>
- Kayagaki, N., Stowe, I. B., Lee, B. L., O'Rourke, K., Anderson, K., Warming, S., Cuellar, T., Haley, B., Roose-Girma, M., Phung, Q. T., Liu, P. S., Lill, J. R., Li, H., Wu, J., Kummerfeld, S., Zhang, J., Lee, W. P., Snipas, S. J., Salvesen, G. S., Morris, L. X., ... Dixit, V. M. (2015).** Caspase-11 cleaves gasdermin D for non-canonical inflammasome signalling. *Nature*, 526(7575), 666–671. <https://doi.org/10.1038/nature15541>
- Kerr, J. F., Wyllie, A. H., & Currie, A. R. (1972).** Apoptosis: a basic biological phenomenon with wide-ranging implications in tissue kinetics. *British journal of cancer*, 26(4), 239–257. <https://doi.org/10.1038/bjc.1972.33>
- Ketelut-Carneiro, N., & Fitzgerald, K. A. (2022).** Apoptosis, Pyroptosis, and Necroptosis-Oh My! The Many Ways a Cell Can Die. *Journal of molecular biology*, 434(4), 167378. <https://doi.org/10.1016/j.jmb.2021.167378>
- Kiewiet, M. B. G., Lupinek, C., Vrtala, S., Wieser, S., Baar, A., Kiss, R., Kull, I., Melén, E., Wickman, M., Porta, D., Gori, D., Gehring, U., Aalberse, R., Sunyer, J., Standl, M., Heinrich, J., Waiblinger, D., Wright, J., Antó, J. M., Bousquet, J., ... Valenta, R. (2023).** A molecular sensitization map of European children reveals exposome- and climate-dependent sensitization profiles. *Allergy*, 78(7), 2007–2018. <https://doi.org/10.1111/all.15689>
- Kim, J., Kim, H. S., & Chung, J. H. (2023).** Molecular mechanisms of mitochondrial DNA release and activation of the cGAS-STING pathway. *Experimental & molecular medicine*, 55(3), 510–519. <https://doi.org/10.1038/s12276-023-00965-7>

- Kischkel**, F. C., Hellbardt, S., Behrmann, I., Germer, M., Pawlita, M., Krammer, P. H., & Peter, M. E. (1995). Cytotoxicity-dependent APO-1 (Fas/CD95)-associated proteins form a death-inducing signaling complex (DISC) with the receptor. *The EMBO journal*, 14(22), 5579–5588. <https://doi.org/10.1002/j.1460-2075.1995.tb00245.x>
- Koshy**, S. T., Cheung, A. S., Gu, L., Graveline, A. R., & Mooney, D. J. (2017). Liposomal Delivery Enhances Immune Activation by STING Agonists for Cancer Immunotherapy. *Advanced biosystems*, 1(1-2), 1600013. <https://doi.org/10.1002/adbi.201600013>
- Krenkel**, O., Puengel, T., Govaere, O., Abdallah, A. T., Mossanen, J. C., Kohlhepp, M., Liepelt, A., Lefebvre, E., Luedde, T., Hellerbrand, C., Weiskirchen, R., Longerich, T., Costa, I. G., Anstee, Q. M., Trautwein, C., & Tacke, F. (2018). Therapeutic inhibition of inflammatory monocyte recruitment reduces steatohepatitis and liver fibrosis. *Hepatology (Baltimore, Md.)*, 67(4), 1270–1283. <https://doi.org/10.1002/hep.29544>
- Krysko**, D. V., Denecker, G., Festjens, N., Gabriels, S., Parthoens, E., D'Herde, K., & Vandenabeele, P. (2006). Macrophages use different internalization mechanisms to clear apoptotic and necrotic cells. *Cell death and differentiation*, 13(12), 2011–2022. <https://doi.org/10.1038/sj.cdd.4401900>
- Kuhl**, N., Linder, A., Philipp, N., Nixdorf, D., Fischer, H., Veth, S., Kuut, G., Xu, T. T., Theurich, S., Carell, T., Subklewe, M., & Hornung, V. (2023). STING agonism turns human T cells into interferon-producing cells but impedes their functionality. *EMBO reports*, 24(3), e55536. <https://doi.org/10.15252/embr.202255536>
- Kuo, C. S., Pavlidis, S., Loza, M., Baribaud, F., Rowe, A., Pandis, I., Sousa, A., Corfield, J., Djukanovic, R., Lutter, R., Sterk, P. J., Auffray, C., Guo, Y., Adcock, I. M., Chung, K. F., & U-BIOPRED Study Group (2017). T-helper cell type 2 (Th2) and non-Th2 molecular phenotypes of asthma using sputum transcriptomics in U-BIOPRED. *The European respiratory journal*, 49(2), 1602135. <https://doi.org/10.1183/13993003.02135-2016>
- Kuriakose**, T., Man, S. M., Malireddi, R. K., Karki, R., Kesavardhana, S., Place, D. E., Neale, G., Vogel, P., & Kanneganti, T. D. (2016). ZBP1/DAI is an innate sensor of influenza virus triggering the NLRP3 inflammasome and programmed cell death pathways. *Science immunology*, 1(2), aag2045. <https://doi.org/10.1126/sciimmunol.aag2045>
- Kuriakose**, T., Zheng, M., Neale, G., & Kanneganti, T. D. (2018). IRF1 Is a Transcriptional Regulator of ZBP1 Promoting NLRP3 Inflammasome Activation and Cell Death during Influenza Virus Infection. *Journal of immunology (Baltimore, Md. : 1950)*, 200(4), 1489–1495. <https://doi.org/10.4049/jimmunol.1701538>
- Lachowicz-Scroggins**, M. E., Dunican, E. M., Charbit, A. R., Raymond, W., Looney, M. R., Peters, M. C., Gordon, E. D., Woodruff, P. G., Lefrançois, E., Phillips, B. R., Mauger, D. T., Comhair, S. A., Erzurum, S. C., Johansson, M. W., Jarjour, N. N., Coverstone, A. M., Castro, M., Hastie, A. T., Bleecker, E. R., Fajt, M. L., ... Fahy, J. V. (2019). Extracellular DNA, Neutrophil Extracellular Traps, and Inflammasome Activation in Severe Asthma. *American journal of respiratory and critical care medicine*, 199(9), 1076–1085. <https://doi.org/10.1164/rccm.201810-1869OC>
- Lahaye**, X., Gentili, M., Silvin, A., Conrad, C., Picard, L., Jouve, M., Zueva, E., Maurin, M., Nadalin, F., Knott, G. J., Zhao, B., Du, F., Rio, M., Amiel, J., Fox, A. H., Li, P., Etienne, L., Bond, C. S., Colleaux, L., & Manel, N.

(2018). NONO Detects the Nuclear HIV Capsid to Promote cGAS-Mediated Innate Immune Activation. *Cell*, 175(2), 488–501.e22. <https://doi.org/10.1016/j.cell.2018.08.062>

Lamers, M. M., & Haagmans, B. L. (2022). SARS-CoV-2 pathogenesis. *Nature reviews. Microbiology*, 20(5), 270–284. <https://doi.org/10.1038/s41579-022-00713-0>

Land WG. Damage-associated molecular patterns in human diseases. Volume 1: Injury-Induced Innate Immune Responses. Cham, Springer International Publishing AG; 2018. <http://link.springer.com/10.1007/978-3-319-78655-1>.

Land WG. Damage-associated molecular patterns in human diseases. Vol. 2: Danger Signals as Diagnostics, Prognostics, and Therapeutic Targets. Cham, Springer International Publishing; 2020. <http://link.springer.com/10.1007/978-3-030-53868-2>.

Larkin, B., Ilyukha, V., Sorokin, M., Buzdin, A., Vannier, E., & Poltorak, A. (2017). Cutting Edge: Activation of STING in T Cells Induces Type I IFN Responses and Cell Death. *Journal of immunology* (Baltimore, Md. : 1950), 199(2), 397–402. <https://doi.org/10.4049/jimmunol.1601999>

Lazear, H. M., Schoggins, J. W., & Diamond, M. S. (2019). Shared and Distinct Functions of Type I and Type III Interferons. *Immunity*, 50(4), 907–923. <https://doi.org/10.1016/j.immuni.2019.03.025>

Lee, B. L., Mirrashidi, K. M., Stowe, I. B., Kummerfeld, S. K., Watanabe, C., Haley, B., Cuellar, T. L., Reichelt, M., & Kayagaki, N. (2018). ASC- and caspase-8-dependent apoptotic pathway diverges from the NLRC4 inflammasome in macrophages. *Scientific reports*, 8(1), 3788. <https://doi.org/10.1038/s41598-018-21998-3>

Lee, J. W., Chun, W., Lee, H. J., Min, J. H., Kim, S. M., Seo, J. Y., Ahn, K. S., & Oh, S. R. (2021). The Role of Macrophages in the Development of Acute and Chronic Inflammatory Lung Diseases. *Cells*, 10(4), 897. <https://doi.org/10.3390/cells10040897>

Lee, S., Karki, R., Wang, Y., Nguyen, L. N., Kalathur, R. C., & Kanneganti, T. D. (2021). AIM2 forms a complex with pyrin and ZBP1 to drive PANoptosis and host defence. *Nature*, 597(7876), 415–419. <https://doi.org/10.1038/s41586-021-03875-8>

Lefrançois, E., Mallavia, B., Zhuo, H., Calfee, C. S., & Looney, M. R. (2018). Maladaptive role of neutrophil extracellular traps in pathogen-induced lung injury. *JCI insight*, 3(3), e98178. <https://doi.org/10.1172/jci.insight.98178>

Lefrançois, E., Mallavia, B., Zhuo, H., Calfee, C. S., & Looney, M. R. (2018). Maladaptive role of neutrophil extracellular traps in pathogen-induced lung injury. *JCI insight*, 3(3), e98178. <https://doi.org/10.1172/jci.insight.98178>

Lemke G. (2019). How macrophages deal with death. *Nature reviews. Immunology*, 19(9), 539–549. <https://doi.org/10.1038/s41577-019-0167-y>

Lewis, H. D., Liddle, J., Coote, J. E., Atkinson, S. J., Barker, M. D., Bax, B. D., Bicker, K. L., Bingham, R. P., Campbell, M., Chen, Y. H., Chung, C. W., Craggs, P. D., Davis, R. P., Eberhard, D., Joberty, G., Lind, K. E., Locke, K., Maller, C., Martinod, K., Patten, C., ... Wilson, D. M. (2015). Inhibition of PAD4 activity is sufficient

to disrupt mouse and human NET formation. *Nature chemical biology*, 11(3), 189–191. <https://doi.org/10.1038/nchembio.1735>

Li, D., & Wu, M. (2021). Pattern recognition receptors in health and diseases. *Signal transduction and targeted therapy*, 6(1), 291. <https://doi.org/10.1038/s41392-021-00687-0>

Li, J., Duran, M. A., Dhanota, N., Chatila, W. K., Bettigole, S. E., Kwon, J., Sriram, R. K., Humphries, M. P., Salto-Tellez, M., James, J. A., Hanna, M. G., Melms, J. C., Vallabhaneni, S., Litchfield, K., Usaite, I., Biswas, D., Bareja, R., Li, H. W., Martin, M. L., Dorsaint, P., ... Bakhoun, S. F. (2021). Metastasis and Immune Evasion from Extracellular cGAMP Hydrolysis. *Cancer discovery*, 11(5), 1212–1227. <https://doi.org/10.1158/2159-8290.CD-20-0387>

Li, L., Yin, Q., Kuss, P., Maliga, Z., Millán, J. L., Wu, H., & Mitchison, T. J. (2014). Hydrolysis of 2'3'-cGAMP by ENPP1 and design of nonhydrolyzable analogs. *Nature chemical biology*, 10(12), 1043–1048. <https://doi.org/10.1038/nchembio.1661>

Li, M., Ferretti, M., Ying, B., Descamps, H., Lee, E., Dittmar, M., Lee, J. S., Whig, K., Kamalia, B., Dohnalová, L., Uhr, G., Zarkoob, H., Chen, Y. C., Ramage, H., Ferrer, M., Lynch, K., Schultz, D. C., Thaïss, C. A., Diamond, M. S., & Cherry, S. (2021). Pharmacological activation of STING blocks SARS-CoV-2 infection. *Science immunology*, 6(59), eabi9007. <https://doi.org/10.1126/sciimmunol.abi9007>

Li, M., Ferretti, M., Ying, B., Descamps, H., Lee, E., Dittmar, M., Lee, J. S., Whig, K., Kamalia, B., Dohnalová, L., Uhr, G., Zarkoob, H., Chen, Y. C., Ramage, H., Ferrer, M., Lynch, K., Schultz, D. C., Thaïss, C. A., Diamond, M. S., & Cherry, S. (2021). Pharmacological activation of STING blocks SARS-CoV-2 infection. *Science immunology*, 6(59), eabi9007. <https://doi.org/10.1126/sciimmunol.abi9007>

Li, M., Lyu, X., Liao, J., Werth, V. P., & Liu, M. L. (2022). Rho Kinase regulates neutrophil NET formation that is involved in UVB-induced skin inflammation. *Theranostics*, 12(5), 2133–2149. <https://doi.org/10.7150/thno.66457>

Li, Q., Tian, S., Liang, J., Fan, J., Lai, J., & Chen, Q. (2021). Therapeutic Development by Targeting the cGAS-STING Pathway in Autoimmune Disease and Cancer. *Frontiers in pharmacology*, 12, 779425. <https://doi.org/10.3389/fphar.2021.779425>

Li, Q., Tian, S., Liang, J., Fan, J., Lai, J., & Chen, Q. (2021). Therapeutic Development by Targeting the cGAS-STING Pathway in Autoimmune Disease and Cancer. *Frontiers in pharmacology*, 12, 779425. <https://doi.org/10.3389/fphar.2021.779425>

Li, S., Hong, Z., Wang, Z., Li, F., Mei, J., Huang, L., Lou, X., Zhao, S., Song, L., Chen, W., Wang, Q., Liu, H., Cai, Y., Yu, H., Xu, H., Zeng, G., Wang, Q., Zhu, J., Liu, X., Tan, N., ... Wang, C. (2018). The Cyclopeptide Astin C Specifically Inhibits the Innate Immune CDN Sensor STING. *Cell reports*, 25(12), 3405–3421.e7. <https://doi.org/10.1016/j.celrep.2018.11.097>

Li, S., Li, H., Zhang, Y. L., Xin, Q. L., Guan, Z. Q., Chen, X., Zhang, X. A., Li, X. K., Xiao, G. F., Lozach, P. Y., Cui, J., Liu, W., Zhang, L. K., & Peng, K. (2020). SFTSV Infection Induces BAK/BAX-Dependent Mitochondrial

DNA Release to Trigger NLRP3 Inflammasome Activation. *Cell reports*, 30(13), 4370–4385.e7. <https://doi.org/10.1016/j.celrep.2020.02.105>

Li, S., Zhang, Y., Guan, Z., Li, H., Ye, M., Chen, X., Shen, J., Zhou, Y., Shi, Z. L., Zhou, P., & Peng, K. (2020). SARS-CoV-2 triggers inflammatory responses and cell death through caspase-8 activation. *Signal transduction and targeted therapy*, 5(1), 235. <https://doi.org/10.1038/s41392-020-00334-0>

Li, X., Shu, C., Yi, G., Chaton, C. T., Shelton, C. L., Diao, J., Zuo, X., Kao, C. C., Herr, A. B., & Li, P. (2013). Cyclic GMP-AMP synthase is activated by double-stranded DNA-induced oligomerization. *Immunity*, 39(6), 1019–1031. <https://doi.org/10.1016/j.immuni.2013.10.019>

Li, X., Zhu, Y., Zhang, X., An, X., Weng, M., Shi, J., Wang, S., Liu, C., Luo, S., & Zheng, T. (2022). An alternatively spliced STING isoform localizes in the cytoplasmic membrane and directly senses extracellular cGAMP. *The Journal of clinical investigation*, 132(3), e144339. <https://doi.org/10.1172/JCI144339>

Li, X., Zhu, Y., Zhang, X., An, X., Weng, M., Shi, J., Wang, S., Liu, C., Luo, S., & Zheng, T. (2022). An alternatively spliced STING isoform localizes in the cytoplasmic membrane and directly senses extracellular cGAMP. *The Journal of clinical investigation*, 132(3), e144339. <https://doi.org/10.1172/JCI144339>

Li, Y., Li, M., Weigel, B., Mall, M., Werth, V. P., & Liu, M. L. (2020). Nuclear envelope rupture and NET formation is driven by PKC α -mediated lamin B disassembly. *EMBO reports*, 21(8), e48779. <https://doi.org/10.15252/embr.201948779>

Liang, J., Hong, Z., Sun, B., Guo, Z., Wang, C., & Zhu, J. (2021). The Alternatively Spliced Isoforms of Key Molecules in the cGAS-STING Signaling Pathway. *Frontiers in immunology*, 12, 771744. <https://doi.org/10.3389/fimmu.2021.771744>

Lim, H. F., & Nair, P. (2018). Airway Inflammation and Inflammatory Biomarkers. *Seminars in respiratory and critical care medicine*, 39(1), 56–63. <https://doi.org/10.1055/s-0037-1606217>

Lin, J., Huang, N., Li, J., Liu, X., Xiong, Q., Hu, C., Chen, D., Guan, L., Chang, K., Li, D., Tsui, S. K., Zhong, N., Liu, Z., & Yang, P. C. (2021). Cross-reactive antibodies against dust mite-derived enolase induce neutrophilic airway inflammation. *The European respiratory journal*, 57(1), 1902375. <https://doi.org/10.1183/13993003.02375-2019>

Lin, W. C., & Fessler, M. B. (2021). Regulatory mechanisms of neutrophil migration from the circulation to the airspace. *Cellular and molecular life sciences : CMLS*, 78(9), 4095–4124. <https://doi.org/10.1007/s00018-021-03768-z>

Linszen, R. S., Chai, G., Ma, J., Kummarapurugu, A. B., van Woensel, J. B. M., Bem, R. A., Kaler, L., Duncan, G. A., Zhou, L., Rubin, B. K., & Xu, Q. (2021). Neutrophil Extracellular Traps Increase Airway Mucus Viscoelasticity and Slow Mucus Particle Transit. *American journal of respiratory cell and molecular biology*, 64(1), 69–78. <https://doi.org/10.1165/rcmb.2020-0168OC>

Liu, C., Xiao, K., & Xie, L. (2022). Advances in the Regulation of Macrophage Polarization by Mesenchymal Stem Cells and Implications for ALI/ARDS Treatment. *Frontiers in immunology*, 13, 928134. <https://doi.org/10.3389/fimmu.2022.928134>

Liu, G., Wang, J., Park, Y. J., Tsuruta, Y., Lorne, E. F., Zhao, X., & Abraham, E. (2008). High mobility group protein-1 inhibits phagocytosis of apoptotic neutrophils through binding to phosphatidylserine. *Journal of immunology (Baltimore, Md. : 1950)*, 181(6), 4240–4246. <https://doi.org/10.4049/jimmunol.181.6.4240>

Liu, H., Zhang, H., Wu, X., Ma, D., Wu, J., Wang, L., Jiang, Y., Fei, Y., Zhu, C., Tan, R., Jungblut, P., Pei, G., Dorhoi, A., Yan, Q., Zhang, F., Zheng, R., Liu, S., Liang, H., Liu, Z., Yang, H., ... Ge, B. (2018). Nuclear cGAS suppresses DNA repair and promotes tumorigenesis. *Nature*, 563(7729), 131–136. <https://doi.org/10.1038/s41586-018-0629-6>

Liu, S., Su, X., Pan, P., Zhang, L., Hu, Y., Tan, H., Wu, D., Liu, B., Li, H., Li, H., Li, Y., Dai, M., Li, Y., Hu, C., & Tsung, A. (2016). Neutrophil extracellular traps are indirectly triggered by lipopolysaccharide and contribute to acute lung injury. *Scientific reports*, 6, 37252. <https://doi.org/10.1038/srep37252>

Liu, Y., Du, X., Chen, J., Jin, Y., Peng, L., Wang, H. H. X., Luo, M., Chen, L., & Zhao, Y. (2020). Neutrophil-to-lymphocyte ratio as an independent risk factor for mortality in hospitalized patients with COVID-19. *The Journal of infection*, 81(1), e6–e12. <https://doi.org/10.1016/j.jinf.2020.04.002>

Liu, Y., Du, X., Chen, J., Jin, Y., Peng, L., Wang, H. H. X., Luo, M., Chen, L., & Zhao, Y. (2020). Neutrophil-to-lymphocyte ratio as an independent risk factor for mortality in hospitalized patients with COVID-19. *The Journal of infection*, 81(1), e6–e12. <https://doi.org/10.1016/j.jinf.2020.04.002>

Livingstone, S. A., Wildi, K. S., Dalton, H. J., Usman, A., Ki, K. K., Passmore, M. R., Li Bassi, G., Suen, J. Y., & Fraser, J. F. (2021). Coagulation Dysfunction in Acute Respiratory Distress Syndrome and Its Potential Impact in Inflammatory Subphenotypes. *Frontiers in medicine*, 8, 723217. <https://doi.org/10.3389/fmed.2021.723217>

Lohard, S., Bourgeois, N., Maillet, L., Gautier, F., Fétiveau, A., Lasla, H., Nguyen, F., Vuillier, C., Dumont, A., Moreau-Aubry, A., Frapin, M., David, L., Loussouarn, D., Kerdraon, O., Campone, M., Jézéquel, P., Juin, P. P., & Barillé-Nion, S. (2020). STING-dependent paracrine shapes apoptotic priming of breast tumors in response to anti-mitotic treatment. *Nature communications*, 11(1), 259. <https://doi.org/10.1038/s41467-019-13689-y>

Low, J. T., Chandramohan, V., Bowie, M. L., Brown, M. C., Waitkus, M. S., Briley, A., Stevenson, K., Fuller, R., Reitman, Z. J., Muscat, A. M., Hariharan, S., Hostettler, J., Danehower, S., Baker, A., Khasraw, M., Wong, N. C., Gregory, S., Nair, S. K., Heimberger, A., Gromeier, M., ... Ashley, D. M. (2022). Epigenetic STING silencing is developmentally conserved in gliomas and can be rescued by methyltransferase inhibition. *Cancer cell*, 40(5), 439–440. <https://doi.org/10.1016/j.ccell.2022.04.009>

Luteijn, R. D., Zaver, S. A., Gowen, B. G., Wyman, S. K., Garelis, N. E., Onia, L., McWhirter, S. M., Katibah, G. E., Corn, J. E., Woodward, J. J., & Raulet, D. H. (2019). SLC19A1 transports immunoreactive cyclic dinucleotides. *Nature*, 573(7774), 434–438. <https://doi.org/10.1038/s41586-019-1553-0>

Ma, R., Li, T., Cao, M., Si, Y., Wu, X., Zhao, L., Yao, Z., Zhang, Y., Fang, S., Deng, R., Novakovic, V. A., Bi, Y., Kou, J., Yu, B., Yang, S., Wang, J., Zhou, J., & Shi, J. (2016). Extracellular DNA traps released by acute

promyelocytic leukemia cells through autophagy. *Cell death & disease*, 7(6), e2283. <https://doi.org/10.1038/cddis.2016.186>

Ma, R., Ortiz Serrano, T. P., Davis, J., Prigge, A. D., & Ridge, K. M. (2020). The cGAS-STING pathway: The role of self-DNA sensing in inflammatory lung disease. *FASEB journal : official publication of the Federation of American Societies for Experimental Biology*, 34(10), 13156–13170. <https://doi.org/10.1096/fj.202001607R>

Ma, Y., Yabluchanskiy, A., Iyer, R. P., Cannon, P. L., Flynn, E. R., Jung, M., Henry, J., Cates, C. A., Deleon-Pennell, K. Y., & Lindsey, M. L. (2016). Temporal neutrophil polarization following myocardial infarction. *Cardiovascular research*, 110(1), 51–61. <https://doi.org/10.1093/cvr/cvw024>

Mackenzie, K. J., Carroll, P., Martin, C. A., Murina, O., Fluteau, A., Simpson, D. J., Olova, N., Sutcliffe, H., Rainger, J. K., Leitch, A., Osborn, R. T., Wheeler, A. P., Nowotny, M., Gilbert, N., Chandra, T., Reijns, M. A. M., & Jackson, A. P. (2017). cGAS surveillance of micronuclei links genome instability to innate immunity. *Nature*, 548(7668), 461–465. <https://doi.org/10.1038/nature23449>

Malireddi, R. K. S., Gurung, P., Kesavardhana, S., Samir, P., Burton, A., Mummareddy, H., Vogel, P., Pelletier, S., Burgula, S., & Kanneganti, T. D. (2020). Innate immune priming in the absence of TAK1 drives RIPK1 kinase activity-independent pyroptosis, apoptosis, necroptosis, and inflammatory disease. *The Journal of experimental medicine*, 217(3), jem.20191644. <https://doi.org/10.1084/jem.20191644>

Malireddi, R. K. S., Gurung, P., Mavuluri, J., Dasari, T. K., Klco, J. M., Chi, H., & Kanneganti, T. D. (2018). TAK1 restricts spontaneous NLRP3 activation and cell death to control myeloid proliferation. *The Journal of experimental medicine*, 215(4), 1023–1034. <https://doi.org/10.1084/jem.20171922>

Malireddi, R. K. S., Kesavardhana, S., & Kanneganti, T. D. (2019). ZBP1 and TAK1: Master Regulators of NLRP3 Inflammasome/Pyroptosis, Apoptosis, and Necroptosis (PAN-optosis). *Frontiers in cellular and infection microbiology*, 9, 406. <https://doi.org/10.3389/fcimb.2019.00406>

Malyshev, I., & Malyshev, Y. (2015). Current Concept and Update of the Macrophage Plasticity Concept: Intracellular Mechanisms of Reprogramming and M3 Macrophage "Switch" Phenotype. *BioMed research international*, 2015, 341308. <https://doi.org/10.1155/2015/341308>

Man, S. M., Karki, R., Malireddi, R. K., Neale, G., Vogel, P., Yamamoto, M., Lamkanfi, M., & Kanneganti, T. D. (2015). The transcription factor IRF1 and guanylate-binding proteins target activation of the AIM2 inflammasome by Francisella infection. *Nature immunology*, 16(5), 467–475. <https://doi.org/10.1038/ni.3118>

Mandal, R., Barrón, J. C., Kostova, I., Becker, S., & Strebhardt, K. (2020). Caspase-8: The double-edged sword. *Biochimica et biophysica acta. Reviews on cancer*, 1873(2), 188357. <https://doi.org/10.1016/j.bbcan.2020.188357>

Mankan, A. K., Schmidt, T., Chauhan, D., Goldeck, M., Höning, K., Gaidt, M., Kubarenko, A. V., Andreeva, L., Hopfner, K. P., & Hornung, V. (2014). Cytosolic RNA:DNA hybrids activate the cGAS-STING axis. *The EMBO journal*, 33(24), 2937–2946. <https://doi.org/10.15252/emboj.201488726>

Mantovani, A., Cassatella, M. A., Costantini, C., & Jaillon, S. (2011). Neutrophils in the activation and regulation of innate and adaptive immunity. *Nature reviews. Immunology*, 11(8), 519–531. <https://doi.org/10.1038/nri3024>

- Mantovani, A.,** Cassatella, M. A., Costantini, C., & Jaillon, S. (2011). Neutrophils in the activation and regulation of innate and adaptive immunity. *Nature reviews. Immunology*, 11(8), 519–531. <https://doi.org/10.1038/nri3024>
- Marani, M.,** Katul, G. G., Pan, W. K., & Parolari, A. J. (2021). Intensity and frequency of extreme novel epidemics. *Proceedings of the National Academy of Sciences of the United States of America*, 118(35), e2105482118. <https://doi.org/10.1073/pnas.2105482118>
- Marichal, T.,** Ohata, K., Bedoret, D., Mesnil, C., Sabatel, C., Kobiyama, K., Lekeux, P., Coban, C., Akira, S., Ishii, K. J., Bureau, F., & Desmet, C. J. (2011). DNA released from dying host cells mediates aluminum adjuvant activity. *Nature medicine*, 17(8), 996–1002. <https://doi.org/10.1038/nm.2403>
- Massberg, S.,** Grahl, L., von Bruehl, M. L., Manukyan, D., Pfeiler, S., Goosmann, C., Brinkmann, V., Lorenz, M., Bidzhekov, K., Khandagale, A. B., Konrad, I., Kennerknecht, E., Reges, K., Holdenrieder, S., Braun, S., Reinhardt, C., Spannagl, M., Preissner, K. T., & Engelmann, B. (2010). Reciprocal coupling of coagulation and innate immunity via neutrophil serine proteases. *Nature medicine*, 16(8), 887–896. <https://doi.org/10.1038/nm.2184>
- Matthay M. A.** (2014). Resolution of pulmonary edema. Thirty years of progress. *American journal of respiratory and critical care medicine*, 189(11), 1301–1308. <https://doi.org/10.1164/rccm.201403-0535OE>
- Matthay, M. A.,** Ware, L. B., & Zimmerman, G. A. (2012). The acute respiratory distress syndrome. *The Journal of clinical investigation*, 122(8), 2731–2740. <https://doi.org/10.1172/JCI60331>
- Matthay, M. A.,** Zemans, R. L., Zimmerman, G. A., Arabi, Y. M., Beitler, J. R., Mercat, A., Herridge, M., Randolph, A. G., & Calfee, C. S. (2019). Acute respiratory distress syndrome. *Nature reviews. Disease primers*, 5(1), 18. <https://doi.org/10.1038/s41572-019-0069-0>
- McKee, A. S.,** Burchill, M. A., Munks, M. W., Jin, L., Kappler, J. W., Friedman, R. S., Jacobelli, J., & Marrack, P. (2013). Host DNA released in response to aluminum adjuvant enhances MHC class II-mediated antigen presentation and prolongs CD4 T-cell interactions with dendritic cells. *Proceedings of the National Academy of Sciences of the United States of America*, 110(12), E1122–E1131. <https://doi.org/10.1073/pnas.1300392110>
- McKnight, K. L.,** Swanson, K. V., Austgen, K., Richards, C., Mitchell, J. K., McGivern, D. R., Fritch, E., Johnson, J., Remlinger, K., Magid-Slav, M., Kapustina, M., You, S., & Lemon, S. M. (2020). Stimulator of interferon genes (STING) is an essential proviral host factor for human rhinovirus species A and C. *Proceedings of the National Academy of Sciences of the United States of America*, 117(44), 27598–27607. <https://doi.org/10.1073/pnas.2014940117>
- McPhillips, K.,** Janssen, W. J., Ghosh, M., Byrne, A., Gardai, S., Remigio, L., Bratton, D. L., Kang, J. L., & Henson, P. (2007). TNF-alpha inhibits macrophage clearance of apoptotic cells via cytosolic phospholipase A2 and oxidant-dependent mechanisms. *Journal of immunology (Baltimore, Md. : 1950)*, 178(12), 8117–8126. <https://doi.org/10.4049/jimmunol.178.12.8117>
- Metzler, K. D.,** Goosmann, C., Lubojemska, A., Zychlinsky, A., & Papayannopoulos, V. (2014). A myeloperoxidase-containing complex regulates neutrophil elastase release and actin dynamics during NETosis. *Cell reports*, 8(3), 883–896. <https://doi.org/10.1016/j.celrep.2014.06.044>

- Mihaila**, A. C., Ciortan, L., Macarie, R. D., Vadana, M., Cecoltan, S., Preda, M. B., Hudita, A., Gan, A. M., Jakobsson, G., Tucureanu, M. M., Barbu, E., Balanescu, S., Simionescu, M., Schiopu, A., & Butoi, E. (2021). Transcriptional Profiling and Functional Analysis of N1/N2 Neutrophils Reveal an Immunomodulatory Effect of S100A9-Blockade on the Pro-Inflammatory N1 Subpopulation. *Frontiers in immunology*, 12, 708770. <https://doi.org/10.3389/fimmu.2021.708770>
- Mincham**, K. T., Bruno, N., Singanayagam, A., & Snelgrove, R. J. (2021). Our evolving view of neutrophils in defining the pathology of chronic lung disease. *Immunology*, 164(4), 701–721. <https://doi.org/10.1111/imm.13419>
- Mishra** P, Pandey N, Pandey R, Tripathi YB. Role of Macrophage Polarization in Acute Respiratory Distress Syndrome. *Journal of Respiration*. 2021; 1(4):260-272. <https://doi.org/10.3390/jor1040024>
- Moffatt**, M. F., Gut, I. G., Demenais, F., Strachan, D. P., Bouzigon, E., Heath, S., von Mutius, E., Farrall, M., Lathrop, M., Cookson, W. O. C. M., & GABRIEL Consortium (2010). A large-scale, consortium-based genomewide association study of asthma. *The New England journal of medicine*, 363(13), 1211–1221. <https://doi.org/10.1056/NEJMoa0906312>
- Mompeán**, M., Li, W., Li, J., Laage, S., Siemer, A. B., Bozkurt, G., Wu, H., & McDermott, A. E. (2018). The Structure of the Necrosome RIPK1-RIPK3 Core, a Human Hetero-Amyloid Signaling Complex. *Cell*, 173(5), 1244–1253.e10. <https://doi.org/10.1016/j.cell.2018.03.032>
- Monteleone**, M., Stow, J. L., & Schroder, K. (2015). Mechanisms of unconventional secretion of IL-1 family cytokines. *Cytokine*, 74(2), 213–218. <https://doi.org/10.1016/j.cyto.2015.03.022>
- Moore**, W. C., Meyers, D. A., Wenzel, S. E., Teague, W. G., Li, H., Li, X., D'Agostino, R., Jr, Castro, M., Curran-Everett, D., Fitzpatrick, A. M., Gaston, B., Jarjour, N. N., Sorkness, R., Calhoun, W. J., Chung, K. F., Comhair, S. A., Dweik, R. A., Israel, E., Peters, S. P., Busse, W. W., ... National Heart, Lung, and Blood Institute's Severe Asthma Research Program (2010). Identification of asthma phenotypes using cluster analysis in the Severe Asthma Research Program. *American journal of respiratory and critical care medicine*, 181(4), 315–323. <https://doi.org/10.1164/rccm.200906-0896OC>
- Moretti**, J., Roy, S., Bozec, D., Martinez, J., Chapman, J. R., Ueberheide, B., Lamming, D. W., Chen, Z. J., Horng, T., Yeretssian, G., Green, D. R., & Blander, J. M. (2017). STING Senses Microbial Viability to Orchestrate Stress-Mediated Autophagy of the Endoplasmic Reticulum. *Cell*, 171(4), 809–823.e13. <https://doi.org/10.1016/j.cell.2017.09.034>
- Morrone**, S. R., Wang, T., Constantoulakis, L. M., Hooy, R. M., Delannoy, M. J., & Sohn, J. (2014). Cooperative assembly of IFI16 filaments on dsDNA provides insights into host defense strategy. *Proceedings of the National Academy of Sciences of the United States of America*, 111(1), E62–E71. <https://doi.org/10.1073/pnas.1313577111>
- Motwani**, M., Pesiridis, S., & Fitzgerald, K. A. (2019). DNA sensing by the cGAS-STING pathway in health and disease. *Nature reviews. Genetics*, 20(11), 657–674. <https://doi.org/10.1038/s41576-019-0151-1>
- Mould**, K. J., Jackson, N. D., Henson, P. M., Seibold, M., & Janssen, W. J. (2019). Single cell RNA sequencing identifies unique inflammatory airspace macrophage subsets. *JCI insight*, 4(5), e126556. <https://doi.org/10.1172/jci.insight.126556>

- Mukai, K., Konno, H., Akiba, T., Uemura, T., Waguri, S., Kobayashi, T., Barber, G. N., Arai, H., & Taguchi, T.** (2016). Activation of STING requires palmitoylation at the Golgi. *Nature communications*, 7, 11932. <https://doi.org/10.1038/ncomms11932>
- Müller-Redetzky, H. C., Suttorp, N., & Witznath, M.** (2014). Dynamics of pulmonary endothelial barrier function in acute inflammation: mechanisms and therapeutic perspectives. *Cell and tissue research*, 355(3), 657–673. <https://doi.org/10.1007/s00441-014-1821-0>
- Münzer, P., Negro, R., Fukui, S., di Meglio, L., Aymonnier, K., Chu, L., Cherpokova, D., Gutch, S., Sorvillo, N., Shi, L., Magupalli, V. G., Weber, A. N. R., Scharf, R. E., Waterman, C. M., Wu, H., & Wagner, D. D.** (2021). NLRP3 Inflammasome Assembly in Neutrophils Is Supported by PAD4 and Promotes NETosis Under Sterile Conditions. *Frontiers in immunology*, 12, 683803. <https://doi.org/10.3389/fimmu.2021.683803>
- Murray, P. J., Allen, J. E., Biswas, S. K., Fisher, E. A., Gilroy, D. W., Goerdts, S., Gordon, S., Hamilton, J. A., Ivashkiv, L. B., Lawrence, T., Locati, M., Mantovani, A., Martinez, F. O., Mege, J. L., Mosser, D. M., Natoli, G., Saeij, J. P., Schultze, J. L., Shirey, K. A., Sica, A., ... Wynn, T. A.** (2014). Macrophage activation and polarization: nomenclature and experimental guidelines. *Immunity*, 41(1), 14–20. <https://doi.org/10.1016/j.immuni.2014.06.008>
- Murthy, A. M. V., Robinson, N., & Kumar, S.** (2020). Crosstalk between cGAS-STING signaling and cell death. *Cell death and differentiation*, 27(11), 2989–3003. <https://doi.org/10.1038/s41418-020-00624-8>
- Nagata, S., & Tanaka, M.** (2017). Programmed cell death and the immune system. *Nature reviews. Immunology*, 17(5), 333–340. <https://doi.org/10.1038/nri.2016.153>
- Nair, P., & Prabhavalkar, K. S.** (2020). Neutrophilic Asthma and Potentially Related Target Therapies. *Current drug targets*, 21(4), 374–388. <https://doi.org/10.2174/1389450120666191011162526>
- Nakashima, K., Arai, S., Suzuki, A., Nariai, Y., Urano, T., Nakayama, M., Ohara, O., Yamamura, K., Yamamoto, K., & Miyazaki, T.** (2013). PAD4 regulates proliferation of multipotent haematopoietic cells by controlling c-myc expression. *Nature communications*, 4, 1836. <https://doi.org/10.1038/ncomms2862>
- Narasaraju, T., Yang, E., Samy, R. P., Ng, H. H., Poh, W. P., Liew, A. A., Phoon, M. C., van Rooijen, N., & Chow, V. T.** (2011). Excessive neutrophils and neutrophil extracellular traps contribute to acute lung injury of influenza pneumonitis. *The American journal of pathology*, 179(1), 199–210. <https://doi.org/10.1016/j.ajpath.2011.03.013>
- Nascimento, M., Gombault, A., Lacerda-Queiroz, N., Panek, C., Savigny, F., Sbeity, M., Bourinet, M., Le Bert, M., Riteau, N., Ryffel, B., Quesniaux, V. F. J., & Couillin, I.** (2019). Self-DNA release and STING-dependent sensing drives inflammation to cigarette smoke in mice. *Scientific reports*, 9(1), 14848. <https://doi.org/10.1038/s41598-019-51427-y>
- Neubert, E., Meyer, D., Rocca, F., Günay, G., Kwaczala-Tessmann, A., Grandke, J., Senger-Sander, S., Geisler, C., Egner, A., Schön, M. P., Erpenbeck, L., & Kruss, S.** (2018). Chromatin swelling drives neutrophil extracellular trap release. *Nature communications*, 9(1), 3767. <https://doi.org/10.1038/s41467-018-06263-5>

- Ning, X., Wang, Y., Jing, M., Sha, M., Lv, M., Gao, P., Zhang, R., Huang, X., Feng, J. M., & Jiang, Z. (2019).** Apoptotic Caspases Suppress Type I Interferon Production via the Cleavage of cGAS, MAVS, and IRF3. *Molecular cell*, 74(1), 19–31.e7. <https://doi.org/10.1016/j.molcel.2019.02.013>
- Nishida, Y., Yagi, H., Ota, M., Tanaka, A., Sato, K., Inoue, T., Yamada, S., Arakawa, N., Ishige, T., Kobayashi, Y., Arakawa, H., & Takizawa, T. (2023).** Oxidative stress induces MUC5AC expression through mitochondrial damage-dependent STING signaling in human bronchial epithelial cells. *FASEB bioAdvances*, 5(4), 171–181. <https://doi.org/10.1096/fba.2022-00081>
- Novosad, J., Krčmová, I., Souček, O., Drahošová, M., Sedlák, V., Kulířová, M., & Králíčková, P. (2023).** Subsets of Eosinophils in Asthma, a Challenge for Precise Treatment. *International journal of molecular sciences*, 24(6), 5716. <https://doi.org/10.3390/ijms24065716>
- Nunokawa, H., Murakami, Y., Ishii, T., Narita, T., Ishii, H., Takizawa, H., & Yamashita, N. (2021).** Crucial role of stimulator of interferon genes-dependent signaling in house dust mite extract-induced IgE production. *Scientific reports*, 11(1), 13157. <https://doi.org/10.1038/s41598-021-92561-w>
- Nye, S., Whitley, R. J., & Kong, M. (2016).** Viral Infection in the Development and Progression of Pediatric Acute Respiratory Distress Syndrome. *Frontiers in pediatrics*, 4, 128. <https://doi.org/10.3389/fped.2016.00128>
- Nyenhuis, S. M., Alumkal, P., Du, J., Maybruck, B. T., Vinicky, M., & Ackerman, S. J. (2019).** Charcot-Leyden crystal protein/galectin-10 is a surrogate biomarker of eosinophilic airway inflammation in asthma. *Biomarkers in medicine*, 13(9), 715–724. <https://doi.org/10.2217/bmm-2018-0280>
- Orning, P., & Lien, E. (2021).** Multiple roles of caspase-8 in cell death, inflammation, and innate immunity. *Journal of leukocyte biology*, 109(1), 121–141. <https://doi.org/10.1002/JLB.3MR0420-305R>
- Pagie, S., Gérard, N., & Charreau, B. (2018).** Notch signaling triggered via the ligand DLL4 impedes M2 macrophage differentiation and promotes their apoptosis. *Cell communication and signaling : CCS*, 16(1), 4. <https://doi.org/10.1186/s12964-017-0214-x>
- Paludan, S. R., Reinert, L. S., & Hornung, V. (2019).** DNA-stimulated cell death: implications for host defence, inflammatory diseases and cancer. *Nature reviews. Immunology*, 19(3), 141–153. <https://doi.org/10.1038/s41577-018-0117-0>
- Paludan, S. R., Reinert, L. S., & Hornung, V. (2019).** DNA-stimulated cell death: implications for host defence, inflammatory diseases and cancer. *Nature reviews. Immunology*, 19(3), 141–153. <https://doi.org/10.1038/s41577-018-0117-0>
- Pan, B. S., Perera, S. A., Piesvaux, J. A., Presland, J. P., Schroeder, G. K., Cumming, J. N., Trotter, B. W., Altman, M. D., Buevich, A. V., Cash, B., Cemerski, S., Chang, W., Chen, Y., Dandliker, P. J., Feng, G., Haidle, A., Henderson, T., Jewell, J., Kariv, I., Knemeyer, I., ... Addona, G. H. (2020).** An orally available non-nucleotide STING agonist with antitumor activity. *Science (New York, N.Y.)*, 369(6506), eaba6098. <https://doi.org/10.1126/science.aba6098>
- Pan, B., Zheng, B., Xing, C., & Liu, J. (2022).** Non-Canonical Programmed Cell Death in Colon Cancer. *Cancers*, 14(14), 3309. <https://doi.org/10.3390/cancers14143309>

- Pan, Y., You, Y., Sun, L., Sui, Q., Liu, L., Yuan, H., Chen, C., Liu, J., Wen, X., Dai, L., & Sun, H. (2021).** The STING antagonist H-151 ameliorates psoriasis via suppression of STING/NF- κ B-mediated inflammation. *British journal of pharmacology*, 178(24), 4907–4922. <https://doi.org/10.1111/bph.15673>
- Pandian, N., & Kanneganti, T. D. (2022).** PANoptosis: A Unique Innate Immune Inflammatory Cell Death Modality. *Journal of immunology (Baltimore, Md. : 1950)*, 209(9), 1625–1633. <https://doi.org/10.4049/jimmunol.2200508>
- Papayannopoulos V. (2018).** Neutrophil extracellular traps in immunity and disease. *Nature reviews. Immunology*, 18(2), 134–147. <https://doi.org/10.1038/nri.2017.105>
- Papayannopoulos, V., Metzler, K. D., Hakkim, A., & Zychlinsky, A. (2010).** Neutrophil elastase and myeloperoxidase regulate the formation of neutrophil extracellular traps. *The Journal of cell biology*, 191(3), 677–691. <https://doi.org/10.1083/jcb.201006052>
- Papi, A., Brightling, C., Pedersen, S. E., & Reddel, H. K. (2018).** Asthma. *Lancet (London, England)*, 391(10122), 783–800. [https://doi.org/10.1016/S0140-6736\(17\)33311-1](https://doi.org/10.1016/S0140-6736(17)33311-1)
- Pastukh, V. M., Zhang, L., Ruchko, M. V., Gorodnya, O., Bardwell, G. C., Tuder, R. M., & Gillespie, M. N. (2011).** Oxidative DNA damage in lung tissue from patients with COPD is clustered in functionally significant sequences. *International journal of chronic obstructive pulmonary disease*, 6, 209–217. <https://doi.org/10.2147/COPD.S15922>
- Persson, E. K., Verstraete, K., Heyndrickx, I., Gevaert, E., Aegerter, H., Percier, J. M., Deswarte, K., Verschueren, K. H. G., Dansercoer, A., Gras, D., Chanez, P., Bachert, C., Gonçalves, A., Van Gorp, H., De Haard, H., Blanchetot, C., Saunders, M., Hammad, H., Savvides, S. N., & Lambrecht, B. N. (2019).** Protein crystallization promotes type 2 immunity and is reversible by antibody treatment. *Science (New York, N.Y.)*, 364(6442), eaaw4295. <https://doi.org/10.1126/science.aaw4295>
- Peters, M. C., McGrath, K. W., Hawkins, G. A., Hastie, A. T., Levy, B. D., Israel, E., Phillips, B. R., Mager, D. T., Comhair, S. A., Erzurum, S. C., Johansson, M. W., Jarjour, N. N., Coverstone, A. M., Castro, M., Holguin, F., Wenzel, S. E., Woodruff, P. G., Bleecker, E. R., Fahy, J. V., & National Heart, Lung, and Blood Institute Severe Asthma Research Program (2016).** Plasma interleukin-6 concentrations, metabolic dysfunction, and asthma severity: a cross-sectional analysis of two cohorts. *The Lancet. Respiratory medicine*, 4(7), 574–584. [https://doi.org/10.1016/S2213-2600\(16\)30048-0](https://doi.org/10.1016/S2213-2600(16)30048-0)
- Peters, M. C., Ringel, L., Dyjack, N., Herrin, R., Woodruff, P. G., Rios, C., O'Connor, B., Fahy, J. V., & Seibold, M. A. (2019).** A Transcriptomic Method to Determine Airway Immune Dysfunction in T2-High and T2-Low Asthma. *American journal of respiratory and critical care medicine*, 199(4), 465–477. <https://doi.org/10.1164/rccm.201807-1291OC>
- Petrasek, J., Iracheta-Vellve, A., Csak, T., Satishchandran, A., Kodys, K., Kurt-Jones, E. A., Fitzgerald, K. A., & Szabo, G. (2013).** STING-IRF3 pathway links endoplasmic reticulum stress with hepatocyte apoptosis in early alcoholic liver disease. *Proceedings of the National Academy of Sciences of the United States of America*, 110(41), 16544–16549. <https://doi.org/10.1073/pnas.1308331110>

- Petretto, A., Bruschi, M., Pratesi, F., Croia, C., Candiano, G., Ghiggeri, G., & Migliorini, P.** (2019). Neutrophil extracellular traps (NET) induced by different stimuli: A comparative proteomic analysis. *PloS one*, 14(7), e0218946. <https://doi.org/10.1371/journal.pone.0218946>
- Pierini, R., Juruj, C., Perret, M., Jones, C. L., Mangeot, P., Weiss, D. S., & Henry, T.** (2012). AIM2/ASC triggers caspase-8-dependent apoptosis in Francisella-infected caspase-1-deficient macrophages. *Cell death and differentiation*, 19(10), 1709–1721. <https://doi.org/10.1038/cdd.2012.51>
- Pillay, J., Kamp, V. M., van Hoffen, E., Visser, T., Tak, T., Lammers, J. W., Ulfman, L. H., Leenen, L. P., Pickkers, P., & Koenderman, L.** (2012). A subset of neutrophils in human systemic inflammation inhibits T cell responses through Mac-1. *The Journal of clinical investigation*, 122(1), 327–336. <https://doi.org/10.1172/JCI57990>
- Pillay, J., Ramakers, B. P., Kamp, V. M., Loi, A. L., Lam, S. W., Hietbrink, F., Leenen, L. P., Tool, A. T., Pickkers, P., & Koenderman, L.** (2010). Functional heterogeneity and differential priming of circulating neutrophils in human experimental endotoxemia. *Journal of leukocyte biology*, 88(1), 211–220. <https://doi.org/10.1189/jlb.1209793>
- Pilszczek, F. H., Salina, D., Poon, K. K., Fahey, C., Yipp, B. G., Sibley, C. D., Robbins, S. M., Green, F. H., Surette, M. G., Sugai, M., Bowden, M. G., Hussain, M., Zhang, K., & Kubes, P.** (2010). A novel mechanism of rapid nuclear neutrophil extracellular trap formation in response to *Staphylococcus aureus*. *Journal of immunology* (Baltimore, Md. : 1950), 185(12), 7413–7425. <https://doi.org/10.4049/jimmunol.1000675>
- Pisetsky D. S.** (2012). The origin and properties of extracellular DNA: from PAMP to DAMP. *Clinical immunology* (Orlando, Fla.), 144(1), 32–40. <https://doi.org/10.1016/j.clim.2012.04.006>
- Place, D. E., Lee, S., & Kanneganti, T. D.** (2021). PANoptosis in microbial infection. *Current opinion in microbiology*, 59, 42–49. <https://doi.org/10.1016/j.mib.2020.07.012>
- Plantinga, M., Guilliams, M., Vanheerswyngheles, M., Deswarte, K., Branco-Madeira, F., Toussaint, W., Vanhoutte, L., Neyt, K., Killeen, N., Malissen, B., Hammad, H., & Lambrecht, B. N.** (2013). Conventional and monocyte-derived CD11b(+) dendritic cells initiate and maintain T helper 2 cell-mediated immunity to house dust mite allergen. *Immunity*, 38(2), 322–335. <https://doi.org/10.1016/j.immuni.2012.10.016>
- Poli, V., & Zanoni, I.** (2023). Neutrophil intrinsic and extrinsic regulation of NETosis in health and disease. *Trends in microbiology*, 31(3), 280–293. <https://doi.org/10.1016/j.tim.2022.10.002>
- Porte, R., Davoudian, S., Asgari, F., Parente, R., Mantovani, A., Garlanda, C., & Bottazzi, B.** (2019). The Long Pentraxin PTX3 as a Humoral Innate Immunity Functional Player and Biomarker of Infections and Sepsis. *Frontiers in immunology*, 10, 794. <https://doi.org/10.3389/fimmu.2019.00794>
- Porto, B. N., & Stein, R. T.** (2016). Neutrophil Extracellular Traps in Pulmonary Diseases: Too Much of a Good Thing?. *Frontiers in immunology*, 7, 311. <https://doi.org/10.3389/fimmu.2016.00311>
- Radermecker, C., Detrembleur, N., Guiot, J., Cavalier, E., Henket, M., d'Emal, C., Vanwinge, C., Cataldo, D., Oury, C., Delvenne, P., & Marichal, T.** (2020). Neutrophil extracellular traps infiltrate the lung airway, interstitial,

and vascular compartments in severe COVID-19. *The Journal of experimental medicine*, 217(12), e20201012. <https://doi.org/10.1084/jem.20201012>

Radermecker, C., Detrembleur, N., Guiot, J., Cavalier, E., Henket, M., d'Emal, C., Vanwinge, C., Cataldo, D., Oury, C., Delvenne, P., & Marichal, T. (2020). Neutrophil extracellular traps infiltrate the lung airway, interstitial, and vascular compartments in severe COVID-19. *The Journal of experimental medicine*, 217(12), e20201012. <https://doi.org/10.1084/jem.20201012>

Radermecker, C., Sabatel, C., Vanwinge, C., Ruscitti, C., Maréchal, P., Perin, F., Schyns, J., Rocks, N., Toussaint, M., Cataldo, D., Johnston, S. L., Bureau, F., & Marichal, T. (2019). Locally instructed CXCR4hi neutrophils trigger environment-driven allergic asthma through the release of neutrophil extracellular traps. *Nature immunology*, 20(11), 1444–1455. <https://doi.org/10.1038/s41590-019-0496-9>

Radermecker, C., Sabatel, C., Vanwinge, C., Ruscitti, C., Maréchal, P., Perin, F., Schyns, J., Rocks, N., Toussaint, M., Cataldo, D., Johnston, S. L., Bureau, F., & Marichal, T. (2019). Locally instructed CXCR4hi neutrophils trigger environment-driven allergic asthma through the release of neutrophil extracellular traps. *Nature immunology*, 20(11), 1444–1455. <https://doi.org/10.1038/s41590-019-0496-9>

Ragnoli, B., Morjaria, J., Pignatti, P., Montuschi, P., Barbieri, M., Mondini, L., Ruggero, L., Trotta, L., & Malerba, M. (2022). Dupilumab and tezepelumab in severe refractory asthma: new opportunities. *Therapeutic advances in chronic disease*, 13, 20406223221097327. <https://doi.org/10.1177/20406223221097327>

Rajput, A., Kovalenko, A., Bogdanov, K., Yang, S. H., Kang, T. B., Kim, J. C., Du, J., & Wallach, D. (2011). RIG-I RNA helicase activation of IRF3 transcription factor is negatively regulated by caspase-8-mediated cleavage of the RIP1 protein. *Immunity*, 34(3), 340–351. <https://doi.org/10.1016/j.immuni.2010.12.018>

Ramanjulu, J. M., Pesiridis, G. S., Yang, J., Concha, N., Singhaus, R., Zhang, S. Y., Tran, J. L., Moore, P., Lehmann, S., Eberl, H. C., Muelbauer, M., Schneck, J. L., Clemens, J., Adam, M., Mehlmann, J., Romano, J., Morales, A., Kang, J., Leister, L., Graybill, T. L., ... Bertin, J. (2018). Design of amidobenzimidazole STING receptor agonists with systemic activity. *Nature*, 564(7736), 439–443. <https://doi.org/10.1038/s41586-018-0705-y>

Rathinam, V. A., Vanaja, S. K., Waggoner, L., Sokolovska, A., Becker, C., Stuart, L. M., Leong, J. M., & Fitzgerald, K. A. (2012). TRIF licenses caspase-11-dependent NLRP3 inflammasome activation by gram-negative bacteria. *Cell*, 150(3), 606–619. <https://doi.org/10.1016/j.cell.2012.07.007>

Ray, C. A., & Pickup, D. J. (1996). The mode of death of pig kidney cells infected with cowpox virus is governed by the expression of the crmA gene. *Virology*, 217(1), 384–391. <https://doi.org/10.1006/viro.1996.0128>

Rehm, M., Dussmann, H., Janicke, R. U., Tavaré, J. M., Kogel, D., & Prehn, J. H. (2002). Single-cell fluorescence resonance energy transfer analysis demonstrates that caspase activation during apoptosis is a rapid process. Role of caspase-3. *The Journal of biological chemistry*, 277(27), 24506–24514. <https://doi.org/10.1074/jbc.M110789200>

Ritchie, C., Cordova, A. F., Hess, G. T., Bassik, M. C., & Li, L. (2019). SLC19A1 Is an Importer of the Immunotransmitter cGAMP. *Molecular cell*, 75(2), 372–381.e5. <https://doi.org/10.1016/j.molcel.2019.05.006>

- Rizzo**, A. N., Haeger, S. M., Oshima, K., Yang, Y., Wallbank, A. M., Jin, Y., Lettau, M., McCaig, L. A., Wickersham, N. E., McNeil, J. B., Zakharevich, I., McMurtry, S. A., Langouët-Astrié, C. J., Kopf, K. W., Voelker, D. R., Hansen, K. C., Shaver, C. M., Kerchberger, V. E., Peterson, R. A., Kuebler, W. M., ... Schmidt, E. P. (2022). Alveolar epithelial glycocalyx degradation mediates surfactant dysfunction and contributes to acute respiratory distress syndrome. *JCI insight*, 7(2), e154573. <https://doi.org/10.1172/jci.insight.154573>
- Robijns**, J., Houthaeve, G., Braeckmans, K., & De Vos, W. H. (2018). Loss of Nuclear Envelope Integrity in Aging and Disease. *International review of cell and molecular biology*, 336, 205–222. <https://doi.org/10.1016/bs.ircmb.2017.07.013>
- Robinson**, N., McComb, S., Mulligan, R., Dudani, R., Krishnan, L., & Sad, S. (2012). Type I interferon induces necroptosis in macrophages during infection with *Salmonella enterica* serovar Typhimurium. *Nature immunology*, 13(10), 954–962. <https://doi.org/10.1038/ni.2397>
- Rochael**, N. C., Guimarães-Costa, A. B., Nascimento, M. T., DeSouza-Vieira, T. S., Oliveira, M. P., Garcia e Souza, L. F., Oliveira, M. F., & Saraiva, E. M. (2015). Classical ROS-dependent and early/rapid ROS-independent release of Neutrophil Extracellular Traps triggered by *Leishmania* parasites. *Scientific reports*, 5, 18302. <https://doi.org/10.1038/srep18302>
- Rodrigues**, D. A. S., Prestes, E. B., Gama, A. M. S., Silva, L. S., Pinheiro, A. A. S., Ribeiro, J. M. C., Campos, R. M. P., Pimentel-Coelho, P. M., De Souza, H. S., Dicko, A., Duffy, P. E., Fried, M., Francischetti, I. M. B., Saraiva, E. M., Paula-Neto, H. A., & Bozza, M. T. (2020). CXCR4 and MIF are required for neutrophil extracellular trap release triggered by Plasmodium-infected erythrocytes. *PLoS pathogens*, 16(8), e1008230. <https://doi.org/10.1371/journal.ppat.1008230>
- Roh**, J. S., & Sohn, D. H. (2018). Damage-Associated Molecular Patterns in Inflammatory Diseases. *Immune network*, 18(4), e27. <https://doi.org/10.4110/in.2018.18.e27>
- Roquilly**, A., Jacqueline, C., Davieau, M., Mollé, A., Sadek, A., Fourgeux, C., Rooze, P., Broquet, A., Misme-Aucouturier, B., Chaumette, T., Vourc'h, M., Cinotti, R., Marec, N., Gauttier, V., McWilliam, H. E. G., Altare, F., Poschmann, J., Villadangos, J. A., & Asehnoune, K. (2020). Alveolar macrophages are epigenetically altered after inflammation, leading to long-term lung immunoparalysis. *Nature immunology*, 21(6), 636–648. <https://doi.org/10.1038/s41590-020-0673-x>
- Rothlin**, C. V., Hille, T. D., & Ghosh, S. (2021). Determining the effector response to cell death. *Nature reviews. Immunology*, 21(5), 292–304. <https://doi.org/10.1038/s41577-020-00456-0>
- Royce**, G. H., Brown-Borg, H. M., & Deepa, S. S. (2019). The potential role of necroptosis in inflammaging and aging. *GeroScience*, 41(6), 795–811. <https://doi.org/10.1007/s11357-019-00131-w>
- Ryu**, C., Sun, H., Gulati, M., Herazo-Maya, J. D., Chen, Y., Osafo-Addo, A., Brandsdorfer, C., Winkler, J., Blaul, C., Faunce, J., Pan, H., Woolard, T., Tzouvelekis, A., Antin-Ozerkis, D. E., Puchalski, J. T., Slade, M., Gonzalez, A. L., Bogenhagen, D. F., Kirillov, V., Feghali-Bostwick, C., ... Trujillo, G. (2017). Extracellular Mitochondrial DNA Is Generated by Fibroblasts and Predicts Death in Idiopathic Pulmonary Fibrosis. *American journal of respiratory and critical care medicine*, 196(12), 1571–1581. <https://doi.org/10.1164/rccm.201612-2480OC>

- Saffar**, A. S., Ashdown, H., & Gounni, A. S. (2011). The molecular mechanisms of glucocorticoids-mediated neutrophil survival. *Current drug targets*, 12(4), 556–562. <https://doi.org/10.2174/138945011794751555>
- Saffarzadeh**, M., Juenemann, C., Queisser, M. A., Lochnit, G., Barreto, G., Galuska, S. P., Lohmeyer, J., & Preissner, K. T. (2012). Neutrophil extracellular traps directly induce epithelial and endothelial cell death: a predominant role of histones. *PloS one*, 7(2), e32366. <https://doi.org/10.1371/journal.pone.0032366>
- Sagulenko**, V., Thygesen, S. J., Sester, D. P., Idris, A., Cridland, J. A., Vajjhala, P. R., Roberts, T. L., Schroder, K., Vince, J. E., Hill, J. M., Silke, J., & Stacey, K. J. (2013). AIM2 and NLRP3 inflammasomes activate both apoptotic and pyroptotic death pathways via ASC. *Cell death and differentiation*, 20(9), 1149–1160. <https://doi.org/10.1038/cdd.2013.37>
- Saitoh**, T., Komano, J., Saitoh, Y., Misawa, T., Takahama, M., Kozaki, T., Uehata, T., Iwasaki, H., Omori, H., Yamaoka, S., Yamamoto, N., & Akira, S. (2012). Neutrophil extracellular traps mediate a host defense response to human immunodeficiency virus-1. *Cell host & microbe*, 12(1), 109–116. <https://doi.org/10.1016/j.chom.2012.05.015>
- Samson**, A. L., Zhang, Y., Geoghegan, N. D., Gavin, X. J., Davies, K. A., Mlodzianoski, M. J., Whitehead, L. W., Frank, D., Garnish, S. E., Fitzgibbon, C., Hempel, A., Young, S. N., Jacobsen, A. V., Cawthorne, W., Petrie, E. J., Faux, M. C., Shield-Artin, K., Lalaoui, N., Hildebrand, J. M., Silke, J., ... Murphy, J. M. (2020). MLKL trafficking and accumulation at the plasma membrane control the kinetics and threshold for necroptosis. *Nature communications*, 11(1), 3151. <https://doi.org/10.1038/s41467-020-16887-1>
- Santos**, J. C., Dick, M. S., Lagrange, B., Degrandi, D., Pfeffer, K., Yamamoto, M., Meunier, E., Pelczar, P., Henry, T., & Broz, P. (2018). LPS targets host guanylate-binding proteins to the bacterial outer membrane for non-canonical inflammasome activation. *The EMBO journal*, 37(6), e98089. <https://doi.org/10.15252/emboj.201798089>
- Sarhan**, J., Liu, B. C., Muendlein, H. I., Weindel, C. G., Smirnova, I., Tang, A. Y., Ilyukha, V., Sorokin, M., Buzdin, A., Fitzgerald, K. A., & Poltorak, A. (2019). Constitutive interferon signaling maintains critical threshold of MLKL expression to license necroptosis. *Cell death and differentiation*, 26(2), 332–347. <https://doi.org/10.1038/s41418-018-0122-7>
- Savio**, L. E. B., de Andrade Mello, P., da Silva, C. G., & Coutinho-Silva, R. (2018). The P2X7 Receptor in Inflammatory Diseases: Angel or Demon?. *Frontiers in pharmacology*, 9, 52. <https://doi.org/10.3389/fphar.2018.00052>
- Scaffidi**, P., & Misteli, T. (2006). Lamin A-dependent nuclear defects in human aging. *Science (New York, N.Y.)*, 312(5776), 1059–1063. <https://doi.org/10.1126/science.1127168>
- Schadt**, L., Sparano, C., Schweiger, N. A., Silina, K., Cecconi, V., Lucchiari, G., Yagita, H., Guggisberg, E., Saba, S., Nascakova, Z., Barchet, W., & van den Broek, M. (2019). Cancer-Cell-Intrinsic cGAS Expression Mediates Tumor Immunogenicity. *Cell reports*, 29(5), 1236–1248.e7. <https://doi.org/10.1016/j.celrep.2019.09.065>
- Schauer**, C., Janko, C., Munoz, L. E., Zhao, Y., Kienhöfer, D., Frey, B., Lell, M., Manger, B., Rech, J., Naschberger, E., Holmdahl, R., Krenn, V., Harrer, T., Jeremic, I., Bilyy, R., Schett, G., Hoffmann, M., &

- Herrmann, M. (2014). Aggregated neutrophil extracellular traps limit inflammation by degrading cytokines and chemokines. *Nature medicine*, 20(5), 511–517. <https://doi.org/10.1038/nm.3547>
- Schenkel**, A. R., Mamdouh, Z., Chen, X., Liebman, R. M., & Muller, W. A. (2002). CD99 plays a major role in the migration of monocytes through endothelial junctions. *Nature immunology*, 3(2), 143–150. <https://doi.org/10.1038/ni749>
- Schmidt**, E. P., Yang, Y., Janssen, W. J., Gandjeva, A., Perez, M. J., Barthel, L., Zemans, R. L., Bowman, J. C., Koyanagi, D. E., Yunt, Z. X., Smith, L. P., Cheng, S. S., Overdier, K. H., Thompson, K. R., Geraci, M. W., Douglas, I. S., Pearse, D. B., & Tuder, R. M. (2012). The pulmonary endothelial glycocalyx regulates neutrophil adhesion and lung injury during experimental sepsis. *Nature medicine*, 18(8), 1217–1223. <https://doi.org/10.1038/nm.2843>
- Schock**, S. N., Chandra, N. V., Sun, Y., Irie, T., Kitagawa, Y., Gotoh, B., Coscoy, L., & Winoto, A. (2017). Induction of necroptotic cell death by viral activation of the RIG-I or STING pathway. *Cell death and differentiation*, 24(4), 615–625. <https://doi.org/10.1038/cdd.2016.153>
- Semeraro**, F., Ammollo, C. T., Morrissey, J. H., Dale, G. L., Friese, P., Esmon, N. L., & Esmon, C. T. (2011). Extracellular histones promote thrombin generation through platelet-dependent mechanisms: involvement of platelet TLR2 and TLR4. *Blood*, 118(7), 1952–1961. <https://doi.org/10.1182/blood-2011-03-343061>
- Serrao**, K. L., Fortenberry, J. D., Owens, M. L., Harris, F. L., & Brown, L. A. (2001). Neutrophils induce apoptosis of lung epithelial cells via release of soluble Fas ligand. *American journal of physiology. Lung cellular and molecular physiology*, 280(2), L298–L305. <https://doi.org/10.1152/ajplung.2001.280.2.L298>
- Seumois**, G., Ramírez-Suástegui, C., Schmiedel, B. J., Liang, S., Peters, B., Sette, A., & Vijayanand, P. (2020). Single-cell transcriptomic analysis of allergen-specific T cells in allergy and asthma. *Science immunology*, 5(48), eaba6087. <https://doi.org/10.1126/sciimmunol.aba6087>
- Shae**, D., Becker, K. W., Christov, P., Yun, D. S., Lytton-Jean, A. K. R., Sevimli, S., Ascano, M., Kelley, M., Johnson, D. B., Balko, J. M., & Wilson, J. T. (2019). Endosomolytic polymersomes increase the activity of cyclic dinucleotide STING agonists to enhance cancer immunotherapy. *Nature nanotechnology*, 14(3), 269–278. <https://doi.org/10.1038/s41565-018-0342-5>
- Shah**, P. I., Bush, A., Canny, G. J., Colin, A. A., Fuchs, H. J., Geddes, D. M., Johnson, C. A., Light, M. C., Scott, S. F., & Tullis, D. E. (1995). Recombinant human DNase I in cystic fibrosis patients with severe pulmonary disease: a short-term, double-blind study followed by six months open-label treatment. *The European respiratory journal*, 8(6), 954–958.
- Shah**, P. L., Scott, S. F., Geddes, D. M., & Hodson, M. E. (1995). Two years experience with recombinant human DNase I in the treatment of pulmonary disease in cystic fibrosis. *Respiratory medicine*, 89(7), 499–502. [https://doi.org/10.1016/0954-6111\(95\)90126-4](https://doi.org/10.1016/0954-6111(95)90126-4)
- Shan**, B., Pan, H., Najafov, A., & Yuan, J. (2018). Necroptosis in development and diseases. *Genes & development*, 32(5-6), 327–340. <https://doi.org/10.1101/gad.312561.118>

Shapouri-Moghaddam, A., Mohammadian, S., Vazini, H., Taghadosi, M., Esmaili, S. A., Mardani, F., Seifi, B., Mohammadi, A., Afshari, J. T., & Sahebkar, A. (2018). Macrophage plasticity, polarization, and function in health and disease. *Journal of cellular physiology*, 233(9), 6425–6440. <https://doi.org/10.1002/jcp.26429>

Sharma, B. R., & Kanneganti, T. D. (2023). Inflammasome signaling in colorectal cancer. *Translational research : the journal of laboratory and clinical medicine*, 252, 45–52. <https://doi.org/10.1016/j.trsl.2022.09.002>

Shaver, C. M., Wickersham, N., McNeil, J. B., Nagata, H., Miller, A., Landstreet, S. R., Kuck, J. L., Diamond, J. M., Lederer, D. J., Kawut, S. M., Palmer, S. M., Wille, K. M., Weinacker, A., Lama, V. N., Crespo, M. M., Orens, J. B., Shah, P. D., Hage, C. A., Cantu, E., 3rd, Porteous, M. K., ... Lung Transplant Outcomes Group (LTOG) (2018). Cell-free hemoglobin promotes primary graft dysfunction through oxidative lung endothelial injury. *JCI insight*, 3(2), e98546. <https://doi.org/10.1172/jci.insight.98546>

She, L., Barrera, G. D., Yan, L., Alanazi, H. H., Brooks, E. G., Dube, P. H., Sun, Y., Zan, H., Chupp, D. P., Zhang, N., Zhang, X., Liu, Y., & Li, X. D. (2021). STING activation in alveolar macrophages and group 2 innate lymphoid cells suppresses IL-33-driven type 2 immunopathology. *JCI insight*, 6(3), e143509. <https://doi.org/10.1172/jci.insight.143509>

Shi, J., Zhao, Y., Wang, K., Shi, X., Wang, Y., Huang, H., Zhuang, Y., Cai, T., Wang, F., & Shao, F. (2015). Cleavage of GSDMD by inflammatory caspases determines pyroptotic cell death. *Nature*, 526(7575), 660–665. <https://doi.org/10.1038/nature15514>

Shi, Q., Zhao, L., Xu, C., Zhang, L., & Zhao, H. (2019). High Molecular Weight Hyaluronan Suppresses Macrophage M1 Polarization and Enhances IL-10 Production in PM2.5-Induced Lung Inflammation. *Molecules (Basel, Switzerland)*, 24(9), 1766. <https://doi.org/10.3390/molecules24091766>

Shin, J. W., Kim, J., Ham, S., Choi, S. M., Lee, C. H., Lee, J. C., Kim, J. H., Cho, S. H., Kang, H. R., Kim, Y. M., Chung, D. H., Chung, Y., Bae, Y. S., Bae, Y. S., Roh, T. Y., Kim, T., & Kim, H. Y. (2022). A unique population of neutrophils generated by air pollutant-induced lung damage exacerbates airway inflammation. *The Journal of allergy and clinical immunology*, 149(4), 1253–1269.e8. <https://doi.org/10.1016/j.jaci.2021.09.031>

Sica, A., & Mantovani, A. (2012). Macrophage plasticity and polarization: in vivo veritas. *The Journal of clinical investigation*, 122(3), 787–795. <https://doi.org/10.1172/JCI59643>

Singh, A. B., & Kumar, P. (2022). Climate change and allergic diseases: An overview. *Frontiers in allergy*, 3, 964987. <https://doi.org/10.3389/falgy.2022.964987>

Singh, J., Boettcher, M., Dölling, M., Heuer, A., Hohberger, B., Leppkes, M., Naschberger, E., Schapher, M., Schauer, C., Schoen, J., Stürzl, M., Vitkov, L., Wang, H., Zlatar, L., Schett, G. A., Pisetsky, D. S., Liu, M. L., Herrmann, M., & Knopf, J. (2023). Moonlighting chromatin: when DNA escapes nuclear control. *Cell death and differentiation*, 30(4), 861–875. <https://doi.org/10.1038/s41418-023-01124-1>

Siu, T., Altman, M. D., Baltus, G. A., Childers, M., Ellis, J. M., Gunaydin, H., Hatch, H., Ho, T., Jewell, J., Lacey, B. M., Lesburg, C. A., Pan, B. S., Sauvagnat, B., Schroeder, G. K., & Xu, S. (2018). Discovery of a Novel cGAMP Competitive Ligand of the Inactive Form of STING. *ACS medicinal chemistry letters*, 10(1), 92–97. <https://doi.org/10.1021/acsmedchemlett.8b00466>

- Sivapalan, P., Bonnesen, B., & Jensen, J. U. (2020).** Novel Perspectives Regarding the Pathology, Inflammation, and Biomarkers of Acute Respiratory Distress Syndrome. *International journal of molecular sciences*, 22(1), 205. <https://doi.org/10.3390/ijms22010205>
- Skopelja-Gardner, S., An, J., & Elkon, K. B. (2022).** Role of the cGAS-STING pathway in systemic and organ-specific diseases. *Nature reviews. Nephrology*, 18(9), 558–572. <https://doi.org/10.1038/s41581-022-00589-6>
- Slee, E. A., Harte, M. T., Kluck, R. M., Wolf, B. B., Casiano, C. A., Newmeyer, D. D., Wang, H. G., Reed, J. C., Nicholson, D. W., Alnemri, E. S., Green, D. R., & Martin, S. J. (1999).** Ordering the cytochrome c-initiated caspase cascade: hierarchical activation of caspases-2, -3, -6, -7, -8, and -10 in a caspase-9-dependent manner. *The Journal of cell biology*, 144(2), 281–292. <https://doi.org/10.1083/jcb.144.2.281>
- Snelgrove, R. J., Goulding, J., Didierlaurent, A. M., Lyonga, D., Vekaria, S., Edwards, L., Gwyer, E., Sedgwick, J. D., Barclay, A. N., & Hussell, T. (2008).** A critical function for CD200 in lung immune homeostasis and the severity of influenza infection. *Nature immunology*, 9(9), 1074–1083. <https://doi.org/10.1038/ni.1637>
- Sollberger, G., Choidas, A., Burn, G. L., Habenberger, P., Di Lucrezia, R., Kordes, S., Menninger, S., Eickhoff, J., Nussbaumer, P., Klebl, B., Krüger, R., Herzig, A., & Zychlinsky, A. (2018).** Gasdermin D plays a vital role in the generation of neutrophil extracellular traps. *Science immunology*, 3(26), eaar6689. <https://doi.org/10.1126/sciimmunol.aar6689>
- Sousa-Rocha, D., Thomaz-Tobias, M., Diniz, L. F., Souza, P. S., Pinge-Filho, P., & Toledo, K. A. (2015).** Trypanosoma cruzi and Its Soluble Antigens Induce NET Release by Stimulating Toll-Like Receptors. *PloS one*, 10(10), e0139569. <https://doi.org/10.1371/journal.pone.0139566>
- Spadaro, S., Park, M., Turrini, C., Tunstall, T., Thwaites, R., Mauri, T., Ragazzi, R., Ruggeri, P., Hansel, T. T., Caramori, G., & Volta, C. A. (2019).** Biomarkers for Acute Respiratory Distress syndrome and prospects for personalised medicine. *Journal of inflammation (London, England)*, 16, 1. <https://doi.org/10.1186/s12950-018-0202-y>
- Stojkov, D., Claus, M. J., Kozłowski, E., Oberson, K., Schären, O. P., Benarafa, C., Yousefi, S., & Simon, H. U. (2023).** NET formation is independent of gasdermin D and pyroptotic cell death. *Science signaling*, 16(769), eabm0517. <https://doi.org/10.1126/scisignal.abm0517>
- Strickland, I., Kisich, K., Hauk, P. J., Vottero, A., Chrousos, G. P., Klemm, D. J., & Leung, D. Y. (2001).** High constitutive glucocorticoid receptor beta in human neutrophils enables them to reduce their spontaneous rate of cell death in response to corticosteroids. *The Journal of experimental medicine*, 193(5), 585–593. <https://doi.org/10.1084/jem.193.5.585>
- Sugita, K., Steer, C. A., Martinez-Gonzalez, I., Altunbulakli, C., Morita, H., Castro-Giner, F., Kubo, T., Wawrzyniak, P., Rückert, B., Sudo, K., Nakae, S., Matsumoto, K., O'Mahony, L., Akdis, M., Takei, F., & Akdis, C. A. (2018).** Type 2 innate lymphoid cells disrupt bronchial epithelial barrier integrity by targeting tight junctions through IL-13 in asthmatic patients. *The Journal of allergy and clinical immunology*, 141(1), 300–310.e11. <https://doi.org/10.1016/j.jaci.2017.02.038>

- Suk, K.,** Chang, I., Kim, Y. H., Kim, S., Kim, J. Y., Kim, H., & Lee, M. S. (2001b). Interferon gamma (IFN γ) and tumor necrosis factor alpha synergism in ME-180 cervical cancer cell apoptosis and necrosis. IFN γ inhibits cytoprotective NF-kappa B through STAT1/IRF-1 pathways. *The Journal of biological chemistry*, 276(16), 13153–13159. <https://doi.org/10.1074/jbc.M007646200>
- Suk, K.,** Kim, S., Kim, Y. H., Kim, K. A., Chang, I., Yagita, H., Shong, M., & Lee, M. S. (2001 a). IFN- γ /TNF- α synergism as the final effector in autoimmune diabetes: a key role for STAT1/IFN regulatory factor-1 pathway in pancreatic beta cell death. *Journal of immunology (Baltimore, Md.: 1950)*, 166(7), 4481–4489. <https://doi.org/10.4049/jimmunol.166.7.4481>
- Sun, L.,** Wu, J., Du, F., Chen, X., & Chen, Z. J. (2013). Cyclic GMP-AMP synthase is a cytosolic DNA sensor that activates the type I interferon pathway. *Science (New York, N.Y.)*, 339(6121), 786–791. <https://doi.org/10.1126/science.1232458>
- Sun, M.,** Wang, T., Zhou, Y., Liu, Q., Sun, M., Li, H., Zhao, Y., Liu, Y., Xu, A., & Liu, Y. (2023). Pulmonary flora-modified diesel particulate matter induced lung injury via cGAS signaling pathway. *The Science of the total environment*, 892, 164490. <https://doi.org/10.1016/j.scitotenv.2023.164490>
- Sun, S.,** Duan, Z., Wang, X., Chu, C., Yang, C., Chen, F., Wang, D., Wang, C., Li, Q., & Ding, W. (2021). Neutrophil extracellular traps impair intestinal barrier functions in sepsis by regulating TLR9-mediated endoplasmic reticulum stress pathway. *Cell death & disease*, 12(6), 606. <https://doi.org/10.1038/s41419-021-03896-1>
- Sundaram, B.,** & Kanneganti, T. D. (2021). Advances in Understanding Activation and Function of the NLRC4 Inflammasome. *International journal of molecular sciences*, 22(3), 1048. <https://doi.org/10.3390/ijms22031048>
- Sundaram, B.,** Pandian, N., Mall, R., Wang, Y., Sarkar, R., Kim, H. J., Malireddi, R. K. S., Karki, R., Janke, L. J., Vogel, P., & Kanneganti, T. D. (2023). NLRP12-PANoptosome activates PANoptosis and pathology in response to heme and PAMPs. *Cell*, 186(13), 2783–2801.e20. <https://doi.org/10.1016/j.cell.2023.05.005>
- Suzuki, J.,** Denning, D. P., Imanishi, E., Horvitz, H. R., & Nagata, S. (2013). Xk-related protein 8 and CED-8 promote phosphatidylserine exposure in apoptotic cells. *Science (New York, N.Y.)*, 341(6144), 403–406. <https://doi.org/10.1126/science.1236758>
- Suzuki, J.,** Umeda, M., Sims, P. J., & Nagata, S. (2010). Calcium-dependent phospholipid scrambling by TMEM16F. *Nature*, 468(7325), 834–838. <https://doi.org/10.1038/nature09583>
- Suzuki, K.,** Okada, H., Takemura, G., Takada, C., Kuroda, A., Yano, H., Zaikokuji, R., Morishita, K., Tomita, H., Oda, K., Matsuo, S., Uchida, A., Fukuta, T., Sampei, S., Miyazaki, N., Kawaguchi, T., Watanabe, T., Yoshida, T., Ushikoshi, H., Yoshida, S., ... Ogura, S. (2019). Neutrophil Elastase Damages the Pulmonary Endothelial Glycocalyx in Lipopolysaccharide-Induced Experimental Endotoxemia. *The American journal of pathology*, 189(8), 1526–1535. <https://doi.org/10.1016/j.ajpath.2019.05.002>
- Sze, A.,** Belgnaoui, S. M., Olganier, D., Lin, R., Hiscott, J., & van Grevenynghe, J. (2013). Host restriction factor SAMHD1 limits human T cell leukemia virus type 1 infection of monocytes via STING-mediated apoptosis. *Cell host & microbe*, 14(4), 422–434. <https://doi.org/10.1016/j.chom.2013.09.009>

Sze, E., Bhalla, A., & Nair, P. (2020). Mechanisms and therapeutic strategies for non-T2 asthma. *Allergy*, 75(2), 311–325. <https://doi.org/10.1111/all.13985>

Szklarczyk, D., Gable, A. L., Lyon, D., Junge, A., Wyder, S., Huerta-Cepas, J., Simonovic, M., Doncheva, N. T., Morris, J. H., Bork, P., Jensen, L. J., & Mering, C. V. (2019). STRING v11: protein-protein association networks with increased coverage, supporting functional discovery in genome-wide experimental datasets. *Nucleic acids research*, 47(D1), D607–D613. <https://doi.org/10.1093/nar/gky1131>

Takaoka, A., Wang, Z., Choi, M. K., Yanai, H., Negishi, H., Ban, T., Lu, Y., Miyagishi, M., Kodama, T., Honda, K., Ohba, Y., & Taniguchi, T. (2007). DAI (DLM-1/ZBP1) is a cytosolic DNA sensor and an activator of innate immune response. *Nature*, 448(7152), 501–505. <https://doi.org/10.1038/nature06013>

Tang, C. H., Zundell, J. A., Ranatunga, S., Lin, C., Nefedova, Y., Del Valle, J. R., & Hu, C. C. (2016). Agonist-Mediated Activation of STING Induces Apoptosis in Malignant B Cells. *Cancer research*, 76(8), 2137–2152. <https://doi.org/10.1158/0008-5472.CAN-15-1885>

Tang, D., Kang, R., Berghe, T. V., Vandenabeele, P., & Kroemer, G. (2019). The molecular machinery of regulated cell death. *Cell research*, 29(5), 347–364. <https://doi.org/10.1038/s41422-019-0164-5>

Tanzer, M. C., Frauenstein, A., Stafford, C. A., Phulphagar, K., Mann, M., & Meissner, F. (2020). Quantitative and Dynamic Catalogs of Proteins Released during Apoptotic and Necroptotic Cell Death. *Cell reports*, 30(4), 1260–1270.e5. <https://doi.org/10.1016/j.celrep.2019.12.079>

Tanzer, M. C., Frauenstein, A., Stafford, C. A., Phulphagar, K., Mann, M., & Meissner, F. (2020). Quantitative and Dynamic Catalogs of Proteins Released during Apoptotic and Necroptotic Cell Death. *Cell reports*, 30(4), 1260–1270.e5. <https://doi.org/10.1016/j.celrep.2019.12.079>

The more one studies ecology, the more obvious it becomes that everything is interconnected.

Thiam, H. R., Wong, S. L., Wagner, D. D., & Waterman, C. M. (2020). Cellular Mechanisms of NETosis. *Annual review of cell and developmental biology*, 36, 191–218. <https://doi.org/10.1146/annurev-cellbio-020520-111016>

Thierry, A. R., & Roch, B. (2020). Neutrophil Extracellular Traps and By-Products Play a Key Role in COVID-19: Pathogenesis, Risk Factors, and Therapy. *Journal of clinical medicine*, 9(9), 2942. <https://doi.org/10.3390/jcm9092942>

Thille, A. W., Esteban, A., Fernández-Segoviano, P., Rodriguez, J. M., Aramburu, J. A., Peñuelas, O., Cortés-Puch, I., Cardinal-Fernández, P., Lorente, J. A., & Frutos-Vivar, F. (2013). Comparison of the Berlin definition for acute respiratory distress syndrome with autopsy. *American journal of respiratory and critical care medicine*, 187(7), 761–767. <https://doi.org/10.1164/rccm.201211-1981OC>

Thorley, A. J., Ford, P. A., Gienbycz, M. A., Goldstraw, P., Young, A., & Tetley, T. D. (2007). Differential regulation of cytokine release and leukocyte migration by lipopolysaccharide-stimulated primary human lung alveolar type II epithelial cells and macrophages. *Journal of immunology (Baltimore, Md.: 1950)*, 178(1), 463–473. <https://doi.org/10.4049/jimmunol.178.1.463>

Tibbitt, C. A., Stark, J. M., Martens, L., Ma, J., Mold, J. E., Deswarte, K., Oliynyk, G., Feng, X., Lambrecht, B. N., De Bleser, P., Nylén, S., Hammad, H., Arsenian Henriksson, M., Saeys, Y., & Coquet, J. M. (2019). Single-

Cell RNA Sequencing of the T Helper Cell Response to House Dust Mites Defines a Distinct Gene Expression Signature in Airway Th2 Cells. *Immunity*, 51(1), 169–184.e5. <https://doi.org/10.1016/j.immuni.2019.05.014>

Toki, S., Goleniewska, K., Zhang, J., Zhou, W., Newcomb, D. C., Zhou, B., Kita, H., Boyd, K. L., & Peebles, R. S., Jr (2020). TSLP and IL-33 reciprocally promote each other's lung protein expression and ILC2 receptor expression to enhance innate type-2 airway inflammation. *Allergy*, 75(7), 1606–1617. <https://doi.org/10.1111/all.14196>

Torchinsky, M. B., Garaude, J., Martin, A. P., & Blander, J. M. (2009). Innate immune recognition of infected apoptotic cells directs T(H)17 cell differentiation. *Nature*, 458(7234), 78–82. <https://doi.org/10.1038/nature07781>

Toussaint, M., Jackson, D. J., Swieboda, D., Guedán, A., Tsourouktsoglou, T. D., Ching, Y. M., Radermecker, C., Makrinioti, H., Aniscenko, J., Bartlett, N. W., Edwards, M. R., Solari, R., Farnir, F., Papayannopoulos, V., Bureau, F., Marichal, T., & Johnston, S. L. (2017). Host DNA released by NETosis promotes rhinovirus-induced type-2 allergic asthma exacerbation. *Nature medicine*, 23(6), 681–691. <https://doi.org/10.1038/nm.4332>

Tsuchiya, K., Nakajima, S., Hosojima, S., Thi Nguyen, D., Hattori, T., Manh Le, T., Hori, O., Mahib, M. R., Yamaguchi, Y., Miura, M., Kinoshita, T., Kushiya, H., Sakurai, M., Shiroishi, T., & Suda, T. (2019). Caspase-1 initiates apoptosis in the absence of gasdermin D. *Nature communications*, 10(1), 2091. <https://doi.org/10.1038/s41467-019-09753-2>

Unterholzner, L., Keating, S. E., Baran, M., Horan, K. A., Jensen, S. B., Sharma, S., Sirois, C. M., Jin, T., Latz, E., Xiao, T. S., Fitzgerald, K. A., Paludan, S. R., & Bowie, A. G. (2010). IFI16 is an innate immune sensor for intracellular DNA. *Nature immunology*, 11(11), 997–1004. <https://doi.org/10.1038/ni.1932>

Upton, J. W., Kaiser, W. J., & Mocarski, E. S. (2012). DAI/ZBP1/DLM-1 complexes with RIP3 to mediate virus-induced programmed necrosis that is targeted by murine cytomegalovirus vIRA. *Cell host & microbe*, 11(3), 290–297. <https://doi.org/10.1016/j.chom.2012.01.016>

Ural, B. B., Yeung, S. T., Damani-Yokota, P., Devlin, J. C., de Vries, M., Vera-Licona, P., Samji, T., Sawai, C. M., Jang, G., Perez, O. A., Pham, Q., Maher, L., Loke, P., Dittmann, M., Reizis, B., & Khanna, K. M. (2020). Identification of a nerve-associated, lung-resident interstitial macrophage subset with distinct localization and immunoregulatory properties. *Science immunology*, 5(45), eaax8756. <https://doi.org/10.1126/sciimmunol.aax8756>

Vajjhala, P. R., Lu, A., Brown, D. L., Pang, S. W., Sagulenko, V., Sester, D. P., Cridland, S. O., Hill, J. M., Schroder, K., Stow, J. L., Wu, H., & Stacey, K. J. (2015). The Inflammasome Adaptor ASC Induces Procaspace-8 Death Effector Domain Filaments. *The Journal of biological chemistry*, 290(49), 29217–29230. <https://doi.org/10.1074/jbc.M115.687731>

Vassallo, A., Wood, A. J., Subburayalu, J., Summers, C., & Chilvers, E. R. (2019). The counter-intuitive role of the neutrophil in the acute respiratory distress syndrome. *British medical bulletin*, 131(1), 43–55. <https://doi.org/10.1093/bmb/ldz024>

Vercammen, D., Beyaert, R., Denecker, G., Goossens, V., Van Loo, G., Declercq, W., Grooten, J., Fiers, W., & Vandenabeele, P. (1998). Inhibition of caspases increases the sensitivity of L929 cells to necrosis mediated by

tumor necrosis factor. *The Journal of experimental medicine*, 187(9), 1477–1485. <https://doi.org/10.1084/jem.187.9.1477>

Verscheure, P., Honnay, O., Speybroeck, N., Daelemans, R., Bruffaerts, N., Devleeschauwer, B., Ceulemans, T., Van Gerven, L., Aerts, R., & Schrijvers, R. (2023). Impact of environmental nitrogen pollution on pollen allergy: A scoping review. *The Science of the total environment*, 893, 164801. <https://doi.org/10.1016/j.scitotenv.2023.164801>

Vestweber D. (2015). How leukocytes cross the vascular endothelium. *Nature reviews. Immunology*, 15(11), 692–704. <https://doi.org/10.1038/nri3908>

Vila, I. K., Chamma, H., Steer, A., Saccas, M., Taffoni, C., Turtoi, E., Reinert, L. S., Hussain, S., Marines, J., Jin, L., Bonnefont, X., Hubert, M., Schwartz, O., Paludan, S. R., Van Simaey, G., Doumont, G., Sobhian, B., Vlachakis, D., Turtoi, A., & Laguet, N. (2022). STING orchestrates the crosstalk between polyunsaturated fatty acid metabolism and inflammatory responses. *Cell metabolism*, 34(1), 125–139.e8. <https://doi.org/10.1016/j.cmet.2021.12.007>

Vince, J. E., De Nardo, D., Gao, W., Vince, A. J., Hall, C., McArthur, K., Simpson, D., Vijayaraj, S., Lindqvist, L. M., Bouillet, P., Rizzacasa, M. A., Man, S. M., Silke, J., Masters, S. L., Lessene, G., Huang, D. C. S., Gray, D. H. D., Kile, B. T., Shao, F., & Lawlor, K. E. (2018). The Mitochondrial Apoptotic Effectors BAX/BAK Activate Caspase-3 and -7 to Trigger NLRP3 Inflammasome and Caspase-8 Driven IL-1 β Activation. *Cell reports*, 25(9), 2339–2353.e4. <https://doi.org/10.1016/j.celrep.2018.10.103>

Volchuk, A., Ye, A., Chi, L., Steinberg, B. E., & Goldenberg, N. M. (2020). Indirect regulation of HMGB1 release by gasdermin D. *Nature communications*, 11(1), 4561. <https://doi.org/10.1038/s41467-020-18443-3>

Vorobjeva, N. V., & **Pinegin**, B. V. (2014). Neutrophil extracellular traps: mechanisms of formation and role in health and disease. *Biochemistry. Biokhimiia*, 79(12), 1286–1296. <https://doi.org/10.1134/S0006297914120025>

Vrolyk, V., & Singh, B. (2020). Animal models to study the role of pulmonary intravascular macrophages in spontaneous and induced acute pancreatitis. *Cell and tissue research*, 380(2), 207–222. <https://doi.org/10.1007/s00441-020-03211-y>

Vrolyk, V., Schneberger, D., Le, K., Wobeser, B. K., & Singh, B. (2019). Mouse model to study pulmonary intravascular macrophage recruitment and lung inflammation in acute necrotizing pancreatitis. *Cell and tissue research*, 378(1), 97–111. <https://doi.org/10.1007/s00441-019-03023-9>

Wang, J., Li, P., Yu, Y., Fu, Y., Jiang, H., Lu, M., Sun, Z., Jiang, S., Lu, L., & Wu, M. X. (2020). Pulmonary surfactant-biomimetic nanoparticles potentiate heterosubtypic influenza immunity. *Science (New York, N.Y.)*, 367(6480), eaau0810. <https://doi.org/10.1126/science.aau0810>

Wang, Q., Imamura, R., Motani, K., Kushiyama, H., Nagata, S., & Suda, T. (2013). Pyroptotic cells externalize eat-me and release find-me signals and are efficiently engulfed by macrophages. *International immunology*, 25(6), 363–372. <https://doi.org/10.1093/intimm/dxs161>

- Wang, X., & Labzin, L. I. (2023).** Inflammatory cell death: how macrophages sense neighbouring cell infection and damage. *Biochemical Society transactions*, 51(1), 303–313. <https://doi.org/10.1042/BST20220807>
- Wang, X., Li, Y., Luo, D., Wang, X., Zhang, Y., Liu, Z., Zhong, N., Wu, M., & Li, G. (2017).** Lyn regulates mucus secretion and MUC5AC via the STAT6 signaling pathway during allergic airway inflammation. *Scientific reports*, 7, 42675. <https://doi.org/10.1038/srep42675>
- Wang, Y., & Kanneganti, T. D. (2021).** From pyroptosis, apoptosis and necroptosis to PANoptosis: A mechanistic compendium of programmed cell death pathways. *Computational and structural biotechnology journal*, 19, 4641–4657. <https://doi.org/10.1016/j.csbj.2021.07.038>
- Watson, F., Gasmi, L., & Edwards, S. W. (1997).** Stimulation of intracellular Ca²⁺ levels in human neutrophils by soluble immune complexes. Functional activation of FcγRIIIb during priming. *The Journal of biological chemistry*, 272(29), 17944–17951. <https://doi.org/10.1074/jbc.272.29.17944>
- Wang, Y., Gao, W., Shi, X., Ding, J., Liu, W., He, H., Wang, K., & Shao, F. (2017).** Chemotherapy drugs induce pyroptosis through caspase-3 cleavage of a gasdermin. *Nature*, 547(7661), 99–103. <https://doi.org/10.1038/nature22393>
- Wang, Y., Gao, W., Shi, X., Ding, J., Liu, W., He, H., Wang, K., & Shao, F. (2017).** Chemotherapy drugs induce pyroptosis through caspase-3 cleavage of a gasdermin. *Nature*, 547(7661), 99–103. <https://doi.org/10.1038/nature22393>
- Webster, S. J., Brode, S., Ellis, L., Fitzmaurice, T. J., Elder, M. J., Gekara, N. O., Turlomousis, P., Bryant, C., Clare, S., Chee, R., Gaston, H. J. S., & Goodall, J. C. (2017).** Detection of a microbial metabolite by STING regulates inflammasome activation in response to *Chlamydia trachomatis* infection. *PLoS pathogens*, 13(6), e1006383. <https://doi.org/10.1371/journal.ppat.1006383>
- Welin, A., Amirbeagi, F., Christenson, K., Björkman, L., Björnsdóttir, H., Forsman, H., Dahlgren, C., Karlsson, A., & Bylund, J. (2013).** The human neutrophil subsets defined by the presence or absence of OLFM4 both transmigrate into tissue in vivo and give rise to distinct NETs in vitro. *PloS one*, 8(7), e69575. <https://doi.org/10.1371/journal.pone.0069575>
- Willemsen, J., Neuhoff, M. T., Hoyler, T., Noir, E., Tessier, C., Sarret, S., Thorsen, T. N., Littlewood-Evans, A., Zhang, J., Hasan, M., Rush, J. S., Guerini, D., & Siegel, R. M. (2021).** TNF leads to mtDNA release and cGAS/STING-dependent interferon responses that support inflammatory arthritis. *Cell reports*, 37(6), 109977. <https://doi.org/10.1016/j.celrep.2021.109977>
- Wong, J. J. M., Leong, J. Y., Lee, J. H., Albani, S., & Yeo, J. G. (2019).** Insights into the immuno-pathogenesis of acute respiratory distress syndrome. *Annals of translational medicine*, 7(19), 504. <https://doi.org/10.21037/atm.2019.09.28>
- Wong, J. J. M., Leong, J. Y., Lee, J. H., Albani, S., & Yeo, J. G. (2019).** Insights into the immuno-pathogenesis of acute respiratory distress syndrome. *Annals of translational medicine*, 7(19), 504. <https://doi.org/10.21037/atm.2019.09.28>

- Woo, Y. D., Jeong, D., & Chung, D. H. (2021).** Development and Functions of Alveolar Macrophages. *Molecules and cells*, 44(5), 292–300. <https://doi.org/10.14348/molcells.2021.0058>
- Woodfin, A., Voisin, M. B., Imhof, B. A., Dejana, E., Engelhardt, B., & Nourshargh, S. (2009).** Endothelial cell activation leads to neutrophil transmigration as supported by the sequential roles of ICAM-2, JAM-A, and PECAM-1. *Blood*, 113(24), 6246–6257. <https://doi.org/10.1182/blood-2008-11-188375>
- Woodruff, P. G., Modrek, B., Choy, D. F., Jia, G., Abbas, A. R., Ellwanger, A., Koth, L. L., Arron, J. R., & Fahy, J. V. (2009).** T-helper type 2-driven inflammation defines major subphenotypes of asthma. *American journal of respiratory and critical care medicine*, 180(5), 388–395. <https://doi.org/10.1164/rccm.200903-0392OC>
- Worthen, G. S., Schwab, B., 3rd, Elson, E. L., & Downey, G. P. (1989).** Mechanics of stimulated neutrophils: cell stiffening induces retention in capillaries. *Science (New York, N.Y.)*, 245(4914), 183–186. <https://doi.org/10.1126/science.2749255>
- Wu, X. N., Yang, Z. H., Wang, X. K., Zhang, Y., Wan, H., Song, Y., Chen, X., Shao, J., & Han, J. (2014).** Distinct roles of RIP1-RIP3 hetero- and RIP3-RIP3 homo-interaction in mediating necroptosis. *Cell death and differentiation*, 21(11), 1709–1720. <https://doi.org/10.1038/cdd.2014.77>
- Xia, P., Wang, S., Ye, B., Du, Y., Huang, G., Zhu, P., & Fan, Z. (2015).** Sox2 functions as a sequence-specific DNA sensor in neutrophils to initiate innate immunity against microbial infection. *Nature immunology*, 16(4), 366–375. <https://doi.org/10.1038/ni.3117>
- Xiao, Q., He, J., Lei, A., Xu, H., Zhang, L., Zhou, P., Jiang, G., & Zhou, J. (2021).** PPAR γ enhances ILC2 function during allergic airway inflammation via transcription regulation of ST2. *Mucosal immunology*, 14(2), 468–478. <https://doi.org/10.1038/s41385-020-00339-6>
- Xie, W., & Patel, D. J. (2023).** Structure-based mechanisms of 2'3'-cGAMP intercellular transport in the cGAS-STING immune pathway. *Trends in immunology*, 44(6), 450–467. <https://doi.org/10.1016/j.it.2023.04.006>
- Xu, B., Sun, Z., Liu, Z., Guo, H., Liu, Q., Jiang, H., Zou, Y., Gong, Y., Tischfield, J. A., & Shao, C. (2011).** Replication stress induces micronuclei comprising of aggregated DNA double-strand breaks. *PloS one*, 6(4), e18618. <https://doi.org/10.1371/journal.pone.0018618>
- Yamasaki, A., Okazaki, R., & Harada, T. (2022).** Neutrophils and Asthma. *Diagnostics (Basel, Switzerland)*, 12(5), 1175. <https://doi.org/10.3390/diagnostics12051175>
- Yang, H., Wang, H., Ren, J., Chen, Q., & Chen, Z. J. (2017).** cGAS is essential for cellular senescence. *Proceedings of the National Academy of Sciences of the United States of America*, 114(23), E4612–E4620. <https://doi.org/10.1073/pnas.1705499114>
- Yang, S. C., Chen, P. J., Chang, S. H., Weng, Y. T., Chang, F. R., Chang, K. Y., Chen, C. Y., Kao, T. I., & Hwang, T. L. (2018).** Luteolin attenuates neutrophilic oxidative stress and inflammatory arthritis by inhibiting Raf1 activity. *Biochemical pharmacology*, 154, 384–396. <https://doi.org/10.1016/j.bcp.2018.06.003>

- Ye, L., Pan, J., Liang, M., Pasha, M. A., Shen, X., D'Souza, S. S., Fung, I. T. H., Wang, Y., Patel, G., Tang, D. D., & Yang, Q. (2020).** A critical role for c-Myc in group 2 innate lymphoid cell activation. *Allergy*, 75(4), 841–852. <https://doi.org/10.1111/all.14149>
- Yeh, Y. T., Serrano, R., François, J., Chiu, J. J., Li, Y. J., Del Álamo, J. C., Chien, S., & Lasheras, J. C. (2018).** Three-dimensional forces exerted by leukocytes and vascular endothelial cells dynamically facilitate diapedesis. *Proceedings of the National Academy of Sciences of the United States of America*, 115(1), 133–138. <https://doi.org/10.1073/pnas.1717489115>
- Ying, S., O'Connor, B., Ratoff, J., Meng, Q., Mallett, K., Cousins, D., Robinson, D., Zhang, G., Zhao, J., Lee, T. H., & Corrigan, C. (2005).** Thymic stromal lymphopoietin expression is increased in asthmatic airways and correlates with expression of Th2-attracting chemokines and disease severity. *Journal of immunology (Baltimore, Md. : 1950)*, 174(12), 8183–8190. <https://doi.org/10.4049/jimmunol.174.12.8183>
- Yoh, S. M., Schneider, M., Seifried, J., Soonthornvacharin, S., Akleh, R. E., Olivieri, K. C., De Jesus, P. D., Ruan, C., de Castro, E., Ruiz, P. A., Germanaud, D., des Portes, V., García-Sastre, A., König, R., & Chanda, S. K. (2015).** PQBP1 Is a Proximal Sensor of the cGAS-Dependent Innate Response to HIV-1. *Cell*, 161(6), 1293–1305. <https://doi.org/10.1016/j.cell.2015.04.050>
- Yona, S., Kim, K. W., Wolf, Y., Mildner, A., Varol, D., Breker, M., Strauss-Ayali, D., Viukov, S., Guilliams, M., Misharin, A., Hume, D. A., Perlman, H., Malissen, B., Zelzer, E., & Jung, S. (2013).** Fate mapping reveals origins and dynamics of monocytes and tissue macrophages under homeostasis. *Immunity*, 38(1), 79–91. <https://doi.org/10.1016/j.immuni.2012.12.001>
- Yoon, S., Kovalenko, A., Bogdanov, K., & Wallach, D. (2017).** MLKL, the Protein that Mediates Necroptosis, Also Regulates Endosomal Trafficking and Extracellular Vesicle Generation. *Immunity*, 47(1), 51–65.e7. <https://doi.org/10.1016/j.immuni.2017.06.001>
- Yu, P., Zhang, X., Liu, N., Tang, L., Peng, C., & Chen, X. (2021).** Pyroptosis: mechanisms and diseases. *Signal transduction and targeted therapy*, 6(1), 128. <https://doi.org/10.1038/s41392-021-00507-5>
- Yu, X., Buttgerit, A., Lelios, I., Utz, S. G., Cansever, D., Becher, B., & Greter, M. (2017).** The Cytokine TGF- β Promotes the Development and Homeostasis of Alveolar Macrophages. *Immunity*, 47(5), 903–912.e4. <https://doi.org/10.1016/j.immuni.2017.10.007>
- Zemans, R. L., & Matthay, M. A. (2017).** What drives neutrophils to the alveoli in ARDS?. *Thorax*, 72(1), 1–3. <https://doi.org/10.1136/thoraxjnl-2016-209170>
- Zhan, C., Huang, M., Yang, X., & Hou, J. (2021).** MLKL: Functions beyond serving as the Executioner of Necroptosis. *Theranostics*, 11(10), 4759–4769. <https://doi.org/10.7150/thno.54072>
- Zhang, A., Yang, H., Yang, Y., & Qian, Z. (1998).** Zhongguo ji sheng chong xue yu ji sheng chong bing za zhi = Chinese journal of parasitology & parasitic diseases, 16(6), 436–440.

- Zhang, X., Shi, H., Wu, J., Zhang, X., Sun, L., Chen, C., & Chen, Z. J. (2013).** Cyclic GMP-AMP containing mixed phosphodiester linkages is an endogenous high-affinity ligand for STING. *Molecular cell*, 51(2), 226–235. <https://doi.org/10.1016/j.molcel.2013.05.022>
- Zhang, Y., Chen, X., Gueydan, C., & Han, J. (2018).** Plasma membrane changes during programmed cell deaths. *Cell research*, 28(1), 9–21. <https://doi.org/10.1038/cr.2017.133>
- Zhang, Z., Yuan, B., Bao, M., Lu, N., Kim, T., & Liu, Y. J. (2011).** The helicase DDX41 senses intracellular DNA mediated by the adaptor STING in dendritic cells. *Nature immunology*, 12(10), 959–965. <https://doi.org/10.1038/ni.2091>
- Zhang, Z., Zhang, Y., Xia, S., Kong, Q., Li, S., Liu, X., Junqueira, C., Meza-Sosa, K. F., Mok, T. M. Y., Ansara, J., Sengupta, S., Yao, Y., Wu, H., & Lieberman, J. (2020).** Gasdermin E suppresses tumour growth by activating anti-tumour immunity. *Nature*, 579(7799), 415–420. <https://doi.org/10.1038/s41586-020-2071-9>
- Zhang, Z., Zhou, H., Ouyang, X., Dong, Y., Sarapultsev, A., Luo, S., & Hu, D. (2022).** Multifaceted functions of STING in human health and disease: from molecular mechanism to targeted strategy. *Signal transduction and targeted therapy*, 7(1), 394. <https://doi.org/10.1038/s41392-022-01252-z>
- Zheng, M., Karki, R., Vogel, P., & Kanneganti, T. D. (2020).** Caspase-6 Is a Key Regulator of Innate Immunity, Inflammasome Activation, and Host Defense. *Cell*, 181(3), 674–687.e13. <https://doi.org/10.1016/j.cell.2020.03.040>
- Zhou, C., Chen, X., Planells-Cases, R., Chu, J., Wang, L., Cao, L., Li, Z., López-Cayuqueo, K. I., Xie, Y., Ye, S., Wang, X., Ullrich, F., Ma, S., Fang, Y., Zhang, X., Qian, Z., Liang, X., Cai, S. Q., Jiang, Z., Zhou, D., ... Xiao, H. (2020).** Transfer of cGAMP into Bystander Cells via LRRC8 Volume-Regulated Anion Channels Augments STING-Mediated Interferon Responses and Anti-viral Immunity. *Immunity*, 52(5), 767–781.e6. <https://doi.org/10.1016/j.immuni.2020.03.016>
- Zhou, D., Huang, C., Lin, Z., Zhan, S., Kong, L., Fang, C., & Li, J. (2014).** Macrophage polarization and function with emphasis on the evolving roles of coordinated regulation of cellular signaling pathways. *Cellular signalling*, 26(2), 192–197. <https://doi.org/10.1016/j.cellsig.2013.11.004>
- Zhou, E., Silva, L. M. R., Conejeros, I., Velásquez, Z. D., Hirz, M., Gärtner, U., Jacquiet, P., Taubert, A., & Hermosilla, C. (2020).** *Besnoitia besnoiti* bradyzoite stages induce suicidal- and rapid vital-NETosis. *Parasitology*, 147(4), 401–409. <https://doi.org/10.1017/S0031182019001707>
- Zhou, W., Whiteley, A. T., de Oliveira Mann, C. C., Morehouse, B. R., Nowak, R. P., Fischer, E. S., Gray, N. S., Mekalanos, J. J., & Kranzusch, P. J. (2018).** Structure of the Human cGAS-DNA Complex Reveals Enhanced Control of Immune Surveillance. *Cell*, 174(2), 300–311.e11. <https://doi.org/10.1016/j.cell.2018.06.026>
- Zhou, Y., Fei, M., Zhang, G., Liang, W. C., Lin, W., Wu, Y., Piskol, R., Ridgway, J., McNamara, E., Huang, H., Zhang, J., Oh, J., Patel, J. M., Jakubiak, D., Lau, J., Blackwood, B., Bravo, D. D., Shi, Y., Wang, J., Hu, H. M., ... Yan, M. (2020).** Blockade of the Phagocytic Receptor MerTK on Tumor-Associated Macrophages Enhances P2X7R-Dependent STING Activation by Tumor-Derived cGAMP. *Immunity*, 52(2), 357–373.e9. <https://doi.org/10.1016/j.immuni.2020.01.014>

- Zhou, Z.,** He, H., Wang, K., Shi, X., Wang, Y., Su, Y., Wang, Y., Li, D., Liu, W., Zhang, Y., Shen, L., Han, W., Shen, L., Ding, J., & Shao, F. (2020). Granzyme A from cytotoxic lymphocytes cleaves GSDMB to trigger pyroptosis in target cells. *Science (New York, N.Y.)*, 368(6494), eaaz7548. <https://doi.org/10.1126/science.aaz7548>
- Zhou, Z.,** Zhang, X., Lei, X., Xiao, X., Jiao, T., Ma, R., Dong, X., Jiang, Q., Wang, W., Shi, Y., Zheng, T., Rao, J., Xiang, Z., Ren, L., Deng, T., Jiang, Z., Dou, Z., Wei, W., & Wang, J. (2021). Sensing of cytoplasmic chromatin by cGAS activates innate immune response in SARS-CoV-2 infection. *Signal transduction and targeted therapy*, 6(1), 382. <https://doi.org/10.1038/s41392-021-00800-3>
- Zhu, K.,** Liang, W., Ma, Z., Xu, D., Cao, S., Lu, X., Liu, N., Shan, B., Qian, L., & Yuan, J. (2018). Necroptosis promotes cell-autonomous activation of proinflammatory cytokine gene expression. *Cell death & disease*, 9(5), 500. <https://doi.org/10.1038/s41419-018-0524-y>
- Zhu, P.,** Ke, Z. R., Chen, J. X., Li, S. J., Ma, T. L., & Fan, X. L. (2023). Advances in mechanism and regulation of PANoptosis: Prospects in disease treatment. *Frontiers in immunology*, 14, 1120034. <https://doi.org/10.3389/fimmu.2023.1120034>
- Zhu, Q.,** Man, S. M., Karki, R., Malireddi, R. K. S., & Kanneganti, T. D. (2018). Detrimental Type I Interferon Signaling Dominates Protective AIM2 Inflammasome Responses during *Francisella novicida* Infection. *Cell reports*, 22(12), 3168–3174. <https://doi.org/10.1016/j.celrep.2018.02.096>
- Zhu, W.,** Wei, L., Dong, C., Wang, Y., Kim, J., Ma, Y., Gonzalez, G. X., & Wang, B. Z. (2022). cGAMP-adjuvanted multivalent influenza mRNA vaccines induce broadly protective immunity through cutaneous vaccination in mice. *Molecular therapy. Nucleic acids*, 30, 421–437. <https://doi.org/10.1016/j.omtn.2022.10.024>
- Zinter, M. S.,** Delucchi, K. L., Kong, M. Y., Orwoll, B. E., Spicer, A. S., Lim, M. J., Alkhouli, M. F., Ratiu, A. E., McKenzie, A. V., McQuillen, P. S., Dvorak, C. C., Calfee, C. S., Matthay, M. A., & Sapru, A. (2019). Early Plasma Matrix Metalloproteinase Profiles. A Novel Pathway in Pediatric Acute Respiratory Distress Syndrome. *American journal of respiratory and critical care medicine*, 199(2), 181–189. <https://doi.org/10.1164/rccm.201804-0678OC>
- Zounemat Kermani, N.,** Saqi, M., Agapow, P., Pavlidis, S., Kuo, C., Tan, K. S., Mumby, S., Sun, K., Loza, M., Baribaud, F., Sousa, A. R., Riley, J., Wheelock, A. M., Wheelock, C. E., De Meulder, B., Schofield, J., Sánchez-Ovando, S., Simpson, J. L., Baines, K. J., Wark, P. A., ... U-BIOPRED Project Team (2021). Type 2-low asthma phenotypes by integration of sputum transcriptomics and serum proteomics. *Allergy*, 76(1), 380–383. <https://doi.org/10.1111/all.14573>
- Zuo, Y.,** Yalavarthi, S., Shi, H., Gockman, K., Zuo, M., Madison, J. A., Blair, C., Weber, A., Barnes, B. J., Egeblad, M., Woods, R. J., Kanthi, Y., & Knight, J. S. (2020). Neutrophil extracellular traps in COVID-19. *JCI insight*, 5(11), e138999. <https://doi.org/10.1172/jci.insight.138999>

Yasmine MESSAOUD NACER

Contribution de la voie de détection de l'ADN STING dans l'exacerbation de l'asthme allergique neutrophilique

Résumé :

Ces dernières années, dans le contexte de la précédente pandémie, des millions de personnes à travers le monde ont éprouvé une détresse respiratoire, dont les conséquences ont parfois été fatales. Cela a été particulièrement préoccupant pour les populations vulnérables telles que les personnes asthmatiques, illustrant l'importance de maintenir la santé des poumons et suscitant d'importants défis pour rétablir l'homéostasie. D'autre part, la combinaison du réchauffement climatique et des risques pandémiques accrus menacent de manière alarmante l'intégrité de notre sphère respiratoire. Il est donc urgent de comprendre les mécanismes responsables de l'exacerbation des pathologies respiratoires, de développer de nouvelles approches thérapeutiques et de tester l'innocuité de ces stratégies. Dans ce travail de thèse, notre objectif était de caractériser (1) la contribution potentielle de l'ADN du soi et de l'activation de la voie STING dans les formes graves du syndrome de détresse respiratoire aiguë (SDRA), telles que survenant lors d'une infection virale respiratoire incontrôlée ou d'une exacerbation d'asthme induite par des infections virales ou l'exposition à la pollution, et (2) l'impact de l'activation de STING sur la modulation de la réponse immune de type 2 lors d'asthme allergique. Nous avons démontré que les agonistes de STING peuvent entraîner des lésions pulmonaires majeures via la libération d'ADN du soi, engendrant une inflammation incontrôlée. D'autre part, nous avons montré qu'une activation accrue de STING durant la réponse allergique entraîne un changement de l'endotype Th2 vers un endotype mixte Th1/Th2 de type sévère neutrophilique, soulignant ainsi l'importance de contrôler l'activation de STING dans les pathologies respiratoires afin de prévenir le développement de formes sévères.

Mots clés : SDRA, exacerbation de l'asthme, STING, agonistes de STING, ADN du soi, NETs, PANoptose.

Contribution of the DNA sensing pathway STING in neutrophilic allergic asthma exacerbation

Summary:

Recently, in the context of the preceding pandemic, millions of people worldwide have experienced respiratory distress, sometimes with fatal consequences. This has raised significant concerns, especially for vulnerable populations such as patients with asthma. These circumstances highlighted the crucial need to maintain the lungs healthy, and presented scientists with considerable challenges to restore homeostasis. Meanwhile, global warming combined with increased pandemic risks and environmental pollution continue to threaten our breathing environment. This highlights the need to understand the mechanisms responsible for exacerbating respiratory pathologies, to develop new therapeutic approaches to test the safety of these strategies. In this thesis work, we aimed at characterizing (1) the potential contribution of self-dsDNA and STING activation to severe forms of acute respiratory distress syndrome (ARDS), such as those occurring during uncontrolled respiratory viral infection, or pollution / viral-induced exacerbation of allergic asthma, and (2) the impact of STING activation on immune modulation of the allergic type 2 immune response during allergic asthma. We show that STING agonists can result in significant lung damage through the release of self-DNA, leading to uncontrolled inflammation. Further, we show that important STING activation during type 2 allergic response may shift the asthma endotype from Th2 asthma toward a mixed severe neutrophilic Th1/Th2 asthma, emphasizing the importance of controlling STING activation in airway inflammatory disease to prevent the development of severe forms.

Keywords: ARDS, asthma exacerbation, STING, STING agonists, self-dsDNA, NETs, PANoptosis.

inem

**Laboratoire d'Immunologie et Neurogénétique
Expérimentales et Moléculaire UMR7355**

3B rue de la Ferrollerie 45100 Orléans



